Bacterial Factors that affect the Inflammatory Response to *Streptococcus pneumoniae*

Jimstan Nerio Periselneris

Submitted for the Degree of Doctor of Philosophy

University College London

2016

Centre for Inflammation & Tissue Repair

Department of Respiratory Research

UCL Division of Medicine

I, Jimstan Periselneris, confirm that the work presented in this thesis is my own.

Where information has been derived from other sources, I confirm this has been indicated in the thesis.

Acknowledgments

This thesis reflects several years of time and input from many people whose hard work and enthusiasm have helped me during the course of my research fellowship. My laboratory skills were honed with the help of members of the pneumococcal research group (Charlie Plumptre, Gabby Szylar, Helina Marshall, Ricardo José, Rob Wilson, Sian Stafford, and Win Yan Chan) who also served as a brilliant sounding board within lab meetings. There are too many people to thank specifically within the wider Department of Respiratory Research and the Innate2Adaptive research group from whom I learned all the essential research skills used during my PhD. A few individuals merit specific thanks: Emilie Camberlein, Alex Dyson, Jennifer Roe, and Gillian Tomlinson were instrumental in helping with specific techniques that were used to obtain some of the data contained within the thesis. The Medical Research Council funded my fellowship; I hope I can repay their support.

Special thanks need to go to my two supervisors. Mahdad Noursadeghi was inspirational in his academic insight, determination, and enthusiasm. Despite his many other commitments always managed to find time for individual tuition. Enormous thanks must go to Jeremy Brown, my primary supervisor, without whom none of this would have come about. He has been an endless source of support and was always available for advice, showing enormous patience whilst steering me right through from writing the initial fellowship application, through to reading this thesis and undoubtedly whilst writing the papers to come.

Lastly I must thank my family. Finn won't remember a time when the PhD was not a major focus of our lives, and Niamh was born in the midst of it. Both have sat in the office at weekends whilst I tended my cells in the lab. Finally my wife, Nuala, without whom I would never have taken the first steps towards looking for research opportunities. She has been ever dependable and shown incredible forbearance as her evenings and weekends have been taken over by either the lab or the laptop. As always she is the best of me, and this thesis is a testament to her support.

Abstract

Streptococcus pneumoniae is an important bacterial pathogen causing significant morbidity and mortality. The host inflammatory response to *S. pneumoniae* plays a critical role in escalating the host defence response to deal with large bacterial numbers, however excess inflammation can cause bystander damage. Macrophages are a key immune cell that mediates recognition of pathogens and initiates inflammatory responses. The polysaccharide capsule and toxin pneumolysin are important virulence factors that affect multiple components of the immune system.

The *S. pneumoniae* capsule increases inflammatory responses *in vitro* tissue culture models, with macrophages providing the main response. This was not dependent on TLR2 signalling, phagocytosis, lectin signalling, or scavenger receptor function. Mouse pneumonia and rat septic shock modelling showed that this had *in vivo* correlates. This data was extended by examining the extent capsule affects inflammatory responses by using other bacteria expressing serotype 4 capsule, and serotype 4 expressing other serotypes' capsules.

Pneumolysin decreases inflammatory responses *in vitro*, this was found to be dependent on phagocytosis and partially by its pore forming ability. This was reflected by the TNF response in mouse bronchoalveolar lavage fluid in a mouse model. Blockade of TNF abrogated differences between wild-type bacteria and pneumolysin deficient mutants. TNF administration to mice increased the ability of bronchoalveolar lavage fluid to restrict the growth of *S. pneumoniae*.

In conclusion, capsule and pneumolysin have opposing roles in their effect on the inflammatory response. The inflammation promoting effects of capsule impact on virulence, and may increase morbidity during infection. The inflammation dampening effects of pneumolysin may be an important immune evasion strategy that explains its evolutionary conservation in *S. pneumoniae*.

Table of Contents

Figures

Tables

Abbreviations used in this thesis

ABC – ATP binding cassette

AEC – alveolar epithelial cells

AIM – absent in melanoma

AM – alveolar macrophage

AP-1 – activator protein 1

ASC - apoptosis-associated speck-like protein containing a caspase activation and recruitment domain

ATP – adenosine triphosphate

BALF – bronchoalveolar lavage fluid

BMDM – bone marrow derived macrophages

BPI - bactericidal/permeability-increasing protein

CAP – community acquired pneumonia

CARD - caspase activation and recruitment domain

CRD – carbohydrate recognition domain

CSF – cerebrospinal fluid

CYLD - cylindromatosis

DAMP – damage associated molecular patterns

DC – dendritic cells

DC-SIGN - dendritic cell-specific ICAM-3 grabbing non integrin

DD – death domain

DUSP - dual specificity protein phosphatases

ER – endoplasmic reticulum

ERK – extracellular signal-regulated kinase

FADD – Fas associated protein with death domain

FBS – Foetal bovine serum

hBD – β defensin

HBEC - human bronchoepithelial cells

IFN - interferon

IFNAR - interferon α/β receptor

Ig - immunoglobulin

IKKγ - IκB kinase γ

IL - interleukin

iNKT - invariant natural killer T cells

iNOS - inducible nitric oxide synthase

IPD – invasive pneumococcal disease

IRAK – interleukin 1 receptor associated kinases

IRE – interferon response elements

IRF – interferon regulatory factor

ITAM - immunoreceptor tyrosine based activation motif

JNK - c-Jun N terminal kinases

KC - keratinocyte chemoattractant

LPS - lipopolysaccharide

LRR – leucine rich repeats

LTA – lipoteichoic acid

MAC – membrane attack complex

MAIT - mucosal associated Invariant T cells

MAL - Myelin and lymphocyte protein

MAPK – mitogen activated protein kinase

MARCO - macrophage receptor with collagenous structure

MDA - melanoma differentiation-associated protein

MDM – monocyte derived macrophages

MHC - major Histocompatibility Complex

MK – mitogen activated protein kinase activated *protein* kinase

MLST - multi-locus sequence typing

MNK – mitogen activated protein kinase-interacting serine/threonine-protein kinase

MOI – multiples of infection

MR – mannose receptor

MSK - mitogen- and stress-activated protein kinase-1

NAG - N-acetylglucosamine

NAM - N-acetylmuramic acid

NEMO - NFκB essential modulator

NFAT - Nuclear factor of activated T cells

NFκB – nuclear factor kappa B

NIK - nuclear factor kappa B inducing kinase

NK – natural killer cells

NLR – like receptor

NLRP - nucleotide-binding oligomerization domain receptor family pyrin containing domain

NO – nitric oxide

NOD - nucleotide-binding oligomerization domain receptor

OD – optical density

OR – odds ratio

PAMP – pathogen associated molecular patterns

PAR – proteinase activated receptor

PBS – phosphate buffered saline

PCho - phosphorylcholine

PCV - pneumococcal conjugated polyvalent vaccine

PG - peptidoglycan

Ply - pneumolysin

PRR – pattern recognition receptor

RelA - v-rel avian reticuloendotheliosis viral oncogene homolog A

RIG - retinoic acid-inducible gene

RIPK - receptor-interacting serine/threonine-protein kinase

RLR - retinoic acid-inducible gene-I-like receptors

ROS – reactive oxygen species

RSK - ribosomal 6S kinase

SAP – serum amyloid

SIRPα - signal regulatory protein α

SP – surfactant protein

SR – scavenger receptor

STAT - signal transducer and activator of transcription

STING – stimulator of interferon genes

TA – teichoic acid

TAK - transforming growth factor β activated kinase

TBK - transforming growth factor β activated kinase binding protein

TCR – T cell receptor

TGFβ – transforming growth factor β

TIR - Toll/interleukin 1 receptor

TIRAP - Toll/interleukin 1 receptor adaptor protein

TLR – toll-like receptor

TNF – tumour necrosis factor

TNFR1&2 – tumour necrosis factor receptor 1 & 2

TRADD – tumour necrosis factor receptor type 1 associated death domain

TRAF – tumour necrosis factor receptor associated factor

1 Introduction

1.1 Background

1.1.1 Microbiology

Streptococcus pneumoniae (or pneumococcus) is a Gram-positive lancet shaped bacterium that usually grows as diplococci, but can also form short chains. Individual cells are between 0.5 and 1.25 μm in diameter. They do not form spores and are non-motile. Like other streptococci, they lack catalase and ferment glucose to lactic acid. When cultured aerobically on blood agar, they are α-haemolytic, giving a characteristic green colour (due to hydrogen peroxide causing the reduction of haemoglobin to methaemoglobin). This is a trait they share with other α-haemolytic streptococci such as the *viridans* species, which also colonise the oropharynx. Tests such as optochin sensitivity or susceptibility to bile salt induced lysis (Garcia-Suarez Mdel, Vazquez et al. 2006) may be required to differentiate *S. pneumoniae* from these commensals. However under anaerobic conditions, β-haemolysis (lysis of red cells resulting in transparent agar) may become evident due to the action of pneumolysin (Ply), which is an oxygen labile cytotoxin. *S. pneumoniae* grows best in culture at 37°C in 5% CO_2, and clinical isolates harbour an enzyme named LytA, which induces autolysis once culture has reached a stationary phase. To grow in culture the *S. pneumoniae* requires a source of catalase (e.g. from blood) to neutralise the hydrogen peroxide it produces.

The structure of *S. pneumoniae* consists of a cell membrane that contains the intracellular material including free circular DNA, and is surrounded by a complex cell wall that allows the bacterium to maintain shape and not lyse due to osmotic pressure. This is then surrounded by a polysaccharide capsule. There are multiple proteins that are attached to the cell membrane and cell wall that contribute to virulence (see chapter 1.5 and table 1.8).

S. pneumoniae cell wall consists of peptidoglycan (PG), lipoproteins, wall teichoic acid (TA), and lipoteichoic acid (LTA). Wall TA is covalently bonded to PG, whereas LTA is non-covalently anchored to the cell membrane via a diacylglycerol-containing lipid anchor

(Weidenmaier and Peschel 2008). Both TA and LTA contain phosphorylcholine (PCho), which serves as an anchor for surface-exposed choline-binding proteins.

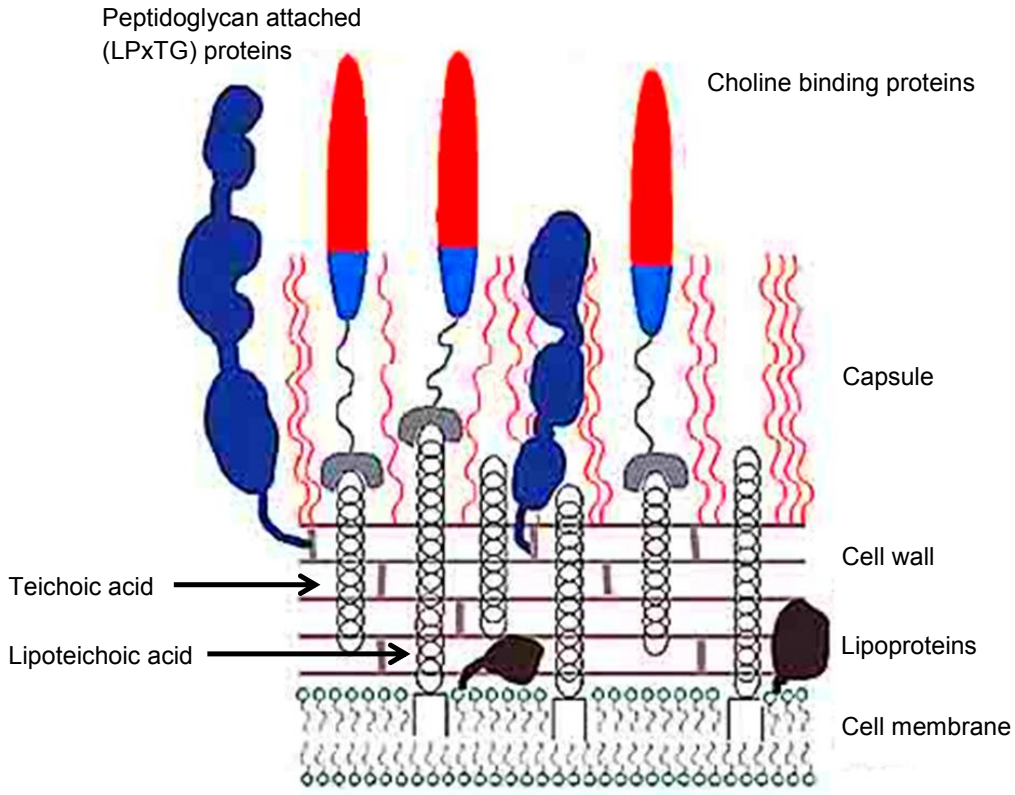

Figure 1.1: Basic *S. pneumoniae* surface structure (Jedrzejas, 2004)
Schematic of how *S. pneumoniae* cell membrane and cell wall are structured.

The first published *S. pneumoniae* genome was for TIGR4, a capsular serotype 4 strain. This has a circular genome containing 2,160,837 base pairs, with 4-6 ribosomal RNA operons depending on strain, and 5% content made up of insertion sequences (Tettelin, Nelson et al. 2001). The genomes of other strains sequenced demonstrate significant genomic heterogeneity between strains, with a core genome of around 50% of the genome (Dopazo, Mendoza et al. 2001, Barocchi, Censini et al. 2007, Lanie, Ng et al. 2007, Donkor, Stabler et al. 2012).

S. *pneumoniae* is genetically and phenotypically closely related to commensal species such as *Streptococcus mitis*, *Streptococcus oralis*, and *Streptococcus infantis*. Population genetic analysis suggests that *S. mitis* has evolved from a common ancestor of *S. pneumoniae* (very similar to the current pneumococcus) but the loss of 15% of its genome including virulence factors results in a harmonious existence with its host. Horizontal transfer of genetic material by *S. pneumoniae* is common, with evidence of periodic transfer of genetic material from *S. mitis* to *S. pneumoniae* (Kilian, Riley et al. 2014). Due to its different epidemiological behaviour compared to other commensals, with frequent short-lived colonisation episodes, *S. pneumoniae* is exposed to a greater number of potential recombination partners. It is possible that a very small population of humans living over 100,000 years ago represent a bottleneck for S. *pneumoniae* and that the recent expansion of the human population allowed lineage-specific expansion of S. *pneumoniae* (Kilian, Poulsen et al. 2008).

1.1.2 Infection & Disease

1.1.2.1 Colonisation

S. pneumoniae is a ubiquitous nasopharyngeal commensal that occasionally spreads beyond its usual ecological niche to cause disease. Over half of children under the age of 2 are colonised, reducing to approximately 8% of adults (Hussain, Melegaro et al. 2005). Colonisation frequently occurs without disease, and asymptomatic carriage induces acquired B cell immunity, as evidenced by circulating serotype specific antibodies (Musher, Groover et al. 1997). However, nasopharyngeal carriage is necessary to progress to disease. In addition, colonisation is thought to be important in horizontal spread, as transmission is via aerosolised droplet. Duration of colonisation reduces with age, likely due to improved immunological memory through exposure to multiple strains, as previous colonisation extends time to subsequent nasopharyngeal carriage by any strain (Turner, Turner et al. 2012).

As the nasopharynx is the natural ecological niche for *S. pneumoniae*, it is likely that most evolutionary pressure is dependent on successful colonisation strategies. Competition

between bacterial species (both pathogenic and non-pathogenic) may be the most important factor that drives the genetic make-up of *S. pneumoniae*, e.g. the production of hydrogen peroxide from *S. pneumoniae* inhibits *Neisseria meningitidis* and *Staphylococcus aureus* growth (Pericone, Overweg et al. 2000).

1.1.2.2 Disease

S. pneumoniae causes a variety of disease phenotypes including non-invasive disease such as otitis media and infective exacerbations of chronic obstructive pulmonary disease. Invasive disease phenotypes include pneumonia, meningitis, and septicaemia. *S. pneumoniae* is responsible for over 800,000 deaths a year in children under 5 (O'Brien, Wolfson et al. 2009), and overall is likely to cause well over a million deaths a year worldwide, leaving it second only to tuberculosis as a cause of bacterial mortality (Walker, Rudan et al. 2013). *S. pneumoniae* is responsible for almost half of pneumonia cases, causing 38% of outpatient treated community acquired pneumonia (CAP), 27% of hospital treated, and 27% of intensive care unit treated CAP (Welte, Torres et al. 2012).

Once *S. pneumoniae* are aspirated into the respiratory tract, if they do not get cleared by the host immune response, bacteria multiple rapidly in the alveolus and spread through the pores of Kohn to cause lobar infection. As a result of local inflammation there is the accumulation of protein-rich fluid in the alveolar compartment, this is accompanied by migration of leukocytes. This thick exudative fluid can solidify to form consolidation and impair gas exchange. Fortunately, if the bacterial infection is cleared, the consolidation can resolve, often without long-term sequelae.

Invasive pneumococcal disease (IPD) requires the movement of bacteria from mucosal surfaces through epithelium into regions of the body that are largely sterile. Less than 1% of *S. pneumoniae* infections achieve invasive bacteraemia, however at this stage mortality rates approach 10%, with rates as high as 25% in patients with predisposing risk factors which are outlined below (Naucler, Darenberg et al. 2013).

1.1.2.3 Risk factors for disease

Host factors can increase the risk of serious *S. pneumoniae* infection; including immune deficiency (Lynch and Zhanel 2010) (HIV, innate immune signalling defects, immunoglobulin (Ig) deficiencies, complement deficiencies, myeloma, post organ transplant), splenic dysfunction (e.g. asplenia, sickle cell disease), and chronic organ dysfunction (Table 1.1). The extremes of age (Table 1.2), smoking, alcohol abuse, and influenza increase the risk of disease mortality.

1.1.2.4 Diagnosis and Treatment

Diagnosis of *S. pneumoniae* infection is reliant on culturing the organism, urine antigen testing, or PCR. The BinaxNOW antigen test is a rapid immunochromatographic test for the use on urine and cerebrospinal fluid that detects TA (Sinclair, Xie et al. 2013). The test is rapid and may be positive in culture negative patients who have already been exposed to antibiotics. Novel multiplex urine capsular antigen tests are also useful (Huijts, Pride et al. 2013). Nucleic acid amplification is also widely available; *lytA* quantitative real-time PCR had a sensitivity of 82.2% and a specificity of 92.0% in respiratory samples (Albrich, Madhi et al. 2012). All these techniques pick up culture negative infection, suggesting epidemiological estimates of disease based on culture are likely to be underestimates.

Antibiotic therapy is the mainstay of treatment for established infection with *S. pneumoniae*. The mortality rates from *S. pneumoniae* pneumonia have dropped from 50% in the pre-antibiotic era to <20% now. Delay of as little as 4 hours in antibiotic administration is associated with increased mortality (Lujan, Gallego et al. 2006). In the clinical setting antibiotics are given empirically for the clinical syndrome before an organism identified, with guidelines tailored for local antibiotic resistant patterns. If there is no suggestion of β-lactam resistance, first line treatment is with a penicillin or a cephalosporin.

Table 1.1: Odds Ratios for IPD compared to individuals with no risk factors, adapted from (van Hoek, Andrews et al. 2012)

Chronic disease	Acquisition of IPD in 2-15 year olds	IPD mortality in 2-15 year olds	Acquisition of IPD in 16-65 year olds	IPD mortality in 16-65 year olds	Acquisition of IPD >65 year olds	IPD mortality in IPD in >65 year olds
Splenic dysfunction	4.7	20.9	2.3	2.0	0.7	0.3
Chronic respiratory disease	12.7	6.6	16.8	3.9	5.1	1.2
Chronic heart disease	4.1	6.5	6.9	4.3	3.0	1.4
Chronic kidney disease	11.7	1.7	6.5	6.2	0.9	1.9
Chronic liver disease	29.6	7.0	33.3	10.3	7.2	2.8
Diabetes mellitus	3.8	Unknown	4.6	3.2	2.3	1.0
Immunosuppression (not HIV)	41	2.0	17.1	3.2	11.7	1.0
HIV	100.8	Unknown	61.2	1.6	5.3	Unknown

Table 1.2: Odds Ratios for 30-day mortality due to IPD, adapted from (Naucler, Darenberg et al. 2013)

Host Factor		Adjusted odds ratio (OR)
Age	>85	29.4
	75-84	11.3
	65-74	7.1
	55-64	4.8
	45-54	2.6
	<45	1 (reference)
Sex	Male	1.55
	Female	1 (reference)
Smoking	Yes	1.79
	No	1 (reference)
Alcohol abuse	Yes	3.82
	No	1 (reference)

1.1.2.5 Vaccine prevention

Vaccination is widely used to reduce the burden of *S. pneumoniae* disease. Vaccines were initially based on a whole cell killed vaccine that did not protect against pneumonia for more than 2 months (Grabenstein and Klugman, 2012), then more recently on the polysaccharide capsule, which was the first non-protein antigen described. A 23-valent vaccine (Pneumovax) covers 23 common disease-causing serotypes (1, 2, 3, 4, 5, 6B, 7F, 8, 9N, 9V, 10A, 11A, 12F, 14, 15B, 17F, 18C, 19F, 19A, 20, 22F, 23F, and 33F). This induces B lymphocytes to create appropriate antibodies by multipoint recognition of polysaccharide. As children have relatively immature B cells this vaccine is not effective in this critical group who host the most colonisation events and facilitate horizontal infection. Conjugating capsular polysaccharide to a carrier protein elicits a more effective response, and this has become the mainstay of childhood vaccination programmes. The most recent pneumococcal conjugated polyvalent vaccine (PCV, Prevenar) covers 13 serotypes (1, 3, 4, 5, 6A, 6B, 7F, 9V, 14, 18C, 19A, 19F, and 23F), though the preceding 10 valent vaccine is still widely used (covering serotypes 1, 4, 5, 6B, 7F, 9V, 14, 18C, 19F and 23F). The capsular polysaccharides are individually conjugated to CRM_{197}, a non-toxic diphtheria toxoid (Song, Dagan et al. 2012) which is expensive and does not afford cover to the other 80 serotypes currently known.

1.1.3 Molecular epidemiology

Given the enormous genetic variation evident in *S. pneumoniae* molecular epidemiology, techniques have been developed to identify subtypes and categorise cultured isolates, allowing for surveillance and tracking of outbreaks.

1.1.3.1 Capsular Serotypes

Variations in capsule composition have led to the identification of at least 93 serotypes of *S. pneumoniae*, grouped into 46 antigenically similar serogroups (Table 1.3), which exhibit different propensities for causing disease. The differential virulence of the serotypes is thought largely to be due to variation in capsule structure. Invasive disease potential of different serotypes can be calculated from rates of invasive disease compared to the

frequency of nasopharyngeal carriage in the population. Serotypes 1, 4, 7F, 18C and 14 have greater invasive disease potential whereas serotypes 6A, 6B, 23F, 9V, and 3 are relatively poor at causing IPD. These data are taken from children in Finland (Hanage, Kaijalainen et al. 2005), when comparing children nasopharyngeal carriage with all invasive isolates in Sweden (Sandgren, Albiger et al. 2004) and Oxford, UK (Brueggemann, Griffiths et al. 2003). However, all 3 groups found different serotypes were overrepresented in the invasive group. This may reflect local prevalence data that could skew the overall interpretation of results. Some authors have also found significant variation in disease induction within serotype, with the same studies noting more similarities in invasive potential associated with clonal type but varying serotype, due to serotype switch events. The mouse studies also noted variation in disease susceptibility by mouse strain, implicating host factors being as, if not more important than serotype (Sandgren, Albiger et al. 2005).

Some serotypes are overrepresented in fatal cases of infection (serotypes 3, 6A, 6B, 9N, 19F, 23F, 31) (Harboe, Thomsen et al. 2009, Weinberger, Harboe et al. 2010). Serotype prevalence varies widely by geographical region (Figure 1.2). Serotypes associated with high carriage prevalence and reduced invasiveness are more heavily encapsulated. Paradoxically invasive serotypes (1, 7F, 14) have relatively reduced mortality rates. This suggests that 'invasive serotypes' act as primary pathogens; more likely to affect the immunocompetent, whereas less invasive serotypes cause infection in patients with underlying disease i.e. causing 'opportunistic infection' (Sjostrom, Spindler et al. 2006).

In a UK study serotypes 14, 1, 8, 3, 19A, 5, 7F, 4 and 6A/C were the commonest causes of CAP, with less invasive serotypes causing more disease and mortality with increasing age (Bewick, Sheppard et al. 2012). Serotype 5 and 14 were overrepresented in non-invasive disease. In American studies serotype1, 7F, 19A and 3 are overrepresented as causes of complicated pneumonia (Fletcher, Schmitt et al. 2014). Serotype 1 was also the commonest cause of CAP in Spain, whereas 19A was more prominent in the Asia-Pacific region. In the UK, serotype1 predominated in causing empyema (McKee, Ives et al. 2011), and serotype3 caused most

bronchopleural fistulas. In another Spanish study serotype1, 5, 7F, and 14 caused most empyemas (Fletcher, Schmitt et al. 2014). Overall cases of complicated *S. pneumoniae* pneumonia and empyema have increased over the past few decades. Though these data may change as all the above serotypes are covered by the PCV13 vaccine. There is less serotype variation in meningitis mortality, suggesting that host factors may be more important in this disease setting, though serotypes 6 and 14 are the most frequently isolated from cerebrospinal fluid (CSF) (Hausdorff, Bryant et al. 2000). Risk factors for IPD associated respiratory failure include: age >50 years, chronic heart or lung disease, and infections by serotypes 3, 19A, and 19F, all of which are heavily encapsulated (Burgos, Lujan et al. 2014). However serotype 8 has a thick capsule and no increase in risk of respiratory failure, indicating that the degree of encapsulation is not the sole factor that is associated with serotype dependent disease.

1.1.3.2 Sequence Typing

S. pneumoniae can also be categorised based on its genetic sequence type. Multi-locus sequence typing (MLST) classifies *S. pneumoniae* based on the sequence of seven core housekeeping gene fragments (Hanage, Kaijalainen et al. 2005). By tracking polymorphisms in these genes, closely related isolates can be identified. A number of isolates responsible for invasive disease from different countries were of the same sequence type, but not necessarily the same serotype (Coffey, Daniels et al. 1999), suggesting clonal expansion with the acquisition of differing capsular polysaccharides by horizontal gene transfer, explaining the variety within serotypes. *S. pneumoniae* strains of different sequence type may therefore have distinct virulence phenotypes independent of capsular polysaccharide (Sjostrom, Spindler et al. 2006). It has been suggested that clonal expansion of *S. pneumoniae* may be more important in isolates responsible for invasive disease than isolates responsible for nasopharyngeal colonisation (Donkor, Stabler et al. 2012).

Table 1.3: Serotypes and serogroups adapted from (Henrichsen 1995)

Type	Cross reactions by capsular reaction	Type	Cross reactions by capsular reaction
1	1a	19C	19a, 19c, 19f, 7h
2	2a	20	20a, 20b, 7g
3	3a	21	21a
4	4a	22F	22a, 22b
5	5a	22A	22a, 22c
6A	6a, 6b	23F	23a, 23b, 18b
6B	6a, 6c	23A	23a, 23c, 15a
6C	6a, 6b	23B	23a, 23b, 23d
7F	7a, 7b	24F	24a, 24b, 24d, 7h
7A	7a, 7b, 7c	24A	24a, 24c, 24d
7B	7a, 7d, 7e, 7h	24B	24a, 24b, 24e, 7h
7C	7a, 7d, 7f, 7g, 7h	25F	25a, 25b
8	8a	25A	25a, 25c, 38a
9A	9a, 9c, 9d	27	27a, 27b
9L	9a, 9b, 9c, 9f	28F	28a, 28b, 16b, 23d
9N	9a, 9b, 9e	28A	28a, 28c, 23d
9V	9a, 9c, 9d, 9g	29	29a, 29b, 13b
10F	10a, 10b	31	31a, 20b
10A	10a, 10c, 10d	32F	32a, 27b
10B	10a, 10b, 10c, 10d, 10e	32A	32a, 32b, 27b
10C	10a, 10b, 10c, 10f	33F	33a, 33b, 33d
11F	11a, 11b, 11e, 11g	33A	33a, 33b, 33d, 20b
11A	11a, 11c, 11d, 11e	33B	33a, 33c, 33d, 33f
11B	11a, 11b, 11f, 11g	33C	33a, 33c, 33e
11C	11a, 11b, 11c, 11d, 11f	33D	33a, 33c, 33d, 33f, 6a
11D	11a, 11b, 11c, 11e	34	34a, 34b
12F	12a, 12b, 12d	35F	35a, 35b, 34b
12A	12a, 12c, 12d	35A	35a, 35c, 20b
12B	12a, 12b, 12c, 12e	35B	35a, 35c, 29b
13	13a, 13b	35C	35a, 35c, 20b, 42a
14	14a	36	36a, 9e
15F	15a, 15b, 15c, 15f	37	37a
15A	15a, 15c, 15d, 15g	38	38a, 25b
15B	15a, 15b, 15d, 15e, 15h	39	39a, 10d
15C	15a, 15d, 15e	40	40a, 7g, 7h
16F	16a, 16b, 11d	41F	41a, 41b
16A	16a, 16c	41A	41a
17F	17a, 17b	42	42a, 20b, 35c
17A	17a, 17c	43	43a, 43b
18F	18a, 18b, 18c, 18f	44	44a, 44b, 12b, 12d
18A	18a, 18b, 18d	45	45a
18B	18a, 18b, 18e, 18g	46	46a, 12c, 44b
18C	18a, 18b, 18c, 18e	47F	47a, 35a, 35b
19F	19a, 19b, 19d	47A	47a, 43b
19A	19a, 19c, 19d	48	48a
19B	19a, 19c, 19e, 7h		

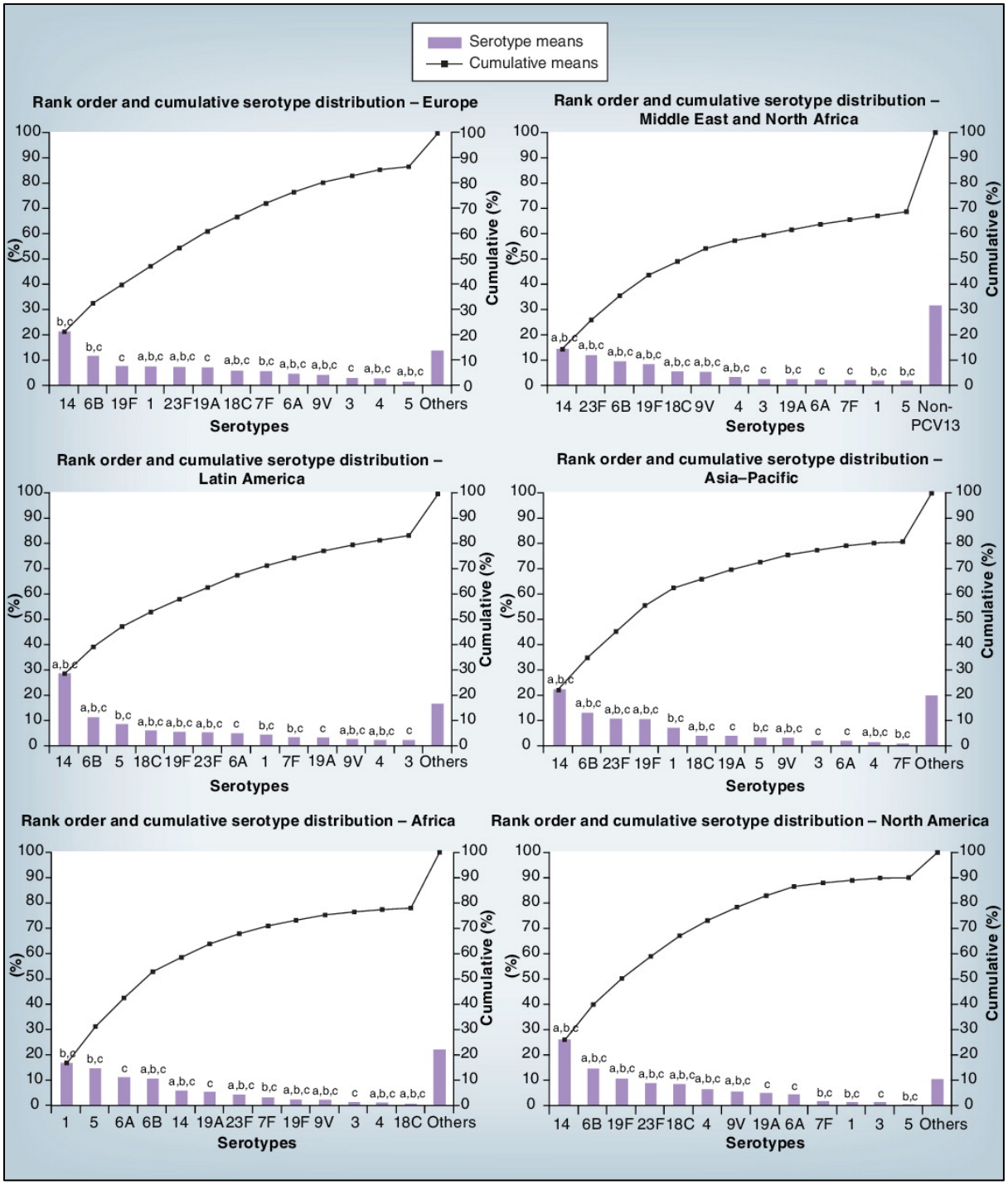

Figure 1.2 Cumulative distribution, by global region, of serotypes causing paediatric IPD for the 13 serotypes in PCV13 and an aggregate estimate for other serotypes, prior to PCV7 introduction (McIntosh and Reinert 2011); a – serotype present in PCV 7, b – serotype present in PCV 10, c – serotype present in PCV 13.

1.1.3.3 Effect of Vaccines on Epidemiology

Multiple studies have examined the effect of the PCV 7 vaccine (which preceded the current 13-valent vaccine) on *S. pneumoniae* infections. While undoubtedly effective in reducing the total burden of pneumococcal disease (by >40%), vaccination has resulted in an increase in nasopharyngeal carriage and disease caused by non-vaccine serotypes (e.g. 11A, 16F, 19A, 22F, 35B) (Hsu, Shutt et al. 2009, Weinberger, Malley et al. 2011). Genetic analysis has shown that existing subpopulations of *S. pneumoniae* have expanded to fill the ecological niche of the vaccine serotypes (Croucher, Harris et al. 2011).

Macrolide resistance has increased in both PCV13 and non PCV 13 serotypes by 2011 in North America, and similarly penicillin non-susceptibility has increased from 3.2 to 11.7% between 1998 and 2011 (Song 2012). There has been particular concern with the expansion of 19A, which accounted for 28-53% of penicillin non-susceptible isolates, and 86% of which are macrolide resistant. Fortunately 19A is covered by PCV13, but there is potential for other non-vaccine serotypes to acquire drug resistance and then spread rapidly.

PCV7 in USA since 2000 has reduced vaccine type invasive disease in young children (by 551 per 100,000 infants) as well as unvaccinated adults (by 1300 per 100,000) (Griffin, Zhu et al. 2013). By 2004 hospitalisations from all cause pneumonia had also reduced in young children. In 2009, decline in hospital admissions for children and adults have continued, with an estimated 168,000 fewer hospitalisations than would have been expected pre PCV.

The introduction of the PCV13 conjugate vaccine has reduced rates of nasopharyngeal carriage of serotypes contained within the vaccine, but not overall carriage rates in children, suggesting replacement by non-vaccine serotypes (van Hoek, Sheppard et al. 2014). The use of the PCV13 vaccine in over 65s has reduced rates of CAP due to *S. pneumoniae,* but not overall CAP rates, over the subsequent year (Bonten, Huijts et al. 2015). However, PCV13 roll out to children in the USA has reduced overall rates of CAP in adults as well as *S. pneumoniae* CAP in children and adults, suggesting that there are herd protective effects of reducing

nasopharyngeal colonisation (Simonsen, Taylor et al. 2014). PCV13 serotypes have a higher incidence of causing IPD compared to non-vaccine serotypes, so PCV13 has had a greater impact on IPD than CAP.

PCV13 roll out in the UK (2010) has coincided with a decrease in incidence rate ratios of total and pneumococcal hospitalised CAP by 0.96 and 0.84 respectively from an incidence in 2008 of 79.9 and 23.4 per 100,000 respectively (Rodrigo, Bewick et al. 2015). *S. pneumoniae* meningitis admission rates have reduced from 4.45 to 2.03 per 100,000 in the UK, septicaemia rates have reduced from 2.81 to 1.12 (Martin, Sadarangani et al. 2014), and the overall incidence of IPD in the UK has decreased from 15.63 to 6.85 per 100,000 (Waight, Andrews et al. 2015). However, there is evidence of a slight increase in non-vaccine serotypes causing invasive disease (Waight, Andrews et al. 2015).

Given the spectre of serotype replacement there continues to be work on *S. pneumoniae* vaccines, ideally that will act across all serotypes. As such there is interest in using protein antigens that are expressed by all *S. pneumoniae* for example, Ply and PspA (Daniels, Rogers et al. 2016). Alternative strategies are also being investigated, such as whole cell vaccines using killed or attenuated bacteria (Chimalapati, Cohen et al. 2011).

1.2 Overview of the Innate Immune Response to *S. pneumoniae*

1.2.1 Mucociliary escalator

Successful adhesion to epithelium is a prerequisite for *S. pneumoniae* causing both colonisation and disease. The initial obstacle is the mucus layer, produced by goblet cells, covering the ciliated pseudostratified columnar epithelial surfaces of nasopharynx or the proximal bronchial tree. The viscous gel layer entraps pathogens, which are then transported by ciliary beating and coughing into the oropharynx. The mucus also contains antimicrobial compounds and mucins, which are glycoproteins coated with negatively charged sialic acid, that serve to bind positively charged bacteria. *S. pneumoniae* expresses several enzymes that cleave sialic acid, e.g. NanA. Inhibition of mucociliary function by cigarette smoke (Nuorti, Butler et al. 2000) or viral co-infection (Pittet, Hall-Stoodley et al. 2010) increases the ability of invading bacteria to establish infection within the lungs.

1.2.2 Epithelial Adhesion & Invasion

S. pneumoniae adheres to cell surface carbohydrates, N-acetyl-glycosamine (GlcNAc), on resting epithelium. This is mediated by cell surface proteins on *S. pneumoniae* binding to receptors on the epithelium and also contributing to hydrophobic and electrostatic surface characteristics contributing to physiochemical interactions (Bogaert, De Groot et al. 2004). The adhesin PspC expressed on the *S. pneumoniae* surface binds to laminin receptor, which is expressed on a variety of cell types including nasopharyngeal epithelium (Zhang, Mostov et al. 2000).

The epithelium acts as a barrier, preventing pathogens from invading into tissue and blood. Damage to the epithelium, in particular through viral infection, increases likelihood of IPD (Kash, Walters et al. 2011). *S. pneumoniae* only enters activated epithelial and endothelial cells; this is mediated by upregulation of cells surface platelet activating factor receptor (PAFr) and GlcNAc expression, induced by pro-inflammatory cytokines (Cundell, Weiser et al. 1995). Adhesion to activated host cells is enhanced by PAFr, which recognises PCho on the

bacterial surface (Cundell, Gerard et al. 1995, Ring, Weiser et al. 1998). PCho bound to PAFr has different effects depending on the cell involved; epithelial cells have an inflammatory response but no uptake whereas endothelial cells internalise *S. pneumoniae* (Fillon, Soulis et al. 2006).

There are 2 routes by which S. pneumoniae has been described as invading through epithelium. It is likely that both occur in parallel. There is evidence that binding to the polymeric Ig receptor also facilitates bacterial uptake, while the majority of *S. pneumoniae* are destroyed in phagolysosomes, a few undergo trancytosis via recycling endosomes through the epithelial layer (Asmat, Agarwal et al. 2014). *S. pneumoniae* also translocates across epithelium by moving through tight junctions between cells (Clarke, Francella et al. 2011). Toll-like receptor (TLR) stimulation induced upregulation of the transcription factor SNAIL1, which downregulated transcription of claudins (7 and 10 particularly), which are important components of tight junctions between epithelial cells. *In vitro,* polarised HBEC monolayers had reduced transepithelial electrical resistance after incubation with *S. pneumoniae*. The host evolutionary imperative for this process is likely to be to allow the egress of host immune cells to the mucosal surface.

1.2.3 Antibacterial peptides

Antibacterial products are found in alveolar lining fluid that assist in bacterial killing. Respiratory secretions inhibit the growth of bacteria, though this is inhibited by the addition of divalent cations, as cationic peptides have an electrostatic attraction to anionic microbial surfaces. Treatment of mice with aerosolised killed non typeable *Haemophilus influenzae* protected mice from subsequent challenge with aerosolised *S. pneumoniae* by increasing levels of multiple proteins with antimicrobial properties in bronchoalveolar lavage fluid (BALF) (Clement, Evans et al. 2008).

Antibacterial compounds include (a) lactoferrin, which sequesters free iron required for bacterial growth and oxidises bacterial cell membranes, (b) lysozyme, which breaks down PG

in bacterial cell walls; and (c) a wide range of antimicrobial peptides (e.g. defensins and cathelicidin) that form pores in bacterial cell surfaces thereby lysing invading pathogens. The efficacy of these soluble components of mucosal defences against *S. pneumoniae* has been poorly defined.

Lactoferrin is an iron binding protein found in neutrophil granules and epithelial secretions. It sequesters iron that is essential for bacterial respiration, but also has direct microbicidal effects. *S. pneumoniae* is relatively resistant to lactoferrin as it is bound by pneumococcal surface protein A (PspA), which blocks its activity (Shaper, Hollingshead et al. 2004).

Similarly, while lysozyme can restrict the growth of *S. pneumoniae,* modifications to its cell wall structure render it relatively resistant to degradation (Lee, Andalibi et al. 2004, Davis, Akinbi et al. 2008). Lysozyme breaks down the glycosidic bond between N-acetylglucosamine (NAG) and N-acetylmuramic acid (NAM), which make up PG. It is highly effective against Gram-positive organisms. Although it is produced by neutrophils, in respiratory fluids the major source is probably airway epithelium and associated glands. Both lysozyme and lactoferrin restrict *S. pneumoniae in vitro*, but have more effect in combination (Andre, Politano et al. 2015).

The α defensins 1-4 also known as human neutrophil peptides (HNP) are small peptides found in neutrophil azurophilic granules whereas 5&6 are found in the secretory granules of Paneth cells, and are important in neutrophil mediated killing of *S. pneumoniae* (Beiter, Wartha et al. 2008). The β defensins (hBD) 1-4 are all found in respiratory fluids, with hBD2 release stimulated by direct activation of epithelial cells, as well as by the cytokines such as interleukin (IL) 1β and tumour necrosis factor (TNF) (Kota, Sabbah et al. 2008, Kim, Min et al. 2010). They act by permeabilising membranes rich in anionic phospholipids (with relative sparing of cholesterol and neutral membranes found in humans), and have antimicrobial activity against bacteria, fungi & viruses. Their effects are inhibited by increasing salt concentrations. They may also act by inducing secretory leukocyte protease inhibitor (SLPI)

and CXCL8 secretion by bronchial epithelial cells. hBD1-3 are the most extensively studied; hBD3 appears to be the most potent. Respiratory epithelial cells constitutively express hBD1, whereas hBD2 & 3 are inducible by *S. pneumoniae*, and both restrict *S. pneumoniae* growth and induce its lysis *in vitro* (Lee, Andalibi et al. 2004, Scharf, Zahlten et al. 2012).

Cathelicidins are mammalian peptides with a varied C terminal peptide sequence that undergo extracellular proteolytic cleavage. LL37 is the only known human member and are found in specific granules of neutrophils and from alveolar epithelium and exhibit broad spectrum microbicidal activities (Ganz 2004). Bactericidal/permeability-increasing protein (BPI) is a cationic protein from azurophilic granules in neutrophils and expressed in mucosal epithelium, and recombinant BPI binds to *S. pneumoniae*. While the addition of recombinant BPI has no effect on growth of *S. pneumoniae*, it increased the association of bacteria with mouse macrophages, increased apoptosis and was protective against pneumonia in a mouse model (Srivastava, Casey et al. 2007).

Surfactant protein A & D (SP-A & D respectively) are constitutively synthesised and secreted into alveolar lining fluid by type II pneumocytes and non-ciliated bronchial epithelial cells. SP-A & D bind to exposed mannose and glucose residues on the surface of bacteria, leading to agglutination of pathogens, inhibition of microbial growth, and increase recruitment of phagocytes. SP-A also functions as an opsonin that increases macrophage phagocytosis of *S. pneumoniae* (Sano, Kuronuma et al. 2006).

1.2.4 Alveolar macrophage

Macrophages are tissue resident phagocytes that play an important role in orchestrating innate immune responses to pathogens. They are characterised by surface expression of multiple proteins, few of which are unique to macrophages; a combination of CD14, CD68 and CD163 have been used to identify human tissue macrophages in the past (Murray & Wynn, 2011). They are able to phagocytose foreign material, coordinate a cytokine response to organisms and act as antigen presenting cells. Macrophages kill pathogens by a variety of

mechanisms. Chief among these are inducible nitric oxide synthase and nicotinamide adenine dinucleotide phosphate (NADPH) oxidase, which enable the generation of reactive oxygen species (ROS). There appear to be subgroups of activated macrophages that display different phenotypes though this may be more akin to a spectrum of phenotypes. Classically activated or M1 macrophages are induced by exposure to interferon gamma (IFNγ) and TNF from Th1 lymphocytes, antigen presenting cells and natural killer (NK) cells. These cells appear to be primed towards microbicidal functions, i.e. to produce more ROS and more pro-inflammatory cytokines, as well as IL12 and IL23. M2 or alternatively activated macrophages are induced by IL4 released from Th2 cells. Their primary role appears to be tissue repair, with increased arginase activity resulting in ornithine, a precursor of collagen thereby contributing to extracellular matrix production. They are also induced by chitinase from parasites and appear to have a role in parasite clearance. A third subset, regulatory macrophages, are induced by IL10 from regulatory T cells, as well as immune complexes and apoptotic cells (Mosser and Edwards 2008). Their function appears to be anti-inflammatory by secreting more IL10 and reducing IL12 secretion, and they express more scavenger receptors and lectins. There appears to be some plasticity in macrophage phenotype, with the ability to switch phenotypes by changes in stimuli.

Foetal monocyte derived alveolar macrophages (AM) make up most of the resident macrophage population in the lung (Hussell and Bell 2014), and recognised by expressing lots of CD11c, little CD11b, and little MHC II on their surface, as well as high amounts of Siglec F, macrophage receptor with collagenous structure (MARCO), mannose receptor (MR), dectin-1 and galectin 3 (Davies, Jenkins et al. 2013, Findlay & Hussell, 2012, Hussell and Bell, 2014). Though, surface expression varies by stimulation state, and some of these receptors are more closely related to M1 or M2 phenotype than AM per se. They are predominantly derived from a low level of replication within the lung and have a long life span (Murphy, Summer et al. 2008). While only 1 in 3 alveoli contain AM, they make up 90-95% of cellular material within the alveoli, and AM can traverse alveoli by pores of Kohn. AM have

characteristics of both classically and alternatively activated phenotypes and can have their phenotype altered by the addition of cytokines. AM exhibit relatively little phagocytic activity and respiratory burst and present antigens relatively poorly. They lack CD86, so are less likely to stimulate T cells, promoting tolerance to innocuous antigens. In addition they may drive differentiation of T cells into a regulatory phenotype by the secretion of transforming growth factor β (TGFβ) and prostaglandins (Gwyer Findlay, Danks et al. 2014).

AM can contain small numbers of bacteria by phagocytosis, with depletion of AM in mouse pneumonia models decreasing bacterial clearance, but more so at low inocula (Camberlein, Cohen et al. 2015). Once their phagocytic capabilities are overcome they institute an inflammatory response that results in leukocyte chemotaxis (Dockrell, Marriott et al. 2003). If the neutrophils are able to clear the infection, macrophages then remove apoptotic neutrophils. If the neutrophils are not cleared, they undergo necrosis with subsequent release of ROS and proteases that cause tissue injury and inflammation.

1.2.5 Cytokines

After cellular recognition of *S. pneumoniae* by PRRs, an inflammatory response is generated by the production of cytokines and chemokines (Table 1.4 and 1.5). In mouse models of intranasal *S. pneumoniae* infection, levels of the pro-inflammatory cytokine TNF are elevated in BALF within an hour of infection followed by IL1β, particularly in lung homogenates, and then IL6 (Calbo and Garau 2010). IL6 is also rapidly elevated in serum. These cytokine responses are associated with neutrophil infiltrate starting from 2 hours onwards, with a later influx of inflammatory monocytes. In meningitis models there is a similar time course of inflammatory cytokine levels in CSF: TNF followed by IL1β, then IL6. Mice deficient in any of these cytokines have increased mortality rates (van der Poll, Keogh et al. 1997, Zwijnenburg, van der Poll et al. 2003, Gerber, Bottcher et al. 2004). These pro-inflammatory cytokines also induce the acute phase response, and upregulate adhesion molecules to facilitate transmigration of leukocytes from the blood; this may also lead to downregulation

of the tight junctions between epithelial cells, facilitating *S. pneumoniae* invasion (Clarke, Francella et al., 2011).

The key cytokines that are important in *S. pneumoniae* responses are discussed in individual sections below.

1.2.5.1 Tumour Necrosis Factor

TNF is one of the cardinal cytokines involved in the inflammatory response. TNF is synthesised in the endoplasmic reticulum (ER) and TNF containing vesicles from the golgi complex fuse with recycling endosomes, which migrate to the cell membrane (Arango Duque and Descoteaux 2014). TNF is expressed by activated macrophages, lymphocytes, natural killer (NK) cells, and epithelial cells; and is generated in its transmembrane form as a 233 amino acid polypeptide (26kDa) and aggregates into homotrimers. TNFα converting enzyme cleaves the transmembrane form to release soluble TNF and the residual portion migrates back to the nucleus. It exerts effects when in either transmembrane or soluble forms. Soluble TNF then acts at distant sites by binding to type I and II TNF receptors (TNF – R1 and R2), whereas the transmembrane form acts in a juxtacrine fashion as a ligand of TNFR2 (Horiuchi, Mitoma et al. 2010).

The TNF receptor family contains 29 members that can be placed into 3 groups: a) induce apoptosis, b) induce inflammatory signalling cascades, and c) act as 'decoys'. Apoptosis is induced by activating caspase 8, which processes downstream caspases (Dempsey, Doyle et al. 2003). Nuclear factor kappa B (NFκB) actively inhibits the death function of TNFR1 by upregulating anti-apoptotic genes such as Bcl-2 and TNF receptor associated factor (TRAF) 1 & 2 (Figure 1.2). TNFR2 does not contain a death domain (DD) but can recruit Fas associated protein with DD (FADD) and/or receptor-interacting serine/threonine-protein kinases (RIPK) to induce apoptosis (Rahman and McFadden 2006).

Table 1.4: Cytokines involved in the immune response to *S. pneumoniae*

Cytokine	Function during *S. pneumoniae* infection	Reference
IFN α/β	Upregulate tight junctions and downregulate PAFr in murine pneumonia models	(Parker, Martin et al. 2011, LeMessurier, Hacker et al. 2013)
IFNγ	Induces inflammatory monocyte infiltrate in murine meningitis model. Induces neutrophil infiltrate by stimulating chemokines in a murine pneumonia model	(Mitchell, Yau et al. 2012) (Sun, Salmon et al. 2007)
IL1β	Endogenous pyrogen, potentiates inflammatory responses in murine pneumonia models	(Marriott, Gascoyne et al. 2012, Zwijnenburg, van der Poll et al. 2003, Jones, Simms et al. 2005)
IL6	Induces acute phase response and potentiates inflammatory responses in murine pneumonia model	(Quinton, Jones et al. 2009, van der Poll, Keogh et al. 1997)
IL10	Inhibits inflammatory responses and inhibits neutrophil recruitment by affecting chemokine expression	(Williams, Jose et al. 2015)
IL12	Induces IFNγ secretion in murine pneumonia models	(Sun, Salmon et al. 2007Yamamoto, Kawakami et al. 2004)
IL17	Potentiates inflammatory responses including neutrophil recruitment, and increases mucosal immunity in murine pneumonia and human colonisation models	(Zhang, Clarke et al. 2009, Li, Moltedo et al. 2012, Wright, Bangert et al. 2013)
IL23	Stimulates T cells, increases IFNγ and IL17 in murine pneumonia models	(Kim, Lee et al. 2013)
IL27	Inhibits IL17 production, so increasing susceptibility in a murine pneumonia model	(Cao, Wang et al. 2014)
TNF	Endogenous pyrogen, and potentiates inflammatory responses in murine pneumonia and meningitis models	(Takashima, Tateda et al. 1997, van der Poll, Keogh et al. 1997, Gerber, Bottcher et al. 2004, Jones, Simms et al. 2005)

In the hypothalamus TNF stimulates corticotropin releasing hormones, suppresses appetite, and induces fever. It stimulates the acute phase response from the liver, vasodilation and increased vascular permeability, and helps regulate chemokine release including inducing CXCL1, 2, and 5 and increasing cell adhesion molecule expression as well as CXCR2 dependent neutrophil migration.

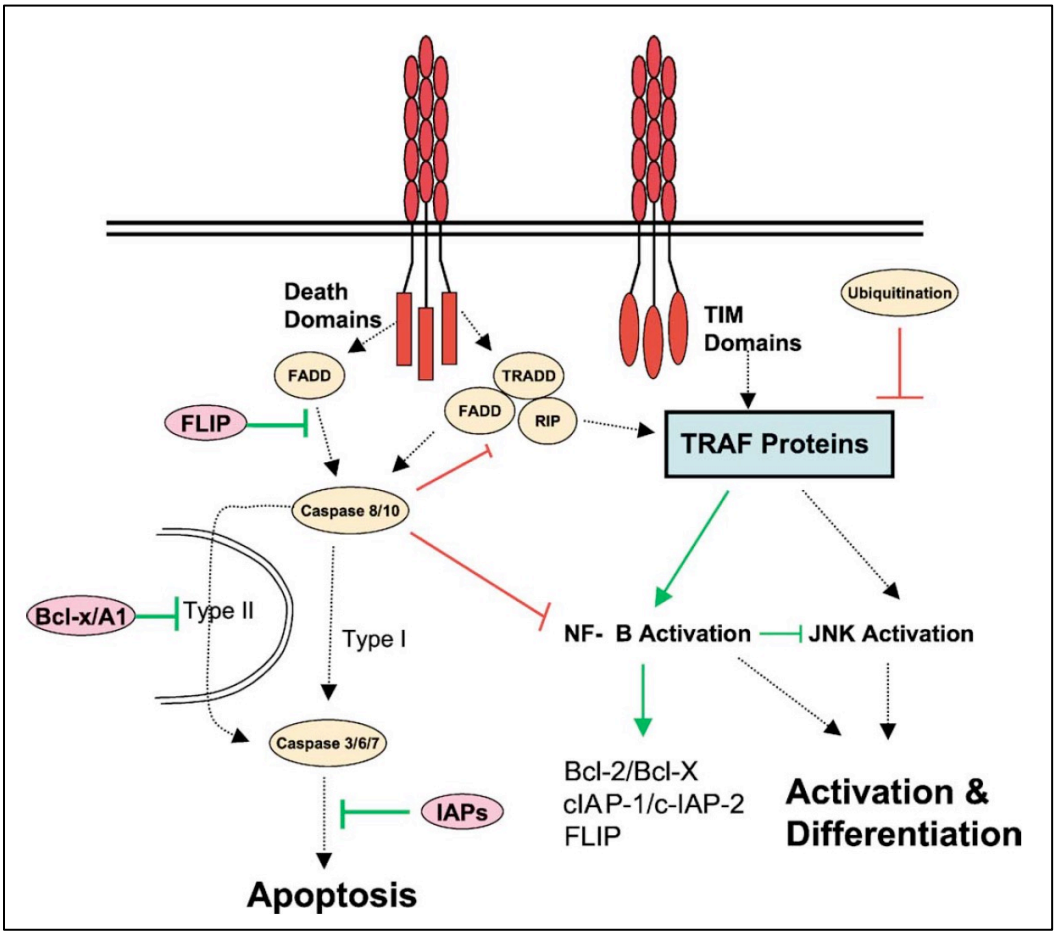

Figure 1.3: **Apoptosis v inflammatory pathways downstream of TNF receptor activation** (Dempsey, Doyle et al. 2003)

TNFR1 labelled in red, upon binding to ligand, induces activation of signalling molecules, such as members of the TRAF family. Signalling cascades induce two main effects; apoptosis or inflammation & differentiation. Anti-apoptotic signalling is labelled in green, whereas pro-apoptotic are in red.

TNF is important in the host response to *S. pneumoniae*. *In vitro* TNF increased the oxidative burst produced by neutrophils in response to *S. pneumoniae* (Kragsbjerg and Fredlund 2001). In addition, TNF deficient mice had poorer bacterial clearance and survival in pneumonia and meningitis models (Gerber, Bottcher et al. 2004, Jeong, Seo et al. 2015) and TNF blockade decreased mouse survival in a pneumonia model (van der Poll, Keogh et al. 1997). This was associated with greater bacteraemia, relative neutropenia, and the development of solid lobar consolidation and pulmonary haemorrhage (Takashima, Tateda et al. 1997).

1.2.5.2 Interleukin 1β

The IL1 gene family consists of the agonists IL1α and IL1β, and the antagonist IL1 receptor antagonist (IL1RA). IL1RA binding to the IL1R fails to recruit an accessory protein, therefore inhibiting the agonists. IL1β is released primarily by monocytes and macrophages, but also NK cells, B cells, DCs, and epithelial cells. IL1β is synthesised as a precursor that is cleaved by caspase-1 after inflammasome activation. Release of IL1β is usually thought to require cell membrane permeabilisation, and occur as a part of the process of subsequent cell death (Martín-Sánchez, Diamond et al. 2016). In neuronal cells, a process of active transport out of the cell by ATP binding cassette (ABC) transporters has been described (Marty V, Medina C et al. 2005). IL1β acts to induce the acute phase response, fever, prostaglandin release from the hypothalamus, and histamine release from mast cells to elicit vasodilation. It is also a chemoattractant for granulocytes, induces expansion of CD4 T cells, and increases adhesion molecules on endothelium and leucocytes. IL1α is active as an intracellular precursor or as its membrane-associated form. It is synthesised de *novo* and can be actively secreted or passively released from apoptotic cells and functions similarly to IL1β (Arango Duque and Descoteaux 2014).

IL1R deficient mice were more susceptible to *S. pneumoniae* colonisation, pneumonia and meningitis (Zwijnenburg, van der Poll et al. 2003, Lemon, Miller et al. 2015). This was associated with higher levels of TNF, IL6, CCL2 and IFNγ in BALF and increased lung bacterial load, but comparable levels of keratinocyte chemoattractant (KC), the mouse homologue of

CXCL8, to infection in wild-type mice. Neutrophil and macrophage numbers and phagocytosis function were also similar. In contrast, deficient mice had reduced levels of fibrinogen. Supplementing IL1R knockout mice with exogenous fibrinogen improved their survival to *S. pneumoniae* challenge (Yang, Ko et al. 2013). In a colonisation model, in IL1R deficient mice there was reduced neutrophil infiltrate at early timepoints, and later reduced macrophage numbers due to less CCL6 compared to wild-type (Lemon, Miller et al. 2015).

After murine intranasal infection IL1β deficient mice had reduced neutrophil numbers in blood compared to wild-type, and worse lung damage on histology, increased bacterial load in lungs, and reduced survival (Kafka, Ling et al. 2008). Administration of recombinant IL1β improved knock out mice survival to equivalence with wild-type.

CXCL8 release from A549 AEC by conditioned media from THP-1 monocytes exposed to *S. pneumoniae* was inhibited by IL1RA suggesting that IL1β is central to chemokine release from epithelial cells. IL1R deficient mice had less neutrophil recruitment after low dose *S. pneumoniae* infection than wild-type, associated with less CXCL1 in BAL at 24 hours, supporting the functional role of the IL1 family in inducing leukocyte recruitment (Marriott, Gascoyne et al. 2012).

1.2.5.3 Interleukin 6

IL6 is a soluble protein synthesised in the ER, that accumulates in the golgi and exits via tubulovesicular carriers (Arango Duque and Descoteaux 2014). IL6 has both pro- and anti-inflammatory functions; inducing the acute phase response and fever as well as promoting B cell differentiation into plasma cells and activation of CD8 cells. IL6 signalling occurs via soluble receptors binding to the ubiquitous gp130, leading to monocyte recruitment, promoting Th17 cell formation, and inhibiting Treg formation. Anti-inflammatory properties occur via classical signalling through the IL6 receptor (expressed on very few cells) to inhibit apoptosis and increase insulin sensitivity. Polymorphisms in IL6 are associated with increased incidence of otitis media, and limiting extrapulmonary spread in *S. pneumoniae*

infection (Schaaf, Rupp et al. 2005). IL6 deficient mice are unable to mount an acute phase response to *S. pneumoniae* pneumonia. This is dependent on IL6 inducing STAT3 activation in hepatocytes (Quinton, Jones et al. 2009). In a pneumonia model IL6 deficient mice had reduced survival, reduced bacterial clearance, but increased levels of both pro- and anti-inflammatory cytokines (van der Poll, Keogh et al. 1997).

1.2.5.4 Interleukin 17

The cytokine IL17 is involved in maintaining mucosal immunity against *S. pneumoniae* (Zhang, Clarke et al. 2009). Polymorphisms in IL17A are associated with increased colonisation and lung infection in humans (Nakada, Russell et al. 2011). Functions include increasing neutrophil recruitment, β defensin production, and expression of polymeric Ig receptor expression on alveolar epithelial cells, which is required for transport of antibodies into epithelial lining fluid. In addition, AM from healthy volunteers have increased uptake and killing of *S. pneumoniae* if incubated with recombinant IL17A (Wright, Bangert et al. 2013). IL17 levels peak 24 hours after *S. pneumoniae* infection and flow cytometry of lung homogenate suggests that γδT cells are the primary source of IL17 (Cao, Wang et al. 2014). IL17 neutralisation reduced neutrophil recruitment and decreased survival in a murine pneumonia model (Cao, Wang et al. 2014); conversely administration of recombinant IL17 reduced bacterial counts. This was associated with increased inflammatory cell infiltrate, increased CCL3 and hBD2 gene expression in lung homogenate, and increased IFNγ in BALF, supporting the central role of IL17 in mucosal immunity in the lung (Chen, Guo et al. 2014).

1.2.5.5 Type I Interferon

Type I IFNs consist of multiple IFNα forms and one IFNβ that bind to a heterodimeric receptor; the interferon α/β receptor (IFNAR). IFNβ mRNA is upregulated in lungs after 24 hours after *S. pneumoniae* infection. IFNAR deficient mice had prolonged nasopharyngeal carriage and increased mortality in lung infection models (Parker, Martin et al. 2011). Type I IFN release from macrophages occurred after phagocytosis and release of bacterial constituents (Kafka, Ling et al. 2008). IFNβ transcription is associated with upregulation of

tight junction proteins and downregulation of PAFr. This was associated with reduced bacterial transmigration across epithelial and endothelial layers in transwell systems. Administration of IFNβ protected mice against systemic disease in a pneumonia model, whereas using blocking antibody to IFNAR increased bacteraemia (LeMessurier, Hacker et al. 2013). This may be strain dependent, as an invasive serotype1 strain upregulated more type 1 IFN genes compared to a non-invasive strain (Hughes, Harvey et al. 2014). In this context IFNAR1 blockade significantly reduced invasion into pleura and blood, i.e. the opposite effect.

1.2.5.6 Interferon γ

IFNγ, secreted by Natural Killer cells and Th1 cells after intracellular PRR activation (Olliver, Hiew et al. 2011), activates macrophages. This usually improves phagocytosis and intracellular killing. However, IFNγ decreased mouse AM binding and internalisation of *S. pneumoniae in vitro* (Mina, Brown et al. 2015). Data on the role of IFNγ during *S. pneumoniae* infection is contradictory; it was largely protective in *S. pneumoniae* pneumonia models (Rubins and Pomeroy 1997, Weber, Tian et al. 2011), but influenza infection in a murine model induced IFNγ that increased susceptibility to subsequent *S. pneumoniae* infection a week later by reducing phagocytosis by AM (Sun and Metzger 2008). In addition, neutralisation of IFNγ was protective in a meningitis model in terms of survival and bacterial clearance due to reduced inflammatory monocyte infiltrate (Mitchell, Yau et al. 2012). Some studies suggest that recruited neutrophils are also an important source of IFNγ (Gomez, Yamada et al. 2015).

1.2.5.7 Other Important Cytokines

IL12 is produced primarily by macrophages and DCs. It synergises with TNF to stimulate Th1 cells by inducing IFNγ and increasing cytotoxicity of NK cells and CD8 cells (Arango Duque and Descoteaux 2014). IL12 deficiency in humans increases risk of *S. pneumoniae* lung infection (Haraguchi, Day et al. 1998). IL12 deficient mice had reduced survival in a pneumonia model (Yamamoto, Kawakami et al. 2004), and supplementary IL12

administration was protective against subsequent *S. pneumoniae* pneumonia in a murine model (Sun, Salmon et al. 2007).

IL22, from Th17 cells, is involved in the induction of inflammation as well as promoting mucosal immunity. *S. pneumoniae* pneumonia induced IL22 production in the lungs of mice, and IL22 production was protective against *S. pneumoniae* in primary infection (Van Maele, Carnoy et al. 2014) as well as in the context of prior sublethal influenza infection (Ivanov, Renneson et al. 2013).

IL23 is closely related to IL12, and is released from DCs and macrophages. It induces IFNγ as well as augmenting IL10 and IL17 production by T cells and chemokine upregulation by respiratory epithelial cells (Arango Duque and Descoteaux 2014). In a mouse pneumonia model, IL23 deficient mice had earlier bacteraemia, associated with lower neutrophil numbers in lungs up to 24 hours after infection. Mononuclear cells isolated from lungs of IL23 deficient mice secreted less IL17A and IFNγ in response to *S. pneumoniae*, and the mice had lower levels of IL6 and IL12 in BALF (Kim, Lee et al. 2013).

IL27 is a heterodimeric cytokine that signals via a receptor complex of T cell cytokine receptor, WSX-1 and gp130 and seems to play a role in regulating Th1/2/17 depending on context. It is produced early by macrophages in response to pathogens, and acts to induce IFNγ and Th1 differentiation, as well as inhibit Th17 differentiation (Arango Duque and Descoteaux 2014). Influenza infection induces a type I IFN mediated increase in IL27 that decreases production of IL17 from γδT cells, and thus increases susceptibility of mice to *S. pneumoniae*. IL27 receptor deficient mice had faster *S. pneumoniae* clearance than wild-type mice but this was only associated with reduced mortality if pre-infected with influenza (Cao, Wang et al. 2014).

The largely anti-inflammatory cytokine, IL10, plays an important role in regulating inflammation during *S. pneumoniae* infections. Deficiency of IL10 in murine models results in increased inflammation that is associated with improved bacterial clearance, but increased

mortality (van Der Poll, Marchant et al. 1997, Penaloza, Nieto et al. 2015). In murine models, IL10 levels were reduced in the lungs of infected aged mice, suggesting that immune dysregulation and enhanced inflammation in these mice is partly due to loss of this anti-inflammatory cytokine resulting in increased levels of chemokines (Williams, Jose et al. 2015). Furthermore the administration of IL10 in combination with antibiotics improves survival of mice infected with *S. pneumoniae* compared to infected mice treated with antibiotics alone (Wang, Bergeron et al., 2005).

1.2.6 Chemokines

The pro-inflammatory cytokines act in concert with chemokines (Table 1.5) to recruit leukocytes to the site of infection. Chemokines are grouped as families by their structure; CC chemokines have two adjacent cysteines, and CXC chemokines have cysteines separated by another amino acids. Chemokine relationships to their receptors are variable with some redundancy; several chemokines bind to the same receptor, and many receptors bind multiple chemokines. In particular, inhibition of CXCR2 (activated by CXCL 1-3, CXCL 5-8), which is expressed on neutrophils and macrophages, appeared to be protective in non-infective acute lung injury and chronic inflammation (Tomankova, Kriegova et al. 2015), but the absence of CXCR2 also compromised host defence (Herbold, Maus et al. 2010). Targeting individual chemokines may prove to be beneficial at attenuating neutrophilic inflammation without compromising host defence (Jose, Williams et al. 2015).

1.2.6.1 CCL Family

CCL2 is upregulated at mRNA and protein level in respiratory epithelial cell lines after exposure to *S. pneumoniae* lysates, this is reflected in transcriptional responses in mouse lung homogenate after inoculation with bacterial lysate (Shin, Yoo et al. 2010). The inability of infant mice to upregulate CCL2 in the nasopharynx in response to *S. pneumoniae* colonisation resulted in reduced macrophage recruitment and delayed clearance (Siegel, Tamashiro et al. 2015). CCL2 deficient mice infected with serotype19F, which results in a resolving

pneumonia phenotype, had reduced survival compared to wild-type, associated with increased bacteraemia. While there was an equivalent neutrophilic infiltrate, CCL2 deficient mice had reduced numbers of parenchymal DCs and inflammatory monocytes and reduced subsequent AM repopulation. This suggests that in less virulent infection, monocyte recruitment is important in preventing bacterial dissemination, that this effect is independent of neutrophil recruitment, and CCL7 and CCL12 cannot fully compensate for lack of CCL2 (Winter, Herbold et al. 2009).

CCL5 is secreted by epithelial cells, lymphocytes and platelets and acts as a chemokine for monocytes, NK cells, eosinophils, memory T cells, DCs and basophils by acting on CCR1, 3, 4 & 5. The expression of CCL5 in nasal associated lymphoid tissue was increased in response to colonisation with *S. pneumoniae,* and was associated with an increase in CCR5 expressing leukocytes, usually Th1 cells. CCL5 blockade reduced transcription of IL4, IL12, IFNγ, and CCR5, which correlated with increased bacterial counts in nasopharynx and lungs and correspondingly low levels of leukocytes in lymphoid tissue and lungs. This protective effect was mediated by increased antibody responses and increased IFNγ from T cells (Palaniappan, Singh et al. 2006). CCL7 is closely related to CCL2 and is primarily known as a monocyte chemoattractant, acting by binding to CCR 1-3, and CCR5. However in a murine pneumonia model, alveolar inhibition of CCL7 inhibited neutrophil recruitment and ameliorated lung injury without affecting bacterial clearance (Jose, Williams et al. 2015).

Table 1.5: Chemokines involved in the immune response to *S. pneumoniae*

Chemokine	Function during *S. pneumoniae* infection	Reference
CCL2 (MCP-1)	Monocyte chemoattractant in a murine pneumonia model	(Winter, Herbold et al. 2009)
CCL5 (RANTES)	Th1 cell chemoattractant	(Palaniappan, Singh et al. 2006)
CCL7	Neutrophil chemoattractant in a murine pneumonia model	(Jose, Williams et al. 2015)
CXCL1 (GRO-1)	Neutrophil chemoattractant in a murine pneumonia model	(Jose, Williams et al. 2015)
CXCL8 (IL8)	Neutrophil chemoattractant in an *in vitro* macrophage/epithelial cell co-culture mouse pneumonia model (KC)	(Marriott, Gascoyne et al. 2012)
CXCR3 (receptor for CXCL9/CXCL10 (IP-10)/CXCL11)	Neutrophil recruitment and lung inflammation in a murine pneumonia model	(Seyoum, Yano et al. 2011)

1.2.6.2 CXC Family

CXCR2 is a receptor for multiple chemokines, and CXCR2 deficient mice have significantly greater mortality than wild-type in a murine pneumonia model, associated with increased bacterial outgrowth in BALF and lungs (Herbold, Maus et al. 2010). The knockout mice had reduced inflammatory monocyte and neutrophil recruitment, greater levels of CXCL1 & 2, CCL2 & 12 suggesting that CXCR2 is important in both neutrophil and monocyte recruitment. In addition neutralisation of systemic CXCL1 inhibited neutrophil recruitment to the lung in a murine pneumonia model (Jose, Williams et al. 2015).

CXCL9, 10, 11 bind to CXCR3, which is expressed on Th1 and NK cells. CXCR3 deficient mice infected with *S. pneumoniae* had better survival, less bacteraemia, less lung neutrophilic infiltrate, more lung AM, and less lung inflammation on histological analysis (Seyoum, Yano et al. 2011). This suggests that these chemokines may be involved, although possibly indirectly, in excessive neutrophil infiltrate.

There is diurnal variation in neutrophil response to *S. pneumoniae*, as mice infected at dusk had greater neutrophil infiltrate at 24 hours than those infected at dawn (Gibbs, Ince et al. 2014). This correlated with lower bacterial counts at 48 hours in lungs and blood. Knocking out expression of clock genes in pulmonary epithelial cells of mice caused greater neutrophil infiltrate and loss of circadian variation; this was associated with CXCL5 upregulation. Human bronchial epithelial cells expressed CXCL5 in response to IL1β. The glucocorticoid receptor binds to the promoter sequence of CXCL5, which may explain why steroids inhibit the neutrophil response to *S. pneumoniae*.

1.2.7 Inflammatory Response to *S. pneumoniae*

Transcriptional analysis of mouse lungs after infection with *S. pneumoniae* shows that IL17 signalling, and NFκB signalling are upregulated at early timepoints in association with the most overrepresented cell types, i.e. granulocytes and macrophages. By 48 hours, IL17 and NFκB pathways are still upregulated but less so, while IFN signalling is also now upregulated (Scicluna, Van Lieshout et al. 2015).

1.2.7.1 Epithelial Cells

As well as secreting soluble antibacterial factors, epithelial cells express PRR that recognise conserved molecular patterns found on the surface of *S. pneumoniae*. While activation of epithelial PRRs can contribute towards the inflammatory response to *S. pneumoniae* (Sorrentino, de Souza et al. 2008), these responses can be also be increased by macrophages in mice, *in vitro* co-culture models (Marriott, Gascoyne et al. 2012), and human *ex vi*vo lung biopsies (Xu, Droemann et al. 2008). BALF from infected mice induced IκB degradation (pro-inflammatory cell signalling) in AECs, but *S. pneumoniae* itself did not. This epithelial cell activation was inhibited by combined IL1β and TNF blockade (Yamamoto, Ferrari et al. 2012). CXCL8 release from an AEC line, A549s, in response to *S. pneumoniae* was greater when in co-culture with a human monocyte cell line, THP-1 or with conditioned media from infected THP-1. This was inhibited by the presence of an IL1 receptor (IL1R) antagonist suggesting that IL1β is key in this communication. This was seen in an *in vivo* setting, as IL1R

deficient mice had less neutrophil recruitment after low dose *S. pneumoniae* infection than wild-type, associated with less CXCL1 in BALF (Marriott, Gascoyne et al. 2012). Culture of primary type II AEC and AM (approximately 5:1 ratio in human lung) from the same donor indicate differential cytokine and chemokine responses in response to lipopolysaccharide (LPS): AM released more IL1β and TNF, but less IL6 and chemokines than AEC (Thorley, Ford et al. 2007). TNF blockade inhibited the release of IL6 and CCL2 from AECs. Conditioned media from either cell type was able to induce migration of monocytes and neutrophils across a transwell. CXCL1 appeared to be the most important chemokine in this context, though CCL2 was more important in AM conditioned media, and CXCL8 in AEC conditioned media. However, a bronchial epithelial cell line, BEAS2B, secreted CXCL8 in response to unencapsulated *S. pneumoniae* in a dose dependent manner after 16 hours (Schmeck, Huber et al. 2006). These data suggests that, while epithelial cells are able to recognise *S. pneumoniae*, AM primarily recognise *S. pneumoniae*, and then stimulate the alveolar epithelium by paracrine or juxtacrine mechanisms to amplify the inflammatory response.

1.2.7.2 Macrophages

AMs must be able to clear debris and limit inflammation for most of the time, but elicit an inflammatory response to pathogens. This may be mediated by juxtaregulation from the alveolar epithelium such that when damaged, there is loss of negative regulators, allowing the AM to respond in an inflammatory manner. Sessile AM communicate with each other via the alveolar epithelium; a subset of AM form gap junctions with alveolar epithelial cells (AEC) via connexin 43 hemichannels. Stimulation of AM induces cyclical synchronised Ca^{2+} release that serves to inhibit excess inflammatory response (Westphalen, Gusarova et al. 2014). AM suppress immune responses by inhibiting dendritic cell (DC) mediated T cell activation, and by secreting TGFβ. αVβ6 integrins on AEC are critical in the activation of secreted non-active TGFβ (Kopf, Schneider et al. 2015). CD200L on epithelial cells interacting with CD200R on AM negatively regulates inflammatory responses, as does signal regulatory protein α (SIRPα)

on AM interacting with SP- A and D. These negative inhibitory signals are overcome by the combined ligation of multiple pattern recognition receptors (PRR).

In mouse models, depleting AM reduced inflammation in low inoculum infection models. This was associated with increased bacterial counts in the lung, and as this was simulated with caspase inhibition, macrophages apoptosis is important in bacterial control (Dockrell, Marriott et al. 2003, Sun and Metzger 2008). Depleting AM in mice, then infecting them with *S. pneumoniae*, induced increased neutrophil infiltrate along with pro-inflammatory cytokine profile and reduced IL10 at 20 and 48 hours post infection (Knapp, Leemans et al. 2003). This is supportive evidence that eventually there will be a pro-inflammatory response from other airway cells, and epithelial cells are the likely candidates. In addition macrophages play a role in clearance of apoptotic neutrophils as increased numbers of apoptotic neutrophils are seen in lungs after macrophage depletion.

1.2.7.3 Non conventional T cells

Non-conventional T cells have T cell receptors (TCR) that only recognise conserved non-peptide antigens and secrete cytokines in response. Invariant natural killer T cells (iNKT) cells express invariant TCR and NK receptors and recognise glycolipid antigens presented by CD1d on antigen presenting cells and produce IFNγ and IL17A in response to α-glucosyldiacylgycerol from *S. pneumoniae* cell wall *in vitro* (Kinjo, Illarionov et al. 2011). They express costimulatory molecules such as CD40L, activate DCs and NK cells and have cytolytic abilities by secreting granzyme B and contribute to FAS ligand induced apoptosis. iNKT cells are found in mucosal sites; making up 0.1-0.2% of T cells in BAL or sputum. Jα18 deficient mice, which lack iNKT had higher bacterial counts and worse survival in *S. pneumoniae* pneumonia(Kawakami, Yamamoto et al. 2003). . This was associated with reduced TNF, CXCL2 and neutrophil recruitment The phenotype was rescued by transfer of cells from wild-type mice, but not for IFNγ knockout mice, suggesting that the IFNγ from iNKT cells was important in the protective effect (Nakamatsu, Yamamoto et al. 2007). They

may also increase antigen presentation by DCs and enhance CD4 T cells ability to induce B cell production of Ig (Ivanov, Paget et al. 2014).

Mucosal associated Invariant T (MAIT) cells, which account for 1-10% of circulating T cells, are found in lung mucosa and secrete IFNγ and TNF (Ivanov, Paget et al. 2014). Their TCR are restricted to antigens presented by Major Histocompatibility Complex (MHC) I related molecule (MR1). They recognise riboflavin metabolites that aren't produced by mammals. Genome analysis of *S. pneumoniae* suggests it may express enzymes involved in riboflavin metabolism. MAIT cells are also stimulated by IL1β, IL12 and IL23.

γδT cells appear to modulate the inflammatory response to other organisms in the respiratory tract despite being present in low numbers. They recognise stress signals via damage associated molecular patterns (DAMPs) through their TCRs, activated via non-classical MHC molecules such as CD1, as well as recognition of other stress molecules by PRRs, NK receptors, and cytokines. Their functions include cytokine release, perforins and granzymes for direct toxicity, and the induction of apoptosis via Fas and TRAIL. γδT cells numbers increased by 30 fold following *S. pneumoniae* intranasal inoculation of mice, peaking at 7-10 days (Ivanov, Paget et al. 2014). Compared to wild-type, γδT cells deficient mice had worse survival associated with reduced CXCL2, TNF, and IL17 with poor neutrophil recruitment to the lungs after *S. pneumoniae* infection. The γδ T cells of influenza infected mice were less able to produce IL17 in response to *S. pneumoniae* and therefore contribute to influenza induced *S. pneumoniae* infection (Li, Moltedo et al. 2012). γδ T cells are probably also involved in the resolution of inflammation by inducing cytotoxic cell death of inflammatory monocytes (Kirby, Newton et al. 2007). However, the mechanism by which *S. pneumoniae* induces their activation remains unclear.

1.2.7.4 Neutrophils

Neutrophils are the first cells recruited to sites of injury and infection, primarily by responding to CXCL1, 2, and 8, and upregulating integrins to allow directed migration

(Kadioglu, De Filippo et al. 2011). The anatomy of the narrow pulmonary microvasculature means that neutrophils have slow intra-pulmonary transit times and hence can respond very rapidly to pulmonary inflammation. Neutrophils primarily engage with pathogens via phagocytosis and intracellular killing in phagolysosomes. They also produce neutrophil extracellular traps by extruding their chromatin, entrapping pathogens and then exposing them to antimicrobial compounds. While required for bacterial clearance in murine pneumonia models, they also induced bystander alveolar epithelial barrier disruption (Jose, Williams et al. 2015).

Neutropenic patients have increased rates of bacteraemia with pneumonia, and while they do not have increased rates of *S. pneumoniae* infection they have very high mortality both after chemotherapy (Carratalà, Marron et al. 1997) and after haematopoetic stem cell transplant (Engelhard, Cordonnier et al. 2002). Steroids also reduce neutrophil function and increase rates of IPD, but have complex effects on the immune system apart from this. The main mechanism of neutrophil antimicrobial function is by the oxidative burst that generates ROS via NADPH oxidase. However, humans with chronic granulomatous disease (exhibit failure of ROS production) don't have excessive rates of *S. pneumoniae* infection. Neutrophils also contain granules with antimicrobial compounds. Azurophilic (or primary) granules contain defensins, myeloperoxidase, BPI and serine proteases such as elastase, cathepsin G and proteinase 3. BPI and defensins disrupt anionic bacterial surface, and serine proteases degrade bacterial proteins. Specific (or secondary) granules contain microbicidal agents like lactoferrin (Kumar and Sharma 2010).

Patients with Chediak-Higashi syndrome have a non-functional lysosomal trafficking protein, leading to failure of phagolysosome formation and reduced lysosomal degranulation. They have increased incidence of *S. pneumoniae* infections amongst other disease forming pathogens. *In vitro* studies suggest that the serine proteases appear to be the predominant method by which neutrophils kill *S. pneumoniae* (Standish and Weiser 2009). Studies with cathepsin G deficient and cathepsin G/neutrophil elastase double knockout mice showed

increased mortality and shorter survival with a non-invasive 19F *S. pneumoniae* pneumonia. This was associated with bacterial outgrowth in the lung, and increased lung permeability and poorer oxygenation in the knockout mice, though this was not related to numbers of recruited neutrophils (Hahn, Klaus et al. 2011).

Neutrophils have a short lifespan due to encoded apoptosis that is regulated by external signals; cross-linking of β2 integrins during the process of transmigration into tissue increases their life span. Other factors that promote survival include IL6, CXCL8, and the complement component C5a, whereas TNF and IL10 induce apoptosis. *S. pneumoniae* causes neutrophil necrosis within 24 hours, though the mechanisms are not fully understood (Zysk, Bejo et al. 2000). Neutrophils also release CXCL8, TNF, CCL3 & 4, and IFNγ that act to recruit monocytes and activate macrophages. Myeloperoxidase released from neutrophils is taken up by macrophages and lead to ROS release and inflammatory cytokine secretion (Kumar and Sharma 2010).

1.2.7.5 Monocytes

Monocytes make up 1-6% of circulating blood cells. They are generated as part of the inflammatory response and can be split into 2 broad groups. 'Patrolling' non-classical monocytes remain amongst the vascular endothelium expressing CD16, CX3CR1 and CXCR1. Non-classical monocytes are effectively 'vascular macrophages', and mainly respond via TLR7 (and are hyporesponsive to LPS). The other 'inflammatory' classical monocytes express CD14 and CCR2 (and Ly6c in mice) and are rapidly mobilised from the subcapsular red pulp and bone marrow. After exiting the circulatory system, they differentiate into inflammatory macrophages. Their main function is to phagocytose foreign organisms, particulate matter, apoptotic cells, and also recycling nutrients (Arango Duque and Descoteaux 2014). Classical monocytes infiltrate inflamed tissue more robustly than non-classical, though after efferocytosis they become less 'classical' and are involved in tissue repair (Italiani and Boraschi 2014).

Recruited inflammatory macrophages undergo Fas-ligand mediated apoptosis, though they may also undergo phenotypic conversion to tissue resident macrophages. Monocyte/ macrophage development is controlled by macrophage colony stimulating factor (or CSF-1), granulocyte macrophage colony stimulating factor is also involved under inflammatory conditions.

Intranasal infection of mice with *S. pneumoniae* results in a 'disappearing macrophage' phenomenon (Taut, Winter et al. 2008). After 24 hours, 60% of the macrophage pool in BALF originates from inflammatory monocytes; this reaches 80% by 7 days (alongside a 10 fold expansion in total macrophage numbers). The decline in numbers of original AM is due to apoptosis and necrosis, with an even higher rate of cell death in the recruited monocyte derived macrophages (MDM). Studies inhibiting chemotaxis of monocytes indicate that monocytes play an important role in amplifying inflammation as well as providing increased phagocytic capability (Winter, Herbold et al. 2009).

1.2.7.6 The Acute Phase Response

The local inflammatory response to *S. pneumoniae* infection in the lungs stimulates a systemic response characterised by increased production of multiple proteins from the liver, many of which play a role in host defence (Gabay and Kushner 1999) (Table 1.6). This acute phase response is vital for effective host defence against *S. pneumoniae*, and is largely mediated by the cytokine IL6, which is produced in large quantities during *S. pneumoniae* pneumonia and reaches the liver via the circulation (Quinton, Jones et al. 2009). It is not clear how the acute phase response boosts immunity; the large increases in circulating levels of complement proteins and pentraxins may improve recognition of *S. pneumoniae* and therefore neutrophil phagocytosis. In addition induction of fever may inhibit optimal bacterial growth. Furthermore, increased permeability of the endothelium allows some of these plasma constituents and cellular infiltrate into affected tissues, thereby promoting immune clearance within the lung during *S. pneumoniae* infection.

Table 1.6 Components of the acute phase response that play a role in host defence

Component	Role in host defence
Complement components: C3,C4,C9, Mannose binding lectin	Opsonisation for phagocytosis Binding of antibody bound to pathogen to effect bacterial agglutination or lysis (Brown, Hussell et al. 2002) Opsonisation for phagocytosis
C reactive protein	Binds to PCho - increasing agglutination, allowing complement binding and phagocytosis (Simons, Loeffler et al. 2014)
Serum amyloid P	Binds to negatively charged carbohydrates – allowing complement binding and phagocytosis
Granulocyte Colony Stimulating Factor	Increases granulopoesis and activates mature granulocytes
Coagulation components: E.g. Fibrinogen	Involved in tissue repair and local containment of bacterial infection (Yang, Ko et al. 2013)
α_1 protease inhibitor	Inhibit proteolytic enzymes and reduces inflammation-induced damage

Complement is a series of host proteins found in serum, epithelial lining fluid and cell surfaces that form protease cascades. When activated by C reactive protein (CRP), serum amyloid P, antibody, or the complement component C1q binding to the *S. pneumoniae* surface, these protease cascades result in the coating of the bacteria with C3b and iC3b molecules, promoting phagocytosis via complement receptors (Brown, Hussell et al. 2002, Hyams, Camberlein et al. 2010), termed the classical pathway. This is important in early lung defence against *S. pneumoniae* (Kerr, Paterson et al. 2005). The alternative pathway is mediated by spontaneous hydrolysis of C3 on cell surfaces, which is inhibited on host cells by host proteins such as factor H. *S. pneumoniae* subverts this by PspC binding factor H (Dave, Carmicle et al. 2004). The proportion of *S. pneumoniae* bound by C3 is dependent on the classical pathway, with the alternative pathway amplifying the C3 deposition once initiated (Brown, Hussell et al. 2002). The mannose binding lectin pathway also activates C3 on binding directly to mannose residues on pathogens, though its role in *S. pneumoniae* infection

is contentious (Brown, Hussell et al. 2002, Roy, Knox et al. 2002). Downstream of C3 activation there is also the cleavage of C5, resulting in the release of the anaphylatoxin C5a, as well as the formation of the membrane attack complex (MAC). The pore forming function of MAC does not seem to play a role in the clearance of *S. pneumoniae* whereas C5a is a powerful inflammatory mediator and effective chemoattractant for monocytes and neutrophils. A polymorphism in C5 is associated with worse outcome in *S. pneumoniae* meningitis in humans and mice (Woehrl, Brouwer et al. 2011). Neutralising C5a antibodies, in conjunction with dexamethasone and antibiotics, had an additional mortality benefit above that of each individual treatment in a murine meningitis model (Kasanmoentalib, Valls Seron et al. 2015).

CRP, which is named after its interaction with *S. pneumoniae* c-polysaccharide (also known as TA), appears to have evolved in response to *S. pneumoniae* and similar bacteria. It binds PCho and can be bactericidal in conjunction with complement. There is no known deficiency of CRP in humans suggesting it has important functions for human survival. Injection of human CRP into mice at the time of infection with *S. pneumoniae* improved survival. CRP deficient mice had reduced survival after intraperitoneal infection with some serotypes, but not with heavily encapsulated mucoid strains originating from patient blood cultures (Simons, Loeffler et al. 2014). This may be due to structural changes on CRP that allow it to bind to factor H (or possibly ficolins) which allow activation of the alternative complement cascade on *S. pneumoniae* (Gang, Hanley et al. 2015).

No natural state of serum amyloid P (SAP) deficiency has been recognised, also suggesting a non-redundant role in host immune function. SAP binds to DNA, chromatin, and apoptotic cells to aid clearance, but also stabilises amyloid fibrils and so promotes amyloidosis. SAP binds to C1q and prevents the inhibitory function of C4BP, and thus may promote classical complement pathway activation. SAP binds PCho and displays calcium dependent binding to *S. pneumoniae* (Yuste, Botto et al. 2007). C3b deposition on *S. pneumoniae* is markedly reduced in serum from SAP deficient mice. SAP deficient mice had impaired survival in a

murine pneumonia model compared to wild-type, associated with reduced bacterial clearance, underlining its importance in *S. pneumoniae* host defence.

Pulmonary infections initiate a pro-coagulant state by activating coagulation pathways, components of which are upregulated by the acute phase response, and inhibiting anticoagulant and fibrinolysis pathways. The tissue factor pathway is the main initiator of inflammation-induced activation of coagulation and the abundance of coagulation proteases can further induce inflammation by activating proteinase-activated receptor (PAR) signalling, in particular PAR-1. PAR-1 antagonism attenuates neutrophilic inflammation and alveolar leak in murine *S. pneumoniae* pneumonia (Jose, Williams et al. 2015). In rodent studies of *S. pneumoniae* pneumonia the use of various anticoagulants (anti-thrombin, activated protein C, tissue factor pathway inhibitor) is beneficial at attenuating inflammation (Choi, Hofstra et al. 2008, Hofstra, Cornet et al. 2009, Schouten, van 't Veer et al. 2011, Van Den Boogaard, Brands et al. 2011), but in human disease these agents have not improved outcomes (Wunderink, Laterre et al. 2011) and are associated with increased bleeding. However, local delivery of these anti-coagulants, limiting systemic effects, may be beneficial (Dixon, Schultz et al. 2010, van den Boogaard, Hofstra et al. 2015). Subgroup analysis of the PROWESS study suggests that activated protein C improved outcome in patients with sepsis secondary to *S. pneumoniae* CAP (Ely, Laterre et al. 2003, Laterre, Garber et al. 2005). So, pathways involved in coagulation-inflammation crosstalk may be amenable to intervention to reduce the lung damage from an excessive inflammatory response without compromising host defence.

1.3 Overview on adaptive response to *S. pneumoniae*

The innate immune response to invading pathogens is generic, able to target conserved microbial structures without the host having had prior exposure to that pathogen. In contrast, the adaptive response is highly specific, depending on recognition of antigens expressed by pathogens. Generating an adaptive immune response can take days after initial exposure to pathogen, but also generates memory cells, which enable a more rapid and

powerful response when that pathogen is subsequently re-encountered. *S. pneumoniae* colonisation of the nasopharynx elicits an adaptive immune response that can help prevent colonisation, pneumonia and invasive disease. Immune deficiencies that cause defects in the adaptive immune response such as antibody deficiency (Martinot, Oswald et al. 2014) and T cell deficiencies (Klein, Lisowska-Grospierre et al. 1993) lead to increased rates of *S. pneumoniae* pneumonia.

1.3.1 Dendritic cells

DC are found in lamina propria, intercalating between epithelial cells, and plasmacytoid DCs are found in the conducting airways. During inflammation, monocyte derived inflammatory DCs are also found (Werner and Steele 2014). Dendritic cells in the submucosa are responsible for phagocytosing pathogens, migrating to regional lymphoid tissue, and presenting antigens to naïve lymphocytes. *S. pneumoniae* phagocytosis stimulates DC maturation as measured by expression of MHC, CD80, and CD86 (Olliver, Spelmink et al. 2013).

1.3.2 B lymphocyte and antibody

Prior infection leads to induction of an antibody response by B lymphocytes to specific bacterial antigens. The high incidence of lung infections in subjects with antibody deficiencies and the efficacy of antibody-inducing vaccines at preventing *S. pneumoniae* pneumonia in children demonstrate an important role for antibody for protection against *S. pneumoniae*. Antibody improves immunity to *S. pneumoniae* by activating complement deposition, so promoting complement-mediated phagocytosis, and by increasing direct phagocytosis by Fcγ receptor recognition of the antibody. They also cause bacterial agglutination (Roche, Richard et al. 2015), which is likely to be how the conjugated vaccine prevents nasopharyngeal colonisation. Adults with antibody deficiencies have increased risk of developing IPD, including those with IgG deficiency, IgA deficiency, isolated IgM deficiency, and paraproteinaemias (Martinot, Oswald et al. 2014).

S. pneumoniae proteins and polysaccharide capsule are recognised as antigens by the adaptive immune system. Polysaccharide antigens generate a poor adaptive immune response as these antigens are unable to stimulate T lymphocytes to assist B cell antibody responses. This type II T cell-independent activation generates rapid B cell proliferation and antibody production (largely IgM, but also IgG) by crosslinking of multiple B cell receptors on the surface of B lymphocyte. While there is some class switch recombination (IgA and IgG3) and somatic hypermutation (Krljanac, Weih et al. 2014), there is no generation of a memory B cell population. So the response is largely limited to antibodies of relatively poor affinity (Coutinho and Moller 1973), and as a result vaccination with capsular polysaccharide alone is ineffective in infants. T cell-independent responses occur primarily in (i) B lymphocytes in the marginal zone of the spleen (Cerruti, Cols et al. 2013), and (ii) B-1 like cells (Verbinnen, Covens et al. 2012) which reside in pleural and peritoneal cavities, but also circulate in the blood and lymphatics (Vos, Lees et al. 2000).

Protein antigens stimulate a T-cell dependent B lymphocyte antibody response that generates a memory B cell population and can therefore lead to a memory response and are effective in infants. Polysaccharide immunogenicity has been improved by conjugation with carrier protein adjuvants to induce a T cell dependent antibody response to the capsule. IgG and IgM titres to capsular polysaccharide are detectable within 6 days of vaccination and weeks of nasopharyngeal colonisation (Musher, Groover et al. 1993, Goldblatt, Hussain et al. 2005).

Patients who have undergone splenectomy have higher incidence of infections with encapsulated bacteria, probably due to reduced levels of IgM memory B cells to capsular polysaccharide in the blood. The presence of IgM memory cells correlates with protection against IPD, and administration of capsule specific IgM is protective in a mouse pneumonia model (Burns, Abadi et al. 2005). A subgroup of patients with common variable immune deficiency who have recurrent IPD have normal total Ig levels, but reduced IgM memory cells (Kruetzmann, Rosado et al. 2003).

IgA is the most common antibody at mucosal surfaces where it primarily functions by agglutinating pathogens. *S. pneumoniae* IgA1 protease removes the Fc domain at the hinge region so it no longer has agglutination ability (Weiser, Bae et al. 2003). In addition the function of IgA is subverted as the cleavage of opsonising IgA allows a neutralisation of surface charge and increased proximity of cell wall epithelial membrane receptors.

1.3.3 T lymphocytes

Cellular adaptive immune responses are driven by T lymphocytes, which recognise internalised antigen presented on MHC II molecules. CD4 expressing helper T cells secrete cytokines to affect cells in the local milieu, while CD8 expressing cytotoxic T cells induce apoptosis of host cells infected with intracellular pathogens. In adaptive immunity, the presentation of antigens to naïve T cells in lymph nodes by DCs drives the activation of T cells and directs their development into specific effector T cells.

Studies with naïve CD4 T cells have found conflicting roles in innate pulmonary *S. pneumoniae* infection. Prior colonisation with *S. pneumoniae* protects against subsequent colonisation by both homologous and heterologous *S. pneumoniae*. Some authors have shown that this protection is dependent on memory CD4 cells and antibody responses are dispensable (Kadioglu, Coward et al. 2004), while other have shown increased survival in mice deficient in CD4 cells (LeMessurier, Hacker et al. 2010). Depletion of CD4 cells at time of infection also reduces protection in some models, suggesting that CD4 T cells need to be present at time of challenge to have a protective effect (Malley, Trzcinski et al. 2005).

Th1 cells are a subset of helper T lymphocytes that secrete IFNγ, the effect of which is to 'activate' macrophages, increasing phagocytosis and intracellular killing. Furthermore, Th1 cells induce B cell isotype switching to IgG2 antibody, which correlates with increased phagocytic ability in mice (Lefeber, Benaissa-Trouw et al. 2003). Live *S. pneumoniae* interact with multiple intracellular receptors to induce IL12 and thus a Th1 response (Olliver, Hiew et

al. 2011), but it is not known whether Th1 responses improve adaptive immune mediated protection against subsequent infection.

CD4 Th17 cells indirectly improve immunity against extracellular pathogens on mucosal surfaces via secretion of IL17, IL17F, and IL22. IL17 induces bronchial epithelium to produce CXCL8 and β-defensins, resulting in neutrophil recruitment and increased mucosal antimicrobial activity respectively. Th17 responses also improve epithelial barrier integrity and increase export of Ig to mucosal surfaces. Patients with hyper IgE syndrome have defects in Th17 cell differentiation and have increased susceptibility to *S. pneumoniae* pneumonia (Milner, Brenchley et al. 2008), and experimental human colonisation with *S. pneumoniae* resulted in detectable Th17 responses in BALF and blood (Wright, Bangert et al. 2013). In animal models Th17 responses to colonisation or vaccination inhibit *S. pneumoniae* colonisation and pneumonia (Zhang, Clarke et al. 2009, Moffitt, Gierahn et al. 2011, Wilson, Cohen et al. 2014), and recombinant IL17F increases CXCL2, β-defensin and IFNγ levels in lung and reduces bacterial load (Chen, Guo et al. 2014). External PRR engagement of monocytes with *S. pneumoniae* or its cell wall constituents skews towards a Th17 response (Olliver, Hiew et al. 2011).

Regulatory T lymphocytes (Treg) are important in host resistance to *S. pneumoniae* pneumonia in mice. Tregs cells limit excessive inflammation by secreting IL10. In murine pneumonia models, CD25 positive T cells migrate preferentially to sites of infection (Kadioglu, Coward et al. 2004). Mice strains that are relatively resistant to infection have more Tregs, TGFβ (which drives the differentiation of naïve T cells into Tregs) and IL10. This is probably because regulation of the inflammatory response during *S. pneumoniae* pneumonia helps prevent the bacteria from penetrating the epithelial layers to cause septicaemia (Neill, Fernandes et al. 2012). *S. pneumoniae* induces TGFβ secretion from human fibroblasts and epithelial cells, suggesting that this drives T cell differentiation in the nasopharynx (Neill, Coward et al. 2014).

CD8 cells are usually associated with responses to intracellular organisms. However genetic mutations in humans affecting transporter associated with antigen processing (TAP) proteins required for CD8 function are associated with an increased incidence of *S. pneumoniae* infection (Gadola, Moins-Teisserenc et al. 2000), and in a mouse model of lung infection CD8 deficient mice had greater levels of bacteraemia with several serotypes of *S. pneumoniae* and poorer survival with serotype 3. The mechanism appears to be the role of CD8 cells in inhibition of CD4 (particularly Th17) mediated inflammation (Weber, Tian et al. 2011), via the secretion of IL10 and TGFβ (Mertens, Fabri et al. 2009). The role of CD8 cells for adaptive immunity to *S. pneumoniae* requires further characterisation.

1.4 Macrophage Biology

1.4.1 Pattern Recognition Receptors

The host immune system recognises *S. pneumoniae* via PRR that recognise pathogen associated molecular patterns (PAMP) such as bacterial virulence factors or DAMPs released by endogenous cells as a result of tissue damage (Figure 1.3 and Table 1.7). Stimulation of PRRs results in cell signalling cascades that result in altered gene transcription to trigger an immune response. PRRs are often situated on cell surface membranes, but are also present on endosomes to recognise phagocytosed PAMPs and the cytosol to recognise intracellular PAMPs. Tissue resident macrophages serve as the surveillance system for the body and as such express an array of receptors that act as PRR. They include opsonic phagocytic receptors such as Fc receptors for Ig and complement receptors. Non-opsonic phagocytic receptors include lectins such as dectin-1 and dendritic cell-specific ICAM-3 grabbing non integrin (DC-SIGN), and scavenger receptors such as scavenger receptor A (SR-A) and MARCO. Non-phagocytic receptors are expressed on cell surface and phagolysosome membranes (toll like receptors [TLRs]) or are found in the cytosol (nucleotide-binding oligomerization domain receptors [NOD], retinoic acid-inducible gene 1 [RIG-I], and the inflammasome).

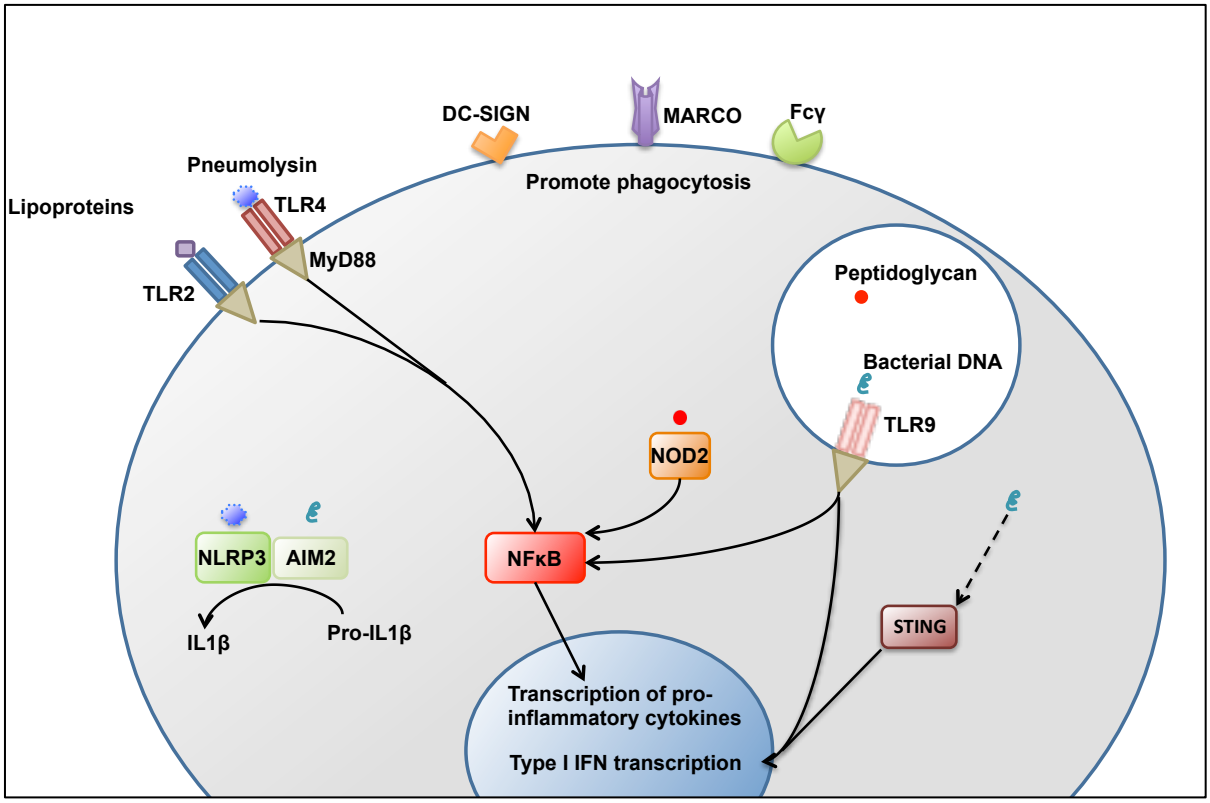

Figure 1.4 Pattern Recognition Receptors expressed by macrophages

Cell surface PRR such as TLR2 and TLR4 induce cell signalling cascades that culminate in NFκB translocating to the nucleus to induce pro-inflammatory cytokine transcription. Non-opsonic PRR such as MARCO and DC-SIGN recognise pathogen constituents that induce phagocytosis. Opsonic PRR such as Fcγ recognise antibody that results in phagocytosis. Endosomal PRR such as TLR9 function like cell surface PRR and initiate cytokine transcription, including pro-inflammatory cytokines and type I IFN. Cytosolic PRR such as NOD2 and STING recognise PG and bacterial DNA respectively to initiate cytokine transcription. NLRP3 and AIM2 recognise the K^+ ion shifts and bacterial DNA respectively and form part of the inflammasome; a multicomponent protein complex that initiate post-translational modifications to activate cytokines such as IL1β.

Table 1.7: Macrophage pattern recognition receptors

PRR	Cellular localisation	*S. pneumoniae* ligand	Consequences of activation	References
TLR 2	Leucocyte and epithelial cell surface	Lipoproteins Cell wall constituents?	Pro-inflammatory cytokine transcription	(Tomlinson, Chimalapati et al. 2014)
TLR 4	Leucocyte and epithelial cell surface	Pneumolysin?	Pro-inflammatory cytokine transcription	(Malley, Henneke et al. 2003)
TLR 9	Leucocyte endosomes	Unmethylated CpG DNA fragments	Pro-inflammatory cytokine transcription Type 1 IFN transcription	(Albiger, Dahlberg et al. 2007)
NOD 2	Leucocyte cytoplasm	Cell wall muramyl dipeptide	Pro-inflammatory cytokine transcription	(Davis, Nakamura et al. 2011)
AIM2	Cytoplasm	Bacterial DNA	Activation of pro IL1β and IL18	(Fang, Tsuchiya et al. 2011)
NLRP3	Cytoplasm	Pore forming function of pneumolysin	Activation of pro IL1β and IL18	McNeela et al. 2010
DC-SIGN / SIGN-R1	Macrophages and dendritic cells (marginal zone of spleen)	Capsular polysaccharide?	Increased phagocytosis Complement activation? Improved natural IgM production?	(Koppel, Wieland et al. 2005)
Unknown	Cytoplasm	Bacterial DNA	Activation of STING to induce Type 1 IFN transcription	(Parker and Prince 2011)
MARCO	Macrophages	Unknown	Increased phagocytosis Amplification of other PRR signalling	(Arredouani , Yang et al. 2004)
Scavenger receptor A	Macrophages	Unknown	Increased phagocytosis	(Arredouani , Yang et al. 2006)
SP-A & SP-D surfactant proteins	Epithelial lining fluid	Surface mannose & glucose residues	Increased phagocytosis	(Jounblat, Clark et al. 2005, Sano, Kuronuma et al. 2006)

1.4.1.1 Toll Like Receptors

Toll like receptors (TLR) are a family of single, membrane-spanning, non-catalytic proteins. There are 10 members in humans. TLR 1, 2, 4, 5, and 6 are situated on the cell surface membrane and the rest reside on endosomes. When they recognise PAMPs they activate signalling pathways by a number of adaptor molecules. TLR2, 4 and 9 are probably the dominant TLRs for driving inflammatory responses to *S. pneumoniae* and are discussed in detail below. TLR3 recognises double stranded RNA, TLR5 recognises flagellin, and TLR7 & 8 recognise single stranded RNA. The function of TLR10 is not entirely clear, though it has been linked to recognition of influenza strains as well as *H. pylori* LPS.

TLR 2 heterodimerises with TLR6 to recognise diacylated lipoproteins from *S. pneumoniae* (Tomlinson, Chimalapati et al. 2014), and heterodimerises with TLR1 to recognise triacylated lipopetides from Gram-negative bacteria (Schenk, Belisle et al. 2009). LTA may activate inflammatory cytokine release by binding to TLR2, but is enhanced by the presence of LPS binding protein (LBP) and CD14 (Schroder, Morath et al. 2003). A human cell line transfected with CD14 and TLR2 had increased NFκB translocation in response to purified PG or heat killed *S. pneumoniae* in a dose dependent manner (Yoshimura, Lien et al. 1999). However the identified TLR2 responses to LTA and PG may be caused by contamination with lipoproteins (Travassos, Girrardin et al. 2004). A cell line transfected with TLR2 were activated by live or heat killed *S. pneumoniae*, and TLR2 neutralising antibodies reduced peripheral blood mononuclear cell secretion of TNF, IL6 and CXCL8 in response to *S. pneumoniae* (Mogensen, Paludan et al. 2006).

There was less IL1β, IL6, and KC in lung homogenates of TLR2 deficient mice compared to wild-type in a murine pneumonia model (Knapp, Wieland et al. 2004). However the mortality rate of the mice and bacterial counts within the lung were similar. AM isolated from knockout mice secreted less TNF and KC after being exposed to heat killed *S. pneumoniae* compared to wild-type. TLR2 deficient mice colonised with *S. pneumoniae* had reduced IL6 transcription in nasopharyngeal tissue compared to wild-type, and less non-

secretory IgG in nasopharyngeal washes indicating less leakage from blood into mucosa. Immunohistochemical analysis demonstrated that this was due to epithelial cell stimulation resulting in Snail1 (downstream of TGFβ signalling) upregulation after infection in wild-type mice, but not TLR2 deficient mice (Beisswenger, Lysenko et al. 2009).

TLR4 is best known as a specific receptor for LPS, but requires the accessory molecule MD-2, which binds to the ectodomain of TLR4 and affects subcellular localisation. Some authors report that TLR 4 recognises Ply (Srivastava, Henneke et al. 2005). TLR4 reporter cells were stimulated by wild-type, but not Ply deficient *S. pneumoniae*. Mice lacking functional TLR4 were more susceptible to nasopharyngeal colonisation and had reduced survival in a pneumonia model (Malley, Henneke et al. 2003). Other authors report that HEK cells transfected with TLR4 did not respond to *S. pneumoniae* (Mogensen, Paludan et al. 2006), and that TLR4 was only protective in a low dose *in vivo* infection (Branger, Knapp et al. 2004).

TLR9 recognises the unmethylated CpG motifs of prokaryotic organisms. Some polymorphisms in TLR9 are associated with reduced production of CXCL8 from AM in response to *S. pneumoniae* (Berenson, Kruzel et al. 2015). In a mouse *S. pneumoniae* pneumonia model, TLR9 deficient mice had reduced survival, increased lung bacterial counts and bacteraemia compared to wild-type. Primary AM and bone marrow derived macrophages (BMDM) from TLR9 deficient mice had reduced ability to phagocytose *S. pneumoniae* (Albiger, Dahlberg et al. 2007). This suggests that TLR9 has a non-redundant role in resident airway macrophage killing of *S. pneumoniae*. HEK cells transfected with TLR9 are activated by live but not heat killed *S. pneumoniae* as well as DNA from *S. pneumoniae*. Peripheral blood mononuclear cell secretion of CXCL10 in response to *S. pneumoniae* was reduced by inhibition of TLR9 (Mogensen, Paludan et al. 2006). TLR9 recognition of CpG also stimulated signalling via myeloid differentiation primary response gene 88 (MyD88) and interferon regulatory factor 7 (IRF7) to initiate type I IFN secretion (Moretti and Blander 2014).

1.4.1.2 NOD

NLRs (NOD like receptors) are a group of intracellular, primarily cytosol-based PRRs, of which 22 have been identified in humans (Koppe, Suttorp et al. 2012). They all contain a centrally located NOD, a C-terminal leucine rich repeat (LRR) that recognises ligands, and a variable N-terminal interaction domain that initiates signalling. The N-terminal can consist of caspase activation and recruitment domain (CARD), pyrin domains, or acidic transactivating domains (Mogensen 2009) (Figure 1.4). NOD 1 & 2 activation results primarily in a pro-inflammatory response as a result of activation of the NFκB pathway. NOD1 recognises diaminopimelic acid, which are cell wall fragments from Gram-negative bacteria, whereas NOD2 recognises PG from all bacteria. NOD1 is expressed in many cell types, but NOD2 is largely restricted to leucocytes and epithelial cells (Opitz, Puschel et al. 2004), where its expression is upregulated by pro-inflammatory cytokines.

NOD2 recognises muramyl dipeptide from the *S. pneumoniae* cell wall, activating a signalling cascade via RIP2 kinase that culminates in NFκB activation (Parker and Prince 2011). *S. pneumoniae* is largely resistant to lysozyme mediated cell lysis due to deacetylation of NAG and *O*-acetylation of NAM (Davis, Nakamura et al. 2011). However, the activation of NOD2 in mice was dependent on LysM (an isoform of lysozyme found on epithelium and in phagosomes of macrophages and neutrophils), with release of NOD2 ligands without lysis of *S. pneumoniae*. This resulted in CCL2 release, and monocyte recruitment in nasopharyngeal colonisation. In mouse nasopharyngeal colonisation double knock out NOD2 and TLR2 deficient mice cleared bacteria less well than single knockout mice (Davis, Nakamura et al. 2011). Additionally, in rat *S. pneumoniae* meningitis NOD2 mRNA and protein were upregulated in brain, associated with elevated NFκB, TNF and IL6 levels (Liu, Han et al. 2014), and NOD2 deficient mice had less inflammation than wild-type (Liu, Chauhan et al. 2010).

NOD1 stimulation by Gram-negative organisms improved neutrophil killing of complement opsonised *S. pneumoniae* (Lysenko, Clarke et al. 2007). Similarly neutrophils from mice

raised in a germ-free environment exhibit reduced killing of *S. pneumoniae* compared to conventionally raised mice, implicating the microbiome as priming neutrophil killing activity. NOD1 deficient mice had increased rates of early sepsis but similar mortality rates to wild-type mice in a *S. pneumoniae* pneumonia model (Clarke, Davis et al. 2010).

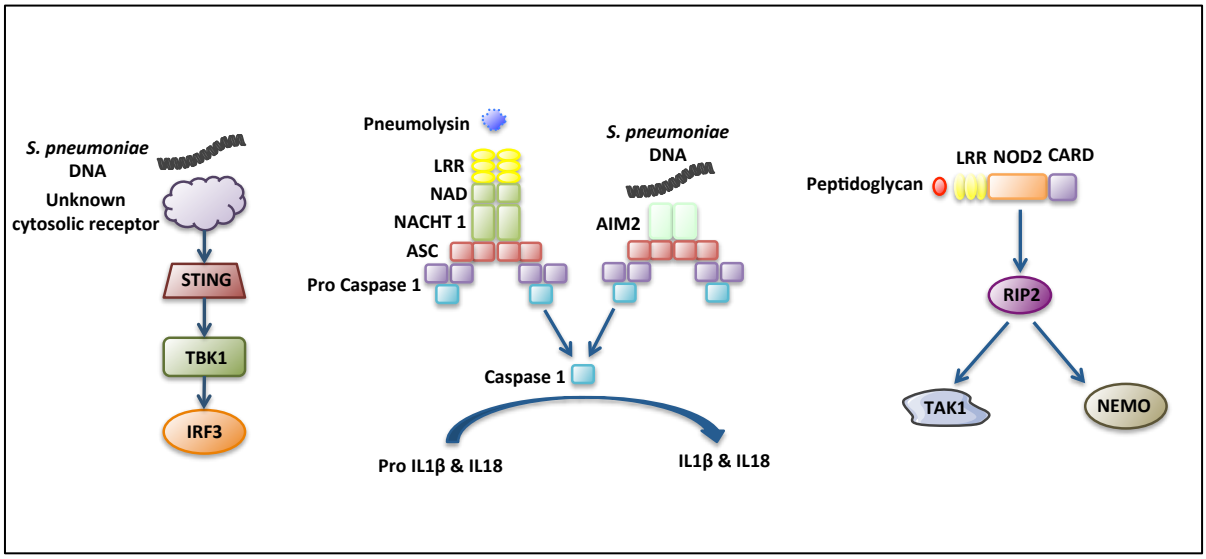

Figure 1.5 Cytosolic PRR signalling

Cytosolic PRR recognise components of *S. pneumoniae* to induce cytokine responses. *S. pneumoniae* DNA is recognised by an unknown PRR to induce STING activation, that activates TBK1 and then IRF3 to induce interferon transcription. LRR are integral to NLRP3 recognition of K^+ efflux induced by Ply. NLRP3 or AIM2 activation (by bacterial DNA), induces caspase 1 activation, which cleaves the zymogen precursors to IL1β and IL18. PG recognition by the LRR of NOD2 induces RIP2 phosphorylation, which stimulates MAPK cascades by TAK1, and NFκB by NEMO, both of which induce pro-inflammatory cytokine transcription.

1.4.1.3 Inflammasome

NLR family pyrin containing domain (NLRP) 1 and 3, and NLR CARD containing domain 4 form cytosolic protein complexes called inflammasomes that promote inflammation by activating post-translational changes to activate IL1β and IL18 by cleaving zymogenic proforms (Figure 1.4). They all contain caspase-1 and the adaptor molecule apoptosis-associated speck-like protein containing a CARD (ASC), which is redistributed from the nucleus to the cytoplasm in activated inflammatory cells (dos Santos, Kutuzov et al. 2012). CARD – CARD interactions between the inactive caspase-1 and ASC induce the activation of caspase-1. NLRP3 and pro-IL1β are expressed minimally in macrophages, but are inducible by inflammatory stimuli; hence two signals are required for inflammasome activation.

NLRP3 knockout mice were more susceptible to pneumonia but have less pathological sequelae in meningitis (Koppe, Suttorp et al. 2012). NLRP3 is activated by pore-forming toxins as well as DAMPs such as uric acid, adenosine triphosphate (ATP), and silica, as well as muramyl dipeptides. Absent in melanoma 2 (AIM2) is activated by cytosolic DNA (Fang, Tsuchiya et al. 2011). Humans with mutations to NLRP3 exhibit a range of dominantly inherited disorders (e.g. Muckle-Wells syndrome, and Familial Cold Urticaria) that involve constitutive activation of the inflammasome and consequent hypersensitivity to exogenous stimuli (Martinon, Agostini et al. 2004).

S. pneumoniae stimulation of the inflammasome is dependent on an initial insult, e.g. TLR2 activation, to induce transcription and synthesis of inflammasome constituents, i.e. two hits are required for IL1β secretion While ASC is the most critical component, NLRP3 deficient BMDM (McNeela, Burke et al. 2010, Witzenrath, Pache et al. 2011), and AIM2 deficient cells also have reduced capacity to secrete IL1β (Fang, Tsuchiya et al. 2011). In a pneumonia model, NLRP3 deficient mice had greater mortality and increased albumin leak into BALF, though no significant difference in BAL cytokines were detected (Witzenrath, Pache et al. 2011). Caspase-1 activation is ablated in a high K^+ medium, suggesting K^+ efflux is critical in activating NLRP3 and ASC (Karmakar, Katsnelson et al. 2015).

CARD8 is implicated in negative regulation of IL1β secretion, and a genome wide association study of bacterial meningitis indicates worse outcomes were associated with a polymorphism in CARD8 that results in translation of a truncated form of the protein (Geldhoff, Mook-Kanamori et al. 2013). IL1β and IL18 levels are elevated in CSF of patients with meningitis, and higher levels are associated with systemic and neurological complications. In murine *S. pneumoniae* meningitis, ASC deficient mice had reduced brain KC, CXCL2, and IL6 compared to wild type; conversely NLRP3 deficient mice had increased brain neutrophil infiltrate and haemorrhage (Geldhoff, Mook-Kanamori et al. 2013). Additionally inflammasome dependent IL18 generation is important in NK cell stimulation and subsequent release of IFNγ in murine meningitis, where the resulting inflammatory monocyte infiltrate drives pathology (Mitchell, Yau et al. 2012).

1.4.1.4 Cytosolic RNA/DNA receptors

Cytosolic DNA sensing may be a means by which a phagocyte distinguishes live bacteria from dead, and so scale inflammatory responses appropriately (Abdullah and Knolle 2014). Cytosolic receptors recognise non-self RNA via RIG-I-like receptors (RLRs), e.g. RIG-I and melanoma differentiation-associated protein 5 (MDA5), resulting in release of type 1 interferon that acts in a para- and autocrine manner to activate IFNα/β receptors to induce transcription of interferon stimulated genes. RNA polymerase III converts A:T rich cytosolic DNA into RNA thus allowing bacterial DNA to be recognised by RLRs (Tam and Jacques 2014). RLR activation is mediated by the adaptor molecule stimulator of interferon genes (STING) (Figure 1.4). Resting dimerised STING is located in the ER or the mitochondria associated membrane, and when activated results in the transcription factor IRF3 being recruited to STING, culminating in IRF3 mediated transcription of IFNβ.

S. pneumoniae or its DNA induces IFNβ transcription in mouse BMDM. Inhibition studies suggest that bacterial DNA is released into the cytosol downstream of phagocytosis or phagolysosome acidification. siRNA knockdown of STING or IRF3 in BMDM inhibited IFN release (Koppe, Hogner et al. 2012). IFNAR deficient mice had reduced levels of CCL5 in

BALF compared to wild-type in a pneumonia model suggesting that this chemokine is dependent on IFN release (Koppe, Hogner et al. 2012). STING also localises with autophagy proteins such as autophagy related gene 9 (Atg9a). The increased susceptibility of aged mice to *S. pneumoniae* pneumonia may be due to increased acetylation of Atg9a, and so decreased STING mediated IFNβ transcription (Mitzel, Lowry et al. 2014). Other DNA sensors such as cyclic GMP-AMP synthase are important in recognition of DNA viruses but have not been implicated in *S. pneumoniae* infection.

1.4.1.5 Lectins

Lectins are carbohydrate-binding proteins that recognise sugar moieties, and serve a multitude of purposes from mediating cell adhesion to glycoprotein synthesis including innate immunity (Geijtenbeek and Gringhuis 2009). Primarily they recognise mannose, fucose, and glucan structures (Werner and Steele 2014). They largely signal via a common adaptor protein, CARD9 (Osorio and Reis e Sousa 2011).

DC-SIGN is a human C-type (i.e. it has a carbohydrate recognition domain [CRD] that requires calcium for binding) lectin, which binds high mannose containing ligands. It is expressed by macrophages and DCs, particularly in the marginal zone of the spleen. SIGN-R1 is a mouse homologue (Pluddemann, Mukhopadhyay et al. 2011). Intravenous bacterial inoculation into mice led to *S. pneumoniae* association with SIGNR1 expressing macrophages in the marginal zone of the spleen (Kang, Kim et al. 2004). In addition, cells from an antigen presenting murine cell line transfected with SIGN-R1 internalised capsular polysaccharide from a variety of *S. pneumoniae* serotypes (Koppel, Wieland et al. 2005). In murine intraperitoneal (Lanoue, Clatworthy et al. 2004) and intranasal infection (Koppel, Wieland et al. 2005) SIGN-R1 deficient mice had poorer survival than wild-type associated with increased bacterial counts and increased levels of IL1β, TNF, and KC in lungs in the pneumonia setting. In addition, B lymphocytes from SIGN-R1 deficient mice produced less anti-PCho IgM than wild-type (Koppel, Litjens et al. 2008), suggesting that B-lymphocytes are stimulated by macrophages that recognise *S. pneumoniae* capsule by DC-SIGN to secrete IgM. In rat meningitis, CD209b

(a homologue of SIGN-R1) is expressed widely on microglia, and uptake of *S. pneumoniae* capsular polysaccharide is abolished by CD209 blockade (Park, Choi et al. 2009). Furthermore, SIGN-R1 mediates complement activation on splenic macrophages after intravenous *S. pneumoniae* infection (Kang, Do et al. 2006).

Collectins are soluble PRRs that increase phagocytosis. This group includes SP-A & D which are constitutively synthesised and secreted into alveolar lining fluid by type II pneumocytes and non-ciliated bronchial epithelial cells. They bind mannose and glucose residues avidly, thus preferentially binding microbial surface ligands over eukaryote glycoproteins. In this manner they agglutinate pathogens, inhibit microbial growth, and recruit phagocytes. SP-A increased AM phagocytosis of *S. pneumoniae,* mediated by increased cell trafficking of SR-A to the cell surface independently of SP-A binding to *S. pneumoniae* (Sano, Kuronuma et al. 2006). SP-A and –D modulate inflammation depending on the orientation of their binding to ligands. If the CRD binds SIRPα, a transmembrane protein, there is inhibition of downstream pro-inflammatory signals. However, if the CRD is bound to pathogen, the collagen region binds to calreticulin/CD91, thus stimulating phagocytosis and pro-inflammatory responses (Kishore, Bernal et al. 2005) with SP-D deficient mice having reduced neutrophil recruitment and *S. pneumoniae* clearance (Jounblat, Clark et al. 2005).

Dectin-1 is a C type lectin that is expressed on myeloid cells and a subset of γδ T cells and recognises the β glucan component of fungal cell walls (Osorio and Reis e Sousa 2011). Binding of its ligand induces activation of Syk and subsequently the NFκB pathway, and stimulates a calcium flux that drives Nuclear factor of activated T cells (NFAT) activation. It also signals in a Syk independent manner via c-Raf to activate NFκB (Osorio and Reis e Sousa 2011). Dectin 2 recognises structures with high mannose concentrations and also subsequently signals via Syk. Dectin-2 deficient mice had reduced survival in a murine *S. pneumoniae* pneumonia model, perhaps due to reduced activation of the IL12-IFNγ axis and subsequent serotype specific antibody production (Akahori, Miyasaka et al. 2016).

MR is a type I integral membrane glycoprotein expressed on macrophages and endothelial cells. It mediates non-opsonic phagocytic uptake of a variety of microbes and endocytosis of soluble glycoconjugates. It recognises mannose, fucose, glucose, and galactose. Direct binding assays suggest that purified polysaccharide of some *S. pneumoniae* serotypes bind to MR (Zamze, Martinez-Pomares et al. 2002), and rat Schwann cell uptake of *S. pneumoniae* was inhibited by competitive inhibition of MR (Macedo-Ramos, Batista et al. 2014). MR is upregulated by IL4 and IL13 and recognition of unopsonised bacteria by MR inhibits AM inflammation, potentially reducing the inflammatory response to commensal bacteria. MR has no recognised signalling motifs, so it is unclear how downstream communication after ligand binding occurs (Drummond and Brown 2013).

1.4.1.6 Scavenger Receptors

Scavenger receptors (SR) include SR-A and MARCO and recognise negatively charged macromolecules, and are best known for binding to low density lipoproteins that have been modified by oxidation or acetylation. They can function as PRRs, this may be because epitopes generated by peroxidation of endogenous proteins and lipoproteins resemble pathogens (Canton, Neculai et al. 2013). The structural features of SRs are varied and membership of this group is determined by functional properties. Overall they recognise and remove unwanted particles by uptake, and their ligand binding sites share similarities in shape and electrostatic charge distribution, possibly explaining their preference for polyanionic ligands (Canton, Neculai et al. 2013). They are able to oligomerise and usually have short cytosolic domains without intrinsic signalling ability. It is likely that heteromultimeric signalling complexes form and that the co-receptors may vary by the ligand bound, resulting in specific downstream effects. CD36 for example binds to diacylated lipoproteins in conjunction with TLR2/6 leading to inflammation, but also mediates uptake of *Plasmodium falciparum* without cytokine release (Canton, Neculai et al. 2013). MARCO and SR-A binding leads to receptor mediated endocytosis. One effect of this process is to remove ligands from the extracellular milieu, so reducing interaction with cell surface PRR, and

increasing interaction with endosomal and cytosolic PRR. Expression of SRs on macrophages vary by polarisation; classical macrophages tend to express MARCO whereas alternative macrophages have more SR-A and less MARCO.

MARCO is expressed on subsets of macrophages as well as endothelial cells and astrocytes, and is inducible by inflammation. MARCO binds to *S. pneumoniae* by non-opsonic mechanisms (Arredouani, Palecanda et al. 2005), and MARCO deficient mice had reduced bacterial clearance and reduced pro-inflammatory cytokines production compared to wild-type in *S. pneumoniae* colonisation and pneumonia models (Arredouani, Yang et al. 2004, Dorrington, Roche et al. 2013). Macrophages isolated from these knockout mice showed reduced internalisation of *S. pneumoniae*. MARCO activation does not induce inflammation by itself, but appears to amplify the response from TLR2 or NOD2 stimulation (Dorrington, Roche et al. 2013). This is probably mediated by the CD14/TLR2 complex and MARCO's role in phagocytosis, for example MARCO appears to bind to *M. tuberculosis* cord factor and present it to TLR2 (Bowdish, Sakamoto et al. 2009). MARCO expression on AMs appears to be downregulated after influenza infection, contributing to secondary *S. pneumoniae* infection (Sun and Metzger 2008).

SR-A also mediates non-opsonic uptake of a variety of pathogens and is expressed on macrophages, and epithelial cells amongst others. SR-A enables phagocytic uptake of apoptotic cells in conjunction with the cell surface receptor MER proto-oncogene tyrosine kinase, whereas interaction with LPS in conjunction with TLR4 results in pro-inflammatory cytokine release. SR-A binding to ligands such as poly I:C can induce endocytosis-mediated TNF production (Coller and Paulnock 2001). In addition SR-A deficient macrophages produced lower levels of inflammatory cytokines in response to TLR3, NOD1, and inflammasome stimulation (Mukhopadhyay, Varin et al. 2011), suggesting that SR-A allows presentation of ligands to endosomal and cytosolic PRR. In a murine *S. pneumoniae* pneumonia model BALF from SR-A deficient mice had reduced levels of neutrophils and pro-inflammatory cytokines and higher bacterial counts (Arredouani, Yang et al. 2006).

1.4.2 Cell Signalling

Intracellular signalling pathways coordinate the macrophage response to PRR from pathogens like *S. pneumoniae*, and also to auto-, para-, and juxtacrine signalling in response to cytokines. These networks are critical in the transcriptional and post translational responses that generate inflammation. Understanding how they work is complicated by the fact that a few receptors stimulate more than one pathway, and multiple receptors initiate signalling events that converge on a few key signalling pathways.

1.4.2.1 MyD88/IRAK4

The binding of a TLR to its ligand induces conformational changes, such that a cytoplasmic Toll/interleukin 1 receptor (TIR) domain is exposed, allowing the recruitment of TIR-containing adaptor proteins (Figure 1.5). Apart from TLR3 and endosomal TLR4, TLR signalling involves the engagement of the adaptor protein MyD88, either directly or in combination with Myelin and lymphocyte protein (MAL), also known as TIR adaptor protein (TIRAP). MyD88 also has a DD which binds to the DD on IL1R associated kinases (IRAK) 4. IRAK4 is a serine/threonine kinase, and phosphorylation induces binding to IRAK1 & 2. The MyD88 and IRAK proteins conglomerate to form the myddosome, which also attracts the E3 ubiquitin ligase TNF receptor-associated factor 6 (TRAF6) as part of a ubiquitin conjugating enzyme complex. This results in the ubiquitination of IκB kinase γ (IKKγ) also known as NFκB essential modulator (NEMO), as well as the ubiquitination of TRAF6 itself. TRAF6 is then recruited to the TGFβ activated kinase (TAK1) complex by binding to TAK1 binding proteins (TAB) 1 & 2, which then initiates the mitogen activated protein kinase (MAPK) pathway (Lee and Kim 2007, Newton and Dixit 2012). In response to TLR1, 2 and 4, TRAF6 also translocates to mitochondria where it associates with Evolutionarily Conserved Signalling Intermediate in Toll pathways, triggering mitochondrial production of ROS, which serves to increase bacterial killing (Vogel, Janssen et al. 2007).

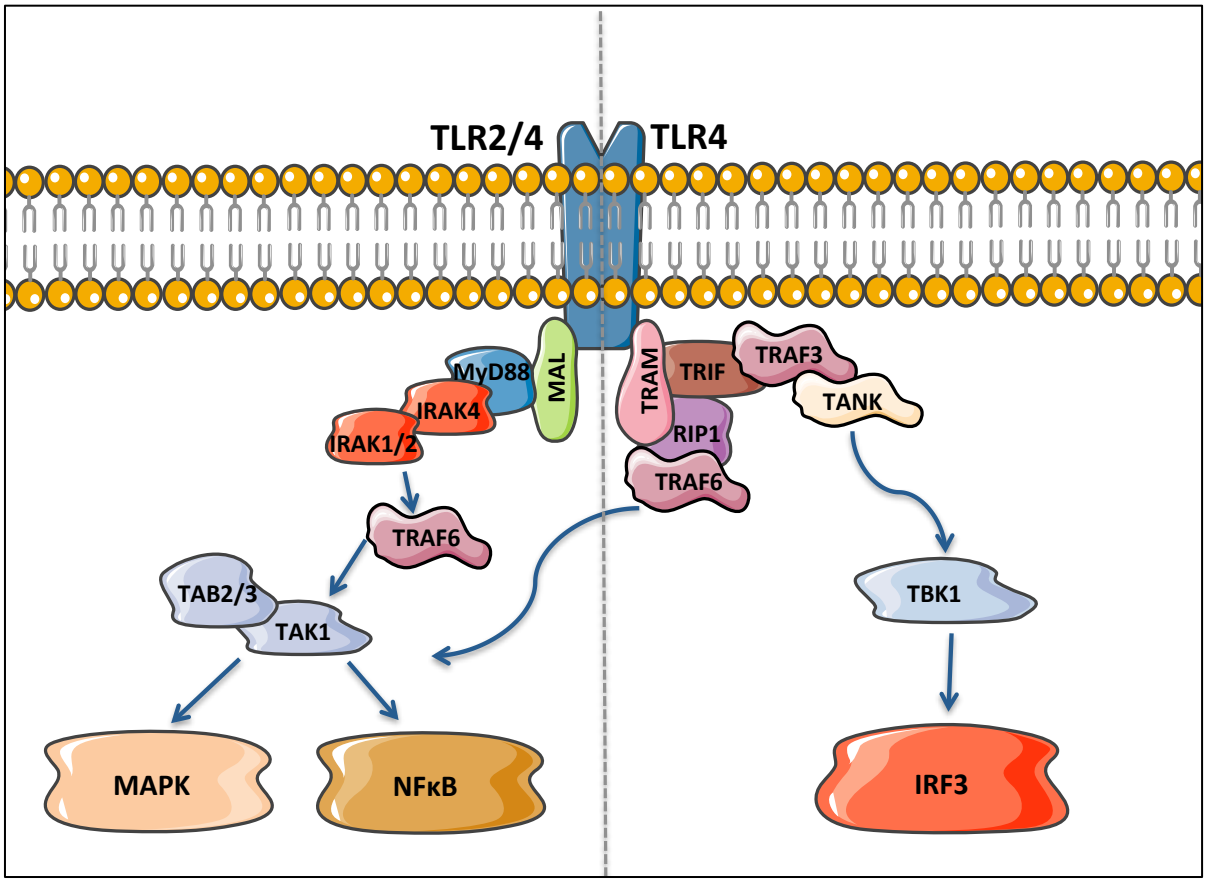

Figure 1.6 TLR signalling

TLR2 and canonical TLR4 signalling induces the recruitment of adaptor proteins such as MAL and MyD88. These activate the IRAK kinases to form the myddosome, which recruits the ubiquitin ligase, TRAF6 that ubiquitinates NEMO to activate NFκB and the TAK proteins that induce the MAPK pathway, both of which are involved in pro-inflammatory cytokine transcription. Meanwhile, TLR3 and endosomal TLR4 activation causes the recruitment of the TRIF and TRAM adaptor proteins that cause the activation of TBK1, and consequently IRF3, which is implicated in IFN transcription.

MyD88 deficient mice had poorer outcomes than either TLR2 or TLR4 deficient mice, with reduced survival and increased bacterial numbers in *S. pneumoniae* CNS infection, nasopharyngeal colonisation, pneumonia and sepsis models (Koedel, Rupprecht et al. 2004, Albiger, Sandgren et al. 2005). Mice with IRAK4 deficiency also had increased susceptibility to *S. pneumoniae* infection and a blunted pro-inflammatory cytokine secretion profile (Pennini, Perkins et al. 2013). *In vitro,* macrophages from mice with deficient phosphorylation of IRAK4 produced less pro-inflammatory cytokines in response to TLR2 agonists, had a partial response to TLR4 agonists compared to wild-type, and produced no inflammatory cytokines from either live or heat-killed *S. pneumoniae.*

The phenotype of humans with MyD88 deficiency is different from mice. Mice have increased susceptibility to many bacteria, as well as some viruses, fungi and protozoa, whereas humans are largely only susceptible to pyogenic bacterial infections, especially *S. pneumoniae* (von Bernuth, Picard et al. 2008). Examination of patients with IRAK4 deficiency and MyD88 deficiency showed that the leading threat was invasive disease including meningitis, septicaemia, deep seated abscesses, lymph node and salivary gland infections (von Bernuth, Picard et al. 2012). *S. pneumoniae* caused the majority of infections, followed by *S. aureus* and *P. aueruginosa*. Systemic signs of inflammation tended to be weak or delayed and in 88% the first infection was before the age of 2 with 72% having recurrent invasive infections. 38% of patients had died due to invasive bacterial disease (primarily IPD) by the age of 8, but after the age of 14 there were no documented cases of invasive disease though there were still incidences of non-invasive disease. Generally there was reduced fever and CRP in response to invasive disease but in some cases there was an exaggerated inflammatory response. In children there was a significant protective effect with prophylactic antibiotics (von Bernuth, Picard et al. 2008, Picard, von Bernuth et al. 2010). The peripheral blood transcriptome of IRAK4 deficient patients in response to *ex vivo* stimulation showed diminished inflammatory cytokine and chemokine responses to synthetic lipoproteins, flagellin, IL1β, IL18, and synthetic TLR7, 8, and 9 agonists. However, exposure of heat killed *S. pneumoniae* still

generated a significant albeit reduced response of inflammatory genes in IRAK4 and MyD88 deficient patients, suggesting further redundancy in recognition of bacteria. Unbiased analysis suggests that this may be mediated by immunoreceptor tyrosine based activation motif (ITAM) signalling (e.g. lectins, Fc receptors, integrins, and complement) (Alsina, Israelsson et al. 2014).

Several members of the IL1 family, e.g. IL1β and IL18 also signal by recruiting the same adaptor proteins as TLRs, i.e. MyD88, IRAKs, and TRAF6. Some of the effects of adaptor protein deficiencies may be therefore linked to IL1 family functions in addition to TLRs.

1.4.2.2 TNF receptor

The binding of members of the TNF family to their receptors can induce both inflammatory responses and apoptotic responses, which are often associated with suppressing inflammation. This depends on the signalling molecules triggered and regulation by other signals received by receptors binding their ligands. TNF-R1 activation usually activates inflammatory pathways by TNF receptor type 1 associated DD (TRADD) activating the TRAFs and RIPKs, whereas when protein synthesis is inhibited TRADD associates with FADD. TRAFs are a major group of intracellular adaptors involved in TNF/IL1/TLR signalling pathways. Distinct but overlapping parts of the protein are responsible for activating differing pathways. This is probably regulated by the binding of differing proteins which stabilise/destabilise the various signalling complexes that TRAF can form.

While the membrane associated complex of RIP1, TRADD and TRAF2, induces rapid NFκB and activator protein 1 (AP-1) activation, the cytosolic complex of RIP1, TRADD, TRAF2, FADD, and caspase 8 and 10 is pro-apoptotic. Therefor TNF signalling leads to rapid NFκB activation, then the dissociation of the complex from the membrane within an hour leads to apoptotic signalling. Apoptosis is only induced when there is insufficient NFκB activation, and therefore failure of induction of anti-apoptotic proteins. TNFR, TRAIL and Fas also induce necroptosis via RIP1 and RIP3 in association with FADD. The deubiquitinase

cylindromatosis (CYLD) promotes apoptosis by increasing RIP1-FADD association; suggesting that the ubiquitin status of RIP1K is critical to which pathway is dominant (Dempsey, Doyle et al. 2003).

1.4.2.3 NFκB

NFκB is a family of 5 proteins that exist as homo- or hetero- dimers in the cytoplasm: v-rel avian reticuloendotheliosis viral oncogene homolog A (RelA) (also known as p65), RelB, c-Rel, p50/p105, p52/p100. RelA mediates the pro-inflammatory functions, whereas p50 has inhibitory effects on inflammation. IκBs bind NFκB to retain the resulting complexes in the cytoplasm. The NFκB pathway can be stimulated by a number of different mechanisms. The canonical pathway of NFκB (Figure 1.6) is initiated after TNF, IL1β, TCR, and LPS stimulation. IκK exists as a complex of IκKα and IκKβ catalytic subunits attached to a regulatory subunit, IκKγ (also known as NEMO). IκK activation phosphorylates IκBα, which results in its ubiquitin mediated degradation. This allows NFκB dimers, primarily RelA bound to p50, to translocate to the nucleus and act as a transcription factor. IκBα bound to NFκB actually translocates to the nucleus but has a nuclear export sequence such that it shuttles out again without binding to DNA.

The non-canonical pathway occurs downstream of specific TNF family members (e.g. B cell activating factor, CD40L, lymphotoxin beta) binding to their receptors. These cause a signal transduction cascade that stimulates NFκB inducing kinase (NIK) to cleave p100 into its active p52 form. p52 heterodimerises with RelB, and translocates into the nucleus to initiate transcription. Dectin-1 also activates NFκB via NIK2, however the signalling pathway has not been completely elucidated (Osorio and Reis e Sousa 2011). There are also atypical IκK independent pathways that result in the dissociation or degradation of IκB (e.g. hypoxia and ultraviolet light stimuli).

NFKBIA/B/E are the genes that encode for the α, β, and ε members of the IκB family respectively. 6 nucleotide polymorphisms in NFKBIA have been associated with protection

from IPD, and one polymorphism in NFKBIE has been associated with susceptibility to IPD (Chapman, Khor et al. 2007). Patients with mutations to NEMO or IκBα suffer from a broad range of infections with some predisposition to *S. pneumoniae* infection. X-linked hypohydrotic ectodermal dysplasia with immunodeficiency is a condition with hypomorphic mutations to *IKBKG* gene that codes for IKKγ, impairing its translocation to the nucleus. They suffer from early life pyogenic infections and have a humoral defect with defective specific antibody production, especially to polysaccharide antigens, and sometimes hypogammaglobulinaemia. This is because CD40 mediated B cell stimulation is dependent on NFκB. Autosomal dominant hypohydrotic ectodermal dysplasia with immunodeficiency is due to a missense gain of function mutation in *NFKBIA* encoding IκBα, preventing its degradation and therefore NFκB activation. Presentation is similar to *IKBKG* mutations, except for the additional presence of T cell immune defects (Turvey and Hawn 2006).

Mice deficient in RelA and TNF receptor had reduced cytokine translation, reduced neutrophil recruitment, and 100-fold more bacteria in the lungs after intranasal *S. pneumoniae* infection (Quinton, Jones et al. 2007). Dexamethasone acts on peripheral blood mononuclear cells to inhibit *S. pneumoniae* mediated CXCL8 secretion by inhibiting IκBα (Mogensen, Berg et al. 2008) partly explaining the inflammation dampening effects of steroids.

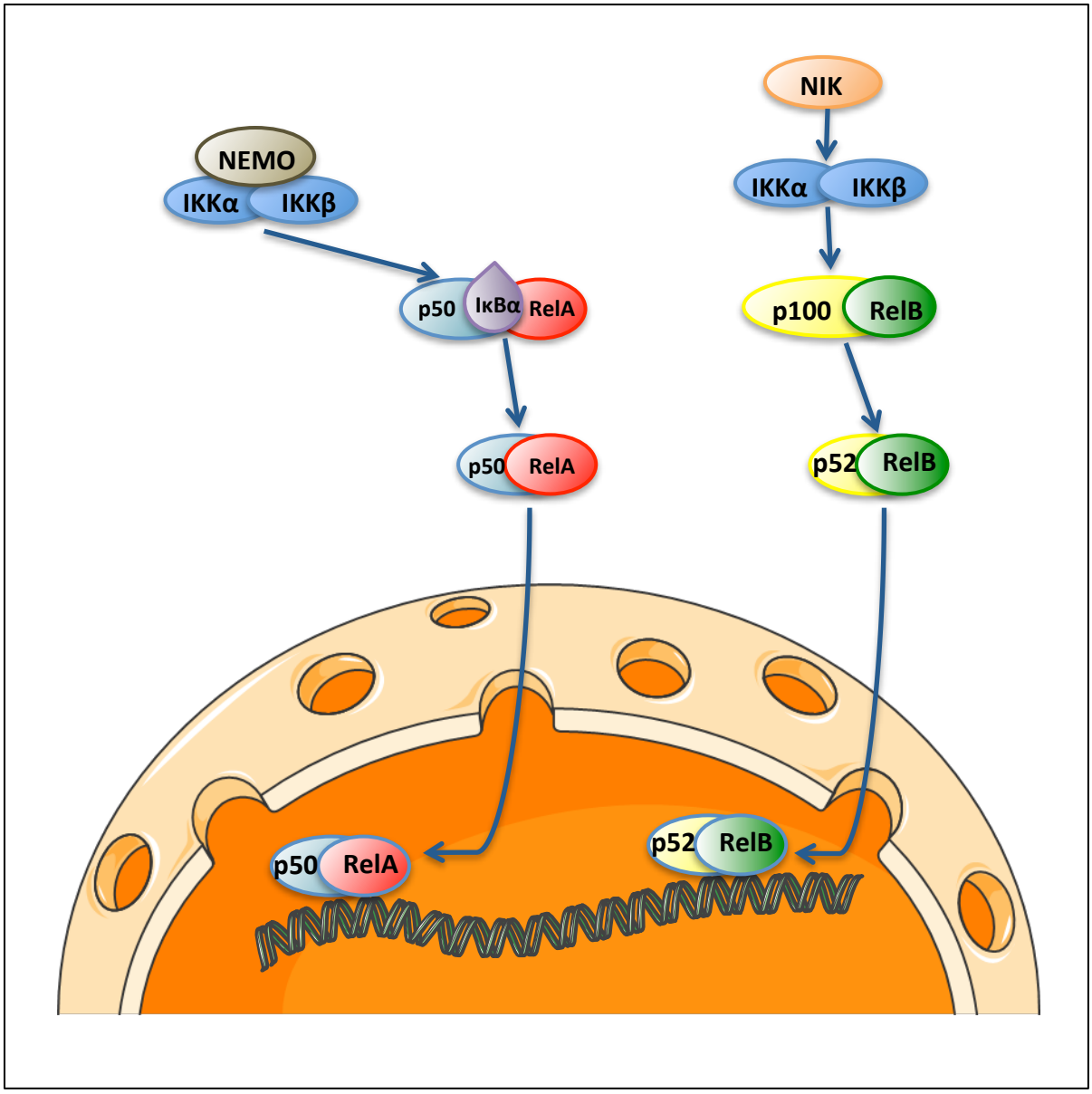

Figure 1.7 NFκB activation

The canonical pathway is activated when the IκK complex (NEMO, IKKα, and IKKβ) is activated to phosphorylate IκBα, allowing its degradation and the consequent translocation of the RelA-p50 dimer into the nucleus to induce transcriptional events. The non-canonical pathway involves NIK activation and subsequent cleavage of p100 into the active p52 form. The p52-RelB dimer translocates into the nucleus to act as a transcription factor.

1.4.2.4 MAPK

MAPK pathways are critical in multiple cellular events from proliferation and metabolism to inflammation. They coordinate multiple receptor–ligand events into 4 conventional signalling cascades where a MAPK kinase kinase (MAP3K) phosphorylates a MAPK kinase (MAP2K), which in turn phosphorylates a MAPK. The best studied pathways are extracellular signal-regulated kinases 1 & 2 (ERK 1/2) which are often stimulated by growth factors, c-Jun N terminal kinases (JNK) 1 & 2, and p38 MAPK (in particular isoform α), both of which are predominantly stimulated by stress pathways and cytokines. The substrates for the MAPK are shared somewhat; ribosomal 6S kinase (RSK) 1-4 are activated by ERK 1/2, whereas MAP kinase-interacting serine/threonine-protein kinase (MNK or MKNK) 1 & 2 and mitogen- and stress-activated protein kinase-1 (MSK) 1 & 2 are activated by ERK 1/2 and p38 MAPK, and MAPK-activated protein kinase (MK) 2 & 3 are stimulated by p38 MAPK and JNK (Figure 1.7).

The RSK proteins are able to phosphorylate IκB, and so induce NFκB activation. The MNKs have been implicated in prostaglandin synthesis, regulate pro-inflammatory cytokine transcription, and stabilise TNF mRNA. The MSKs may have an effect on acetylation of RelA, and thus increase its DNA affinity, but also target IL10 and IL1RA, so may be important in regulation of inflammation. MK2 and the closely related MK3 act to stabilise pro-inflammatory cytokine mRNA as well as induce their transcription directly (Moens, Kostenko et al. 2013). The MSKs, and ERK directly, increase transcription of dual specificity protein phosphatases (DUSP) such as DUSP1, which inactivates JNK and p38 MAPK.

JNK deficient macrophages have reduced expression of classically activated M1 genes in response to LPS indicating that JNK has pro-inflammatory roles. ERK activation increases production of TNF, IL1β, and IL10, but reduces production of IL12, IFNγ, and inducible nitric oxide synthase (iNOS). P38 MAPK induces TNF, IL10, and type I IFN production, but also initiates feedback mechanisms by inhibiting TAK1 effects on NFκB activation. Some of the MAPK functions are also by direct transcriptional control; translocation of ERK to the nucleus

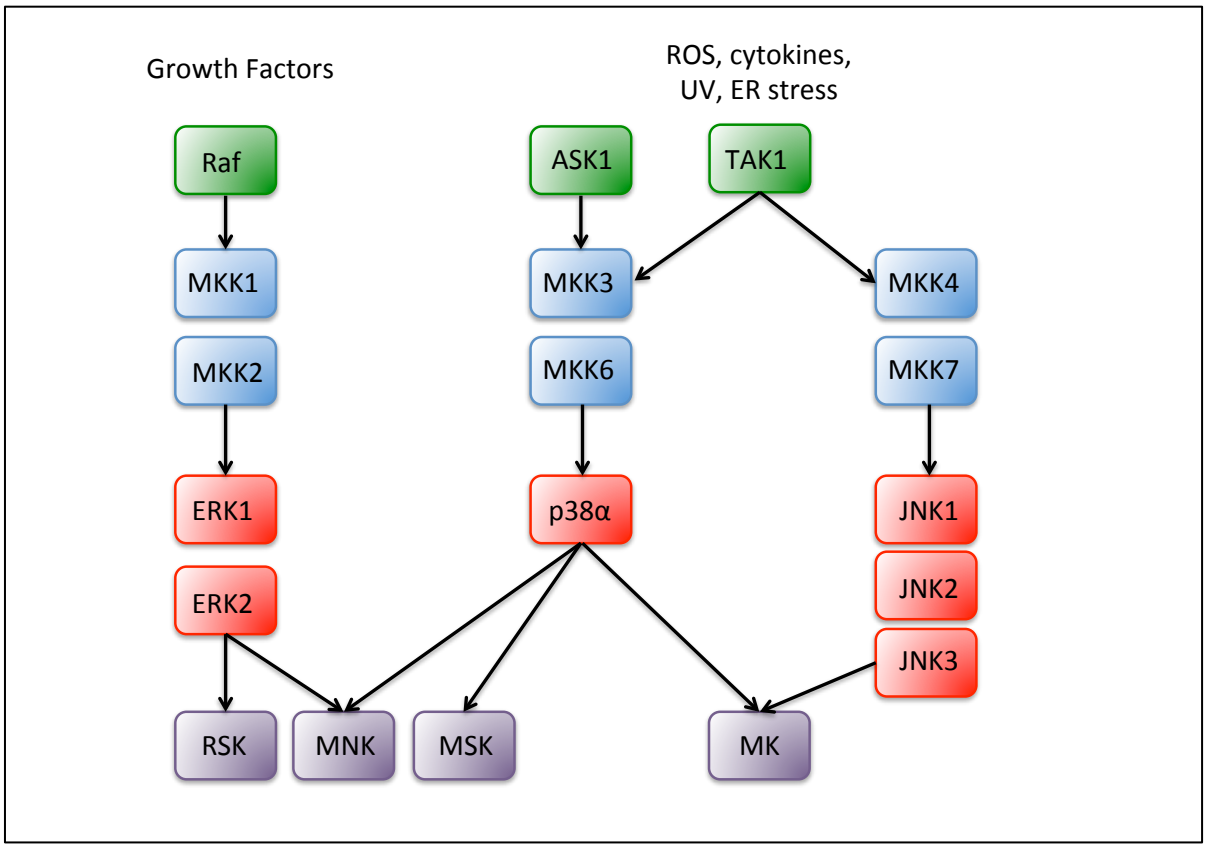

Figure 1.8 MAPK signalling

MAPK signalling pathways involve at least 3 kinases. MAP3K (in green) activate MAP2K (in red), which then activate MAPK (in red). Raf is stimulated by growth factor and antigen receptor activation. TLR, TNFR1, and IL1R activation induces TAK1 activation. ROS action on cell membrane liberates apoptosis signal-regulating kinase 1 (ASK1). The terminal MAPK have multiple isoforms; those most involved in inflammatory signalling are shown above. The terminal MAPK then activate further kinases and induce transcriptional effects.

induces the phosphorylation of Elk-1, stimulating the transcription of *fos*. JNK causes phosphorylation of c-Jun, which translocates to the nucleus and combines with c-Fos to form the transcription factor AP-1. AP-1 has pleiotropic effects, including transcription of pro-inflammatory genes and chemokines (Foletta, Segal et al. 1998, Whitmarsh 2007).

S. pneumoniae is known to induce some MAPK activation. When incubated *in vitro* with AM, *S. pneumoniae* induced phosphorylation of p38 MAPK and ERK pathways (Thorley, Ford et al. 2007). In a bronchial epithelial cell line, defensin release was mediated by the JNK/AP-1 pathway (Scharf, Zahlten et al. 2012).

1.4.2.5 IRF3

Type 1 IFN are primarily involved in antiviral immunity and also mediate induction of co-stimulatory molecules on antigen presenting cells. IRF 3 and 7 are transcription factors that regulate type 1 IFN transcription, with IRF3 constitutively expressed in most cells. Phosphorylation of a serine/threonine cluster at the C terminal of IRF3 causes conformational change allowing dimerisation of IRF3 and DNA binding at the relevant promoters. This change also allows association with co-activators cAMP response element-binding protein (CREB) binding protein (CBP) and p300 to prevent export of IRF3 from the nucleus. IRF3 effects transcription of IFNβ in cooperation with other transcription factors such as NFκB. IFNβ activates the IFN stimulated gene factor 3 complex (signal transducer and activator of transcription [STAT] 1, STAT2, IRF9), which in turn induces IRF7 transcription - and thus IFNα and β transcription.

Multiple receptors induce IRF functions, including TLR3 and TLR4, when activated on an endosomal membrane rather than at the cell surface. This occurs via activation of TIR-domain-containing adaptor inducing interferon-beta (TRIF). TLR3 interacts directly with TRIF but TLR4 requires the bridging adaptor TRIF related adaptor molecule (TRAM). TRIF activates TRAF3 to induce IKKε and TRAF family member-associated NF-kappa-B activator (TANK) binding kinase 1 (TBK1) mediated phosphorylation of IRF3. In addition, TRIF

activation of TRAF-6 leads to delayed NFκB activation. RIG-I or MDA5 recognition of cytoplasmic non-self RNA induces IRF3 via TRAF3 and TBK1, in these instances the adaptor mitochondrial antiviral protein (MAVS) is also involved (Moynagh 2005, Newton and Dixit 2012).

The relationship between interferon and inflammatory cytokine induction is complex. While Rel A can form dimers with IRF3 to act as cofactors in transcription of both NFκB and interferon response elements (IRE), p50 homodimers may bind to IRE in competition with IRFs so inhibiting their transcription (Oeckinghaus, Hayden et al. 2011). In hepatocytes IRF3 signalling inhibited IKKβ by interacting with its kinase domain while in the cytoplasm, thereby inhibiting downstream signalling (Wang, Zhang et al. 2014). Bioinformatic analysis of transcription factor binding sites indicated that NFκB activation can directly compete with and inhibit IRF3 mediated transcription. IRF3 activation similarly inhibited NFκB function, but indirectly, possibly through cooperation with other transcription factors such as AP-1 (Iwanaszko and Kimmel 2015). TBK1 and IKKε can phosphorylate the catalytic domains of IKKα and β, resulting in less IKK complex activity and lower expression of NFκB dependent gene expression. IKKε and TBK1 phosphorylation of TANK may also be involved in this regulation of canonical IKK activity (Oeckinghaus, Hayden et al. 2011).

1.4.2.6 Syk

Spleen tyrosine kinase (Syk) is an important signalling molecule that is activated by a number of receptors including TCR, BCR, lectins, and Fc receptors. Several lectins including dectin-1, dectin-2, and Mincle signal via Syk. Lectin meditated Syk signalling usually requires ITAM containing adaptor proteins, though a few signal directly through hemITAM intracellular domains (Osorio and Reis e Sousa 2011). Downstream of Syk phosphorylation, the adaptor protein CARD9 is recruited, which recruits Mucosa-associated lymphoid tissue lymphoma translocation protein 1 (MALT-1) and B cell leukaemia/lymphoma 10 (Bcl-10), which activates the IKK complex. CARD9 is recruited to phagosomes, but also appears to act at the cell membrane. c-Rel is preferentially activated by MALT-1, and is the only subunit of

NFκB that is activated by dectin-2, whereas dectin-1 activates all subunits (Drummond and Brown 2013). Syk also activates the inflammasome via ROS and thus leads to IL1β activation and in addition stimulates calcium flux that drives NFAT activation (Geijtenbeek and Gringhuis 2009).

1.4.2.7 c-RAF

DC-SIGN is known to have a pro-inflammatory role in other infections. Once mannose is bound on the cell surface, Syk-independent pathways cause cellular Rapidly Accelerated Fibrosarcoma (cRAF) (a serine/threonine protein kinase) to phosphorylate RelA. cRAF, best known as a primary member of MAPK signalling, does not signal via ERK for this function. RelA phosphorylation allows histone acetyltransferases such as CREB-binding protein or p300 to acetylate RelA, when it is already in the nucleus. This increases its DNA binding affinity thus prolonging pro-inflammatory cytokine transcription (Gringhuis, den Dunnen et al. 2007). Acetylation of RelA also results in the formation of RelA-RelB dimers, which cannot bind DNA. This can limit the function of RelB-p52 dimers, which usually inhibit inflammatory cytokine transcription (Geijtenbeek and Gringhuis 2009).

1.4.3 Phagocytosis

Phagocytosis is the receptor-mediated uptake of particles ≥0.5 μm into cells. These receptors include non-opsonic PRRs such as MR, MARCO, CD14, and opsonic receptors such as Fcγ, complement receptors, and apoptosis receptors such as $\alpha_V\beta_5$ integrin. The effectiveness of these receptors depends on the density of receptor expression, and their affinity to their ligand. Usually receptors cluster on the cell membrane to tether the pathogen to overcome low affinity and active movement of the microbe.

The best understood phagocytosis receptor is the Fc family, which binds antibody. Antibody coated particles bind to the Fcγ receptor, leading to clustering of Fcγ receptors that leads to actin-driven extension of pseudopodia, and further receptor binding. Once the target engages with the receptors on all sides engulfment begins. Multivalent ligand binding is

required to trigger intracellular signalling, which requires lateral clustering such that the cytosolic domains (containing ITAM regions) are brought together to be phosphorylated by intracellular kinases, then leading to actin polymerisation by recruitment of adaptor proteins. Rho family GTPases, located on the inner layer of the cell membrane regulate actin polymerisation. Dectin 1 recognition of fungal wall ligands also signals via Syk to have a similar effect. CR3 signals via different pathways dependent on RhoA, which activates Rho kinase and subsequently myosin. Unlike other members of its family, FcγRIIB contains an immunoreceptor tyrosine-based inhibition motif (ITIM), which recruits kinases that inhibit phagocytosis (Moretti and Blander 2014).

Once engulfment is complete, a phagosome matures. Vesicle traffic to the phagosome is mediated by Rab GTPases. As proton pumps are acquired, the interior of the phagosome becomes acidic. Lysosomal associated membrane proteins (LAMP) are integral membrane proteins associated with lysosomes and mature phagosomes that are essential for recruitment of Rab7, a small GTPase essential for full maturation of the phagosome. Lysosomes fuse with the phagosome to make a phagolysosome, and by this stage the vacuole contents are very acidic.

NOX2, an NADPH oxidase, forms at the membrane in response to inflammatory stimuli and shuttles electrons across the phagolysosomal membrane, allowing the production of ROS. The formation of reactive nitrogen species (RNS) is then catalysed by iNOS. Nitric oxide (NO) is synthesised on the cytosolic face of the membrane and diffuses into the phagolysosome and react with ROS to form reactive nitrogen intermediates (RNI). Cytoplasmic granules containing antibacterial peptides then fuse with the phagolysosome. Specific cathepsins work at differing pH ranges and need to be delivered to the phagosome at the right maturation phase to allow effective function.

TLR stimulation and consequent p38 MAPK activation results in increased macropinocytosis. TLR stimulation may also increase phagosomal assembly and increase NADPH mediated

microbicidal function. Activation of inflammasomes allows the accumulation of caspase 1 around phagosomes, which hydrolyses components of NOX2 and encourages acidification of the phagolysosome (Moretti and Blander 2014). The circumstances under which a phagosome forms affect the receptors present on the phagosome membrane, and thus subsequent signalling events. Blocking actin polymerisation and thus phagocytosis increased cytokine production by macrophages, as did frustrated phagocytosis of fungal wall particles too large to internalise (Rosas, Liddiard et al. 2008), possibly due to increased engagement with cell surface PRR.

1.4.4 Apoptosis

Apoptosis of alveolar macrophages is found after *S. pneumoniae* infection. Bacterial uptake of *S. pneumoniae* and subsequent apoptosis contributes to bacterial clearance. Macrophage apoptosis results in intracellular bacterial death while minimising inflammatory signalling, with downregulation of pro-inflammatory cytokine secretion compared to necrotic cell death (Haslett 1999, Marriott, Hellewell et al. 2006). Once phagolysosomal capacity for bacterial killing is exceeded, lysosomal permeabilisation and cathepsin D activation results in macrophage apoptosis. Cathepsins cleave members of the Bcl-2 family and increase degradation of the anti-apoptotic protein Mcl-1, to trigger either the mitochondrial pathway of apoptosis or directly activate caspases (Bewley, Marriott et al. 2011). Inhibition of cathepsins decreases late phase macrophage-mediated killing of *S. pneumoniae* (Dockrell, Marriott et al. 2003).

Apoptotic cell death results in phosphatidylserine accumulation at the cell surface, which increases scavenger receptor mediated recognition by other macrophages. The uptake of apoptotic bodies, i.e. efferocytosis, is into efferosomes where the dead cell is broken down (Martin, Peters et al 2014). This results in anti-inflammatory cytokine secretion such as TGFβ and IL10 in addition to limiting pro-inflammatory cytokine secretion. Though this also

results in reduced phagocytic and microbicidal ability of the remaining macrophages (Medeiros, Serazani et al. 2009)

1.5 *S. pneumoniae* virulence factors and macrophages

S. pneumoniae has a number of genetically conserved factors that contribute to its virulence. Two of the best-described virulence factors are the extracellular polysaccharide capsule and toxin Ply and are described in detail. For context some of the other important virulence factors are described in brief below and summarised in table 1.8.

Table 1.8: Major *S. pneumoniae* virulence factors (modified from Ferreira and Gordon, 2015)

Virulence factor	Function
Autolysin A	Autolysis by PG breakdown, releasing inflammatory bacterial components
Capsule	See 1.5.1
Hyaluronate	Breaks down hyaluronan in extracellular matrix allowing tissue invasion
IgA1 protease	Cleaves human IgA
Neuraminidase A	Cleaves sugars from host cell surfaces, revealing adhesion sites
Phosphorylcholine	Binds to PAFr on epithelial cells, increasing adhesion
Pneumolysin	See 1.5.2
Pneumococcal adherence and virulence factor A	Binds to fibronectin, allowing adhesion
Pneumococcal surface antigen A	Resistance to oxidative stress by mediating metal ion uptake
Pneumococcal surface protein A	Inhibits complement binding by blocking alternate pathway C3 convertase
Pneumococcal surface protein C	Binds factor H to limit complement deposition, and binds pIgR to increase invasion

Choline binding proteins (CBP) are a family of 15 *S. pneumoniae* proteins that are non-covalently anchored to the cell surface via choline present in the cell wall. Autolysin A (LytA) is the major *S. pneumoniae* autolysin, and is required for virulence (Martner, Skovbjerg et al. 2009). LytB and CbpE are involved in nasopharyngeal colonisation (Mitchell and Mitchell 2010). PspA interferes with complement binding to *S. pneumoniae* and binds to lactoferrin, thus inhibiting host-mediated killing of the bacteria (Ricci, Gerlini et al. 2013). PspA also inhibits complement deposition (Tu, Fulgham et al. 1999). PspC (also known as CbpA) acts as an adhesin to PAFr as well as binding to factor H, thus inhibiting the alternative complement pathway (Dave, Carmicle et al. 2004). During colonisation PspC interacts with epithelial cells by the polymeric Ig receptor, facilitating invasion.

S. pneumoniae expresses around 50 lipoproteins that possess an acyl group, allowing them to be anchored to cell membrane phospholipids. Lipoproteins have multiple functions including adhesion, transport, nutrient uptake, and signal transduction. Lipoproteins are translated with a characteristic signal sequence and exported to the cell membrane, where post-translational conformational changes occur. Action by the enzyme lipoprotein diacylglyceryl transferase (Lgt) adds an acyl group, this prolipoprotein is further modified by lipoprotein signal peptidase (Lsp), to leave mature lipoprotein in Gram-positive organisms. The acyl moiety of lipoproteins interacts directly with TLR2 (Kovacs-Simon, Titball et al. 2011). Lgt deficient *S. pneumoniae* have been used to confirm that lipoproteins are the dominant PAMP inducing TLR2 stimulation and thus inflammatory response in *S. pneumoniae* infection (Khandavilli, Homer et al. 2008, Basavanna, Khandavilli et al. 2009, Chimalapati, Cohen et al. 2012, Tomlinson, Chimalapati et al. 2014). Lgt deficient mutants are also cleared less well than wild-type from the nasopharynx (Moffitt, Skoberne et al. 2014). The majority of *S. pneumoniae* lipoproteins are components of ABC transporters required for import of micronutrients into the bacteria. For example pneumococcal surface antigen (Psa) A is a manganese binding lipoprotein that is part of an ABC transporter that imports manganese, and is important for resistance to oxidative stress (Kadioglu, Weiser et al. 2008).

S. pneumoniae has several surface proteins that are covalently attached to PG in the cell wall via sortase peptidases that recognise the amino acid sequence LPXTG, including hyaluronidase, neuraminidases, and pili. Hyaluronidase (Hyal) breaks down mammalian connective tissue and extracellular matrix, possibly aiding bacterial spread once the organism has reached the basement membrane. Neuraminidase (NanA) cleaves glycolipids, lipoproteins, and oligosaccharides by removing sialic acid from soluble proteins, causing direct damage to the host or possibly exposing binding sites to aid adherence. Some strains of *S. pneumoniae* express a pilus-like structure encoded by the pathogenicity island *rlrA*. Pili bind to components of host extracellular matrix, and Δ*rlrA* mutants have reduced adherence to epithelial cells and cause lower mortality in a lung infection model (Barocchi, Ries et al. 2006).

As discussed in the adaptive immunity section, *S. pneumoniae* possesses an IgA1 protease that cleaves the mucosally abundant IgA, the main function of which is to neutralise and agglutinate pathogens. Pneumococcal adherence and virulence factor A (PavA) binds to fibronectin, thus mediating attachment to endothelium and facilitates transmigration through the basement membrane (Mitchell and Mitchell 2010). PavB is a surface exposed multi-domain protein that similarly binds to components of extracellular matrix (Jensch, Gamez et al. 2010)

1.5.1 Capsule Biology

S. pneumoniae is surrounded by a capsule that is vital for full virulence. The capsule is usually a polyanionic highly hydrated shell consisting of chains of polysaccharide. Electron microscopy demonstrates that the capsule size varies between strains but is usually 200 to 400nm in thickness (Skov Sorensen, Blom et al. 1988). Capsular polysaccharide consists of mono- or oligo- saccharide repeats and is usually covalently bonded to the cell wall (except for serotype 3), which nuclear magnetic resonance data suggests forms an extended flexible

ribbon-like structure with no stabilisation of secondary structure (Rutherford, Jones et al. 1994).

S. pneumoniae undergo spontaneous phase switching between transparent (low capsule expression, and increased cell wall TA) and opaque (high capsule expression, and less TA) phenotypes. These differences are visible in oblique light on an agar plate. The ability to switch phenotypes allows expansion of *S. pneumoniae* expressing a phenotype that is better able to cope with the present bacterial environment. For example, transparent variants are more efficient at colonisation and adhere more strongly to epithelial cells and predominate during colonisation, whereas opaque variants have greater virulence and survive longer in blood and are the dominant phenotype amongst bacteria recovered from blood in mouse models of infection (Kim and Weiser 1998). The ability to dynamically vary the amount of capsule expressed is important in causing disease in a mouse model; mutants that constitutively overexpress or underexpress the capsule are attenuated in mouse models compared to wild-type bacteria (Shainheit, Mule et al. 2014). Table 1.9 summarises the recognised functions of the capsule on the host immune system.

1.5.1.1 Structure

The carbohydrate chain structure is defined by; i) the nature and number of mono- or oligo-saccharide units, ii) the sequence and ring size of the monosaccharides, iii) the type and configuration of glycosidic linkages, and iv) non-sugar substituents (Yother 2011). The outer surface of *S. pneumoniae* exhibits various degrees of negative charge, primarily due to acidic sugars, pyruvate or phosphate in the capsular polysaccharide. This may play a role in repulsion from anionic mucus and phagocytes. There is a correlation between increased net negative charge, resistance to neutrophil mediated killing, and increased nasopharyngeal carriage (Li, Weinberger et al. 2013).

Table 1.9: Effects of *S. pneumoniae* capsule (Jonsson, Musher et al. 1985, Musher 1992, Nelson, Roche et al. 2007, Wartha, Beiter et al. 2007, Hyams, Camberlein et al. 2010)

Effects of *S. pneumoniae* capsule on host immune response
Inhibition of complement mediated phagocytosis
Inhibition of antibody binding to cell surface proteins
Inhibition of phagocyte engagement with opsonins on cell surface
Inhibition of opsonin-independent phagocytosis
Inhibition of mucus entrapment
Inhibition of neutrophil extracellular traps

1.5.1.2 Capsule synthesis

Capsular biosynthesis requires the synthesis of a monosaccharide, attachment of each monosaccharide to a nucleotide precursor, coordinated transfer of each sugar to the capsule chain, export and attachment to the cell surface of the finished product in succession. There are two main mechanisms of capsule synthesis, with most serotypes using Wzy-dependent pathway, and serotype 3 and 37 having a synthase dependent pathway.

Capsule production is controlled by the *cps* portion of the bacterial genome and is highly conserved amongst most serotypes. These genes lie between the homologous sequences *dexB* and *aliA*. Conserved genes are *cps A – D* which encode assembly and export proteins, a gene coding for a flippase that transports the repeat unit from inside the cell to the external surface of the cell membrane, and the gene encoding a polymerase that links the repeat units together. Non-conserved genes are those genes coding for specific glycosyl transferases (Lopez and Garcia 2004, Kadioglu, Weiser et al. 2008). CpsA appears to be responsible for the covalent bonding of the polysaccharide to cell wall. However, if *cpsA* is inactivated, LytR (another enzyme involved in cell wall assembly, particularly TA to PG) takes over responsibility of retaining the capsule at the cell wall (Eberhardt, Hoyland et al. 2012). Two

proteins involved in sugar metabolism are also critical for capsule formation. Phosphoglucomutase (Pgm) catalyses the conversion of G-6-P to G-1-P, and G-1-P uridyltransferase (GalU) catalyses the formation of UDP-Glc from G-1-P. Mutations in the genes encoding either protein result in almost no capsule and limited growth.

Amongst synthase-dependent serotypes a single enzyme initiates, polymerises, and transports the sugars. In serotype 3, the locus for the synthase genes is also between *dexB* and *aliA*, however the common region is not transcribed. The 3' end of the locus is also truncated with only 2 genes required for capsule synthesis: C*ps3D* encodes UDP-glucuronyl dehydrogenase and *cps3S* encodes the synthase (Yother 2011). Type 3 capsule is synthesised by the addition of alternating glucose and glucuronic acid after initiation onto a lipid primer. The chain is terminated when either constituent drops below the necessary concentrations (Lopez and Garcia 2004). Serotypes with less metabolically demanding capsules generate thicker capsules in metabolically restricted environments, giving them an advantage in nasopharyngeal colonisation (Hathaway, Brugger et al. 2012).

1.5.1.3 Effect on colonisation

Nasopharyngeal colonisation of mice with isogenic unencapsulated strains of *S. pneumoniae* occurs at much lower density and is cleared more quickly than encapsulated strains (Magee and Yother 2001). Apart from serotype 1, 7A, 7F, 15, 33F, and 37, which have a neutral overall charge, all other serotypes of *S. pneumoniae* are negatively charged by virtue of their capsule make up. The capsular serotype is thus the strongest factor in determining surface charge, which allows movement through mucus and correlates with carriage (Nelson, Roche et al. 2007, Li, Weinberger et al. 2013). Strongly negatively charged serotypes (4, 6A, 23F) and opaque phenotype variants are bound less by mucus than less strongly charged serotypes (7F, 14) and transparent mutants (Nelson, Roche et al. 2007). The difference in bacterial clearance between wild-type and unencapsulated strains is preserved in the absence of AM, further evidence that capsule has an effect on physical defences (Camberlein, Cohen et al. 2015).

Capsule expression is reduced, albeit temporarily, during tissue invasion. Unencapsulated mutants adhere more strongly to epithelial cells than wild-type *S. pneumoniae* (Morona, Morona et al. 2006). Electron microscopy confirms reduced capsular material upon adhesion to epithelium, and subculture of the internalised bacteria shows increased ability to both adhere to and invade epithelial cells (Hammerschmidt, Wolff et al. 2005). While transparent *S. pneumoniae* adhere better than opaque variants to resting buccal cells by GlcNAcb1-3Gal, lung epithelial and endovascular cells needed to be stimulated by IL1β and TNF respectively to increase adherence by upregulation of PAFr and GlcNAc (Cundell, Weiser et al. 1995). This again had a more pronounced effect in transparent phenotypes than opaque variants. Similarly, opaque *S. pneumoniae* are taken up less by endothelium and are more likely to be degraded in the internalised vacuole (Ring, Weiser et al. 1998).

1.5.1.4 Effect on phagocytosis

The capsule of *S. pneumoniae* inhibits opsonophagocytosis, by inhibiting deposition of complement, IgG and CRP, and inhibits neutrophil phagocytosis mediated by Fcγ, complement receptors, and non-opsonic receptors (Hyams, Camberlein et al. 2010). *In vivo*, mouse AM internalised unencapsulated *S. pneumoniae* more than wild-type, particularly at high inocula. The use of capsule switch mutants confirms that capsule makeup affects resistance to neutrophil killing. This correlates with degree of encapsulation. However, generating thick capsule has a metabolic cost (Weinberger, Trzcinski et al. 2009). In specific circumstances capsule increases bacterial uptake; SIGN-R1 positive macrophages allow recognition of capsular polysaccharide from a variety of serotypes to be phagocytosed in mice (Koppel, Wieland et al. 2005), and the human homologue DC-SIGN similarly binds to capsular polysaccharide, though it also binds some heat killed strains suggesting non capsular polysaccharides may also be recognised by DC-SIGN (Koppel, Saeland et al. 2005). Similarly neutrophil binding to SP-D varies by capsular serotype (Jounblat, Kadioglu et al. 2004), meaning that capsule may affect binding to the bacterial ligand or that capsular polysaccharide may be a ligand itself depending on the oligosaccharide makeup. However,

neutrophil killing of internalised *S. pneumoniae* by α defensins is decreased in unencapsulated *S. pneumoniae*, due to alteration in surface charge, as surface exposed LTA is positively charged (Beiter, Wartha et al. 2008).

1.5.1.5 Effect on complement

Capsule also plays a role in binding of complement to *S. pneumoniae*. The capsule inhibits deposition of C3b/iC3b as well as inhibiting the conversion of bound C3b to iC3b (Hyams, Camberlein et al. 2010). Cleavage of bound IgG still results in increased C3b binding, suggesting the alternative pathway is inhibited in addition to the classical pathway. C3 deposition on *S. pneumoniae* varies by capsular serotype, this difference persists in capsule switch strains, even in IgG depleted systems. The strains with increased complement deposition were phagocytosed more readily by neutrophils and had reduced virulence in a mouse sepsis model (Hyams, Yuste et al. 2010). However, variation in C3b deposition on *S. pneumoniae* did not correlate with capsular thickness, and varies between different isolates of the same serotype. Binding of C3b correlates with C1q, and less so with IgG binding. This suggests that capsule independent variation between strains is important in complement recognition (Hyams, Opel et al. 2011). Similarly factor H binding (mainly to PspC) varies by capsular serotype; this is inversely correlated with factor B binding, C3 deposition, and neutrophil association (Hyams, Trzcinski et al. 2013). These differences are abrogated when PspC mutant strains are used, suggesting that variations in complement resistance are driven by the degree of factor H binding due to variations in capsular makeup but not thickness, probably by affecting PspC access to circulating factor H (Hyams, Trzcinski et al. 2013).

1.5.1.6 Effect on inflammation

There is some evidence that capsular serotype affects inflammation. A 13-year single centre Spanish study looked at cases of CAP caused by *S. pneumoniae*. Serotype 3 was overrepresented, and serotype 1 was underrepresented in cases presenting with shock compared to those without shock (Garcia-Vidal, Ardanuy et al. 2010), with a OR of 2.2 for serotype 3 causing shock on multivariate analysis. However, only 10 serotypes were found

in 650 patients, with serotype 3 being far the commonest, and only a handful of cases with shock due to other serotypes, possibly underestimating their predisposition to cause shock. Additionally an analysis of the patients with bacteraemia, i.e. true septic shock, only showed a correlation with steroid treatment. Immunosuppressed patients were also largely excluded, which may have skewed the data. Given the variation in serotype prevalence by region, ideally similar data from other countries and from multiple centres would be considered to confirm the serotype association with shock.

A 3-year, country wide study of bacterial meningitis in adults from the Netherlands gathered 211 CSF samples from patients infected with *S. pneumoniae*. The authors suggest that IL1β and IL18 levels in CSF of patients with meningitis vary by the serotype causing the infection (Geldhoff, Mook-Kanamori et al. 2013), however there are 16 serotypes identified, and a further 50 cases not categorised by serotype. For several of the serotypes, they were only identified in a handful of cases. In addition the cytokine data shows a lot of variation within serotype, and although Kruskal-Wallis analysis suggests variation between strains, no multiple comparison tests were undertaken that suggest specific serotypes cause more or less inflammation than others.

In a mouse model of sepsis serotypes 1 and 7F induced less serum TNF than 6B and 19F (Sandgren, Albiger et al. 2005). In a rabbit model of meningitis serotypes 5 and 7F developed a milder phenotype than serotypes 6B, 14, and 23F as measured by leucocytes, protein concentration, lactate levels, and cytokine response in CSF (Engelhard, Pomeranz et al. 1997). In a mouse pneumonia model serotype3 induced greater lung inflammation and mortality than serotype8 (Seyoum, Yano et al. 2011).

Despite the evidence for the capsule serotype affecting inflammatory responses, capsular polysaccharide itself does not appear to provoke a profound inflammatory response. Purified polysaccharide only causes pro-inflammatory cytokine release from whole blood at much higher concentrations than heat killed bacteria (Jagger, Huo et al. 2002), and RAW

macrophages require longer to release TNF after stimulation with purified capsular polysaccharide compared to heat killed *S. pneumoniae* (Simpson, Singh et al. 1994). Similarly, injection of purified capsular polysaccharide does not generate an inflammatory response in a rabbit meningitis model when compared to purified cell wall or equivalent numbers of heat-killed bacteria (Tuomanen, Tomasz et al. 1985). CXCL8 release from human epithelial and monocyte cell lines is lower with wild-type bacteria than isogenic unencapsulated strains (Marriott, Gascoyne et al. 2012). There are however data suggesting that the presence of capsule increases inflammatory responses. In a mouse model of meningitis, unencapsulated mutants induced less inflammation than wild-type (Ricci, Gerlini et al. 2013). Additionally, mice infected intranasally with wild-type *S. pneumoniae* had greater lung TNF, IL6, and CXCL8 than unencapsulated mutants, though levels of IL1β were similar. However, in MyD88 deficient mice, the difference was markedly reduced (De Vos, Dessing et al. 2015). However data from mouse models are likely to be confounded by differences in bacterial counts, as unencapsulated bacteria are cleared more rapidly.

1.5.2 Pneumolysin Biology

Ply is a 53kDa cytosolic protein expressed by most strains of *S. pneumoniae,* with upregulated expression in clinical strains, (Hu, Liu et al. 2015). Ply is released on bacterial lysis, although it also localises to the bacterial cell wall (Price, Greene et al. 2012) independently of autolysis. The bacterial cell wall inhibits Ply activity as the branched peptides of mature PG inhibit Ply release extracellularly from the cell wall, and this is dependent on remodelling of PG by choline binding proteins (Greene, Narciso et al. 2015).

Ply has multiple functional effects (table 1.10). Ply is a cholesterol-binding toxin, and best known for inducing pore formation in host cell membranes and therefore host cell lysis. Multiple monomers of Ply bind to cell membranes and oligomerise into a circular barrel structure of 30-50 monomers, which unfolds and penetrates the membrane to create the pore. This appears to be related to interactions with actin within the cell (Hupp, Fortsch et al.

2013). Neuroblastoma cells incubated with purified Ply exhibit membrane depolarisation within 60 seconds of exposure, and cell morphological changes within 8 minutes. The morphological changes were dependent on voltage gated calcium channel mediated calcium influx and consequent Rho GTPase activation (Iliev, Djannatian et al. 2007). This was dependent on Ply binding cholesterol, and occurred even at sub-lytic concentrations.

1.5.2.1 Effects *in vivo*

Mice infected intranasally, intraperitoneally or intravenously with *S. pneumoniae* lacking Ply (Δ*ply*) had longer median survival than if infected with wild-type bacteria (Berry, Yother et al. 1989). Similarly wild-type bacteria induced more protein leak in a pneumonia model, and invaded the blood much more rapidly than a Δ*ply* strain (Rubins, Charboneau et al. 1995). The co-administration of purified Ply with the Δ*ply* strain replicated the wild-type phenotype. Purified Ply induced vascular leakage and lung oedema in mice when administered intratracheally. This was associated with neutrophil recruitment and early depletion of AM. Pre-depleting AM had no effect on this phenomenon, suggesting other cell types, such as epithelium are involved in this response (Maus, Srivastava et al. 2004). Ply also causes elevation of pro-inflammatory cytokines in BALF and leukocyte trafficking that was mediated by CXCL2 (Rijneveld, van den Dobbelsteen et al. 2002). Purified Ply caused alveolar epithelial damage when instilled intranasally (Kadioglu, Taylor et al. 2002). Sublytic doses of Ply also elicited significant epithelial barrier damage (Los, Randis et al. 2013). Ply is also implicated in breaching the endothelial barrier prior to causing meningitis. Intravenous administration of wild-type *S. pneumoniae* into mice induced more systemic IL6 than intravenous administration of the Δ*ply* strain, with Δ*ply* leading to a chronic bacteraemic phenotype rather than an acute sepsis phenotype (Benton KA, VanCott JL et al. 1998). In this context, the role of Ply occurs early in infection, with early host resistance to Δ*ply* being dependent on TNF. Large amounts of Ply are released by *S. pneumoniae* on exposure to antibiotics, with perhaps potentially negative consequences for the host.

Table 1.10: Effects of Pneumolysin (Bewley, Naughton et al. 2014, Davis, Nakamura et al. 2011, Ferrante, Rowan-Kelly et al. 1984, Los, Randis et al. 2013, Malley, Henneke et al. 2003, McNeela, Burke et al. 2010, Paton, Rowan-Kelly et al. 1984)

Effects of pneumolysin on host immune response
Activates TLR4
Activates inflammasome & NOD
Reduces neutrophil killing of *S. pneumoniae*
Breaks down epithelial tight junctions
Induces apoptosis
Activate and deplete host complement
Activate memory T cell responses
Inhibit T cell inflammatory responses

1.5.2.2 Non haemolytic pneumolysin

Although virtually all clinical isolates of *S. pneumoniae* produce Ply, some invasive strains express allelic variants of the *ply* gene that encode non-haemolytic Ply. For example, 50% of serotype 1 clinical isolates in Scotland have a mutation in the pore-forming region of the pneumolysin gene, rendering it non-haemolytic (Kirkham, Jefferies et al. 2006). These non-haemolytic strains are of MLST sequence type 306, whereas the normal Ply expressing strains were sequence type 227. Ply from serotypes 7 & 8 strains can have a threonine to isoleucine substitution at position 172 that reduces haemolytic activity (Kirkham, Jefferies et al. 2006). Non-haemolytic alleles are also found in some serotype 8 (sequence type 53) strains, and may be overrepresented in outbreak causing strains (Jefferies, Johnston et al. 2007). Relatively little epidemiological data about non-haemolytic Ply exists elsewhere, though isolates have been found in Australia (Lock, Zhang et al. 1996) and France (Garnier, Janapatla et al. 2006). In mouse infection models the non cytotoxic strain induced less lung oedema and leukocyte trafficking, and caused less mortality but had better survival in blood

than both wild-type and Δ*ply* strains (Harvey, Hughes et al. 2014, Harvey, Ogunniyi et al. 2011, Maus, Srivastava et al. 2004, Rijneveld, van den Dobbelsteen et al. 2002). This suggests that the non-cytolytic functions of Ply enhance survival of the bacterium in blood.

1.5.2.3 Effect on inflammation

Multiple mechanisms have been described by which Ply affects inflammation, most of which lead to enhanced inflammatory responses (figure 1.8). Purified Ply induces secretion of TNF and IL1β in human monocytes, as well as inhibiting H_2O_2 release, suggesting that it inhibits the respiratory burst (Houldsworth, Andrew et al. 1994).

TLR4

Purified Ply induces TNF and IL6 secretion from mouse macrophages that is abrogated in macrophages from MyD88 deficient mice (Malley, Henneke et al. 2003). Ethanol-killed *S. pneumoniae* induced CXCL8 secretion in HEK cells transfected with TLR4 and NFκB nuclear translocation in mouse macrophages incubated with purified Ply was TLR4 dependent. *In vivo*, mice infected with *S. pneumoniae* had improved survival when infected with *Δply* compared to wild-type bacteria, however the virulence of wild-type was reduced in mice that did not express TLR4. In addition, purified Ply coated onto ELISA plates bound to TLR4 but not TLR2 (Srivastava, Henneke et al. 2005). These data all support the hypothesis that Ply stimulates TLR4 dependent inflammatory responses. However, other data suggest Ply is not recognized directly by TLR4 *in vitro* (McNeela Burke et al. 2010) and low dose purified Ply induced mild leukocytosis in BALF as well as raised levels of TNF, CXCL2 and KC when given to mice intranasally. These effects were also seen in in TLR2 deficient mice, and, apart from reduced KC, in TLR4 deficient mice (Dessing, Hirst et al. 2009), suggesting that inflammation may be TLR4 independent. As such, the concept of TLR4 recognition of Ply remains contentious. Indirect effects of Ply on TLR4 could possibly explain these discrepancies.

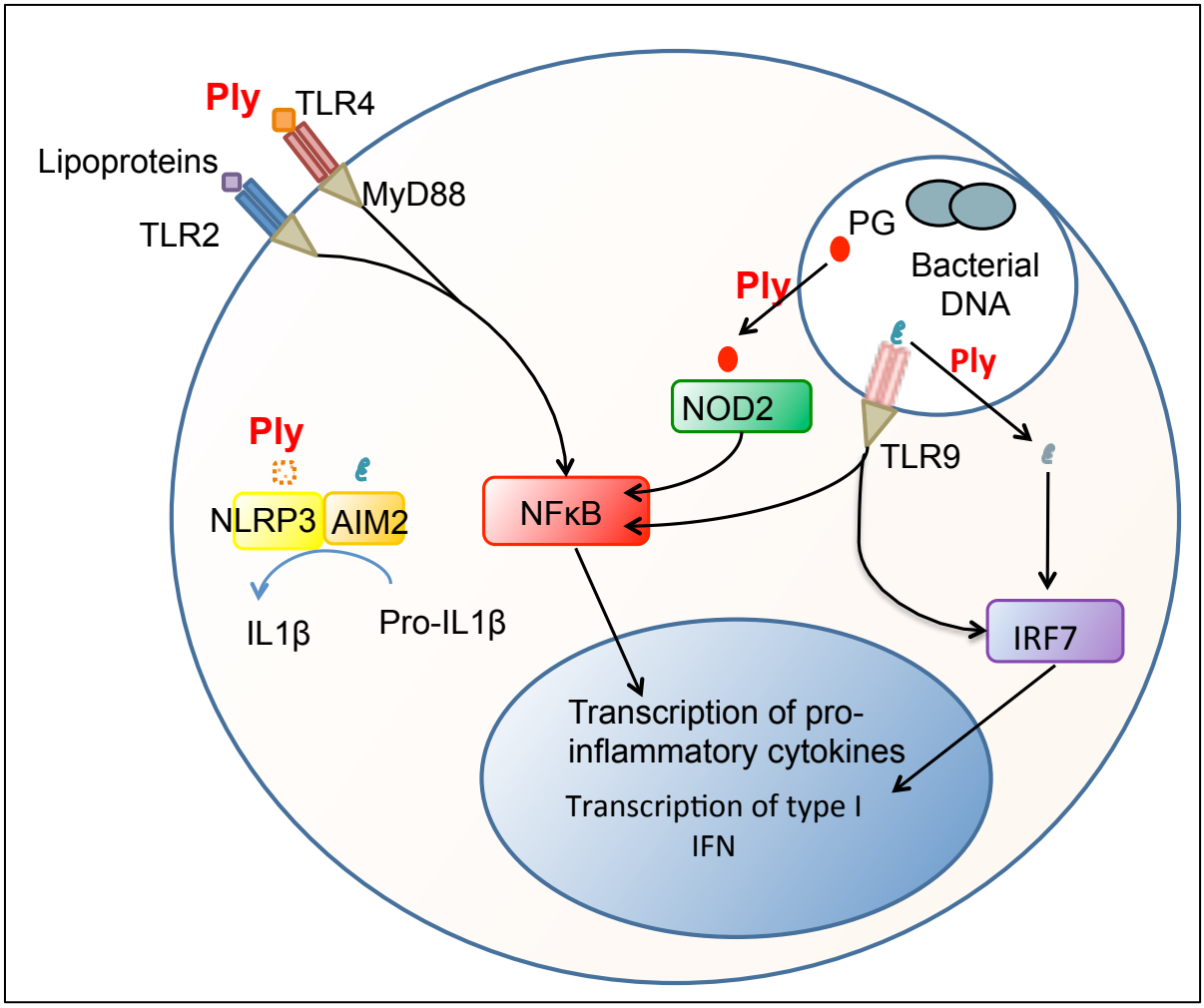

Figure 1.9 Effects of pneumolysin on inflammation

Ply is thought to activate TLR4 and so induce NFκB mediated transcription of pro-inflammatory cytokines. In addition due to its pore-forming effects, it allows the penetration of PG and bacterial DNA into the cytosol. Here PG activates NOD2 and hence pro-inflammatory cytokines. Bacterial DNA entering the cytosol by means of Ply induces IRF7 and type 1 IFN transcription. Additionally the pore forming effects of Ply are thought to lead to ion shifts that result in the activation of NLRP3, a component of the inflammasome, such that post-translational activation of IL1β occurs.

NOD2

The ability of *S. pneumoniae* to induce NOD2 activation is dependent on the pore-forming effect of pneumolysin, allowing delivery of PG fragments in the phagosome into the cytosol, resulting in chemokine release and leucocyte recruitment (Davis, Nakamura et al. 2011)

Inflammasome

Ply activates the inflammasome independently of TLR4. While purified Ply at up to 1μg/ml did not induce cytokine production from murine DC or BMDM, and caused cell death at greater concentrations, the addition of purified Ply to heat killed *S. pneumoniae* increased the secretion of IL1β, IL12, IL23, TNF, and IL6 from DCs, and IL6 and TNF from BMDM (McNeela, Burke et al. 2010), with an initial signal required to upregulate inflammasome expression before a second signal causing its activation. Caspase 1 inhibition reduced the amount of IL1β released due to Ply in combination with a TLR2 agonist, while DC from caspase 1 and NLRP3 deficient mice also exhibited reduced IL1β secretion in response to purified Ply. However non-haemolytic Ply induced less IL1β secretion that wild type Ply suggesting that the pore-forming component is critical. Inhibition of potassium efflux and phagosome rupture also inhibited IL1β secretion from DC. In mouse pneumonia, while infection with the Δ*ply* strain resulted in reduced bacterial lung counts compared to wild-type, this was less evident in NLRP3 deficient mice (McNeela, Burke et al. 2010, Witzenrath, Pache et al. 2011). NLRP3 deficient BMDM had a reduced capacity to secrete IL1β, and ASC deficient cells had complete abrogation of IL1β and 18 release in response to *S. pneumoniae.* This was recapitulated with AIM2 deficient macrophages, but not Δ*ply* mutants, suggesting that Ply plays a role in delivering bacterial DNA to AIM2 (Fang, Tsuchiya et al. 2011). Additionally fibroblast and epithelial cell secretion of TGFβ in response to *S. pneumoniae* is dependent on Ply-dependent ion fluxes and likely NLRP3 (Neill, Coward et al. 2014).

MAPK

Low doses of purified Ply induced rapid phosphorylation of p38 MAPK in A549 cells, and induced CXCL8 release, as well as TNF and IL1β transcription (Lu, Sun et al. 2014). This was

recapitulated with live wild-type *S. pneumoniae*, but not Δ*ply* strains. This effect was dependent on the pore forming ability of Ply, and not mediated by TLR2 or 4. P38 MAPK activation is inhibited by dextran, indicating that pores induce osmolar changes that are responsible for this effect (Ratner, Hippe et al. 2006).

The deubiquitinating enzyme CYLD acts as a negative regulator of the MAPK pathway (Lim, Stirling et al. 2007), and was upregulated in mouse lungs after administration of intranasal *S. pneumoniae* or purified Ply but not after infection with the Δ*ply* strain. CYLD deficient mice had reduced mortality and protein leak, as well as less bacteraemia than wild-type. NFAT is a rapidly inducible transcription factor that requires dephosphorylation to translocate to the nucleus, which then binds to the IL2 promoter as well as inflammatory cytokines. NFAT phosphorylation, mediated by p38 MAPK and calcineurin, was stimulated by *S. pneumoniae* lysate but not a lysate made with the Δ*ply* strain (Koga, Lim et al. 2008). The NFAT dependent genes COX-2 and IL6 were also upregulated in A549 by *S. pneumoniae* lysate, and this was also seen in mouse lungs after intranasal instillation. Calcium chelation, calcineurin, and p38 MAPK inhibition all reduced NFAT induction in response to bacterial lysate. Conversely NFAT activation was increased in CYLD deficient cells, dependent on its deubiquitinating function.

CCL2 was upregulated at mRNA and protein level in respiratory epithelial cell lines and mouse lungs after exposure to *S. pneumoniae* lysate. Δ*ply* mutants did not induce CCL2, whereas purified Ply did (Shin, Yoo et al. 2010). This was inhibited by a p38 MAPK inhibitor; conversely DUSP-1 inhibition increased Ply mediated p38 phosphorylation, suggesting that Ply also induces DUSP-1, which acts as a negative regulator of CCL2 release. Wild-type *S. pneumoniae* culture supernatant induced more CXCL8 from nasopharyngeal cells than Δ*ply* (Dogan, Zhang et al. 2011). Intracellular Ca^{2+} chelation reduced CXCL8 release, as did inhibition of MEK, p38 MAPK, and JNK.

These data suggest that Ply can both promote and inhibit MAPK signalling. While Ply induces NFAT-dependent pro-inflammatory cytokine production, it also upregulates CYLD, so inhibiting MAPK pathways. Similarly Ply stimulates MAPK-dependent chemokine release whilst also inducing DUSP-1.

Interferons

Mouse macrophages pre-incubated with IFNγ then with *S. pneumoniae* produced significantly more NO in response to the wild-type compared to the Δ*ply* strain (Braun, Novak et al. 1999). Purified Ply also induced NO from wild-type macrophages, but not in macrophages from mice deficient in IFNγ or IRF1. Type I IFN is released by macrophages after phagocytosis of *S. pneumoniae* and Ply dependent release of bacterial DNA or PG from the phagosome into the cytosol for recognition in a STING or NOD dependent manner respectively (Kafka, Ling et al. 2008). Mouse lungs produce more IFNβ, less IL6 and have a reduced neutrophil infiltrate in response to intranasal infection with wild-type *S. pneumoniae* compared to the Δ*ply* strain. Mouse nasopharyngeal epithelial cells also upregulate IFNβ after incubation with *S. pneumoniae*, mediated by LytA and the pore forming function of Ply. In addition, DNAse treatment, inhibition of phagocytosis, inhibition of phagolysosome acidification or inhibition of STING, TBK1, and IRF3 all inhibit IFNβ, suggesting that Ply allows delivery of bacterial DNA into the cytosol to induce IFNβ (Parker, Martin et al. 2011). *In vivo* IFNAR deficient mice produced less CCL5 in BAL in response to wild-type but not Δ*ply* suggesting that this chemokine is dependent on IFN release (Koppe, Hogner et al. 2012).

Anti-inflammatory effects

The above data largely show Ply induces an enhanced inflammatory response either directly (e.g. via TLR4 stimulation or activation of the inflammasome) or indirectly (e.g. by releasing DNA and PG from phagolysosomes into the cytosol to activate NODs and RIGs). *In vitro, S. pneumoniae* induces TNF and IL1β transcription relatively late, and there are limited data suggesting Ply has an anti-inflammatory effect instead. Ply acts via DUSP1 to act as a negative regulator of p38 MAPK and thus reduces early TNF transcription (Shin, Yoo et al.

2010). Human DC produced less IL12 and CXCL8 in the presence of Ply expressing strains than those without. Ply is also required for activation of caspase 1, 3, and 8, and subsequent apoptosis and cell death, with slightly less apoptosis in strains producing non-haemolytic Ply (Littmann, Albiger et al. 2009). Interestingly the Δ*ply* strain also induced more IL1β at both transcriptional and secreted protein levels in this model of primary human DCs. It is unclear whether this discrepancy is explained by type of cell, or the species origin, and whether this could be replicated *in vivo*.

1.5.2.4 Effect on Apoptosis

There is considerable evidence that Ply promotes host cell apoptosis. Purified Ply caused dose-dependent increase in apoptosis of RAW macrophages at 18 hours and this was inhibited by a TLR4 inhibitor. Similarly HEK TLR4 cells underwent more apoptosis in response to Ply than HEK TLR2 cells. This effect was partially inhibited by ZVAD-FMK indicating that Ply induction of apoptosis is at least partially caspase dependent. In mice infected intranasally, there was greater nasopharyngeal apoptosis with wild-type *S. pneumoniae* than the Δ*ply* strain, and again this difference was abrogated in TLR4 knockout mice. Wild-type mice pretreated with ZVAD had increased mortality, indicating that the apoptotic response is important in protection from infection (Srivastava, Henneke et al. 2005). Human MDM incubated with *S. pneumoniae* had increased iNOS expression and NO production, which resulted in mitochondrial membrane permeabilisation (Marriott, Ali et al. 2004). This NO is expressed adjacent to internalised bacteria, not in mitochondria. iNOS inhibition reduced killing of internalised bacteria, reduced MDM apoptosis, and increased necroptosis. Δ*ply* induced less mitochondrial membrane permeabilisation and apoptosis than wild-type suggesting that Ply is involved in apoptosis induction. Ply did not contribute to apoptosis if added exogenously, and *S. pneumoniae* expressing Ply must be phagocytosed in conjunction with TLR stimulation to induce programmed cell death; this occurred independently of its cytolytic and inflammasome activating functions (Bewley, Naughton et al. 2014).

1.5.2.5 Effects on antimicrobial peptides

Incubation of *S. pneumoniae*, but not the Δ*ply* strain, with A549 cells induced upregulation of HBD2 mRNA. This was dependent on p38 MAPK signalling, but Ply also induced DUSP1 that then rapidly inhibited HBD2 expression (Kim, Shin et al. 2013). The host immunity peptide BPI increased TNF release caused by *S. pneumoniae* from mouse macrophages, which caused apoptosis; this effect on TNF response to BPI was Ply dependent but TLR4 independent (Srivastava, Casey et al. 2007). These data suggest that Ply is important in inducing epithelial-derived antimicrobial peptides, which may have an impact on inflammation as well as their recognised role in bacterial killing.

1.6 Summary

In summary, generation of an inflammatory response is key in the human host response to clear *S. pneumoniae*. Alveolar macrophages are the sentinels of the lung and are crucial to the initial phagocytosis of *S. pneumoniae* and orchestration of the inflammatory response to help augment bacterial clearance. The capsule and Ply are central to the virulence of *S. pneumoniae*, though their effects on inflammation have not been fully explored.

Most data regarding the effect of capsule on the inflammatory response suggest that it has little role, particularly in comparison to cell wall lipoproteins. Ply on the other had appears to have pleiotropic pro-inflammatory effects. However, there are some data that suggests it may play a more complex role, including some anti-inflammatory effects. In both cases, the roles of the purified components have been explored fully in the past, but less so in the context of live bacteria and particularly in early infection. Further exploration of the initial host-pathogen interactions and how specific bacterial components affect inflammation may improve understanding of pathogenesis and possibly identify factors that could be used in adjunctive treatment of *S. pneumoniae* infection.

1.7 Aims

S. pneumoniae expresses several factors that are important in promoting virulence, foremost of which are the polysaccharide capsule and toxin pneumolysin. The capsule is best recognised as a mechanism for evading opsonophagocytosis, with little and conflicting data on its effects on inflammation. As it inhibits host recognition of bacterial surface molecules it would be predicted to reduce inflammatory responses to *S. pneumoniae*. Pneumolysin has pleiotropic effects on the host immune response, which previous data suggest are largely pro-inflammatory, but there are some conflicting data and the effects of pneumolysin on early macrophage responses have on the whole not been investigated.

The aim of this thesis is to address the hypothesis:

'The polysaccharide capsule inhibits and pneumolysin stimulates the macrophage inflammatory response to live *S. pneumoniae*.'

The specific aims are:

1. To compare the effects of encapsulated and unencapsulated *S. pneumoniae* on the inflammatory response of macrophages and epithelial cells, and in murine infection models.

2. To characterise the effects of pneumolysin on the inflammatory response to live *S. pneumoniae* of macrophages and epithelial cells in culture and in murine infection models.

3. To identify the mechanisms causing any capsule or pneumolysin dependent effects on the macrophage inflammatory response.

4. To assess the functional consequences of any capsule or pneumolysin dependent effects on the macrophage inflammatory response for disease development using rodent infection models.

2 Materials and Methods

Many thanks should go to others in UCL who helped with generating some of the data in this thesis. Emilie Camberlein performed some of the initial mouse experiments, Alex Dyson performed the instrumentation for the rat sepsis experiments, and Gillian Tomlinson performed some of the MDM transcription experiments. The relevant experiments are noted in the results when presented. All data was analysed by myself. General reagents were largely supplied by Sigma Aldrich (Gillingham).

2.1 Bacterial Culture and Strains

2.11Growth conditions and media

Streptococcus pneumoniae was grown in autoclaved THY medium; Todd Hewitt broth (Oxoid, Basingstoke) supplemented with 0.5% yeast extract (Sigma Aldrich, Gillingham) at 37°C in 5% CO_2 till mid log phase. This was considered to be when optical density (OD) measured at 580nm by spectrophotometer (Amersham Pharmacia, Amersham) reached 0.4-0.5. Stocks were archived in 10% glycerol at -80°C. *S. pneumoniae* strains were cultured on 5% blood Columbia agar (Sigma Aldrich, Gillingham) plates made with defibrinated horse blood (E&O Laboratories, Bonnybridge, UK). Mutant strains were streaked and grown in antibiotic supplemented media (table 2.1 – list of all strains used in thesis). For a number of experiments (involving Δ*pab* strains) bacteria were grown to an OD of 0.8 in 50ml of THY, pelleted and resuspended in smaller volumes of sterile phosphate buffered saline (PBS) (Gibco, Loughborough) with 10% glycerol to create concentrated stocks.

Stock concentrations were confirmed by defrosting glycerol stocks, centrifuging for 10 minutes at 13,000 g, and resuspending the pellet in PBS. This suspension was serially diluted and plated on blood agar and incubated overnight at 37°C in 5% CO_2.

The strains used in animal experiments (excepting the Δ*pabB*) were grown from animal passaged isolates obtained from mouse spleen homogenates after infection to ensure

virulence. All strains used in this thesis were additionally sent for whole genome sequencing at the Sanger Centre, with no significant mutations noted. Phenotype was not, however checked for each experiment. Though the encapsulated strains were visually distinct from unencapsulated strains and haemolytic function of Δ*ply* strains were checked several times during the course of my PhD.

Table 2.1 Strains used in this thesis

Strain	Serotype	Phenotype	Resistance	Source
TIGR4	4	Wild-type	Nil	
D39	2	Wild-type	Nil	
OXC-1417-23F	23F	Wild-type	Nil	
	3	Wild-type	Nil	
6A	6A	Wild-type	Nil	
14	14	Wild-type	Nil	
TIGR4Δ*cps*	4	Unencapsulated	Kan	
D39Δ*cps*	2	Unencapsulated	Kan	
3Δ*cps*	23F	Unencapsulated	Kan	
23FΔ*cps*	3	Unencapsulated	Kan	
S. mitis	NCTC		Nil	F Peterson
S. mitis Δ*cps*	12261	Unencapsulated	Kan	F Peterson
S. mitis + TIGR4cps		Express TIGR4 capsule	KanEry	F Peterson
TIGR4 + 6A	4	Express 6A capsule	Strep	J Weiser
TIGR4 + 7F	4	Express 7F capsule	Strep	J Weiser
TIGR4 + 14	4	Express 14 capsule	Strep	J Weiser
TIGR4 + 23F	4	Express 23F capsule	Strep	J Weiser
TIGR4Δ*ply*	4	Lack pneumolysin	Ery	T Mitchell
TIGR4Δ*cps*Δ*ply*	4	Lack pneumolysin and capsule	EryKan	
D39Δ*ply*	2	Lack pneumolysin	Ery	J Weiser
D39	2	Wildtype		
D39 complemented	2	Pneumolysin complemented	Strep	J Weiser
3Δ*ply*	3	Lack pneumolysin	Ery	
23FΔ*ply*	23F	Lack pneumolysin	Ery	
INV104B	1	Wild-type		
03.3038	1	Wild-type – non-lytic pneumolysin		
NCTC7465	1	Wild-type – lacks pneumolysin		
TIGR4Δ*pabB*	4	Non-replicating *in vivo*	Kan	
TIGR4Δ*pabB*Δ*cps*	4	Unencapsulated and non replicating *in vivo*	KanEry	

2.12 FAM-SE labelling

S. pneumoniae was labelled fluorescently for uptake experiments using 6-carboxyfluorescein succinimidyl ester (FAM-SE, Molecular Probes, Eugene, USA) (Yuste, Sen et al. 2008). Bacteria were grown in THY till an OD of 0.6-0.7. The bacteria were pelleted by centrifugation, then washed and resuspended in sterile filtered 0.1M $NaHCO_3$. 50µl of FAM-SE solution (10mg/ml in dimethyl sulphoxide - DMSO) was added and the resulting solution was incubated at 37°C in 5% CO_2 for 1 hour. This was then washed by centrifugation and resuspension in PBS till the supernatant was free of dye. The FAM-SE stocks were then resuspended in PBS with 10% glycerol and stored as above.

2.13 Opsonisation & IgG Binding

S. pneumoniae was opsonised in human serum or intravenous immunoglobulin by defrosting an aliquot, centrifugation, and then resuspension in diluted human serum for 30 minutes at 37°C in 5% CO_2, then centrifuging and resuspended in required media for experiment.

IgG binding to bacteria was assessed (Yuste, Sen et al. 2008) by pelleting 5×10^6 CFU of *S. pneumoniae*, resuspending in 25µl of anti-human IgG conjugated to PE (Sigma Aldrich, Gillingham) at 1:100 dilution for 20 minutes at 4°C. The bacteria were then washed twice by centrifugation and resuspension in PBS, then resuspending in 4% paraformaldehyde (PFA, Sigma Aldrich, Gillingham), and transferred to FACS tubes. Binding was assessed on the FACS Verse (Becton Dickinson, Oxford) by relative fluorescence and analysed on Flojo.

2.14 Bacterial DNA extraction (Wizard Promega kit)

A loop of bacterial stock was plated and incubated overnight at 37°C, 5% CO_2. This was inoculated into THY broth and grown till OD_{580} was 0.4-0.6. This was split into eppendorf tubes and centrifuged for 10 mins at 13000*g.* The supernatant was aspirated and the pellet resuspended in 200µl of 50mM EDTA+0.1% DOC (deoxycholic acid) (Sigma Aldrich, Gillingham). This was incubated for 10 minutes at 37°C, then 200µl of 50mM EDTA + 300µl of nuclei lysis buffer was added and incubated for a further 10 minutes at 80°C, then allowed

to cool to room temperature. 1.5µl of RNAse was added and incubated at 37°C for 40mins. Then 100µl of protein precipitation solution was added and vortex vigorously for 20s. This was then incubated on ice for 5 minutes and centrifuged at 13000*g*. The supernatant was then aspirated, added to 600µl of isopropanol in a new eppendorf, then gently mixed by inverting the tube, till thread-like DNA formed a solid mass. This was centrifuged at 13000*g* for 10 minutes. The supernatant was discarded and 750µl of 70% ethanol was added. This solution was then centrifuged at 13000*g* for 10 minutes and the supernatant discarded. The DNA was left open overnight at room temperature. Hours later, 25µl of rehydration solution was added and incubated at 1 hour for 65°C, while periodically mixing the solution by gently tapping the tube. The DNA was then stored at -20°C.

2.15 Bacterial Transformation to Create TIGR4 Δ*cps* Δ*ply*

TIGR4 Δ*ply* was grown from a fresh colony till OD_{580} 0.015 in 20ml THY pH 6.8 (the acidic nature delays entry of *S. pneumoniae* into its natural competence state). The bacteria were transferred into eppendorfs and centrifuged at 13000*g* at 4°C for 10 minutes. The supernatant was then discarded and the pellets resuspended and combined in 1ml of pre-warmed (to 37°C) filtered THY pH 8.0 supplemented with 1mM CaCl, 0.2% BSA. The bacterial suspension was split into 'positive' and 'negative' marked conical tubes and 20µl CSP 2 added, allowed to sit for 5 minutes at room temperature, then 5-10µl of TIGR4 Δ*cps* DNA was added to the positive tube (Havarstein, Coomaraswamy et al. 1995). This was incubated for 2 hours at 37°C in 5%CO_2. All of transformant was plated onto double antibiotic (Kanamycin and erythromycin) selection plates (and 200µl of control) overnight at 37°C 5% CO_2. The colonies were then grown in double antibiotic containing THY and archived as normal. Transformation was confirmed by picking colonies across single and double antibiotic impregnated agar plates. Additionally DNA was isolated and sent to the Sanger Institute in Cambridge for DNA sequencing.

2.16 Haemolysis assay

100 µl of 2% horse blood was added to U-bottomed 96 well plates, then serial dilutions of bacteria, purified pneumolysin, or 0.5% saponin (positive control) in PBS were added at 100µl volumes. The plate was incubated at 37°C 5% CO_2 for 30 minutes then centrifuged at 1000*g* for 1 minute. The supernatant was aspirated and placed in a flat-bottomed 96 well plate (Brand, Wertheim, Germany) and absorbance at 540nm was measured on a microplate reader. Absorbance reflected free haemoglobin liberated from lysed cells, with 0.5% saponin considered to be 100% haemolysis (Kirkham, Kerr et al. 2006).

2.2 Cell culture

2.21 Monocyte Derived Macrophages

MDM were used to simulate AM as obtaining sufficient numbers of human AM from healthy volunteers would pose both ethical and practical difficulties. Given the plasticity of macrophages, it was hoped that similar effects would be seen with MDM in terms of bacterial phagocytosis, transcription, and inflammatory cytokine secretion. 50 ml of healthy volunteer blood was obtained with consent into heparinised syringes along with 10 ml of blood into separation tubes. The heparinised blood was diluted 1:2 with sterile PBS, then layered onto Ficoll-Paque Plus (GE Healthcare Life Sciences, Hatfield) (20ml blood onto 15ml of Ficoll) in 50ml conical tubes. This was centrifuged at 800*g* for 20 minutes with minimal brake. The resulting Buffy coats, made up of peripheral blood mononuclear cells (PBMCs) were aspirated with a Pasteur pipette, pooled and topped up with PBS. The resulting suspension was centrifuged at 800*g* for 10 minutes with maximum brake. The resulting pellet was washed 3 times in PBS by resuspension then centrifuging at 400*g* for 5 minutes. The resulting pellet was resuspended in Roswell Park Memorial Institute (RPMI) media supplemented with 5% AB serum and 2mM L-glutamine at 1×10^7 cells/ml. This single cell suspension was added to tissue culture plates (Nunc, Roskilde, Denmark) and incubated at 37°C 5% CO_2 for 1 hour. Meanwhile, the coagulated blood in separation tubes was centrifuged at 3000*g* for 20 minutes to obtain autologous serum, which was heat inactivated by incubation at 56°C for 30 minutes. Non-adherent cells were aspirated at this time, then adherent cells were washed gently in PBS 3 times, then RPMI supplemented with 10% autologous serum, 2mM L-glutamine and 20ng/ml human macrophage colony stimulating factor (M-CSF). After 3 days the medium was removed, the cells washed again 3 times in PBS, and RPMI supplemented with 10% autologous serum and 2mM L-glutamine was added. After a further 3 days the resulting monocyte derived macrophages were ready for experiments.

This method has been long established in the Noursadeghi lab. Previous members have confirmed cell surface expression of CD14 and CD68, and lab experience is that morphological change from rounded cells to flattened enlarged adherent cells is consistent with a macrophage phenotype (Tsang, Chain et al. 2009). Further confidence was built by evidence of transcriptional signature of characteristically expressed molecules such as CXCL5.

MDM viability was assessed during culture and at end of experiments by visual inspection. Confirmatory data on cell death during incubation with bacteria was obtained using LDH assays (Cayman Chemical, Michigan). This showed significant cell death at 24 hours with Ply containing strains (figure 2.1). This cytokine suggested that data at 24 hours would not necessarily be reliable as cell death could be a confounder. Ideally this would have been confirmed across a range of bacterial concentrations, but holds true for the majority of MDM data contained within this thesis.

Experiments using MDM were approved by the joint University College London/University College Hospitals National Health Service Trust Human Research Ethics Committee (Ref: 3076/001), and written informed consent was obtained from all participants.

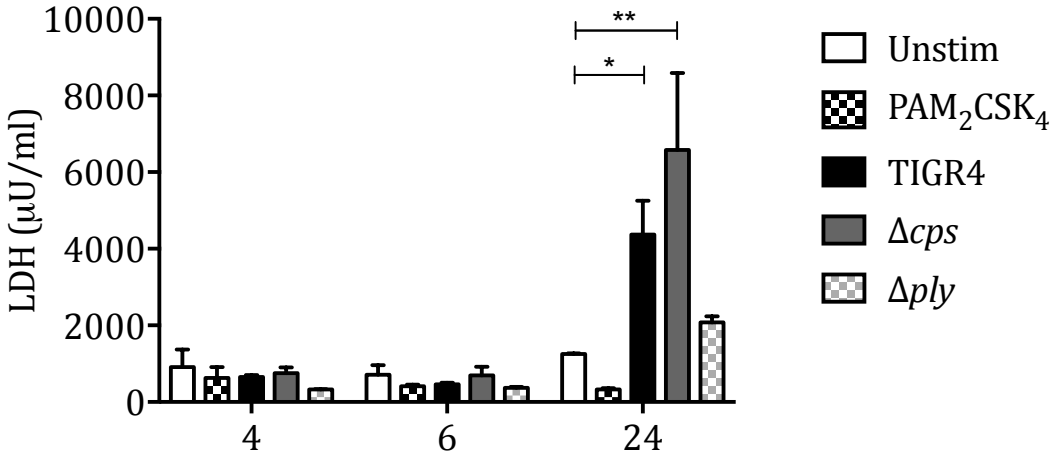

Figure 2.1 LDH assay of MDM during incubation with bacteria

Supernatants of MDM incubated with control media, positive control, or bacteria at MOI 10 taken at various timepoints were analysed for LDH content by a commercial ELISA kit. Data presented are mean +/- SEM of 4 experiments and analysed by 2 way ANOVA with Tukey's multiple comparison test.

2.22 RAW Macrophages

RAW 264.7 cells, a murine Abelson murine leukaemia virus transformed cell line with macrophage-like phenotype, were cultured in RPMI media (Gibco, Loughborough) supplemented with 10% foetal bovine serum (Lonza, Blackley, UK) and 2mM L-glutamine. They were passaged at 70-80% confluence by rinsing in sterile PBS then gentle scraping into PBS. The cell suspension was centrifuged at 400*g* for 5 minutes, then resuspended in supplemented RPMI and seeded into T175 tissue culture flasks (Nunc, Roskilde, Denmark) and incubated at 37°C at 5% CO_2. Cells were archived in RPMI with 20% foetal bovine serum (FBS) and 10% DMSO in cryovials in liquid nitrogen.

2.23 A549 Alveolar Epithelial Cells

A549 cells, a human adencarcinomic human alveolar basal epithelial cell line, were cultured in F12 media (Gibco, Loughborough) supplemented with 10% FBS and 2mM L-glutamine. They were passaged at 70-80% confluence by rinsing in sterile PBS then detaching with 0.05% Trypsin/EDTA (Gibco, Loughborough) and incubation at 37°C. Once cells were observed to be detached under an inverted light microscope, the suspension was centrifuged at 300*g* for 5 minutes, then resuspended in supplemented F12 and seeded into T175 tissue culture flasks (Nunc, Roskilde, Denmark) and incubated at 37°C at 5% CO_2. Cells were archived in F12 with 20% FBS and 10% DMSO in cryovials in liquid nitrogen.

2.24 HEK TLR2 Reporter Cells

HEK 293 cells, a human embryonic kidney cell line, stably transfected with TLR2 and CD14 (Invivogen, San Diego) were cultured in Dulbecco's Modified Eagle's Medium (DMEM) (Gibco, Loughborough) supplemented with 10% FBS and 2mM L-glutamine. They were passaged at 70-80% confluence by rinsing in sterile PBS then gentle scraping into PBS. The cell suspension was centrifuged at 300*g* for 5 minutes, then resuspended in supplemented DMEM and seeded into T175 tissue culture flasks (Nunc, Roskilde, Denmark) and incubated at 37°C

at 5% CO_2. Cells were archived in DMEM with 20% FBS and 10% DMSO in cryovials in liquid nitrogen.

2.3 Tissue Culture Assays

2.31 Antibiotic Protection Assay

MDM or RAW cells were incubated with specified bacterial concentrations for 1 hour at 37°C 5% CO_2, then supernatant was removed, plated for external CFU and replaced with PBS or PBS containing gentamicin 200μg/ml. After 1 hour the supernatant was removed and washed twice in PBS. The cells were lysed with sterile water and lysate plated for internalised bacteria (Ring, Weiser et al. 1998).

2.32 Adhesion Assay

A549 cells were incubated with specified bacterial concentrations for 2 hours at 37°C 5% CO_2, then washed twice in PBS. Cells were then lysed with sterile water and plated to establish numbers of adherent bacteria (Suri, Periselneris et al. 2016).

2.33 Phagocytosis of Fluorescent Bacteria By MDM

MDM were seeded into a 96 well optical cell carrier plate (Perkin Elmer, Wokingham) at 5×10^4 per well. FAM-SE labelled bacteria were defrosted, and resuspended in pooled human serum for 30 minutes at 37°C in the dark. They were then centrifuged again and resuspended in media at the required concentration. Medium was aspirated from the MDM and replaced with opsonised bacteria. At specified timepoints medium was aspirated, cells were washed once in PBS, then fixed in 4% PFA for 15 minutes at room temperature in the dark. The MDM were then washed 3 times in PBS. Then the wells were blocked with 10% goat serum in PBS for 30 minutes at room temperature in the dark. The blocking solution was then replaced with PE labelled goat anti human IgG (Sigma Aldrich, Gillingham) in PBS with 10% goat serum. This was incubated in the dark for 1 hour at room temperature; the cells were then washed 3 times in PBS. DAPI at 2 μg/ml in PBS was added to the wells for 5 minutes; the cells were then washed again in PBS three times and stored in 0.01% sodium azide (Sigma Aldrich, Gillingham) in PBS at 4°C in foil until imaging on HERMES microscope (Biotech-Europe, Prague, Czech Republic). Plates were imaged with ×20 objective using 3

LED sources at DAPI, GFP, and RFP settings; with nuclei in blue, fluorescent bacteria in green, and external bacteria in red (bound with serum IgG). Images were analysed on Metamorph (Metamorph Inc) software.

2.34 Phagocytosis of Fluorescent Bacteria By RAW Cells

RAW macrophages were incubated with FAM-SE labelled bacteria at specified concentrations for 1 hour at 37°C 5% CO_2. Supernatant was aspirated and replaced by PBS or 0.5% Trypan blue (Thermo Fisher Scientific, Loughborough) for 15 minutes at room temperature. The cells were then washed twice with PBS then 300µl 0.25% Trypsin-EDTA was added to each well, pipetted vigorously, and incubated at 37 °C till cells were detached (visualised under inverted microscope). The cell suspension was transferred to FACS tubes, centrifuged at 400*g* for 5 minutes, then supernatant was removed and replaced with 200µl 4% PFA, vortexed and stored under foil at 4°C till analysis (Hyams, Camberlein et al. 2010).

2.35 TLR2 reporter assay

HEK TLR2 transfected cells had a SEAP reporter gene placed under control of IFN-β minimal promoter fused to NFκB and AP-1 binding sites, such that with the addition of substrate a colorimetric change was induced to reflect TLR2 activation, as per manufacturer instructions.

HEK TLR2 cells were resuspended in HEK-Blue detection media (Invivogen, San Diego) at 5 × 10^5 cells/ml and added to 96 well tissue culture plates (Nunc, Roskilde, Denmark); 100µl per well. Then 100µl of stimulant, e.g. bacterial suspension or PAM_2CSK_4 (Invivogen, San Diego), as a positive control, was added. The cells were incubated at 37°C at 5% CO_2 for 16-24 hours and optical density was measured on a microplate reader (Versamax, Sunnyvale, USA).

2.36 Nuclear density Analysis by High Throughput Microscopy

MDM were cultured on Cell Carrier optical plates, then incubated with bacteria for specified timepoints, the supernatant was removed, then the cells were fixed in 4% PFA for 15 minutes. The cells were washed 3 times in PBS, then DAPI (2µg/ml in PBS) was added. The cells were then washed in PBS 3 times and stored in PBS 0.01% sodium azide at 4°C in foil till

imaging. The cells were imaged on the HERMES microscope with the ×10 objective. Nuclear counts, size, and density were measured with Metamorph software.

2.37 Transcription Factor Translocation Analysis by High Throughput Microscopy

MDM cultured in 96 well Cell carrier plates were incubated with bacteria or controls for the specified times. The media was aspirated, then the cells were fixed for 15 minutes in 4% PFA. The cells were then washed 3 times in PBS, then stored at 4°C in PBS + 0.01% sodium azide in foil till staining. The cells were permeabilised with 0.2% Triton-X100 (Sigma Aldrich, Gillingham) for 10 minutes at room temperature, then washed 3 times with PBS. The cells were blocked with 10% goat serum in PBS for 30 minutes at room temperature, then primary antibody diluted 1 in 100 in 10% goat serum was added to each well and incubated overnight at 4°C. The cells were then washed 3 times in PBS, then incubated with secondary antibody; goat anti-rabbit conjugated to AF488 (Invitrogen, Loughborough) for 1h at room temperature. The cells were then washed 3 times in PBS, and then incubated with DAPI (2µg/ml in PBS) for 5 minutes. The cells were washed 3 more times in PBS, then stored at 4°C in the dark in PBS + 0.01% sodium azide in foil till imaging. The cells were imaged on the HERMES microscope ×20 objective with 3 lasers (Noursadeghi, Tsang et al. 2008). Images were analysed with Metamorph nuclear translocation software.

ImageJ was used to collate and overlay images.

2.4 Enzyme-Linked Immunosorbent Assay (ELISA) for cytokines

Cytokines levels in cell culture supernatant, mouse bronchoalveolar lavage fluid, and lung homogenate supernatant were measured using ELISA as per manufacturer instructions. Coating antibody diluted in PBS was added to 96 well plates (Brand, Wertheim, Germany) and incubated at room temperature overnight. The next morning plates were washed 3 times using wash buffer: PBS with 0.05% Tween 20 (Fisher Scientific, Loughborough). The wells were then blocked with 1% BSA in PBS for 1 hour. Samples were added diluted in 1% BSA in PBS (reagent diluent) if necessary, then added to the wells in duplicate. A standard curve was also added using serial two fold dilutions, with reagent diluent as a blank. The plates were allowed to incubate at room temperature for 2 hours then washed 3 times in wash buffer. Then detection antibody diluted in reagent diluent and added, and incubated for a further 2 hours at room temperature. Plates were washed 3 times in wash buffer, then streptavidin-horseradish peroxidase (HRP) diluted in reagent buffer was added to the wells, and incubated for 30 minutes at room temperature. Plates were washed again 3 times in wash buffer then substrate, tetramethylbenzidine (TMB) (Life Technologies, Loughborough), was added. This was incubated in the dark till sufficient colour change occurred, at which point 2N H_2SO_4 was added to stop the reaction. Absorbance was measured at 450 nm and 540 nm using a microplate reader (Versamax, Sunnyvale, USA). Samples were compared to standard curve (formulated by 2 fold serial dilution in reagent diluent of a supplied standard) to obtain cytokine concentrations.

ELISAs were carried out using R&D Systems kits (Abingdon) to measure human TNF, IL1β, IL6, CXCL8, and murine TNF, IL1β, and IL6. Lower limits of detection were: hTNF 100pg/ml, hIL1β 10pg/ml, hIL6 50pg/ml, hCXCL8 200pg/ml, mTNF 100pg/ml, mIL1β 100pg/ml, mIL6 50pg/ml. These were carried out as above except as follows. In the human CXCL8 kit, blocking was carried out with 1% BSA in PBS with 0.05% NaN3, and reagent diluent was made up as 0.1% BSA in 0.05% Tween 20 in Tris buffered saline (TBS) (Sigma Aldrich,

Gillingham). In the murine IL1β kit reagent diluent was also made up as 0.1% BSA in 0.05% Tween 20 in TBS.

Rat TNF, IL1β, and IL6 were measured using Peprotech kits (lowers limits of detection were 100pg/ml). These were carried out as above, except reagent diluent was made up as 0.05% Tween 20, 0.01% BSA in PBS. Human CXCL10 was measured with an Insight Biotechnology kit, (lower limit of detection was 10pg/ml). ELISAs were carried out as above, except reagent diluent was made up as 0.05% Tween 20, 0.01% BSA in PBS. Mouse lavage albumin levels (lower limit of detection 500pg/ml) were measured with a Bethyl Laboratories kit and differed from the other ELISA protocols as follows. Coating antibody was diluted in 0.05M Carbonate-bicarbonate, pH 9.6, and once added to the plate, was incubated for 1 hour at room temperature. Washes were performed as other ELISAs. Blocking was performed as other ELISAs for an hour, then the plate was washed. Sample and standard was added, diluted in diluent buffer (1% BSA 0.05% Tween 20 in PBS), and incubated at room temperature for 1 hour. Plates were washed then detection antibody (directly conjugated to HRP) diluted in diluent buffer was added to the plates. The plate was washed again, then TMB was used as a substrate. The reaction was stopped and measured as other ELISA kits.

IFNβ was measured with a Verikine kit (PBL Assay Science, Piscataway Township, USA) using pre-coated wells in strips, lower limit of detection was 50pg/ml. Wash buffer was diluted 1 in 10 in distilled water. A standard curve was constructed by dilution to 4000pg/ml in sample diluent. Samples of standard were applied to pre-coated wells and incubated for 1 hour at room temperature. Wells were then washed 3 times in wash buffer. Detection antibody was defrosted 15 minutes before use, and dilute in dilution buffer then added to each well. Wells were then washed 3 times in wash buffer. HRP conjugated detection antibody was diluted in dilution buffer 15 minutes prior to use, and added to each well, and incubated for 1 hour. Wells were washed 3 times in wash buffer. Then TMB was added to each well and incubated in the dark at room temperature for 15 minutes. Stop solution was added, and the plate read at 450nm on a microplate reader.

2.5 Quantitative polymerase chain reaction (qPCR)

RNA extraction of MDM was performed with Quiagen RNeasy Mini kit (Quiagen, Hilden, Germany) as per manufacturer instructions. MDM were cultured at 4 ×10^5 cells per well in a 12 well plate and incubated with bacteria or media. At specified timepoint supernatant was aspirated, and cells washed twice with ice-cold PBS. 350µl of RLT buffer (supplemented with 1% 14.3 M β mercaptoethanol) was added to each well in an ice bucket. MDM were scraped, pipette mixed, and lysate was aspirated and stored at -80°C.

Lysate was defrosted on ice and vortex mixed, then 350µl of 70% ethanol was added. The sample was then transferred to a spin column in a collecting tube and centrifuged at 8000*g* for 30s at 4°C. The flow through was discarded and 700µl of RW1 buffer and centrifuged at 8000*g* for 30s at 4°C. 500 ml RPE buffer (with ethanol) was added to the column, and centrifuged at 8000*g* for 30s at 4°C. This was repeated once but centrifuged for 2 minutes. The spin column was placed in a new collection tube and 30µl of RNAse free water added to the column and centrifuged at 8000*g* for 1 minute. The resulting RNA was stored at -80°C.

Contaminating DNA was eliminated with Precision DNase (Primer Design, Southampton) by adding 1.5µl buffer to 0.5µl nuclease free water, and 0.5µl DNAse to 12.5µl RNA. This was placed in a PCR machine at 30°C for 10 minutes then 55°C for 5 minutes. Nanodrop 3000 was used to measure RNA concentration and quality established using ratio of absorbance at 260:280 (aiming for 2.0).

cDNA was synthesised in clear PCR plates (Thermoscientific, Loughborough) on ice. 4µl of 5× qScript cDNA SuperMix (QuantaBiosciences, Beverley, USA) was added to 1µg RNA and made up to 20µl with nuclease free water. A sealplate (Thermo Scientific, Loughborough) was used to seal the plate, which was then vortexed for 1 minute at 1000rpm, then centrifuged 1000*g* for 1 minute. This was placed in a PCR machine (Tetrad, Ramsey, USA) for 5 minutes at 25°C, then 30 minutes at 42°C, then 5 minutes at 85°C. The product was diluted by adding 40µl nuclease free water then stored at 4°C till qPCR.

TaqMan gene expression assays were thawed on ice, vortexed and pulse centrifuge. The Universal master mix II (Life Technologies, Loughborough) was warmed to room temperature. A master mix was made with enough volume for required samples in duplicate: 5.0µl of 2× TaqMan Universal Master Mix II, 0.5 µl of specified 20× Taqman Gene Expression Assay and 2.5µl of nuclease free water. 8µl of mastermix and 2µl of cDNA was then added per well in white PCR plates (Thermoscientific, Loughborough), then sealed with optical film, vortexed at 1000rpm for 1 min, then centrifuged at 1000*g* for 1 minute. The qPCR was run on a Realplex Mastercycler (Eppendorf, Stevenage) and run for 2 minutes at 50°C, then for 10 min at 95°C, followed by 40 cycles of 15 seconds at 95°C, then 1 minute at 60°C. Cycle threshold (CT) was determined for all samples and analysed by ΔΔCT for relative expression values, with GAPDH as a housekeeping gene (Tomlinson, Cashmore et al. 2010).

2.6 Western Blotting

2.61 DC Assay (Biorad)

This assay was used to determine protein concentrations in lysates as per manufacturer instructions. If detergent was in the lysate (e.g. after nuclear extraction), 20µl of reagent S was added to 1 ml of reagent A. A standard curve was made by making twofold serial dilutions of bovine serum albumin (Alpha diagnostics) in PBS, with a top concentration of 2µg/ml. 5µl of lysate or standard curve was added in duplicate to a microtitre plate. Then 25µl of reagent A solution (i.e. with or without reagent S) was added to each well, followed by 200µl of reagent B. This was mixed for 5 seconds then incubated for 15 minutes at room temperature. OD was measure on a microplate reader.

2.62 Western Blot

MDM at 4×10^6 cells per well in 12 well plates were incubated with bacteria for the required time then washed twice in ice cold PBS in an ice bucket and lysed in RIPA buffer (Sigma Aldrich, Gillingham) supplemented with 100× phosphatase inhibitor (Thermo Scientific) and

100× phosphatase inhibitor (Thermo Scientific, Loughborough). The lysate was stored at -80°C till required.

Lysate concentration was equalised in RIPA buffer. Then 2.5µl of 4× sample buffer (Thermo Scientific, Loughborough) and 1µl of 10× reducing buffer (Thermo Scientific, Loughborough) was added to the lysates. Deionised water was added to make the final volume 20µl. Samples were then heated to 70 °C for 10 minutes. 50ml of NuPage 20× MES buffer (Thermo Scientific, Loughborough) was added to 950ml deionised water to make running buffer. The combs were removed from a NuPage BisTris mini gel (Thermo Scientific, Loughborough) and the wells were rinsed with running buffer. The gel was placed in the tank, clamped in place, then running buffer was added. PageRuler Plus Protein ladder (Thermo Scientific, Loughborough) and samples were loaded into the wells. Electrophoresis of the gel was run at 200V for 30-60 minutes. Once the gel had run, the gel was extracted from its cassette then an iBlot gel transfer device (Thermo Scientific, Loughborough) was used to transfer separated proteins to a membrane.

Membranes were blocked in 5% BSA in 0.1% Tween20 in TBS for one hour at room temperature on a rocker. Then primary antibody was added in 5% TBST in a conical tube and placed on a roller at 4°C overnight. The membrane was then washed 3 times in TBST for 10 minutes on a rocker. Then secondary antibody (conjugated to HRP) was added to 5% BSA in TBST in a new conical tube and placed on a roller at room temperature for 1 hour. The membrane was then washed 3 times again in TBST. 1 ml of Luminata Crescendo Western HRP substrate (Merck, Readington, USA) was added to the membrane, incubated at room temperature for a minute, then excess substrate was drained off. The blot was imaged and analysed on an Imagequant (GE Healthcare, Hatfield). All steps performed as per manufacturer instructions.

2.63 Phosphoarray (R&D Systems, Abingdon)

MDM were cultured in 6 well plates at 1×10^6 cells per well. Bacteria were added at specified concentrations, and incubated at 37°C in 5% CO_2. After half an hour the cells were placed on ice, rinsed with PBS, then Lysis Buffer 6 was added. This was incubated at 4 degrees on a rocking platform for 30 minutes. The samples were then placed in eppendorfs and centrifuged at 14000*g* for 5 minutes, and the supernatants stored at -80 till required.

Array buffer 5 was placed in a 4 well multi dish, and one nitrocellulose membrane printed with capture antibodies placed in each well. This was incubated for an hour at room temperature on a rocking platform. Meanwhile samples were diluted in array buffer 1 so that all samples were at equivalent concentrations. Detection antibody cocktail was added to each sample and incubated at room temperature for 1 hour. The array buffer was then removed from the membranes and replaced with the sample antibody mixture. This was incubated overnight at 4°C on a rocking platform. The membranes were then removed to individual containers and washed 3 times in washing buffer, 10 minutes at a time. Streptavidin-HRP was diluted in array buffer 5 and placed in the 4 well multidish. The membranes were placed back in the wells and incubated on a rocking platform for 3 minutes. The membranes were then washed again 3 times in wash buffer. After excess wash buffer was removed from the membranes, chemi-reagent mix was added to each membrane, then the membranes were placed in an autoradiography cassette till imaging on hyperfilm (GE Healthcare, Hatfield) by exposure to an autoradiography film developer (Kodak, UK). All steps carried out as per manufacturer instructions.

2.7 Transcription Factor Array

The Protein/DNA array (Panomics, Fremont, USA) allows examination of multiple transcription factors' function. Biotin labelled DNA binding oligonucleotides were incubated with nuclear extract, to bind to transcription factors bound to DNA. The bound probes were separated by columns, then eluted and incubated with an oligonucleotide spotted membrane. Chemiluminescence was used to identify bound transcription factors.

2.71 Nuclear Extraction

Nuclear extraction of MDM was performed with a Panomics kit as per manufacturer instructions. MDM in a 6 well plate had media aspirated, and were washed twice with ice-cold PBS. 250µl Reagent A (750µl buffer A, 7.5µl phosphatase inhibitor I, 7.5µl phosphatase inhibitor II, 7.5µl protease inhibitor, and 7.5µl DTT) added per well. The plate was placed on an ice bucket and transferred to a rocker at 200rpm. Cells were scraped and lysate transferred to eppendorfs and centrifuged at 14,000*g* for 5 minutes at 4°C. The superntatants were discarded and 50µl of reagent B was added to each pellet, while on ice. This was vortexed and incubated on ice for 1 hour, with intermittent agitation by hand. The nuclear extract was centrifuged again at 14,000*g* for 5 minutes at 4°C. The pellets were stored at -80°C till required.

2.72 Protein/DNA Array

Nuclear extracts and DNA binding oligonucleotides (probe mix) were thawed on ice. Meanwhile array membranes were incubated in pre-treatment buffers at 45°C then hybridisation buffer at 42°C in hybridisation bottles. 10µl of nuclear extract (concentration of different donors and conditions equalised in distilled water) was added to 10µl of TransSignal probe mix and incubated at 15°C for 30 minutes. The spin columns were washed in incubation buffer, then the transcription factor probe mix was added to the spin column and incubated on ice for 30 minutes. The spin column was then centrifuged at 6000*g* for 30 seconds at 4°C, the flow through discarded and the column was then washed through 3 times

with column wash buffer. Then 60µl of column elution buffer was added and incubated at room temperature for 5 minutes. The spin column was then centrifuged at 8500*g* for 1 minute at room temperature, and the eluate was collected on ice. The eluate was then heated to 95°C for 3 minutes then chilled on ice for 2 minutes. The eluate was then added to the hybridisation bottles and incubated overnight in a rotating hybridisation oven at 42°C overnight. The membranes were then washed in hybridisation wash I and II, then removed to a container holding blocking buffer for 15 minutes with gentle agitation. Then Strepavidin-HRP was added to the container and incubated under gentle agitation at room temperature for 15 minutes. The membranes were then washed in wash buffer 3 times and then 20ml of detection buffer was added and allowed to incubate for 5 minutes at room temperature. The substrate solution was then added to the membrane for 5 minutes, excess solution removed, then the membrane was imaged on an Imagequant (GE Healthcare, Hatfield). All steps were carried out as per manufacturer instructions.

2.8 Microarray genome wide transcriptional assessment

Microarray (Agilent, Santa Clara, USA) analysis was used to perform whole genome transcriptional analysis of MDM incubated with bacteria for specified timepoints at 1×10^6 cells per well in 6 well plates. RNA was extracted as above and purity was established on a bioanalyser with an Agilent RNA 6000 kit.

2.81 Bioanalyser (Agilent 2100)

Nano dye concentrate was allowed to equilibrate to room temperature and 1µl was added to 65µl filtered gel matrix, vortexed, then centrifuged at 13,000*g* for 10 minutes. Nanochips were placed in a chip priming station and 9 µl gel/dye mix added to specified wells, then the chip is primed with a plunger. 9µl gel/dye mix was added to the remaining control wells. 5 µl of marker was added to each well, 1µl of sample was added to sample wells, and 1µl of ladder to the ladder well. The chip was then vortexed in an IKA vortexer for 1 minute at 2400rpm. The bioanalyser was cleaned with RNAzap then RNAse free water, and then the chip was run and analysed with 2100 Expert software.

2.82 Microarray Labelling & Scanning

Low input quick amp labelling kit was used for two colour microarray based gene analysis. Spike A (Cy3) and spike B (Cy5) mix was diluted in dilution buffer for the appropriate RNA mass. RNA was diluted to the required concentration with RNA free water. 2µl spike A mix was added to half the samples and 2µl spike B mix to the other half. T7 promoter primer master mix was diluted in nuclease free water and 1.8µl added to each sample. This was placed in a PCR machine and heated at 65°C for 10 minutes, then cooled to 4°C for 5 minutes. Meanwhile strand buffer was warmed to 80°C for a few minutes to adequately resuspend, and make cDNA mastermix (2µl 5× strand buffer, 1µl 0.1M DTT, 0.5µl dNTP, and 1µl Affinity script RNAseblock mix). 4.7µl of the cDNA mastermix was added to each sample and then it was placed in a PCR machine, then it was heated to 40°C for 2hours, then 70 °C for 15 minutes, then cooled to 4°C for 5 minutes, then stored at -80°C.

A transcription master mix was prepared (0.75µl nuclease free water, 3.2µl 5× transcription buffer, 0.6µl 0.1M DTT, 1µl NTP mix, 0.21µl T7 RNA polymerase blend, and 0.24µl Cyanine 3-CTP or 0.24µl Cyanine 5-CTP for 'A ' or 'B' samples respectively). 6µl of transcription mastermix was added to each sample and pipette mixed. This was heated to 40 °C for 2 hours in a PCR machine, then cooled to 4°C (or stored at -80°C).

The RNA was then purified with a Quiagen kit (Hilden, Germany). 84µl nuclease-free water was added to each sample and pipette mixed with 350µl RLT buffer. Then 250µl 100% ethanol was added with further pipette mixing. This was transferred to an RNeasy spin column, centrifuged at 10,000*g* for 30 seconds at 4°C. The flow through was discarded then 500µl RPE (with ethanol) added, then centrifuged again, and repeated. The spin column was placed in a new tube and 30µl RNAse free water was added. After 30 seconds the spin column was then centrifuged at 10,000*g* for 30 seconds at 4°C. The eluate RNA was measured on a nanodrop; RNA concentration and Cy3 or Cy5 concentration was determined.

Next 300ng Cy3 labelled RNA was added to 300ng Cy5 labelled (paired sample) RNA, 5µl 10× blocking agent, 1µl 25× fragmentation mix, and made up to 25µl with nuclease free water. This was vortexed gently then heated to 60 °C for 30 minutes, then cooled immediately in ice for 1 minute. 25µl of 2× GE hybridisation buffer HI-RPM was added to each sample then pipette mixed gently, then centrifuged at 10,000*g* for 1 minute and placed on ice.

A gasket slide was loaded onto an Agilent SureHyb chamber base and 40µl of hybridisation sample was dispensed and gently dragged down the slide. An array slide was then placed face down, and then a chamber cover was clamped to the sandwiched slide. This was then placed in a rotisserie hybridisation oven for 17 hours at 65 °C 10rpm. The gasket slide was placed in a slide rack and washed in Gene expression wash buffer I, then the array separated from the gasket slide while submerged. The array slide was then placed in fresh Gene expression wash buffer I and washed, then placed in a third staining dish containing pre-warmed Gene expression wash buffer II. This was washed again then transferred in a holder

to an Agilent Microarray Scanner. All steps were carried out as per manufacturer instructions.

2.83 Multi Experiment Viewer

Data from the microarray was normalised (Chain, Bowen et al. 2009) and analysed using multi experiment viewer (Sourceforge) and Bioagilent insert for R (R-project). Bioinformatic analysis was using the online analysis tools Innate DB (Breuer, Foroushani et al. 2013) and OPOSSUM (Kwon, Arenillas et al. 2009).

2.9 *In vivo* models

Murine work was carried out within Home Office guidelines under project license PPL70/7361. The rat sepsis model was carried out under project license PPL70/7028.

2.91 Mouse pneumonia

S. pneumoniae stocks were defrosted, centrifuged, and resuspended in sterile PBS. Concentration was adjusted (1×10^7 or 1×10^8 CFU/ml). Female CD1 5 week old mice were anaesthetised with inhaled isoflurane, and then 50µl of bacterial suspension was administered via one nostril. Bacterial inoculum was then plated to ensure consistency. In specific experiments, antibodies or inhibitors were administered intranasally under isoflurane anaesthesia or intraperitoneally. At specified timepoints the mice were euthanised with intraperitoneal pentobarbital, and death was confirmed by severing the inferior vena cave. Blood was obtained for bacterial counts at this time into heparinised tubes. Cannulation of the trachea was then performed, and the bronchial tree was flushed with 3 times with 1ml of PBS to obtain bronchoalveolar lavage fluid (BALF). Lastly lungs were dissected out carefully. The lungs were homogenised using cell strainers (Falcon, Corning, USA) and the homogenate was diluted in 3ml PBS. Blood, BALF and lung homogenate was plated at serial dilution to obtain bacterial counts if required. BALF was centrifuged at 300*g*, the supernatant was stored for further analysis, and the cell pellet resuspended in PBS. The cell suspension was counted using a haemocytometer to obtain BALF cell counts, and 200µl was centrifuged onto slides using a cytospin (700rpm for 7 minutes), then stained with Romanowsky's solutions to examine under a light microscope for cell morphology. Lung homogenate was centrifuged at 600*g*, supernatant was stored for analysis and bacterial counts. Blood was allowed to clot, then centrifuged at 2000*g* for 20 mins; the resulting serum supernatant was stored for downstream analysis. As seen in figure 6.20 to 6.22, intranasal PBS does not induce an inflammatory response in mice.

2.92 Alveolar Macrophage Association with Fluorescent Bacteria

CD1 mice were infected intranasally with $5*10^6$ CFU FAM-SE labelled bacteria and culled at 4 hours, then bronchoalveolar lavage fluid was recovered (in PBS) and placed on ice. The lavage fluid was centrifuged at 700*g* for 5 minutes and resuspended in 100µl of 1% FBS in PBS with 1 in 10 rat anti F4/80 conjugated to APC (Biolegend, San Diego). They were incubated in the dark in FACS tubes for 30 minutes at room temperature, then washed twice in 1% FBS in PBS (by centrifuging at 700*g* for 5 minutes, decanting the supernatant, then resuspending in 1% FBS). They were then fixed in 200µl 4% PFA for 15 minutes at room temperature (in the dark). The cells were then washed twice in 1% FBS in PBS and left in 200µl 1% FBS in the fridge till FACS analysis.

2.93 Rat sepsis

Male Wistar rats had PVC tubes inserted into the right jugular vein and left carotid artery and tunnelled subcutaneously to emerge at the nape of the neck under 2% isoflurane anaesthesia. These were mounted on a swivel-tether system so that the rats had unimpeded movement. After 24 hours, 1×10^9 CFU non-replicating TIGR4Δ*pab* were injected via the tunnelled lines over 10 minutes. Fluid resuscitation was carried out with 1:1 0.9% NaCl and 6% glucose at 10 ml/kg/hr. Blood pressure and heart rate were continually measured using the arterial line (Brealey, Karyampudi et al. 2003).

Blood was withdrawn into capillary tubes from the tunnelled lines at baseline, 1 and 4 hours, where the lines remained patent. When lines were not patent 4 hour blood was taken via terminal cardiac puncture. Blood gas measurements were obtained using an ABL800 FLEX (Radiometer, Crawley). Blood was also plated for CFU, allowed to clot and centrifuged at 4000*g* for 20 minutes to obtain serum. Serum was frozen at -20°C until cytokine analysis.

2.10 Statistics

Statistical analyses of data were performed with Graphpad Prism V 7 (La Jolla, USA). Data in this thesis are largely presented as means +/- SEM (e.g. cytokines, qPCR, cell counts). When two groups were compared an unpaired t-test was used. When several groups were compared, a one way analysis of variance (ANOVA) with Tukey's multiple comparison test was used. When several pairs of grouped data were compared, a two way ANOVA with Tukey's multiple comparison test was used.

Non-parametric data (e.g. CFU data) are presented as individual data points and median values. Two groups were compared with a Mann Whitney U test. Multiple groups were analysed with a Kruskal-Wallis test, with Dunn's multiple comparison test.

Significance is denoted as follows:

*=$p<0.05$

**=$p<0.01$

***=$p<0.001$

****=$p<0.0001$

3 Effect of capsule on the inflammatory response to *S. pneumoniae*

S. pneumoniae capsule has an important role in reducing antibody and complement binding and so inhibits phagocytosis (Hyams, Camberlein et al. 2010). As the capsule inhibits engagement with the host, it should also inhibit interaction with PRR. Hence I investigated the hypothesis that the capsule would reduce the inflammatory response of the host to *S. pneumoniae*.

To explore this, wild-type and isogenic unencapsulated mutants were used, allowing investigation of the effect of capsule with live bacteria. A serotype 4 strain, TIGR4 was used in the majority of experiments, along with an unencapsulated strain, Δ*cps*, with an antibiotic resistance cassette inserted in place of the capsule locus. Macrophages are the sentinel cells of the immune system so in prime position to initiate inflammatory responses, so primary human monocyte derived macrophages (MDM) from volunteers were the primary cell type used to investigate the inflammatory response to *S. pneumoniae*.

3.1 Effects of capsule on inflammatory response of macrophages

To assess the inflammatory response, supernatant levels of the pro-inflammatory cytokines TNF, IL1β, and IL6 were measured in primary human MDM cultures after incubation with TIGR4 or TIGR4Δ*cps* at different timepoints (figure 3.1) and varying concentrations of bacteria (figure 3.2). Unstimulated MDM levels of TNF, IL1β, and IL6 were undetectable. There was a trend towards increased pro-inflammatory cytokine release during the timecourse, most evident across the analysed cytokines at 6 and 12 hours. Others have shown that there is large scale MDM cell death after 16 hours (Dockrell, Marriott et al. 2003), and indeed LDH data (figure 2.1) suggested significant cell death at 24 hours in my datasets, so earlier timepoints were used to reflect the initial inflammatory response to *S. pneumoniae*. At 6 hours wild-type bacteria induced higher inflammatory cytokine levels than unencapsulated at all multiples of infection (MOI) for TNF, and at low MOIs for IL6. There was little difference in IL1β levels, though these were possibly too low to interpret effectively. Interestingly IL1β and IL6 release gradually decreased with more bacteria, possibly reflecting cell death with higher concentrations of bacteria. qPCR results at 4 hours replicated this pattern (figure 3.3), indicating that the differences between bacterial strains in inflammatory response are likely to be transcriptionally regulated.

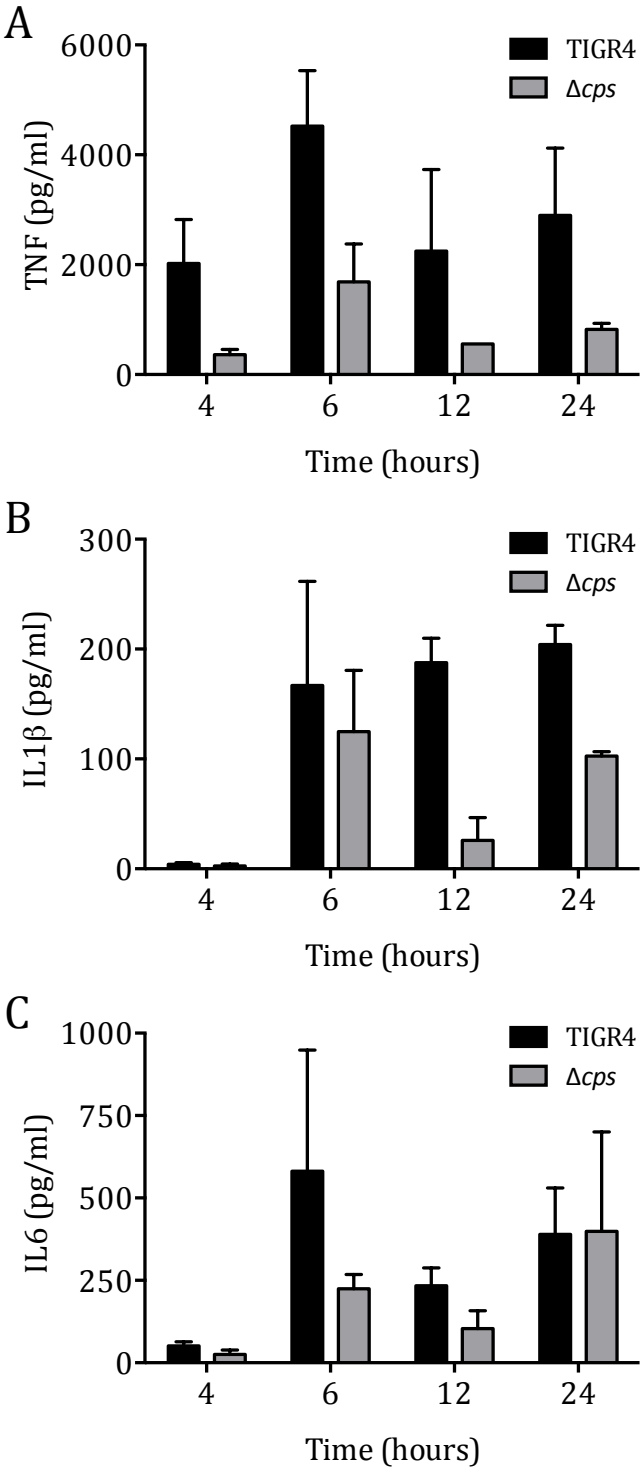

Figure 3.1 Timecourse of cytokine response of MDM to TIGR4 and unencapsulated mutant

MDM were incubated with TIGR4 or TIGR4Δ*cps* in tissue culture plates, with 10 bacteria per cell (multiples of infection - MOI 10). Supernatant was aspirated at 6 hours and later analysed for A) TNF, B) IL1β, and C) IL6. The data from 3 different donors are analysed by 2 way ANOVA and Tukey's multiple comparison test, with no significant differences seen.

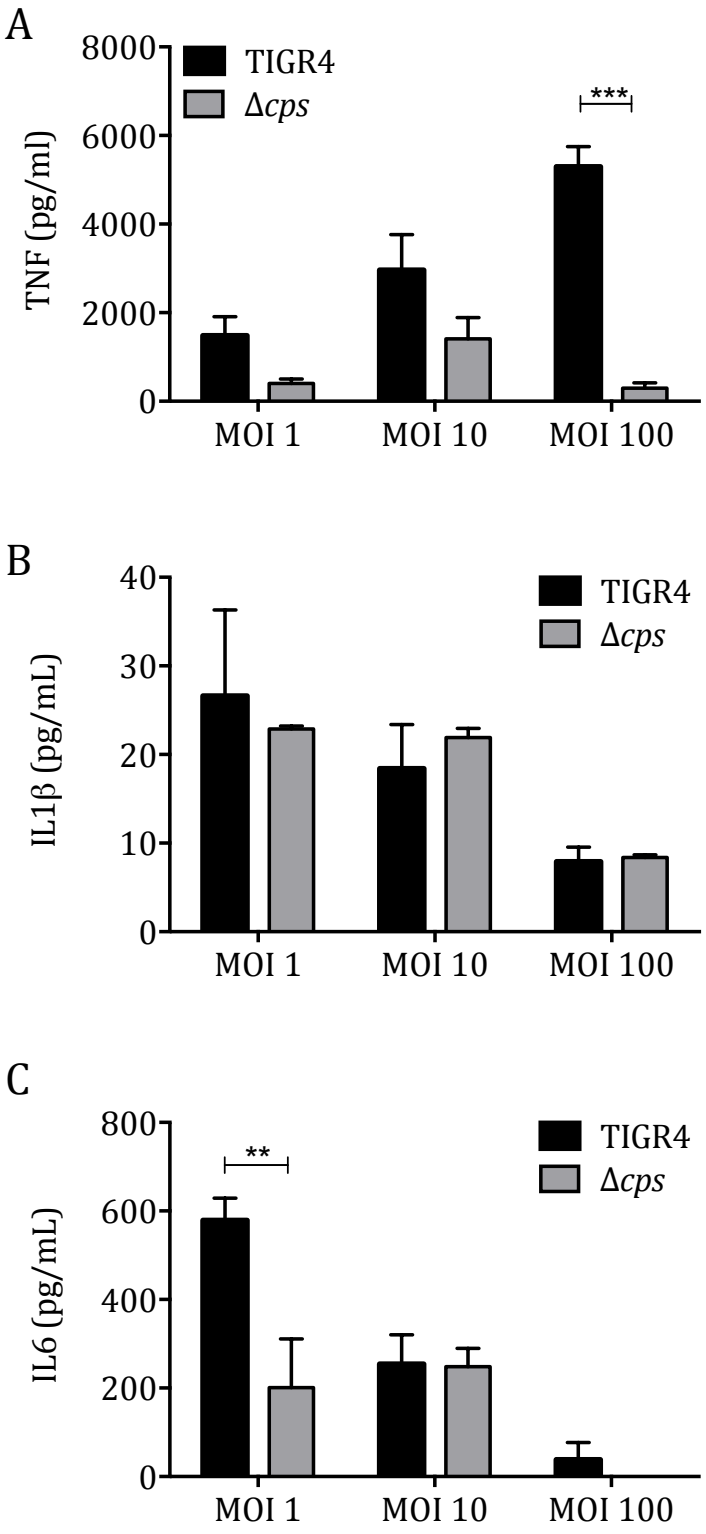

Figure 3.2 MDM cytokine responses to varying numbers of bacteria

MDM were incubated with TIGR4 or Δ*cps* at varying concentrations; from MOI 1 to 100. After 6 hours, supernatant was removed, and later analysed for A) TNF, B) IL1β, and C) IL6. The data obtained are from 3 different donors, and analysed by 2 way ANOVA and Tukey's multiple comparison test.

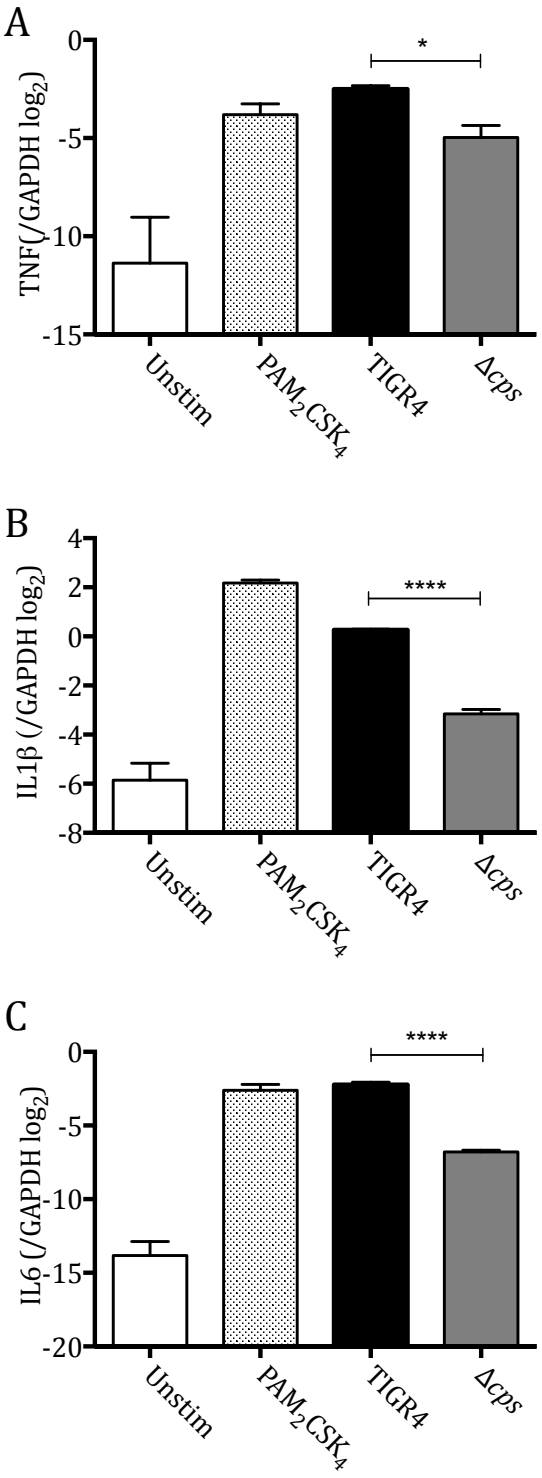

Figure 3.3 MDM qPCR response to TIGR4 and unencapsulated mutant

Pro-inflammatory cytokine (A) TNF, B) IL1β, and C) IL6 transcriptional response of MDM after 4 hours incubation with TIGR4 or Δ*cps* at MOI 10 as measured by Taqman qPCR of cell lysate. Results from 3 donors presented as change in cycle threshold with GAPDH as a housekeeping gene, and analysed by 1 way ANOVA and Tukey's multiple comparison test.

3.2 Effects of capsule on inflammatory response of epithelial cells

Alveolar epithelial cells are another important cell type that might recognise *S. pneumoniae* and induce an inflammatory response in the context of pneumonia. Owing to the difficulty of obtaining primary alveolar epithelial cells, a transformed cell line was used (A549s). The capsule inhibited adhesion of *S. pneumoniae* to an epithelial cell layer (figure 3.4), which is a potential confounder of epithelial inflammatory responses. No internalisation was detected by antibiotic protection assay (data not shown). A 1 hour timepoint was used as per previously established assay in the Brown lab (Suri, Periselneris et al. 2015).

Direct incubation of bacteria with A549s for up to 24 hours induced minimal inflammatory responses compared to unstimulated cells (figure 3.5). Again, by 24 hours, there may well have been some significant cell death, that could have confounded the data. At higher MOIs, there was a suggestion of some cytokine response to bacteria, but much less than that of MDM (figure 3.6). However, MDM conditioned media induced significant IL6 and CXCL8 release, and detectable TNF (figure 3.7), with no detectable IL1β (data not shown). The cytokine response here reflected that of MDM, i.e. more TNF and IL6 (and trend toward more CXCL8) with TIGR4 compared to Δ*cps*. Although this may reflect the cytokines initially produced by the MDM, the levels of TNF for example are significantly less than that produced by MDM (possibly due to either uptake of TNF by TNF receptors or TNF decay in media) with less of a difference in IL6, suggesting downstream effects of the secreted products of MDM.

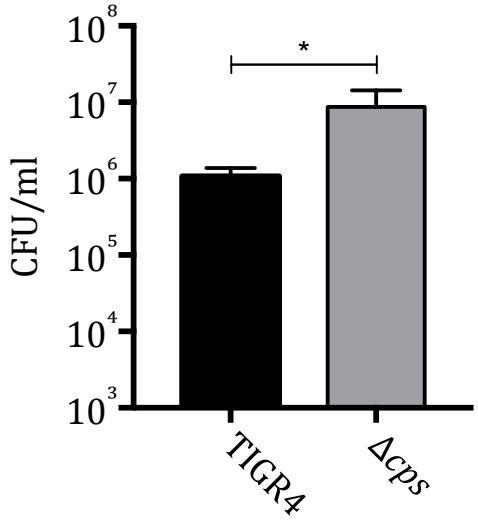

Figure 3.4 Adhesion of bacteria to A549 cells

The number of TIGR4 and Δ*cps* adhering to an A549 cell layer after 1 hour is shown. A representative experiment of 3 is shown, presented as median +/- range, and analysed by Mann-Whitney U test.

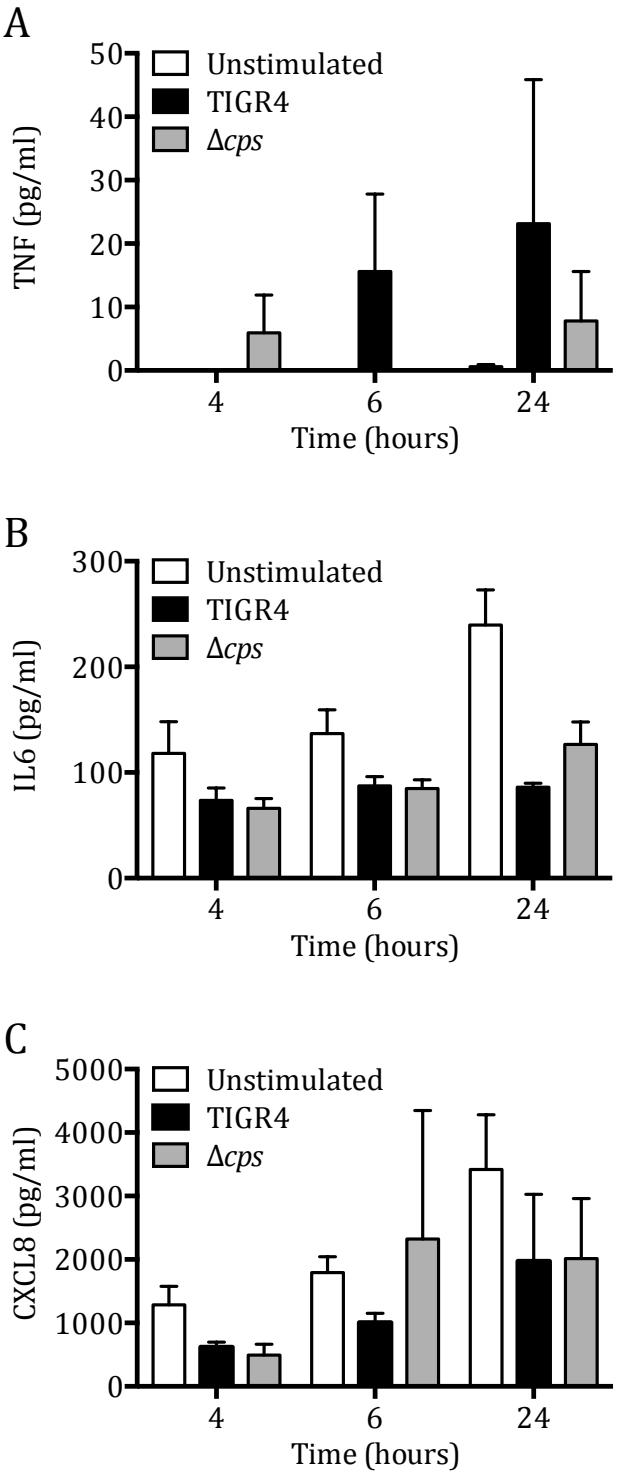

Figure 3.5 Timecourse of cytokine release by A549 alveolar epithelial cells incubated with bacteria

Mean +/- SEM of 3 experiments at MOI 1, at various timepoints supernatant was analysed for cytokine secretion. Panel A shows TNF, B shows IL6, and C shows CXCL8 (IL1β was undetectable). Data were analysed by 2 way ANOVA and Tukey's multiple comparison test, with no significant differences seen.

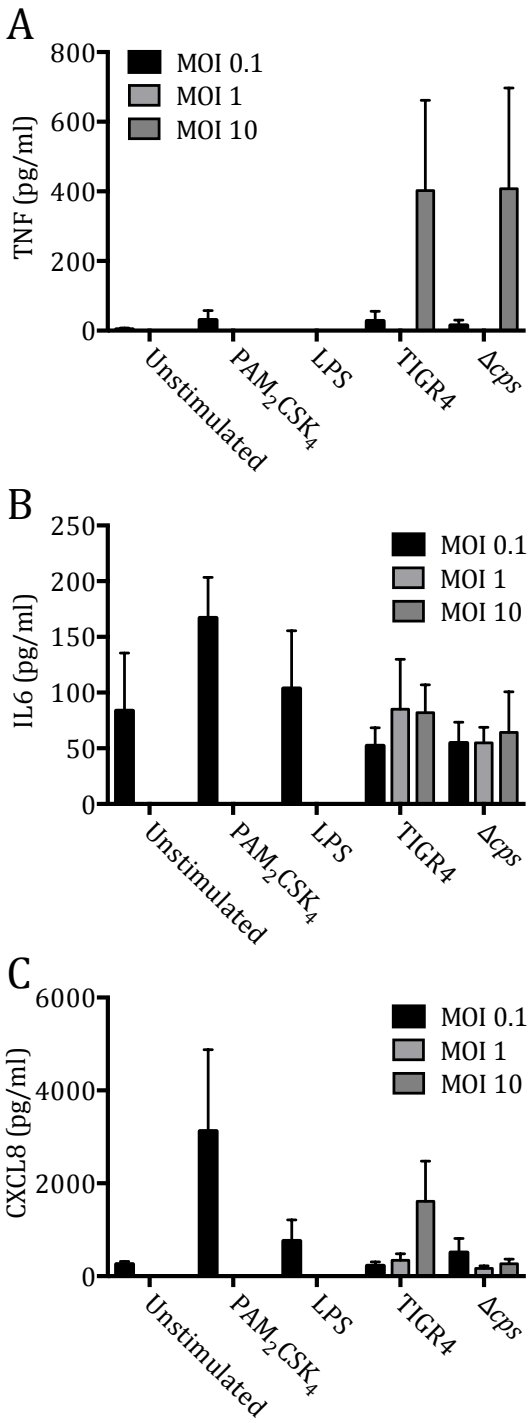

Figure 3.6 Cytokine release by A549 cells in response to different numbers of bacteria

A549 cells were incubated with positive controls and varying multiple infections of TIGR4 or Δ*cps.* Supernatant was analysed for cytokines after 6 hours. Mean +/- SEM of 3 experiments shown. Panel A shows TNF, B shows IL6, and C shows CXCL8. Data were analysed by 2 way ANOVA and Tukey's multiple comparison test, with no significant differences seen.

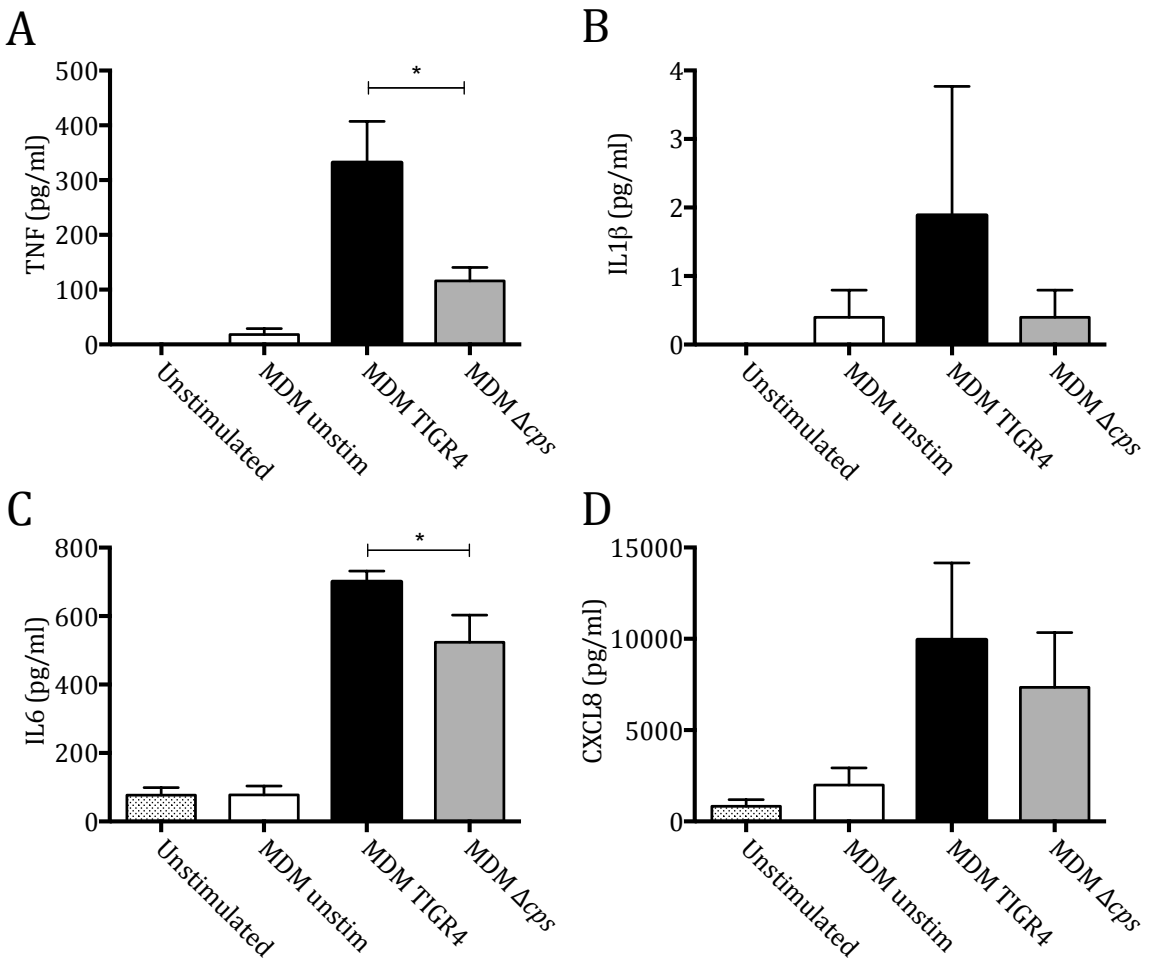

Figure 3.7 Cytokine release by A549 cells in response to conditioned media from MDM
A549 cells were incubated with pooled conditioned media from MDM incubated TIGR4 or Δ*cps* (4 separate experiments were pooled) at MOI 10. The conditioned media was diluted 1 in 5 in media before adding to A549 cells. Supernatant was analysed for cytokines after 6 hours. Mean +/- SEM of 3 experiments shown. Panel A shows TNF, B shows IL1β, C shows IL6, and D shows CXCL8. Data were analysed by 1 way ANOVA and Tukey's multiple comparison analysis.

3.3 Effect of capsule on macrophage internalisation of *S. pneumoniae*

The capsule has been shown to inhibit phagocytosis of *S. pneumoniae* in human neutrophils *in vitro* (Hyams, Camberlein et al. 2010) and mouse AM recovered after intranasal infection (Camberlein, Cohen et al. 2015). Primary human MDM also phagocytose unencapsulated bacteria more readily as shown below in a high throughput microscopy experiment with fluorescently labelled bacteria. FAM-SE labelled bacteria were opsonised in pooled human serum, and added to MDM. After fixation, PE labelled anti human IgG was added. Internalised bacteria fluoresce green, whereas external bacteria are yellow due to colocalised FAM-SE and PE. The results showed that double the number of unencapsulated mutant were internalised after 2 hours compared to encapsulated *S. pneumoniae* (figure 3.8, A & B). This was also confirmed using the mouse RAW macrophage cell line and a flow cytometry assay of association of cells with fluorescent bacteria, though this assay measures both internalised and adherent bacteria. Again greater numbers of unencapsulated bacteria were associated with RAW macrophages than wild-type (figure 3.8 C & D).

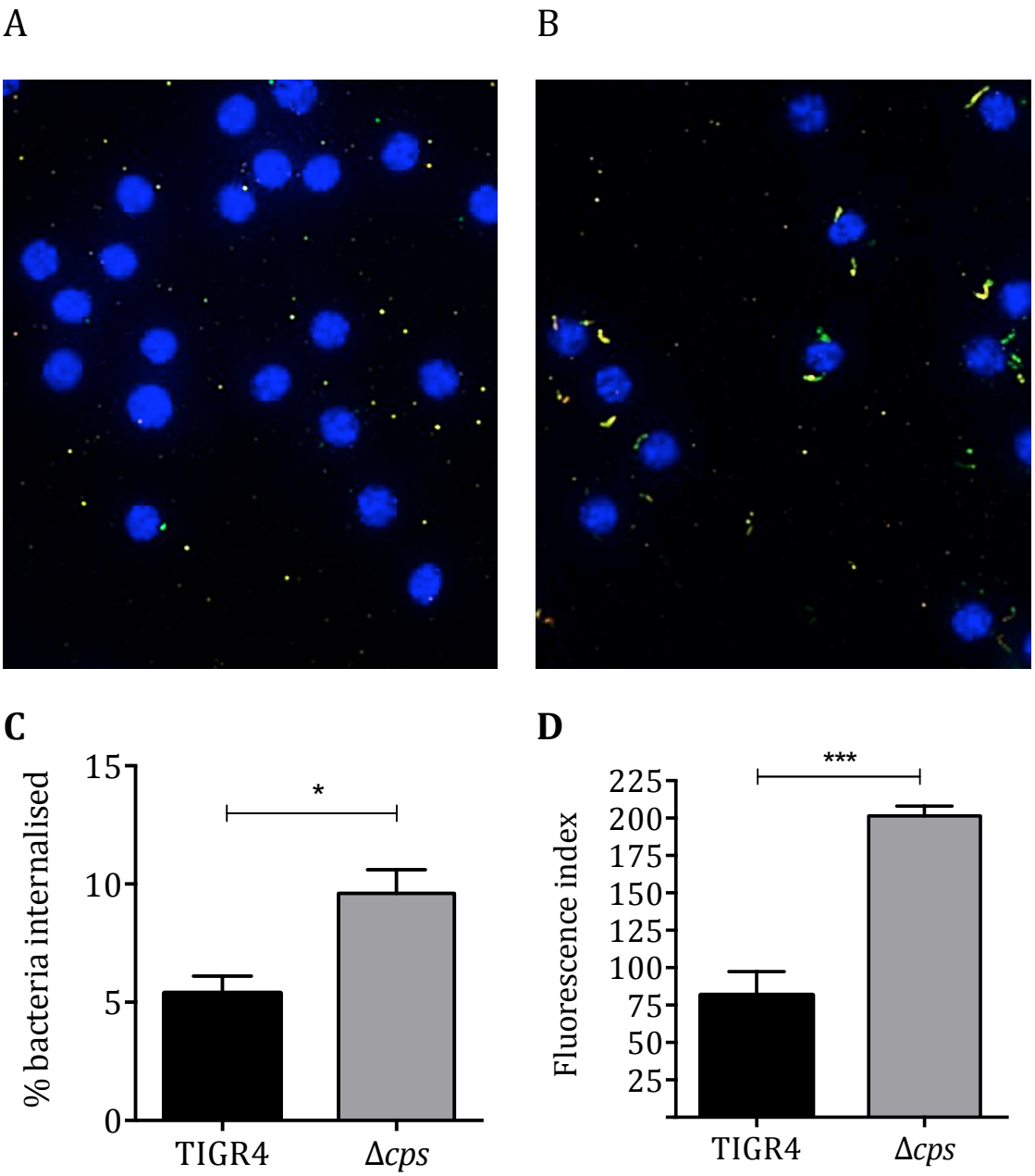

Figure 3.8 Macrophage uptake of FAM-SE labelled bacteria

MDM were incubated with FAM-SE labelled bacteria for 2 hours before fixing in PFA. Nuclei stained with DAPI are in blue, internalised bacteria are in green, and external bacteria are labelled in yellow. Panel A shows TIGR4, panel B Δ*cps*, and C shows the percentage of bacteria internalised, analysed on metamorph software. The displayed results are the means +/- SEM of 3 donors. Panel D is flow cytometry analysis of RAW macrophages incubated with FAM-SE labelled bacteria for 2 hours presented as mean fluorescence index (product of number of FITC positive cells and the geometric mean of their fluorescence). The displayed data is the mean +/- SEM of 4 experiments. Data were analysed by t test.

3.4 Effects of capsule on bacterial counts

As the capsule is known to affect opsonophagocytosis and therefore there is likely to be increased clearance of unencapsulated bacteria, one possible explanation for difference in inflammatory response is that encapsulated bacteria are cleared less well and therefore there are present in greater numbers to elicit a greater inflammatory response than unencapsulated bacteria.

Bacterial counts in MDM supernatant show that wild-type bacteria are present in significantly greater numbers than unencapsulated by 6 hours (figure 3.9). To see if the bacterial numbers accounted for the variation in inflammatory response, penicillin was added to the supernatant to kill the bacteria. Plating supernatant within 1 hour of the addition of penicillin confirmed no surviving bacteria (data not shown). If antibiotics were added 30 minutes after the addition of bacteria the inflammatory response was largely abrogated when incubated with both strains (figure 3.10). Antibiotics added after 4 hours allowed the bacteria sufficient time to elicit an inflammatory response, though much reduced compared to live replicating bacteria, the difference between wild-type and unencapsulated organisms was preserved (figure 3.11). This suggests that bacterial count differences are not sufficient to explain all the difference between the strains. Of note, penicillin is thought to cause cell lysis and may have been expected to cause inflammation from disgorgement of cell contents, though this was not seen in this series of experiments. This may suggest that ongoing bacterial replication is the most important factor in causing an inflammatory response.

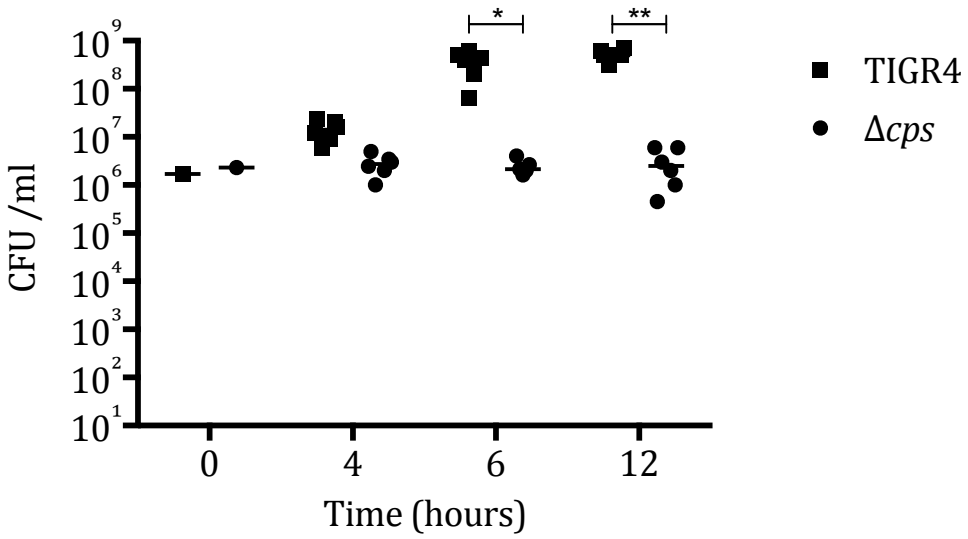

Figure 3.9 Bacterial counts in supernatant of MDM

Bacteria were added to MDM at MOI 10, then supernatant was plated at specified timepoints. The data shown is from 6 different experiments, individual values and means are presented. Data are analysed by Kruskal-Wallis and Dunn's multiple comparison test.

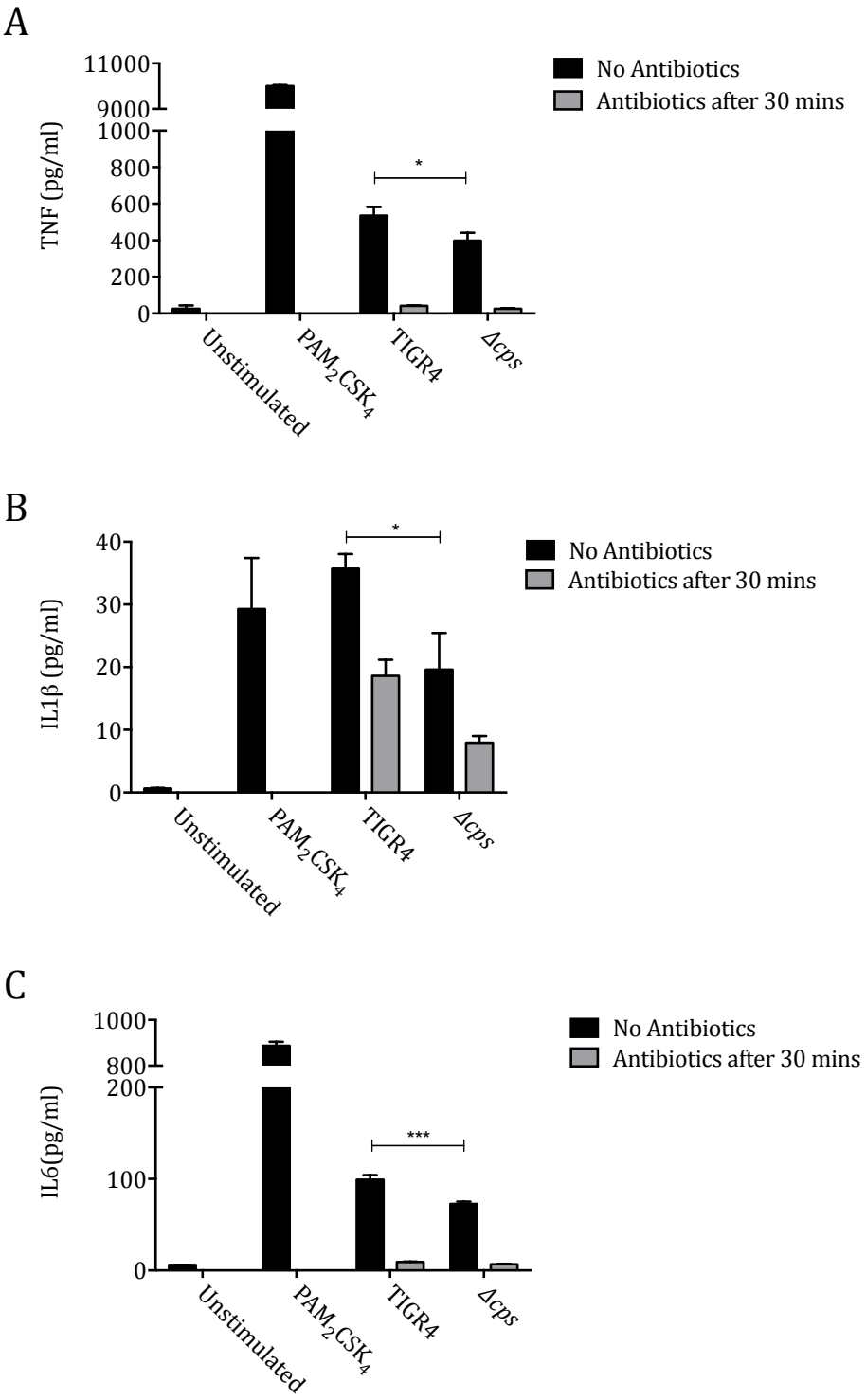

Figure 3.10 MDM response to bacteria with the addition of antibiotics after 30 minutes

MDM were incubated with TIGR4 or Δ*cps* at MOI 10, some wells had penicillin (Sigma Aldrich, Gillingham) added after 30 minutes . After 4 hours, supernatant was removed, and later analysed for A) TNF, B) IL1β, and C) IL6. The data obtained are from 3 different donors, and analysed by 2 way ANOVA and Tukey's multiple comparison test.

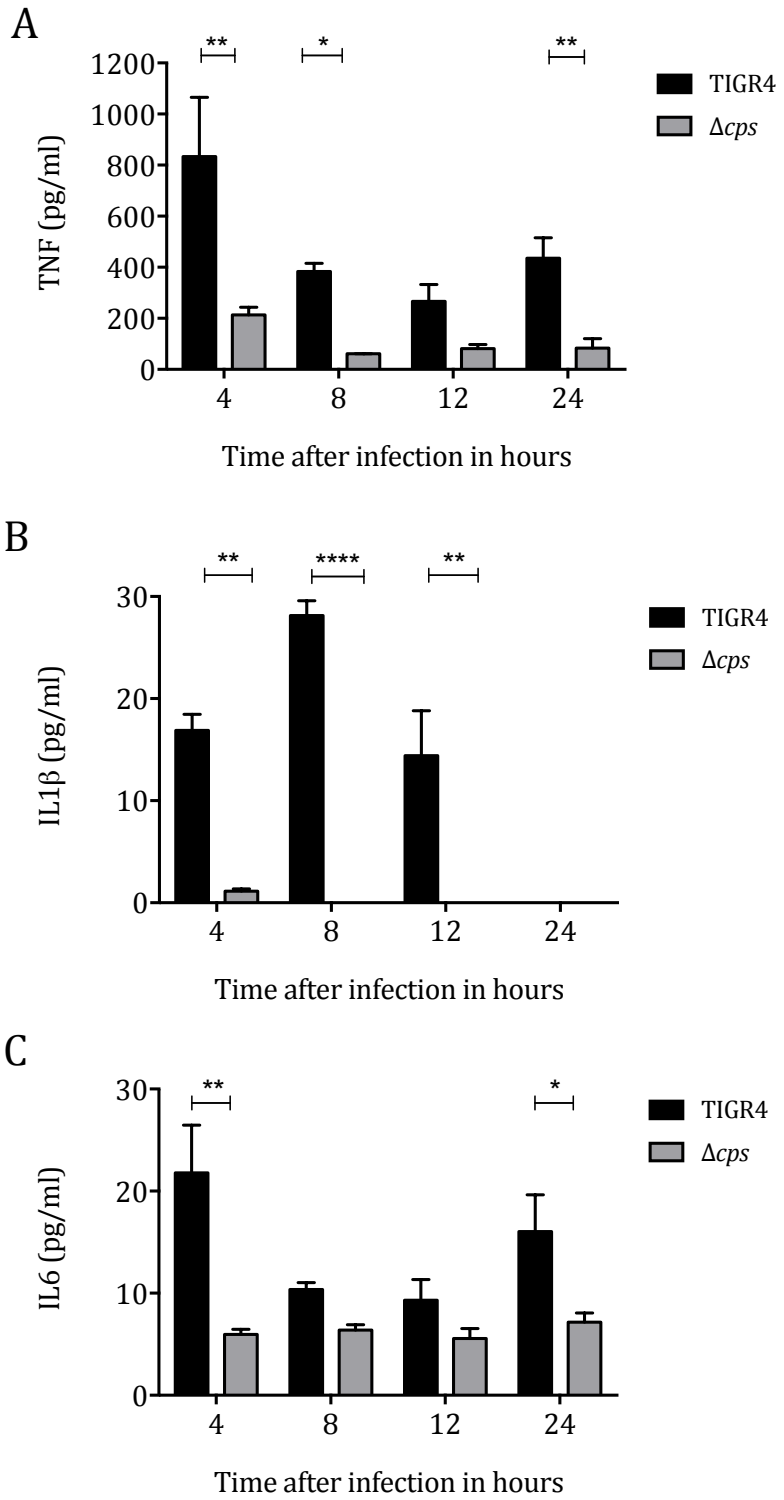

Figure 3.11 MDM response to bacteria with antibiotics added after 4 hours

MDM were incubated with TIGR4 or Δ*cps* at MOI 10, some wells had penicillin (Sigma Aldrich, Gillingham) added after 4 hours. At various timepoints, supernatant was removed, and later analysed for A) TNF, B) IL1β, and C) IL6. The data obtained are from 3 different donors, presented as mean +/- SEM, and analysed by 2 way ANOVA and Tukey's multiple comparison test.

3.5 Purified Capsule

To establish whether capsular polysaccharide induced inflammatory cytokine directly, purified polysaccharide was incubated with MDM. Purified serotype 4 capsular polysaccharide (ATCC) induced a dose dependent release of inflammatory cytokines from MDM (figure 3.12). It has been estimated that 10^5 bacteria equates to 0.2μg of capsular material (Tuomanen, Tomasz et al. 1995), so MOI 10 infection is roughly equivalent to 5μg/ml. Importantly the secretion of pro-inflammatory cytokines was abrogated by the use of polymyxin B (figure 3.13), suggesting that the pro-inflammatory effect of purified capsular polysaccharide was likely due to LPS contamination. Polymyxin B is a cationic basic peptide that binds to the negatively charged lipid A portion of LPS, and thus has a dose-dependent inhibitory effect. These data suggest that capsular polysaccharide does not directly induce an inflammatory response, but that capsule modifies how other factors within the bacterium interact with host cells to induce cytokine release.

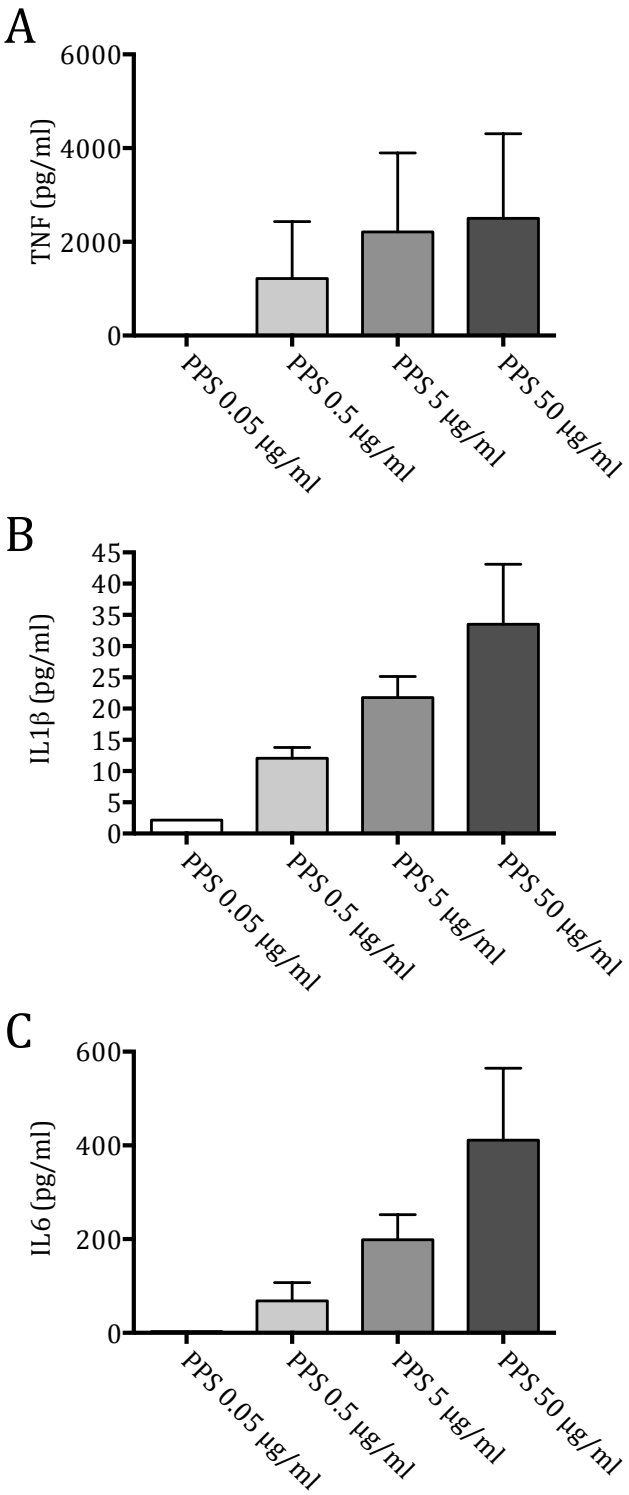

Figure 3.12 Inflammatory response to purified polysaccharide

Purified polysaccharide (PPS) was incubated with MDM at various concentrations and supernatant analysed for A) TNF, B) IL1β, and C) IL6 after 6 hours. Data from 3 donors are presented as mean +/- SEM and analysed by 1 way ANOVA and Tukey's multiple comparison test, with no significant differences seen.

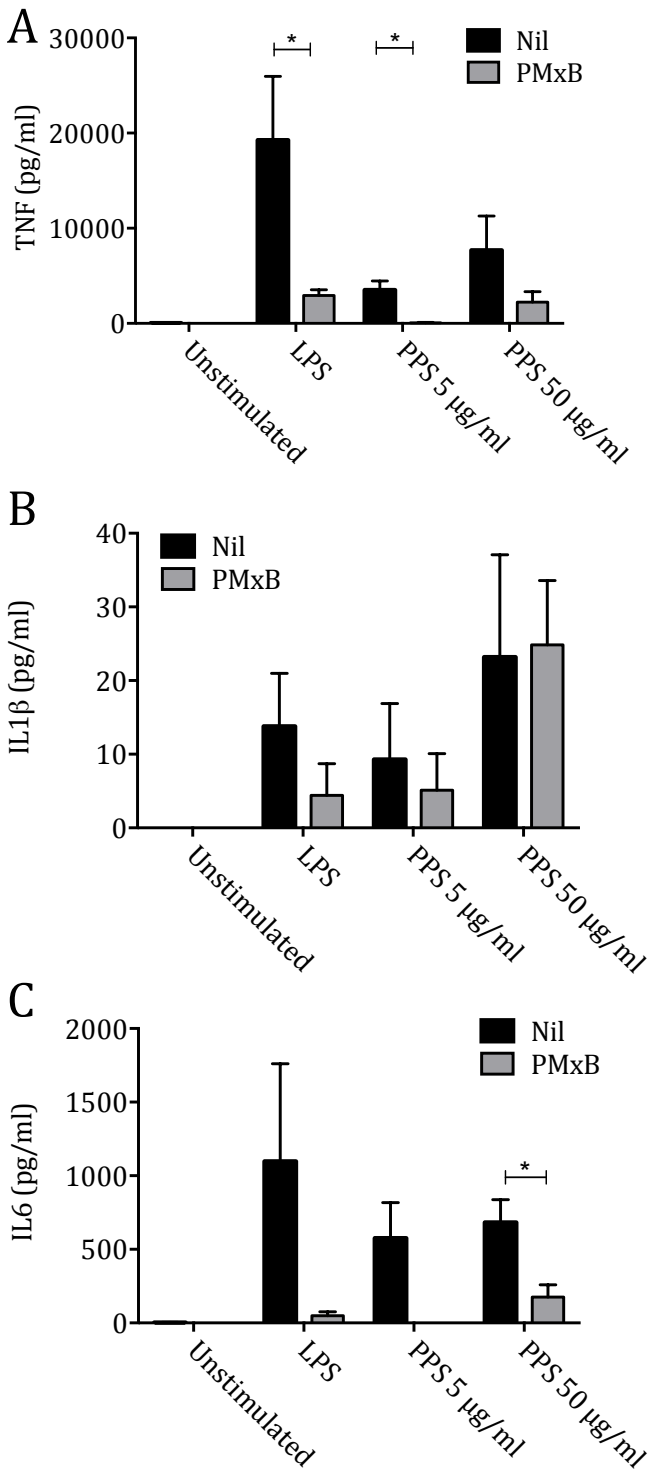

Figure 3.13 Effect of polymyxin B on purified capsular polysaccharide

In panels A, B, and C MDM were incubated with PPS with or without 30 µg/ml polymyxin B (PMxB), and TNF, IL1β, and IL6 measured respectively. LPS at 100ng/ml was used as a positive control, and both sets of experiments are represented as means +/- SEM of 3 experiments. Analysis was by 2 way ANOVA and Tukey's multiple comparison test.

3.6 Effects of capsule on pneumonia in mice

A well-established model of mouse pneumonia was used to assess whether the differences in inflammatory response between wild-type and unencapsulated bacteria seen in a tissue culture model translated into physiological effects. This model results in bacterial replication in the alveolar space, invasion into the lungs and into the blood stream. The host response includes local inflammation and a neutrophil influx. Early timepoints were examined to correlate with initiation of the inflammatory response.

The animal work for this experiment was carried out by Dr Emilie Camberlein, from the Brown laboratory. Even by 30 minutes, recovery of wild-type bacteria from BALF was a $\log_{10}$ fold greater than unencapsulated bacteria (figure 3.14). Inflammatory cytokine levels in BALF showed different temporal patterns, with TNF levels rising very early, then dipping again, with later modest increases in IL1β, and later increases in IL6 (figure 3.15). At 2 hours there was significantly more TNF with the encapsulated bacteria, and a similar pattern seen at 4 hours with IL1β and IL6. This reflects the *in vitro* data, but may be confounded by bacterial numbers.

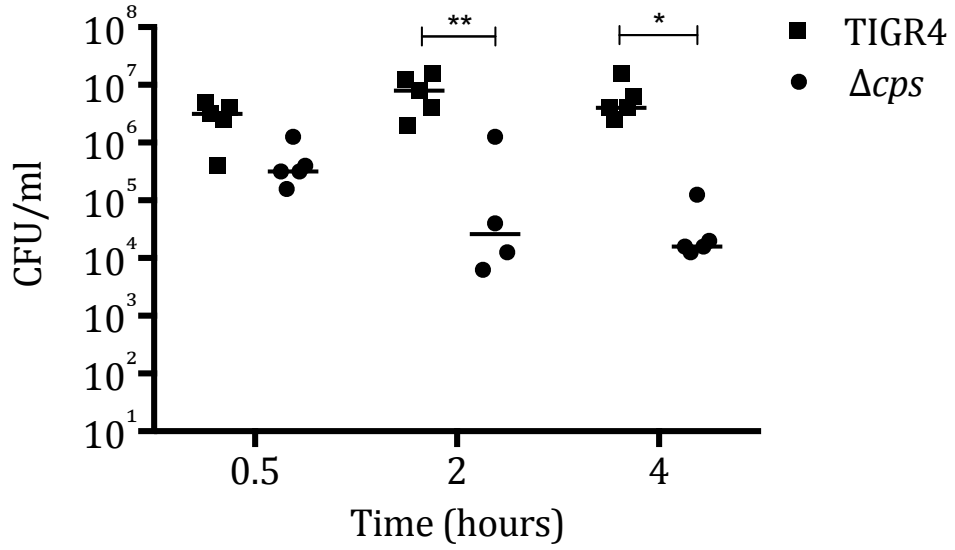

Figure 3.14 Bacterial counts in BALF after intranasal infection

5 week old female CD1 mice were inoculated intranasally with 5×10^6 CFU bacteria under isoflurane anaesthesia. The mice were culled at specified timepoints, bronchoalveolar lavage was performed and plated to ascertain bacterial numbers. There were 5 mice per group, analysis by Kruskal-Wallis and Dunn's multiple comparison test.

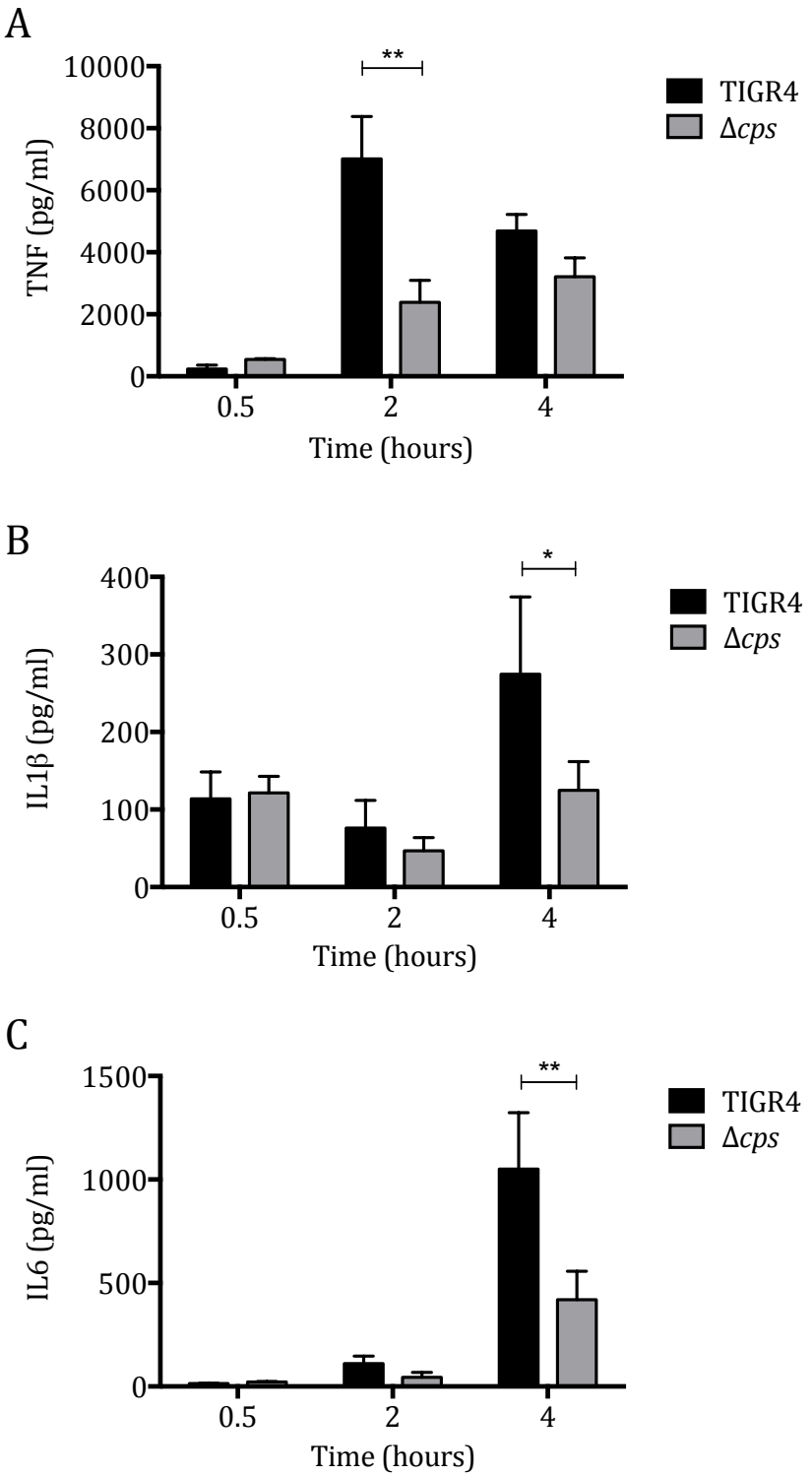

Figure 3.15 Cytokine levels in BALF after intranasal infection

5 week old female CD1 mice were inoculated intranasally with 5×10^6 CFU bacteria under isoflurane anaesthesia. The lavage fluid of mice was stored and the cytokines levels were measured by ELISA. Three were 5 mice per group, and results are presented as mean +/- SEM and analysed by 2 way ANOVA and Tukey's multiple comparison test.

3.7 Effects of alveolar macrophages depletion on capsule effects on mouse pneumonia

The *in vitro* data suggested that macrophages were critical in initial inflammatory responses to *S. pneumoniae*, as well as being important in initial clearance of bacteria. So the mouse experiments were repeated with liposomal clodronate, which induces apoptosis of phagocytes. Groups of mice had AM depleted by the administration of intranasal clodronate 72 hours prior to infection. The mouse work was, again carried out by Dr Emilie Camberlein. Depletion of macrophages with lysosomal clodronate (from the van Rooijen lab) reduced clearance of bacteria by 4 hours in both groups (figure 3.16). The efficacy of intranasal clodronate was confirmed by examining AM counts in PBS sham-infected animals. This confirmed approximately 80% reduction of AM numbers (performed by Emily Camberlein and data not shown).

At 4 hours TNF levels were decreased in response to both strains by depletion of macrophages, though the difference between the strains was preserved (figure 3.17 A). At the same timepoint IL1β levels (figure 3.17 B) were decreased in response to the wild-type strain, but there was little difference with the unencapsulated strain, albeit from an already low starting point. In this experiment there was non-significant differences in IL6 between the strains (figure 3.17 C), though removal of macrophages markedly reduces IL6 release.

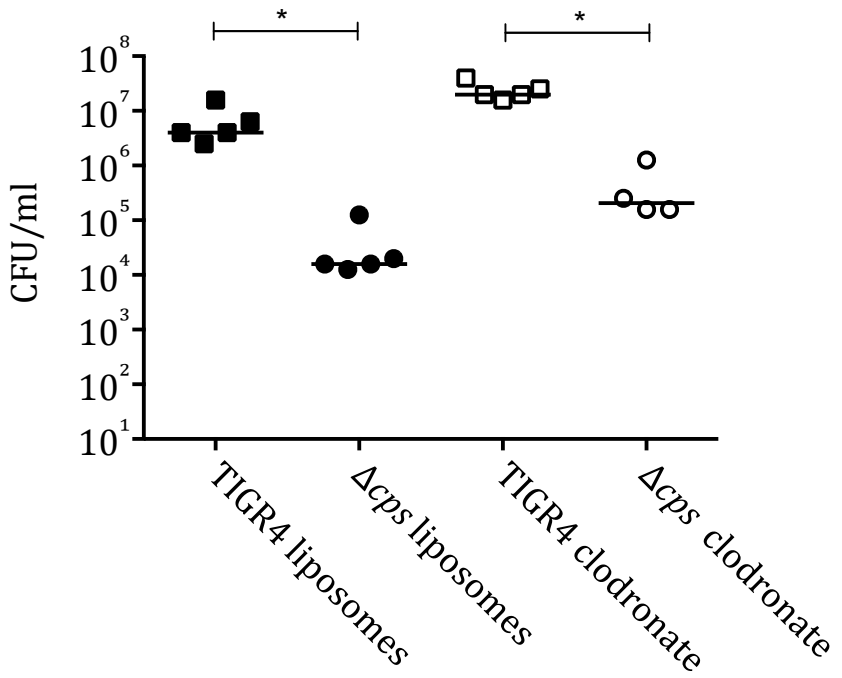

Figure 3.16 Bacterial counts in lavage fluid at 4 hours after intranasal infection

5 week old female CD1 mice were inoculated intranasally with 5×10^6 CFU bacteria under isoflurane anaesthesia. Mice were culled after 4 hours, bronchoalveolar lavage was performed and plated to ascertain bacterial numbers. There were 5 mice per group, and data is presented as mean +/- SEM. Analysed by Kruskal-Wallis and Dunn's multiple comparison test.

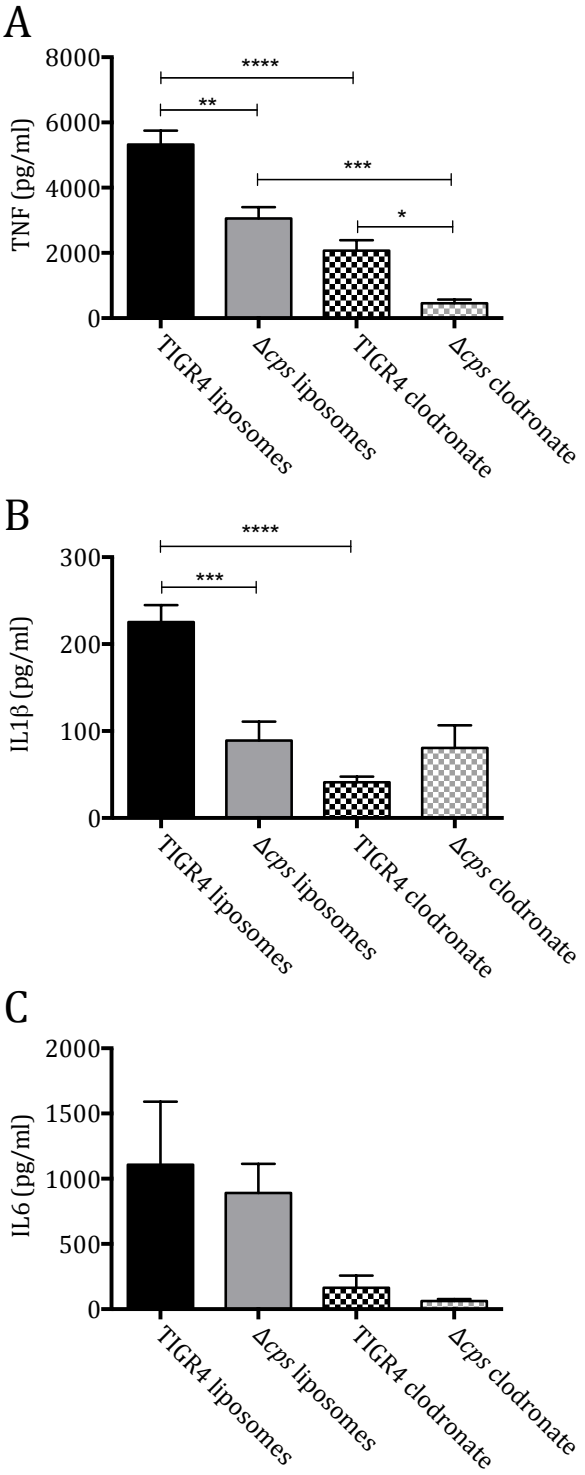

Figure 3.17 Cytokine levels in BALF at 4 hours after intranasal infection

5 week old female CD1 mice were inoculated intranasally with 5×10^6 CFU bacteria under isoflurane anaesthesia. The lavage fluid of mice was stored and the cytokines levels were measured by ELISA. Three were 5 mice per group, and results are presented as mean +/- SEM and analysed by 1 way ANOVA and Tukey's multiple comparison test.

3.8 Effects of capsule and macrophage in low inoculum respiratory infection

The effect of macrophages appears to be most pronounced with low numbers of bacteria, so the inflammatory response was assessed in a low inoculum mouse pneumonia model where *S. pneumoniae* is usually cleared 24 hours after intranasal infection, with mice that had been treated with liposomal clodronate or a liposome only control.

At 2 hours there was rapid clearance of unencapsulated bacteria in comparison to wild-type from the alveolar compartment (figure 3.18, A), with a log fold increase in both groups in macrophage-depleted mice. By 4 hours there was less difference between wild-type and unencapsulated bacteria, but in macrophage-depleted mice there was a 2 $\log_{10}$ increase in wild-type bacteria compared to unencapsulated, indicating that AM are important in clearance of encapsulated bacteria at low numbers, but non-phagocyte defences are more important in dealing with unencapsulated bacteria. Bacterial numbers in lung homogenate are much lower than in the alveolar compartment, with no significant differences between groups (figure 3.18, B).

Cytokine levels were generally much lower in BALF than with the higher inoculum experiments, probably due to better control of replicating bacteria. Here TNF levels in BALF were higher in wild-type bacteria at 2 and 4 hours (figure 3.19), and the depletion of alveolar macrophages reduced TNF secretion in response to wild-type but not unencapsulated bacteria at 2 hours, though by 4 hours there was little difference. Wild-type bacteria induced more IL1β secretion than unencapsulated at 2 hours, though IL1β levels were very low. There was very little difference between groups in IL6 secretion.

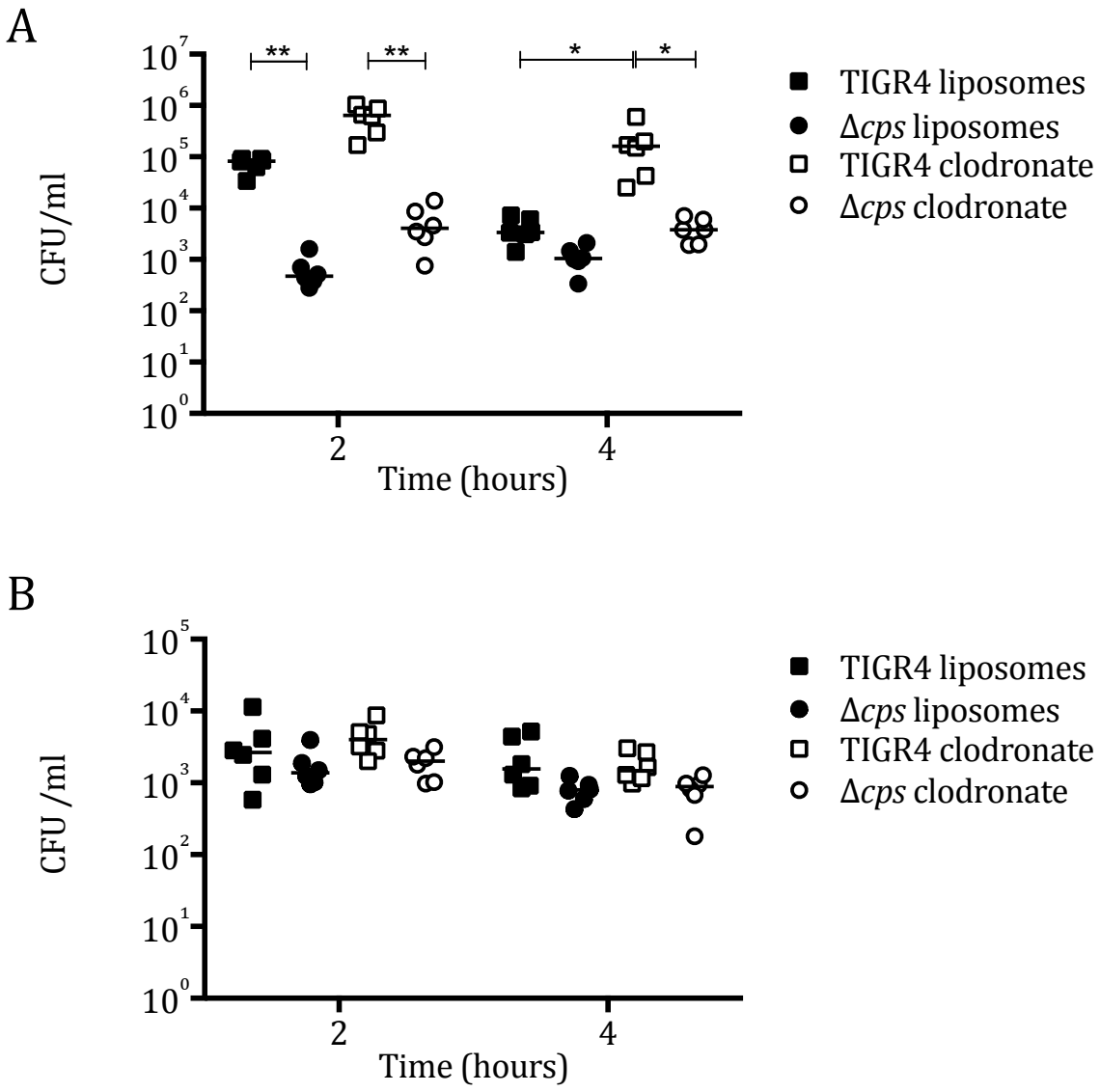

Figure 3.18 Bacterial counts at specified timepoints after low inoculum intranasal infection

5 week old female CD1 mice were inoculated intranasally with 5×10^5 CFU bacteria under isoflurane anaesthesia. The lavage fluid of mice was stored and the cytokines levels were measured by ELISA. There were 6 mice per group, and results are presented as individual mouse results with medians in BALF (panel A) and lung homogenate (panel B) and analysed by Kruskal-Wallis and Dunn's multiple comparison test, with no significantly different results in lung homogenate.

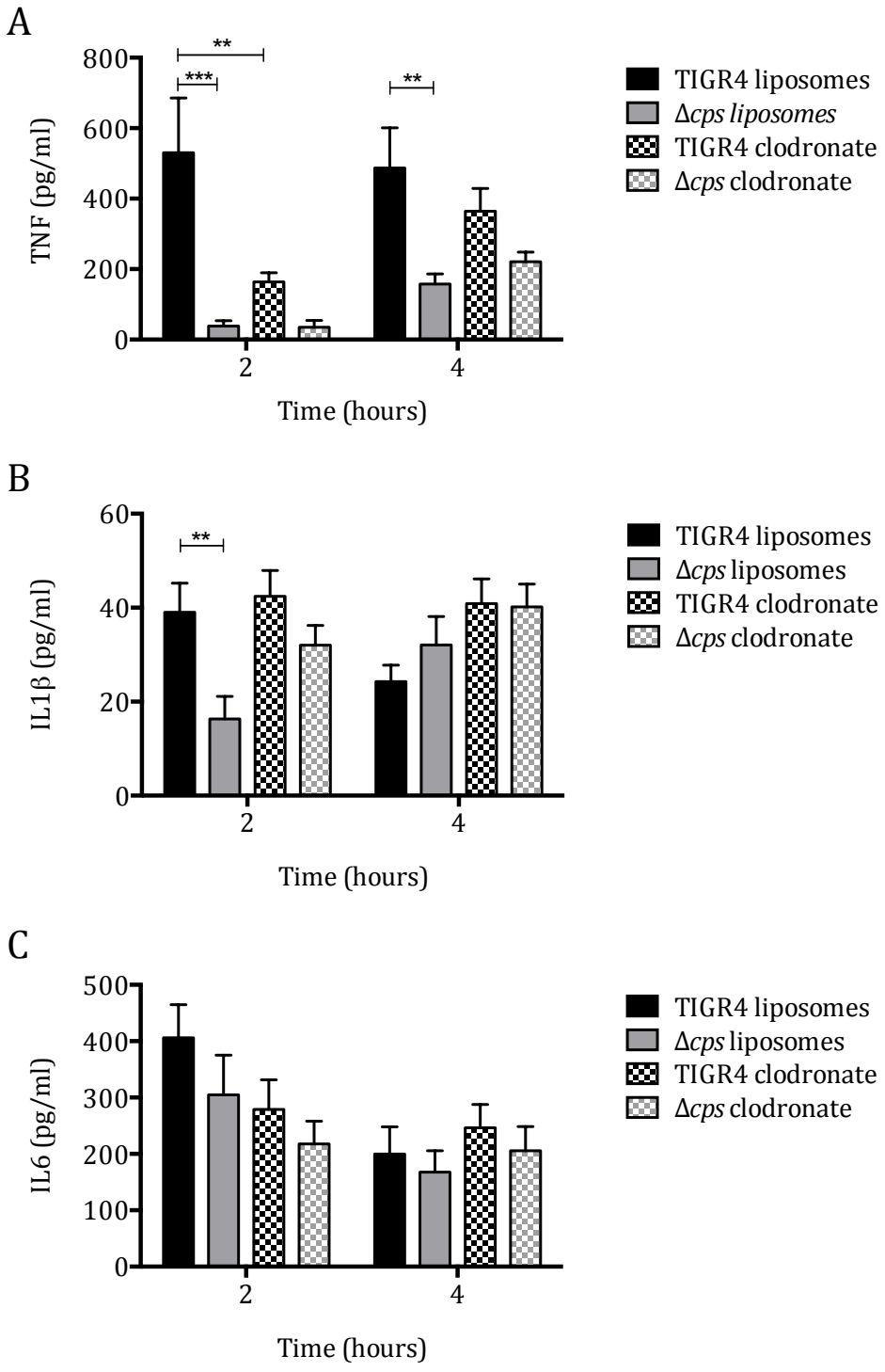

Figure 3.19 Cytokines in BALF after low inoculum intranasal infection

5 week old female CD1 mice were inoculated intranasally with 5×10^5 CFU bacteria under isoflurane anaesthesia. The cytokine levels in lavage fluid of the mice were measured by ELISA. Three were 6 mice per group, and results are presented as mean +/- SEM and analysed by 1 way ANOVA and Tukey's multiple comparison test.

In lung homogenates the cytokine pattern was quite different (figure 3.20). TNF levels were low in all groups except with wild-type bacteria in liposome treated mice at 4 hours, suggesting that macrophage responses to encapsulated *S. pneumoniae* are important in this compartment. IL1β levels were much higher in lungs than BALF, with only a trend towards greater levels with encapsulated bacteria. There was, however, a significant decrease in IL1β levels after macrophage depletion with complete abrogation of the difference between the strains. This suggests that AM are important in inducing inflammatory responses in lung parenchyma, possibly by crosstalk with epithelium. IL6 levels were also increased after exposure to wild-type bacteria compared to unencapsulated, with macrophage depletion attenuating these differences, in particular reducing IL6 secretion in response to wild-type bacteria.

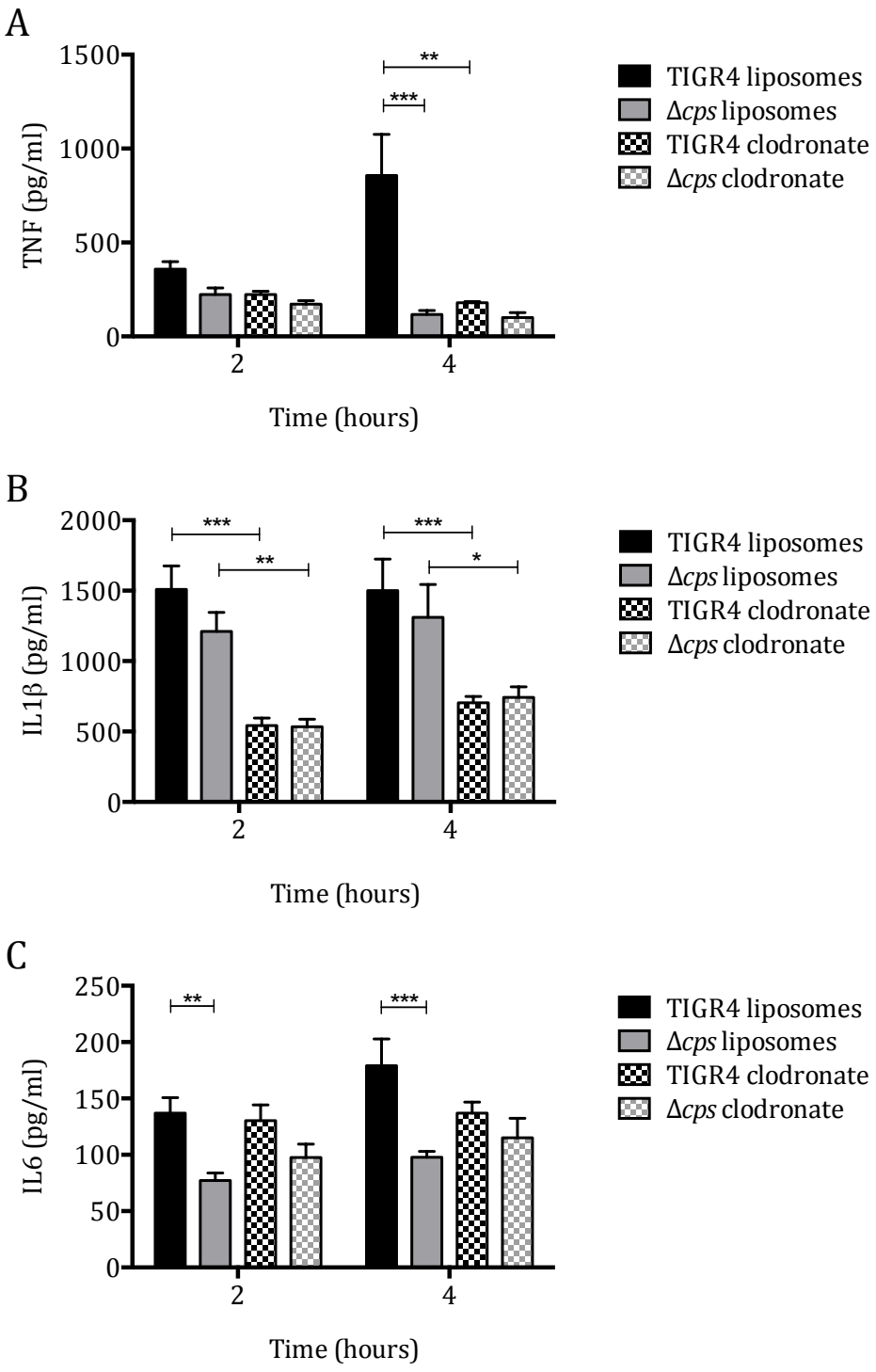

Figure 3.20 Cytokines in lung homogenate after low inoculum intranasal infection

5 week old female CD1 mice were inoculated intranasally with 5×10^5 CFU bacteria under isoflurane anaesthesia. The cytokine levels in lung homogenate of the mice were measured by ELISA. There were 6 mice per group, and results are presented as mean +/- SEM and analysed by 1 way ANOVA and Tukey's multiple comparison test.

3.9 Effects of capsule on septic shock in rats

To see if the physiological difference between wild-type and unencapsulated bacteria were maintained in other disease states, a model of rat septic shock was used, with the help of Dr Alex Dyson, from Professor Mervyn Singer's lab. To account for differences in clearance between wild-type and unencapsulated bacteria, non-replicating bacteria were used. These had a mutation in the *pabB* gene, meaning that the bacteria cannot replicate in organic environments unless supplemented. As clearance from blood is rapid, high inoculums were required to induce a septic shock phenotype (figure 3.21). Although there was no significant difference between the bacterial strains, there was a trend towards a greater drop in systolic blood pressure and rise in lactate with the wild-type strain, suggesting that the greater inflammatory response to encapsulated organisms may also be replicated in this model.

There was great variability in cytokine levels, possibly due to the instrumentation required to insert the indwelling catheters. With this in mind there is a trend towards greater TNF and IL6 levels induced by wild-type organisms, reflecting *in vitro* data and the mouse pneumonia data.

Overall the data using this model lack significance and specific conclusions should not be drawn from them. With more biological replicates, a clearer picture may have developed.

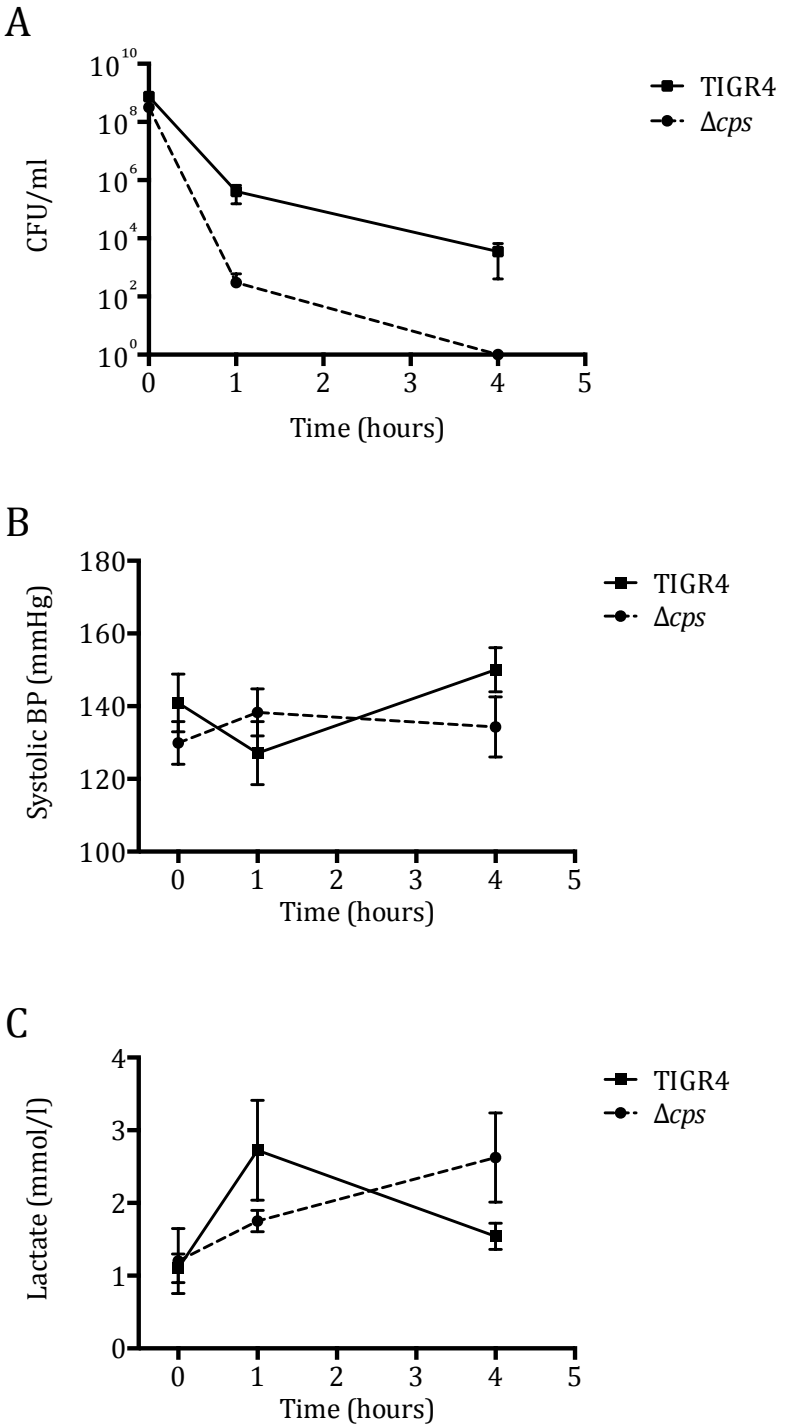

Figure 3.21 Bacterial counts and physiological data of intravenous infection of rats

Male Wistar rats (5 per group) were injected intravenously with non-replicating bacteria. Panel A shows bacterial counts in blood taken at specified timepoints. Panel B shows systolic blood pressure measure by arterial line, and panel C shows lactate level as measured by arterial blood gas analysis. CFU data are shown as median and IQR, analysed by Mann-Whitney U test. Physiological data are shown as mean +/- SEM, and analysed by t-test. There were no signifcant differences seen.

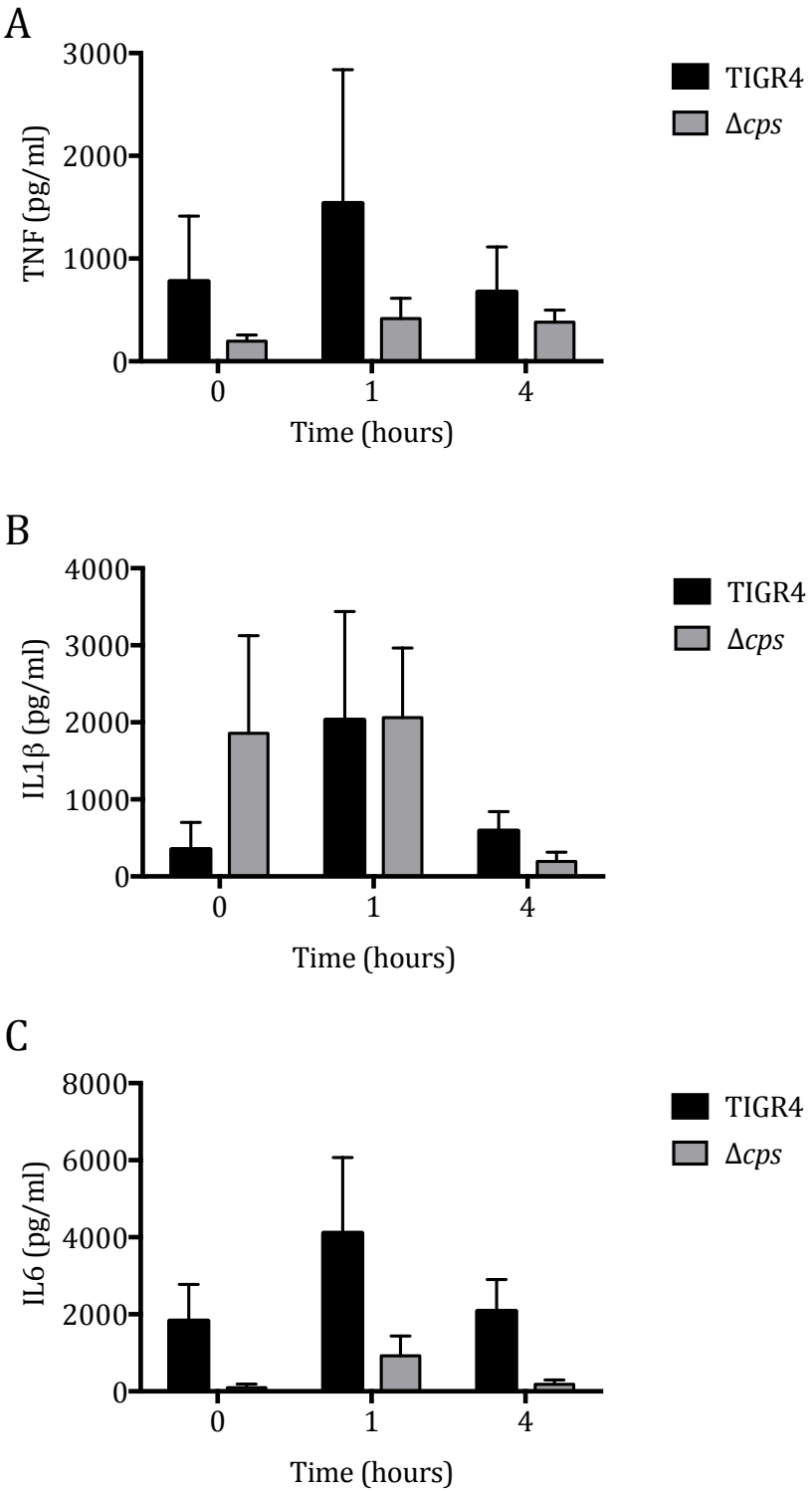

Figure 3.22 Cytokine levels in serum from intravenous infection of rats

Male Wistar rats (5 per group) were injected intravenously with non-replicating bacteria. Cytokine levels were measured by ELISA in serum obtained at specified timepoints. Data are presented as mean +/- SEM and analysed by 2 was ANOVA and Tukey's multiple comparison test, with no significant differences seen.

3.10 Chapter Summary

This chapter has explored the role of *S. pneumoniae* capsule on the inflammatory cytokine response in cell culture models using monocyte derived macrophages and an alveolar epithelial cell line. This data was extended to *in vivo* models of mouse pneumonia and rat septic shock to ensure there are physiological effects correlating with the inflammatory cytokines seen in the tissue culture model.

The pro-inflammatory cytokine response to purified capsule is abolished by the addition of polymyxin B, suggesting that this is due to LPS contamination. The effect of polymyxin B could have had unanticipated effects, for example on any anionic charge from the capsule. Despite this, encapsulated TIGR4 induces more pro-inflammatory cytokine transcription and secretion than the isogenic unencapsulated mutant. Bacterial stimulation of pro-inflammatory cytokine release from alveolar epithelial cells is limited, whereas the products of macrophages exposed to bacteria induce significant cytokine release, particularly CXCL8. This reflects the differences in macrophage stimulation due to the presence of capsule.

The capsule is known to have an important role in inhibiting opsonophagocytosis, and it is clear from MDM internalisation data that the capsule inhibits internalisation in this model. Similarly capsule inhibited bacterial clearance by MDM from cell culture supernatant. Both may contribute to explaining the difference in inflammatory responses between strains.

It was also noted that the difference between inflammatory responses to TIGR4 and Δ*cps* was not so marked in some experiments, particularly evident in later chapters (e.g. figure 5.1 and 6.7). The data had large inter-donor variation noted, and this may explain the lack of significant difference. This is likely due to variation in between experiments, possibly due to variation in MDM numbers, activation state perhaps due to differences in plasticware, different batches of AB serum and RPMI used during the course of my PhD. In addition there could be variation in bacterial virulence (though this was minimised by using bacteria grown form animal passaged archived master stocks). There is undoubtedly donor variation in

responses to bacteria and so conclusions would ideally be drawn from greater number of replicates. Ideally I would have made greater efforts to confirm MDM expression of cell surface markers to ensure consistency. To account for this all TIGR4 v Δ*cps* cytokine data obtained at MOI 10 for 6 hours were combined (60 experiments in total) and can be seen in figure 3.23. Overall there was a significant difference seen by t-test giving confidence to the overall pattern that capsule contributes to pro-inflammatory inflammation.

In a mouse pneumonia model wild-type encapsulated *S. pneumoniae* also induced greater inflammatory cytokine release than unencapsulated. The unencapsulated bacteria were also cleared more quickly from lavage fluid. While removal of AM reduced bacterial clearance, the effect was similar in both strains. Similarly inflammatory cytokine levels were reduced in macrophage-depleted mice but the difference between strains largely persisted (except IL1β, though levels were very low so is of doubtful significance). However in a low inoculum infection model, where macrophages are thought to play a more pivotal role, it was clear that clearance of encapsulated organisms is more dependent on macrophages than unencapsulated organisms. Inflammatory cytokine levels were much lower, but there was still more cytokine secretion seen with encapsulated *S. pneumoniae*, though the differences were less impressive. When AM were depleted the cytokine profile between both strains was very similar, suggesting that macrophages are key to the difference in inflammatory response noted both *in vitro* and *in vivo*. The presence of capsule magnifies the inflammatory response at the transcriptional and secreted cytokine level. It is difficult to draw conclusions from the lung homogenate data, mainly because the lung compartment is complex. Lung homogenate includes lung parenchyma, blood vessels, and also what is left in the airways after the lavage was taken. Although there are clear differences from the alveolar lavage, it is difficult to pick apart the causes of those differences with such a heterogeneous population of cells. It is clear that TNF is the dominant cytokine in the alveolar compartment, and IL1β is much more prominent in the lungs, but these data cannot discern which cell type is responsible for this.

A rat septic shock model with intravenous infection of non-replicating bacteria showed no significant differences between the strains, but there was a trend towards more inflammatory cytokine release with wild-type bacteria and physiological sequelae of sepsis such as hypotension and lactataemia.

In summary, the data indicate that unexpectedly the macrophage inflammatory response to *S. pneumoniae* was greater to encapsulated than unencapsulated bacteria.

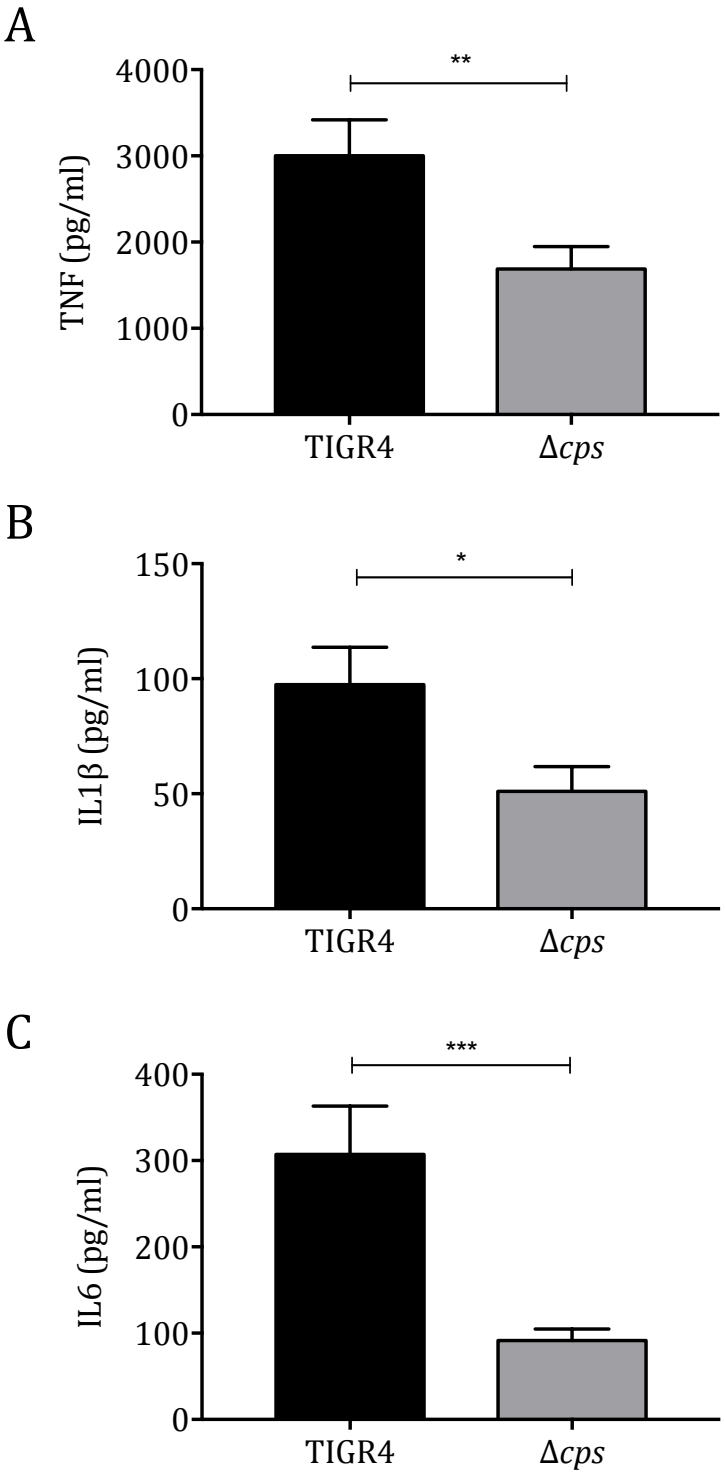

Figure 3.23 Combined cytokine response of MDM to TIGR4 and unencapsulated mutant
MDM were incubated with TIGR4 or TIGR4Δ*cps* in tissue culture plates, at MOI 10. Supernatant was aspirated at 6 hours and later analysed for A) TNF, B) IL1β, and C) IL6. The data from 60 different donors are analysed by t-test.

4 Mechanisms of pro-inflammatory effects of capsule

After establishing that capsule had pro-inflammatory effects *in vitro* and *in vivo*, I carried out a series of experiments to try and explore the mechanisms by which they occur.

4.1 Transcriptional response of monocyte derived macrophages

To further explore the response of MDM to *S. pneumoniae* and how the capsule modifies this response, I undertook whole genome transcriptional analysis. Some of the datasets were obtained by Gillian Tomlinson (from the Noursadeghi lab), who performed the LPS and PAM_2CSK_4 control experiments as well as obtained data for TIGR4 and Δ*cps* infection experiments from 3 donors each. However I extracted and analysed the data. I carried out the microarray experiments with unstimulated controls, and the TIGR4 and Δ*cps* infection experiments for an additional three donors. In total there were 3 replicates each for unstimulated, LPS and PAM2CSK4 incubated MDM, and 6 each for TIGR4 and Δ*cps* infected MDM. These data were obtained at the same time as the transcriptional data presented in chapters 4.4, 7.1 and 7.3. The data were analysed by T tests on MultiExperiment Viewer v 4.6.0 and significance was set at $p<0.05$. A false discovery rate was not used as the number of biological replicates was low (3 to 6), and confidence was built by comparison to historical group data and bioinformatic analysis confirmation with other experimental data.

Figure 4.1 A shows all the genes on the microarray, with relative expression values plotted for MDM incubated with TIGR4 versus unstimulated MDM. As relatively few points lie outside the red lines, this indicates that a small proportion of recognised genes are altered by incubation with TIGR4. The Venn diagram in panel C indicates that after infection with TIGR4, 298 genes are differentially expressed by more than 2 fold compared to unstimulated controls, and 294 genes with Δ*cps*. Of these genes showing differential expression compared to unstimulated controls, 194 genes were shared between the two bacterial strains. Stimulation of MDMs with the TLR2 agonist PAM_2CSK_4 caused two-fold changes in expression of 2863 genes, 135 of which were also affected by MDM infection with TIGR4 and / or Δ*cps S.*

pneumoniae. Figure 4.2, panel A compares the gene expression between MDM exposed to TIGR4 and the Δ*cps* mutant. Here, only 50 genes were differentially expressed by more than 2 fold. Panel B shows the 20 genes that were most overexpressed by TIGR4 in relation to Δ*cps*, with $\log_2$ difference in gene expression displayed. Pro-inflammatory cytokines are prominent in this gene list, supporting the previous data that the encapsulated bacteria promote increases in the inflammatory responses at the transcriptional level. Figure 4.3 illustrates the top 20 genes upregulated by TIGR4, and how the mean expression values compare to the other conditions. Again pro-inflammatory genes are prominent, and the heat map shows that the Δ*cps* strain upregulated similar genes, but to a lesser extent. The fold change column shows a direct comparison of the two strains for this gene signature. While the differences were modest, pro-inflammatory cytokines such as ILβ, IL6, and IL23 as well as chemokines such as CXCL1, 2, & 8 were more upregulated by MDMs after infection with the wild-type strain in comparison to the unencapsulated strain.

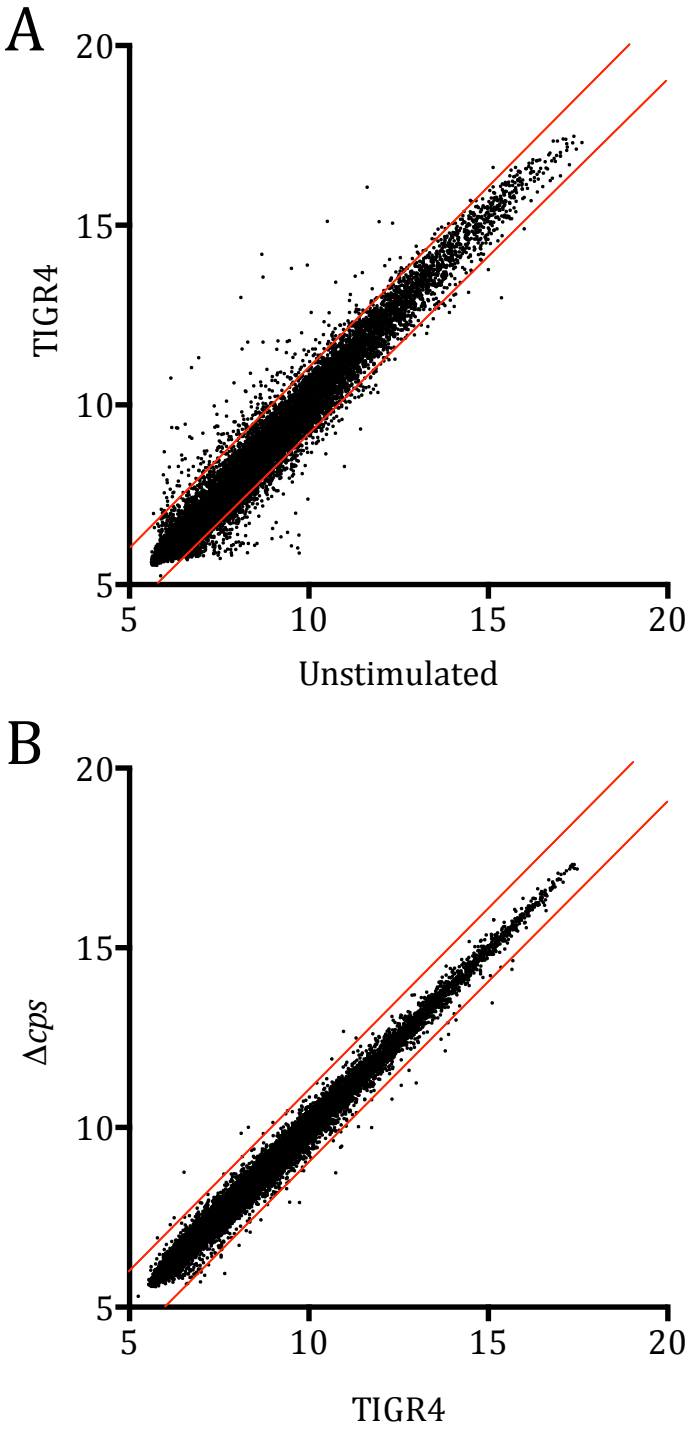

Figure 4.1 Comparative transcriptome response of MDMs to *S. pneumoniae* and Δ*cps*

Panel A plots expression values of all genes on a microarray comparing TIGR4 v unstimulated, whereas B compares TIGR4 v Δ*cps.* In both, the red lines indicate 2 fold differences. Each gene on the microarray is expressed as a data point. Data points falling outside these lines indicate significantly different gene expression between conditions.

A

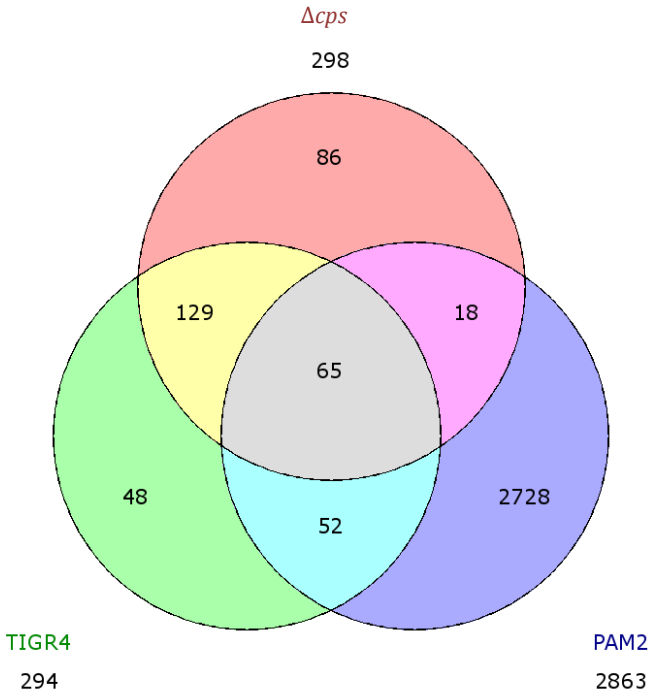

B

Gene Symbol	T4-Δ*cps*
IL6	2.01
EREG	1.82
IL23A	1.76
IL8	1.75
FAM198A	1.72
CXCL1	1.66
IL1B	1.64
PTGS2	1.55
DUSP1	1.53
IL7R	1.44
TNFAIP6	1.43
BIRC3	1.40
HILPDA	1.36
CSF3	1.34
CXCL2	1.30
ATE1	1.28
PCDHB6	1.28
NFKBIA	1.26
MMP1	1.23
ADM	1.22

Figure 4.2 Comparative transcriptome response of MDM to TIGR4 and Δ*cps* – most upregulated genes

Panel A is a Venn diagram showing the number of genes upregulated by more than 2 fold compared to unstimulated for the two strains and the positive control. Panel B shows the genes most upregulated when comparing the response of TIGR4 with Δ*cps* directly; the values indicating $\log_2$ of the difference in expression values between the conditions.

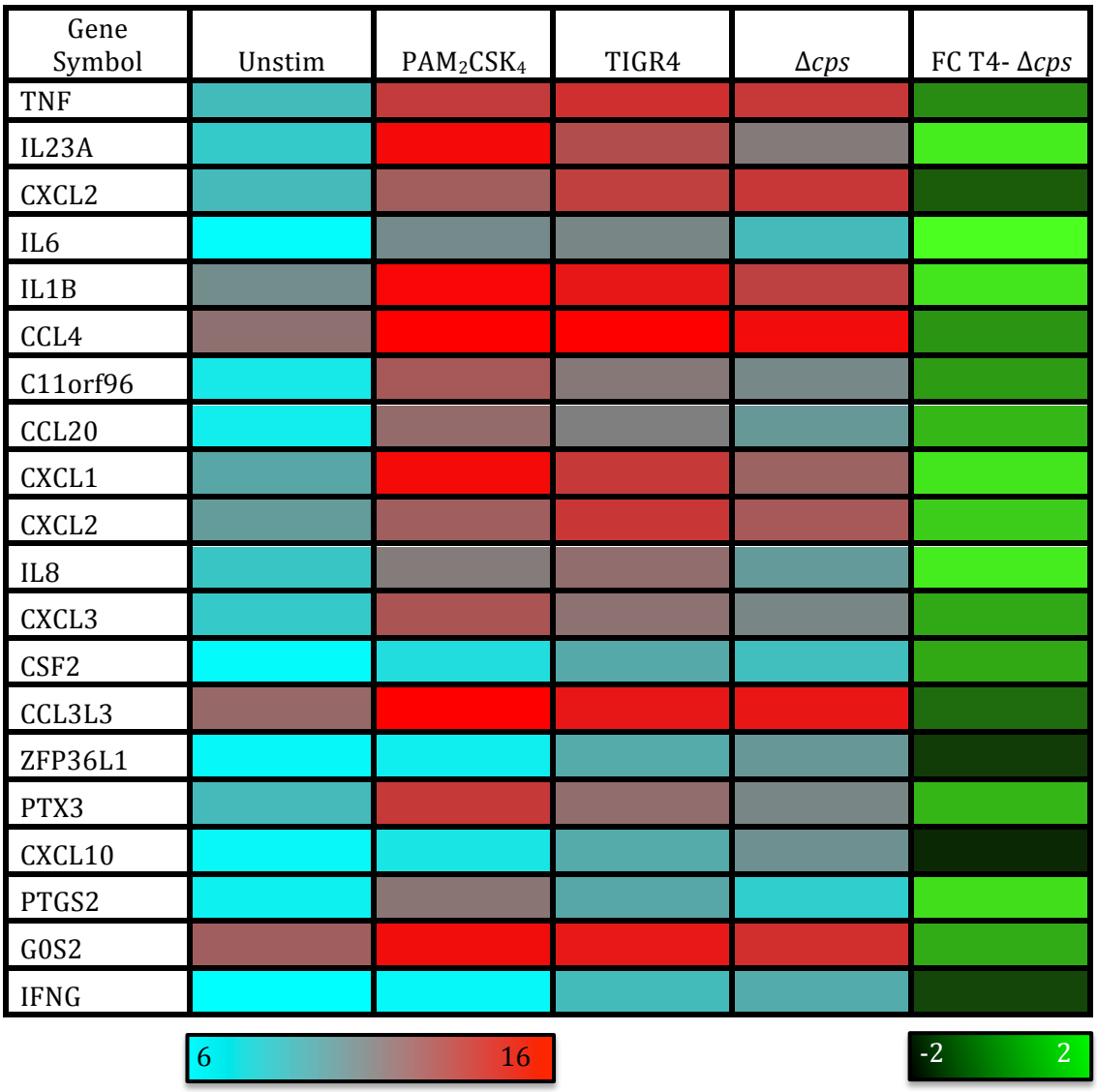

Figure 4.3 Comparison of genes upregulated by PAM_2CSK_4, TIGR4 and Δ*cps*

This heat map shows mean relative expression values of the top 20 genes upregulated by wild-type TIGR4 when compared to unstimulated MDM. The results displayed are from experiments of 6 donors. The most upregulated genes are displayed as relative expression with the most upregulated in red, and the least upregulated in blue. The last column shows a direct comparison of gene upregulation of these genes between TIGR4 and the Δ*cps* mutant, displayed as $\log_2$ fold change (FC) with green being the most upregulated genes, and black the most downregulated.

Analysis of the same data by non-biased principle component analysis (PCA) was confounded as the experiments carried out by colleagues were performed on an older microarray chip platform with differences in the genes included as well as the oligonucleotides spotted on the membranes. As a consequence PC1 (accounting for 45% of variation) primarily separated the data by differences between the two microarray chips. PC2 (accounting for 24% of variation) mostly separated the LPS control from the other conditions, but PC3 (accounting for 19% of variation) is composed primarily of pro-inflammatory genes. The results of the PCA indicated that both LPS and PAM_2CSK_4 induced a greater inflammatory response than *S. pneumoniae*, and that wild-type bacteria induced higher transcriptional responses of pro-inflammatory genes than unencapsulated bacteria (figure 4.4).

Bioinformatic analysis of the transcriptome with oPOSSUM software extracts information about predicted transcription factor binding sites on upregulated genes. Analysis of the genes differentially upregulated by TIGR4 over Δ*cps* is illustrated in figure 4.5. A z-score of >10 is considered to be significant, and panel A shows the transcription factors predicted to be activated by TIGR4 and Δ*cps* compared to unencapsulated, whereas panel B shows the transcription factors predicted to be activated by TIGR4 compared to Δ*cps* in rank order. These largely involved the NFκB complex and stimulation of interferon stimulated response elements (e.g. IRF1), as well as response to cytokines and proliferation/differentiation/apoptosis responses (e.g. AP1). The Innate DB database of genes, proteins, and signalling pathways is a curated resource of experimentally verified interactions. Innate DB analysis of the difference in upregulated genes identified overrepresented functional pathways. The most significantly overrepresented pathways in MDM exposed to TIGR4 compared to unstimulated MDM are shown in figure 4.6, panel A. They include PRR signalling, and inflammatory cytokine recognition. Pathways overrepresented during infection with encapsulated wild-type compared to Δ*cps* bacteria are shown in panel B.

A

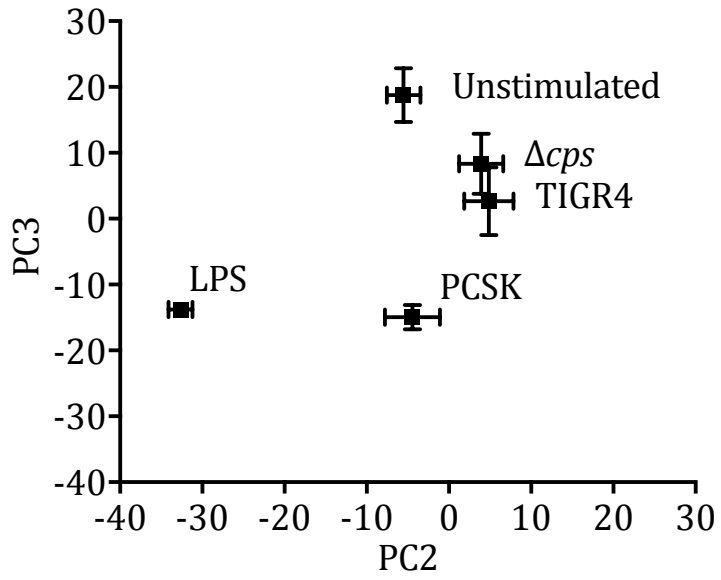

B

PC3 negative
IL6
TNF
CCL20
CSF3
CXCL1
TNFAIP6
IL1B
IL23A
CCL5
PTGS2
VCPIP1
CSF2
CCR7
TNIP3
KGFLP2
SOCS3
PTX3
CXCL3
IL1A
CCL4

Figure 4.4 Principle component analysis of transcriptome of MDM incubated with TIGR4 or Δ*cps*

The transcriptome of MDM exposed to wild-type, unencapsulated TIGR4, or controls for 4 hours was analysed by non-biased principle component analysis illustrating expression of co-correlated genes in the global gene expression profile. Panel A shows mean +/- SEM scores of principle components 2 and 3, for 3 donors of controls, and 6 each of TIGR4 and Δ*cps*. The top 20 genes contributing the most towards the negative deflection of PC3 are shown in panel B.

A

	TIGR4	Δ*cps*
EWSR1-FLI1		
HIF1A::ARNT		
IRF1		
IRF2		
Klf4		
NF-kappaB		
NFYA		
PAX4		
REL		
RELA		
Sox2		
ZNF354C		

B

TIGR4-Δ*cps*
RELA
IRF1
NF-kappaB
AP1
RXR::RAR_DR5
NFKB1
HOXA5
FEV
Gfi
NFE2L2
REL
Pdx1
IRF2
Sox17
SRY

Figure 4.5 Bioinformatic analysis – transcription factor binding sites

Panel A shows oPOSSUM analysis of the most upregulated genes in MDM when incubated with TIGR4 or Δ*cps* compared to unstimulated cells, which predict the transcription factors activated in those conditions. Z-score indicating significantly overrepresented transcription factor binding sites are illustrated; the darker the panel the more genes upregulated that are activated by the transcription factor in question. Panel B shows the transcription factors most differentially activated between wild-type and unencapsulated in rank order.

A

TIGR4 > Unstimulated	p value
IL23-mediated signalling events	1.14^{-4}
TLR signalling pathway	3.17^{-4}
Staphylococcus aureus infection	3.52^{-4}
IL12-mediated signalling events	3.68^{-4}
Cytokine-cytokine receptor interaction	9.36^{-4}
IFN α/β signalling	0.0012
Chemokine receptors bind chemokines	0.0013
Cytosolic DNA-sensing pathway	0.0016
IFNγ signalling	0.0016
NOD-like receptor signalling	0.0025

B

TIGR4 > Δ*cps*	p value
NOD-like receptor signalling pathway	8.24^{-6}
IL23-mediated signalling events	5.04^{-5}
Signal transduction through IL1R	4.93^{-4}
Validated transcriptional targets of AP1 family members Fra1 and Fra2	5.96^{-4}
CD40/CD40L signalling	0.0017
Cytokine –cytokine receptor interaction	0.0021
NFκB activation by nontypeable *Haemophilus influenzae*	0.0022
TNFR2 signalling pathway	0.0023
AP-1 transcription factor network	0.0041
Chagas disease pathways	0.0041

Figure 4.6 Bioinformatic analysis of transcriptome – overrepresented pathways

This shows the 10 most significantly overrepresented pathways analysis by innateDB software. This shows the pathways predicted to be activated by analysing clusters of genes more expressed in one group than the other. Panel A shows the pathways overrepresented by incubation with wild-type over unstimulated cells whereas B shows the pathways overrepresented by incubation with wild-type over incubation with unencapsulated cells.

4.2 Effect of opsonisation and on the inflammatory response to capsule

As the primary role of the capsule appears to be to inhibit phagocytosis, I investigated the effect of phagocytosis on MDM inflammatory responses. The media MDM were incubated in contained 10% pooled human serum, which contains enough human antibody to cause detectable IgG binding to *S. pneumoniae* (figure 4.7). Figure 4.7 also demonstrates that there was increased binding of human antibody to unencapsulated mutants in MDM media as well as with pooled human immunoglobulin (IVIG) compared to wild-type. This may have indicated that serum in media could confound the inflammatory responses from MDM, particularly as Fcγ receptors are known to play a role in inflammatory signalling (Clatworthy and Smith, 2004). However, repeating the MDM infection experiments in serum-free media (removing the effects of antibody) showed that wild bacteria still induced more inflammatory cytokine than unencapsulated mutants when assessed using qPCR at 3 hours (Figure 4.8). In contrast, pre-opsonisation of bacteria before incubating with MDMs to increase bacterial phagocytosis reduced the inflammatory response to *S. pneumoniae* and abrogated the differences between the TIGR4 and Δ*cps* strains.

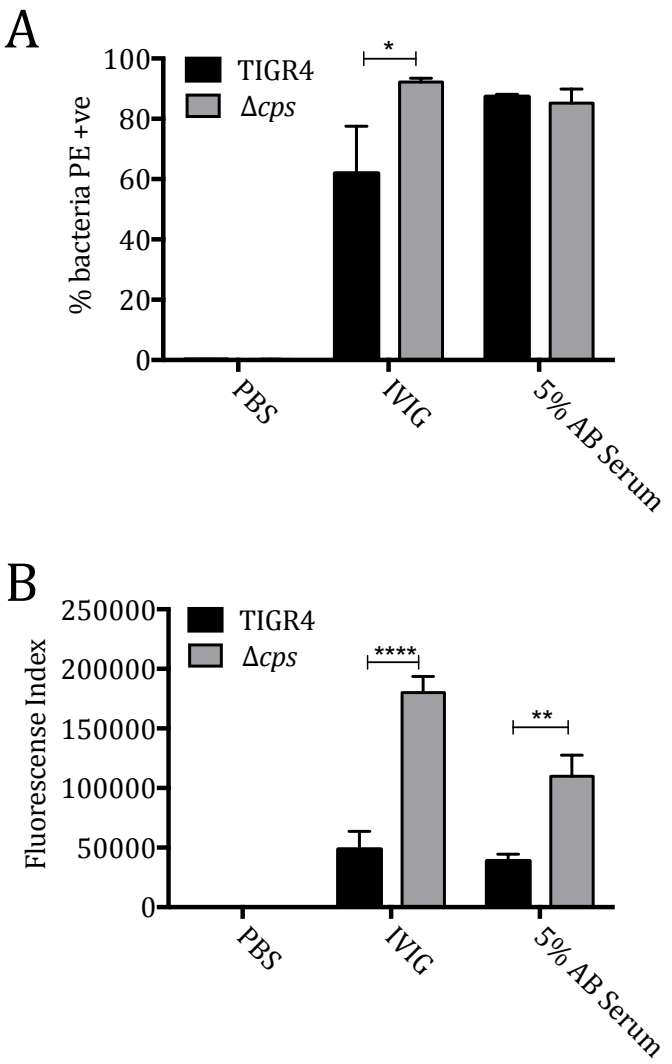

Figure 4.7 IgG binding to bacteria

Bacteria were suspended in PBS, 10% IVIG in media or 5% AB serum media for 30 minutes. Fixed bacteria were stained for PE conjugated to an anti human IgG antibody. Panel A shows the number of bacteria that bound IgG and panel B display the fluorescence index, a product of the amount of bacteria that fluoresce, with degree of fluorescence (measured by geometric mean of fluorescence), indicating the quantity of antibody binding to each bacterium. Results displayed are mean +/- SEM of 3 separate experiments, and analysed by 2 way ANOVA and Tukey's multiple comparison test.

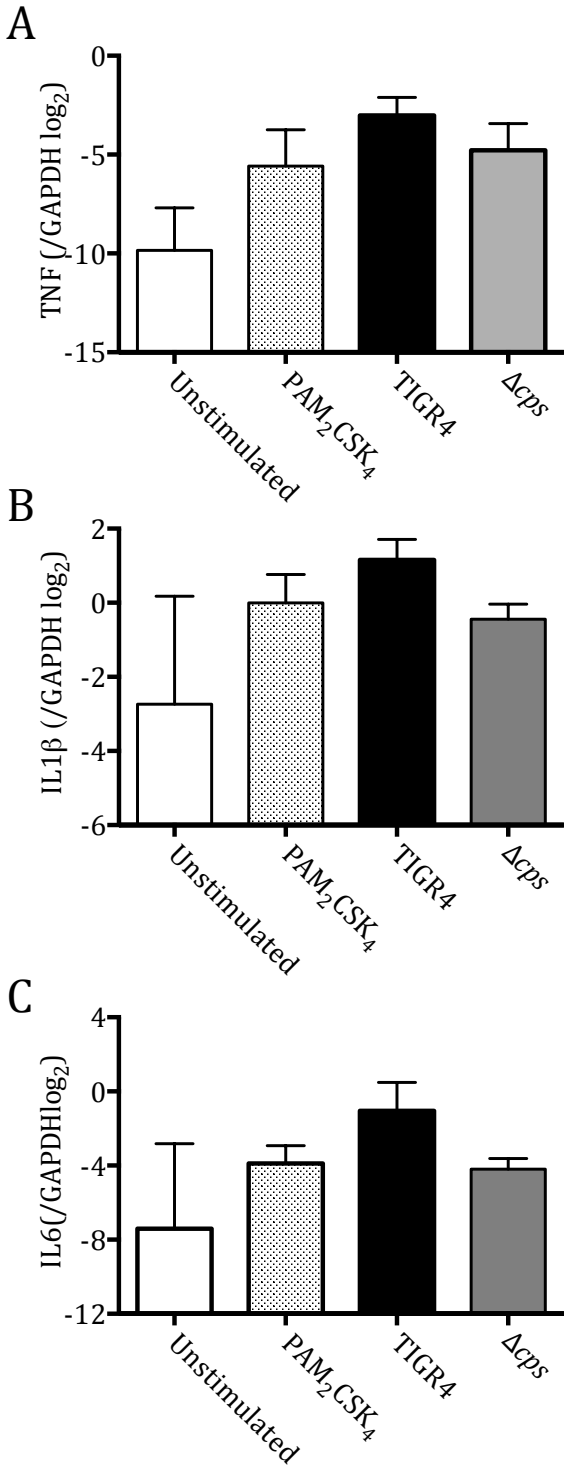

Figure 4.8 MDM cytokine responses to bacteria in serum free media

MDM were incubated with controls or bacteria at MOI 10 in RPMI supplemented with L-glutamine only for 3 hours. RNA was extracted from cells after 3 hours and results of 3 experiments are depicted as mean +/-SEM, with panel A showing TNF, B, showing IL1β, and C, IL6. Data were analysed by 1 way ANOVA, and Tukey's multiple comparison test with no significant differences found.

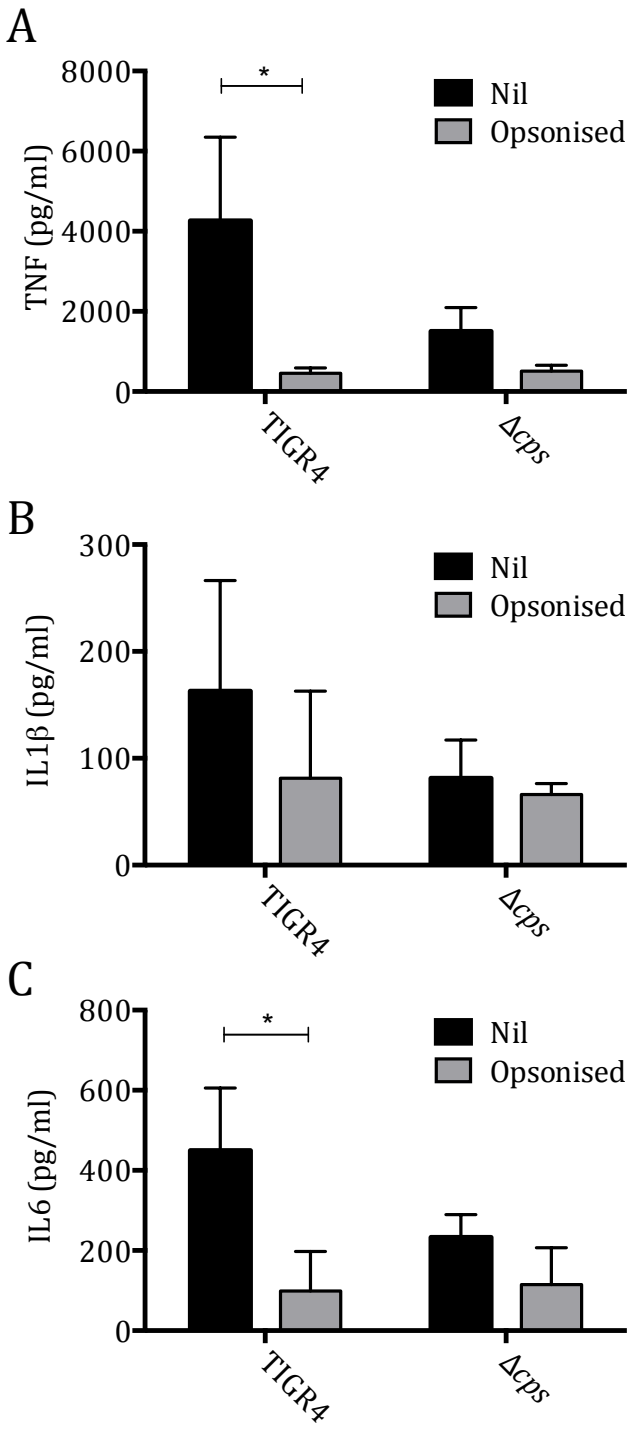

Figure 4.9 Effect of opsonisation on inflammatory response

Bacteria were opsonised in pooled human serum for 30 minutes before being diluted to the required concentration and added to MDM. Analysis from 3 experiments with supernatants 6 hours after infection are shown as mean +/- SEM. Panel A is TNF, B is IL1β, and C is IL6. Statistical analysis was with 2 way ANOVA and Tukey's multiple comparison test.

4.3 Effect of phagocytosis on the inflammatory response to capsule

The above results indicated that the increase in inflammatory responses to TIGR4 compared to the Δ*cps* strain was driven by non-phagocytosed bacteria. To further establish whether the effect of capsule on the inflammatory response to *S. pneumoniae* was driven by bacteria external to the host cell, phagocytosis was inhibited by pre-incubation of MDM with 10 μM cytochalasin D, an actin polymerisation inhibitor, for 30 minutes. Pre-incubation of MDM with cytochalasin D reduced internalisation of *S. pneumoniae* (figure 4.10, panel A) as measured by internalised bacteria in an antibiotic protection assay. Similarly fluorescent microscopy with labelled bacteria and anti IgG to label external bacteria, showed fewer green internalised bacteria with cytochalasin D (figure 4.10, panel B&C). Inhibiting phagocytosis had relatively limited effects on the cytokine response to *S. pneumoniae*, with a trend towards increasing responses (most evident with IL1β) especially for encapsulated organisms although this did not achieve statistical significance ($p=0.07$ for IL1β) (figure 4.11). Importantly, the increased inflammatory response due to encapsulated organisms compared to unencapsulated was preserved, best seen by qPCR (figure 4.12). Interestingly cytochalasin D appeared to reduce the inflammatory effect of PAM_2CSK_4. While this was not significant, it potentially suggests that cytochalasin D has off target effects that may effect the generation of an inflammatory response, as TLR2 stimulation does not require actin polymerisation or phagocytosis.

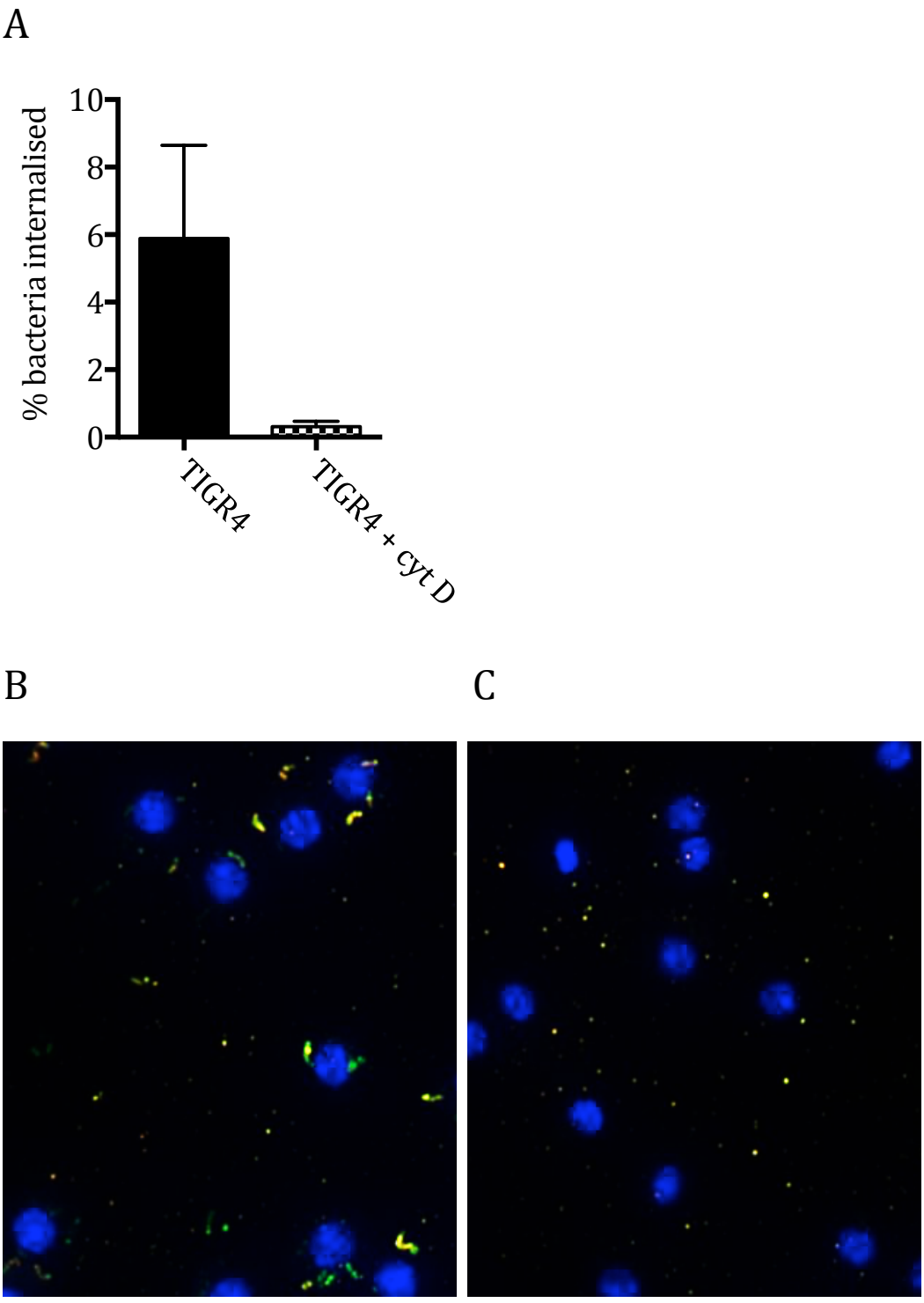

Figure 4.10 The effect of cytochalasin D on bacterial internalisation

Panel A shows the percentage of bacteria internalised using an antibiotic protection assay. Data were analysed by Mann Whitney U test, with no significant differences seen. Panel B shows MDM in a culture plate incubated with FAM-SE labelled TIGR4 Δ*cps* (in green). Bacteria external to the cells are also labelled with PE conjugated anti IgG (in red), colocalisation leads to a yellow colour. Panel C shows MDM pre-treated with 10μM cytochalasin D.

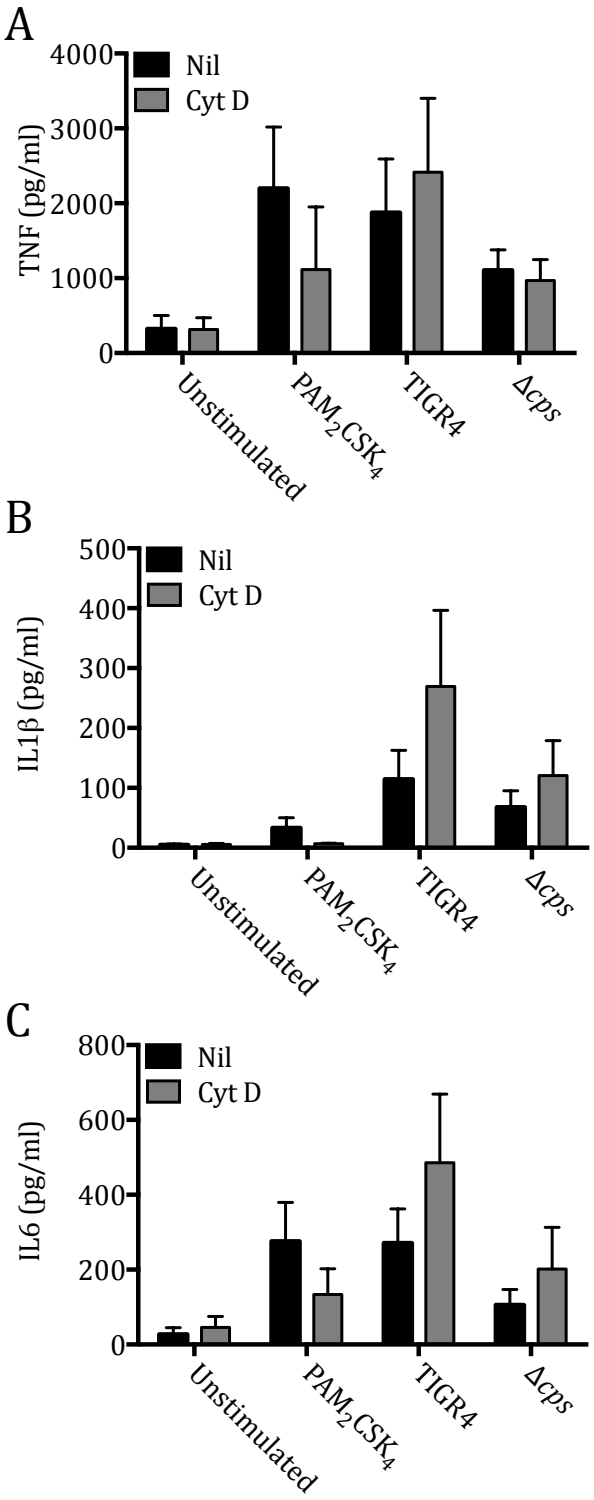

Figure 4.11 Effects of inhibiting phagocytosis on the inflammatory response

MDM were incubated with controls or bacteria at MOI 10, and supernatants were analysed for A) TNF, B) IL1β, and C) IL6 after 6 hours. The presented results are mean +/- SEM of 3 experiments, analysed by 2 way ANOVA and Tukey's multiple comparison test, with no significant differences seen.

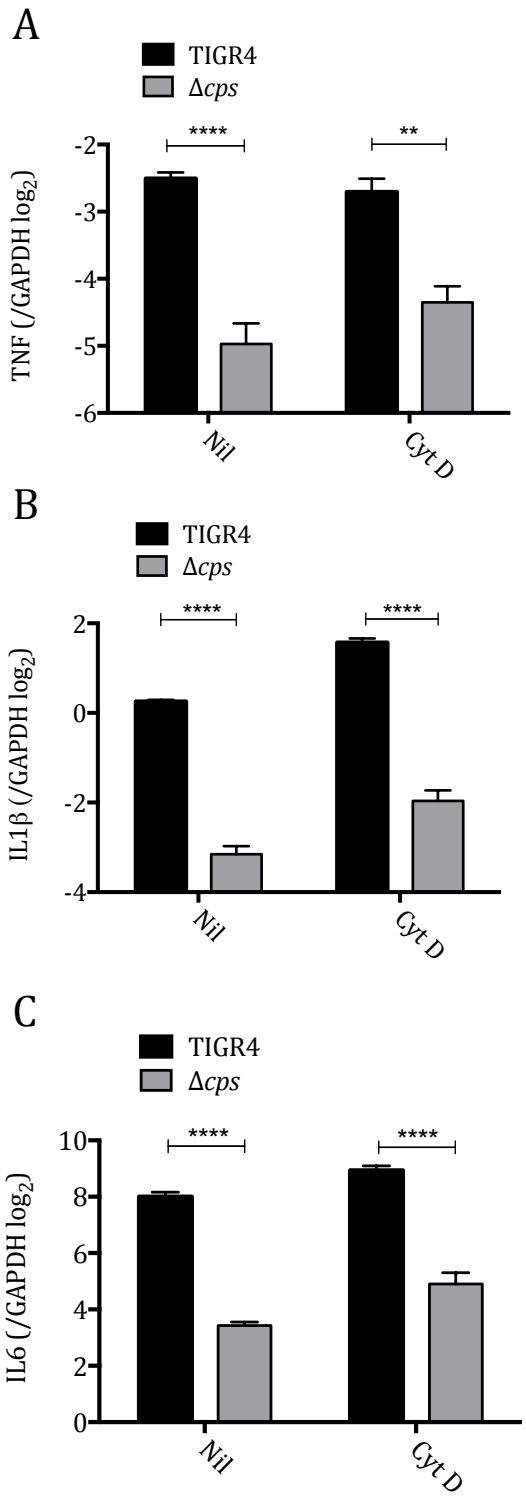

Figure 4.12 Effects of inhibiting phagocytosis on transcription of inflammatory cytokines

MDM were incubated with bacteria at MOI 10 for 4 hours, and then RNA extracted from cells. Data from 3 experiments is presented as mean +/- SEM and analysed by 2 way ANOVA and Tukey's multiple comparison test. Panel A is TNF, B is IL1β, and IL6 is seen in panel C. GAPDH was used as a housekeeping gene.

4.4 Effects of inhibiting phagocytosis on the transcriptome

The genome wide microarray analyses of MDM responses to incubation with TIGR4 or Δ*cps* were examined with and without pre-incubation with cytochalasin D to prevent phagocytosis. These data were obtained at the same time as the transcriptional data presented in chapters 4.1, 7.1, and 7.3. Cytochalasin D had some effect on MDM incubated with *S. pneumoniae*, and this was more marked for TIGR4 than the Δ*cps* strains (figure 4.13). Incubation with cytochalasin D increased the number of genes differentially regulated by TIGR4 compared to Δ*cps* (figure 4.13C, compare to figure 4.1 panel B). Of note, there was very little effect of cytochalasin D on gene expression in unstimulated cells.

Figure 4.14 and 4.15 demonstrate that pro-inflammatory genes are more highly upregulated by both wild-type and unencapsulated bacteria in the presence of cytochalasin D. In addition, while inhibiting phagocytosis increased the inflammatory response of MDM, the difference in scale of inflammatory response is maintained between wild-type and unencapsulated strains. Interestingly more genes are upregulated with the encapsulated wild-type, than unencapsulated with inhibition of phagocytosis. However the genes that were upregulated did not map to any specific pathways, many of them had unknown functions.

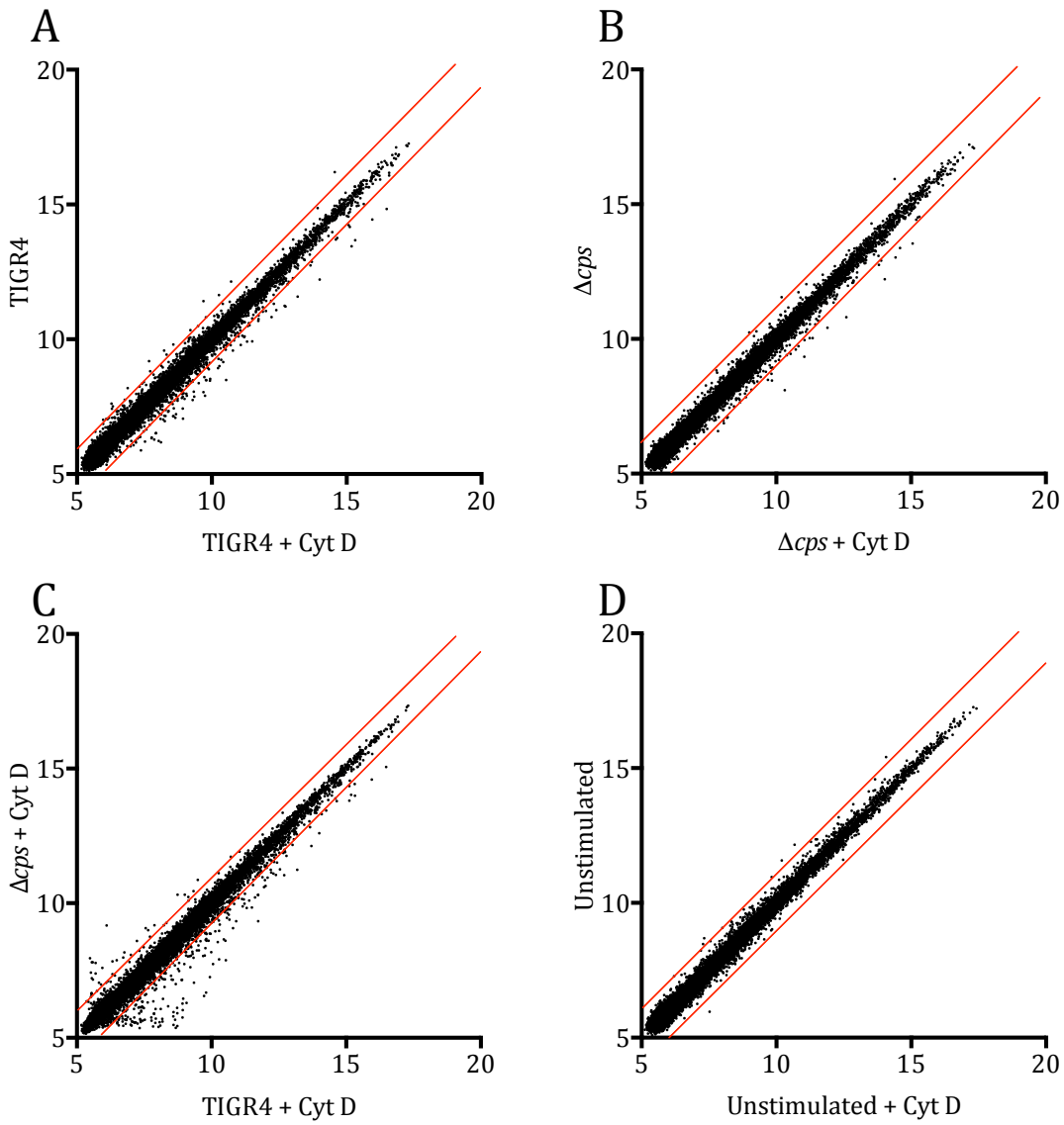

Figure 4.13 Gene expression of MDM by genome wide analysis

Relative gene expression is plotted by condition for all genes on a microarray. The mean of 3 experiments for each condition is plotted. The red lines indicated $\log_2$ of 2 fold differences in expression.

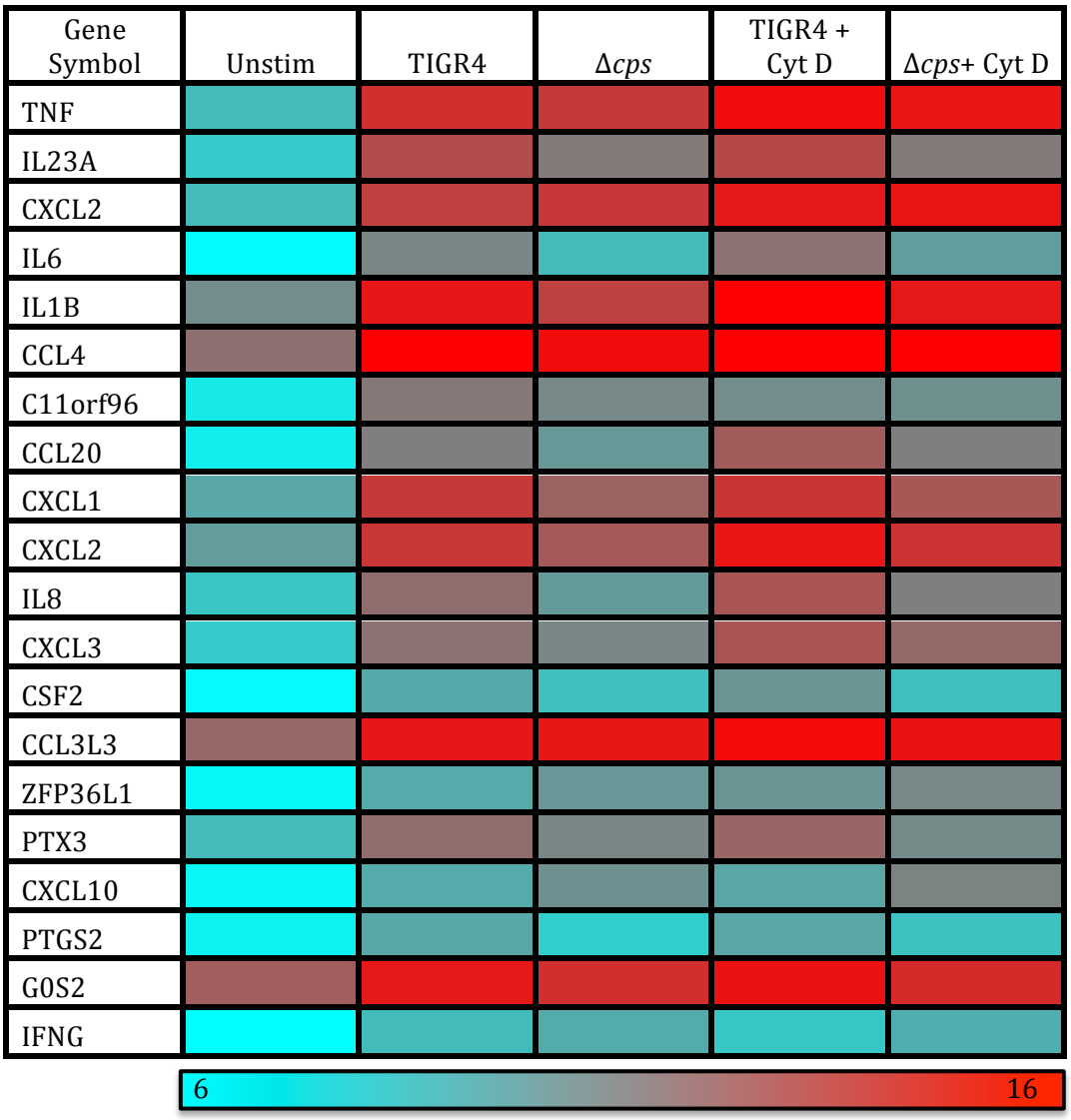

Figure 4.14 Heat map of gene expression of top 20 genes upregulated byTIGR4

Mean gene expression of MDM incubated with TIGR4 or Δ*cps* (3 donors each), with least expressed in blue, and most expressed in red. Gene order by most upregulated genes with TIGR4 compared to unstimulated. In the relevant experiments, MDM were pre-incubated with 10μM cytochalasin D for 30 minutes, which was washed off, before the addition of bacteria at MOI 10.

Gene Symbol	FC T4> Δ*cps*	FC T4+ cytD- Δ*cps* + cytD	FC T4 + CytD > T4	FC Δ*cps* + Cyt D > Δ*cps*
TNF				
IL23A				
CXCL2				
IL6				
IL1B				
CCL4				
C11orf96				
CCL20				
CXCL1				
CXCL2				
IL8				
CXCL3				
CSF2				
CCL3L3				
ZFP36L1				
PTX3				
CXCL10				
PTGS2				
G0S2				
IFNG				

Figure 4.15 Fold change in relative gene expression of top 20 upregulated genes by TIGR4

Heat map of relative differences in expression between MDM incubated with TIGR4 or Δ*cps* +/- pre-incubation with cytochalasin D. Values expressed as $\log_2$ differences in gene expression (fold change, FC), colour coded such that the most upregulated are in green, and most downregulated in black. Mean of 3 experiments displayed.

4.5 Effects of capsule on Transcription factors

NFκB is a key transcription factor that coordinates pro-inflammatory gene transcription. NFκB is induced to translocate into the nucleus to engage promoter sequences as a culmination of multiple different signalling pathways, such as TLR signalling and MAPK signalling. I therefore investigated whether MDM NFκB location after infection with *S. pneumoniae* was affected by the presence of the capsule using single cell analysis in optical tissue culture plates read on a high throughput fluorescent microscope (figure 4.16 & 4.17). Surprisingly NFκB activation in MDMs at one hour after incubation with bacteria was greater with the unencapsulated bacteria than wild-type, although by 2 hours the difference was minimal.

A commercially available transcription factor array (Panomics) was used to assess which other transcription factors were engaged with gene promoters at a protein/DNA level in MDMs infected with *S. pneumoniae*. These data were obtained from a single analysis of pooled DNA extracts. Visual inspection of the protein/DNA arrays shows that far more transcription factors were actively bound to DNA in Δ*cps* infected MDM than TIGR4 (figure 4.18). This was further analysed by Imagequant analysis software, and differences between membranes accounted for by normalising data by using the placement dots. The effect of TIGR4 appears to be largely downregulation of transcription factors that are active in unstimulated cells (i.e. metabolic and cell function pathways), with the Δ*cps* upregulating more transcription factors than wild-type (figure 4.19). However, key transcription factors such as NFκB and IRF1, which were predicted to be activated from the microarray data, were not detected, suggesting this array system lacked sensitivity.

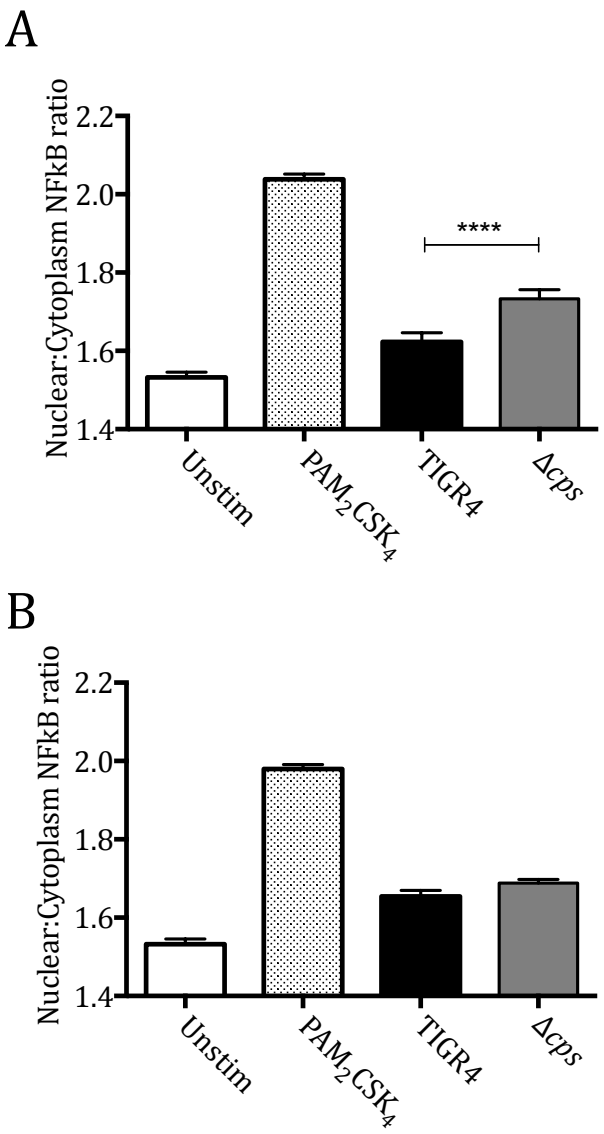

Figure 4.16 Nuclear: Cytoplasm ratio of NFκB in MDM after stimulation with bacteria or controls

Panels A & B show the ratio of NFκB between the nucleus and cytoplasm in MDM, with the data from 3 different donors at 1 and 2 hours respectively, analysed by 1 way ANOVA and Tukey's multiple comparison test.

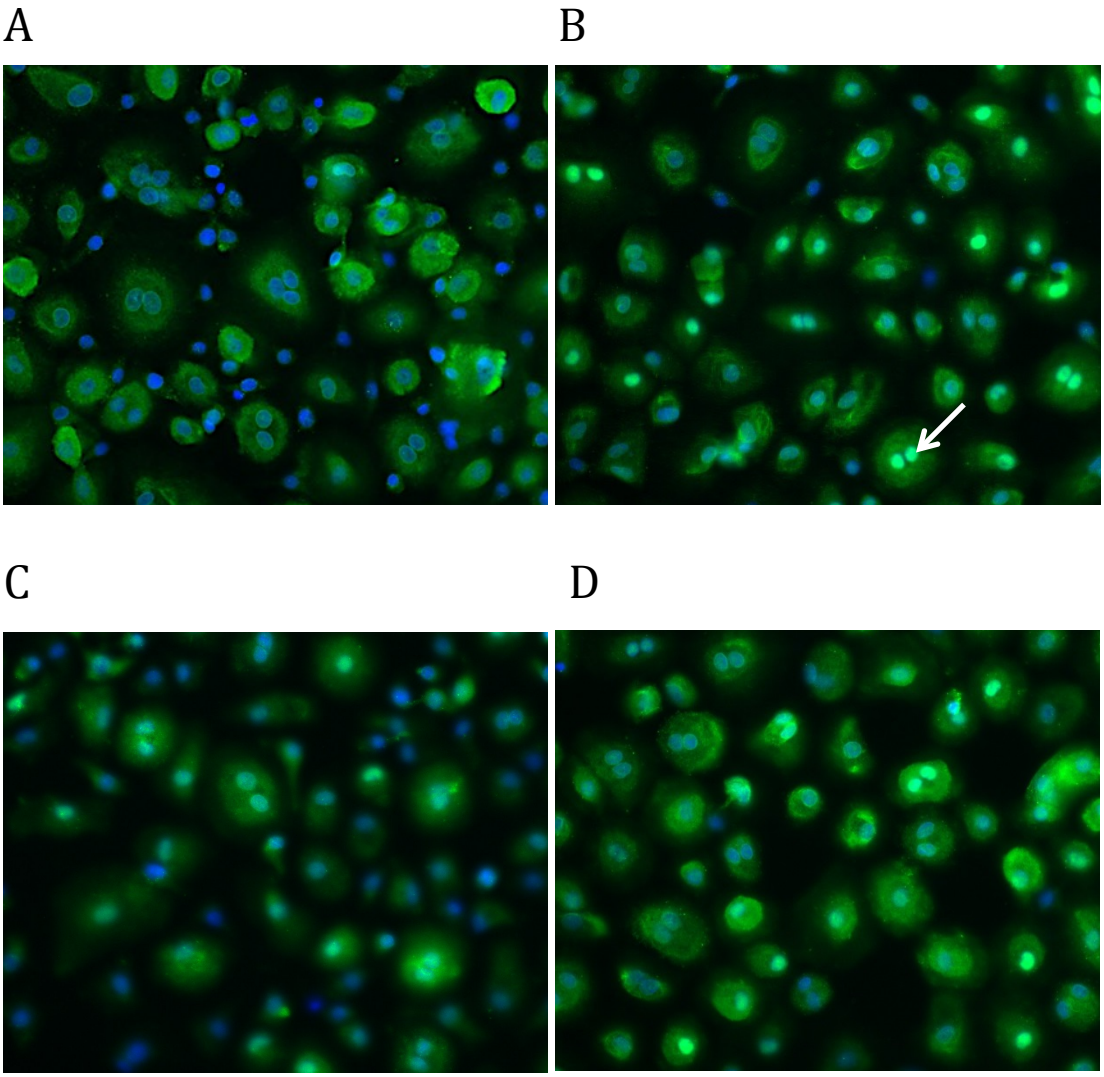

Figure 4.17 NFκB translocation 1 hour after infection

Microscopy images of high throughput optical 96 well plates with MDM incubated with bacteria. Panel A (Unstimulated), B (PAM_2CSK_4), C (TIGR4), and D (Δ*cps*) are representative images of MDM. Here the nucleus is DAPI stained, in blue, and NFκB is in green. High amounts of nuclear translocation are indicated by colocalisation of blue and green, an example is indicated by the white arrow.

A

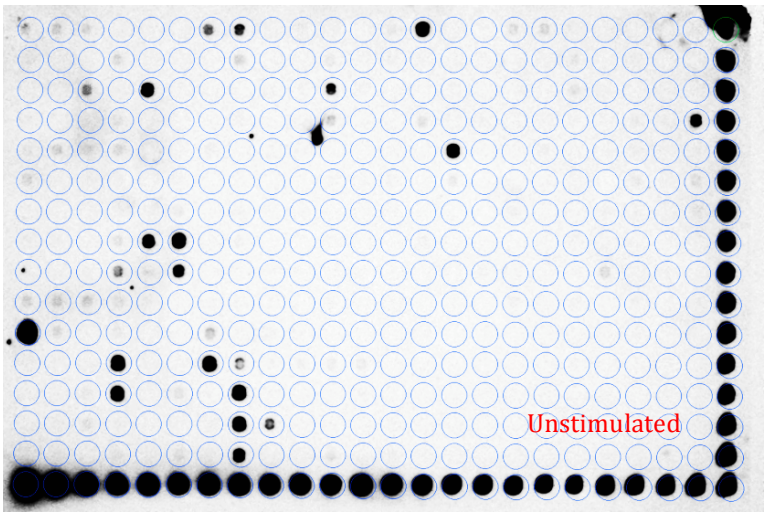

B

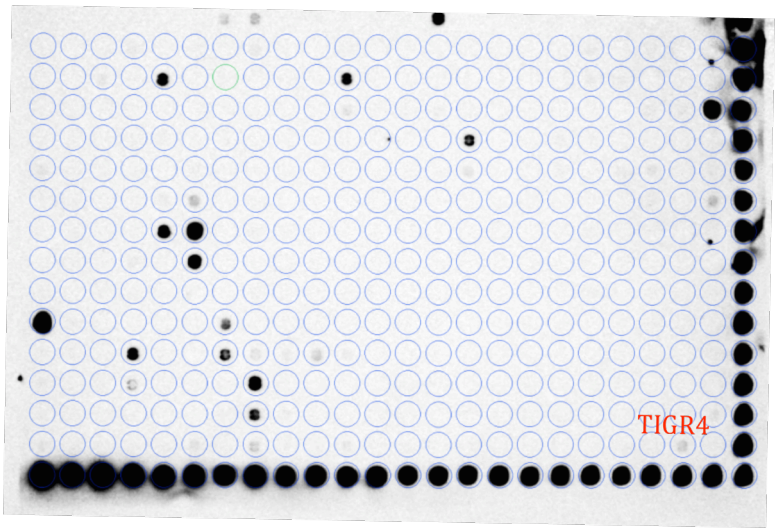

C

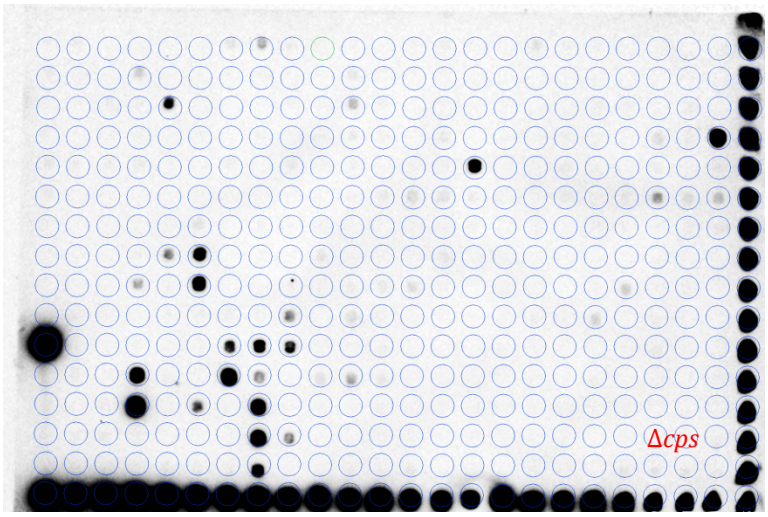

Figure 4.18 Transcription Factor Array

MDM were incubated with media or bacteria at MOI 10 for 1 hour. Nuclear extracts were isolated, then combined between 4 donors, and transcription factors bound to DNA were bound to oligonucleotide spotted membranes. Panel A is of unstimulated MDM, B, MDM incubated with TIGR4, and C, Δ*cps.*

A

TIGR4	Δ*cps*
Tat	PAX-1
TEF1	GATA2
GATA 1/2	XBP-1
GATA 2	ISRE
	PAX-2
	XRE
	ERE
	L-III BP
	HMG
	AP-3
	GFI-1
	TEF-1

B

TIGR4	Δ*cps*
HFH-3	Pbx1
MT-Box	HFH-3
PPUR	PPUR
CEF-1	PPAR
CEF-2	CEF-2
CP-1B	E12
MEF-1	RAR/DR-5
RAR/DR-5	CBF
WTI	E47
ADR-1	GATA-1/2
NF-E1/YY!	CREB
Elk-1	SMAD-3/4
Antioxidant RE	
L-III BP	
PAX-3	
AP-3	
PAX-4	
PAX-6	
AFP-1	
Beta-RE	
HFH-2	
PAX-8	
c-Fos BP	

Figure 4.19 Active Transcription Factors

After quantification of chemiluminescence on protein/DNA membranes (figure 3.20), relative activity of transcription factors was estimated. Panel A shows transcription factors that are >2 fold upregulated compared to unstimulated MDM, and panel B, the transcription factors that are <2 fold downregulated.

4.6 Effect of capsule on MAPK signalling response of macrophages

As MAPK signalling is critical in multiple responses downstream of PRR activation and cytokine-cytokine receptor interaction, western blotting was used to assess the activity of these pathways. Although there was more pro-inflammatory cytokine production at both transcriptional and secretion level with the TIGR4 strain, there appears to be much more activation of all 3 MAPK cascades with the Δ*cps* mutant compared to TIGR4 by 60 minutes (figure 4.20 & 4.21) suggesting greater PRR activation by the Δ*cps* strain. In contrast, a phosphoarray at 30 minutes after incubation of bacteria with MDM showed no significant differences between the strains across a range of kinase pathways (figure 4.22 & 4.23). This timepoint was chosen because there was significant NFκB activation evident by 1 hour and to avoid confounding by any autocrine activation by pro-inflammatory cytokines, so that the initial engagement of MDM with bacteria would be the most important factor in the phosphorylation events detected. Overall, the data shows no suggestion that the increased inflammatory response seen by encapsulated organisms can be attributed to increases in MAPK signalling. Rather the data indicate there might be greater MAPK signalling in response to the unencapsulated strain.

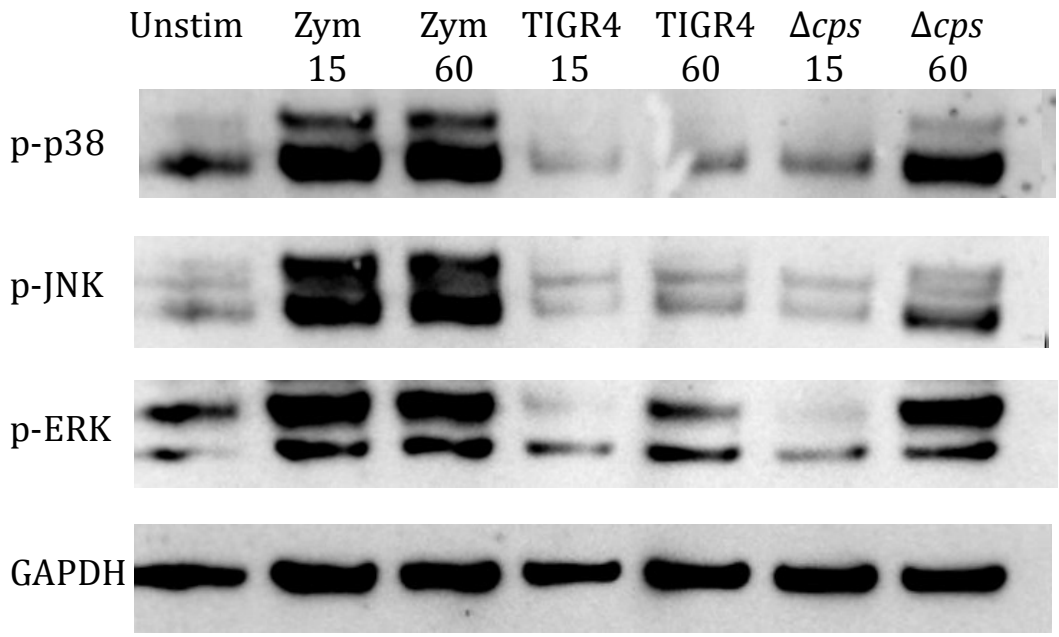

Figure 4.20 Western blot of MDM for MAPK

Western blot of 4 pooled MDM lysates with TIGR4 or Δ*cps*, with zymosan as a positive control and media only as an unstimulated negative control. Lysates were probed for phospho-MAPK and GAPDH was used as a loading control. One example of 2 separate western blots shown.

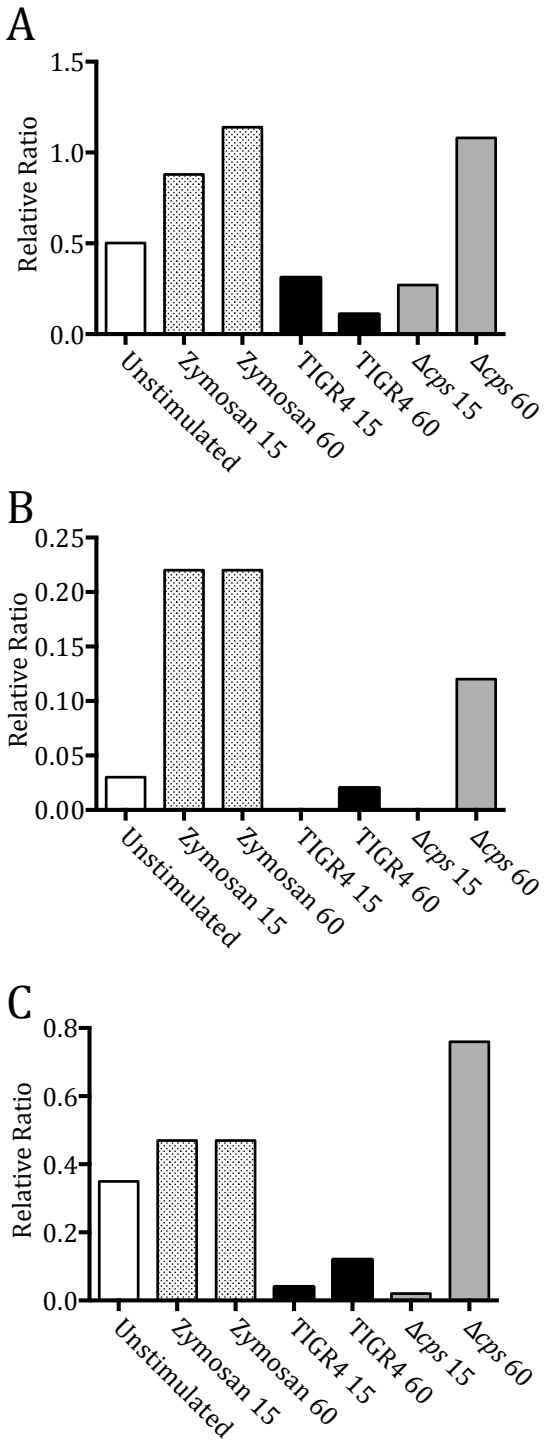

Figure 4.21 Quantification of MAPK Western blots

Western blots from figure 4.20 were quantified by Imagequant and presented as relative density normalised to GAPDH. A) phospho-p38, B) phospho–JNK, and C) phospho-ERK.

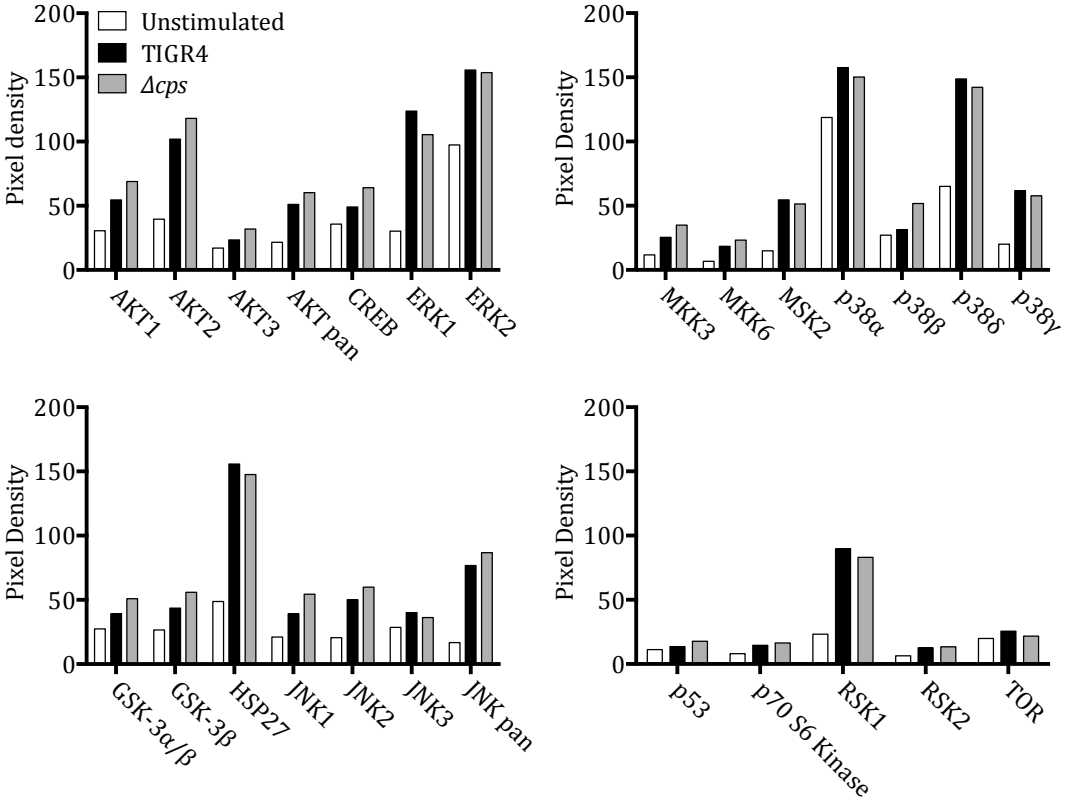

Figure 4.22 Analysis of phosphoarray

Panel A shows relative pixel density analysed by ImageJ of a phosphoarray of 4 pooled MDM lysates at 30 minutes of incubation.

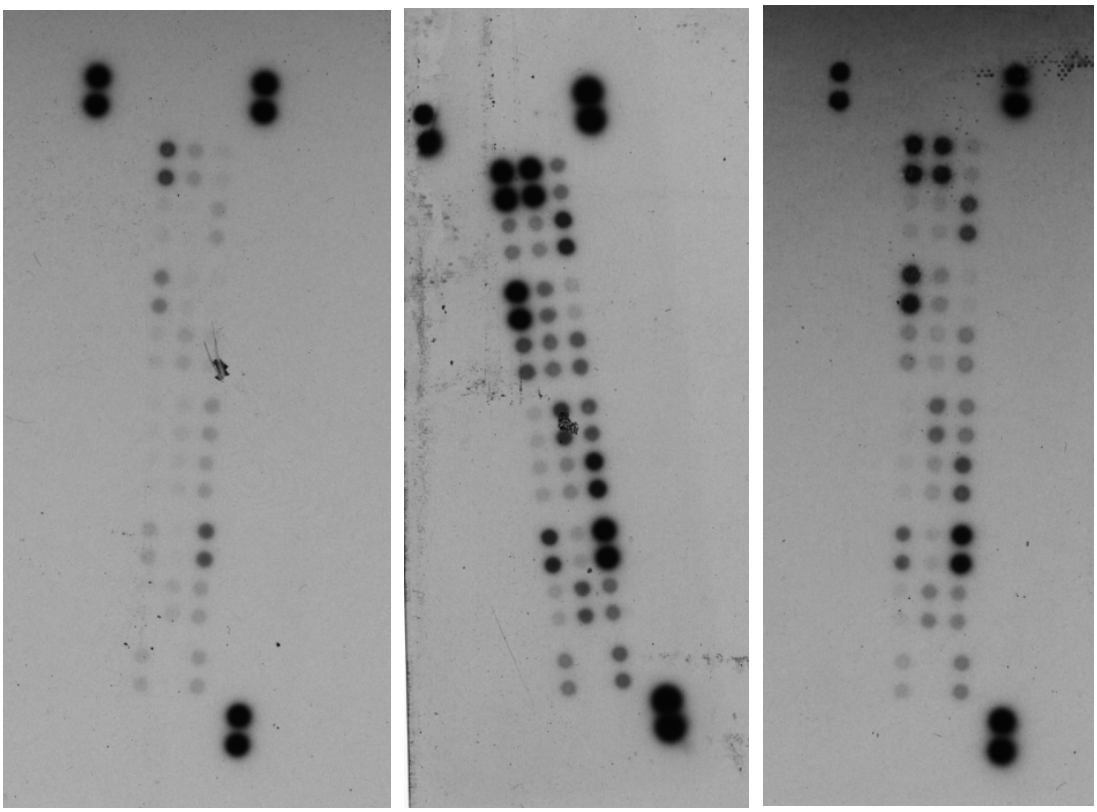

Figure 4.23 Phosphoarray of MDM at 30 minutes of incubation

Images of phosphoarray membranes of exposed for 45 seconds of MDM lysates after incubation with: A) media only, B) TIGR4, and C) Δ*cps* are shown.

4.7 Effect of capsule on TLR2 stimulation, lectin stimulation, and scavenger receptors

As inhibiting phagocytosis preserved the difference between TIGR4 and Δ*cps*, specific cell surface PRR that might explain this difference were investigated to see if they could explain the difference between strains.

TLR2 is recognised as an important PRR that recognises lipoproteins of *S. pneumoniae* (Tomlinson, Chimalapati et al, 2014). Purified capsule, even at very high concentrations, did not induce TLR2 activation in a reporter cell assay (figure 4.24, A). Interestingly after incubation with whole bacteria there was less TLR2 activation with TIGR4 compared to Δ*cps* strains at MOI 10, with no significant differences seen at other MOI (figure 4.24, B). However, transfected HEK cells may not represent TLR2 function in professional phagocytic immune cells such as macrophages.

Lectins are a group of receptors that recognise carbohydrate motifs, some of which serve as PRRs, for example in the recognition of fungal cell wall products, and could potentially recognise *S. pneumoniae* capsular polysaccharide. Lectins are a diverse group of receptors, but they largely signal through either the Syk or c-Raf pathways. Syk is also activated downstream of immunoglobulin recognising Fc receptors, as well as B and T cell receptors. As the media used for MDM culture is usually supplemented with human serum, which would contain antibodies, the experiments looking for phosphorylation events in these pathways were performed in serum free conditions. Immunoblots showed constitutive phosphorylation of both Syk and c-RAF, with no evidence of differential activation between TIGR4 and Δ*cps* (figure 4.25 & 4.26). Furthermore Syk inhibition had no inhibitory effect on the inflammatory response to either TIGR4 or Δ*cps* (figure 4.27). It was a surprise to find marked basal activation of both these signalling molecules. This suggests that the experimental setup or processing of the lysates induced some lectin activation or that there was poor specificity of the antibodies to the phosphorylated kinases. This means that these

data may require more parallel experiments to confirm no lectin involvement in capsule recognition.

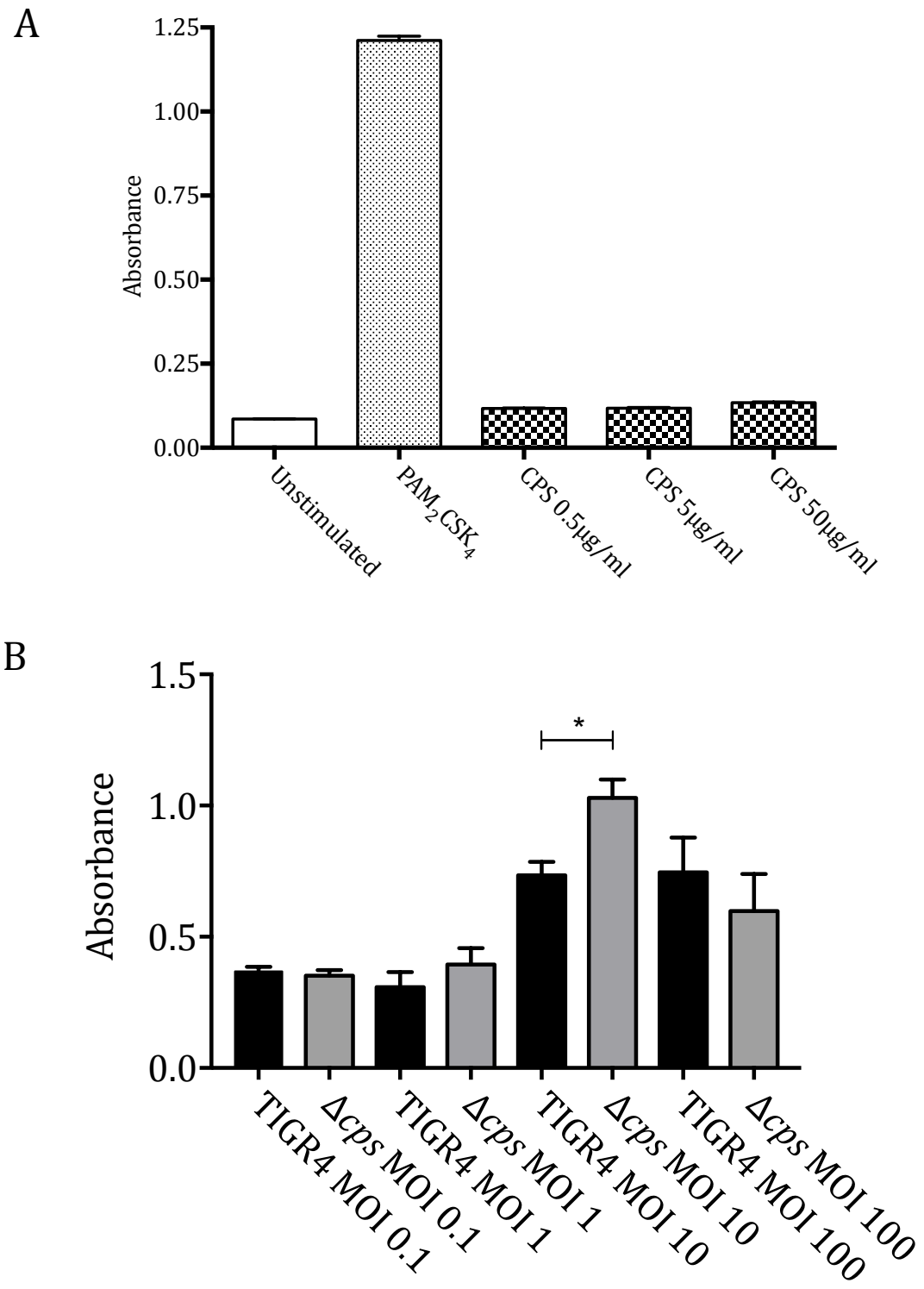

Figure 4.24 HEK TLR2 activation

HEK cells, transfected with TLR2 linked to a NFκB SEAP reporter, were incubated with A) purified capsular polysaccharide at varying concentrations, positive control, or B) bacteria at varying MOI. Supernatant removed and analysed on a microplate reader. Mean +/-SEM of 5 experiments shown and analysed by 1 way ANOVA with Tukey's multiple comparison test.

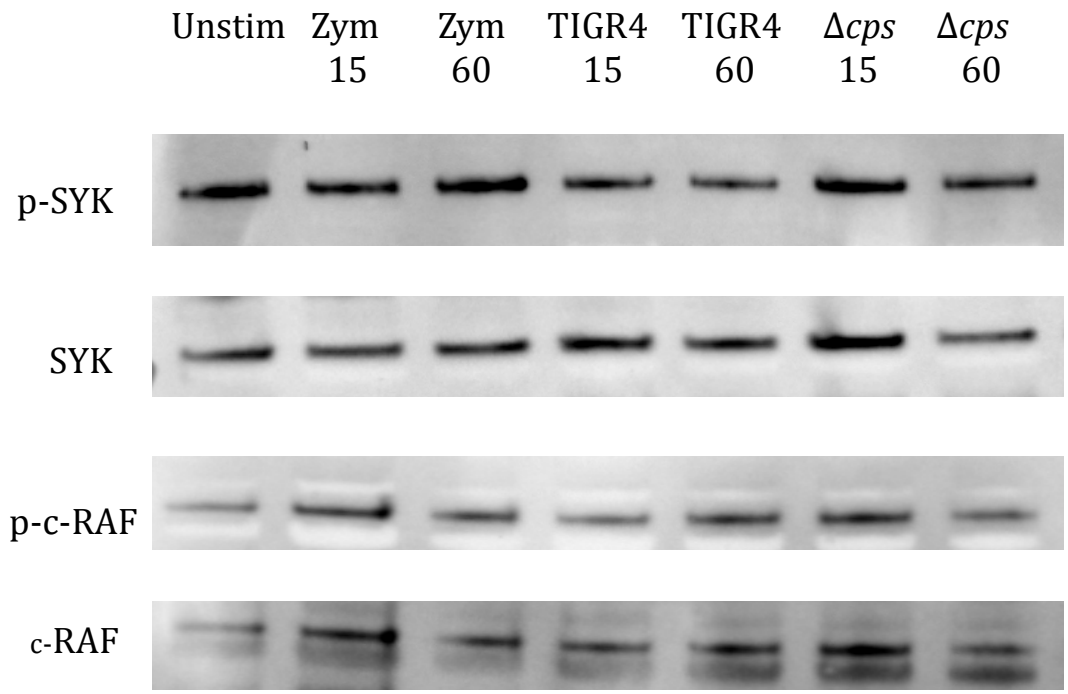

Figure 4.25 Western blots of MDM lysates for lectin signalling

Western blot of 4 MDM lysates with TIGR4 or Δ*cps*, with zymosan as a positive control and media only as an unstimulated negative control. Lysates were probed for phospho-SYK and c-RAF, with total SYK and c-RAF used as loading controls. Representative blot of 2 experiments shown.

A

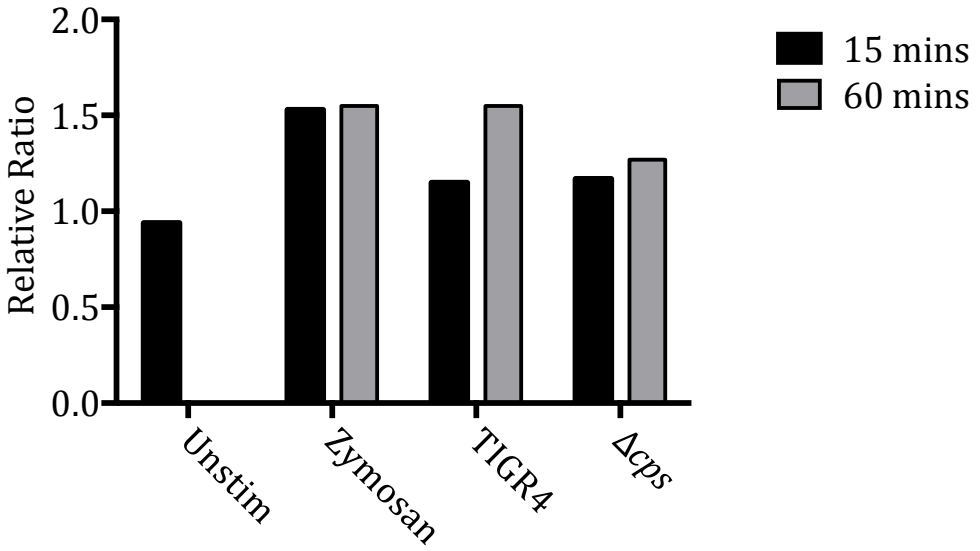

B

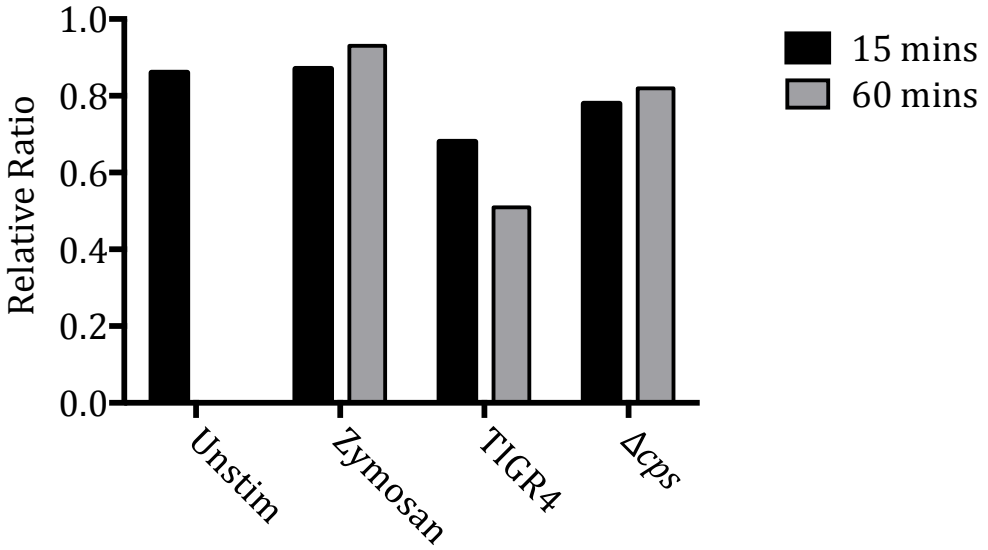

Figure 4.26 Westerns of SYK and c-RAF phosphorylation

Western blot of 4 MDM lysates with TIGR4 or Δ*cps*, with zymosan as a positive control and media only as an unstimulated negative control shown in panel A. Lysates were probed for phosphorylated SYK (at 525) and total SYK, phosphorylated c-RAF and total c-RAF. This was quantified by Imagequant; phospho-SYK presented in panel A, and phospho-c-RAF presented in panel B.

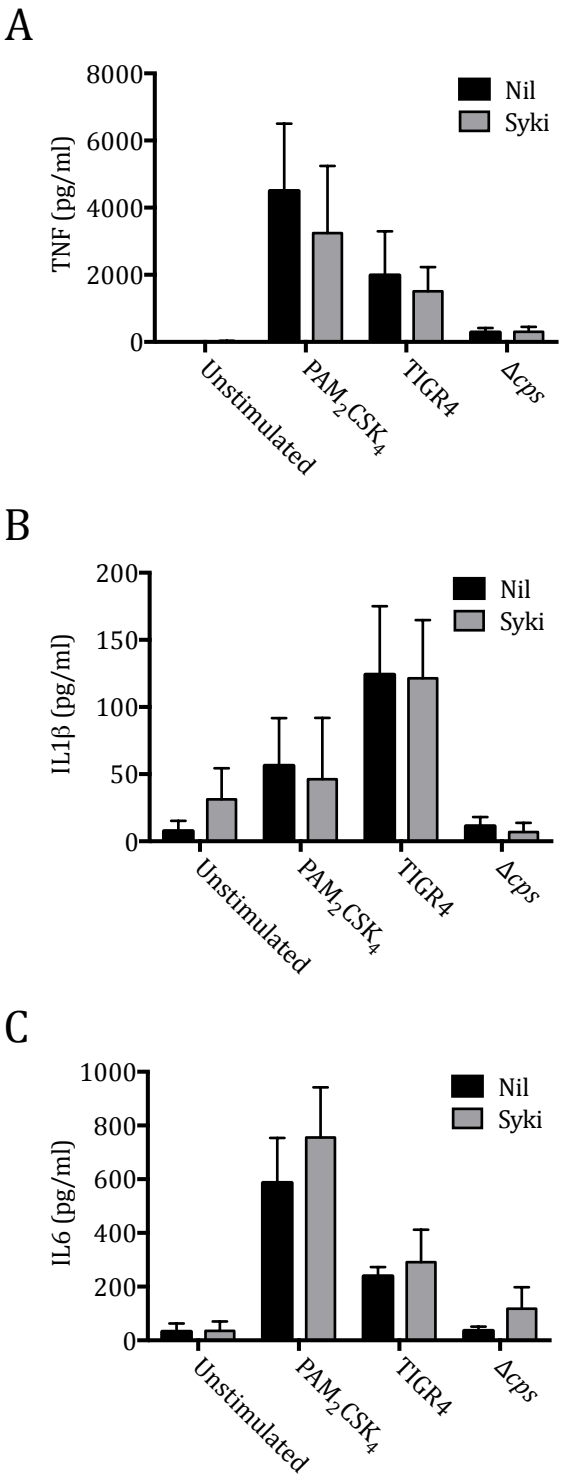

Figure 4.27 The effect of Syk inhibition of MDM cytokine secretion

Mean +/- SEM of 3 MDM experiments with cytokines measured in cell culture supernatants 6 hours after stimulation with positive control or bacteria at MOI 10. Cells pre-incubated with Syk inhibitor (Oxindole, Sigma Aldrich, Gillingham at 2μM) for 1hour. Panel A shows TNF, panel B shows IL1β, and panel C shows IL6. Analysed by 2 way ANOVA and Tukey's multiple comparison test with no significant differences seen.

Similarly scavenger receptors are a heterogeneous group of receptors that recognise anionic structures. Previous work has shown that MARCO in particular is important for the recognition of *S. pneumoniae* capsule, and that it facilitates non-opsonic phagocytosis. In addition, MARCO recognition of components of other organisms such as *Mycobacterium tuberculosis* cord factor, have been shown to increase TLR2 responses. However, neutralisation of MARCO with antibody failed to reduce the inflammatory response of MDM (figure 4.28). Similarly, competitive blockade of all type A scavenger receptors with dextran sulphate failed to significantly reduce the inflammatory response to either encapsulated or unencapsulated strains (figure 4.29).

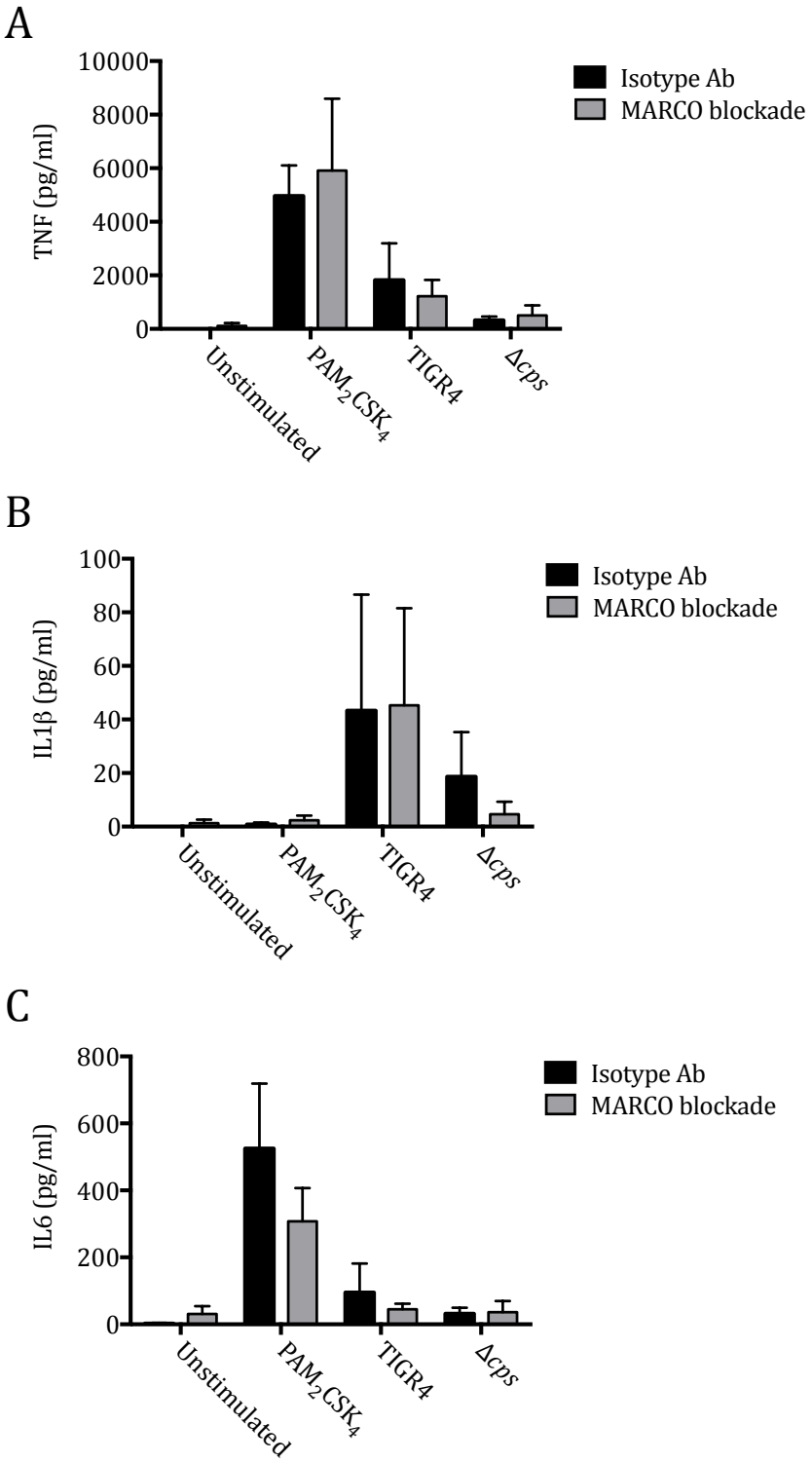

Figure 4.28 Effect of MARCO blockade on MDM cytokine secretion

Mean +/- SEM of 3 MDM experiments with cytokines measured in cell culture supernatants 6 hours after stimulation with positive control or bacteria at MOI 10. Cells pre-incubated with mouse anti-human monoclonal MARCO antibody (eBioscience) or isotype control (both at 25 μg/ml) for 1hour. Panel A shows TNF, panel B shows IL1β, and panel C shows IL6. Analysed by 2 way ANOVA and Tukey's multiple comparison test with no significant differences seen.

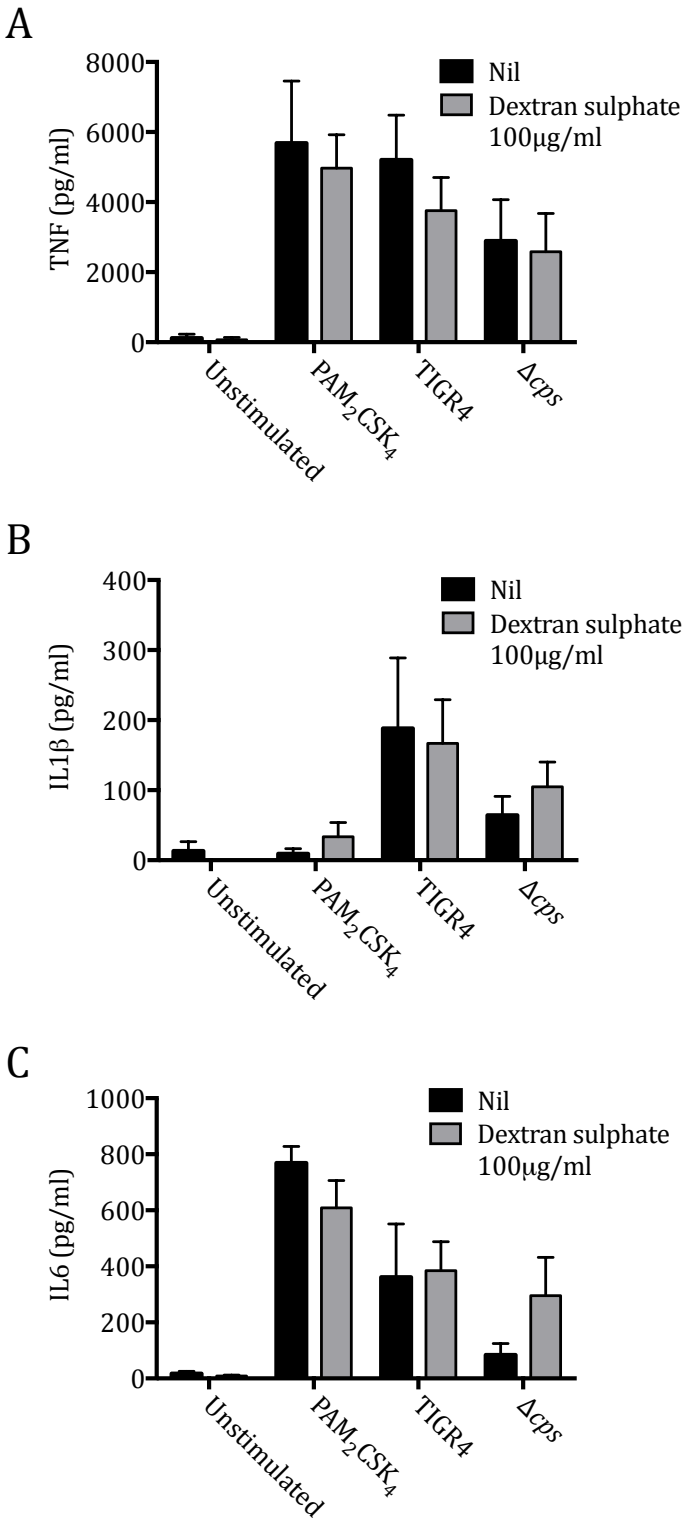

Figure 4.29 The effect of scavenger receptor blockade on MDM cytokine secretion

Mean +/- SEM of 4 MDM experiments with cytokines measured in cell culture supernatants 6 hours after stimulation with positive control or bacteria at MOI 10. Some cells pre-incubated with dextran sulphate at 100µg/ml for 1hour to block class A scavenger receptors. Panel A shows TNF, panel B shows IL1β, and panel C shows IL6. Analysed by 2 way ANOVA and Tukey's multiple comparison test with no significant differences seen.

4.8 Chapter Summary

Whole genome transcriptional analysis indicates that the most upregulated genes in MDM incubated with *S. pneumoniae* involve pro-inflammatory cytokines and chemokines. The wild-type strain induced a very similar upregulated gene signature to the unencapsulated mutant, but to a greater extent. Bioinformatic analysis suggests that NFκB and IFN stimulating transcription factors are the most active on MDM exposure to *S. pneumoniae*, and that TLR, NOD, and cytokine signalling pathways are the most stimulated intracellular signalling pathways.

The best-recognised role of capsule is to evade phagocytosis, and this was confirmed in both human and mouse macrophages. Pre-opsonisation of bacteria reduced the inflammatory sequelae, more evident in the wild-type encapsulated organism. The reduced inflammatory response to unencapsulated bacteria is not solely due to more rapid internalisation, as complete inhibition of phagocytosis with an actin polymerisation inhibitor preserved the differences between the strains. These observations suggest that the presence of capsule at the host cell surface could modify the inflammatory response to other components of the bacteria, as without phagocytosis the bacteria would remain at the cell surface, and thus able to stimulate more prolonged activation of cell surface receptors (frustrated phagocytosis). The genome-wide transcriptional response to bacteria after inhibition of phagocytosis supports this, as the differences between wild-type and unencapsulated strains were minimally affected by cytochalasin D. Cytochalasin D could have other effects on the inflammatory response: bacterial uptake and subsequent bacterial breakdown may stimulate inhibitory pathways that would not been seen with phagocytosis inhibition, it is also known to cause p53 mediated cell cycle arrest therefore may affect inflammatory signalling directly, and its effects on actin polymerisation could have unintended pro-inflammatory effects as the cell continues to signal the cell to move. These are potential confounders for the effects of cytochalasin D on MDM responses to *S. pneumoniae*.

NFκB, a critical transcription factor that regulates pro-inflammatory cytokine transcription, is activated by *S. pneumoniae*. Despite this the unencapsulated strain induced more NFκB translocation and also stimulated the activation of more transcription factors than TIGR4. The unencapsulated strain also induced more activation of MAPK than wild-type within 60 minutes of incubation with MDM. It should be noted that GAPDH has been used as a control to account for total protein, but this does not account for upregulation of unphosphorylated proteins, and it can be argued that total amount of MAPK is a better control. These data indicate that the recognition of polysaccharide capsule may inhibit multiple pathways that culminate in transcription factor activation. However this transcription factor activation did not correlate with pro-inflammatory gene transcription, possibly reflecting the complex interplay between transcription factors, some of which may inhibit the downstream consequences of NFκB activation. This discordance could also be explained by longer duration of or amplification of transcription factor action within the nucleus driven by alternative signalling pathways. The transcription factor array assay had poor sensitivity so strong conclusions should not be drawn from the results.

TLR2, lectin, and scavenger receptor activation was similar between strains, so it is as yet unclear if a cell surface PRR actively recognises capsular polysaccharide to cause this effect. It should be noted that the transfected HEK cell line, while effective for simple TLR2 stimulation, may not be generalizable in the context of complex infection. These cells do not phagocytose bacteria and therefore there is less dynamic effect on bacterial cell numbers, which would only be restricted by the nutrient content of the media. In addition, the length of the incubation required to generate a colorimetric change (16 hours), may result in some cell death that could confound the results. I did not assess bacterial counts for adherence or invasion, which could additionally have confounded the data. So they are a blunt tool to assess TLR2 activation, and may not be reflective of what happens in MDM, and ore particularly *in vivo*. The immunoblots of Syk and cRAF activation showed no difference between negative and positive controls. This means that they are very difficult to interpret.

It may be that there is constitutional lectin activation in MDM in sugar containing media in tissue culture plates. However, non-specificity of the antibody to phospho Syk and c-Raf (i.e. off target binding to total Syk and Raf) could also explain the lack of difference between negative and positive control. As such, more supportive data is required to definitively state there is no difference in lectin signalling due to capsule.

It remains unclear how the capsule is recognised to have this effect, and an alternative hypothesis is that capsule may rather act as a physical barrier to recognition of other cell surface ligands, which then have inhibitory effects on the inflammatory response.

5 Effects of serotype 4 capsule expression on other *S. pneumoniae* serotypes and *Streptococcus mitis*

5.1 Effect of capsule on inflammatory response to various serotypes

To ensure the difference in inflammatory response between TIGR4 and Δ*cps* strain was not serotype specific, the experiments were repeated with 3 other serotypes and their isogenic unencapsulated mutant strain derivatives. For all three serotypes, MDM supernatant pro-inflammatory cytokine levels were not significantly different between encapsulated and unencapsulated strains. There were relatively large differences in some pro-inflammatory cytokine responses to wild type serotype2 and 23F compared to their isogenic unencapsulated mutants, but inter donor variability prevented the results from being statistically significant (figure 5.1). For the serotype 3 strain the presence of the capsule showed a trend towards reduction in the levels of pro-inflammatory cytokines, perhaps as a consequence of its heavily mucoid phenotype.

The absence of capsule affected TLR2 stimulation, with increased TLR2 activation for TIGR4 and serotype 2, but less with serotype 3 (figure 5.2). There were variations between serotypes in TLR2 stimulation with serotypes 2, 3, and 23F showing increased TLR2 stimulation compared to the serotype 4 strain. Interestingly these differences were no longer evident between unencapsulated strains. As data in chapter 4 indicated that capsular material does not directly induce TLR2 stimulation, this is more evidence that capsule is likely to modify how bacterial surface components interact with TLR2 on host cell membranes.

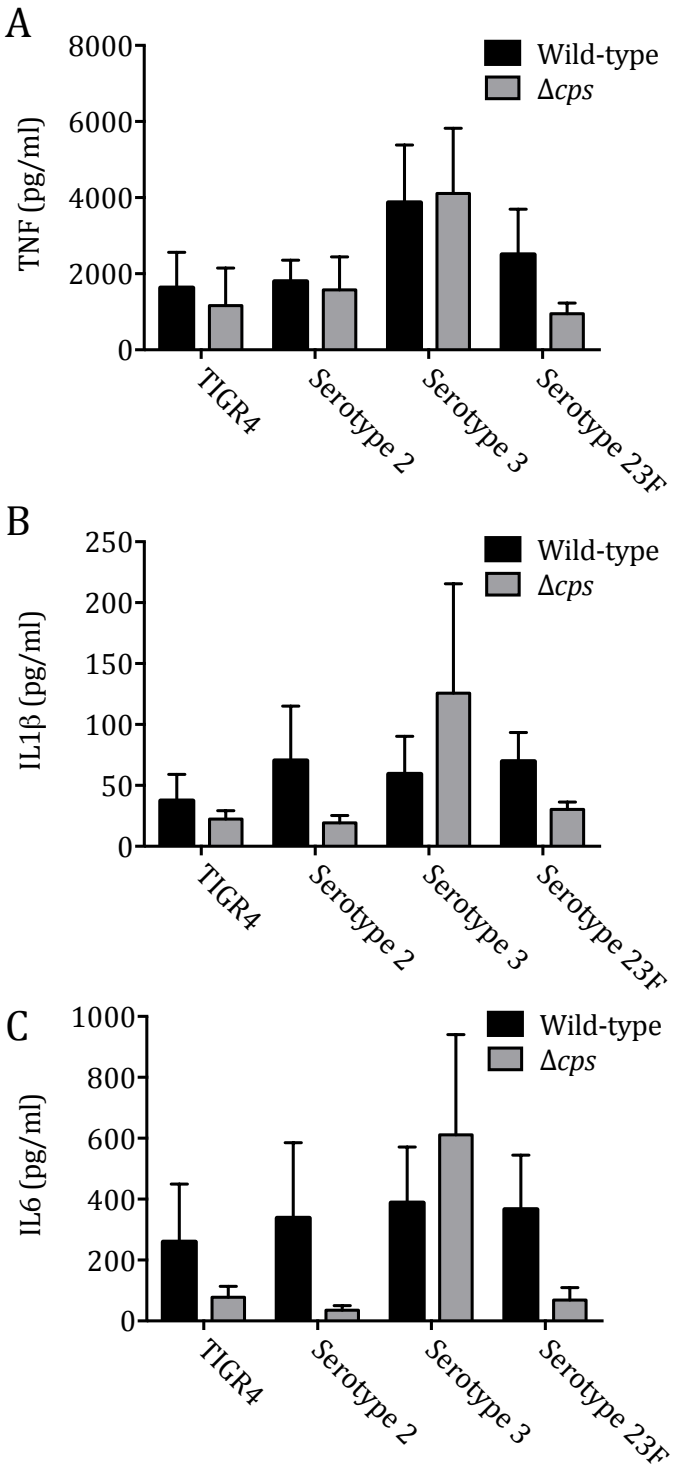

Figure 5.1 MDM cytokine response to different serotypes and their isogenic unencapsulated mutants

MDM were incubated with 4 different serotypes and their isogenic unencapsulated mutants at MOI 10 for 6 hours. Supernatants were removed and analysed for A) TNF, B) IL1β, and C) IL6. Data are presented as mean +/- SEM. No results were significantly different by 2 way ANOVA and Tukey's multiple comparison test.

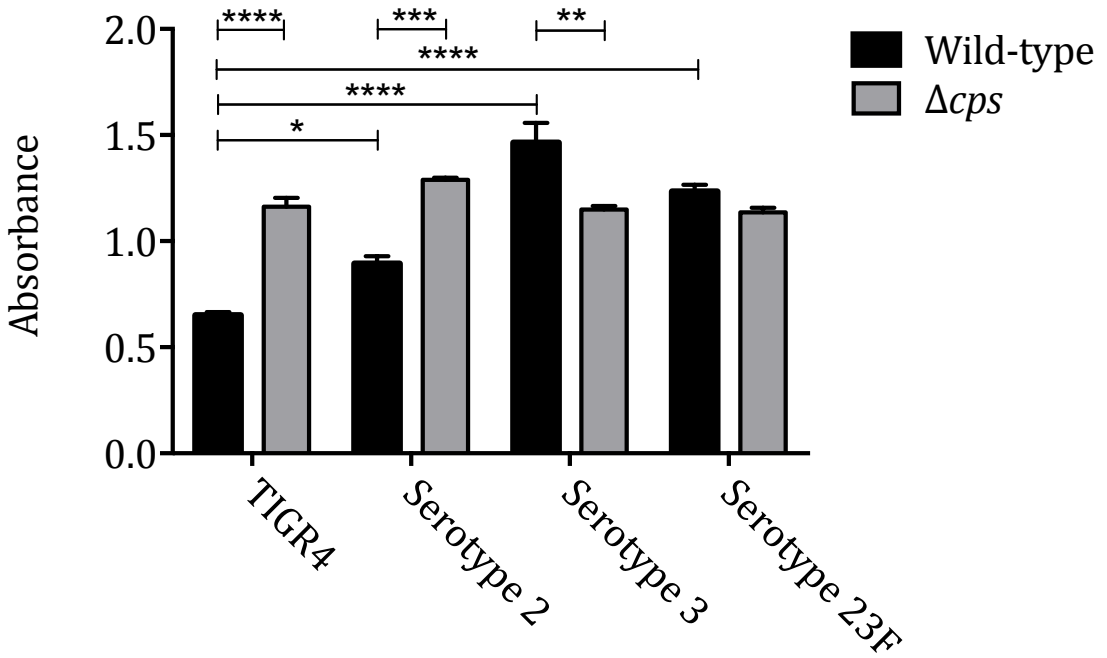

Figure 5.2 TLR2 reporter cell responses to different serotypes and their isogenic unencapsulated mutants

HEK 293 cells transfected with TLR2 and NFκB linked to a SEAP reporter were incubated with several wild-type (WT) *S. pneumoniae* serotypes and their isogenic unencapsulated mutants at MOI 10 for 20 hours. Supernatant colorimetric change is expressed as absorbance. Data are presented as the mean +/- SEM of 3 separate experiments. Analysed by 2 way ANOVA and Tukey's multiple comparison test.

5.2 Inflammatory response of capsule switch *S. pneumoniae* strains

To investigate whether capsular serotype directly affected MDM inflammatory response to *S. pneumoniae*, capsule switch strains based on the TIGR4 background were incubated with MDM. Again donor variation made data interpretation difficult. When comparing results for non-isogenic strains there was a significantly increased IL6 release by MDMs in response to a serotype 6A strain compared to TIGR4 (figure 5.3), with a trend towards more TNF from 6A compared to the other serotypes. While other differences were not statistically significant, both 6A and 14 appeared to induce more IL1β than TIGR4. 23F appeared to generate relatively similar inflammatory responses to TIGR4. This may suggest that serotype differences influence specific cytokines differentially, so multiple PRR are likely to be involved to account for variation in response to serotype.

There were differences between TIGR4 strains expressing different capsular serotypes, showing that the capsule itself affects inflammatory responses (figure 5.4), and that non-capsular differences between serotypes do not account for all the variation in inflammatory response between serotypes. TIGR4 + 6A induced more TNF and IL6 than TIGR4, and TIGR4 + 23F induced more IL6 than TIGR4, though IL1β levels were again quite variable.

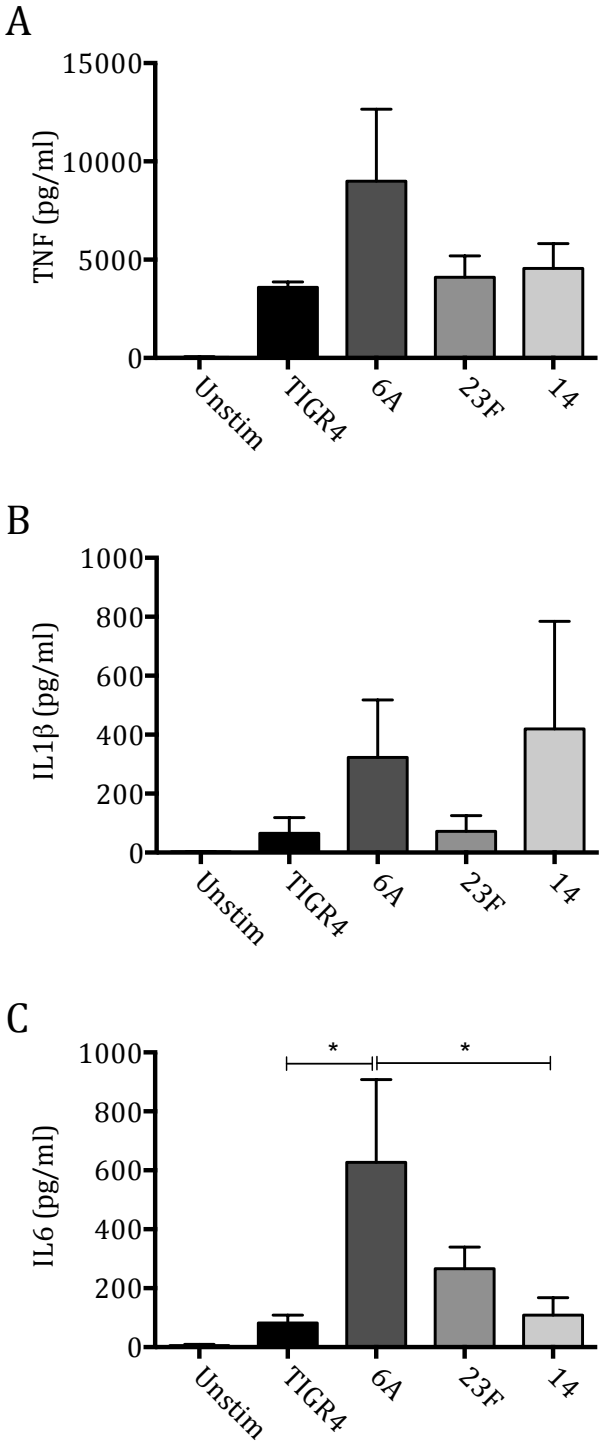

Figure 5.3 MDM cytokine response to varied serotypes

MDM were incubated with different serotypes. Supernatants were removed after 6 hours and analysed for A) TNF, B) IL1β, and C) IL6. Data are presented as mean +/- SEM. Results were analysed by 1 way ANOVA and Tukey's multiple comparison test.

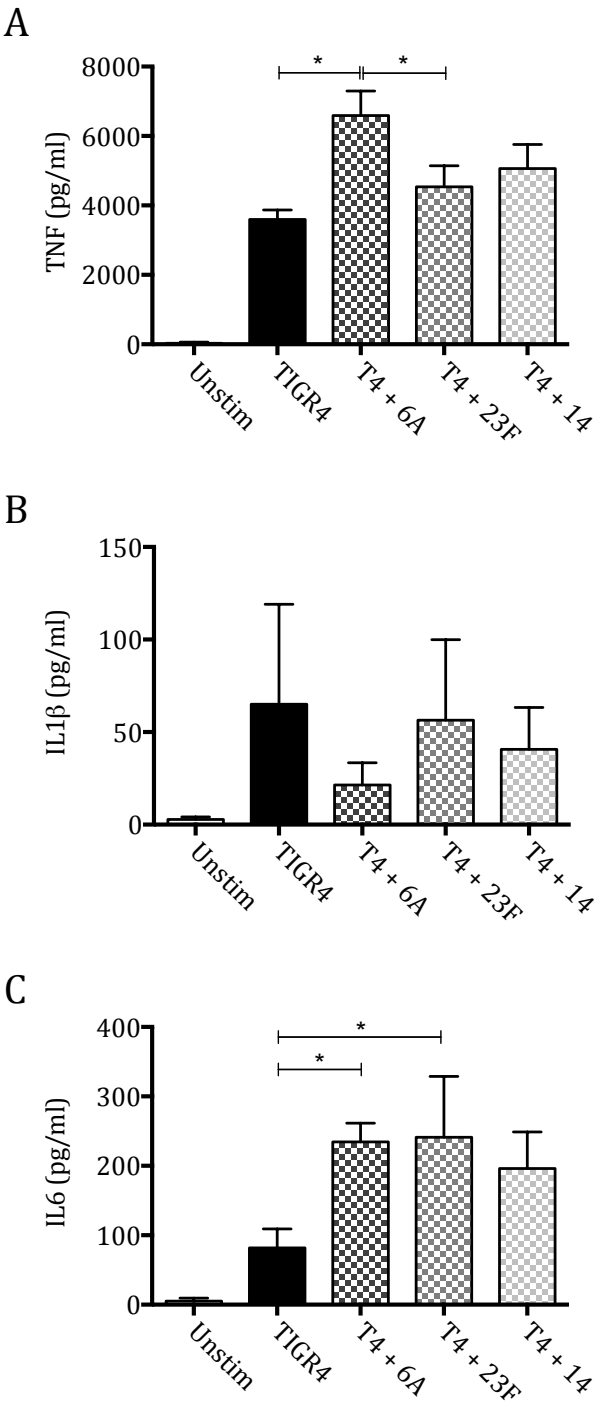

Figure 5.4 MDM cytokine response to capsule switch strains

MDM were incubated with capsule switch strains where the other serotype is expressed on TIGR4 bacteria. Supernatants were removed after 6 hours and analysed for A) TNF, B) IL1β, and C) IL6. Data are presented as mean +/- SEM. Results were analysed by 1 way ANOVA and Tukey's multiple comparison test.

The HEK TLR2 reporter assay was used to assess whether the differences in MDM inflammatory responses identified above were due to differences between strains in TLR2 stimulation. Sian Hutchings, a BSc student, performed these experiments under my supervision. The data from HEK TLR2 cells incubated with TIGR4, other clinical isolates and the TIGR4 capsular serotype switched strains showed differences in TLR2 responses between wild-type strains but none between the TIGR4 capsular switch strains (figure 5.5). These results indicate that expression of varying capsule does not alter TLR2 recognition of TIGR4. The differences in TLR2 stimulation between clinical strains did not correlate with the results from MDM pro-inflammatory cytokine release e.g. despite reduced TLR2 responses to the serotype 23F strain, infection of MDMs with this strain resulted in higher levels of IL6 compared to infection with the TIGR4 strain (figures 5.3 and 5.5).

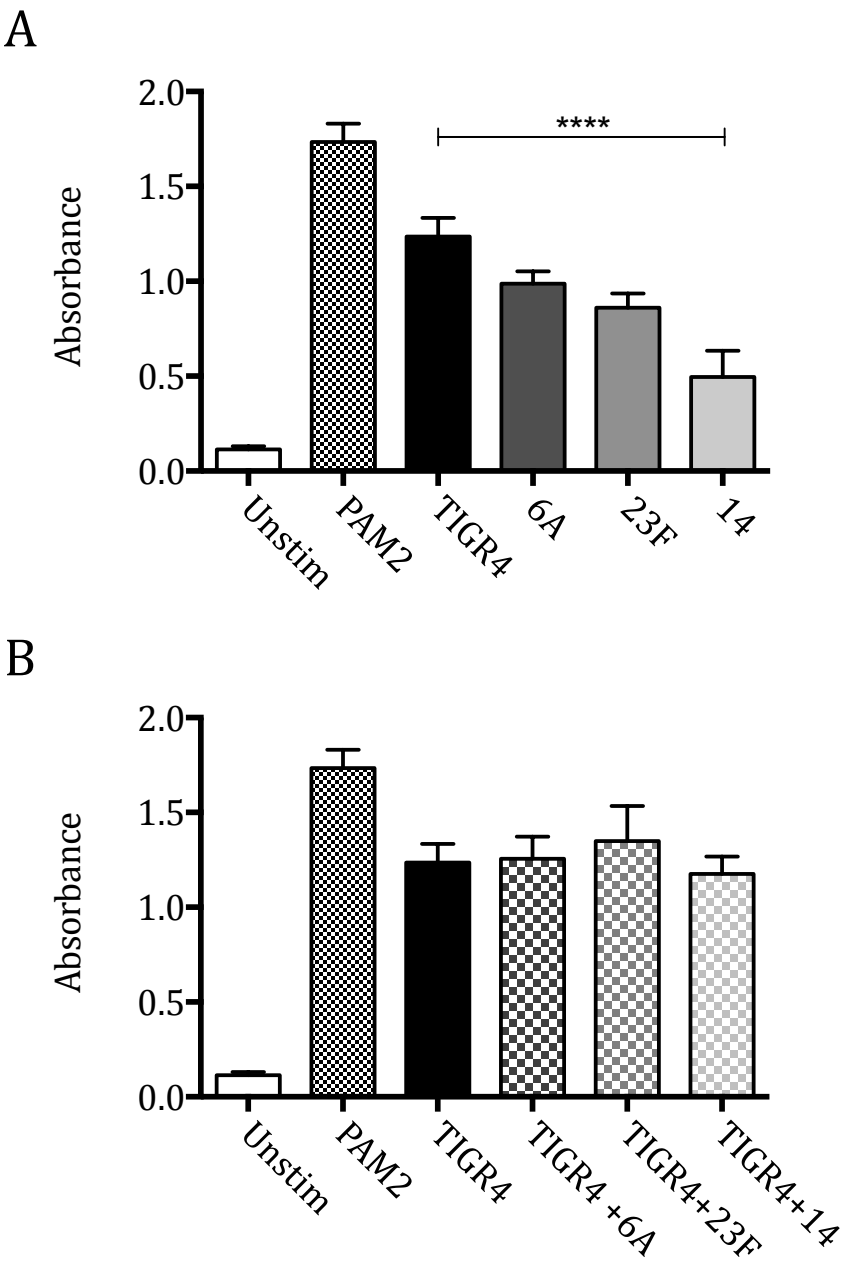

Figure 5.5 TLR2 reporter cell responses to varied serotypes and capsule switch strains
HEK 293 cells transfected with TLR2 and NFκB linked to a SEAP reporter were incubated with several *S. pneumoniae* serotypes (panel A) and capsule switch strains where the other serotype is expressed on TIGR4 bacteria (panel B) at MOI 10 for 20 hours. Supernatant colorimetric change is expressed as absorbance. Data are presented as the mean +/- SEM of 4 separate experiments and analysed by 1 way ANOVA and Tukey's multiple comparison test.

5.3 Effect of capsule on the inflammatory response to *S. mitis*

To extend the data on capsule, with collaborators from Oslo, we used the closely related bacteria *Streptococcus mitis* to assess the effect of its capsule on the inflammatory response. In addition to assess whether the S. pneumoniae serotype 4 capsule is directly pro-inflammatory we compared the MDM response to wild-type *S. mitis* (expressing its natural polysaccharide capsule) to an *S. mitis* strain expressing the TIGR4 *cps* locus (Rukke, Kalluru et al. 2014). Data from our group also show that *S. mitis* is taken up into RAW macrophages, that its naturally expressed capsule is protective against uptake, and that expression of TIGR4 capsule provides even greater protection (Rukke, Kalluru, et al. 2014) as evidenced by association with fluorescent cells, intracellular bacterial numbers, and electron micrography.

The data were heterogeneous, but the most obvious difference was that all the *S. mitis* strains induced more TNF and IL6 than *S. pneumoniae*, though again the IL1β response was muted in this model (figure 5.6). There was no significant difference between *S. mitis* and *S. mitis* Δ*cps* except in IL1β, although the levels were so low that this difference is unlikely to have functional significance. Importantly, expression of the *S. pneumoniae* serotype 4 capsule by *S. mitis* did not increase the inflammatory response, with in fact a significantly increased IL6 in response to *S. mitis* compared to *S. mitis* + TIGR4 capsule. This suggests that the pro-inflammatory effect of TIGR4 capsule lies in modification of a response to another component of *S. pneumoniae* rather than a direct effect of the capsule material.

The HEK TLR2 reporter assay showed no difference between TIGR4 and *S. mitis*, and no difference between *S. mitis* and either the capsule deficient mutant or the mutant expressing the TIGR4 capsule (figure 5.7).

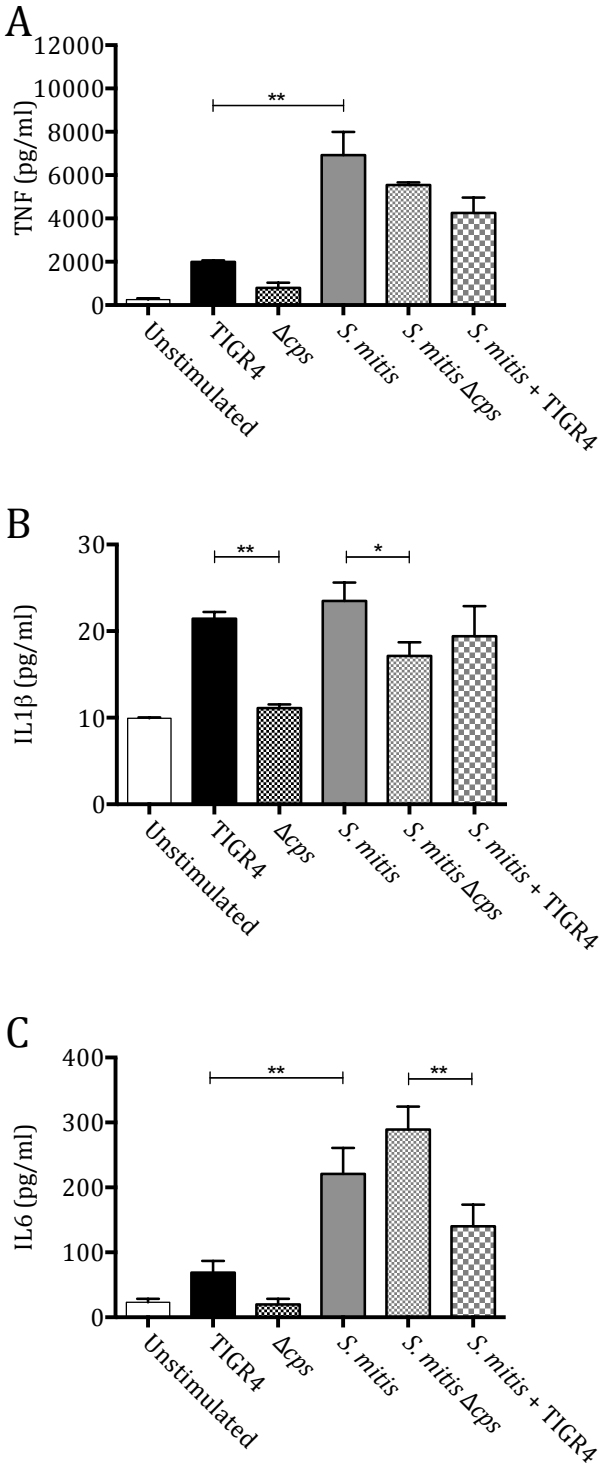

Figure 5.6 MDM cytokine response to TIGR4 and *S. mitis* strains

MDM were incubated with TIGR4, and *S. mitis* wild-type, capsule deficient strains, and *S. mitis* expressing the TIGR4 capsule. Supernatants were removed after 6 hours and analysed for A) TNF, B) IL1β, and C) IL6. Data are presented as mean +/- SEM. Analysis was by 1 way ANOVA and Tukey's multiple comparisons test.

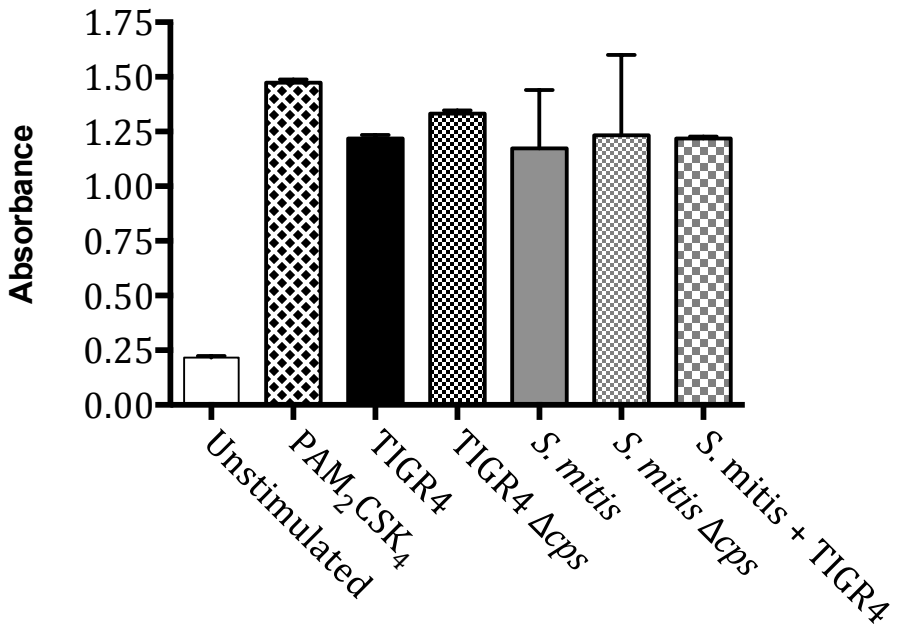

Figure 5.7 TLR2 reporter cell responses to TIGR4 and *S. mitis* strains

HEK 293 cells transfected with TLR2 and NFκB linked to a SEAP reporter were incubated with TIGR4 and *S. mitis* wild-type, capsule deficient strains, and *S. mitis* expressing the TIGR4 capsule, and capsule switch strains where the other serotype is expressed on TIGR4 bacteria at MOI 10 for 20 hours. Supernatant colorimetric change is expressed as absorbance. Data are presented as the mean +/- SEM and analysed by 1 way ANOVA and Tukey's multiple comparisons test, with no significant differences seen.

5.4 Effects of *S. mitis* expressing TIGR4 capsule in a mouse pneumonia model

To assess the role of capsule of *S. mitis in vivo* we used *S. mitis*, its isogenic capsule deficient mutant, and *S. mitis* expressing the TIGR4 capsule in a pneumonia model, and mice were culled at 4 hours to evaluate inflammatory responses in early infection.

In the first set of experiments, mice were treated with empty liposomes as a control for liposomal clodronate used in the experiments in chapter 5.6. By 4 hours there was already significantly more *S. mitis* + TIGR4*cps* than *S. mitis* in both lavage fluid and lung homogenate (figure 5.8). However, TIGR4 caused significantly more neutrophil recruitment to lavage fluid than the *S. mitis* strains, but the expression of TIGR4 capsule had little effect on the inflammatory cell infiltrate caused by *S. mitis* (figure 5.9). Similarly, while TIGR4 induced similar TNF levels in lavage fluid to the *S. mitis* strains, it induced significantly more IL1β and a trend to more IL6 than all the *S. mitis* strains (figure 5.10). In lung homogenate, TNF levels were similar between strains but there was significantly more IL6 and a trend to more IL1β with TIGR4 (figure 5.11). Again, the TIGR4 capsule had little bearing when expressed on *S. mitis* in both lavage fluid and lung homogenate.

These data support the *in vitro* data that TIGR4 capsule has little effect on inflammatory response in the context of *S. mitis*. This provides more evidence that the TIGR4 capsule's pro-inflammatory effects must be driven by modification of host cell interaction with other *S. pneumoniae* components.

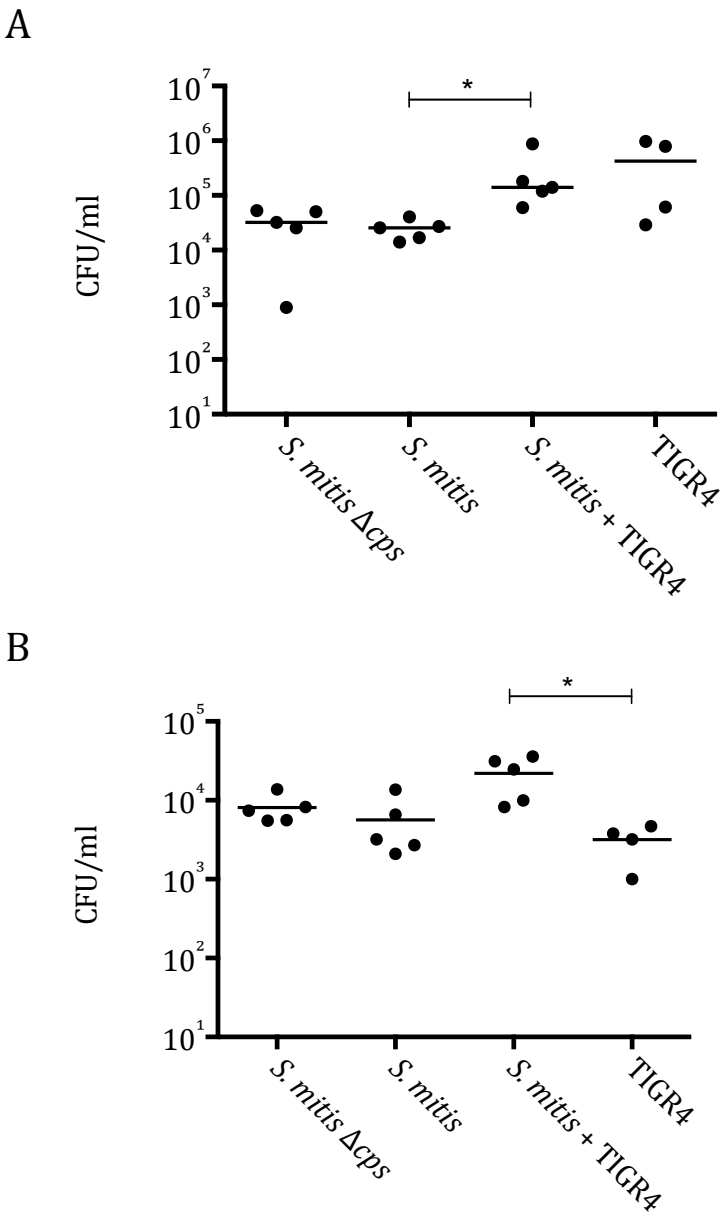

Figure 5.8 Mouse lavage and lung homogenate bacterial counts 4 hours after infection
5 week old female CD1 mice had intranasal liposomes administered 72 hours before intranasal infection with 5×10^6 CFU bacteria; either TIGR4, *S. mitis*, *S. mitis* Δ*cps*, or *S. mitis* + TIGR4*cps*. Mice were culled at 4 hours and bronchoalveolar lavage and lung homogenate was obtained and plated to assess bacterial counts, shown in panel A and B respectively. Data from individual mice and medians values are presented. Analysed by Kruskal-Wallis and Dunn's multiple comparisons test.

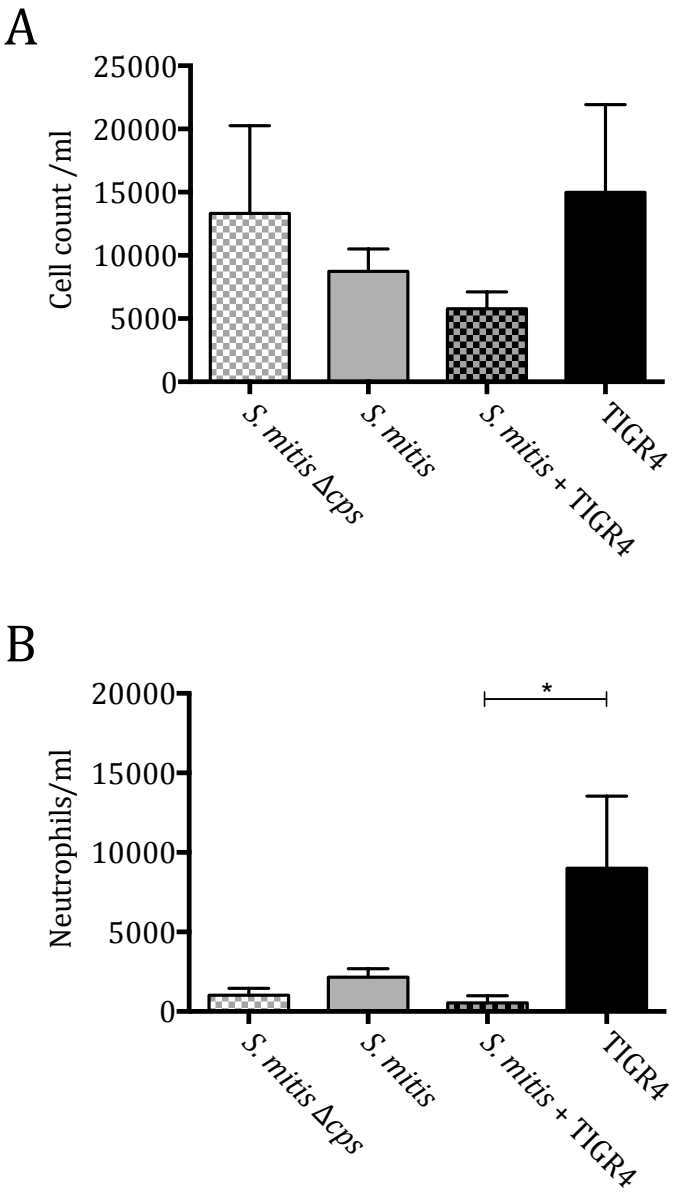

Figure 5.9 Mouse lavage cell counts 4 hours after infection

5 week old female CD1 mice had intranasal liposomes administered 72 hours before intranasal infection with 5×10^6 CFU bacteria; either *S. mitis* Δ*cps*, *S. mitis*, *S. mitis* + TIGR4*cps* or TIGR4. Mice were culled at 4 hours and cell count and neutrophil numbers in bronchoalveolar lavage fluid determined by haemocytometer and cytospin, shown in panel A and B respectively. Data shown as mean +/-SEM and analysed by 1 way ANOVA and Tukey's multiple comparisons test.

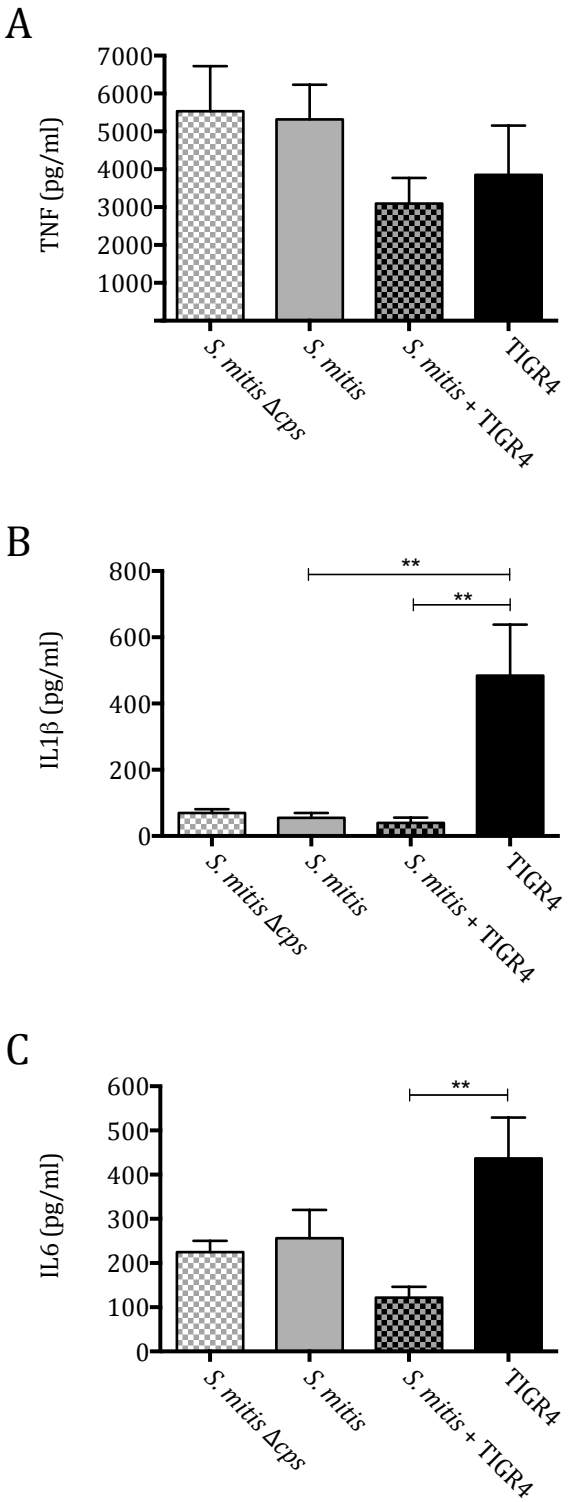

Figure 5.10 Mouse lavage cytokine levels 4 hours after infection in mice given liposomes

5 week old female CD1 mice had intranasal liposomes administered 72 hours before intranasal infection with 5×10^6 CFU bacteria; either, *S. mitis* Δ*cps*, *S. mitis*, *S. mitis* + TIGR4*cps* or TIGR4. Mice were culled at 4 hours and cytokine levels in lavage fluid were determined by ELISA. TNF, IL1β, and IL6 shown in panels A, B and C respectively. Data are shown as mean +/-SEM and analysed by 1 way ANOVA and Tukey's multiple comparisons test.

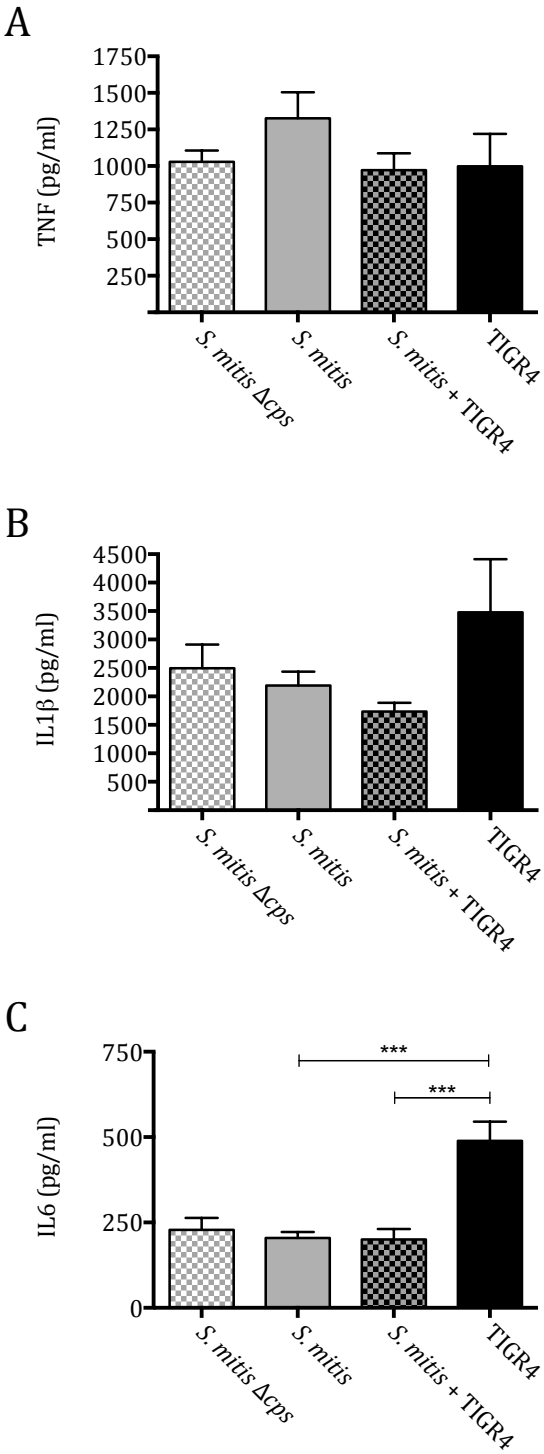

Figure 5.11 Mouse lung homogenate cytokine levels 4 hours after infection

5 week old female CD1 mice had intranasal liposomes administered 72 hours before intranasal infection with 5×10^6 CFU bacteria; either, *S. mitis* Δ*cps*, *S. mitis*, *S. mitis* + TIGR4*cps* or TIGR4. Mice were culled at 4 hours and cytokine levels in lung homogenate were determined by ELISA. TNF, IL1β, and IL6 shown in panels A, B and C respectively. Data are shown as mean +/-SEM and analysed by 1 way ANOVA and Tukey's multiple comparison test.

5.5 Effect of macrophage depletion on *S. mitis* strains

This series of experiments was then repeated in mice that had been pre-treated with intranasal clodronate to deplete AM. After clodronate, there were no longer any significant differences in bacterial counts between strains in either lavage fluid or lung homogenate (figure 5.12). While it is difficult to compare directly with the liposome treated mice, there appears to be a similar order of bacteria found in lavage fluid, but more bacteria in lung homogenate in clodronate treated mice. This suggests increased invasion in the absence of AM, though the effect may be minimised because of the high inoculum, as previous data indicates that the role of the AM is more important in bacterial clearance in low inoculum models (Dockrell, Marriott et al. 2003).

Despite the similarities in bacterial counts, again TIGR4 induced a greater leucocytosis (figure 5.13), though *S. mitis* Δ*cps* counts also increased in this system, suggesting that *S. mitis* capsule may have a role like *S. pneumoniae* capsule in inhibiting macrophage mediated bacterial clearance (Camberlein, Cohen et al. 2015, Rukke, Kalluru et al. 2014).

Interestingly, macrophage depletion appeared to have a larger effect on lavage fluid cytokines in the *S. mitis* strains. There was now a trend to greater TNF production with TIGR4 (figure 5.14) although differences were preserved for IL1β and IL6 the magnitudes of cytokine response were reduced. This reduction in cytokine responses has been noted in other clodronate experiments within the Brown laboratory. Within lung homogenate, AM depletion had little effect on the pattern of responses, though levels of TNF and IL1β were somewhat reduced overall (figure 5.15). A direct comparison of the liposome treated and clodronate treated mice can be seen in figures 5.16 (CFU and neutrophil counts), 5.17 (BALF cytokines) and 5.18 (Lung homogenate cytokines).

These data suggest that while macrophages are important in cytokine responses to inhaled bacteria, other tissue such as epithelial cells can take over some of this role. They also

suggest that while macrophage depletion has effects on the inflammatory response to *S. pneumoniae*, there is little effect in the context of *S. mitis*.

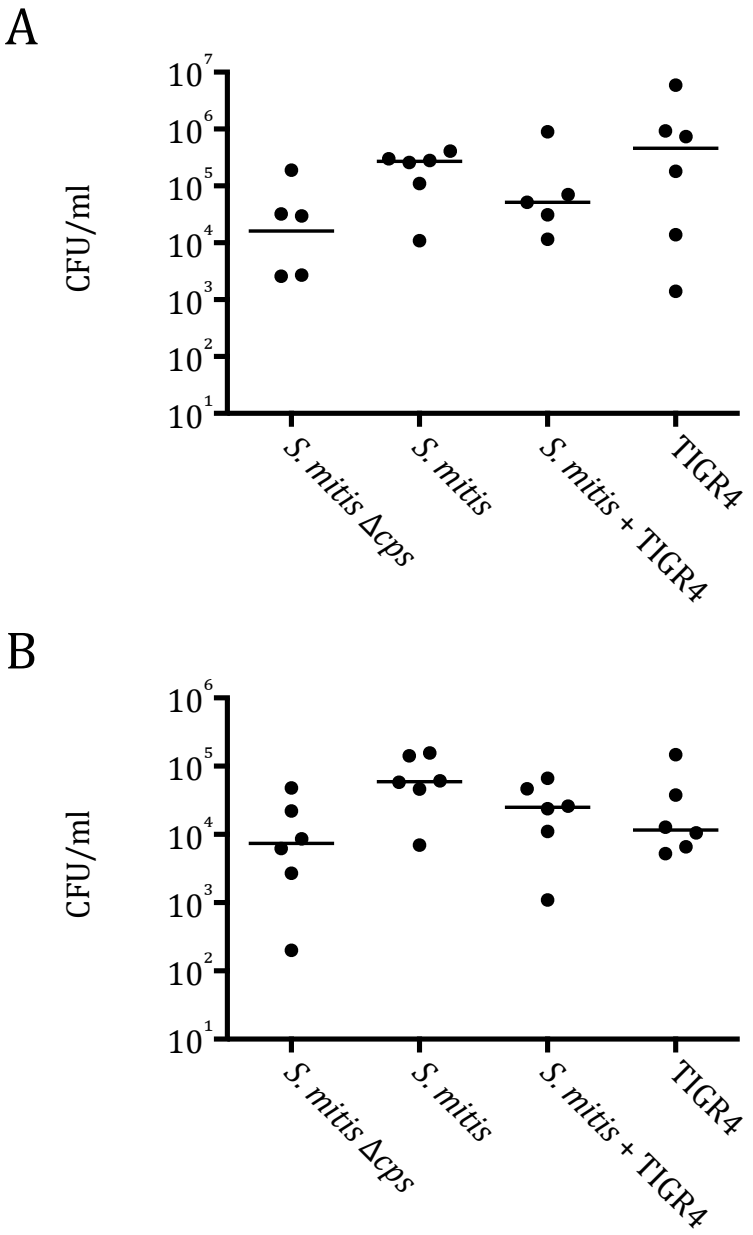

Figure 5.12 Mouse lavage and lung homogenate bacterial counts at 4 hours in macrophage depleted mice

5 week old female CD1 mice had intranasal clodronate administered 72 hours before intranasal infection with 5×10^6 CFU bacteria; either, *S. mitis* Δ*cps*, *S. mitis*, *S. mitis* + TIGR4*cps* or TIGR4. Mice were culled at 4 hours and bronchoalveolar lavage and lung homogenate was obtained and plated to assess bacterial counts, shown in panel A and B respectively. Data from individual mice and medians values are presented. Analysed by Kruskal-Wallis and Dunn's multiple comparisons test with no significant difference found.

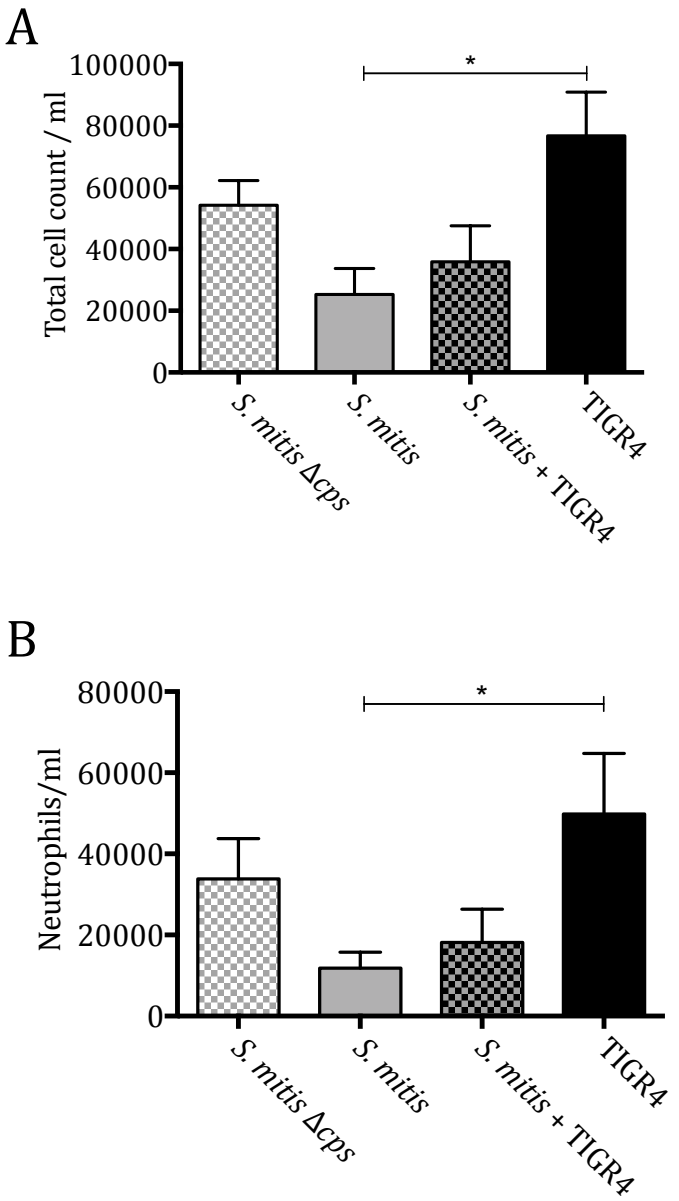

Figure 5.13 Mouse bronchoalveolar lavage cell counts 4 hours after infection in clodronate treated mice

5 week old female CD1 mice had intranasal clodronate administered 72 hours before intranasal infection with 5×10^6 CFU bacteria; either, *S. mitis* Δ*cps*, *S. mitis*, *S. mitis* + TIGR4*cps* or TIGR4. Mice were culled at 4 hours and cell count and neutrophil numbers in bronchoalveolar lavage fluid determined by haemocytometer and cytospin, shown in panel A and B respectively. Data are shown as mean +/-SEM and analysed by 1 way ANOVA and Tukey's multiple comparisons test.

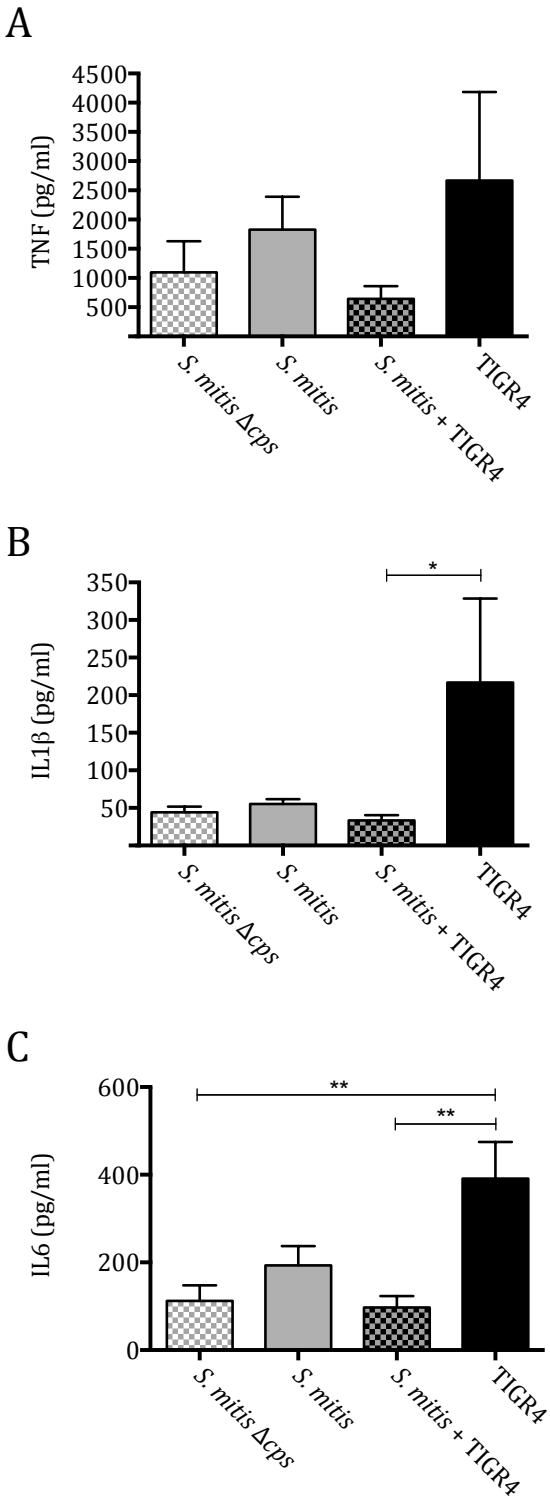

Figure 5.14 Mouse bronchoalveolar lavage cytokine levels 4 hours after infection in clodronate treated mice

5 week old female CD1 mice had intranasal clodronate administered 72 hours before intranasal infection with 5×10^6 CFU bacteria; either, *S. mitis* Δ*cps*, *S. mitis*, *S. mitis* + TIGR4*cps* or TIGR4. Mice were culled at 4 hours and cytokine levels in lavage fluid were determined by ELISA. TNF, IL1β, and IL6 shown in panels A, B and C respectively. Data are shown as mean +/-SEM and analysed by 1 way ANOVA and Tukey's multiple comparisons test.

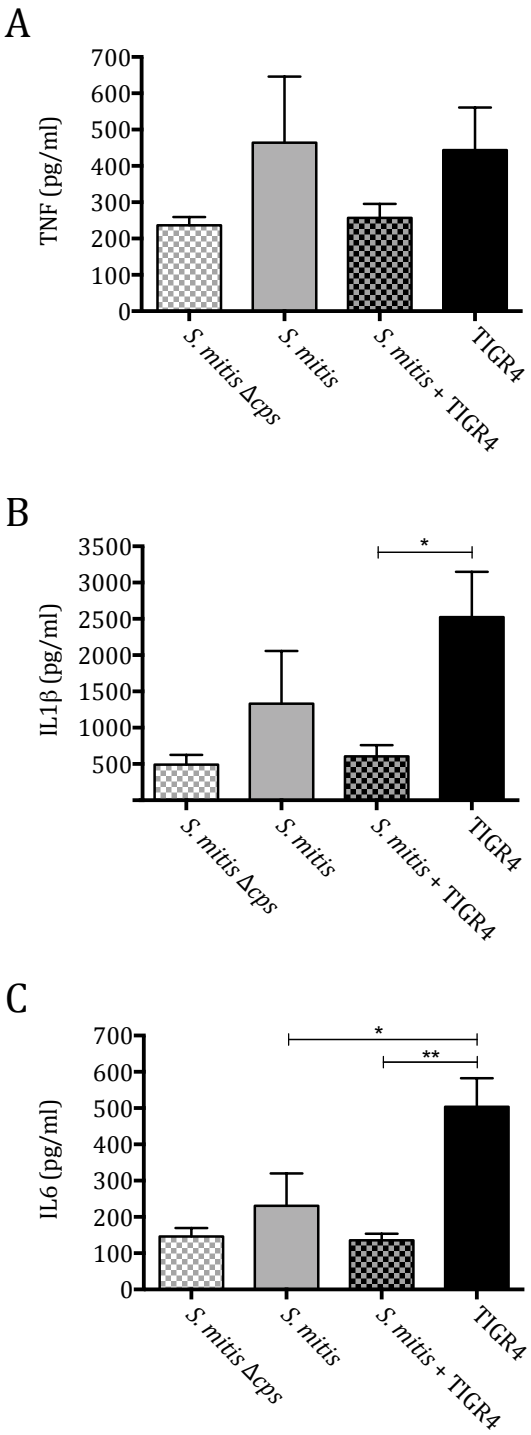

Figure 5.15 Mouse lung homogenate cytokine levels 4 hours in clodronate treated mice

5 week old CD1 mice had intranasal clodronate administered 72 hours before intranasal infection with 5×10^6 CFU bacteria; either, *S. mitis* Δ*cps*, *S. mitis*, *S. mitis* + TIGR4*cps* or TIGR4 Mice were culled after 4 hours and cytokine levels in lung homogenate were determined by ELISA. TNF, IL1β, and IL6 shown in panels A, B and C respectively. Data are shown as mean +/-SEM and analysed by 1 way ANOVA and Tukey's multiple comparisons test.

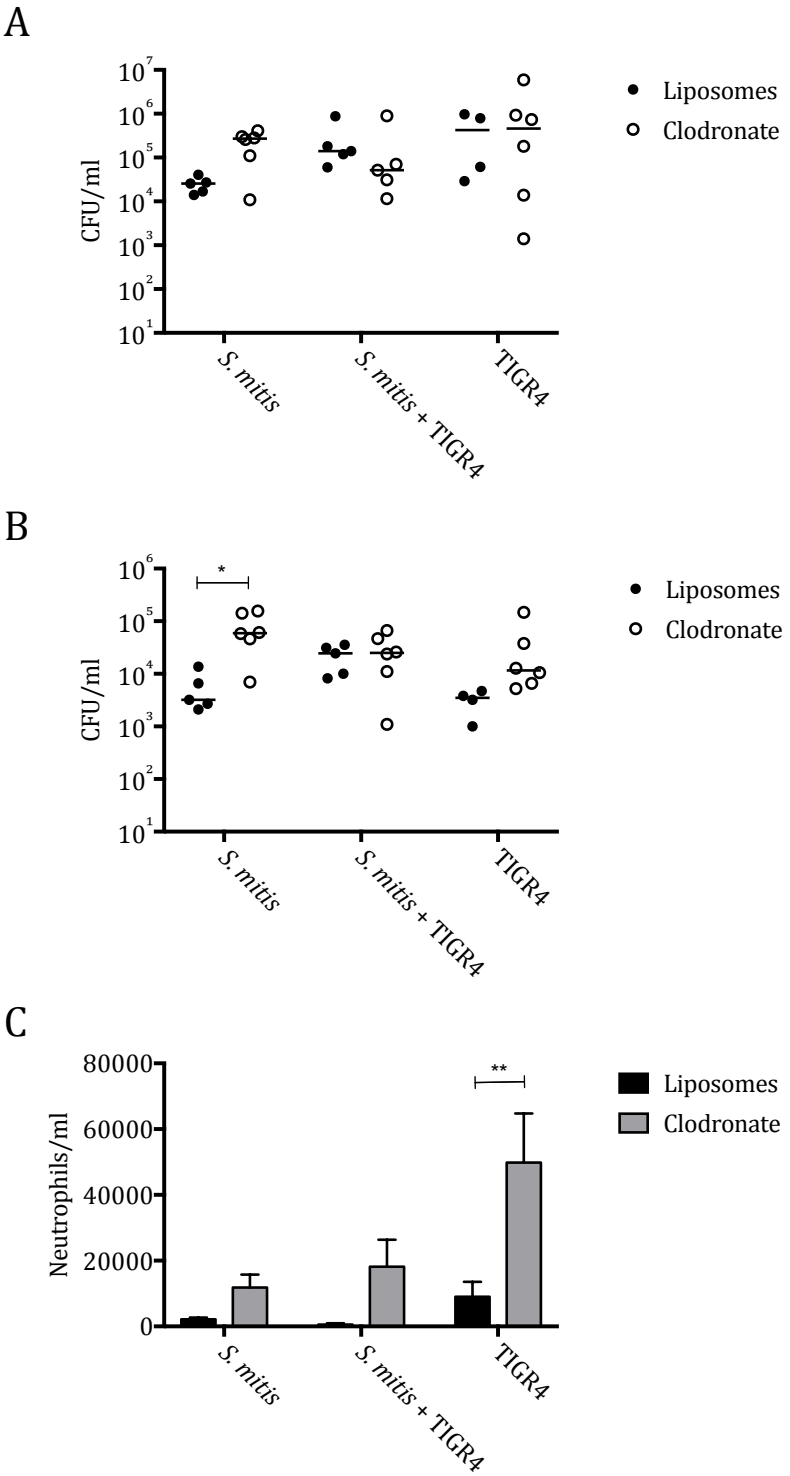

Figure 5.16 Mouse lavage & lung bacterial counts, and lavage neutrophil numbers after infection in liposome or liposomal clodronate treated mice

These data are a combination of figures 5.8, 5.9, 5.12, and 5.13. CFU data from individual mice and medians values are presented and analysed by Dunn's multiple comparisons test. Panel C shows BALF neutrophil numbers as determined by haemocytometer and cytospin. Data are shown as mean +/-SEM and analysed by 1 way ANOVA and Tukey's multiple comparisons test.

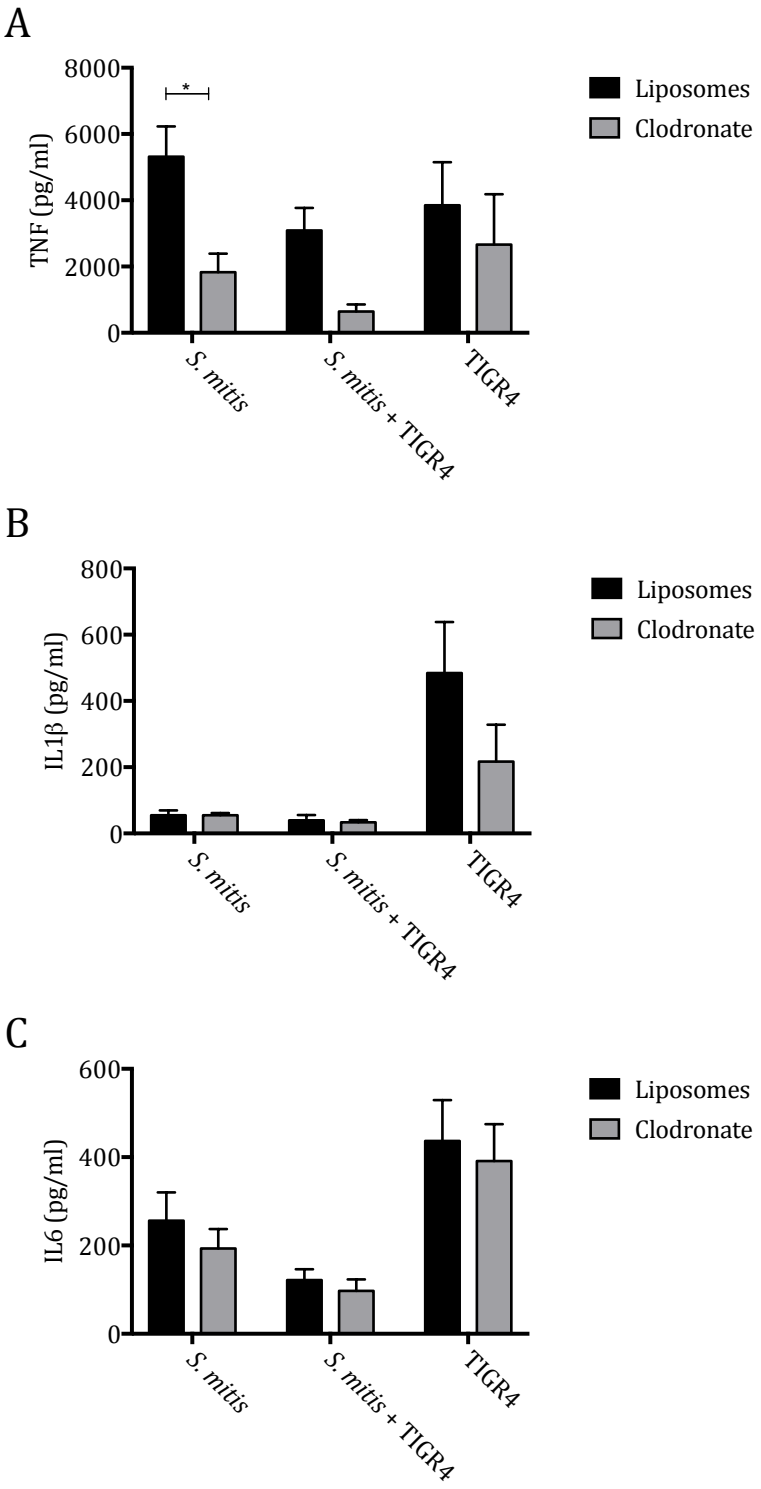

Figure 5.17 Mouse bronchoalveolar lavage cytokine levels 4 hours after infection in liposome or liposomal clodronate treated mice

These data are a combination of figures 5.10 & 5.14. BALF levels of TNF, IL1β, and IL6 shown in panels A, B and C respectively. Data are shown as mean +/-SEM and analysed by 2 way ANOVA and Tukey's multiple comparisons test.

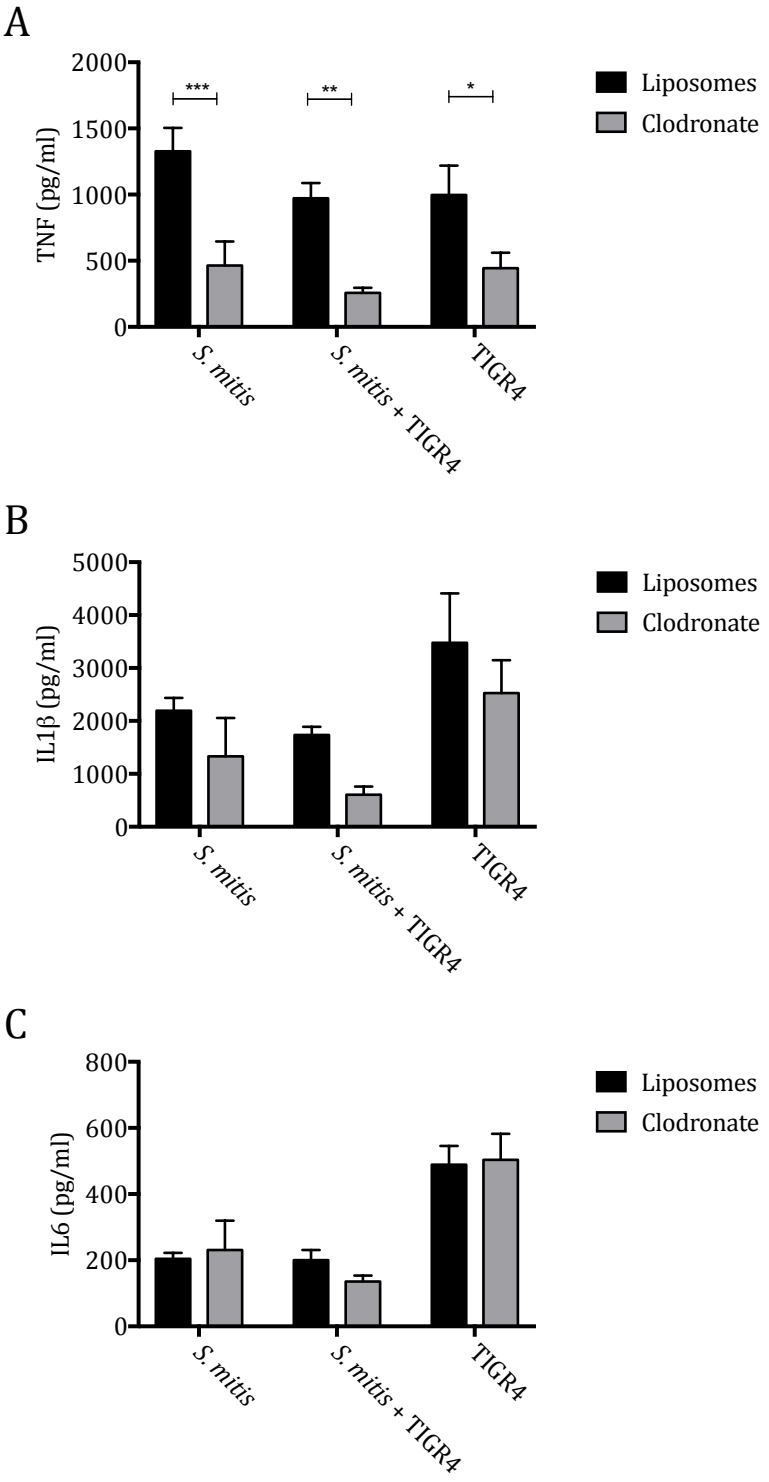

Figure 5.18 Mouse lung homogenate cytokine levels 4 hours after infection in liposome or liposomal clodronate treated mice

These data are a combination of figures 5.11 & 5.15. Lung homogenate levels of TNF, IL1β, and IL6 are shown in panels A, B and C respectively. Data are shown as mean +/-SEM and analysed by 2 way ANOVA and Tukey's multiple comparisons test.

5.6 Chapter Summary

This chapter explored the effect of the capsule role in inflammatory response in other *S. pneumoniae* serotypes, the effect of capsule on a closely related species, *S. mitis*. and to assess how much individual serotypes' capsule contributes to differences in the inflammatory response.

The initial experiments suggested that the effect of capsule is not restricted to TIGR4, though serotype 3 with its unusual mucoid capsule behaves differently. Interestingly the serotypes examined had different propensities to induce TLR2 stimulation, but the unencapsulated forms were all similar. This suggests that different capsule structure may modify how common cell wall ligands interact with host PRR. The use of capsule switch strains, where TIGR4 expressed the capsule of other serotype, was aimed at assessing how much capsular differences accounted for variation in inflammatory responses by serotype. However, a detailed accounting for confounding variables such as how capsule affects adhesion to and phagocytosis by MDM was not carried out, and could explain some of the variation.

Interestingly when the closest relative of *S. pneumoniae*, *S. mitis*, is examined, its native capsule does not consistently promote inflammatory responses from MDM *in vitro*. If TIGR4 capsule was expressed on *S. mitis*, there was no increase in inflammatory response, if anything there was a trend to reduced inflammatory response. Both the native and TIGR4 capsule had no obvious effect on TLR2 stimulation. Intriguingly, *S. mitis* strains appeared to cause more inflammatory responses than TIGR4 from MDM.

In the context of mouse pneumonia, native capsule has no effect on leukocyte recruitment, and no significant effect in cytokine levels in lavage fluid. The addition of TIGR4 capsule to *S. mitis*, was not sufficient to make it as virulent as TIGR4. At 4 hours, despite having fewer bacteria than *S. mitis* + TIGR4*cps*, the inflammatory cytokine response was convincingly higher in response to TIGR4. The inflammatory response to *S. mitis* strains compared to TIGR4 *in vivo* was in the opposite direction to that of MDM *in vitro* data, which may be

explained by human/murine differences, or more likely that the exposure of bacteria to macrophages *in vitro* does not reflect the complexities of the cell-cell interaction *in vivo* and that greater changes in bacterial dynamics may play a more important role in the cytokine responses seen *in vivo*.

At 4 hours *in vivo*, in mouse pneumonia, TIGR4 induced significantly more neutrophilia than the *S. mitis* strains. This was accompanied by greater IL1β and in particular IL6. This pattern was preserved when alveolar macrophages were depleted by the use of liposomal clodronate, though overall cytokine levels were marginally lower.

In general, it may be expected that pneumococcal capsule expression on *S. mitis* does not have similar effects to that seen in *S. pneumoniae*; despite the close genetic ancestry, there are many differences in protein expression that may bear on inflammation and virulence. As such, if a positive effect of TIGR4 capsule on *S. mitis* had been noted, this would have been strong evidence of its effect, but the lack of effect merely confirms the phenotypic difference between a largely avirulent bacterium and its pathogenic cousin.

In summary, the pro-inflammatory effect of *S. pneumoniae* capsule largely persists for other strains. However, differences in inflammatory response between serotypes are largely driven by non-capsular factors. The capsule of *S. mitis* does not promote pro-inflammatory responses, and neither does TIGR4 capsule expressed on *S. mitis*.

6 Effects of pneumolysin on the inflammatory response to *S. pneumoniae*

Ply is a cytosolic protein that can localise to the bacterial cell wall and is best known as pore-forming toxin. In addition pleiotropic pro-inflammatory effects have been described for Ply (Davis, Nakamura et al. 2011, Malley, Henneke et al. 2003, Witzenrath, Pache et al. 2011). However many of these effects were defined using purified Ply or occur late during infection. For this work I have investigated the early Ply dependent effects on the macrophage inflammatory response using infection of MDM cultures with wild-type and Ply deficient bacteria and an *in vivo* model of mouse infection.

6.1 Haemolysis assays

Ply activity is measure by ability to haemolyse red blood cells, and this assay was used to confirm the Ply phenotype of the proteins and strains used in this chapter. Purified Ply (kind gift from Prof Tim Mitchell) induces significant haemolysis down to 125 ng/ml (figure 6.1, A). Purified non-haemolytic Ply (also gift from Professor Tim Mitchell) with an amino acid substitution that allows the toxin to be inserted into cholesterol containing membranes but prevents oligomerisation to form pores, does not induce haemolysis unless present at very high concentrations (>5 μg/ml). Whole bacteria, including TIGR4 cause haemolysis, but isogenic Δ*ply* strains do not (figure 6.1, B). Bacterial supernatants also cause haemolysis, indicating some liberation of Ply from *S. pneumoniae* during normal log phase growth (figure 6.1 C). Haemolysis occurs in the presence of other *S. pneumoniae* serotypes such as D39 (figure 6.2, A), serotype 3 and serotype 23F (figure 6.2, B) with varying efficacy, but not with their isogenic Δ*ply* strains. The *ply* complemented D39 strain regained its haemolytic ability. Some serotype 1clinical isolates express a variant of Ply that is non-haemolytic (03.3038, 306) and some that do not express Ply at all (NCTC7465, ST615) (figure 6.2, C).

A

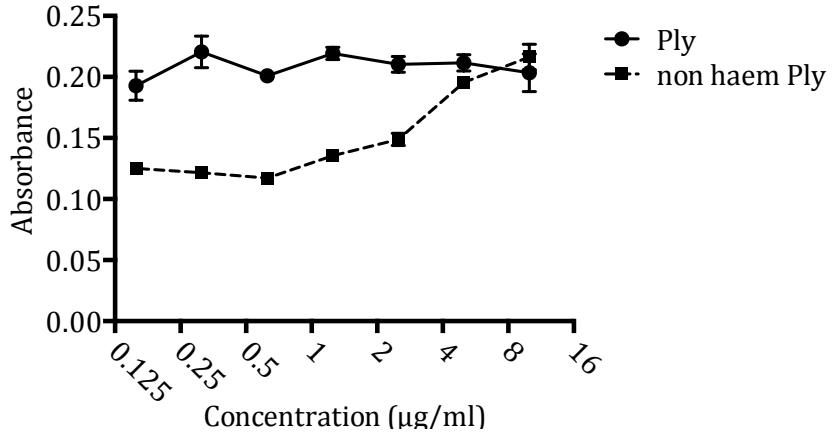

B

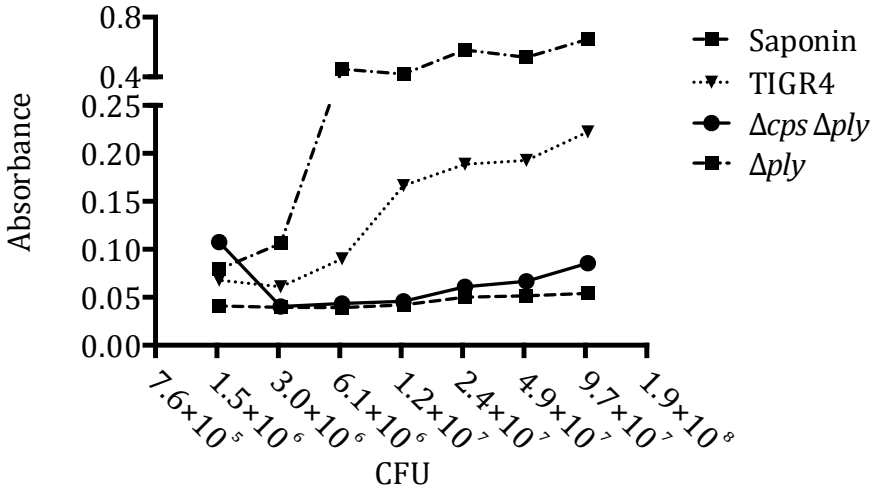

C

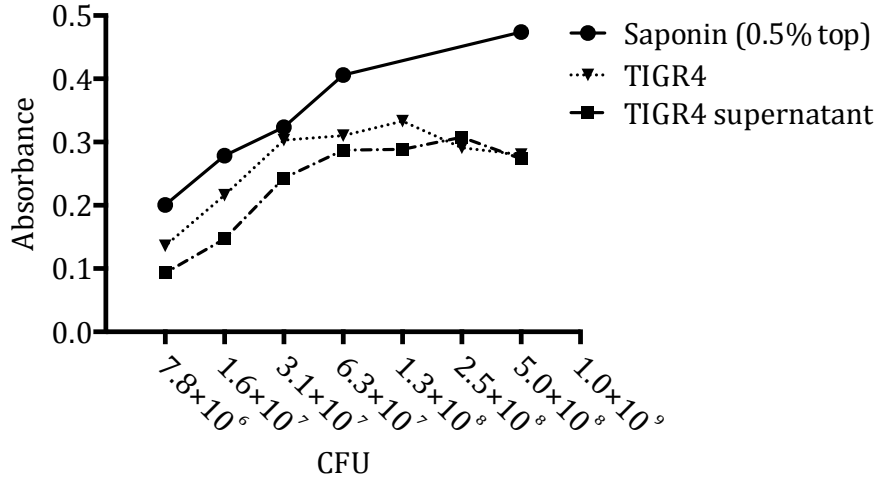

Figure 6.1 Haemolysis assays: TIGR4 strains

Bacteria and pneumolysin at different concentrations were assessed for haemolysis ability. Liberated pigments from haemolysed red blood cells were measured by microplate spectrophotometer. Panel A shows purified Ply and a non-haemolytic mutant Ply. Panel B shows saponin as a positive control as well as TIGR4 strains with isogenic strains deficient in capsule and Ply. Panel C shows whole bacteria and supernatant from whole bacteria.

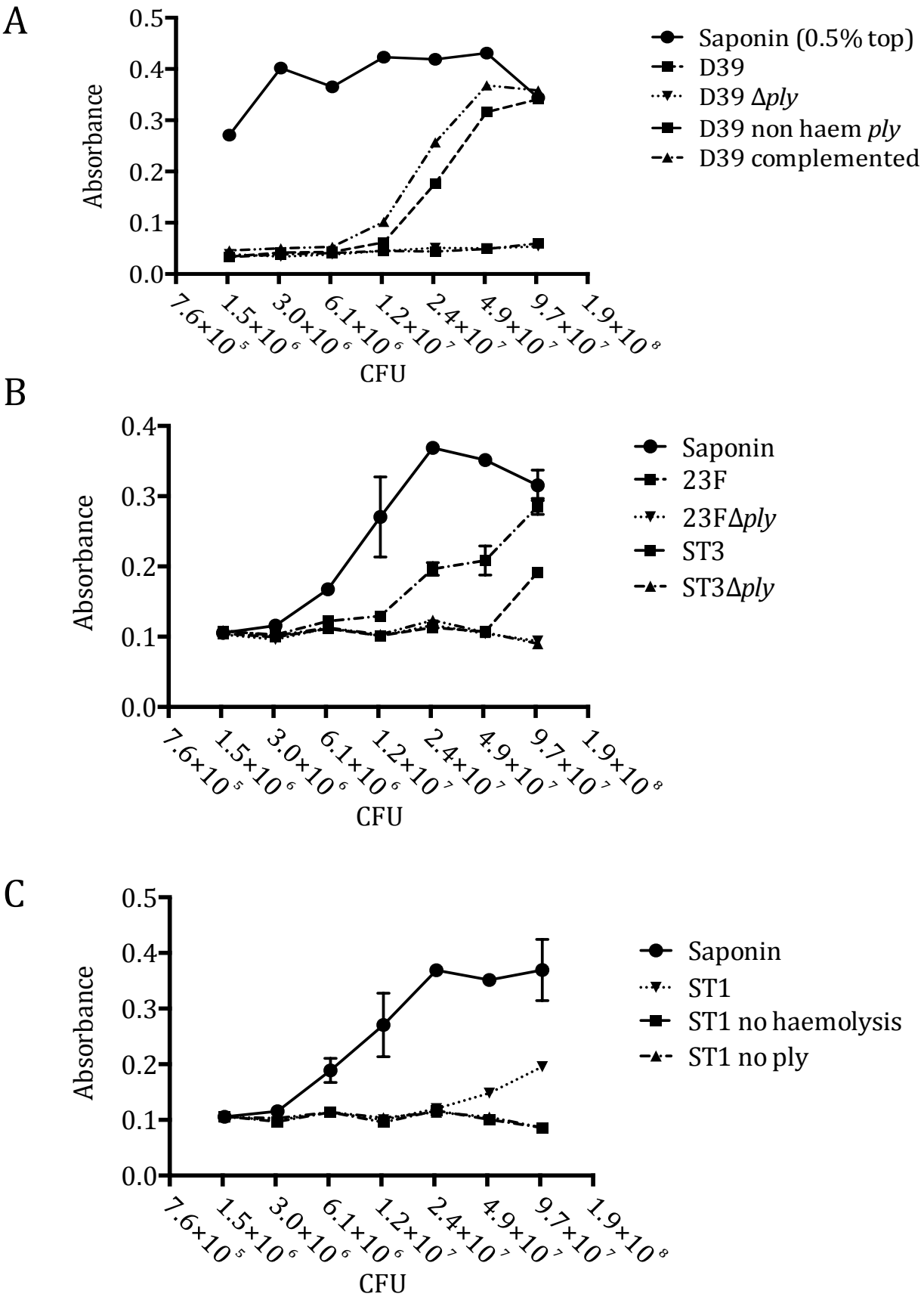

Figure 6.2 Haemolysis assays: other serotypes

Haemolysis assays with other strains, panel A) D39, panel B) serotype 3 and 23F, panel C) 1.

6.2 Effect of pneumolysin on inflammatory response of macrophages

To assess the effects of Ply on macrophage inflammatory responses, MDMs were incubated with the TIGR4 wild-type and Δ*ply* strains and the levels of pro-inflammatory cytokines measured in the culture supernatants. Surprisingly, when whole TIGR4 bacteria were incubated with MDM the wild-type strains induced less inflammatory responses than isogenic Δ*ply* bacteria. This was particularly evident with TNF and IL6, especially at later timepoints (figure 6.3) and across a range of multiples of infection (figure 6.4). However data at 24 hours may have been confounded by significant cell death in wild-type infected MDM (figure 2.1). These data suggest that despite the large body of literature showing that Ply induces pro-inflammatory responses, during early macrophage infection with live bacteria Ply might actively inhibit pro-inflammatory cytokine responses.

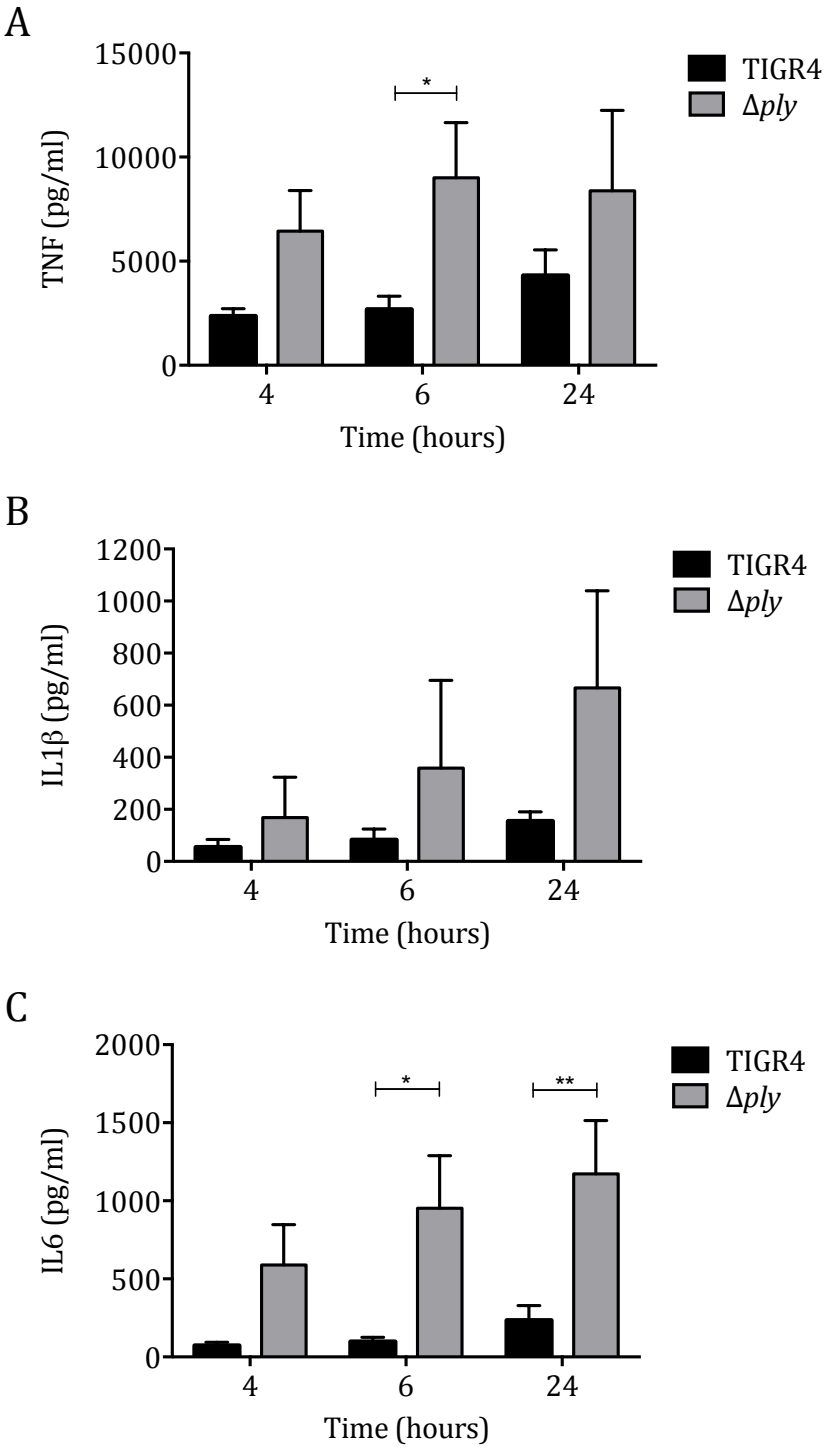

Figure 6.3 Timecourse of cytokine response of MDM to TIGR4 and Δ*ply* mutant

MDM were incubated with TIGR4 or TIGR4Δ*ply* in tissue culture plates, with 10 bacteria per cell. Supernatant was aspirated at 6 hours and later analysed for A) TNF, B) IL1β, and C) IL6. The data are presented as mean +/- SEM, with results from 4 different donors, with results analysed by 2 way ANOVA and Tukey's multiple comparisons test.

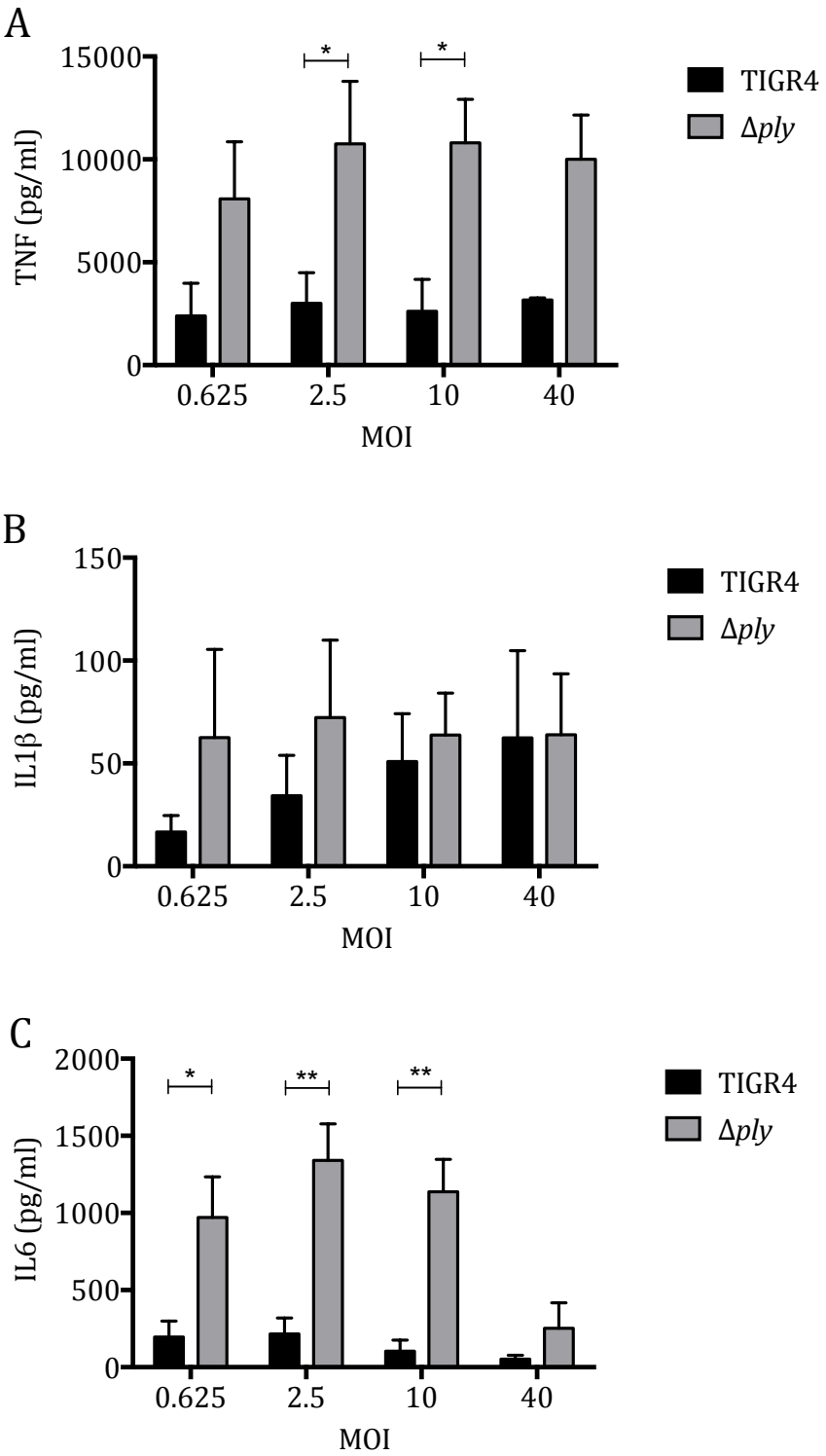

Figure 6.4 MDM cytokine response to varying numbers of bacteria

MDM were incubated with TIGR4 or Δ*cps* at varying concentrations; from 0.625 to 40 bacteria per cell. After 6 hours, supernatant was removed, and later analysed for A) TNF, B) IL1β, and C) IL6. The data obtained are from 3 different donors, presented as mean +/- SEM, and analysed by 2 way ANOVA and Tukey's multiple comparisons test.

6.3 Effects of pneumolysin on inflammatory response of epithelial cells

Previous studies have indicated that purified Ply induces epithelial cell damage in mouse pneumonia, and that this was due to its pore-forming ability inducing an inflammatory response (Kadioglu, Taylor et al. 2002, Maus, Srivastava et al. 2004). To establish whether there was a pro-inflammatory response to whole bacteria containing Ply, I incubated TIGR4 wild-type and Δ*ply* bacteria with A549 cells. The presence of Ply did not affect how well bacteria adhered to epithelial cells (figure 6.5). As shown in chapter 4, whole bacteria induced very little in the way of inflammatory cytokine response with no significant difference between the wild-type and Δ*ply* strains (figure 6.6 and figure 6.7), though there was a trend towards increased CXCL8 at high MOI with wild-type compared to Δ*ply*. Unstimulated MDM media induced similar cytokine responses to conditioned media from MDMs incubated with wild-type TIGR4, and the chemokine CXCL8 responses were similar for conditioned media from unstimulated MDM and those incubated with wild type or Δ*ply* bacteria. This very high basal release of CXCL8 from MDM conditioned media may be an artefact due to the effect of the MDM media or basally secreted factors on A549 cells. However conditioned media from MDM incubated with Δ*ply* induced greater TNF and IL6 responses than conditioned media from MDM incubated with wild-type TIGR4 (figure 6.8).

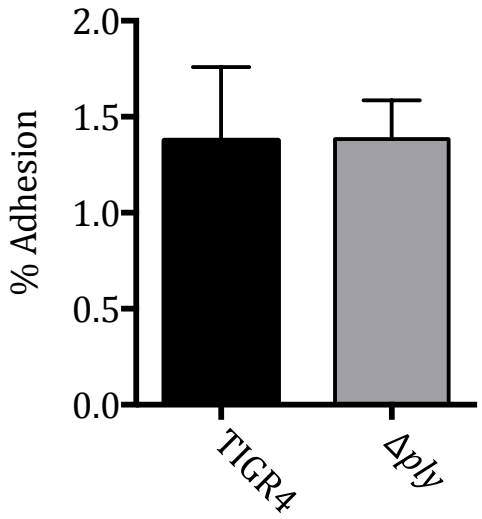

Figure 6.5 Adhesion of bacteria to A549 cells

This compares the number of TIGR4 and Δ*ply* adhering to an A549 cell layer after 1 hour expressed as percentage of all bacteria present in the well. A representative experiment of 3 is shown, presented as mean +/-SEM, with no significant differences by paired t test.

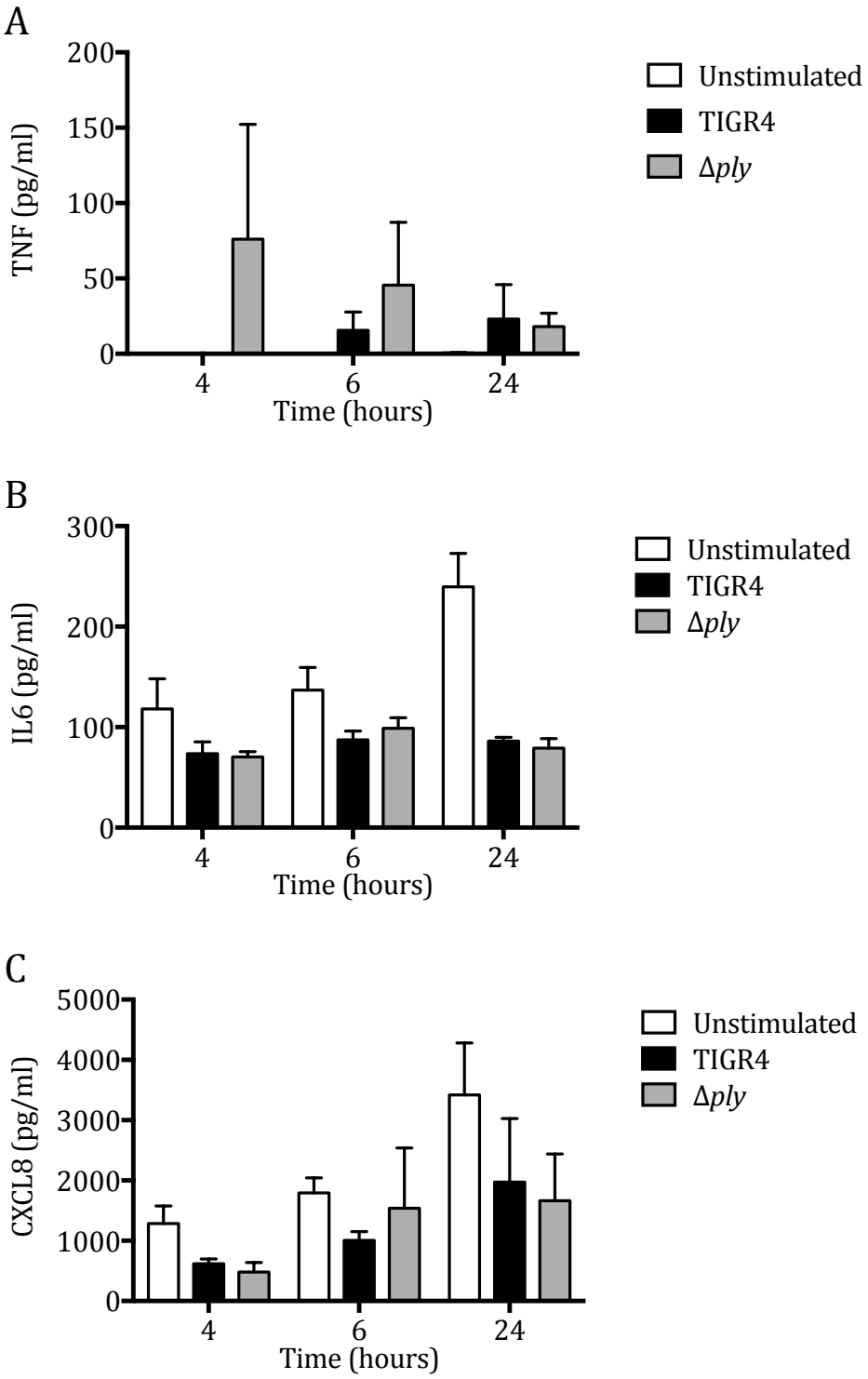

Figure 6.6 Timecourse of cytokine release by A549 alveolar epithelial cells incubated with bacteria

A549 were incubated with approximately 1 bacterium per cell, at various timepoints supernatant was analysed for cytokine secretion. Panel A shows TNF, B shows IL6, and C shows CXCL8 (IL1β levels were undetectable). Data are presented as mean +/- SEM of 3 experiments and were analysed by 2 way ANOVA and Tukey's multiple comparisons test, with no significant differences noted. Controls are also shared with figure 3.5

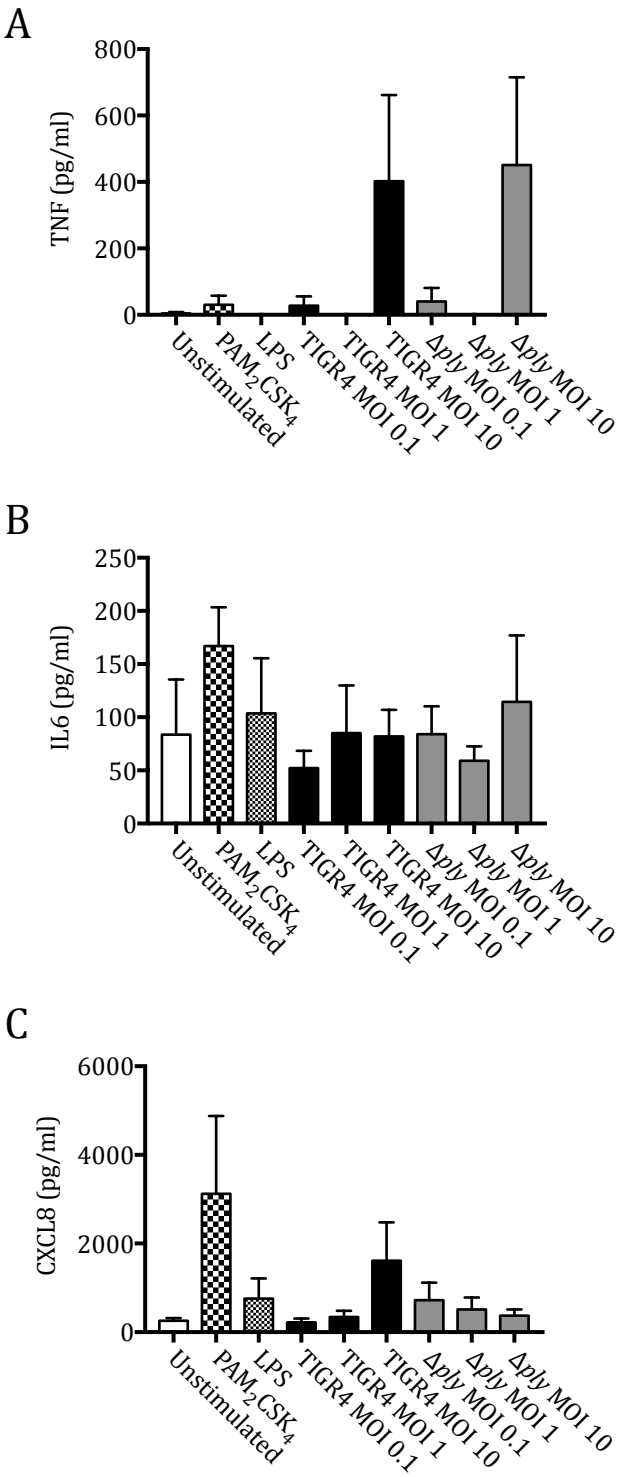

Figure 6.7 Cytokine release by A549 cells in response to different numbers of bacteria

A549 cells were incubated with positive controls and varying multiple infections of TIGR4 or Δ*ply*. Supernatant was analysed for cytokines after 6 hours. Mean +/- SEM of 3 experiments shown. Panel A shows TNF, B shows IL6, and C shows CXCL8. There were no differences between wild-type and Δ*ply* when analysed by 1 way ANOVA and Tukey's multiple comparisons test.

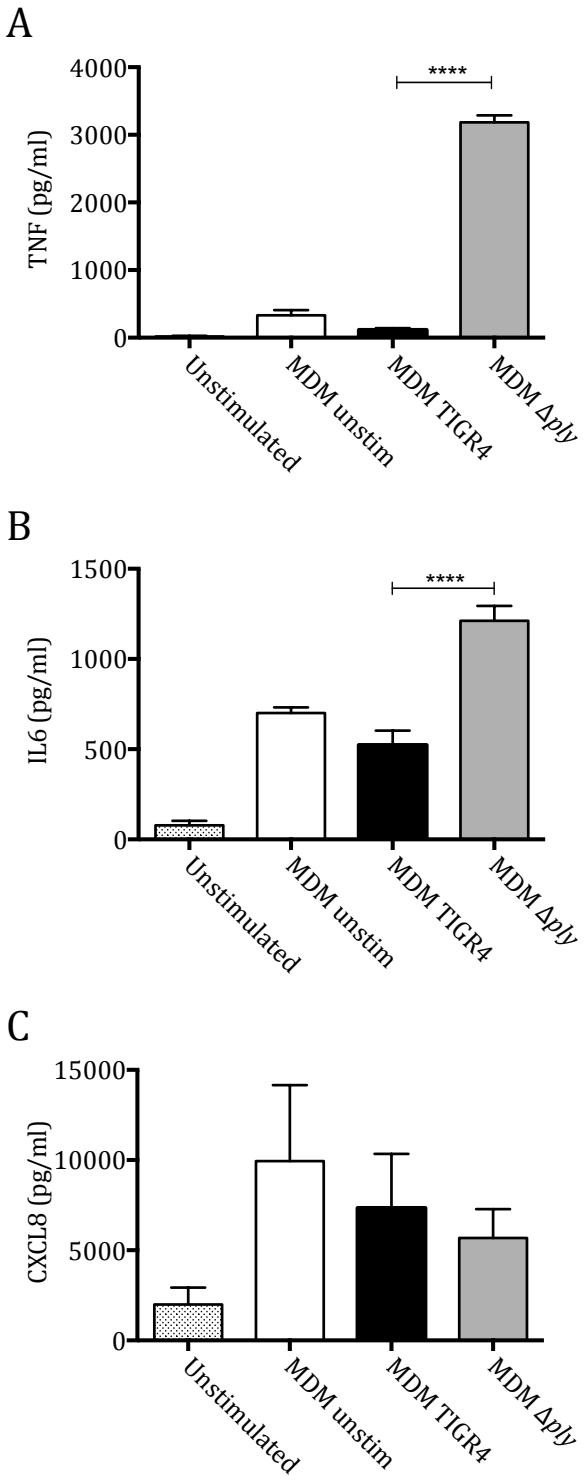

Figure 6.8 Cytokine release by A549 cells in response to conditioned media from MDM

A549 cells were incubated with pooled conditioned media from MDM incubated TIGR4 or Δ*ply* (4 separate experiments were pooled) at MOI 10. The conditioned media was diluted 1 in 5 in media before adding to A549 cells. Supernatant was analysed for cytokines after 6 hours. Mean +/- SEM of 3 experiments shown. Panel A shows TNF, B shows IL6, and C shows CXCL8. The data was analysed by 1 way ANOVA and Tukey's multiple comparisons test.

6.4 Effects of purified pneumolysin

The effect of purified Ply was measured to establish whether extracellular Ply had different effects from cytosolic Ply in the context of a whole bacterium. Purified Ply induced a dose related increase in pro-inflammatory cytokine secretion from MDM (figure 6.9), although cytokine release was only seen at high concentrations of Ply. This was more evident with high concentrations of non-haemolytic Ply, though this may be due to the cytotoxic effects of very high concentrations of purified Ply causing cell death; in these experiments 10μg/ml caused significant numbers of MDM to become non-adherent within 6 hours (data not shown). The experiments were replicated in the presence of polymyxin B to ensure that the inflammatory responses were not caused by contaminating endotoxin. There appeared to be a significant effect of polymyxin B on the MDM TNF response to Ply and a trend towards an effect with IL6 (figure 6.10), suggesting that there may be an effect of endotoxin contamination at high concentrations of Ply contributing to its inflammatory effect. This was not evident in CXCL8 responses, and a trend towards the opposite response in IL1β suggested that high concentrations of Ply have an intrinsic pro-inflammatory effect on the inflammasome as previously described (McNeela, Burke et al. 2010). The inflammatory response from epithelial cells was again limited, and IL1β remained undetectable (figure 6.11).

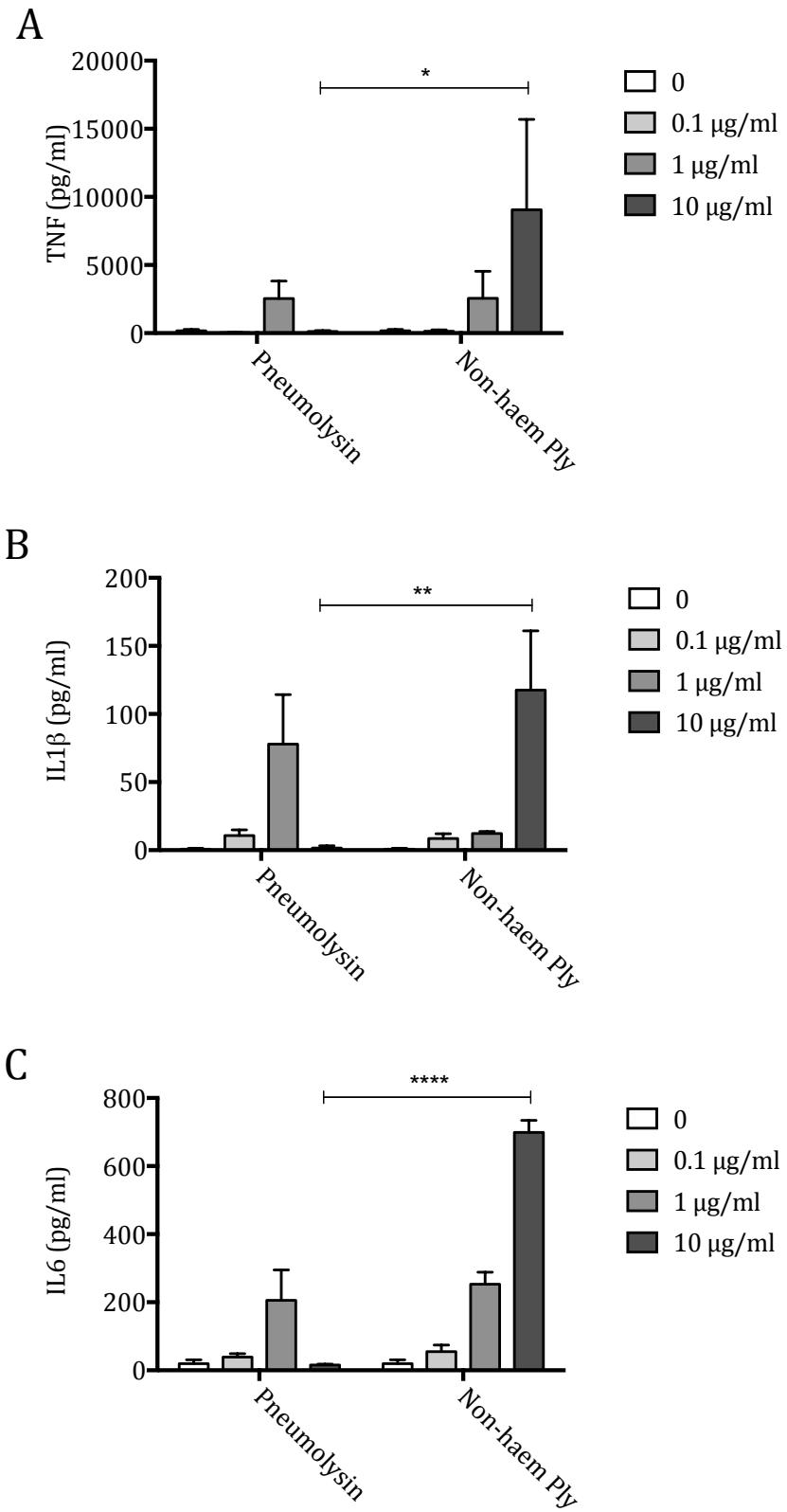

Figure 6.9 Inflammatory response to purified pneumolysin

Purified Ply and a non-haemolytic variant were incubated with MDM at various concentrations and supernatant analysed for A) TNF, B) IL1β, and C) IL6 after 6 hours. Results are presented as mean +/- SEM, and analysed by 2 way ANOVA and Tukey's multiple comparisons test.

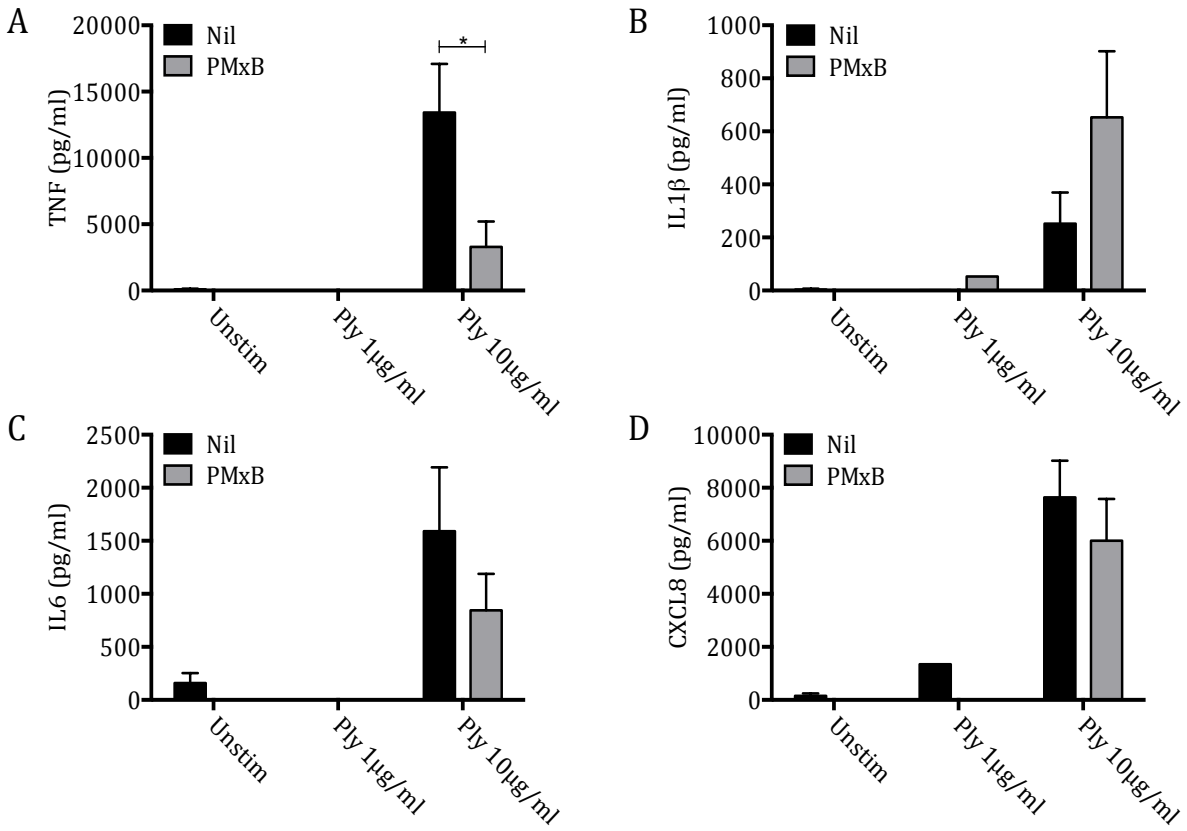

Figure 6.10 Effect of polymyxin B on purified pneumolysin

In panels A, B, C, and D MDM were incubated with purified Ply with or without 30 µg/ml polymyxin B (PMxB), and TNF, IL1β, and IL6 measured respectively. Both sets of experiments are represented as means +/- SEM of 3 experiments. Analysis was by 2 way ANOVA and Tukey's multiple comparisons test.

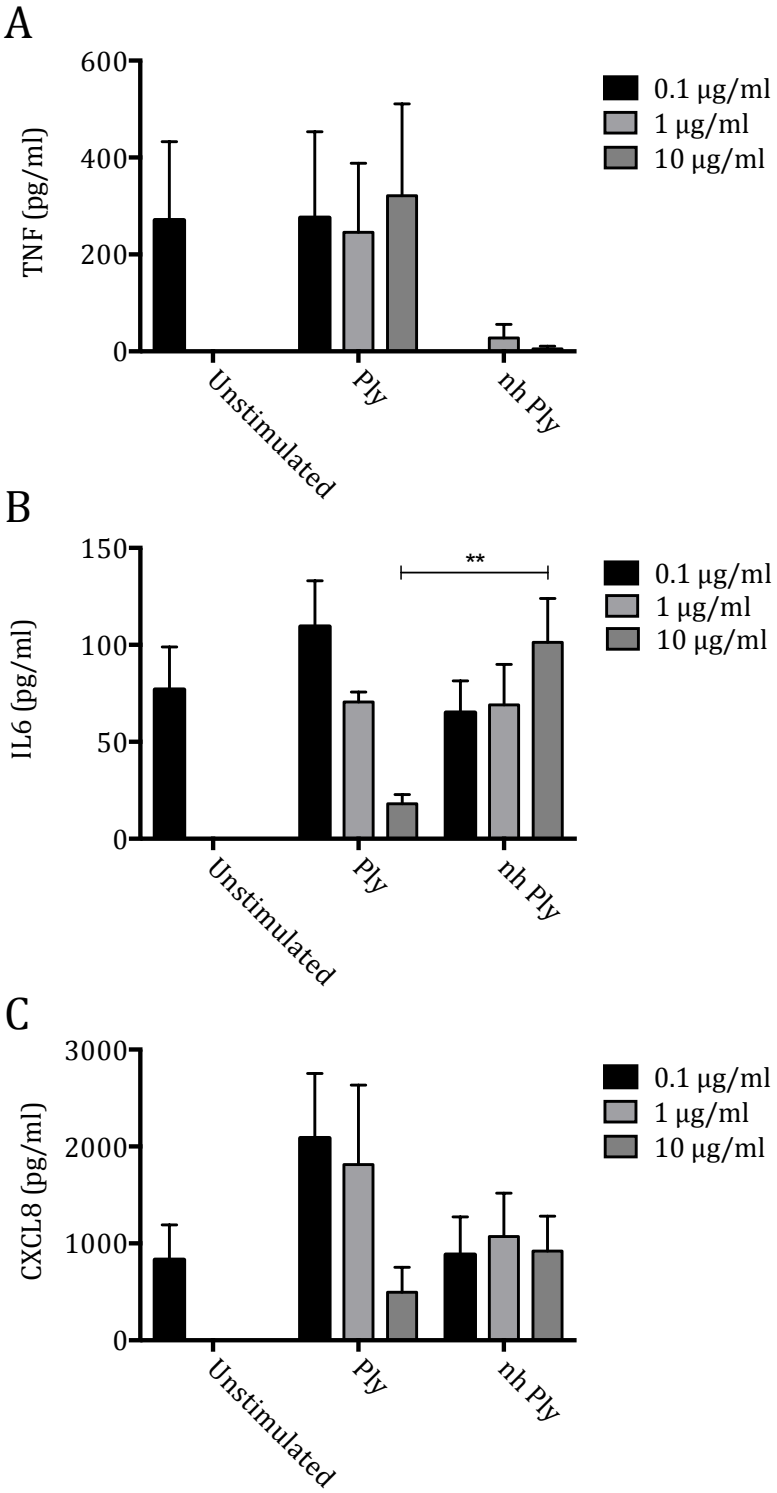

Figure 6.11 Inflammatory response of epithelial cells to purified pneumolysin

Purified Ply and a non-haemolytic variant was incubated with A549 at various concentrations and supernatant analysed for A) TNF, B) IL6 and C) CXCL8 (IL1β levels were undetectable) after 6 hours. Results are presented as mean +/- SEM, and analysed by 2 way ANOVA and Tukey's multiple comparison test.

6.5 Effect of pneumolysin on *S. pneumoniae* survival and macrophage internalisation

As Ply is thought to be important in virulence, the effect on bacterial viability was assessed. As phagocytosis is the main mechanism by which *S. pneumoniae* is killed by the host, and this could affect the inflammatory response, the effect of Ply on bacterial phagocytosis was also ascertained. TIGR4 and Δ*ply* CFU in MDM supernatant were similar, indicating similar growth in media and rate of killing by MDM in culture (figure 6.12, panel A). The gentamicin protection assay demonstrated similar levels of bacterial adherence and uptake to MDM for both strains (figure 6.12, panel B), i.e. no differences in internalisation. So the differences in inflammatory response between the strains were not explained by differences in bacterial numbers. This was supported by data in mouse AM after intranasal infection with fluorescently labelled bacteria and flow cytometry of AM in recovered BALF, with similar numbers of bacteria associated with cells 4 hours after inoculation (figure 6.12, panels C and D).

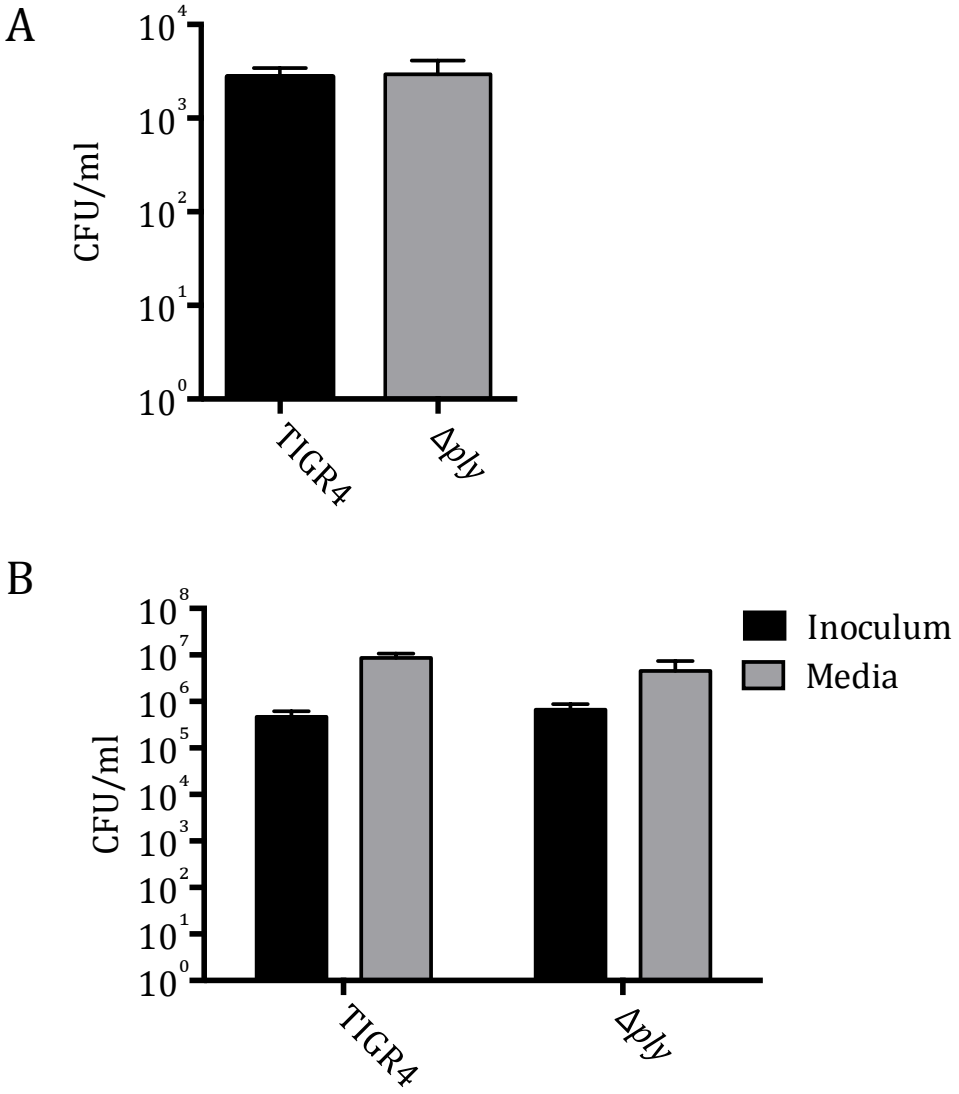

Figure 6.12 The effect of pneumolysin on bacterial numbers

Bacterial counts (CFU/ml) of MDM supernatants at 6 hours are shown in panel A as median +/- IQR of 4 experiments and analysed by Mann-Whitney U test. Panel B shows growth of wild-type and mutant bacteria (CFU/ml) in media in tissue culture plates containing no cells as median +/- IQR of 4 experiments. These data are analysed by Kruskal-Wallis and Dunn's multiple comparisons test. No significant differences were noted.

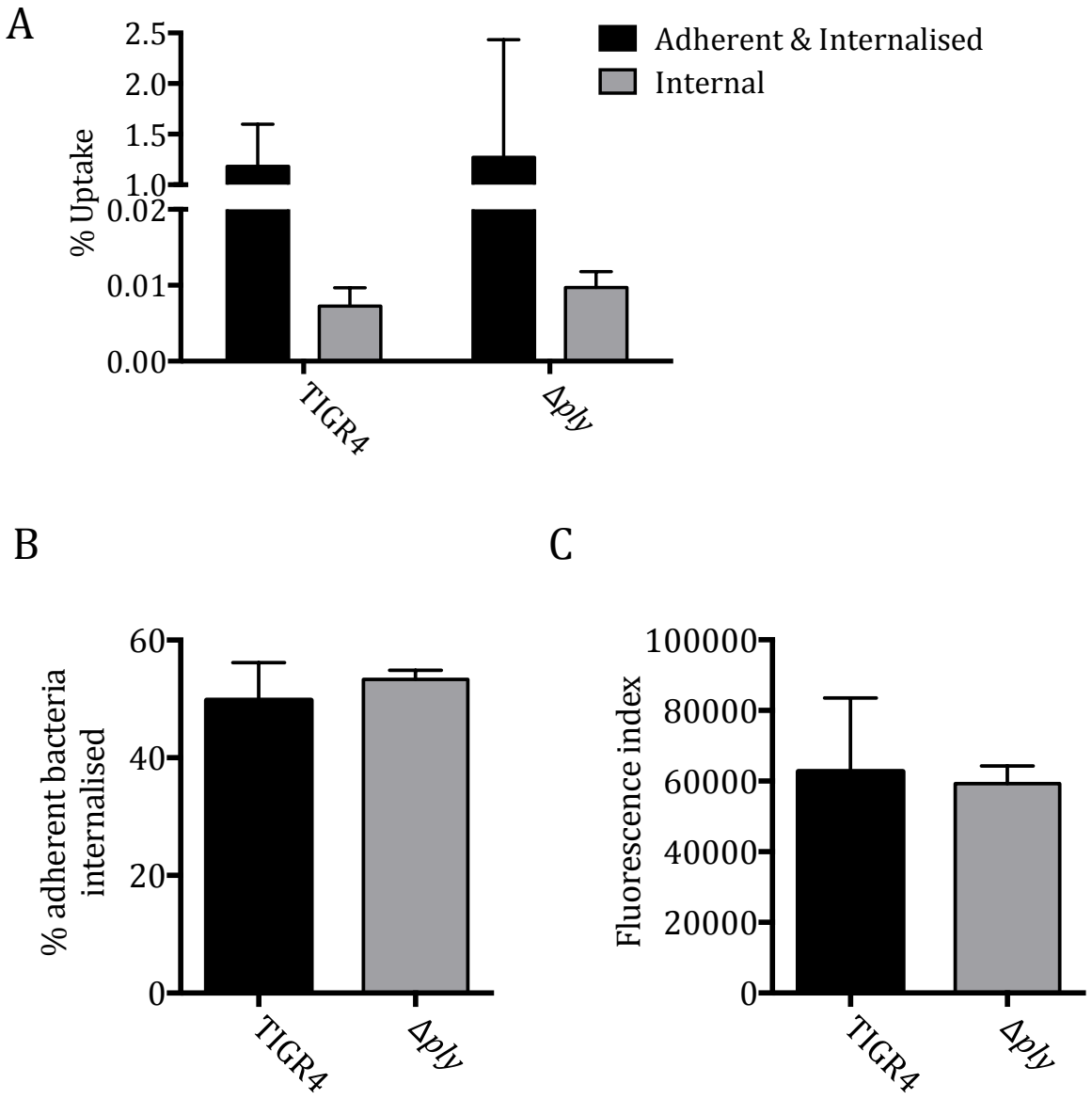

Figure 6.13 The effect of pneumolysin on bacterial uptake and association

Panel A shows numbers of bacteria adherent and internalised in MDM after 1 hour, measured by gentamicin protection assay, presented as mean +/- SEM of 3 experiments. Panel B & C show recovered mouse AM association with FAM-SE labelled bacteria after 4 hours, presented as mean +/- SEM and analysed by t-test.

6.6 Effect of pneumolysin in other serotypes

To ensure that the pro-inflammatory effect of Ply on MDM was replicated across other serotypes, MDM responses were assessed by 3 other serotypes along with their isogenic Ply deficient mutants. The effects on TNF, IL1β, and IL6 for the serotype 2, 3, and 23F strains were broadly similar to those seen with the TIGR4 stains, with the Δ*ply* mutants causing increased TNF and IL6 levels for all three strains and increased IL1β levels for the serotype 2 and 3 strains (figure 6.14).

MDM cytokine responses to naturally occurring non-isogenic Ply expressing and deficient serotype 1 strains also suggested that Ply also dampens TNF and IL6 secretion in this context (figure 6.15). In addition serotype 1 strains expressing a non-haemolytic Ply caused an intermediate phenotype, suggesting that both insertion of Ply into cell membranes and oligomerisation to form pores are important for the anti-inflammatory this response on MDMs (Korchev, Bashford et al, 1998).

Using isogenic D39 strains, these effects of Ply were confirmed (figure 6.16), with the non-haemolytic Ply having a similar partial phenotype as that seen with the serotype 1 clinical isolates. In addition, a complemented strain recapitulated the effects of wild-type D39, linking the phenotype directly to the Ply mutation.

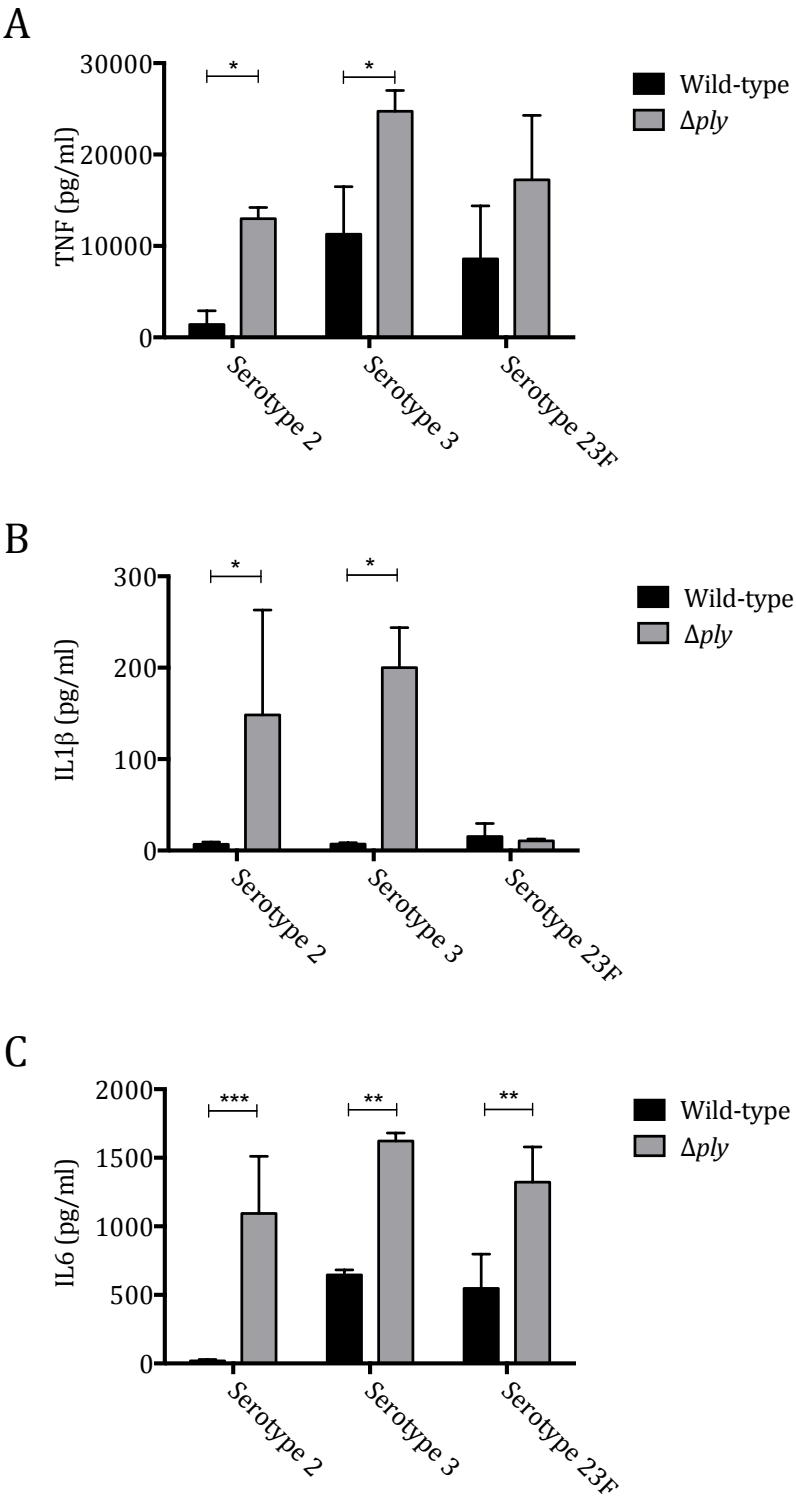

Figure 6.14 MDM cytokine response to different serotypes and their isogenic pneumolysin deficient mutants

MDM were incubated with 4 different serotypes and their isogenic Ply deficient mutants at MOI 10 for 6 hours. Supernatants were removed and analysed for A) TNF, B) IL1β, and C) IL6. Data are presented as mean +/- SEM. Results were analysed by 2 way ANOVA and Tukey's multiple comparisons test.

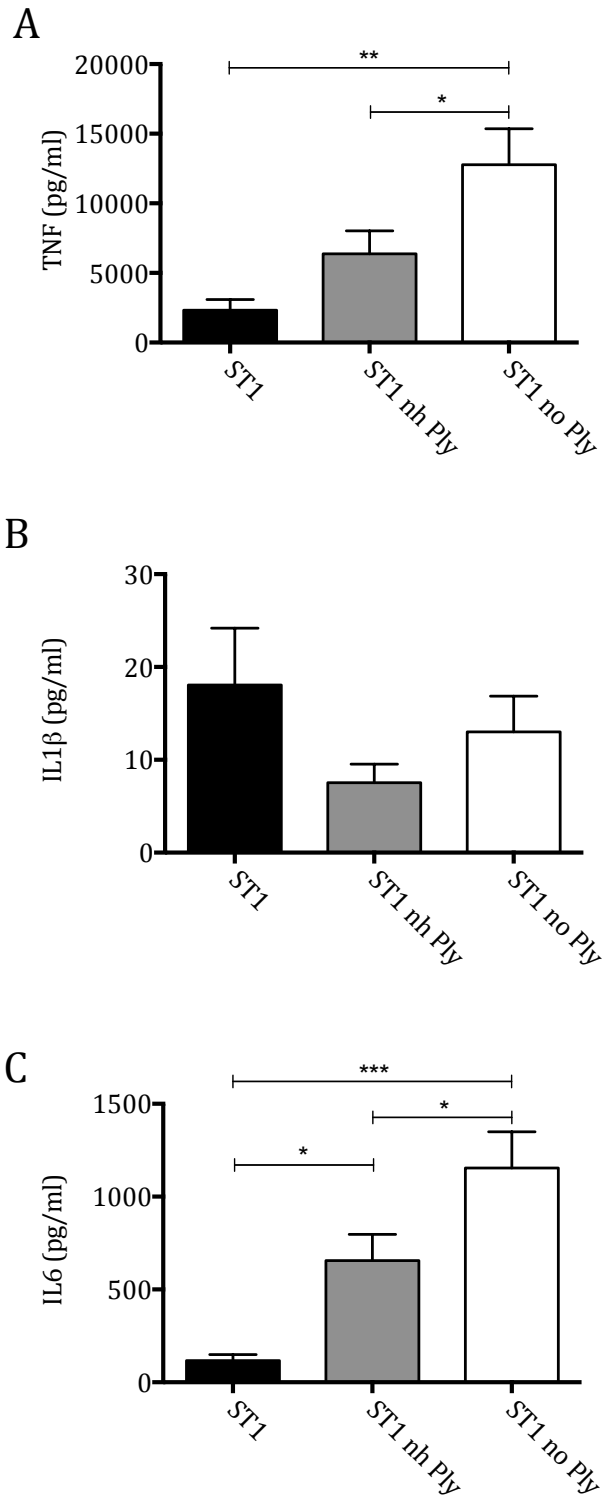

Figure 6.15 MDM cytokine response to Serotype 1 strains

MDM were incubated with serotype 1 strains at MOI 10 for 6 hours. The 3 clinical isolates express Ply normally, express non-haemolytic Ply, or no Ply at all respectively. Supernatants were removed and analysed for A) TNF, B) IL1β, and D) IL6. Data are presented as mean +/- SEM. Results were analysed by 1 way ANOVA and Tukey's multiple comparisons test.

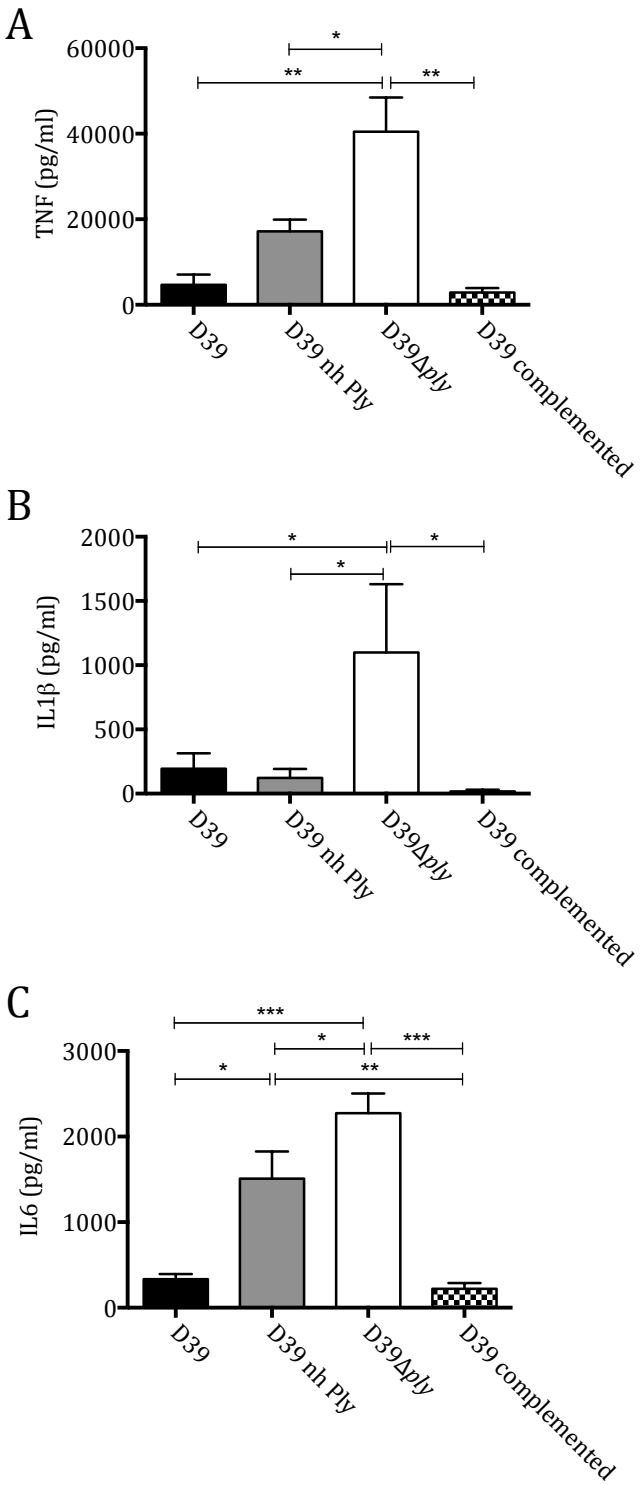

Figure 6.16 MDM cytokine response to D39, D39 expressing no pneumolysin, D39 expressing non-haemolytic pneumolysin, and a complemented strain

MDM were incubated with a D39 strain, its isogenic Ply deficient mutant, a mutant expressing non-haemolytic Ply, and a complemented strain (i.e. the Ply gene has been reinserted after removal) at MOI 10 for 6 hours. Supernatants were removed and analysed for A) TNF, B) IL1β, C) IL6, and D) CXCL8. Data are presented as mean +/- SEM. Results were analysed by 1 way ANOVA and Tukey's multiple comparisons test.

6.7 Effect of capsule and pneumolysin together on inflammation

The data from chapter 3 and 6 indicate that capsule is pro-inflammatory, and that Ply is anti-inflammatory. To establish if these two components affect each other, a double mutant lacking capsule and Ply was created and incubated with MDM to obtain supernatant cytokine levels. The results showed that the effect of Ply deletion largely eclipsed the pro-inflammatory effect of capsule with similar levels of TNF, IL6 and IL1β in the supernatants of MDMs incubated with the Δ*ply* and Δ*cps*Δ*ply* mutant strains (figure 6.17). Similar changes were seen for TNF, IL6 and IL1β gene expression levels (figure 6.18). It is not clear why the difference between TIGR4 and Δ*cps* is not evident in this data set (compared to figure 3.3). Potential explanations include differential MDM numbers and their activation status, as well as differences in individual host responses. The data are not easily combinable with that of figure 3.3 with different CT values, partially due to the use of an alternative qPCR reader in this experiment due to refurbishment of the lab. However, the data does support that the anti-inflammatory effects of Ply are greater than the pro-inflammatory effects of capsule.

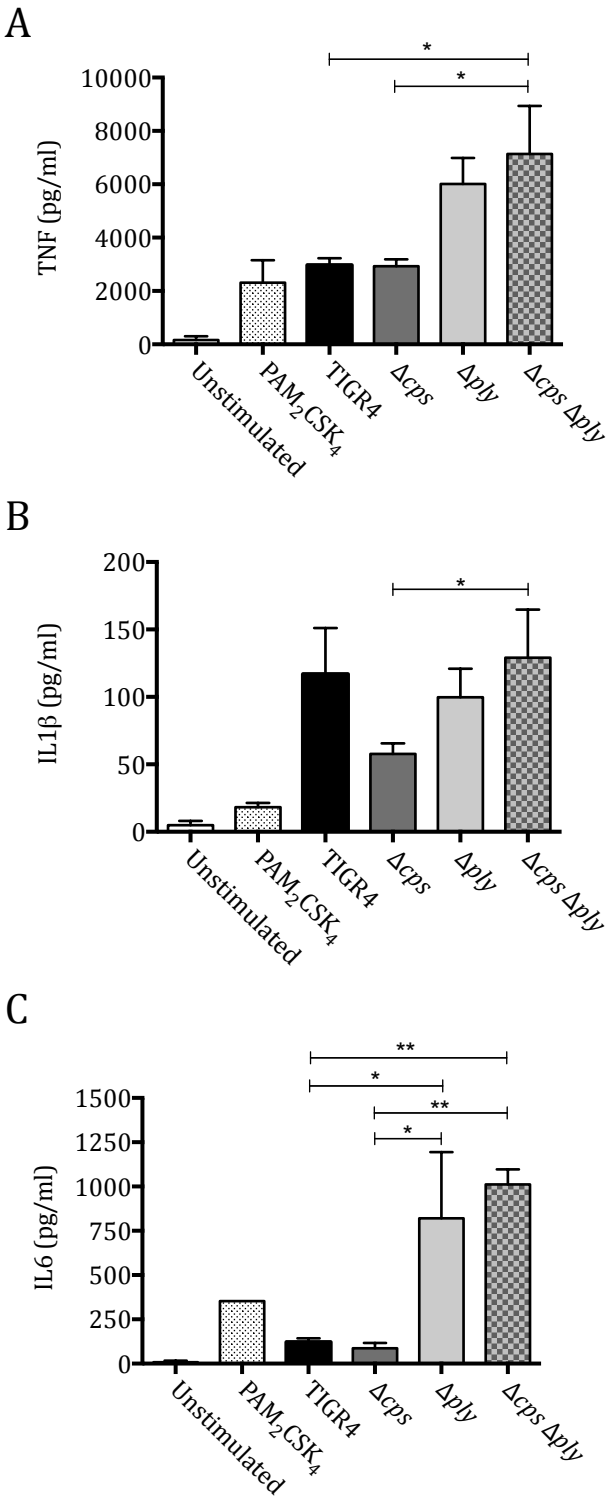

Figure 6.17 MDM cytokine response to TIGR4, Δ*cps*, Δ*ply*, and Δ*cps*Δ*ply* double mutants

MDM were incubated with TIGR4, an isogenic capsule deficient strain, a Ply deficient strain, and a mutant deficient in both capsule and Ply. They were incubated at MOI 10 for 6 hours. Supernatants were removed and analysed for A) TNF, B) IL1β, and D) IL6. Data are presented as mean +/- SEM. Results were analysed by 1 way ANOVA and Tukey's multiple comparisons test.

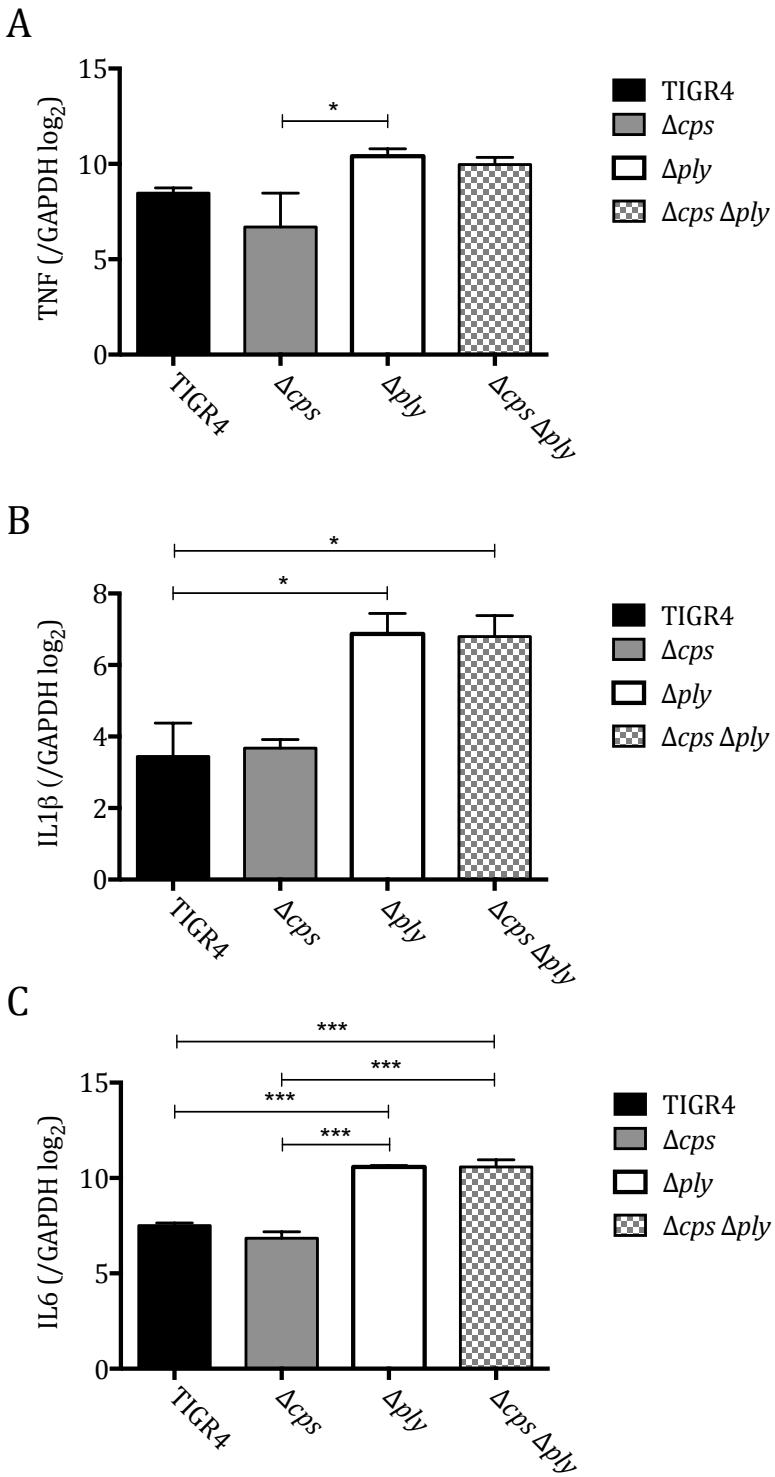

Figure 6.18 MDM cytokine gene expression in response to TIGR4, Δ*cps*, Δ*ply*, and Δ*cps*Δ*ply* double mutants

MDM were incubated with TIGR4, an isogenic capsule deficient strain, a Ply deficient strain, and a mutant deficient in both capsule and Ply. They were incubated at MOI 10 for 4 hours. RNA was extracted from cell lysates and analysed for A) TNF, B) IL1β, and D) IL6 by qPCR. Data are presented as mean +/- SEM. Results were analysed by 1 way ANOVA and Tukey's multiple comparisons test.

6.8 Effect of pneumolysin in mouse pneumonia

The mouse pneumonia model was used to establish whether the *in vitro* findings had *in vivo* correlates. By 4 hours after intranasal infection there was a $\log_{10}$ more TIGR4 CFU recovered from BALF than Δ*ply* CFU (figure 6.19) reflecting increased virulence. There were no statistically significant differences in lung homogenate CFU at 4 hours, or in BALF and lung CFU at 24 hours by which time both strains bacteria had largely been cleared.

At 4 hours there were similar numbers of neutrophils found in lavage fluid, despite the differences in bacterial numbers (figure 6.20). By 24 hours in mice infected with the wild-type TIGR4 there were significantly more recruited neutrophils and increased alveolar leak, as measured by albumin concentrations. BALF TNF levels at 4 hours reflected *in vitro* data, with significantly lower TNF levels for mice infected with the TIGR4 strain compared to those infected with the Δ*ply* strain. By 24 hours BALF TNF levels were much lower with no differences between mice infected with the TIGR4 and Δ*ply* strains (figure 6.21). In contrast to the TNF data, BALF IL1β levels at 4 and 24 hours were greater in mice infected with the TIGR4 wild-type strain compared to those infected with the Δ*ply* strain. BALF IL6 levels were not significantly different between the 2 strains. Levels of TNF in lung homogenates were much lower, and similar between the 2 strains, whereas lung levels of IL1β were much greater than BALF, with higher levels in mice infected with Δ*ply* compared to those infected with TIGR4 the strain (figure 6.22), opposing the IL1β patterns in BALF. Lung IL6 levels opposed this pattern, with higher levels in mice infected with the TIGR4 strain compared to those infected with Δ*ply* strain at 4 hours. Overall, these data suggest there is an anti-inflammatory effect of Ply during early lung infection with marked suppression of early BALF TNF responses, but that there was also a pro-inflammatory effect in increasing IL1β in some compartments compatible with the described data on Ply activation of the inflammasome (McNeela, Burke et al. 2010).

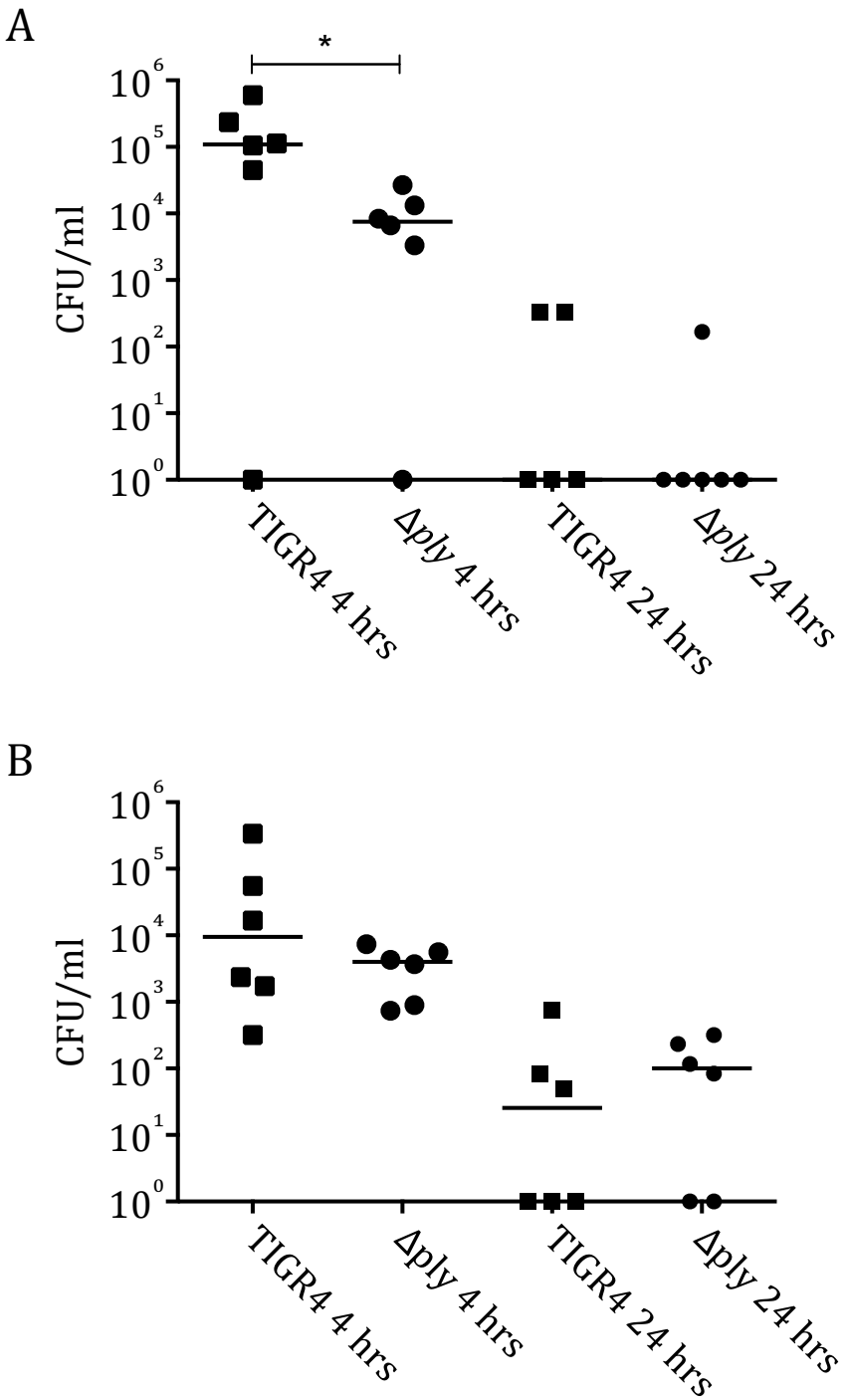

Figure 6.19 Bacterial counts in BALF and lung homogenate after intranasal infection with TIGR 4 or Δ*ply*

5 week old female CD1 mice were inoculated intranasally with 5×10^6 CFU bacteria under isoflurane anaesthesia. Mice were culled at specified timepoints, bronchoalveolar lavage was performed (panel A), and lungs removed and homogenised (panel B). Both were then plated to ascertain bacterial numbers. There were 6 mice per group. Data presented as per individual mouse and medians; analysed by Kruskal-Wallis and Dunn's multiple comparisons test.

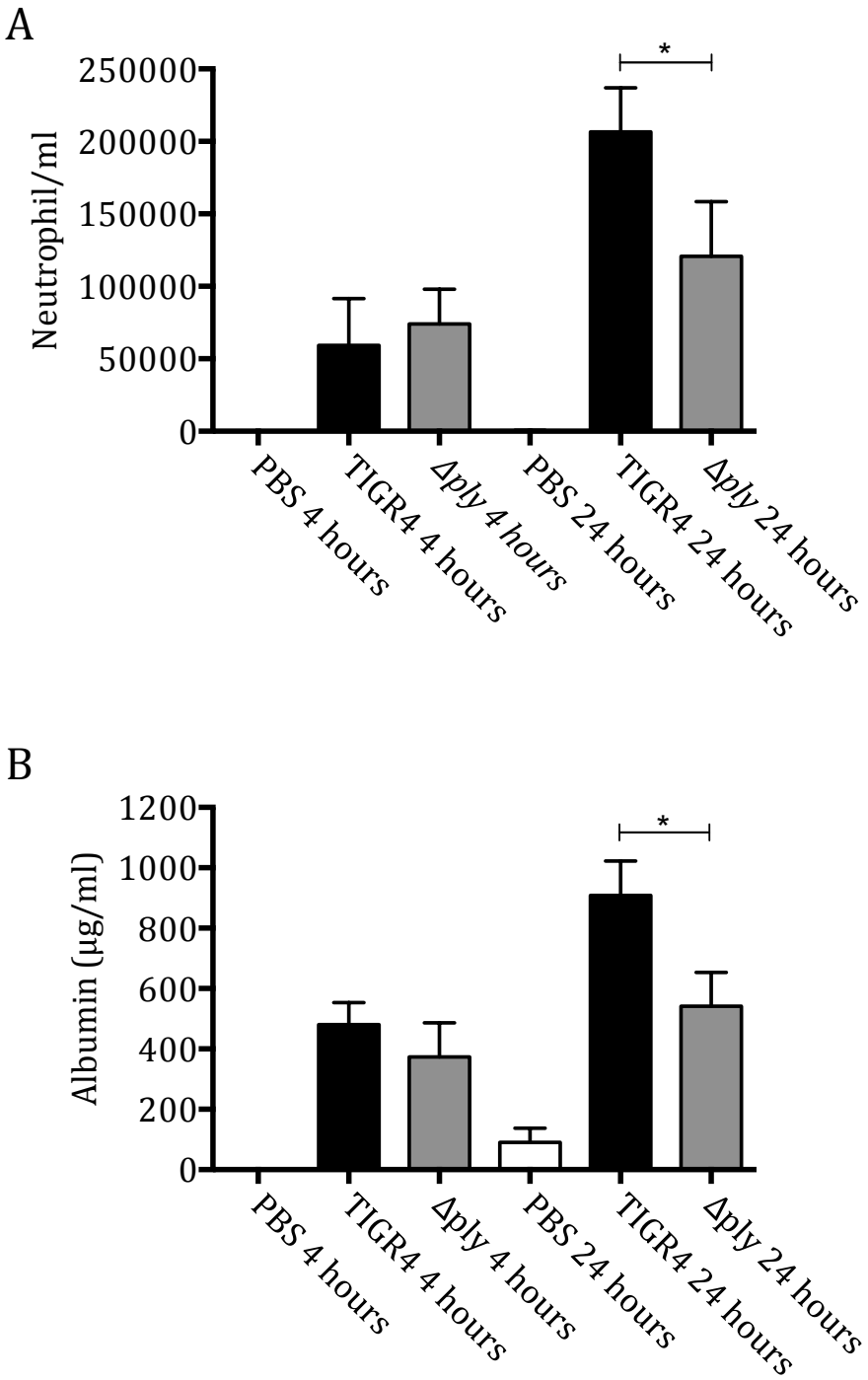

Figure 6.20 Neutrophil counts and albumin in BALF after intranasal infection with TIGR4 or Δ*ply*

5 week old female CD1 mice were inoculated intranasally with 5×10^6 CFU bacteria under isoflurane anaesthesia. Mice were culled at specified timepoints, bronchoalveolar lavage was performed and neutrophil numbers were determined (panel A), as well as albumin levels (panel B). There were 6 mice per group. Data presented as mean +/- SEM; analysed by 1 way ANOVA and Tukey's multiple comparisons test.

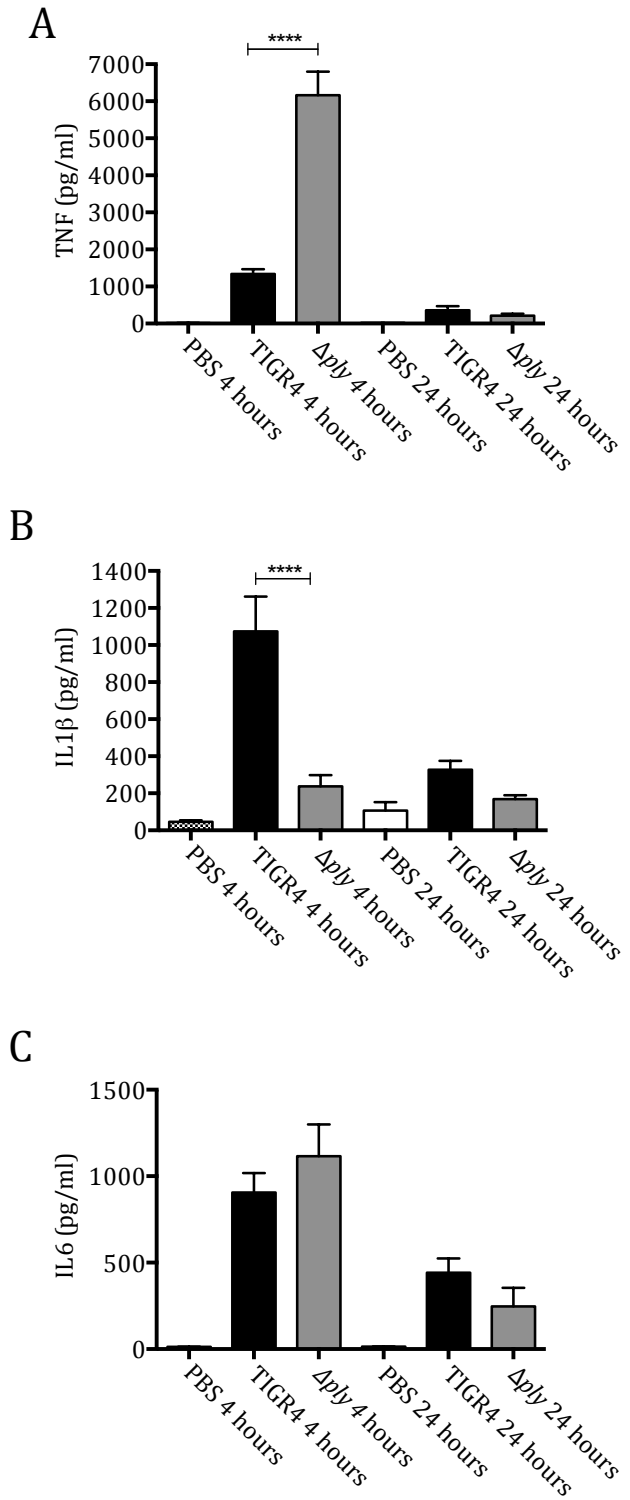

Figure 6.21 Cytokine levels in BALF after intranasal infection with TIGR 4 or Δ*ply*

5 week old female CD1 mice were inoculated intranasally with 5×10^6 CFU bacteria under isoflurane anaesthesia. Mice were culled at specified timepoints, bronchoalveolar lavage was performed and TNF (panel A), IL1β (panel B), and IL6 (panel C) levels were measured. There were 6 mice per group. Data are presented as mean +/- SEM; analysed by 1 way ANOVA and Tukey's multiple comparisons test.

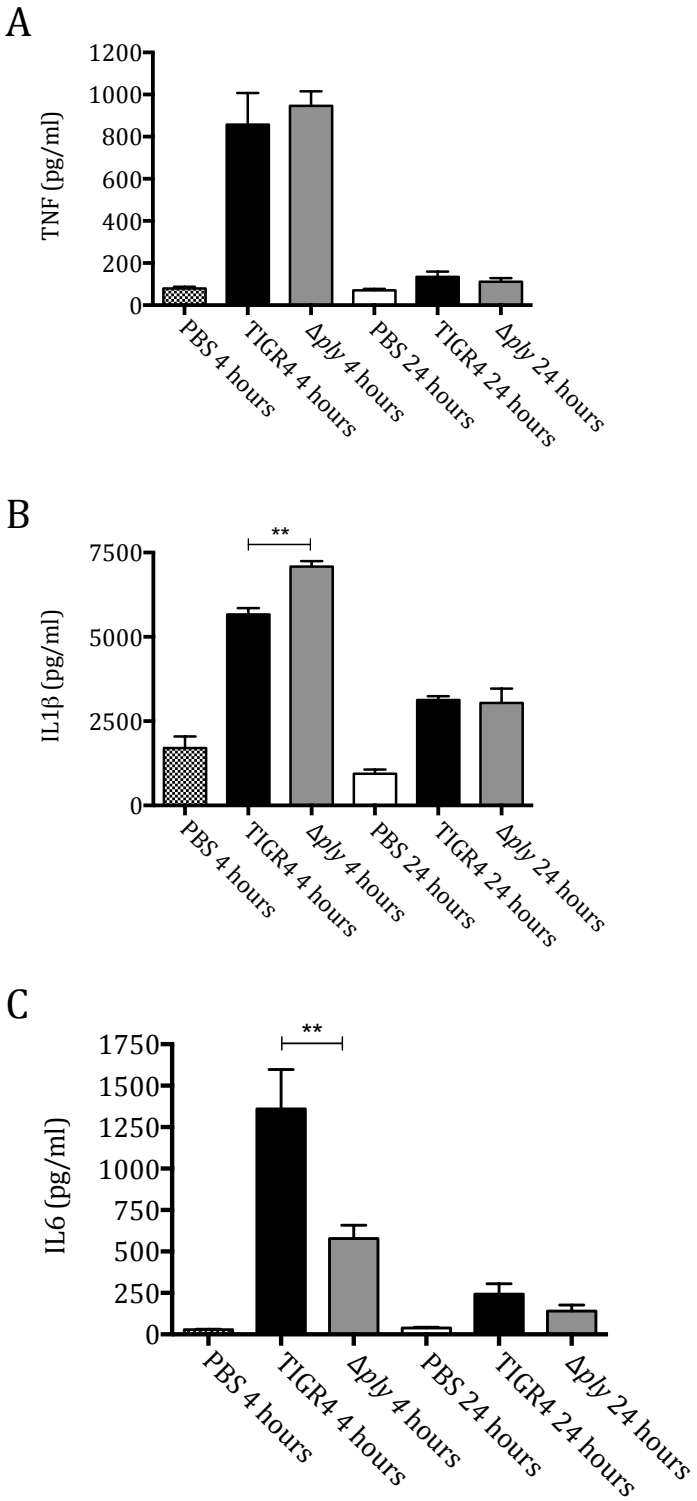

Figure 6.22 Cytokine levels in lung homogenate after intranasal infection with TIGR4 or Δ*ply*

5 week old female CD1 mice were inoculated intranasally with 5×10^6 CFU bacteria under isoflurane anaesthesia. Mice were culled at specified timepoints, lung homogenate retrieved, and TNF (panel A), IL1β (panel B), and IL6 (panel B) levels were measured. There were 6 mice per group. Data are presented as mean +/- SEM; analysed by 1 way ANOVA and Tukey's multiple comparisons test.

6.9 Effects of pneumolysin in D39 in mouse pneumonia

To ensure the effects of Ply *in vivo* were not serotype specific, the mouse pneumonia model was used to assess D39, D39Δ*ply*, and complemented D39. For these strains, 4 hours after inoculation there were similar numbers of bacteria recovered in BALF and lung homogenate. The complemented D39 induced higher BALF neutrophil infiltrate, with no differences between D39 and D39Δ*ply* strains (figure 6.25). Similar to the TIGR4 experiments, compared to the results for D39 there was an increase in BALF TNF levels in mice infected with the Δ*ply* strain and lower BALF IL1β levels. These differences were lost between D39 and the complemented Δ*ply* strain. There were no differences in BALF IL6 levels (figure 6.26) between the strains. There were no significant differences in TNF or IL1β in lung homogenate, but complemented D39 induced significantly more IL6 than Δ*ply* (figure 6.27).

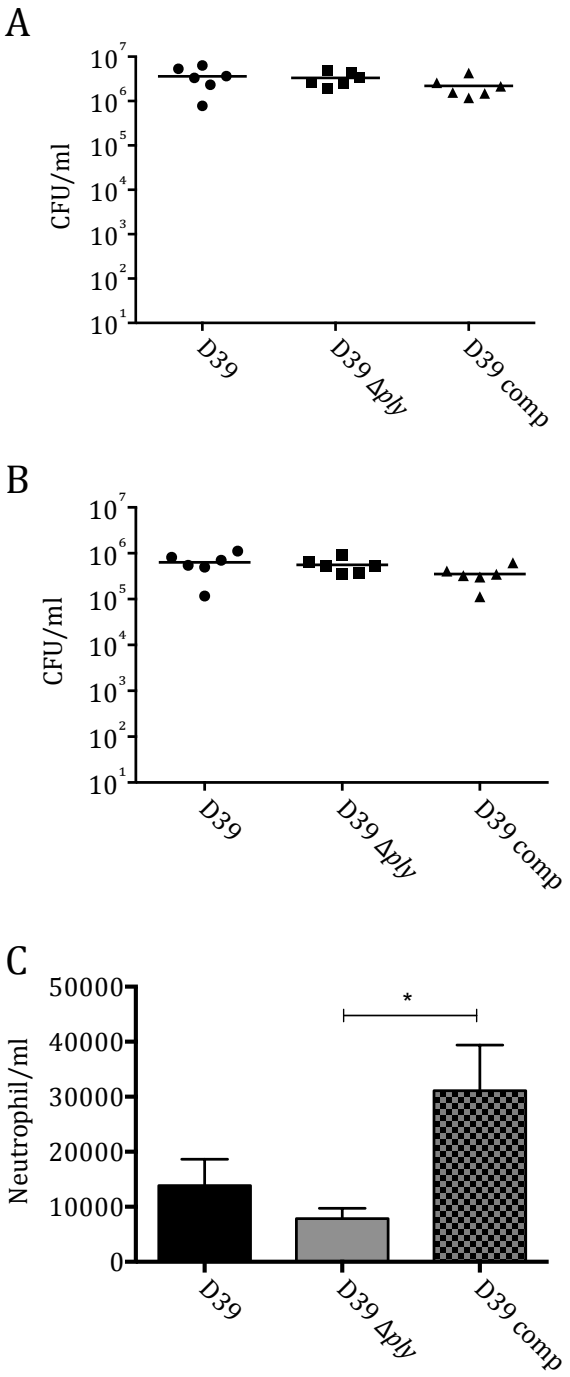

Figure 6.23 Bacterial and neutrophil counts in BALF and bacterial numbers in lung homogenate, and after intranasal infection with TIGR4 or Δ*ply*

5 week old female CD1 mice were inoculated intranasally with 5×10^6 CFU bacteria under isoflurane anaesthesia. Mice were culled at specified timepoints, bronchoalveolar lavage was performed (panel A), and lungs removed (panel B). Both were plated to ascertain bacterial numbers. Neutrophil numbers were measured in BALF. Data presented as per individual mouse and medians; analysed by Kruskal-Wallis with Dunn's multiple comparisons test for bacterial counts, and by 1 way ANOVA and Tukey's multiple comparisons test for neutrophil numbers (*=$p<0.05$).

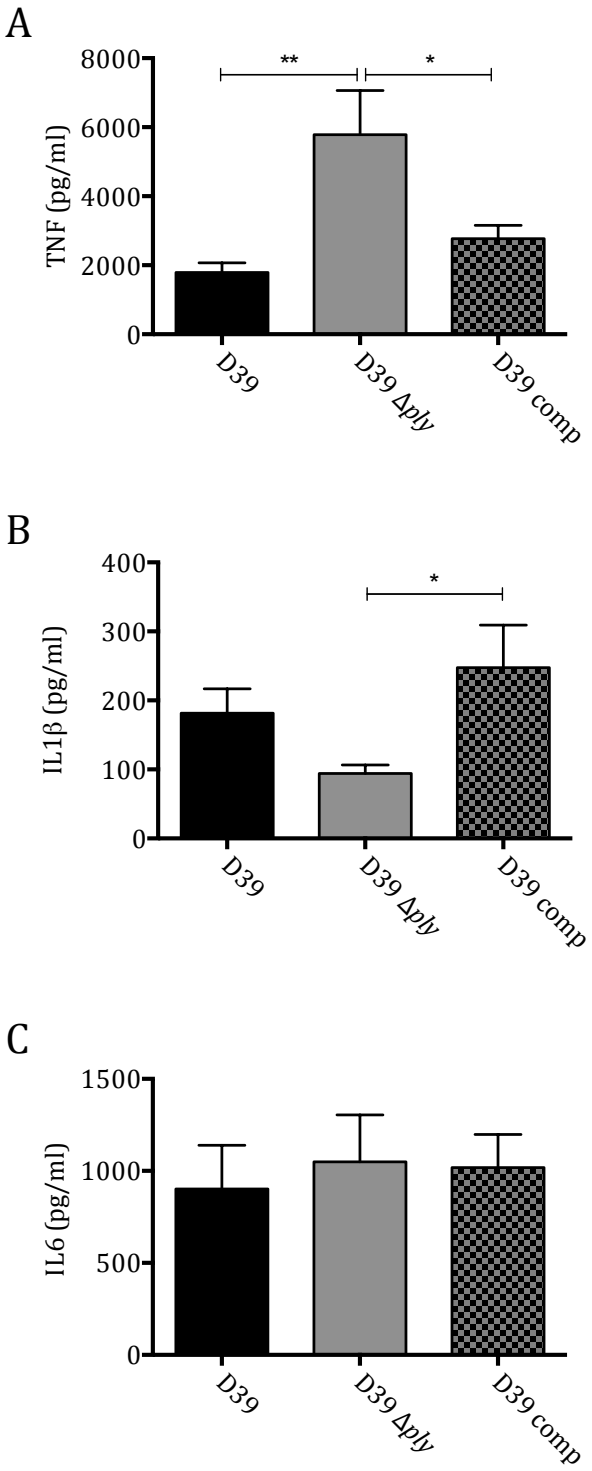

Figure 6.24 Cytokine levels in BALF after intranasal infection with D39, Δ*ply*, or complemented strain

5 week old female CD1 mice were inoculated intranasally with 5×10^6 CFU bacteria under isoflurane anaesthesia. Mice were culled at specified timepoints, BALF retrieved, and TNF (panel A), IL1β (panel B), and IL6 (panel C) levels were measured. There were 6 mice per group. Data are presented as mean +/- SEM and analysed by 1 way ANOVA with Tukey's multiple comparisons test.

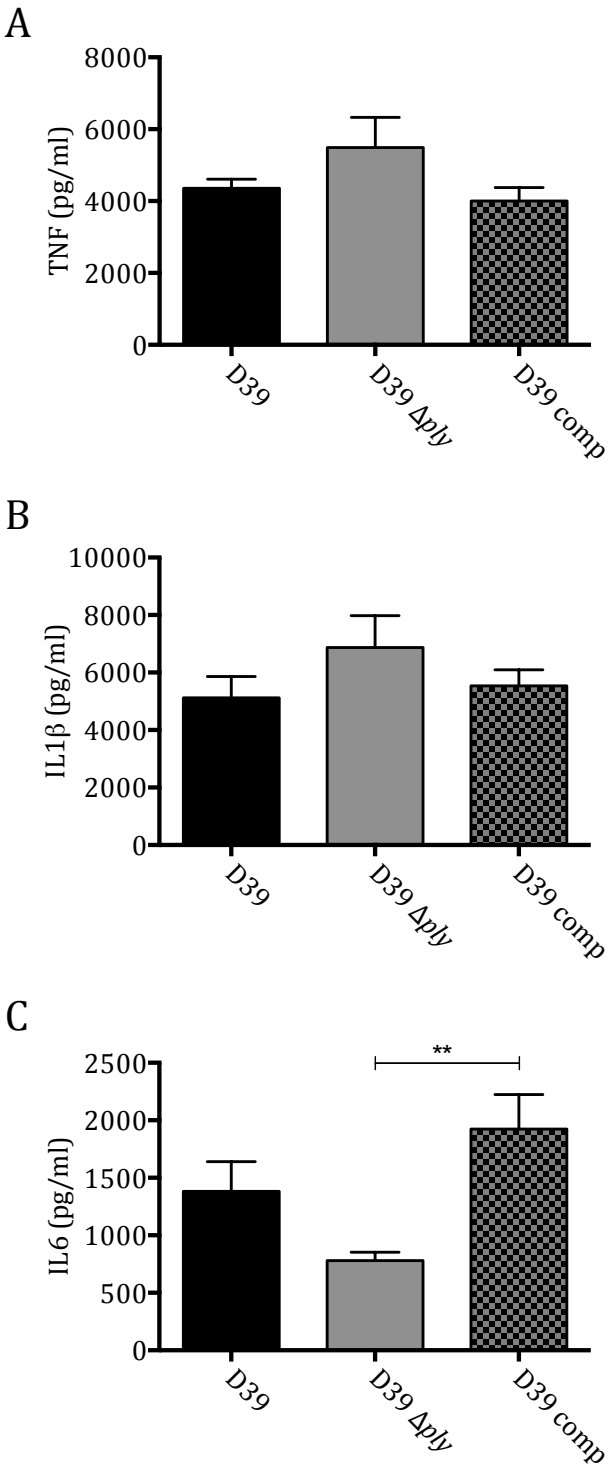

Figure 6.25 Cytokine levels in lung homogenate after intranasal infection with D39, Δ*ply*, or complemented strain

5 week old female CD1 mice were inoculated intranasally with 5×10^6 CFU bacteria under isoflurane anaesthesia. Mice were culled at specified timepoints, lung homogenate obtained, and TNF (panel A), IL1β (panel B), and IL6 (panel B) levels were measured. There were 6 mice per group. Data are presented as mean +/- SEM; analysed by 1 way ANOVA with Tukey's multiple comparisons test.

6.10 Chapter Summary

Ply is an important virulence factor in *S. pneumoniae* pathogenesis with pleiotropic effects on the host immune response. Previous data have largely held that Ply has pro-inflammatory effects, particularly through activation of TLR4, the inflammasome, and the delivery of bacterial breakdown products to cytosolic PRR. Much of these data had been derived from models using purified Ply.

Purified Ply induced significant cell death at high concentration, and did induce MDM pro-inflammatory responses, albeit at quite high concentrations (which could be directly due to the pore-induced cell death),, in line with other investigators. Not all of this inflammation can be explained my contamination by endotoxin, suggesting high concentrations of purified Ply in the external environment of cells are indeed pro-inflammatory.

The rest of the data presented above, using whole bacteria and isogenic mutants, suggests that Ply has important anti-inflammatory effects. Human macrophages produced less pro-inflammatory cytokine response to Ply containing wild-type bacteria than Δ*ply*. At this same early timepoint, alveolar epithelial cells secrete little pro-inflammatory cytokine in response to bacteria, but conditioned media from macrophages indicates that the Ply driven macrophage-phenotype increased the release of inflammatory cytokines by epithelial cells. The most contentious section of these data are the increased IL1β levels seen with Δ*ply* strains, suggesting that Ply inhibits the inflammasome. This phenomenon may be explained by the early timepoint, meaning less exogenous Ply both in cell culture and *in vivo* so less pore formation and so less inflammasome activation. The release of IL1β without Ply could be explained by more pro-IL1β synthesis due to other components of the bacteria, and then inflammasome activation by DAMPs such as ATP, or bacterial DNA activation of AIM. That is, the Ply does not inhibit the inflammasome directly, rather it inhibits production of the inflammasome components and IL1β, so taking longer for any K+ shifts due to Ply-related pore formation to have an effect.

Mutation of *ply* does not appear to affect rates of bacterial adhesion to epithelial cells, phagocytosis by MDM, or growth rates in cell culture supernatant, suggesting that different bacterial numbers between strains were unlikely to be a confounding factor.

The phenotype of increased inflammatory responses by MDM to the Ply strain was preserved across four other *S. pneumoniae* strains, and complementation replicated the wild-type phenotypes. These data suggest the differences seen were not due to genetic manipulation of the bacteria but directly linked to the inflammatory phenotype. The effect of non-haemolytic Ply seemed to be half that of haemolytic Ply suggesting that the pore-forming effect is partially implicated in the mechanism by which Ply alters early MDM inflammatory responses. possibly due to membrane insertion of Ply either singly or in oligomers to form pores.

Using a double capsule/Ply deficient mutant, I confirmed that capsule had little effect on Ply driven anti-inflammatory responses, and indeed the effect of capsule on inflammation was on a much smaller scale than that of Ply.

In an *in vivo* mouse pneumonia model some of the anti-inflammatory effects of Ply were replicated, specifically increases in BALF TNF levels. TNF is the quickest cytokine response seen and important in protection against *S. pneumoniae* infection. The increased IL1β levels in wild-type BALF probably reflect the pore-forming effect of Ply, which may be seen more quickly *in vivo* with more cell types and tissues involved in host response. Similar data was obtained using mice infected with the D39 strains.

7 Mechanisms of anti-inflammatory functions of pneumolysin

Once I had established the surprising anti-inflammatory effects of Ply *in vitro* and *in vivo*, I carried out a series of experiments to try and explore the mechanisms by which they occur.

7.1 Transcriptional response of monocyte derived macrophages

I carried out whole genome transcriptional analysis of MDM responses to wild-type TIGR4 and Δ*ply* to explore potential mechanisms that explain the differential inflammatory responses between the strains. Again the positive control, PAM_2CSK_4 data was obtained by Gillian Tomlinson. These data were obtained at the same time as the transcriptional data presented in chapters 4.1, 4.4, and 7.3. The data were analysed by T tests on MultiExperiment Viewer v 4.6.0 and significance was set at $p<0.05$. A false discovery rate was not used as the number of biological replicates was low (3 to 6), and confidence was built by comparison to historical group data and bioinformatic analysis confirmation with other experimental data.

Figure 7.1 shows all the genes on the microarray, with relative expression values plotted for MDM incubated with TIGR4 versus Δ*ply*. The red lines indicate 2 fold gene changes. A relatively small proportion of genes were differentially expressed between MDM incubated with either strain, but more genes were downregulated in the presence of Ply than upregulated, and to a greater extent.

A Venn diagram of upregulated genes indicates that after infection with TIGR4 or Δ*ply,* 294 or 314 genes respectively were upregulated compared to unstimulated controls (figure 7.2, panel A). 102 of these genes were shared between the two bacterial strains. Figure 7.2 panel B shows the 20 genes that were most overexpressed by TIGR4 in relation to Δ*ply*, with difference $\log_2$ in gene expression displayed. The most prominent genes in this list include IL12, important in stimulating Th1 responses, as well as genes stimulated as a consequence

of interferon signalling e.g. IFIT2, CXCL9, 10 & 11. Pro-inflammatory cytokines and chemokines were also upregulated by incubation with Δ*ply* e.g. IL6 and CCL2.

When gene upregulation was ranked by the genes most upregulated by wild-type TIGR4, comparison of the top 20 upregulated genes, shows that many were more upregulated by Δ*ply*. In particular, pro-inflammatory genes such as TNF, IL6, and chemokines such as CXCL10 were all upregulated in the absence of Ply (figure 7.4).

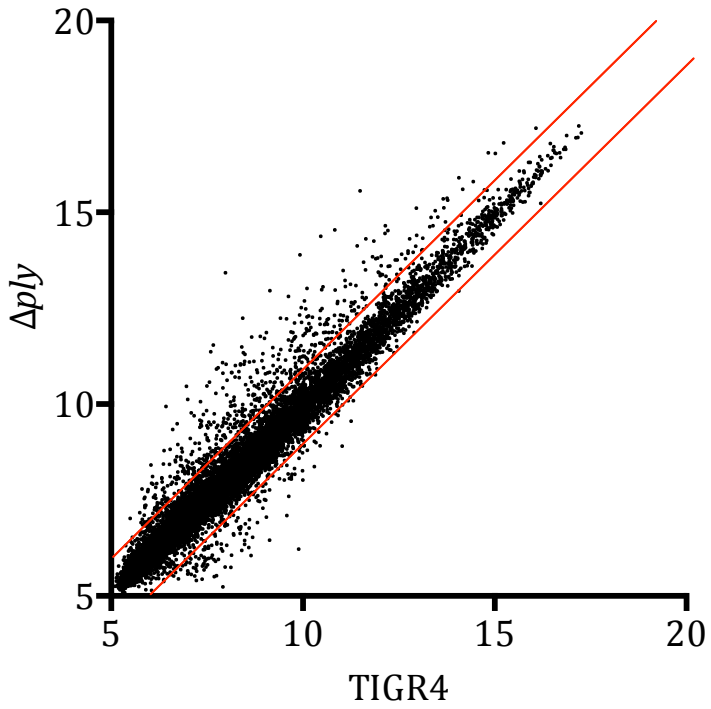

Figure 7.1 Transcriptome Response of MDMs to TIGR4 and Δ*ply*

The graph plots expression values of all genes on a microarray comparing TIGR4 v Δ*ply*. In both, the red lines indicate 2 fold differences. Each gene on the microarray is expressed as a data point. Data points falling outside these lines indicate significantly different gene expression between TIGR4 and Δ*ply*, with greater expression after incubation with Δ*ply* above the superior line and greater expression after incubation with TIGR4 below the lower line.

A

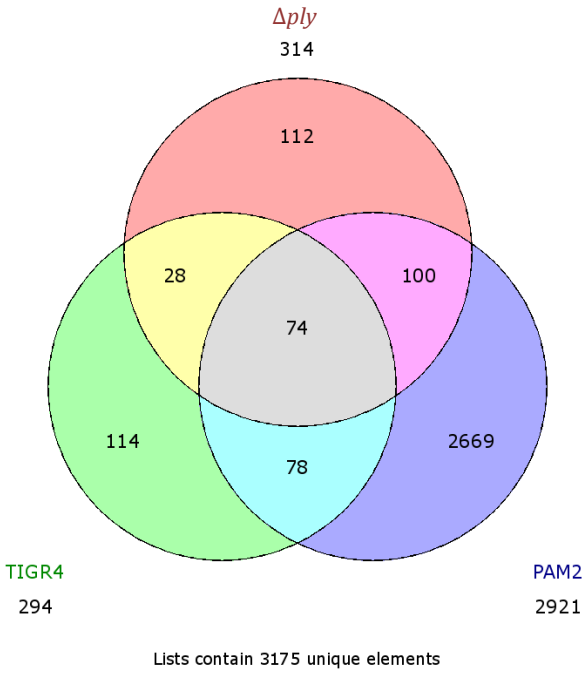

B

Gene Symbol	Δ*ply* - TIGR4
IL12B	6.00
SERPINB2	4.06
CCL5	4.00
CLCF1	3.79
CCR7	3.76
RSAD2	3.73
ISG20	3.69
IFITM1	3.68
CXCL10	3.62
CD38	3.51
SLAMF1	3.31
CXCL9	3.26
CCL2	3.23
EDN1	3.20
IL6	3.14
IFIT2	3.04
CSF3	3.02
CXCL11	3.00
IFI44L	2.95
LAMP3	2.93

Figure 7.2 Comparative transcriptome response of MDM to TIGR4 and Δ*ply* – most upregulated genes

Panel A is a Venn diagram showing the number of genes upregulated by more than 2 fold compared to unstimulated MDM for the two strains and the positive control. Panel B shows the genes most upregulated when comparing the MDM responses to the Δ*ply* strain with TIGR4 directly; the values indicating $\log_2$ of the difference in expression values between the conditions.

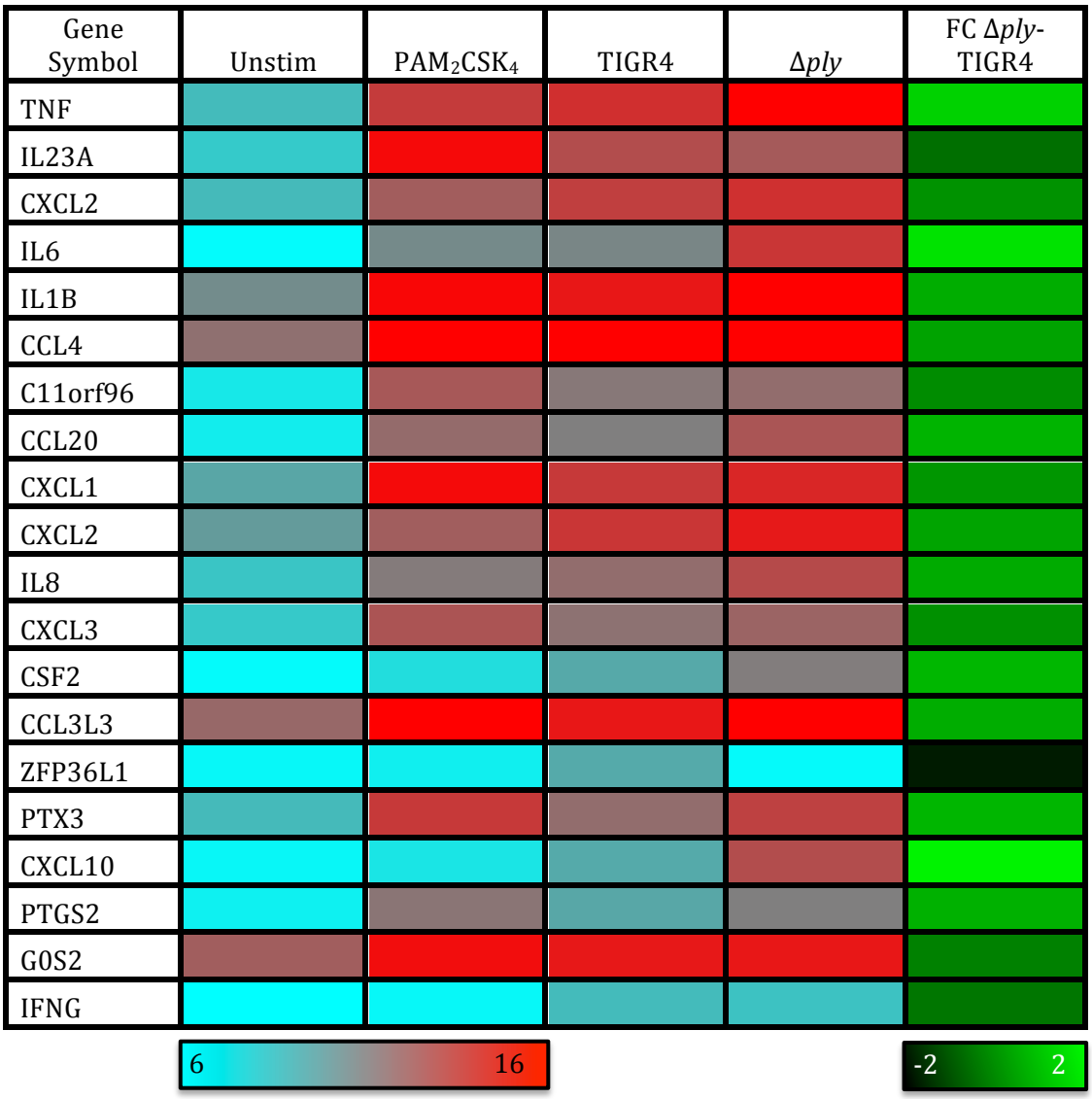

Figure 7.3 Comparison of genes upregulated by PAM_2CSK_4, TIGR4 and Δ*ply*

This heat map shows mean relative expression values of the top 20 genes upregulated by wild-type TIGR4 when compared to unstimulated MDM. The results displayed are from experiments of 3 donors. The most upregulated genes are displayed as relative expression with the most upregulated in red, and the least upregulated in blue. The last column shows a direct comparison of gene upregulation of these genes between TIGR4 and the Δ*ply* mutant, displayed as log_2 fold change with green being the most upregulated genes, and black the most downregulated.

A non-biased principle component analysis of the data shows that the Δ*ply* strain induces a similar pattern of gene transcription to PAM_2CSK_4 by PC2 and 3 (as previously, PC1 segregates data by the specific array used) (figure 7.4, panel A). As mentioned in chapter 4.1, PC1 accounts for 45% of variation seen, PC2 for 24%, and PC3 for 19%. This suggests that Ply acts to inhibit, mask, or counteract the transcriptional response to bacterial TLR2 activation, in the context of whole bacteria. In particular Ply inhibits inflammatory cytokine transcription, as shown by the genes that contribute to a negative deflection in PC 3 (figure 7.4, panel B).

oPOSSUM bioinformatics analysis of differentially upregulated genes reveals that the predicted transcription factors activated in response to Δ*ply* compared to unstimulated MDM were largely from the NFκB family (figure 7.5, panel A). In addition, the presence of Ply appeared to restrict the number of pathways upregulated by TIGR4. On direct comparison between the 2 strains, again the NFκB family followed by IRE were the most upregulated transcription factors stimulated by Δ*ply* (figure 7.5, panel B).

Innate DB software analysis of the pathways most upregulated by Δ*ply* compared to TIGR4 (figure 7.6) indicated that cytokine and IFN signalling pathways were prominent followed by innate immune signalling pathways.

A

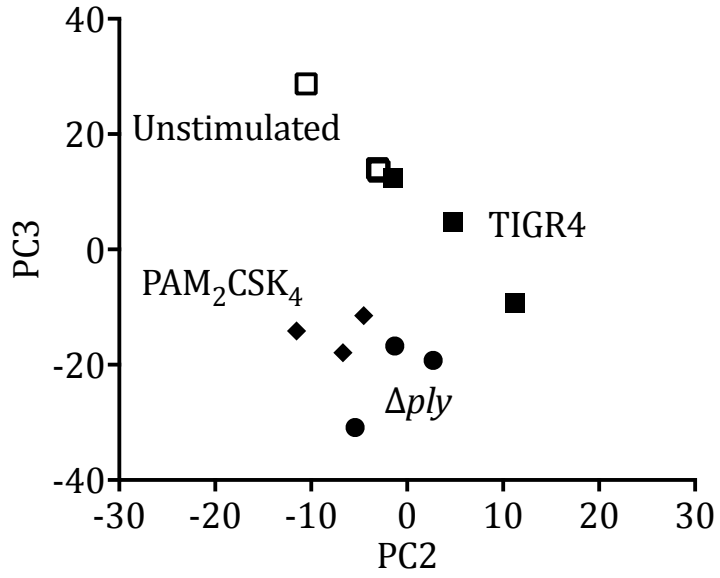

B

PC3 negative
IL6
TNF
CCL20
CSF3
CXCL1
TNFAIP6
IL1B
IL23A
CCL5
PTGS2
VCPIP1
CSF2
CCR7
TNIP3
KGFLP2
SOCS3
PTX3
CXCL3
IL1A
CCL4

Figure 7.4 Principle component analysis of transcriptome of MDM incubated with TIGR4 or Δ*ply*

The transcriptome of MDM exposed to wild-type, TIGR4Δ*ply*, or controls for 4 hours was analysed by non-biased principle component analysis illustrating expression of co-correlated genes in the global gene expression profile. Panel A shows individual donor scores of principle components 2 and 3 for unstimulated cells, PAM_2CSK_4, TIGR4 and Δ*ply*. The top 20 genes contributing the most towards the negative deflection of PC3 are shown in panel B.

A

	TIGR4	Δ*ply*
Egr1		
ELF5		
ELK1		
EWSR1-FLI1		
FEV		
GABPA		
HIF1A::ARNT		
IRF1		
IRF2		
Klf4		
MZF1_1-4		
MZF1_5-13		
NF-kappaB		
NFKB1		
NFYA		
NHLH1		
PAX4		
REL		
RELA		
RUNX1		
Sox2		
SP1		
SPI1		
SPIB		
Tcfcp2l1		
TP53		
Zfp423		
ZNF354C		

B

Δ*ply* - TIGR4
RELA
REL
NF-kappaB
IRF1
NFKB1
SPIB
IRF2
ELK1
TP53
SPI1
FEV
ELF5
GABPA
MZF1_5-13
MZF1_1-4
RUNX1
SP1

Figure 7.5 Bioinformatic analysis– transcription factor binding sites

Panel A shows oPOSSUM analysis of the most upregulated genes in MDM when incubated with TIGR4 or Δ*ply* compared to unstimulated cells, which predict the transcription factors activated in those conditions. Z-score indicating significantly overrepresented transcription factor binding sites are illustrated. Panel B shows the transcription factors most differentially activated between wild-type and Δ*ply* in order.

Δ*ply* – TIGR4	p value
Cytokine signalling in immune system	5.28^{-23}
Cytokine-cytokine receptor interaction	1.72^{-19}
Interferon alpha/beta signalling	9.41^{-17}
Interferon signalling	3.98^{-17}
Immune system	1.19^{-16}
Interferon gamma signalling	6.66^{-11}
JAK STAT pathway and regulation	7.10^{-10}
Toll-like receptor signalling pathway	4.72^{-9}
Jak-STAT signalling pathway	1.93^{-7}
IL23-mediated signalling events	1.79^{-7}

Figure 7.6 Bioinformatic analysis of transcriptome

This shows the 10 most significantly overrepresented pathways analysis by innateDB software. This shows the pathways predicted to be activated by analysing clusters of genes more expressed in one group than the other. This list shows the top pathways significantly overrepresented by incubation with Δ*ply* over incubation with wild-type.

7.2 Effect of opsonisation and phagocytosis on the inflammatory response to pneumolysin

The effect of bacterial opsonisation and uptake by macrophages on the differential inflammatory response to wild-type *S. pneumoniae* and Δ*ply* was investigated. Pre-opsonisation of bacteria in human serum, which would serve to increase engagement with Fc receptors as well as increase bacterial uptake, caused a reduction in TNF responses to wild-type and Δ*ply* (figure 7.7). There was a trend to reduction in IL6, but a trend to increased IL1β. Pre-incubation of MDM with cytochalasin D interestingly increased TNF and IL6 responses from wild-type bacteria, but decreased the same cytokines with Δ*ply* (figure 7.8) at least partially abrogating the differences between the 2 strains. These data suggest that the effect of Ply on pro-inflammatory cytokine release is dependent on bacterial uptake.

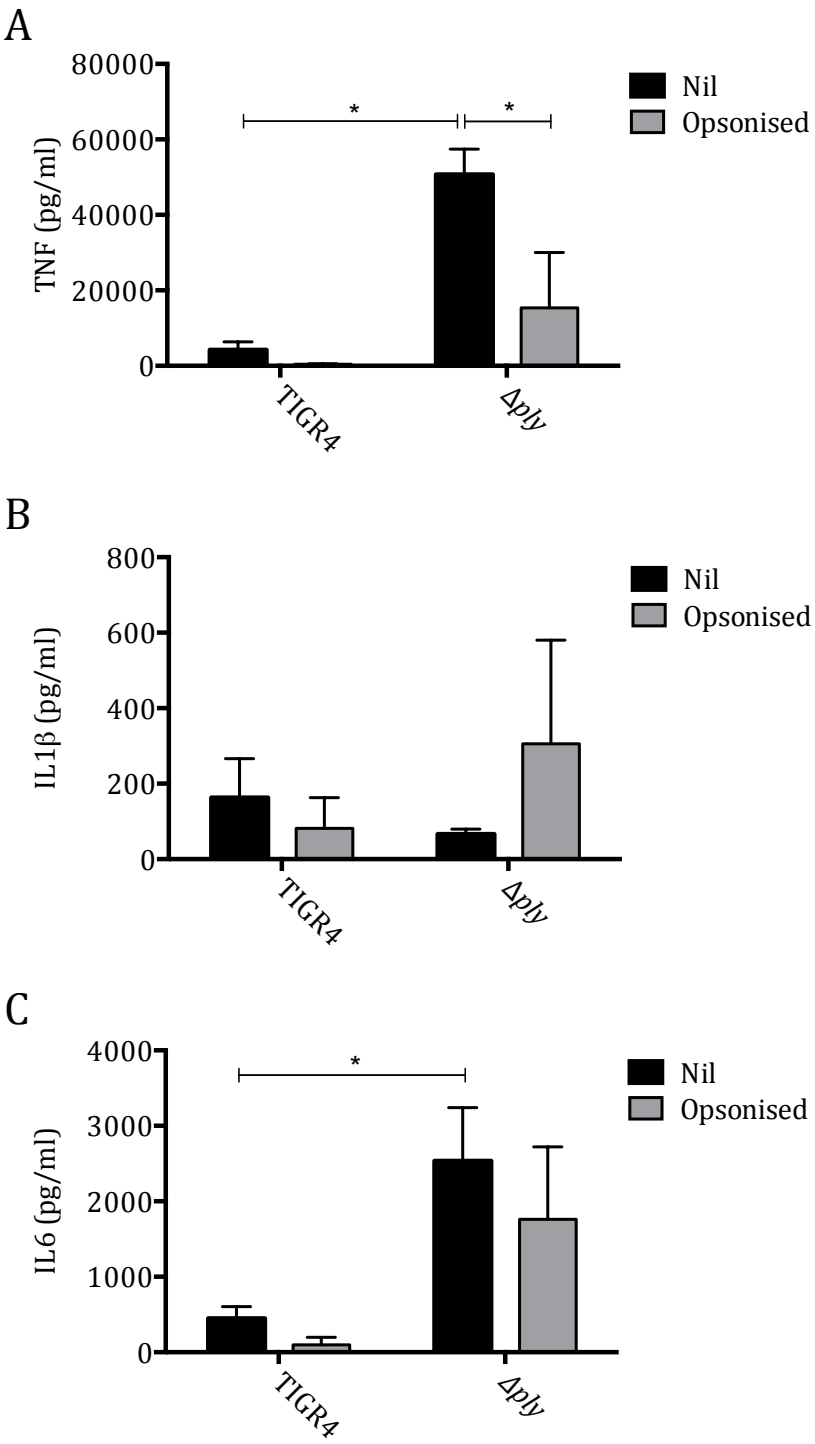

Figure 7.7 Effect of opsonisation on inflammatory response

Bacteria were opsonised in pooled human serum for 30 minutes before being diluted to the required concentration and added to MDM. Analysis from 3 experiments with supernatants 6 hours after infection are shown as mean +/- SEM. Panel A is TNF, B is IL1β, and C is IL6. Statistical analysis was with 2 way ANOVA and Tukey's multiple comparisons test. These experiments were run at the same time as figure 4.9.

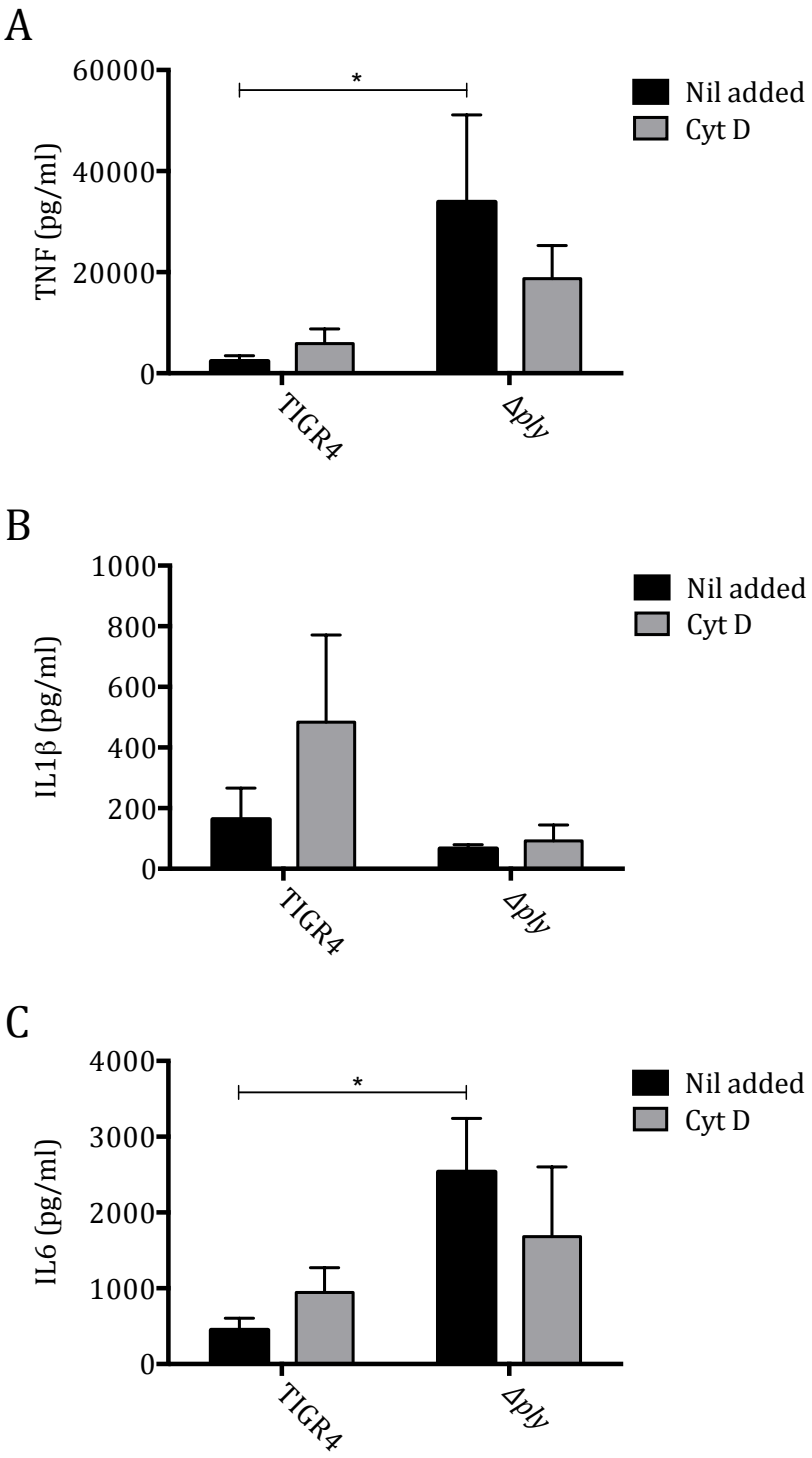

Figure 7.8 Effects of inhibiting phagocytosis on the inflammatory response

MDM were incubated with controls or bacteria at MOI 10, and supernatants were analysed for A) TNF, B) IL1β, and C) IL6 after 6 hours. The presented results are mean +/- SEM of 3 experiments, analysed by 2 way ANOVA and Tukey's multiple comparisons test.

7.3 Effect of inhibiting phagocytosis on transcriptional response

As the data above indicated that phagocytosis was key to the effects on inflammatory cytokine release, the effect of phagocytosis inhibition on the response to wild-type and Ply deficient bacteria was explored by whole genome transcription analysis. MDM were incubated with either media or 10μM cytochalasin D for an hour prior to the addition of bacteria. These data were obtained at the same time as the transcriptional data presented in chapters 4.1, 4.4, and 7.1.

The number of genes that were upregulated after 4 hours by more than 2 fold due to Δ*ply* was reduced by the addition of cytochalasin D (figure 7.9 panel A). In addition the number of genes differentially expressed between wild-type and Δ*ply* was reduced when both were in the presence of cytochalasin D (figure 7.9, panel B). Heat map representation (ranked by the most expressed genes induced by TIGR4 over unstimulated controls) suggests that inhibition of phagocytosis greatly inhibited the transcriptional response to Δ*ply*, whereas there was an increase in responses to wild-type TIGR4 (figure 7.10). In a direct comparison of MDM genes expression between Δ*ply* and TIGR4 in the presence of cytochalasin D, inhibition of phagocytosis considerably reduced the difference between the 2 strains (figure 7.11).

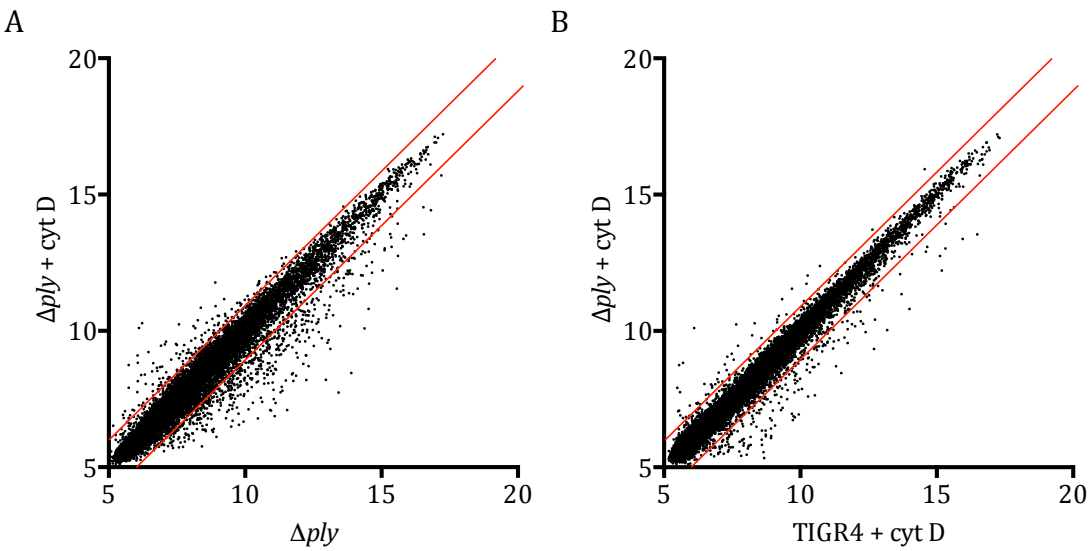

Figure 7.9 Gene expression of MDM by genome wide analysis

Relative gene expression is plotted by condition for all genes on a microarray. The mean of 3 experiments for each condition is plotted. Panel A plots the effect of cytochalasin D on the Δ*ply* strain, and panel B compares TIGR4 v Δ*ply* once phagocytosis had been inhibited with cytochalasin D. The red lines indicated $\log_2$ of 2 fold differences in expression

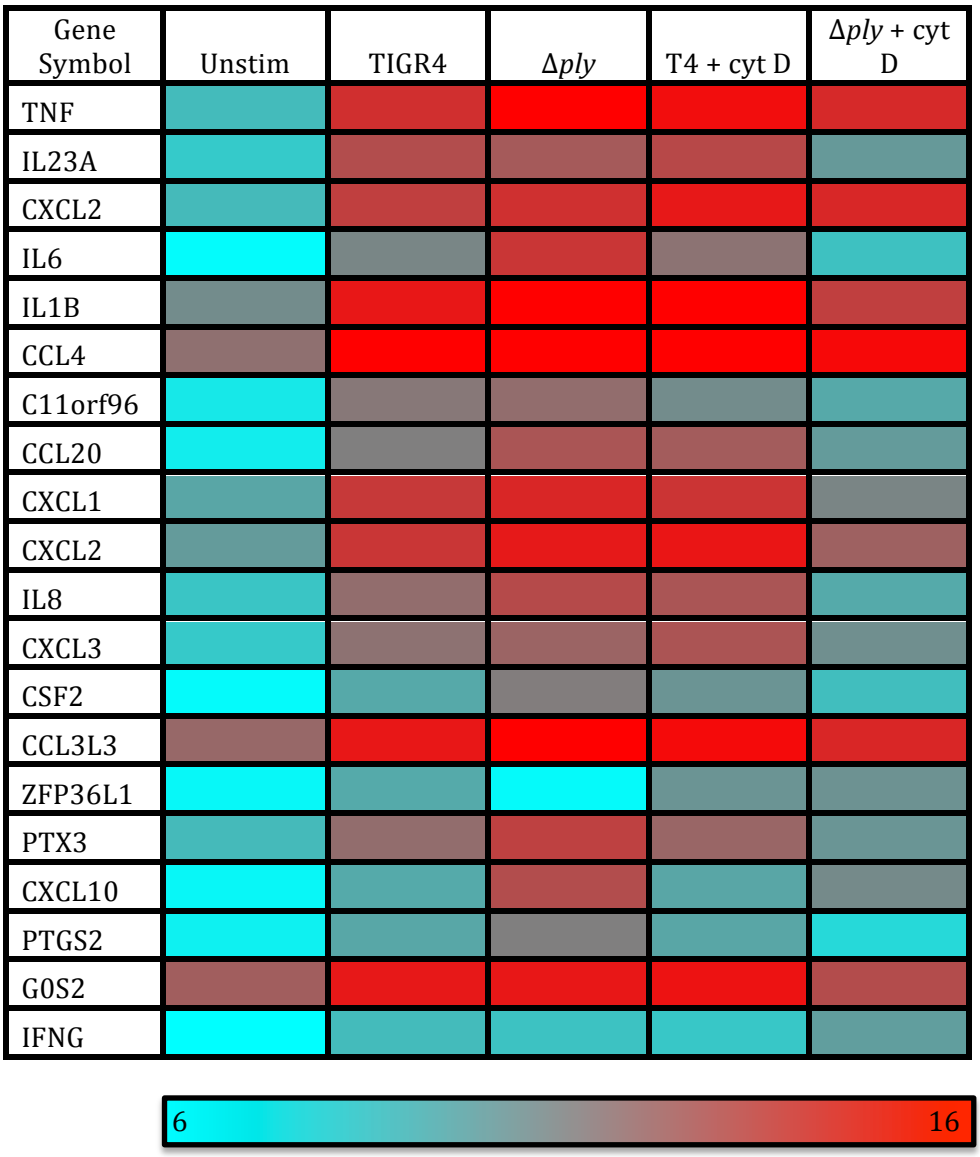

Figure 7.10 Heat map of gene expression of top 20 genes upregulated byTIGR4

Mean gene expression of MDM incubated with TIGR4 or Δ*ply* (3 donors each), with least expressed in blue, and most expressed in red. Gene order by most upregulated genes with TIGR4 compared to unstimulated. In the relevant experiments, MDM were pre-incubated with 10μM cytochalasin D for 30 minutes, which was washed off, before the addition of bacteria at MOI 10.

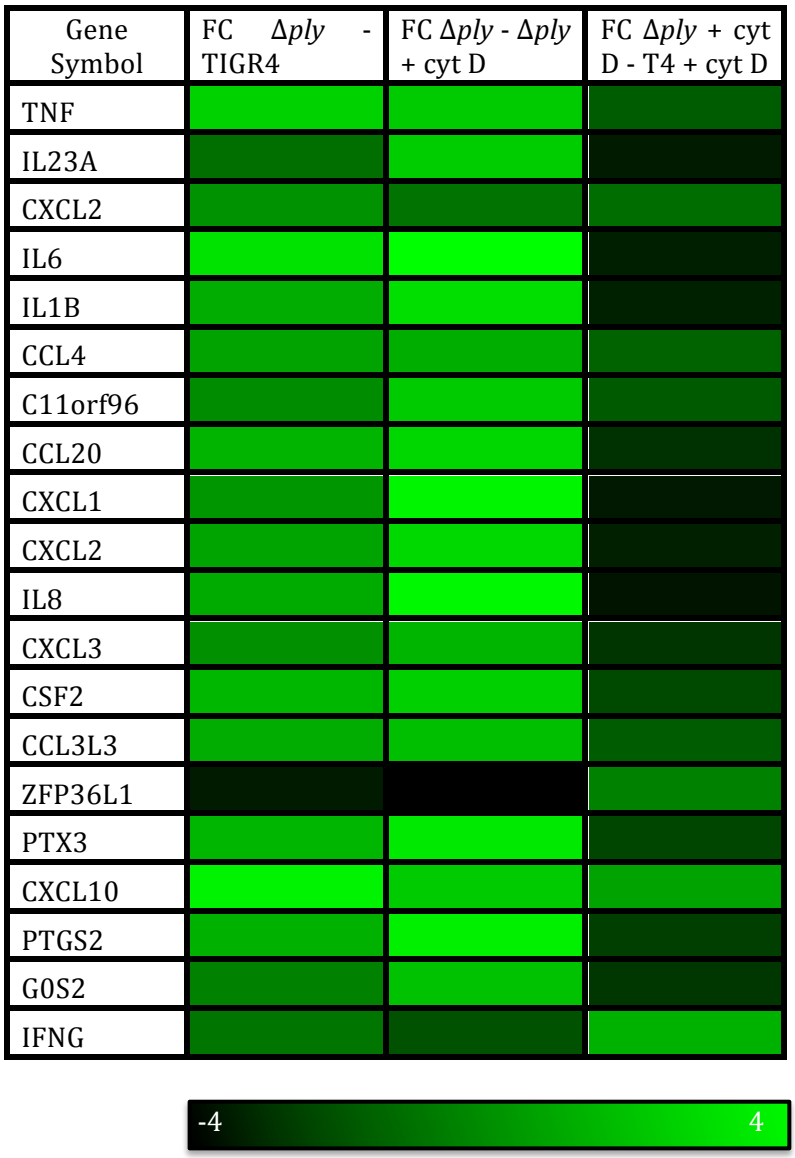

Figure 7.11 Fold change in relative gene expression of top 20 upregulated genes by TIGR4

Heat map of relative differences in expression between MDM incubated with TIGR4 or Δ*ply* +/- pre-incubation with cytochalasin D. Values expressed as $\log_2$ differences in gene expression, colour coded such that the most upregulated are in green, and most downregulated in black. Mean of 3 experiments displayed.

7.4 Effect of pneumolysin on MAPK signalling

Western blotting of important components of MAPK signalling was used to assess differences in signalling activation in MDM as a consequence of Ply. There did seem to be differences in signalling cascades activated, as Δ*ply* appeared to induce greater phosphorylation of p38 and to a lesser extent ERK (figure 7.12 & 7.13). Whereas JNK phosphorylation was broadly similar between the MDM incubated with either strain. This suggests that Ply may selectively inhibit some pro-inflammatory pathways that are triggered by specific MAPK cascades.

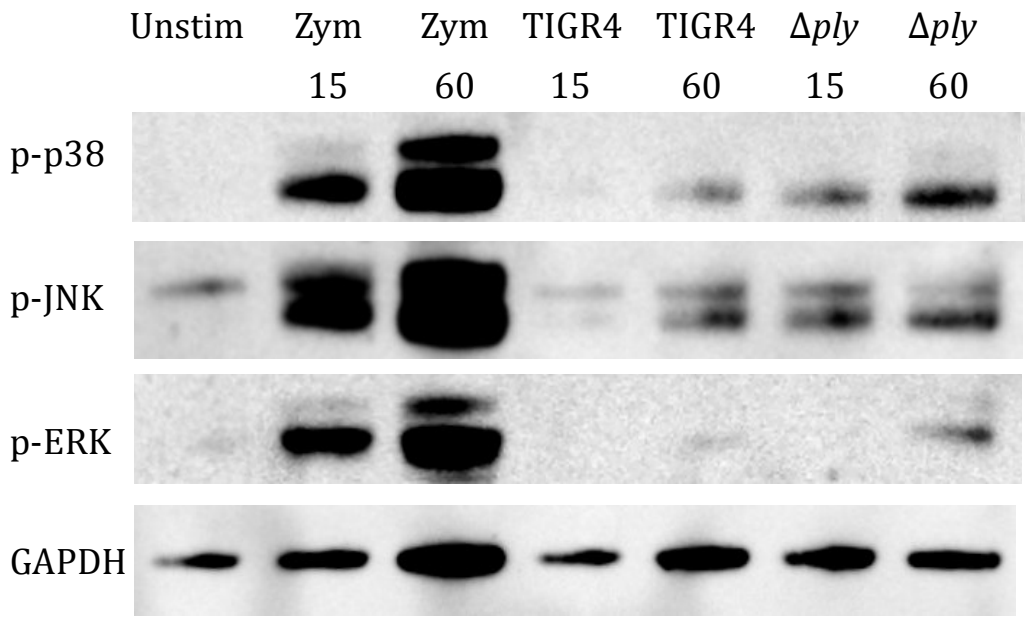

Figure 7.12 Western blot of MDM for MAPK

Western blot of 4 pooled MDM lysates with TIGR4 or Δ*ply*, with zymosan as a positive control and media only as an unstimulated negative control. Lysates were probed for phospho-MAPK and GAPDH was used as a loading control. A representative immunoblot of 2 replicates is shown. These experiments were run at the same time as those in figure 4.20, though the Western blots were run separately.

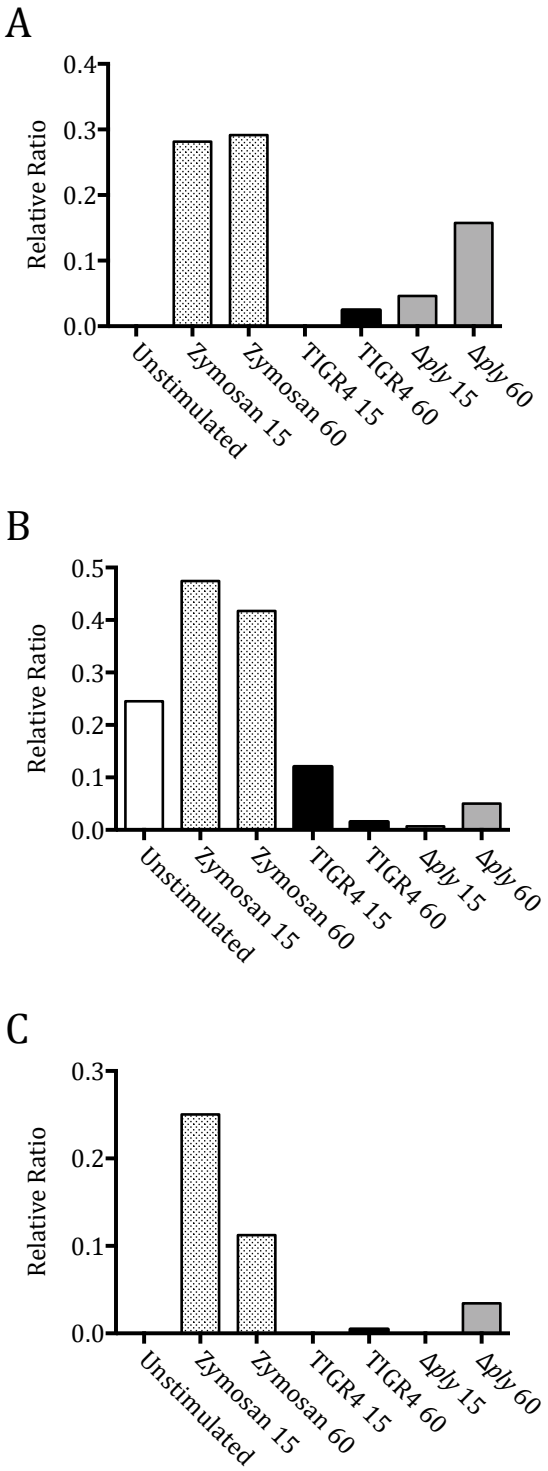

Figure 7.13 Quantification of Western blots

Western blots from figure 7.13 were quantified by Imagequant and presented as relative density normalised to GAPDH. A) phospho-p38, B) phospho–JNK, and C) phospho-ERK.

7.5 Effect of pneumolysin on transcription factors

As NFκB is central to how multiple PRR and cytokine-receptor interaction pathways impact on the regulation of pro-inflammatory cytokine transcription, the translocation of NFκB to the nucleus was measured as a marker of activation in MDM. This was measured using high throughput microscopy techniques and analysed on software to look at the intensity of NFκB protein in nucleus compared to cytoplasm.

NFκB translocation was greater at both 1 and 2 hours when MDM were incubated with Δ*ply* in comparison to TIGR4 (figure 7.14 & 7.15). This indicates that the presence of Ply significantly decreases NFκB activation. As previous investigators have suggested that Ply engages with TLR4 (Malley, Henneke et al. 2003), I also looked at the transcription factor IRF3, which is activated by phagolysosomal TLR4 activation (Moynagh 2005). IRF3 translocated into the nucleus significantly more in MDM incubated with TIGR4 than Δ*ply* at 1 hour (though they were similar by 2 hours) possibly indicating that phagolysosomal release of Ply may engage with TLR4, which could conceivably inhibit pathways that activate NFκB.

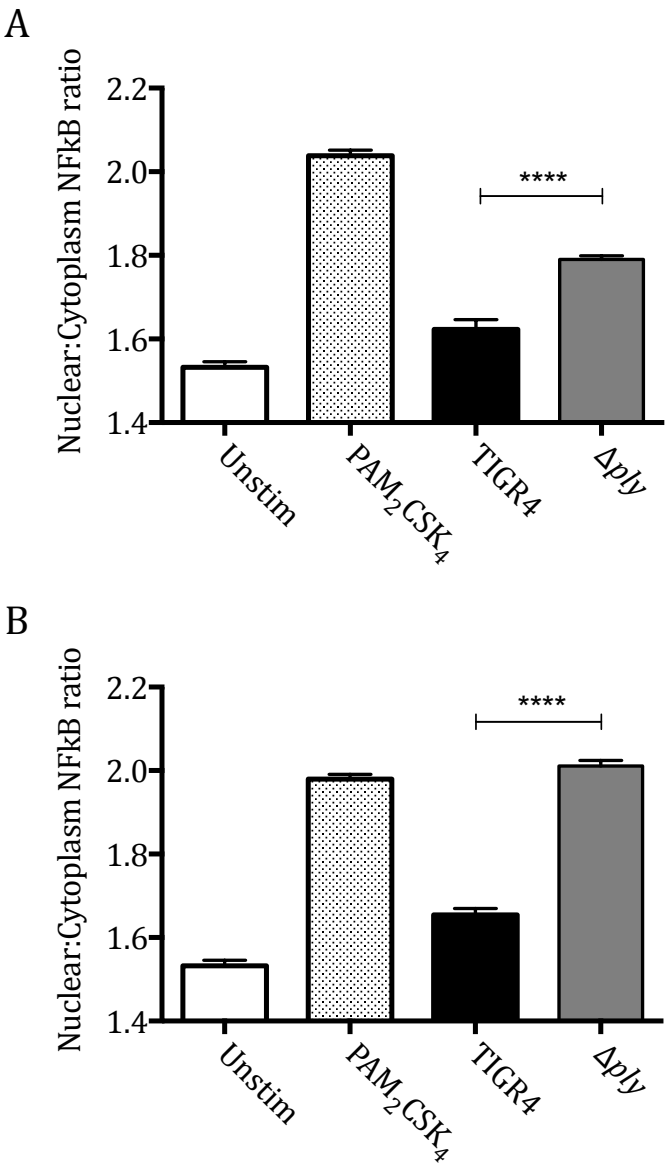

Figure 7.14 Nuclear: Cytoplasm ratio of NFκB in MDM after stimulation with bacteria or controls

Panels A & B show the ratio of NFκB between the nucleus and cytoplasm in MDM, with the data from 3 different donors at 1 and 2 hours respectively, analysed by 1 way ANOVA, and Tukey's multiple comparisons test. These experiments were run at the same time as those in figure 4.16.

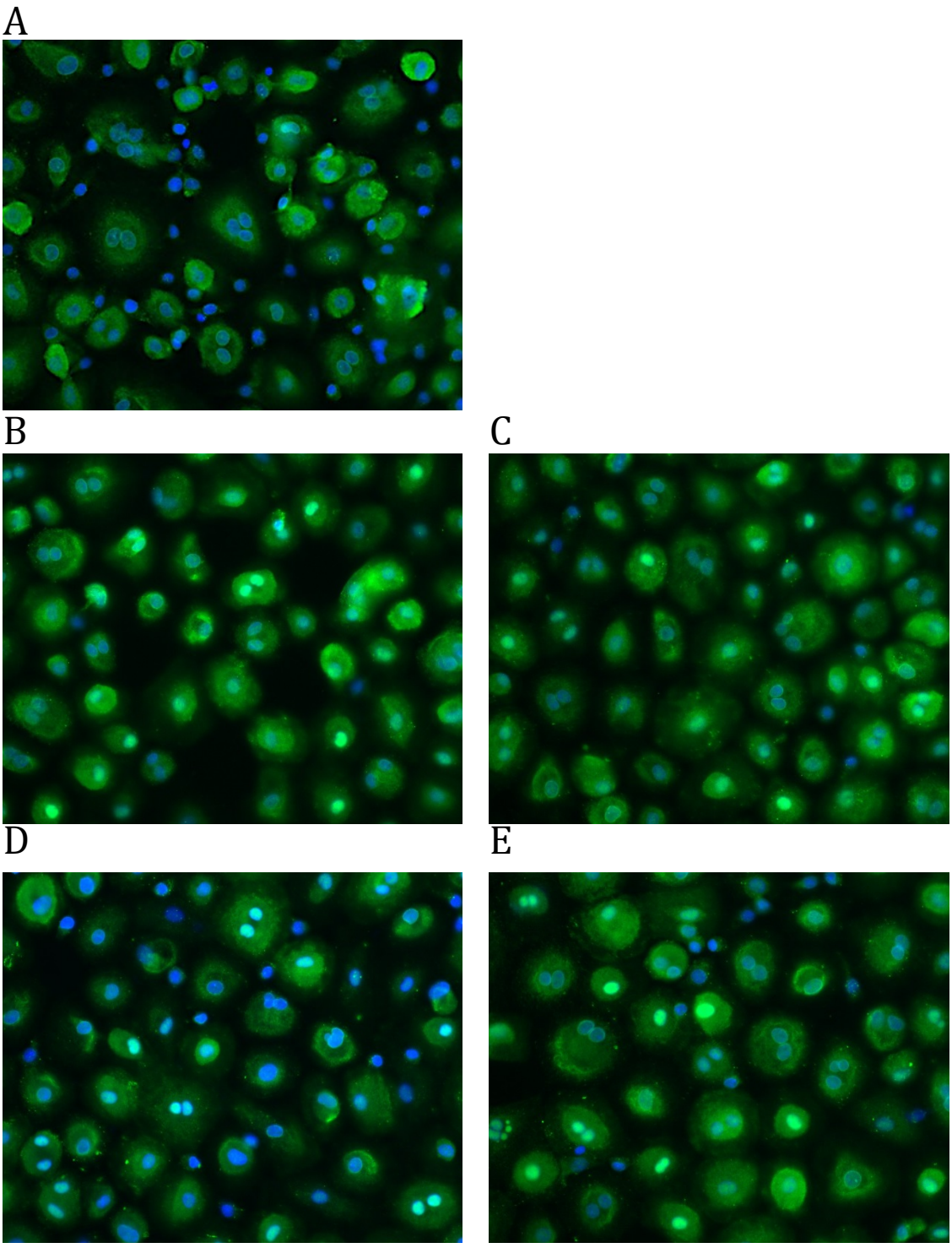

Figure 7.15 NFκB translocation

Microscopy images of high throughput optical 96 well plates with MDM incubated with bacteria. Panel A (unstimulated), B (TIGR4 1 hour), C (TIGR4 2 hours), D (Δ*ply* 1 hour), and E (Δ*ply* 2 hours) are representative images of MDM. Here the nucleus is DAPI stained, in blue, and NFκB is in green.

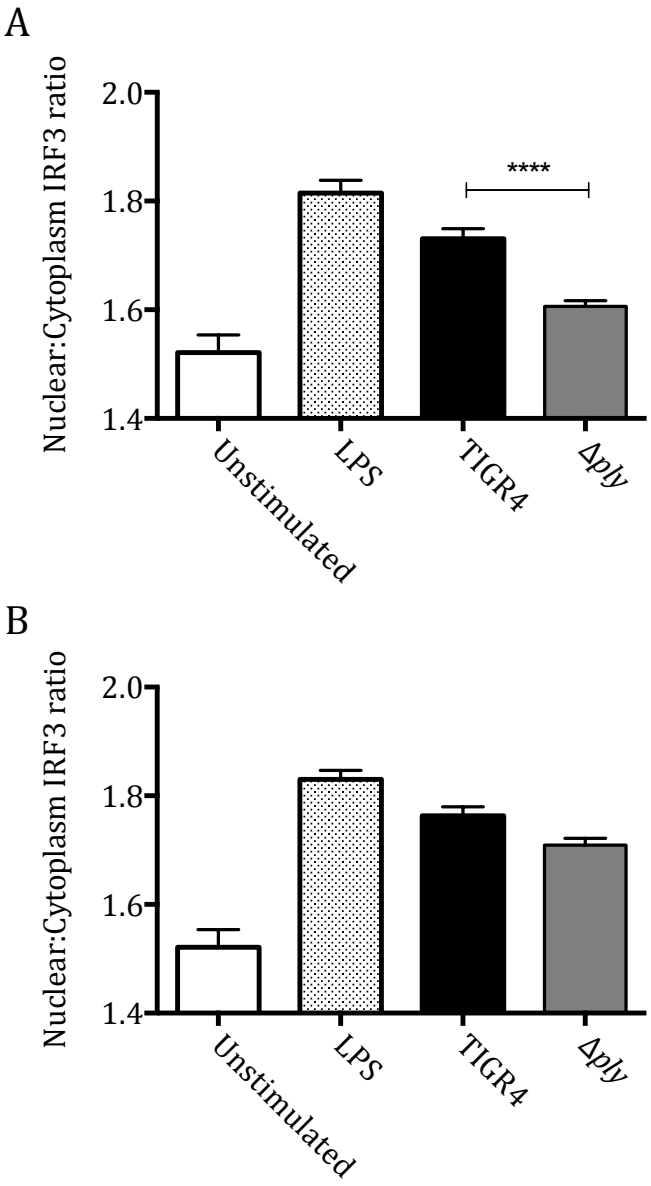

Figure 7.16 Nuclear: Cytoplasm ratio of IRF3 in MDM after stimulation with bacteria or controls

Panels A & B show the ratio of IRF3 between the nucleus and cytoplasm in MDM, with the data from 3 different donors at 1 and 2 hours respectively shown as mean +/-SEM, and analysed by 1 way ANOVA and Tukey's multiple comparisons test.

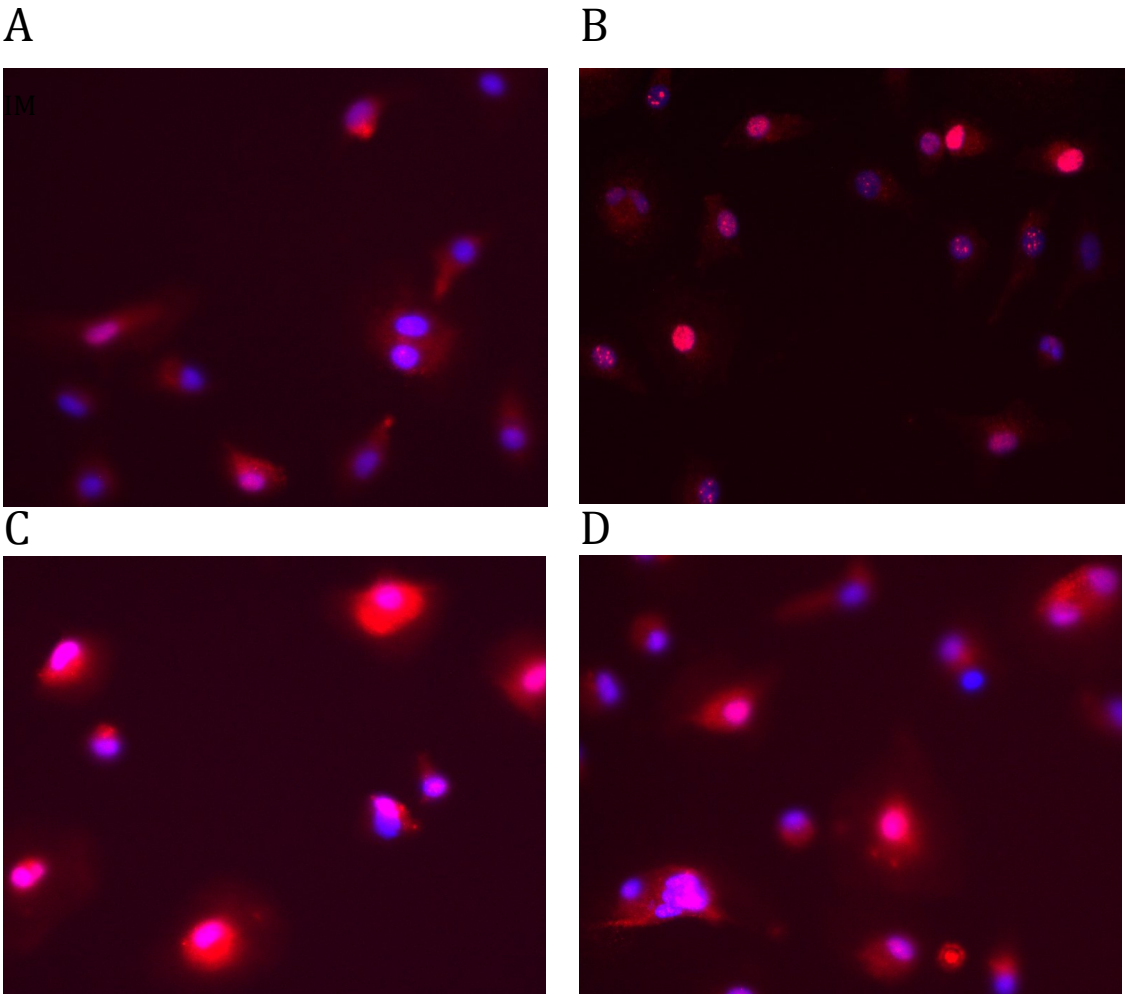

Figure 7.17 IRF3 translocation

Microscopy images of high throughput optical 96 well plates with MDM incubated with bacteria. Panel A (Unstimulated), B (LPS), C (TIGR4), and D (Δ*ply*) are representative images of MDM after 1 hour. Here the nucleus is DAPI stained, in blue, and IRF3 is in red.

7.6 Effect of pneumolysin on apoptosis, inflammasome and TLR4 mediated signalling

Other authors have shown that Ply has multiple effects on inflammatory pathways, pre-eminent amongst these are induction of apoptosis (Marriott, Ali et al. 2004), activation of inflammasome pathways (McNeela, Burke et al. 2010), and interaction with TLR4 (Malley, Henneke et al. 2003). By 24 hours, incubation with live wild-type TIGR4 (or the positive control staurosporin) induces nuclear condensation, but Δ*ply* strains do not, confirming that Ply is involved in inducing macrophage apoptosis (figure 7.18, panel A), but at 6 hours the differences between the strains were not significant (figure 7.18, panel B). This indicates that apoptosis is not morphologically evident at 6 hours, analagous to the early stages of infection. However this does not exclude pathways upstream of apoptosis being involved in cross talk with inflammatory pathways.

To explore specific pathways in the *in vitro* model of human MDM responses to *S. pneumoniae*, specific inhibitors were employed. ZVAD-FMK (Invivogen), a pan caspase inhibitor and so inhibitor of apoptosis, did not affect inflammatory cytokine release (figure 7.19) suggesting Ply-dependent inhibition of inflammation does not depend on increasing apoptosis. Similarly, YVAD-FMK (Invivogen), a caspase 1 inhibitor that inhibits the inflammasome reduced IL1β release due to LPS and calcium pyrophosphate crystals, but had no impact on the release of pro-inflammatory cytokines induced by TIGR4, irrespective of the presence of Ply (figure 7.20).

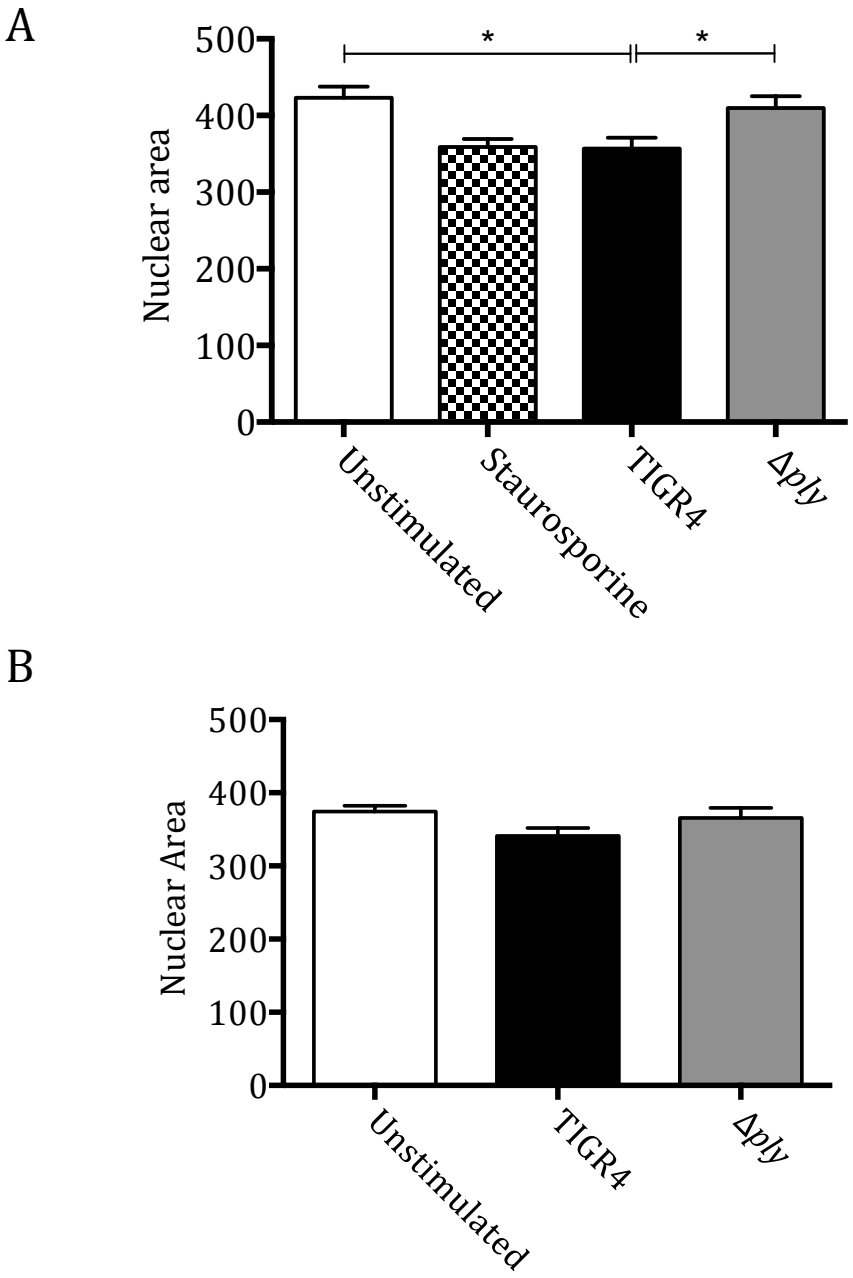

Figure 7.18 MDM apoptosis after incubation with bacteria

MDM in optical plates were incubated with controls or bacteria at MOI 10 for 24 (panel A) or 6 hours (panel B). Cells were fixed and stained with DAPI to assess nuclei. Nuclear area was used as a proxy for apoptosis mediated nuclear condensation. Data are presented as mean +/-SEM of 3 experiments, and analysed by 1 way ANOVA and Tukey's multiple comparisons test.

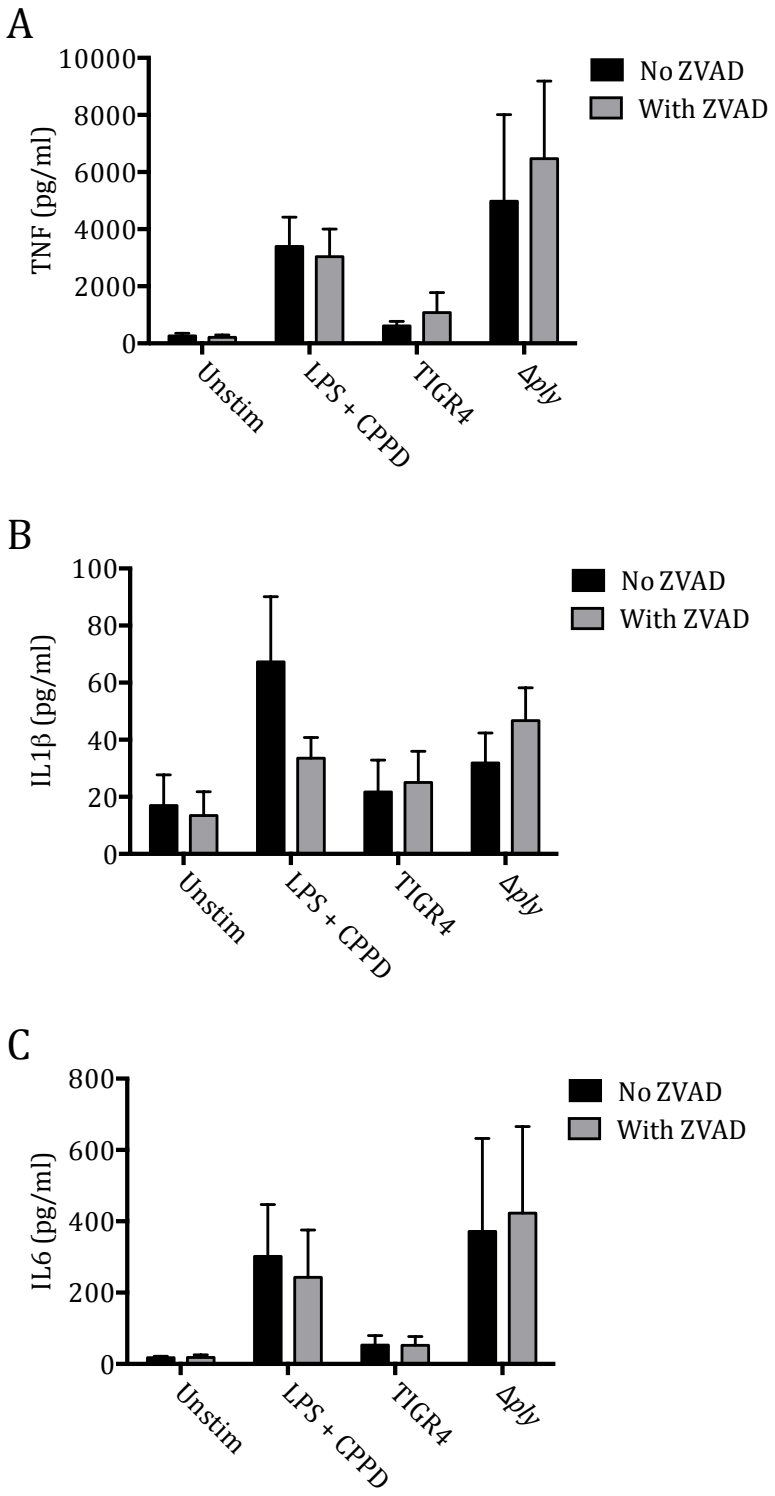

Figure 7.19 MDM cytokine response after apoptosis inhibition

MDM were incubated with 20μM ZVAD FMK, a pan caspase inhibitor, or media for 1 hour, then bacteria or controls were added. Supernatants were removed at 6 hours and analysed for pro-inflammatory cytokine levels. Data are presented as mean +/- SEM of 3 experiments and analysed by 2 way ANOVA and Tukey's multiple comparisons test with no significant differences seen.

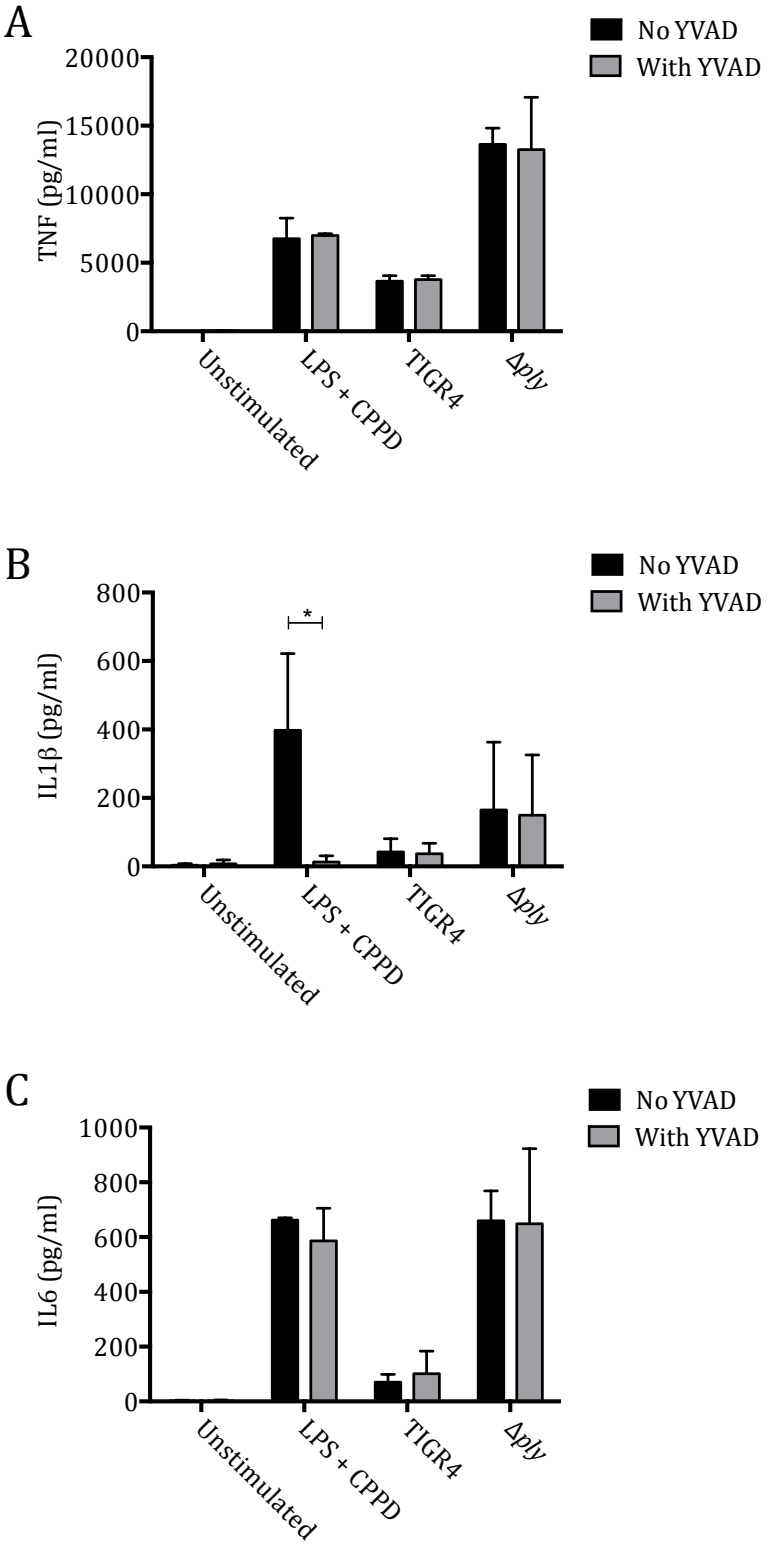

Figure 7.20 MDM cytokine response after inflammasome inhibition

MDM were incubated with 50μM YVAD FMK, a caspase 1 inhibitor, or media for 1 hour, then bacteria or controls were added. Supernatants were removed at 6 hours and analysed for pro-inflammatory cytokine levels. Data are presented as mean +/- SEM of 3 experiments and analysed by 2 way ANOVA with Tukey's multiple comparisons test, with no significant differences seen.

As data from transcription factor translocation indicated that IRF3 was more rapidly activated by the Ply containing wild-type strain, and this pathway is stimulated by lysosomal TLR4 activation, potential crosstalk between these pathways was investigated. TBK1 is an adaptor protein that is an important intermediary between TLR4 activation and IRF3 activation. A small molecule inhibitor BX795 (Invivogen) was used to inhibit TBK1, to see if this would increase the inflammatory response to wild-type TIGR4. BX795 slightly reduced IFNβ, and significantly reduced CXCL10, which is induced by interferon signalling (figure 7.21). However, MDM secretion of pro-inflammatory cytokines was not affected, in particular the response to wild-type TIGR4 was not decreased by BX795 (figure 7.22). Similarly, the converse approach of addition of poly I:C (Invivogen), a TLR3 agonist that also stimulates TRIF-mediated signalling cascades that act via TBK1 to stimulate IRF3, did not reduce the inflammatory response to Δ*ply* bacteria (figure 7.23). Interpretation of this experiment may have been confounded by the direct pro-inflammatory properties of poly I:C.

As data from *S. pneumoniae* expressing non-haemolytic Ply suggested that the pore-forming functions of Ply were at least partially involved in inhibiting the inflammatory response, inhibition of voltage gated calcium channels was performed with SKF96365 (Sigma Aldrich, Gillingham). Blockade of these channels inhibits the early membrane depolarisation effects of Ply, and if Ply insertion into membrane was involved in inhibiting the inflammatory response, SKF96365 would be expected to increase the MDM inflammatory cytokine response to wild-type bacteria. However, there was a trend to reduced inflammatory cytokine release across all strains (figure 7.24).

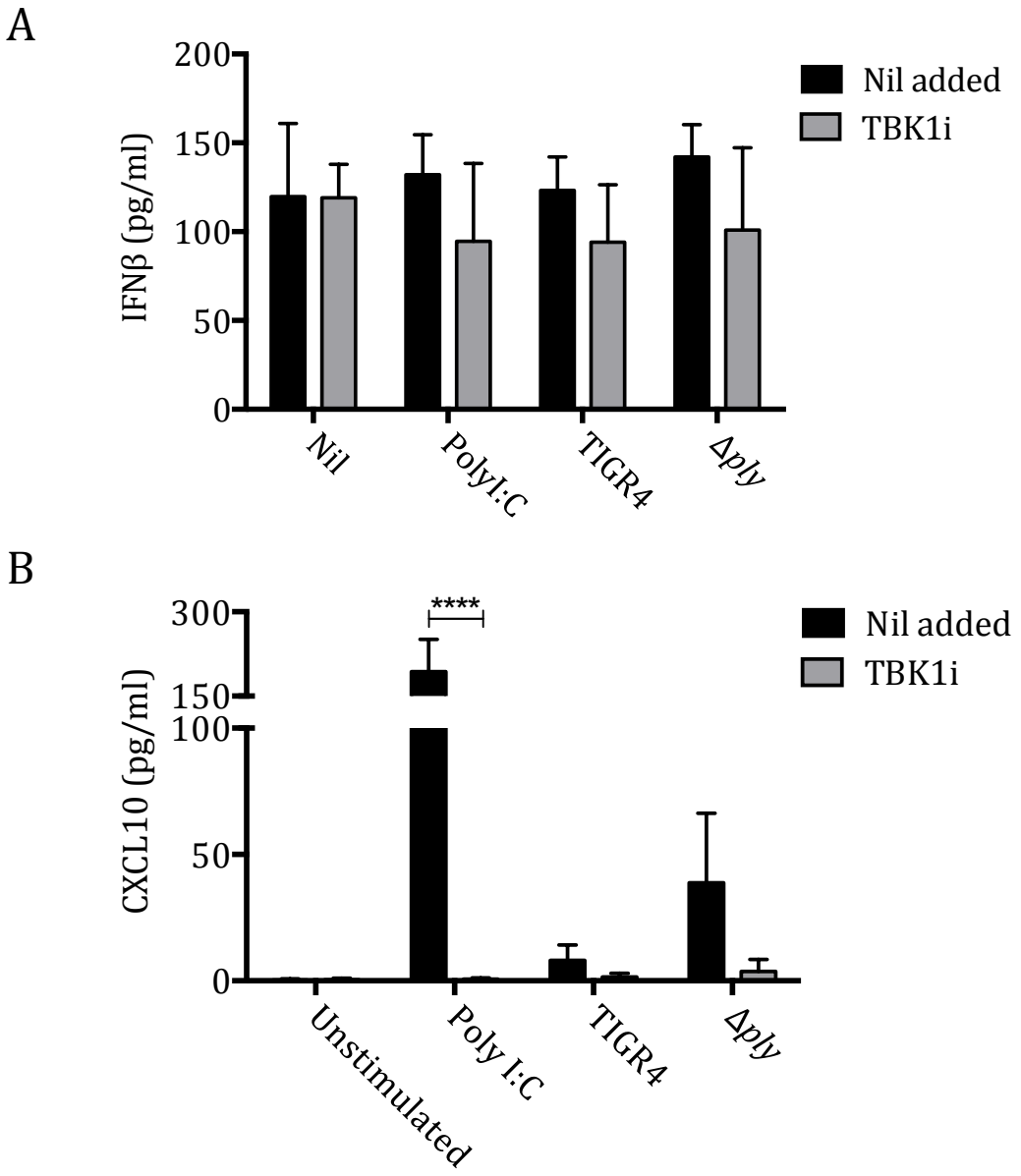

Figure 7.21 MDM IFN response to TBK1 inhibitor

MDM were incubated with 1μM BX-795, a TBK1 inhibitor, or media, then bacteria and controls were added and supernatant removed after 6 hours. These were analysed for IFNβ (panel A) and CXCL10 (panel B), which are downstream of TBK1. Mean +/- SEM of 3 experiments are shown. Results were analysed by 2 way ANOVA and Tukey's multiple comparisons test.

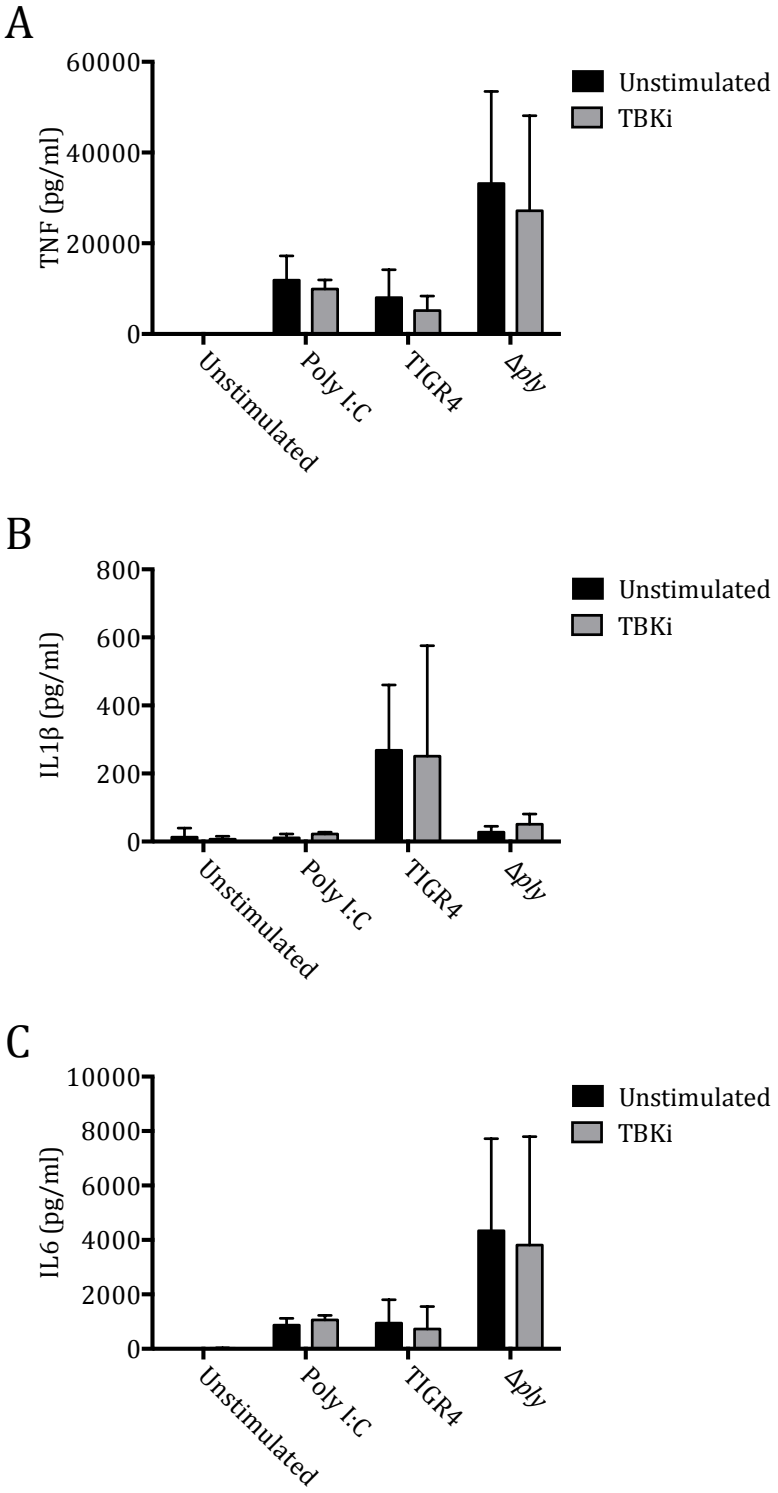

Figure 7.22 MDM cytokine response to TBK1 inhibitor

MDM were incubated with 1μM BX-795, a TBK1 inhibitor, or media for 1 hour, then bacteria and controls were added and supernatant removed after 6 hours. These were analysed for pro-inflammatory cytokines. Data are presented as mean +/- SEM of 3 experiments and analysed by 2 was ANOVA and Tukey's multiple comparisons test, with no significant differences seen.

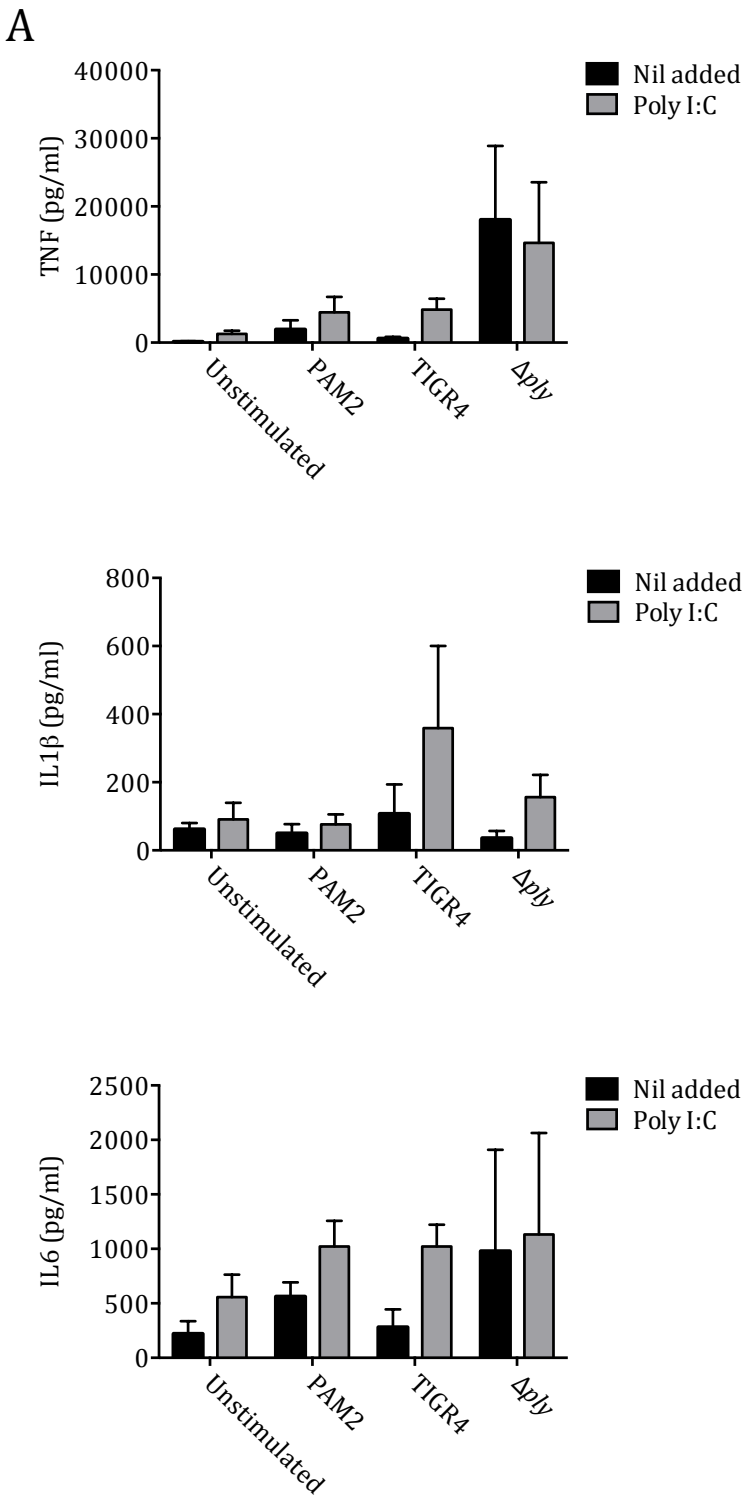

Figure 7.23 MDM cytokine response after the addition of Poly I:C

MDM were incubated with bacteria or controls +/- 10μg/ml poly I:C (Invivogen) and supernatant removed after 6 hours. These were analysed for pro-inflammatory cytokines. Data are presented as mean +/- SEM of 3 experiments and analysed by 2 way ANOVA and Tukey's multiple comparisons test with no significant differences seen.

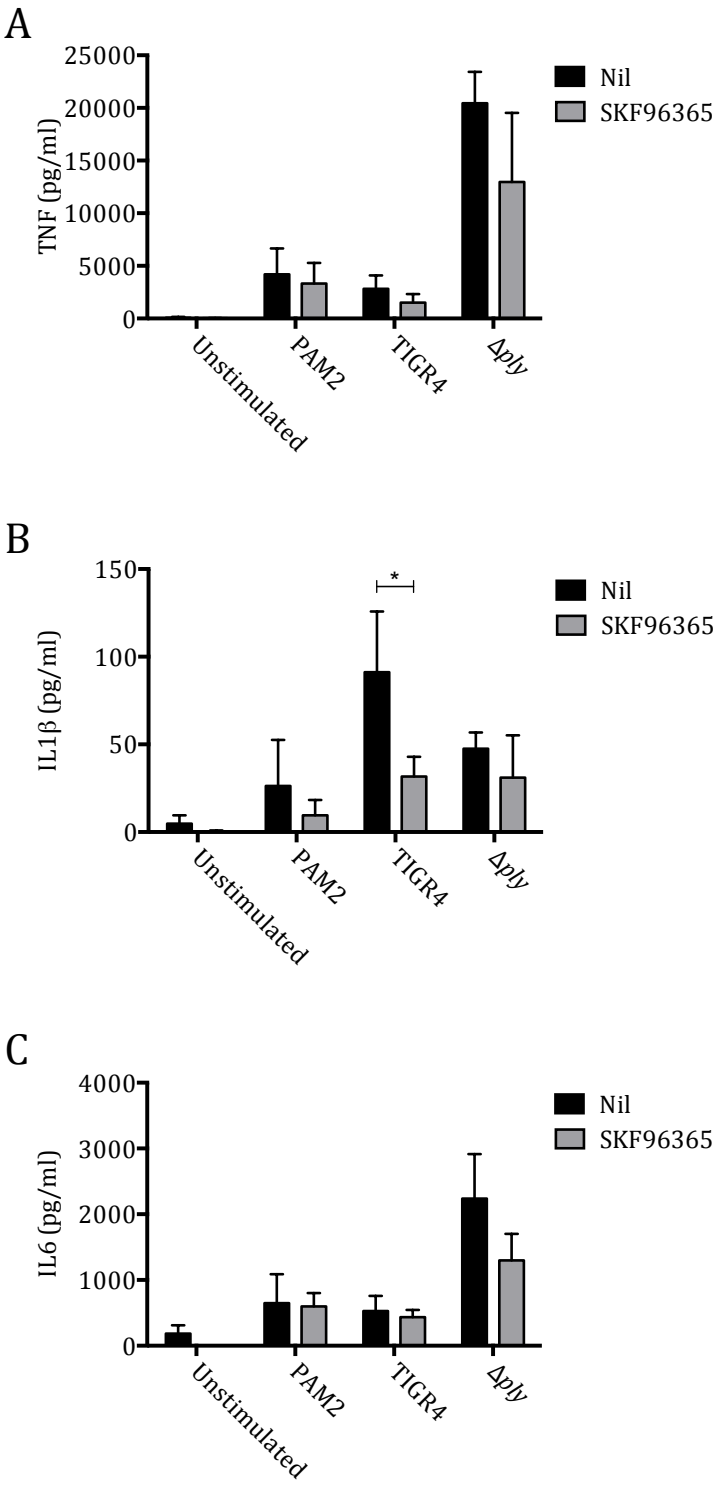

Figure 7.24 MDM cytokine response after voltage gated calcium channel blocker

MDM were incubated with 40μM SKF96365, a voltage gated calcium channel blocker, or media for 1 hour, then bacteria and controls were added and supernatant removed after 6 hours. These were analysed for pro-inflammatory cytokines. Mean +/- SEM of 3 experiments are shown. Data were analysed by 2 way ANOVA and Tukey's multiple comparisons test.

7.7 Effects of TNF blockade on pneumolysin in mouse pneumonia

In the murine intranasal infection model, wild-type TIGR4 reduced TNF secretion in the bronchoalveolar compartment in comparison to Δ*ply*. To see if this reduction in TNF release had physiological effects, TNF activity was inhibited in the bronchoalveolar compartment with a neutralising antibody (Biolegend). The antibody was administered intranasally at the same time as bacteria to only inhibit TNF secreted locally as a result of bacterial infection.

Bacterial counts in BALF show that TNF inhibition abrogated the difference between TIGR4 and Δ*ply* (figure 7.25), suggesting Ply mediated reduction of early TNF release in the bronchoalveolar compartment is important in controlling bacterial numbers. This abrogation of difference was also seen in neutrophil counts (figure 7.25, panel C).

Cytokines in BALF show that TNF blockade had little effect on IL1β, but that it may attenuate the difference in IL6 between the strains, though this was not statistically significant (figure 7.26). Interestingly TNF blockade reduced the Ply dependent release of IL1β in lung homogenate (figure 7.27). Similarly, there was a reduction in Ply dependent TNF and IL6 release in this compartment suggesting that the other cytokines may compensate somewhat for Ply mediated TNF inhibition.

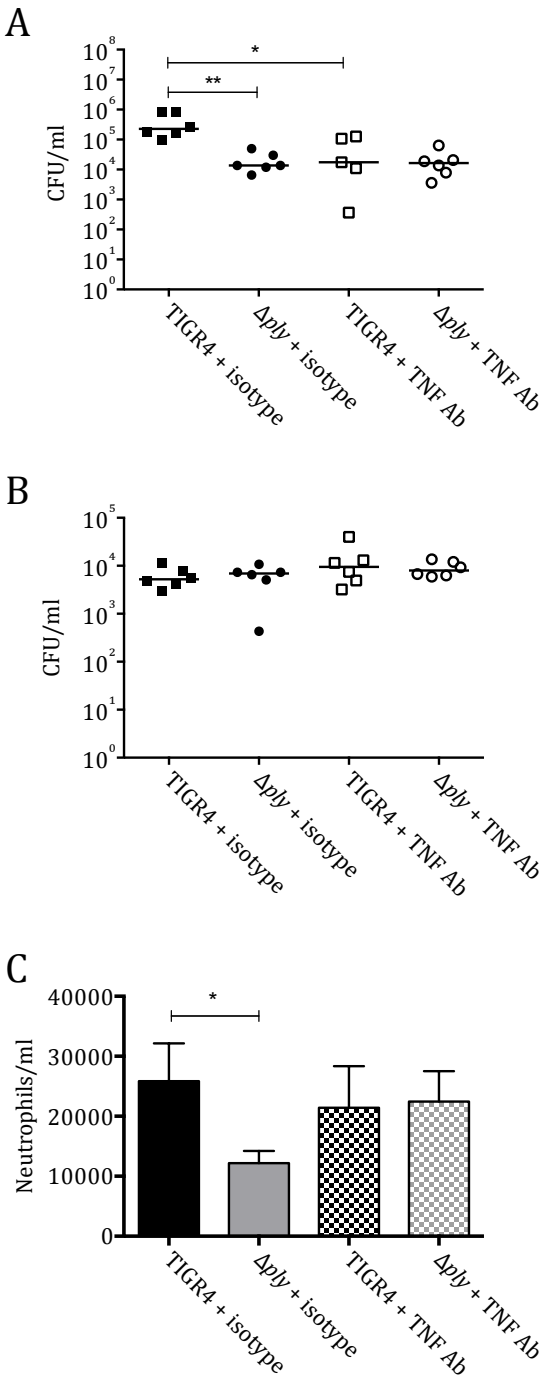

Figure 7.25 Bacterial counts at 4 hours in mouse pneumonia with and without TNF blocking antibody

5 week old female CD1 mice were inoculated intranasally with 5×10^6 CFU bacteria under isoflurane anaesthesia, mixed with either 20μg TNF blocking antibody (Biolegend) or isotype control (Biolegend). BALF and lung homogenates were obtained after 4 hours with 6 mice per group. CFU are presented as individual mouse results with medians in BALF (panel A) and lung homogenate (panel B) and analysed by Kruskal-Wallis with Dunn's multiple comparison test. Neutrophil counts are presented as mean +/- SEM and analysed by 2 way ANOVA with Tukey's multiple comparisons test.

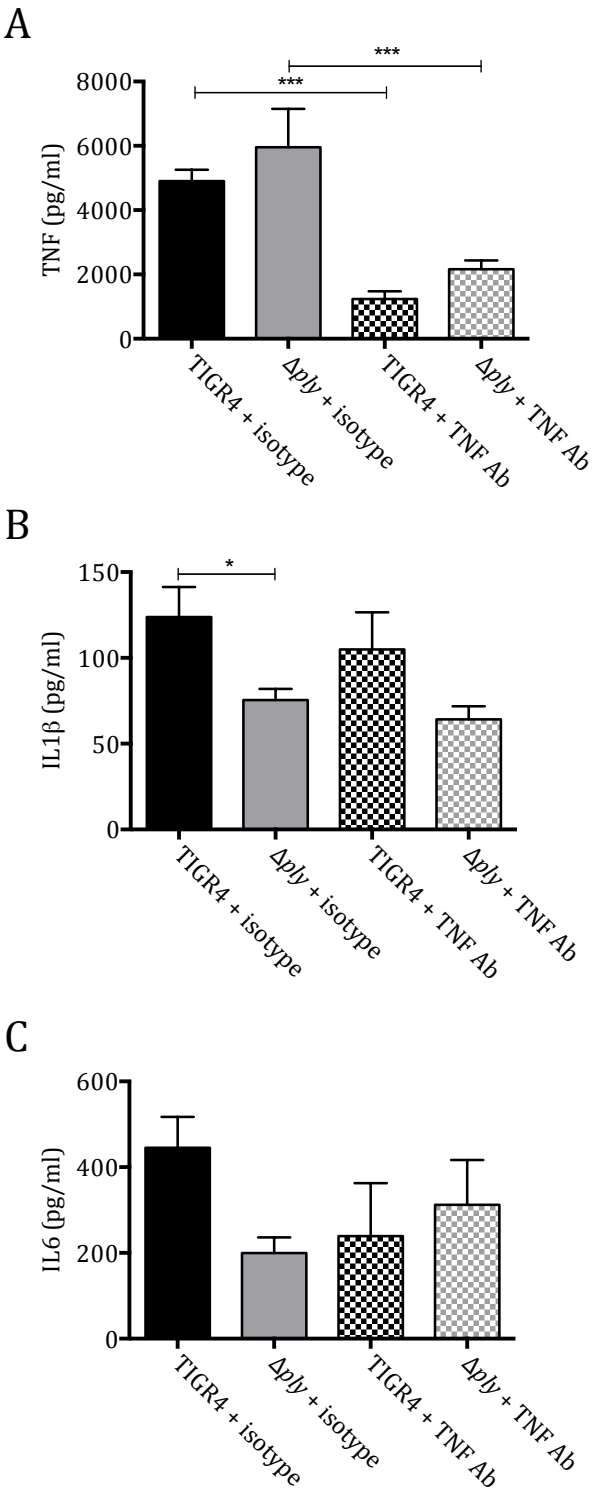

Figure 7.26 Cytokines in BALF with TNF blockade

5 week old female CD1 mice were inoculated intranasally with 5×10^6 CFU bacteria under isoflurane anaesthesia. The cytokine levels in lavage fluid of the mice at 4 hours were measured by ELISA. Three were 6 mice per group, and results are presented as mean +/- SEM and analysed by 1 way ANOVA and Tukey's multiple comparisons test.

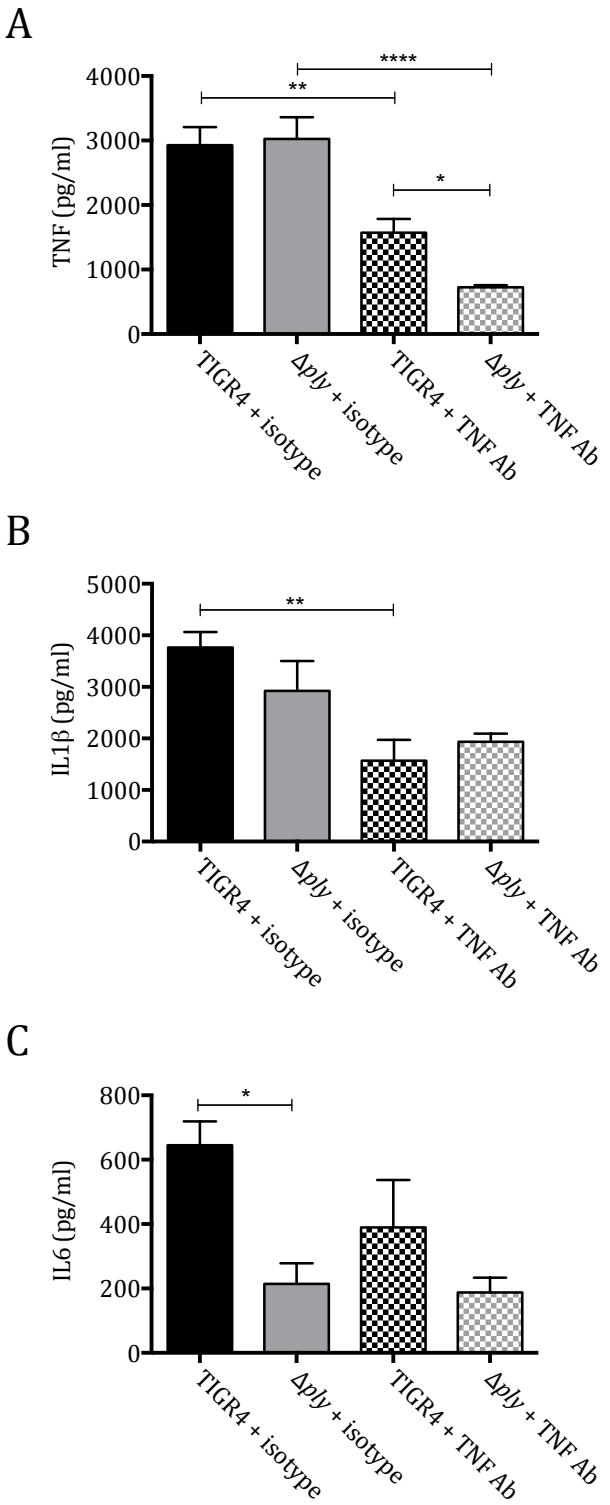

Figure 7.27 Cytokines in lung homogenate with TNF blockade

5 week old female CD1 mice were inoculated intranasally with 5×10^6 CFU bacteria under isoflurane anaesthesia. The cytokine levels in lavage fluid of the mice at 4 hours were measured by ELISA. Three were 6 mice per group, and results are presented as mean +/- SEM and analysed by 1 way ANOVA and Tukey's multiple comparisons test.

7.8 Early timepoint mouse pneumonia

As the neutrophil infiltrate was similar between the 2 strains at 4 hours, an earlier timepoint was assessed to ascertain whether the Δ*ply* strain caused more early inflammation, potentially facilitating early neutrophil ingress and bacterial clearance. By 2 hours there was already a small but significant difference in bacterial numbers in BALF, with greater numbers seen with the wild-type (figure 7.28). There were significantly more neutrophils recruited in response to the Δ*ply* strain by this stage. Cytokine levels were not significantly different between the strains (figure 7.29), though the trends replicated those seen by the 4 hour timepoint with wild-type inducing lower BALF TNF and greater IL1β levels.

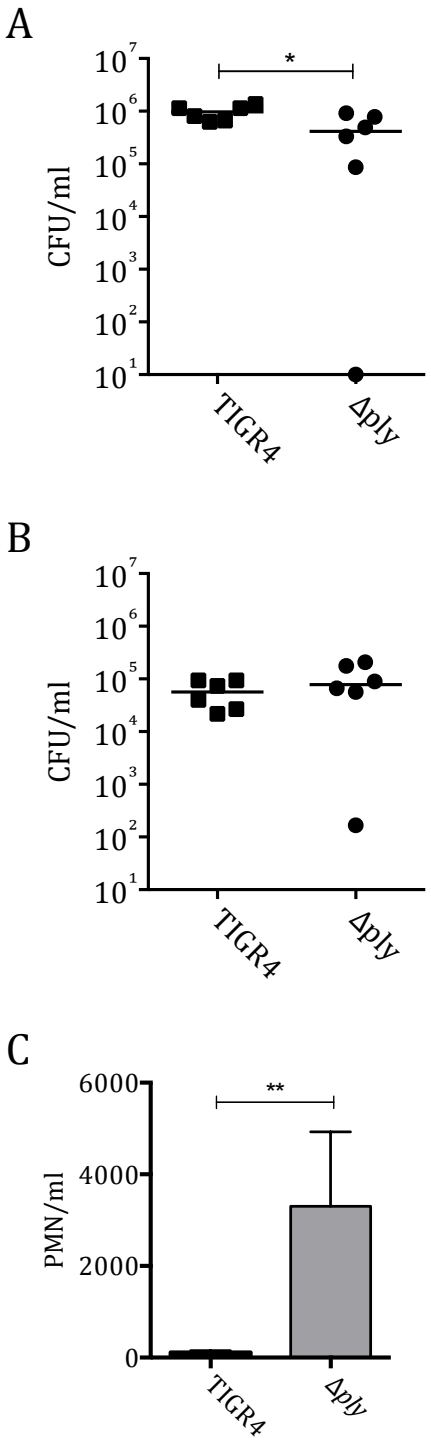

Figure 7.28 Bacterial and neutrophil counts in BALF and bacterial numbers in lung homogenate, and after intranasal infection with TIGR 4 or Δ*ply*

5 week old female CD1 mice were inoculated intranasally with 5×10^6 CFU bacteria under isoflurane anaesthesia. Mice were culled after 2 hours, bronchoalveolar lavage was performed (panel A), and lungs removed (panel B). Both were plated to ascertain bacterial numbers. Neutrophil numbers were measured in BALF. Data presented as per individual mouse and medians; analysed by Mann Whitney test for bacterial counts, and by t-test for neutrophil numbers.

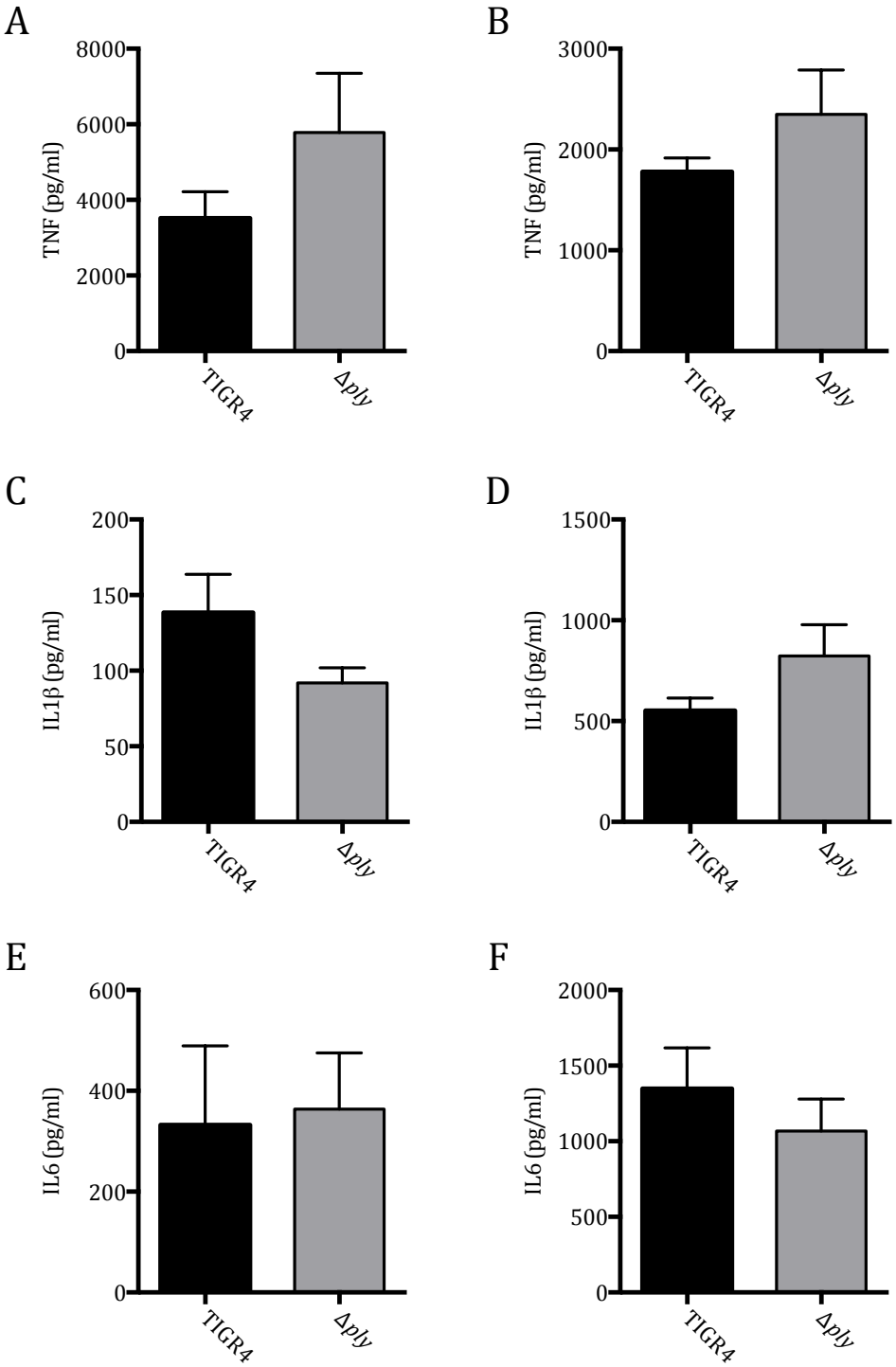

Figure 7.29 Cytokine levels in BALF or lung homogenate 2 hours after intranasal infection with TIGR4 or Δ*ply*

5 week old female CD1 mice were inoculated intranasally with 5×10^6 CFU bacteria under isoflurane anaesthesia. Mice were culled after 2 hours. BALF was obtained, and TNF (panel A), IL1β (panel C), and IL6 (panel E) levels were measured. TNF, IL1β, and IL6 were also measured in lung homogenate (panels B, D, and F respectively). There were 6 mice per group. Data are presented as mean +/- SEM and analysed by paired t-test with no significant differences seen.

7.9 Effects of neutrophil depletion on pneumolysin in mouse pneumonia

As there was a rapid neutrophil influx into BALF at 2 hours after infection with Δ*ply* compared to wild-type, and TNF induced a neutrophil influx, I explored the possibility that Ply's impact on bacterial numbers and thus virulence was due to the effect of TNF on neutrophil recruitment to BALF. This was carried out by depleting neutrophils from mice prior to intranasal infection with 600μg Ly6G (clone 1A8) antibody (BioXcell) or isotype control administered intraperitoneally 24 hours prior to infection, which reduced BALF neutrophil numbers by 80% (figure 7.30, panel A). However, despite this differences in TIGR4 and Δ*ply* BALF and lung CFU at 4 hours were similar after neutrophil depletion (figure 7.30, panel B & C), indicating neutrophils were not required for Ply dependent differences in bacterial CFU in BALF. TNF and IL1β levels in BALF were increased with both strains after neutrophil depletion, possibly reflecting increased bacterial numbers (figure 7.31, panel A & B). Interestingly IL6 levels were increased after Δ*ply* infection, but not wild-type (figure 7.31, panel C). TNF levels in lung homogenate were increased after neutrophil depletion with wild-type but not Δ*ply* infection, however there were no differences in IL1β or IL6 (figure 7.32).

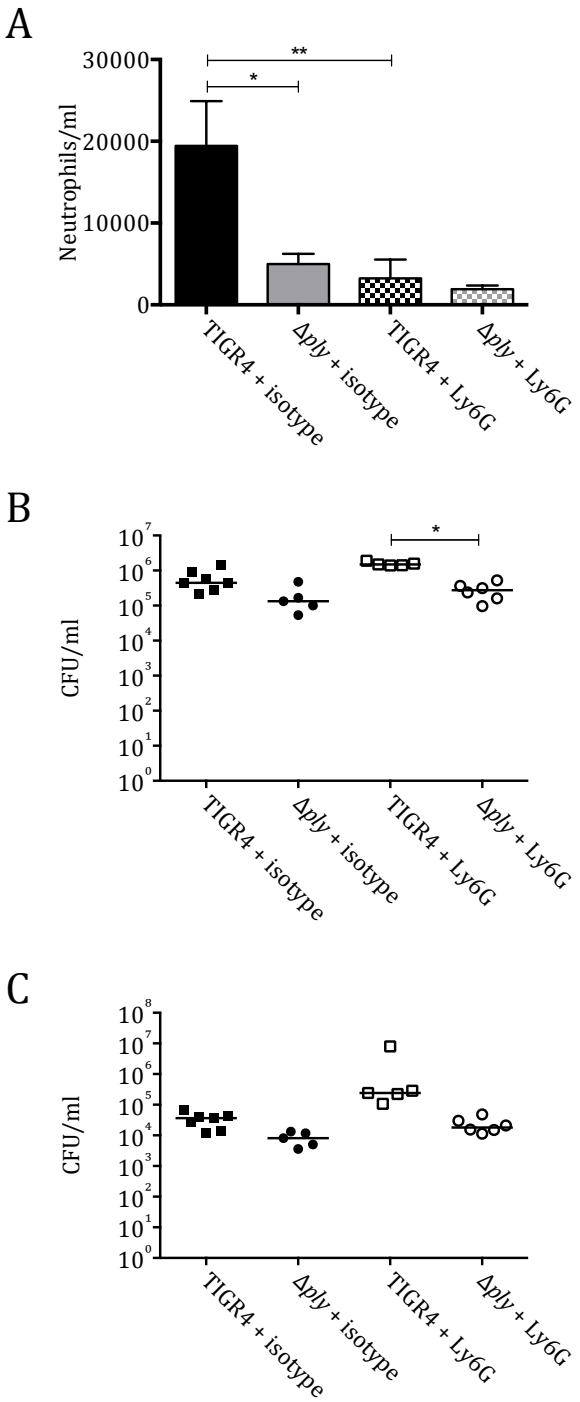

Figure 7.30 Neutrophil and bacterial counts in BALF and bacterial numbers in lung homogenate, after neutrophil depletion

5 week old female CD1 mice were inoculated intranasally with 5×10^6 CFU bacteria 24 hours after intraperitoneal Ly6G antibody. After 4 hours, neutrophil depletion was confirmed in bronchoalveolar lavage (panel A), and bacterial counts measured in BALF (panel B), and lung homogenate (panel C). Neutrophil numbers presented as mean +/- SEM, and CFU presented as per individual mouse and medians; analysed by 1 way ANOVA and Tukey's multiple comparisons test for neutrophil numbers and Kruskal-Wallis with Dunn's multiple comparisons test for CFU.

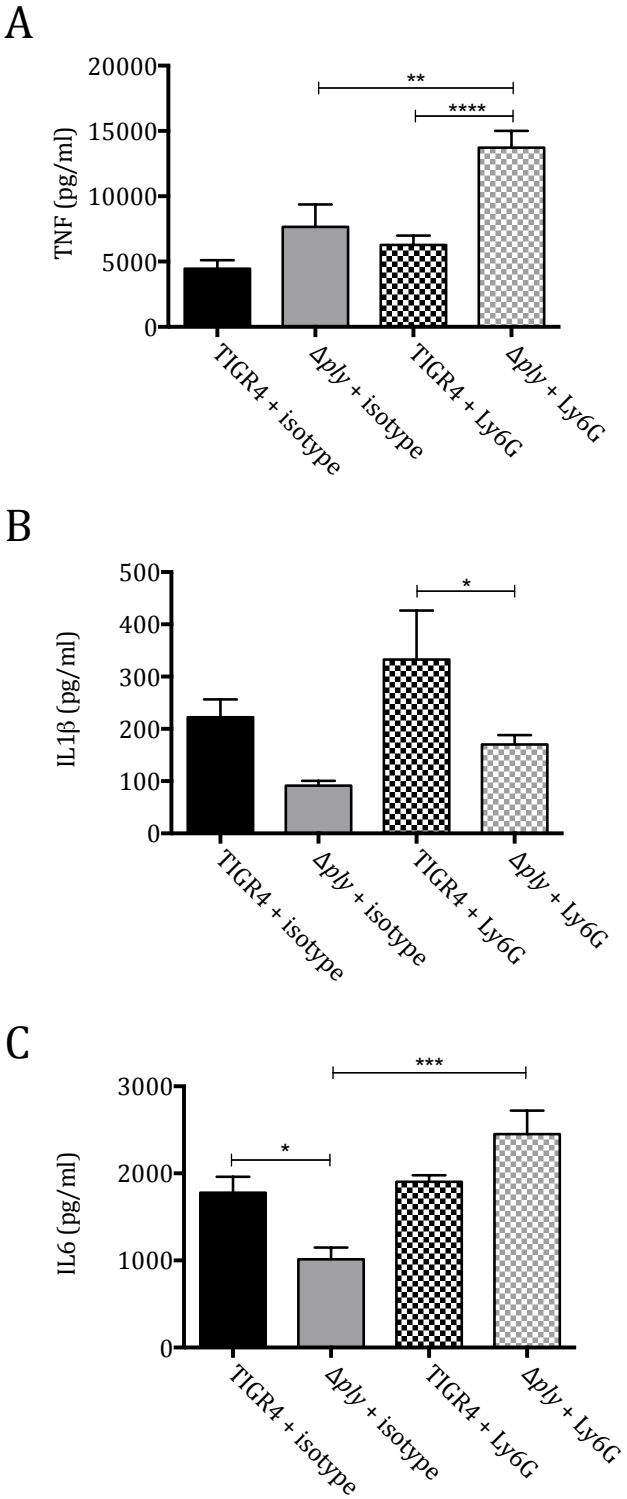

Figure 7.31 Cytokines in BALF with neutrophil depletion

5 week old female CD1 mice were inoculated intranasally with 5×10^6 CFU bacteria under isoflurane anaesthesia, some had been pre-depleted of neutrophils with Ly6G antibody. The cytokine levels in lavage fluid of the mice after 4 hours were measured by ELISA. Data are presented as mean +/- SEM and analysed by 1 way ANOVA and Tukey's multiple comparisons test.

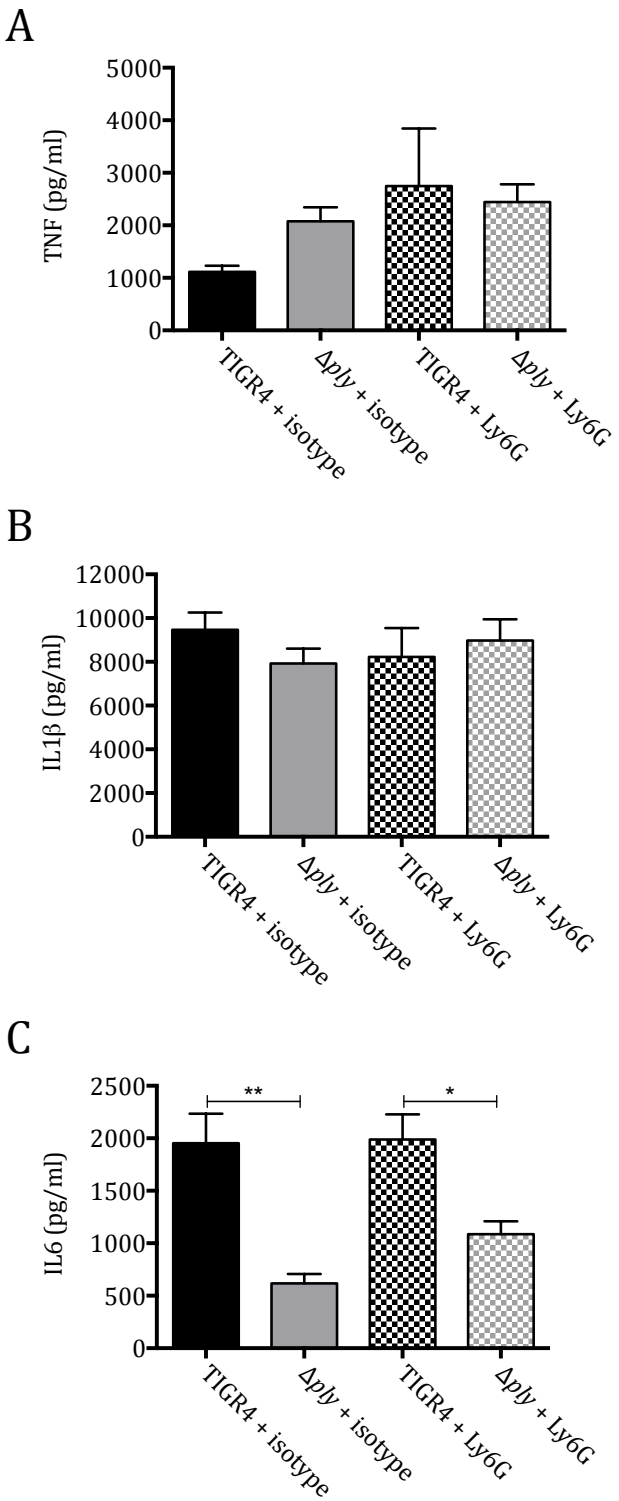

Figure 7.32 Cytokines in lung homogenate after neutrophil depletion

5 week old female CD1 mice were inoculated intranasally with 5×10^6 CFU bacteria under isoflurane anaesthesia, some had been pre-depleted of neutrophils with Ly6G antibody. The cytokine levels in the lung homogenate of the mice after 4 hours were measured by ELISA. Data are presented as mean +/- SEM and analysed by 1 way ANOVA and Tukey's multiple comparisons test.

7.10 Effects of TNF *in vitro* and *in vivo*

To further characterise the role of TNF in early host defence against *S. pneumoniae*, TNF was directly instilled intranasally into mice and the BALF recovered. The administration of 50ng of TNF per mouse had little inflammatory effects (data not shown). However, after administration of 200ng of TNF in 50µl per mouse a significant leucocytosis was induced, in particular a BALF neutrophilia (figure 7.33 panels A, C, and E). Similarly there was an increase in pro-inflammatory cytokines (figure 7.33 panels B, D, and F), suggesting that TNF by itself induces other cytokine release. This could be an early host protective response that is subverted by the actions of Ply.

As TNF is thought to activate macrophages and increase killing of intracellular organisms (Bekker, Freeman et al. 2001 et al) and is known to increase oxidative burst mediated killing of *S. pneumoniae* by neutrophils (Kragsbjerg and Fredlund 2001). 10µg/ml TNF (similar to the concentrations produced by MDM after incubation with Δ*ply*) was added to media of MDM and the effect on *S. pneumoniae* growth assessed. At a variety of bacterial concentrations there was no significant increase in restriction of *S. pneumoniae* growth by the addition of TNF (figure 7.34).

To investigate whether TNF induces release of soluble factors into BALF that could inhibit *S. pneumoniae* survival or growth, BALF from PBS or TNF treated mice were passed through a cell strainer and pooled. BALF from PBS treated mice supported growth of TIGR4. In contrast, at all timepoints TIGR4 CFU in BALF from TNF treated mice was at least one $\log_{10}$ lower that in BALF from PBS treated mice and there was no increase over time (figure 7.35). These data indicate that TNF stimulates soluble immunity to *S. pneumoniae* and the TNF inhibiting properties of Ply may thus allow bacterial proliferation and thus contribute to virulence of *S. pneumoniae*.

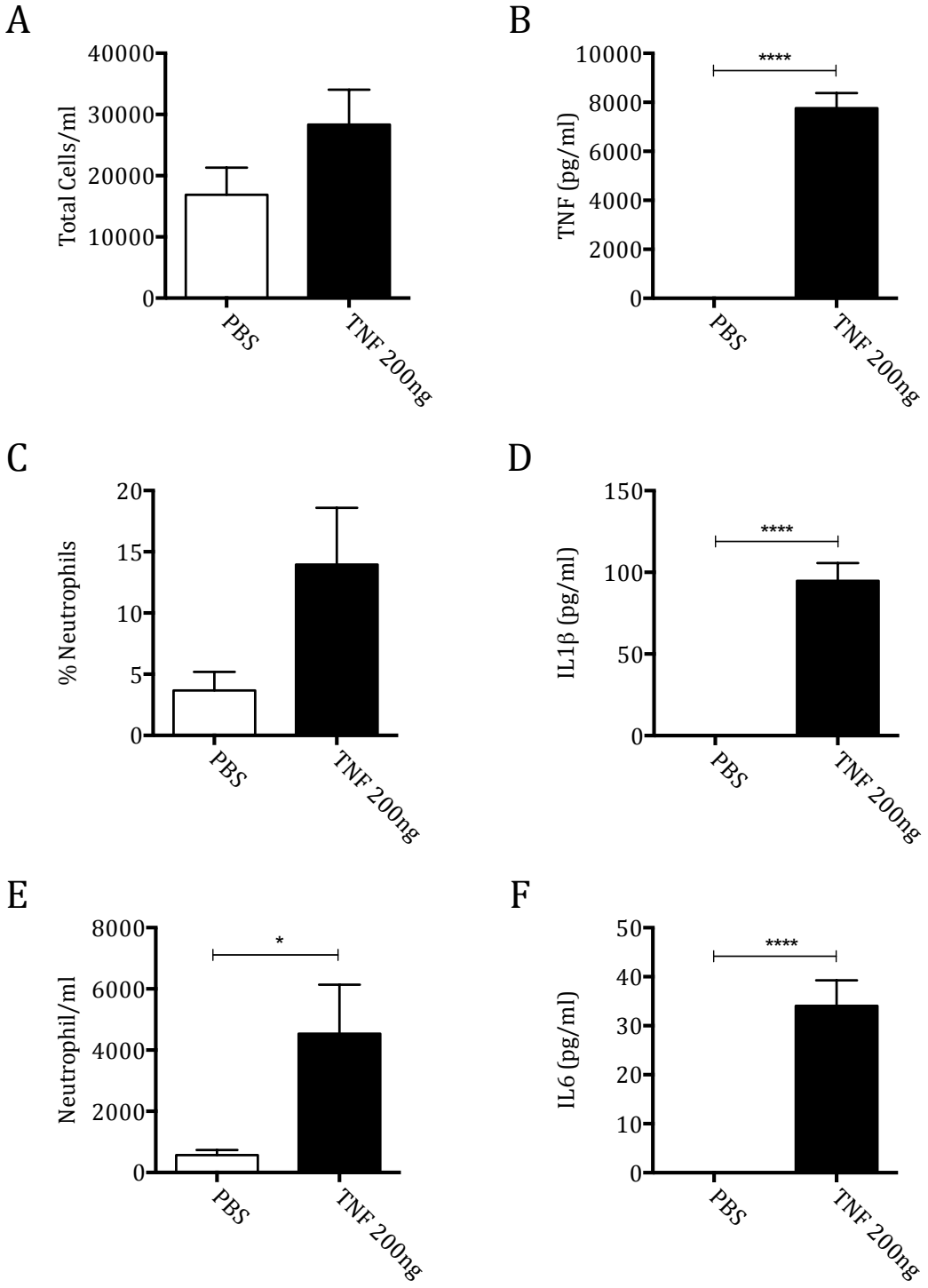

Figure 7.33 Mouse Lavage fluid 4 hours after instillation of 200ng TNF

5 week old female CD1 mice were given PBS or 200ng murine TNF (Miltenyi Biotech) intranasally. 4 hours later, lavage was retrieved and analysed for total cell count (panel A), neutrophil percentage (panel C) and neutrophil numbers (panel E). BALF was then analysed for TNF (panel B), IL1β (panel D), and IL6 (panel F). There were 6 mice in each group, with data presented as mean +/- SEM and analysed by t-test.

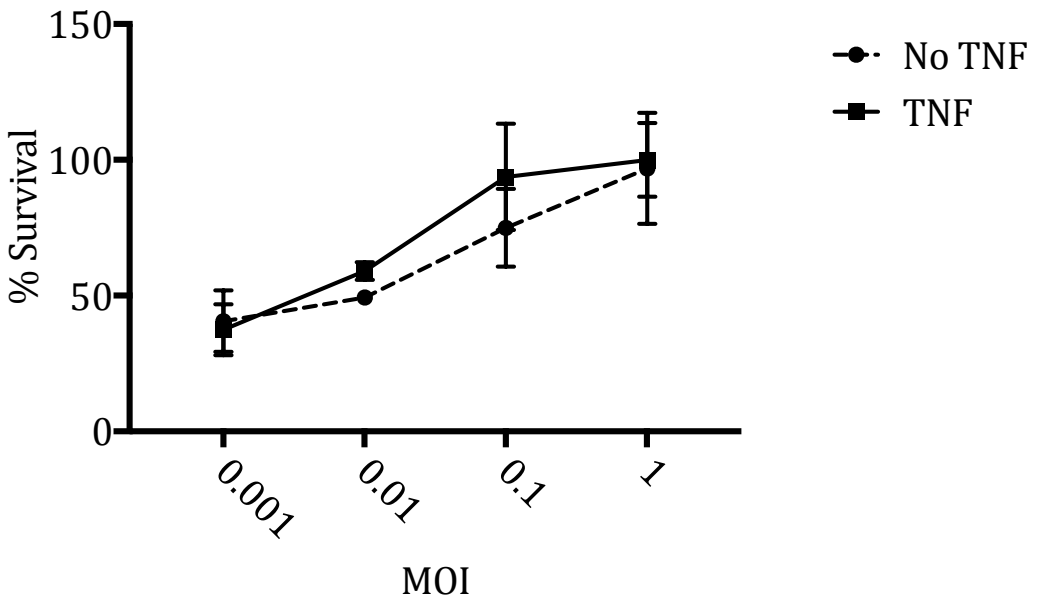

Figure 7.34 TIGR4 survival in the presence of macrophages with TNF

MDM were incubated with various concentrations of TIGR4, and bacterial numbers counted in culture supernatant after 1 hour. Data presented were representative of 3 experiments, and displayed as mean +/- SEM.

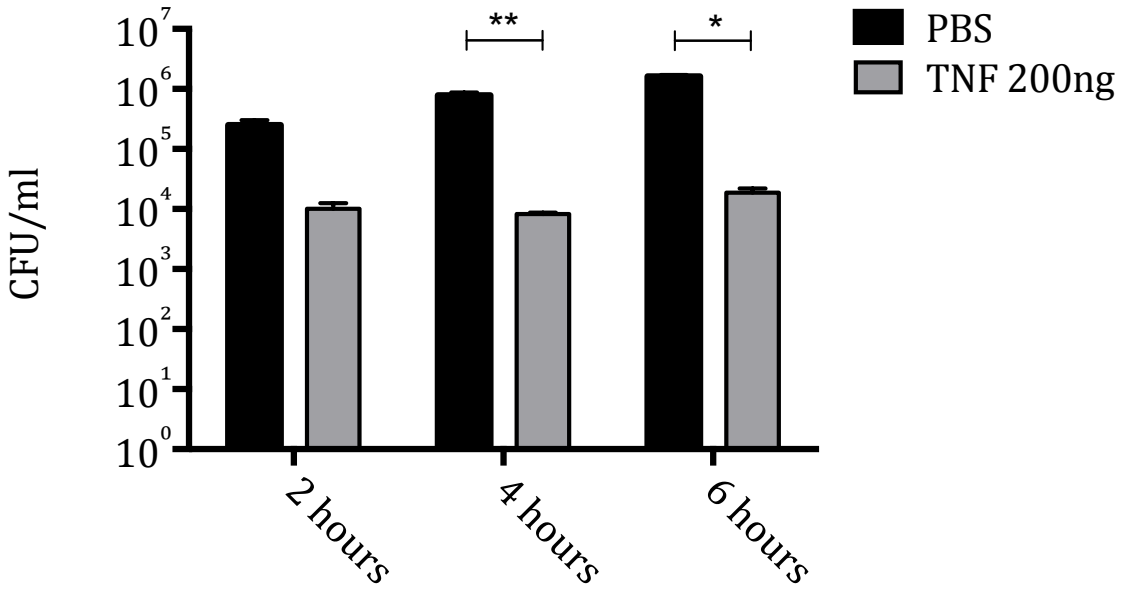

Figure 7.35 TIGR4 growth in BALF from PBS treated or TNF treated mice

BALF from CD1 mice (5 per group) was retrieved 4 hours after intranasal administration of PBS or 200ng TNF. The samples were centrifuged, pooled and passed through a cell strainer. Then TIGR4 was added to both pooled BALF samples and bacterial counts measured at various timepoints. Data presented is a representative of 3 experiments (one performed by Gabriella Szylar), and analysed by Kruskal-Wallis and Dunn's multiple comparisons test.

7.11 Chapter Summary

Whole genome transcriptional analysis of MDM after exposure to wild-type or Δ*ply* strains suggest that Ply downregulates immune gene expression, including IL12, interferon stimulated genes and pro-inflammatory cytokines. Principle component analysis suggests that without Ply MDM responses to *S. pneumoniae* segregate more closely with those to the TLR2 agonist PAM_2CSK_4, suggesting that Ply suppresses some of the inflammatory responses that are induced by *S. pneumoniae* surface lipoproteins. Bioinformatic analysis suggests that wild-type bacteria induce less NFκB and interferon regulated pathways than Δ*ply.*

S. pneumoniae clearance is dependent on phagocytosis, and opsonisation (which facilitates bacterial uptake) reduced inflammatory responses from MDM suggesting that improving bacterial clearance, and thereby reducing external bacterial numbers, reduces inflammatory responses. Interestingly inhibition of phagocytosis with cytochalasin D increased the inflammatory response to wild-type bacteria but reduced the response to Δ*ply*. This suggests that Ply-dependent inhibition of inflammation is dependent on bacterial uptake. In addition these data indicate a role for intracellular PRR to amplify inflammatory responses to *S. pneumoniae*. Whole genome analysis of MDM responses to both strains suggested that inhibition of phagocytosis reduced the upregulation of pro-inflammatory genes to the Δ*ply* strain, decreasing the differences with the wild-type strain and further supporting that the effects of Ply are dependent on bacterial uptake.

Signalling events upstream of transcription were also inhibited by Ply, with wild-type inducing less p38 and ERK phosphorylation and translocation of NFκB to the nucleus, indicating that the effects of Ply inhibit NFκB activation. Interestingly, wild-type bacteria induced more IRF3 activation than Δ*ply*, suggesting that Ply actively induces this pathway. This could be explained by lysosomal TLR4 stimulation that induces TBK1 mediated pathways, which may also inhibit NFκB. However, inhibition of TBK1 does not replicate the pro-inflammatory phenotype of the Δ*ply* strain. Another explanation for the IRF3 data could

be Ply allowing bacterial DNA to enter the macrophage cytoplasm and stimulate cytosolic PRR.

Similarly inhibition of apoptosis and inflammasome did not impact on the 6 hour inflammatory response from MDM. Though further evidence would have provided more support, for example with intracellular stains for apoptosis markers. However, while caspase 1, an important step in the apoptosis pathway was inhibited with no effect on inflammation, opposing the data seen by Littman et al (Littman, Albiger et al. 2009), this does not preclude earlier points in the signalling cascade that stimulate apoptosis being involved. In addition, though the cytolytic component of Ply may contribute to inhibition of inflammation, voltage gated calcium channels were not implicated.

In vivo, in a mouse model of pneumonia, the Δ*ply* strain caused increased BALF TNF and neutrophil levels and was more rapidly cleared that the wild type strain. Inhibiting TNF abrogated the differences in bacterial CFU at 6 hours, suggesting that TNF in BALF is important in control of bacterial numbers early in infection. It is not clear why TNF blockade reduced the amount of bacteria in BALF; possible reasons include a) TNF blockade allowing greater invasion and movement of bacteria into lungs and blood and b) the pleiotropic effects of TNF making direct inferences difficult.

Although at very early timepoints the Δ*ply* strain induced an early neutrophil influx, neutrophil depletion did not alter the differences in bacterial BALF CFU indicating that this was not the main mechanism of bacterial control. The addition of TNF to MDM did not increased bacterial killing suggesting, suggesting the difference in survival between the Δ*ply* and wild-type strains was not due to TNF effects on phagocytes. Rather, BALF recovered from mice treated with TNF restricted *S. pneumoniae* growth, implicating TNF driven soluble factors such as antimicrobial peptides, lysozyme or lactoferrin in the early control of bacterial numbers in the bronchoalveolar compartment. Hence, inhibition of early

inflammatory responses to *S. pneumoniae* by Ply would allow increased bacterial replication in the bronchoalveolar space thereby supporting virulence.

8 Discussion

S. pneumoniae causes an enormous amount of morbidity and mortality worldwide. Since Sir William Osler used Bunyan's phrasing to refer to pneumonia as the captain of the men of death (Osler 1904), antibiotics and vaccination programmes have improved the outlook for long-term disease control. However despite antibiotics and vaccination programmes *S. pneumoniae* is still a common cause of infectious disease, and a proportion of people who develop infection go on to develop severe disease characterised by local and systemic infection. It is likely that the pattern of excessive inflammation is established early within the course of infection, which manifests as consolidation and lung injury, septic shock or meningitis. Thus elucidating the pathogenesis of the inflammatory response and the reason for its propagation remain key targets in tackling *S. pneumoniae* related morbidity.

8.1 Effect of Capsule on Inflammatory Response to *Streptococcus pneumoniae*

The capsule has been long recognised as the most important virulence factor for *S. pneumoniae* but the primary characterised functions have been to reduce recognition and thus engagement with the host immune system. Unencapsulated *S. pneumoniae* are cleared quickly by the innate immune response so are rarely found as a cause of invasive infections, although they are present as colonisers of the nasopharynx and can cause conjunctivitis (Haas, Hesje et al. 2011) and otitis media (Keller, Robinson et al. 2016).

Variation in capsular makeup has resulted in over 90 serotypes, some of which are more likely to cause invasive disease than others (Brueggemann, Griffiths et al. 2003, Hanage, Kaijalainen et al. 2005, Sandgren, Albiger et al. 2005). Interestingly the different serotypes also seem to have differing propensities to cause inflammation in terms of septic shock (Garcia-Vidal, Ardanuy et al. 2010), and meningitis (Geldhoff, Mook-Kanamori et al. 2013). Similarly in animal models, there is serotype dependent variation in inflammatory response (Engelhard, Pomeranz et al. 1997, Seyoum, Yano et al. 2011). This suggests that the capsule certainly plays a role in modifying the inflammatory response to *S. pneumoniae*.

Previous work has shown that purified capsule itself is not pro-inflammatory (Tuomanen, Tomasz et al. 1985), and considerable human and animal data demonstrates that inflammation is necessary for host immunity to *S. pneumoniae*. Hence, it would follow that a physical barrier such as the capsule that reduces engagement of host PRR with bacterial PAMPs should reduce inflammation, and this might allow greater bacterial survival. I therefore set out to assess how the capsule affects inflammatory responses to *S. pneumoniae* using MDMs.

8.1.1 *Streptococcus pneumoniae* capsule promotes inflammatory responses *in vitro* and *in vivo*

I have investigated how the presence of capsule in live *S. pneumoniae* affected inflammatory responses *in vitro* and *in vivo* using macrophage cell culture and murine models of infection.

When primary human MDM were incubated with live *S. pneumoniae*, unexpectedly encapsulated wild-type strains induced greater pro-inflammatory cytokine secretion than isogenic capsule deficient strains. Despite significant variation in individual responses, overall there was a strong pro-inflammatory signal due to encapsulated strains. While this variation may well have been due to variations in individual response to bacteria, more time and effort should have gone into ensuring standardisation across experiments, e.g. by ensuring similar cell numbers and activation states, ensuring no contaminating T cells, perhaps by more regular cell surface/intracellular marker staining. Additionally, MDM were differentiated with M-CSF, and a more regulatory phenotype (perhaps more similar to AM) could have been investigated using GM-CSF differentiated cells. While it is likely that exposure to pathogens does induce a more M1 phenotype, initial responses that I examined during this thesis may be different using differently differentiated MDM. Ideally a few key experiments could have been performed with primary human alveolar macrophages.

This effect was also seen at transcriptional level as measured by qPCR and whole genome transcriptional analysis. The whole genome transcriptional microarrays of primary human MDM responses to *S. pneumoniae* showed that a relatively small proportion of the whole genome was differentially expressed by the addition of TIGR4. The differentially expressed genes were largely pro-inflammatory genes and chemokines, and transcription of many of these was reduced in response to the unencapsulated strain. While these data were obtained from relatively few individuals, they support the secreted cytokine data, and suggest a transcriptionally regulated difference between encapsulated and unencapsulated strains. These data reflect epithelial transcription responses to TIGR4 and TIGR4Δ*cps*, with similarly greater gene upregulation in response to wild-type strains, and more pro-inflammatory

signalling (Bootsma, Egmont-Petersen, et al. 2007). Additionally the genes commonly upregulated by the strains examined are similar to that of my data.

The results seen with MDMs were partially replicated in a mouse pneumonia model. TNF production in the bronchoalveolar compartment was evident within 2 hours, and IL1β and IL6 within 4 hours. Wild-type TIGR4 induced greater pro-inflammatory cytokine release than unencapsulated TIGR4. However, these results were confounded by bacterial numbers as bacterial clearance is heavily influence by the presence of capsule (Camberlein, Cohen et al. 2015). These differences were also partially reflected in physiological effects and serum cytokine levels in a rat septic shock model, although these data were largely statistically non-significant due to few biological replicates and large error bars. The early mouse infection model used is relevant as inflammation is induced, bacteria are not entirely cleared, and previous data from the Brown laoratory have shown that left longer, many of the mice would succumb to bacteraemia and often die. Hence the unencapsulated strain induced weaker proinflammatory responses when measured at the protein and gene level, with some evidence of this effect being relevant in murine models of infection.

Similar to others (Tuomanen, Tomasz et al. 1998), I found that the relatively pro-inflammatory effect of encapsulated bacteria compared to unencapsulated *S. pneumoniae* was not caused directly by capsular material, as inhibiting contaminating endotoxin abolished pro-inflammatory cytokine release due to high concentrations of capsular material. LPS contamination could also explain the cytokine response seen in response to high concentrations of purified polysaccharide seen in others' work (Jagger, Huo et al. 2002, Simpson, Singh et al. 1994).

In the *in vitro* model, capsule inhibited phagocytosis corroborating previous data (Hyams, Camberlein et al. 2010). Phagocytosis by MDM restricted bacterial replication in media, and CFU of the unencapsulated strains were therefore restricted more effectively than encapsulated strains. As a result by 6 hours there were significantly more TIGR4 than Δ*cps* in

media which could confound the results reflecting MDM inflammatory responses. However, when penicillin was added to the MDMs, although the cytokine response was vastly diminished, differences between wild-type and unencapsulated strains were preserved. At 4 hours, when there was already a non-signifcant smaller difference in bacterial counts between the strains, again the cytokine response was blunted but the difference between strains was preserved. These data suggest that while bacterial numbers may account for some of the difference in inflammatory response between strains, they do not explain all of the pro-inflammatory effect of the encapsulated bacteria versus unencapsulated bacteria. In addition, unpublished data from the Brown group with non-replicating bacteria in a mouse pneumonia model suggests that the difference in early lung TNF inflammatory responses between encapsulated and unencapsualted bacteria is preserved when differential bacterial bacterial numbers are accounted for.

During pneumonia the two main resident cell populations that encounter *S. pneumoniae* are the respiratory epithelium and alveolar macrophages. As the cytokine response from alveolar epithelial cells was limited with direct exposure to *S. pneumoniae,* macrophages are likely to be the predominant cell type that initiate early inflammatory responses during pneumonia. Conditioned media from macrophages induced a slightly greater cytokine response from epithelial cells, but even this was at a much lower level than that of macrophages themselves. This supports a model of AM being key sensors of pathogens, initiating inflammatory responses, and activating nearby epithelial cells to amplify this response until pathogens are dealt with. Depletion of AM in a low inoculum model of infection in mice by the instillation of lysosomal clodronate diminshed inflammatory responses, confirming that macrophages are the key cell type involved in capsule-dependent inflammatory responses *in vivo*. However the difference between TIGR4 and Δ*cps* was preseved with respect to TNF in high inoculum infection. At lower inocula, the pro-inflammatory effects of encapsulated bacteria were diminshed somewhat. The patterns of inflammatory responses were different in lung homogenate, in particular while TNF and IL6 levels were slightly lower, IL1β levels were an

order of magnitude greater, suggesting differential responses by compartment. Importantly the pro-inflammatory effects of the capsule were preserved in both compartments overall.

Thus both *in vitro* and *in vivo* models suggest that the presence of capsule on *S. pneumoniae* has pro-inflammatory effects early during host-pathogen interaction. While bacterial numbers may contribute to this, they are not the sole reason for the effect seen.

8.1.2 Exploration of mechanisms underpinning the pro-inflammatory effects of *S. pneumoniae* capsule

There are multiple potential explanations as to why capsule exerts a pro-inflammatory effect. My hypotheses included:

(i) The capsule allows greater exposure of pro-inflammatory bacterial ligands to cell surface PRRs by preventing bacterial phagocytosis

(ii) Capsule recognition by cell surface PRRs amplifies the inflammatory response driven by other bacterial ligands such as lipoproteins

(iii) Antibody binding to the capsule increases inhibitory signalling due to engagement with Fcγ receptors on the cell surface

(iv) Increased activation of intracellular PRR by internalised bacteria with inhibitory effect

Further interrogation of the whole genome transcriptional responses showed that the TLR2 agonist PAM_2CSK_4 induced far more differential gene expression than bacteria, though this may have been distorted by the differences in platforms used between the positive controls and the unstimulated cells. The most upregulated genes in response to PAM_2CSK_4 were largely an inflammatory gene set but the levels of upregulation were greater and more genes were upregulated by more than 2 fold (data not shown in thesis). The difference between wild-type and unencapsulated strains was limited to an even smaller gene set, and the difference in gene expression was surprisingly small given the effects seen in culture supernatant and *in vivo*. Bioinformatic analysis suggested that the transcription factors

involved in generating this gene signature were largely restricted to the NFκB family and some interferon response genes, which would be predicted to occur as a result of PRR and cytokine receptor stimulation. Interestingly the pathway predicted to be most overrepresented by TIGR4 compared to unencapsulated bacteria was the NOD-like receptor signalling pathway. This pathway is stimulated by cytosolic recognition of PAMPs, which would be unexpected as the capsule reduces rates of *S. pneumoniae* phagocytosis.

Nuclear NFκB translocation was greater with unencapsulated bacteria compared to wild-type at 1 hour, but there was little difference by 2 hours. This may indicate a slightly delayed kinetic of signalling responses with encapsulated bacteria, possibly due to slower engagement of cell surface host PRR with bacterial ligands due to the shielding effect of the capsule. These data were strengthened by the single cell nature of the analysis, and had little variation between donors, suggesting a conserved response. Importantly, this was discordant with the transcriptional findings at 4 hours or protein data at subsequent timepoints. This implicates capsule driven, non-NFκB mediated pathways affecting cytokine transcription and secretion. The phosphoarray and MAPK data suggested that similar activation patterns between the strains, indicating that the capsule did not affect these pathways, although there was greater signalling seen with Δ*cps*. Although the transcription factor array was not necessarily sensitive enough to detect all transcription factor effects (for example, this array did not identify NFκB), there was the suggestion of more transcription factors being activated by the unencapsulated strain, possibly indicating that the unencapsulated organism activates more pathways than wild-type bacteria. Indeed much of the effect of *S. pneumoniae* appeared to be to downregulate transcription factor activation. This may be the macrophage responding to pathogen by amplifying anti-pathogen functions while reducing regulatory functions. Conclusions from this array must be viewed with caution given the lack of sensitivity, and may reflect that some transcription factors can have profound effects despite a lack of abundance, although could also reflect timepoint issues or the effect of transcription regulators magnifying small effects.

The media used to culture MDM contained pooled human serum, which is likely to contain anti-pneumococcal antibodies. Both wild-type and unencapsulated bacteria bound to antibodies in serum, but unencapsulated bacteria had a greater mean fluorescence index, indicating that on average more antibodies bound to each unencapsulated bacterium. Antibody responses can have an effect on inflammation over and above that on the effect on phagocytosis as Fc receptor engagement are implicated in inflammatory signalling pathways (Clatworthy and Smith, 2004). However, in serum free media at early timepoints wild-type bacteria still induced a trend to more inflammatory cytokine transcription than unencapsulated bacteria. Deliberately opsonising bacteria in higher concentration pooled serum reduced inflammatory cytokine responses, and reduced the differences between the two strains, likely due to increased phagocytosis and enhanced clearance of bacteria by opsonisation. Given the strength of this correlation, it may well be that the largest part of the difference in inflammatory response seen between encapsulated and unencapsulated strains is due to variation in bacterial uptake. This is logical as lack of adherent bacteria would serve to reduce external PRR engagement, and successful phagocytosis could therefore switch off pro-inflammatory signalling.

Hence I examined the effect on inflammatory responses of phagocytosis using the actin polymerisation inhibitor, cytochalasin D, to inhibit phagocytosis. The antibiotic protection assay and fluorescent microscopy data indicated that phagocytosis was almost completely abrogated by the use of 10μM cytochalasin D. Interestingly, inhibition of phagocytosis with cytochalasin D increased the inflammatory responses to TIGR4, and to a lesser extent Δ*cps,* with increases in the number of genes differential expressed by MDM after incubation with wild-type and unencapsulated bacteria. However, the relative expression of inflammatory cytokines and supernatant cytokine levels was very similar to those seen with MDMs not treated with cytochalasin D, and with preserved differences between the strains. Hence the differences in inflammation were not due to differences in ratios of internal to external bacteria for encapsulated and unencapsulated *S. pneumoniae*. Rather as inhibition of

phagocytosis maintained the difference in inflammatory cytokine production, this suggests that cell surface receptors are responsible for the difference seen.

These data would be compatible with the hypothesis that capsule modifies and amplifies external PRR signalling due to other components of bacteria although TLR2, probably the most important cell surface PRR, activation was similar between the two strains. Alternatively the capsule could be relatively selective in inhibiting engagement of bacterial cell surface ligands with host surface PRR that are anti-inflammatory compared to pro-inflammatory PRRs. However, there was no difference seen in lectin-mediated signalling or after scavenger receptor blockade, suggesting that although several members of these receptor families have been linked to recognition of *S. pneumoniae*, they are not implicated in capsule-mediated pro-inflammatory signalling. Hence the increase in inflammatory cytokine release attributable to capsule is not explained by differences in phagocytosis, TLR2 activation, Fc receptor, lectin, or scavenger receptor activation, so the mechanism remains unexplained. Alternative mechanisms that need investigation include capsule induced amplification of pro-inflammatory signals or reductions in inhibitory signals at the cell surface (figure 8.1) perhaps due to non-NFκB mediated transcriptionally regulated events.

8.1.3 Serotype affects inflammatory responses of human macrophages to *S. pneumoniae*

Expression of a capsule saw a trend towards increased inflammatory cytokine from MDMs after incubation with a number of different *S. pneumoniae* serotypes. The exception was serotype 3, which expresses a particularly mucoid capsule. These data indicate that the presence of a capsule affects inflammation across a variety of strains, usually increasing the inflammatory response. For encapsulated wild-type strains there were differences in inflammatory responses between serotypes, with for example serotype 6A inducing more TNF and IL6 than TIGR4. Interestingly while TLR2 simulation varied between serotypes, there was little difference between different capsule deficient strains. This suggests that

while the capsule does not directly activate TLR2, it may modify how TLR2 ligands such as bacterial surface lipoproteins engage with this surface PRR.

As the inflammatory phenotype differed between *S. pneumoniae* strains expressing different capsular serotypes, I used isogenic capsule switch strains to determine how much of these differences were due to variations in the capsule rather than non-capsular differences between strains. Similar to wild-type strains the expression of 6A capsule on TIGR4 induced more IL6 and TNF than serotype 4 capsule. These data suggest that at least part of the difference in inflammatory response between strains is driven directly by capsular structure. However, the TLR2 activation did not vary between isogenic capsule switch variants suggesting that these serotype effects are not TLR2 dependent.

8.1.4 The expression of *S. pneumoniae* capsule on *S. mitis* does not affect inflammatory responses

S. mitis is closely related to *S. pneumoniae*, and has been suggested to be a descendent that has lost multiple virulence factors. It is a successful coloniser of the oropharynx that rarely causes disease. Recently it has been established that some strains express a capsule, and the capsule genetic locus has been manipulated so that the *S. pneumoniae* serotype 4 capsule is expressed by *S. mitis* (Rukke, Hegna et al. 2012). This enabled me to assess the effect of *S. pneumoniae* capsule on inflammatory responses to another organism. MDM responses to *S. mitis* strains (perhaps surprisingly) showed that they induced more TNF and IL6 than TIGR4 strains. Importantly the addition of TIGR4 capsule did not appear to affect the inflammatory response. Along with the data that showed capsular polysaccharide does not induce inflammation by itself, these results suggest that the capsule modifies how macrophages interact with another pneumococcal virulence factor not shared with *S. mitis*.

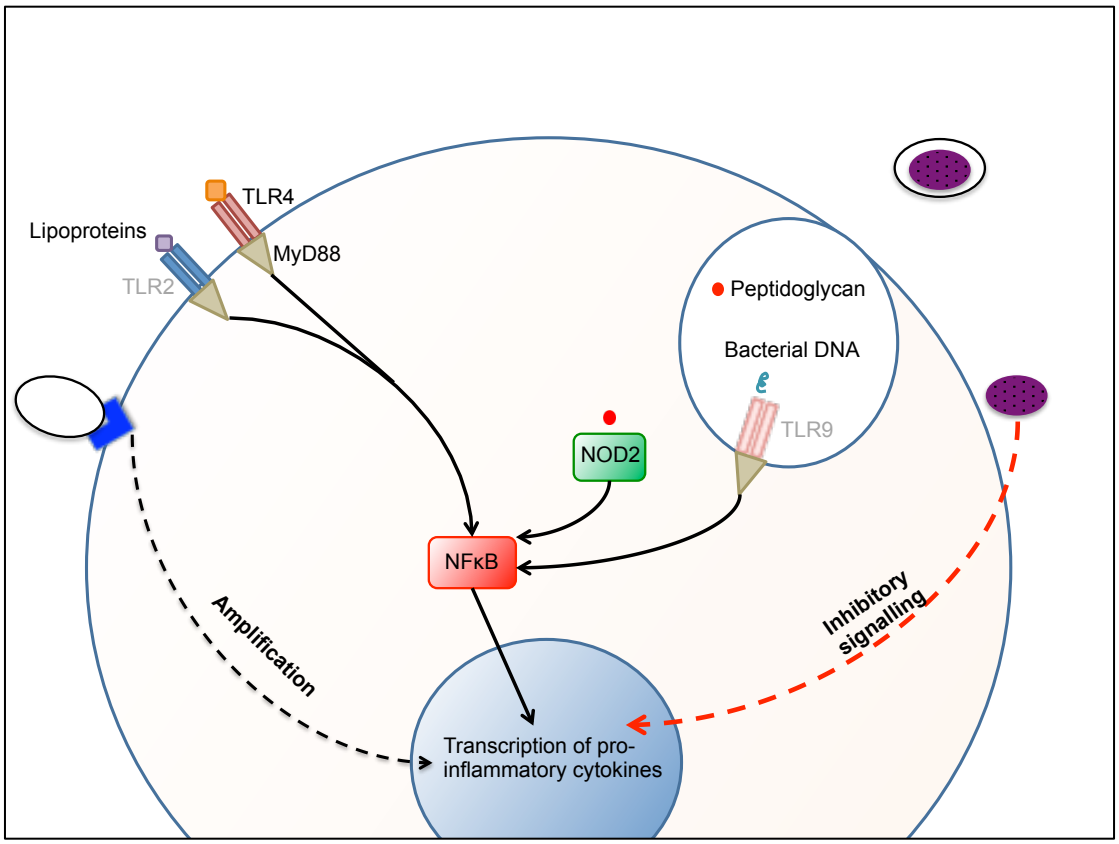

Figure 8.1 Possible pro-inflammatory mechanisms of *S. pneumoniae* capsule

Pro-inflammatory components of *S. pneumoniae* stimulate PRR, and largely converge via NFκB to induce pro-inflammatory cytokine transcription. Capsule does not directly induce inflammation, but as yet unrecognised PRR may allow signalling such that transcription is amplified, but not via NFκB. Alternatively, as the surface and internal constituents of *S. pneumoniae* may engage more PRR, which could either compete with or directly inhibit NFκB, so effectively the capsule may streamline macrophage responses through the pro-inflammatory pathways.

In a mouse pneumonia model, the addition of the TIGR4 capsule to *S. mitis* reduced bacterial clearance, confirming the effect of TIGR4 capsule on inhibiting phagocytosis. However, there was no effect on neutrophil infiltrate or cytokine levels in lavage fluid or lung homogenate. In contrast to human MDM cytokine levels, during murine pneumonia *S. mitis* strains induced similar levels of BAL TNF but far less IL1β and IL6 than infection with *S. pneumoniae*. The reasons for these differences are not known, but the mouse pneumonia model involves bacterial interactions with multiple cell types and a very active innate immune response, and is a much more complex situation than cell culture infection.

8.1.5 Summary

The most important role of *S. pneumoniae* capsule is clearly the inhibition of phagocytosis, which is the main mechanism of bacterial clearance. The data presented in this thesis indicates that the capsule also has pro-inflammatory effects which may contribute to the morbidity and mortality associated with the over-exuberant inflammatory response seen in disease caused by *S. pneumoniae*. Many other major bacterial pathogens express a polysaccharide capsule, including *Neisseria meningitides, Klebsiella pneumoniae, Haemophilus influenzae*, and *Streptococcus pyogenes*. In addition *Cryptococcus neoformans*, a bacteria-sized yeast expresses a capsule. In all these species the capsule is a virulence factor that primarily inhibits opsonophagocytosis. When the inflammatory properties of the capsule in other species have been studied, in contrast to my data for *S. pneumoniae* generally they dampen the response to the organism (Yoshida, Matsumoto et al. 2000; Ellerbroek, Walenkamp et al. 2004; Regueiro, Campos et al. 2006; Raffatellu, Santos et al. 2007; Frank, Reguerio et al. 2013; Monari et al. 2005), presumably improving evasion of host immune responses. The exceptions are purified *Staphylococcus aureus* and *Neisseria meningitidis* capsular polysaccharide that induced pro-inflammatory cytokines secretion from PBMC (Soell, Diab et al. 1995) or human macrophages in a TLR2 and TLR4 dependent manner (Zughaier, Tzeng et al. 2004) respectively, producing a similar functional effect to the *S. pneumoniae* capsule effects but by a different mechanism. As loss of the capsule has multiple other effects on host

- bacterial interactions the biological significance of the effect of the capsule on inflammatory responses to *S. pneumoniae* during actual infection remains unclear. The *in vitro* data would suggest that it maybe partially responsible for the marked inflammatory response that is characteristic of acute *S. pneumoniae* infections.

8.2 Effect of Pneumolysin on Inflammatory Response to *Streptococcus pneumoniae*

Ply is an important virulence factor expressed by the majority of virulent *S. pneumoniae* strains. There is little variation in Ply proteins between strains, though some serotypes express a form that does not induce pore formation and therefore do not cause cytolysis. This particularly occurs in some serotype 1 strains (Kirkham, Jefferies et al. 2006); serotype 1 has an unusual capsular structure (Mertens, Fabri et al. 2009), possibly accounting for the loss of Ply as a compensatory measure. Ply has no recognised export sequence, and is thought to be released extracellularly by bacterial lysis although it has recently been reported to also be cell wall associated (Price, Greene et al. 2012).

Since its initial discovery, Ply has proven to have pleiotropic effects on the immune system, mostly pro-inflammatory (Malley, Henneke et al. 2003) and often linked to its pore-forming function (Davis, Nakamura et al. 2011, McNeela, Burke et al. 2010). As initiation of the innate immune response and inflammation is important in host defence to *S. pneumoniae*, it is unclear why if Ply is strongly pro-inflammatory it has been retained in the *S. pneumoniae* genome. In contrast to the data on pro-inflammatory effects of Ply, at least one group suggest that human DCs incubated with wild-type bacteria secrete less pro-inflammatory cytokine than Δ*ply* (Littman, Albiger et al. 2009).

8.2.1 Pneumolysin inhibits inflammatory responses

I investigated whether the early macrophage inflammatory response to live *S. pneumoniae* was affected by Ply by incubating primary human MDM with wild-type and Ply deficient *S. pneumoniae*. Contrary to most of the existing Ply literature (Davis, Nakamura et al. 2011, Malley, Henneke et al. 2003, McNeela, Burke et al. 2010), wild-type strains induced less pro-inflammatory cytokine release than Δ*ply* strains. This finding was quite striking, and much more obvious than the difference seen with capsule. Δ*ply* strains were found in similar numbers in culture supernatant with similar bacterial uptake suggesting adhesion and

phagocytosis by macrophages are not affected by Ply, so differences in bacterial numbers were not likely to confound the results.

Whole genome transcriptome analysis suggested quite a significant increase in upregulated genes with Δ*ply* over wild-type, supporting an inhibitory role for Ply at the transcriptional level. Direct comparison of the genes upregulated showed that Δ*ply* increased expression of IL12, chemokines, interferon stimulated genes and pro-inflammatory cytokines. NFκB translocation was increased in the presence of Δ*ply* compared to wild-type, confirming the predicted transcription factor activation from the genome wide transcriptional data. Interestingly others have examined transcriptional responses of THP-1 cells, a monocytic cell line, to D39 and D39Δ*ply* (Rogers, Thornton et al.) and found much less effect on inflammation and no striking pattern that Ply inhibits inflammation despite a similar timepoint. The differences could be explained by the effects of differentiation of my cells into macrophages, alternatively they could be a function of cell line versus primary cells.

In a mouse pneumonia model, the Δ*ply* strain was clearly less virulent by 4 hours but by 24 hours both strains had largely been cleared. At this timepoint neutrophil recruitment and albumin leak were similar despite a $\log_{10}$ less Δ*ply s*uggesting that each individual Δ*ply* bacterium induced more inflammatory response than wild-type. Despite there being fewer bacteria, early TNF responses in BALF were significantly greater with Δ*ply* suggesting that Ply inhibits TNF release from AM, the primary cell type that initiate inflammatory responses in the bronchoalveolar compartment. Ideally the central role of the AM to this response could have been confirmed with a clodronate-mediated macrophage depletion. Although clodronate also appears to induce neutrophil infiltrate directly, which could confound any data.

The effects of Ply on MDM inflammatory responses were conserved across a number of different serotypes and their isogenic Δ*ply* mutants, as well as naturally occurring variants within serotype 1, suggesting that this effect is not serotype dependent, and therefore

unlikely to be due to bacterial uptake or affected by bacterial association with the cell surface. The data from D39 strains *in vivo* suggests that the virulence effects of Ply are less pronounced in this strain background. Despite this, the effects of loss of Ply on TNF and IL1β levels were similar to those seen for the TIGR4 data. Importantly, the complemented D39 strain had similar effects to wild-type suggesting that the antibiotic resistance cassette alone was not responsible for differences in cytokine response seen. Much larger cytokine responses were also obtained from epithelial cells incubated with MDM conditioned media obtained using the Δ*ply* strain compared to MDM conditioned media obtained using wild-type bacteria. Again, this reflects the primary importance of the AM in generating inflammatory responses. A double deletion Δ*cps*Δ*ply* mutant showed similar effects on inflammatory cytokines as Δ*ply*. This suggests that the effect of Ply outweighs that of capsule, and that there was no obvious effect of one component on the response to the other, though in these experiments the pro-inflammatory effects of capsule were blunted so perhaps not generalisable.

One reason that the data described in this thesis is at odds with the bulk of published data may be the use of live bacteria rather than purified Ply. Purified Ply induced dose-dependent pro-inflammatory cytokine release, which in the case of TNF and IL6 was greatly reduced by removing endotoxin contamination, though it may be that polymyxin B could have been off-target effects. However, at the highest concentrations of purified Ply there was still significant TNF and IL6 secretion in the presence of polymyxin B indicating some direct Ply pro-inflammatory effects, though with higher concentrations, IL1β levels fell with probably due to significant cell death. More experiments to confirm this cell death, and its manner, would have been useful to build confidence in this narrative. Purified non-haemolytic Ply induced inflammatory cytokine release in a dose-dependent manner. These data confirm that IL1β release is stronger upon exposure to the pore-forming effects of extracellular Ply, which would be consistent with inflammasome activation (McNeela, Burke et al. 2010) but that some of the inflammatory responses to extracellular Ply occur independently of this function.

Another important reason for the discrepancy in my data compared to previous publications were the early timepoints I used to examine initial host-pathogen interaction. Furthermore, most previous data were largely derived from murine models and cell lines, whereas my data involved primary human macrophages similar to the data from primary human DCs that also suggested an anti-inflammatory effect of Ply (Littman, Albiger et al. 2009). This paper used Δ*cps* and Δ*cps*Δ*ply* to facilitate uptake, and used monocyte-derived DCs, which only differ from MDMs in that monocyte differentiation was induces with GM-CSF and IL4. Interestingly they noted that expression of Ply affected bacterial uptake in the context of unencapsulated bacteria. This may have not been apparent in my data as the capsule has a more profound effect on bacterial uptake. They looked at IL12 and CXCL8 with similar effects to my dataset, as well as similar effects on apoptosis. Secreted IL1β levels were also similar, and differences clearer at later timepoints. They also showed that Ply murine DCs had the opposite pattern in respect to IL1β secretion, further suggesting that murine responses to Ply may be different from humans'.

Principle component analysis of the whole genome transcriptome showed that Δ*ply* induced similar upregulation patterns to PAM_2CSK_4, a lipoprotein that signals via TLR2, suggesting that Ply inhibits the host response to bacterial TLR2 ligands. Transcription factor enrichment binding analysis predicted increased NFκB-dependent gene transcription in response to the Δ*ply* strain, which is also consistent with signalling via TLR2 (but not limited to this PRR). The other group of transcription factors that Δ*ply* induced were the IRFs, suggesting increased interferon responses. Previous data suggests that Ply is instrumental in inducing IFN responses by allowing bacterial DNA to enter the cytosol (Parker, Martin et al. 2011). This function of Ply seems to occur later in infection, as there are data suggesting that Ply only enters the cytosol of macrophages after 8 hours (Bewley, Naughton et al. 2014). As interferon responses may also be induced by phagolysosomal membrane PRR stimulation, e.g. TLR9 (Moretti and Blander 2014), Ply could conceivably interfere with the engagement of bacterial DNA with these PRR.

Of the MAPK signalling molecules upstream of inflammatory transcriptional responses, the Δ*ply* strain induced more ERK and, in particular, p38 phosphorylation, but had little effects on JNK phosphorylation compared to wild-type. ERK is stimulated by lectins, growth factors, and calcium signalling, whereas p38 is stimulated by TLRs, IL1β, and TNF. This is likely to mean greater responses to external PRR signalling, possibly TLR2, after exposure to Δ*ply.*

In the mouse pneumonia model, while there were clear anti-inflammatory effects of Ply at 4 hours, by 24 hours there was significantly more neutrophil infiltrate and corollary albumin leak after wild-type infection. This may reflect the persistence of wild-type bacteria or the pore forming pro-inflammatory effects of Ply may be becoming evident at this later timepoint.

TNF is the quickest responder of the pro-inflammatory cytokines, which may explain why transcriptional inhibition of release by Ply *in vivo* may most easily be seen with TNF compared to IL6. Unlike MDM, IL1β levels were also reduced in response to the Δ*ply* strain during lung infection. This may be because of increased Ply liberation in the context of other host defence mechanisms such as antibacterial peptides, but also may reflect the interplay between macrophages and epithelial cells being key for the two step process required for IL1β secretion.

Interestingly in lung homogenate the differences in cytokine responses between the Δ*ply* and wild-type strains were not so clear. The process of obtaining lung homogenates means that the tissues involved include alveolar and parenchymal cells, but also includes cells in the vasculature including circulating immune cells. Compared to BALF, TNF levels were lower in lung homogenate, whereas IL1β responses were much greater, and IL6 of a similar magnitude. IL1β levels were raised after infection with Δ*ply* infection suggesting that the pro-inflammatory effects in the alveolus may cause enough of a stimulus to induce IL1β without requiring the pore-forming functions of Ply. IL6 levels were greater after infection with wild-type, which is at odds with the other cytokine data.

Overall, the data show that Ply inhibits inflammation when live bacteria are incubated with MDM, and has similar effects in a mouse pneumonia model particularly in respect to BALF TNF levels.

8.2.2 Exploration of mechanisms underpinning the anti-inflammatory effects of pneumolysin

To investigate the possible mechanisms by which Ply may exert its anti-inflammatory effects, I investigated bacterial and cellular mechanisms using the *in vitro* model, and investigated the downstream sequelae in the mouse pneumonia model.

The expression of non-haemolytic Ply by *S. pneumoniae* induced more TNF and IL6 from MDM than wild-type bacteria but less than Ply deficient strains, suggesting that Ply inhibition of macrophage inflammation is partially mediated by pore formation. This would suggest that insertion into the cell membrane is key to triggering the inhibitory effects on inflammation, with a more obvious effect once pores are formed.

Opsonisation of bacteria, which facilitates more rapid phagocytosis, largely reduced inflammatory cytokine release, indicating that external PRR are probably more responsible for induction of pro-inflammatory cytokines than phagolysosomal and cytosolic PRR. However, inhibition of phagocytosis with cytochalasin D had divergent effects on the inflammatory response to the two strains; it increased the response to wild-type and decreased the response to Δ*ply*, with the differences between the strains largely abolished in the presence of cytochalasin D. Genome wide transcriptional responses confirmed that the difference in gene expression was reduced between the two strains in the presence of cytochalasin D, and in particular that differences between inflammatory cytokines were abrogated. This suggests that the anti-inflammatory effects of Ply are dependent on bacterial phagocytosis.

Although the wild-type bacteria, but not the Δ*ply* strain, induced nuclear condensation reflecting Ply's ability to cause apoptosis (Marriott, Ali et al. 2004), these differences were

not evident at 6 hours. Hence the inflammation dampening effects of Ply were not due to downstream effects of apoptosis. This was confirmed when inhibition of all caspases with ZVAD FMK made little difference to inflammatory cytokine release, in contrast to Littman *et al* (Littman, Albiger et al. 2009). Inhibition of caspase-1, which functions downstream of inflammasome activation, also made little difference to cytokine release. This is surprising as Ply is known to activate the inflammasome after pore-formation; however these experiments involved relatively early timepoints and this may be before the IL1β response is evident.

As TLR4 is thought to be activated by Ply (Malley, Henneke et al. 2003), and TLR4 acts via different adaptors proteins and signalling pathways when situated on the phagolysosome compared to cell surface, I investigated IRF3 translocation which occurs downstream of endosomal TLR4 activation, and subsequent engagement with TRIF and TRAM (Newton and Dixit 2012). At 1 hour there was more IRF3 activation by wild-type than Δ*ply,* though this was similar by 2 hours. This suggested that Ply might indeed activate TLR4 (or TLR3) directly, and that this might cause inhibition of pro-inflammatory pathways. However inhibition of TBK1, an adaptor protein that is activated by lysosomal TLR4, reduced IFN-dependent responses but did not affect inflammatory cytokine release. Similarly co-stimulation of TLR3 did not reduce the inflammatory cytokine responses to bacteria. This suggests that while IRF3 activation may be induced by Ply, this does not have a downstream inhibitory effect on pro-inflammatory cytokine release. This may be due to alternative mechanisms by which IRF3 is stimulated, e.g. cytosolic DNA sensors, being affected by TBK1 inhibition, rather than TLR4.

As the pore-forming effects partially affected inflammatory cytokine release, I assessed the effects of insertion of Ply into the cell membrane. As both haemolytic and non-haemolytic Ply inserts into cholesterol-containing membranes to cause membrane depolarisation very quickly, this may be the mechanism mediating the inhibitory effects of Ply on pro-inflammatory responses. Voltage-gated calcium channels are activated within minutes of Ply inserting into a cell membrane (Iliev, Djannatien et al. 2006), and their blockade attenuates

calcium influx and consequent actin polymerisation responses to Ply. However, inhibition of voltage gated calcium channels did not increase inflammatory cytokine responses to wild-type strains. Rather, it decreased IL1β responses to wild-type, suggesting that membrane destabilisation and calcium flux is important in driving Ply-mediated inflammasome activation. Better understanding of whether calcium channels were inhibited would strengthen these negative data.

As TNF responses in bronchoalveolar lavage fluid of mice were diminished after infection with wild-type bacteria compared to Δ*ply*, I assessed the functional effects of TNF during early infection. Blockade of TNF in the bronchoalveolar space abrogated the difference in bacterial counts recovered in lavage fluid between wild-type and Δ*ply*, indicating that TNF plays an important role in protection in early infection. Unexpectedly the effect of TNF blockade was to decrease the virulence of wild-type, rather than as expected increasing the virulence of Δ*ply*. The explanation for this is not clear. In addition, TNF blockade reduced levels of TNF and IL6 in lavage fluid, and TNF, IL1β, and IL6 in lung homogenate, indicating that TNF has important secondary inflammatory effects that promote inflammation. This was confirmed by the direct administration of intranasal TNF to mice, which also induced a neutrophil influx as well as pro-inflammatory cytokine secretion. Clearly the effects of TNF do not directly reflect the complex effects of inflammatory bacterial infection, but the downstream effects of TNF may be to stimulate inflammatory effects from macrophages and epithelial cells that then somewhat replicate the early stages of infection.

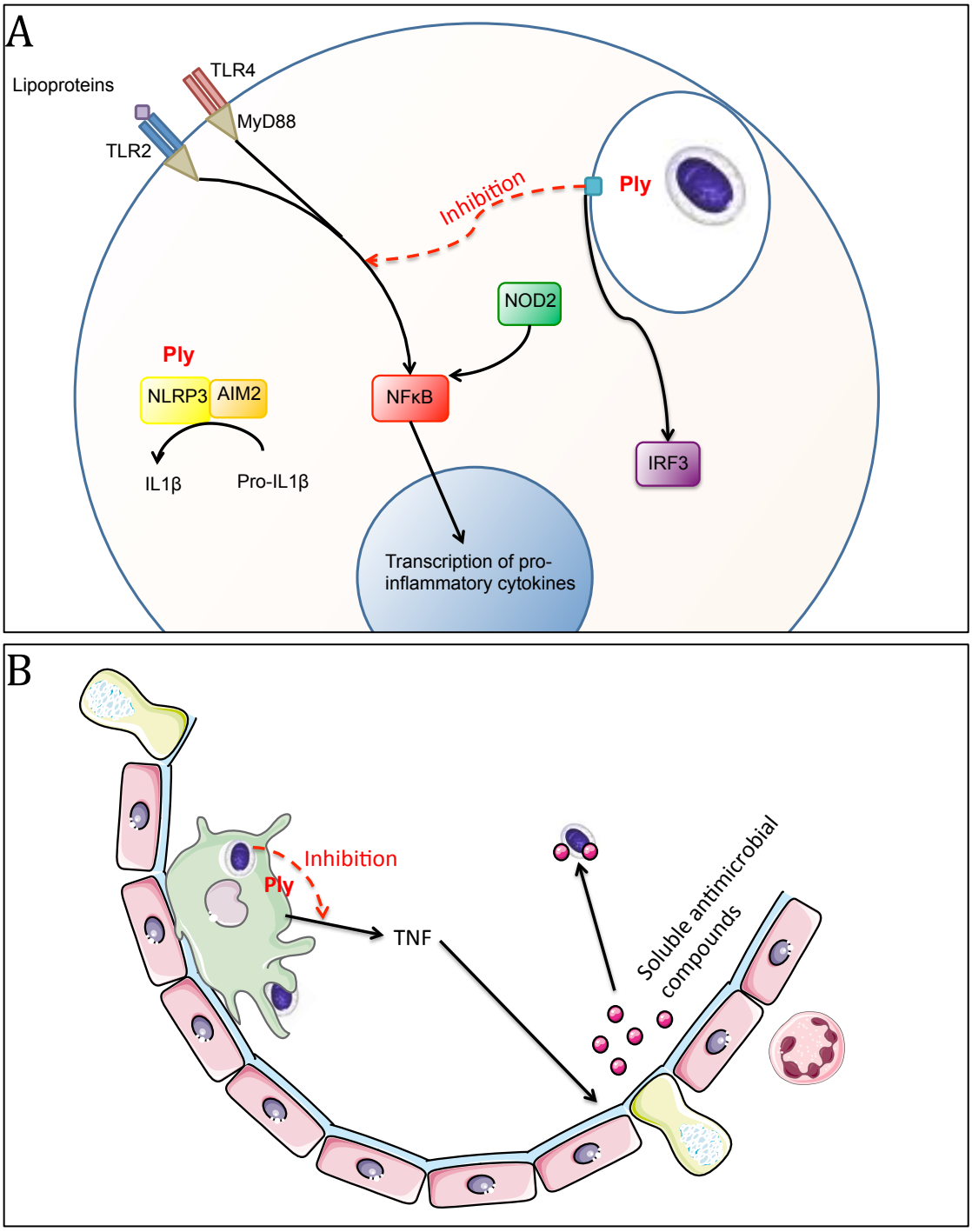

Figure 8.2 Mechanisms of anti-inflammatory effects of Ply

A) The insertion of Ply in the phagolysosomal membrane inhibits inflammatory signalling, possibly downstream of surface TLR activation. This inhibits NFκB mediated transcription of pro-inflammatory cytokines. Ply also induces inflammasome activation and IRF3, though these do not directly impact on early inflammation.

B) Ply inhibits AM release of TNF in early infection in response to *S. pneumoniae.* TNF induces epithelial derived release of soluble antibacterial compounds, which in turn inhibit early bacterial replication.

As TNF was a driver of neutrophil influx, and neutrophil numbers in lavage fluid were similar between strains at 4 hours despite there being $\log_{10}$ more wild-type bacteria than Δ*ply*, an earlier timepoint was examined. This was to ascertain whether the greater TNF secretion Δ*ply* induced caused a brisker neutrophil influx that allowed more rapid clearance of bacteria. Indeed, at 2 hours there was already more rapid bacterial clearance of Δ*ply*, along with a significant neutrophil infiltrate, suggesting that the elevated TNF levels did contribute to quicker leucocyte recruitment. To confirm the role of neutrophils in early bacterial clearance, 4 hour experiments were repeated in neutrophil depleted mice. After neutrophil depletion the difference in virulence between the 2 strains was preserved, indicating that at this early timepoint the differences in neutrophil numbers do not explain the difference in bacterial clearance. Interestingly there was greater TNF and IL6 release in the absence of neutrophils, indicating that without increased phagocytic capacity, pro-inflammatory signalling was increased. This may mean simply that macrophages were being overwhelmed, causing them to send more 'help' signals, and could also mean that non-cellular defence mechanisms were more upregulated in response to the increased cytokine secretion.

Other potential downstream effects of TNF that could promote host defence include activating macrophages to increase phagocytic and/or killing capacity. However TNF administration did not improve MDM mediated *S. pneumoniae* killing *in vitro*. Whilst *in vitro,* mouse lavage fluid recovered from mice after administration of TNF was less able to support TIGR4 growth in comparison to PBS treated mice. This suggests that non-cellular mechanisms are upregulated by TNF that may account for host defence improvements early infection. This may include soluble antimicrobial compounds, such as defensins or lactoferrin.

Overall, my data show that Ply inhibits early macrophage-dependent inflammatory responses to *S. pneumoniae* by phagocytosis dependent mechanism(s), and partially due to its pore-forming abilities. This inhibition of TNF secretion in the bronchoalveolar compartment seems to reduce the efficacy of secreted antibacterial factors that would otherwise usually

inhibit bacterial growth during early lung infection. Hence Ply contributes to virulence by inhibiting inflammation-dependent mucosal soluble immune mechanisms (figure 8.2).

8.2.3 Summary

Understanding how Ply inhibits inflammatory responses, and dissection of the cellular mechanisms could have implications beyond that of understanding the pathogenesis of *S. pneumoniae*. Anti-inflammatory treatments with fewer side effects are needed for a multitude of chronic diseases, and the ability to selectively inhibit inflammatory pathways in phagocytes could be an attractive therapeutic strategy.

Pore forming toxins are relatively common among bacteria, and are known to cause a variety of different functions. Several aid immune evasion by causing death of immune cells. Group A Streptococci (i.e. *Streptococcus pyogenes*), group B Streptococci (*Streptococcus agalectiae*), *Staphylococcus aureus,* and *Mycobacterium tuberculosis* possess toxins (streptolysin O, β-haemolysin, α-toxin, and ESAT-6 respectively) that induce programmed cell death (Los, Randis et al. 2013), whereas streptolysin S from group B *Streptococci* causes direct neutrophil toxicity. Many of the toxins are also described to induce barrier dysfunction, which allows bacterial invasion and dissemination into deeper tissues. While this causes host damage, and in some bacteria allows them to access their preferred ecological niche, *S. pneumoniae*'s preferred home is the nasopharynx. This is easily accessed without invasion, and inducing host cell damage may be counter-productive as this initiates and/or amplifies host innate immune responses. Innate immune signalling is important in protection from invasive pneumococcal disease. The data presented in this thesis shows that *S. pneumoniae* possesses anti-inflammatory properties that allow bacterial replication, and so allows bacterial dissemination. In evolutionary terms, this would allow horizontal transmission from the nasopharynx, but has the unintended effect of increasing bacterial replication at other body sites and so increasing pathogenicity.

Previous studies have indicated that Ply is important in virulence and ascribed pleiotropic functions that promote disease. Many of these functions are pro-inflammatory, and while they explain how Ply contributes to the negative consequences of infection, they don't explain why Ply is a ubiquitous *S. pneumoniae* virulence factor. The data presented in this thesis suggests that Ply has anti-inflammatory properties during early infection with downstream consequences for epithelial innate immunity, and this may explain its persistence in the majority of *S. pneumoniae* genomes.

8.3 Limitations

The main limitations of the data presented in this thesis are the inherent weaknesses of the models used. *In vitro* cell culture work is useful for teasing out cell-specific responses and cellular mechanisms but can miss the complexities of cell-cell interactions and may not be physiologically relevant as it cannot replicate how organs function; for example cell culture models of interactions between macrophages and respiratory epithelial immune mechanisms such as cilia and antimicrobial peptides have not yet been properly developed. Largely, primary cells from healthy volunteers were used, which helps account for the heterogeneity in human responses and that primary cells are less likely to have changed the way they interact with pathogens. However, the inherent variety of responses for primary cells meant that finding significant consistent differences between conditions was sometimes difficult.

Murine models are useful when trying to model disease states, but *S. pneumoniae* is not a natural coloniser or pathogen of mice or rats, suggesting that there are important differences in the ecological niches explored such as the nasopharynx and lungs. In addition it is likely that there are significant differences in how both the innate and adaptive immune of mice respond to *S. pneumoniae* compared to humans. Despite this, the introduction of bacteria into the respiratory tract of mice does induce a neutrophil infiltrate and consolidation, as well as causing bacteraemia and eventually death, which is a similar pattern to severe human pneumonia. Obtaining data from the rat sepsis model was made difficult by the rapid clearance of *S. pneumoniae* after intravenous inoculation, especially when non-replicating bacteria were used to overcome differences in bacterial uptake due to the capsule. As a result very high inocula were necessary to generate an inflammatory response, and even then there was only a relatively narrow window of effect.

The use of isogenic deficient mutants is an advantage in that it ensures that the role of specific bacterial components can be studied in the context of a whole bacterium rather than purified components, which are often contaminated. However, unexpected effects of these

mutations may affect the interactions studied. The antibiotic resistance cassette may exert a burden that affects bacterial growth, and the lack of capsule or Ply could result in compensatory gene expression that may affect the interaction between host and bacteria and confound the data obtained.

8.4 Future Work

The data in this thesis points towards several conclusions, but more work is necessary to support these conclusions. In addition, some intriguing points came up that warrant further investigation.

To improve the link between the *in vitro* and *in vivo* data, I carried out preliminary work on a neutrophil migration model, where I was investigating whether the pro-inflammatory cytokine release of MDM had functional correlates in increasing human neutrophil migration across an epithelial layer seeded onto transwells. This work needed more time to develop fully, and ideally would incorporate a dual layer of endothelial and epithelial cells to mimic the alveolar interface with blood vessels. Similarly I had carried out preliminary studies on mouse lung slices where whole mouse lungs were sliced and placed in tissue culture wells but maintaining a complex mix of cell types and some tissue structure. Ideally this work would be extended to human lung biopsy cores to mimic complex human tissue responses to *S. pneumoniae*. Potentially *ex vivo* human lungs that were not usable for transplant could be a more advanced model for lung infection.

The mechanism by which capsule exerts its pro-inflammatory effects still need defining. The effect of capsule in its structured form needs exploring, perhaps by layering capsular material on inert beads, as 3 dimensional recognition of capsule may trigger PRR when a suspension does not. If contamination was possible to eradicate, the serial addition of other bacterial components could identify how capsule modifies interaction with other virulence factors. It is also possible that some of the methods I used did not completely eliminate possible mechanisms, i.e. there are many PRR belonging to the lectin and scavenger groups that have not been fully explored, which may not signal via Syk or be inhibited by dextran respectively. There are also other classes of PRR that could conceivably recognise capsular polysaccharide. Immunopreciptation experiments with macrophages and labelled capsular polysaccharide (in the context of live bacteria) may allow greater exploration of other receptors that

recognise capsule, and then phosphoproteomic approaches could be used to understand which signalling molecules are activated to further explore the mechanisms underpinning the pro-inflammatory effects of capsule.

The differences between strains within the same serotype also merit exploration. Significant differences would lend support to non-capsular factors being the dominant explanation of variation in inflammation. These data could also be correlated with *in vivo* differences in inflammation between serotypes and capsule switch strains.

The murine Ply data indicated that TNF release increase non-cellular mechanisms that limit bacterial replication. Protein expression in lavage fluid and/or mRNA of lung tissue would be useful in identifying the specific components that are upregulated in response to TNF. The identified elements could then be tested to establish if they effectively inhibit bacterial growth, so confirming one mechanism by which Ply contributes to virulence.

The Ply data from the microarray pointed to important differences between wild-type and Δ*ply* that I did not get the chance to follow up. Some of the differences involved IL12, which is important in the generation of Th1 responses, suggesting that Ply may play a role in inhibiting the adaptive immune response as well as the innate. In addition IFN responses were much increased in response to Δ*ply*, and exploring the mechanisms by which this occur would also be interesting.

Further work is also required to establish the molecular mechanism by which Ply exerts these effects. This could be carried out by creating mutants where Ply is expressed and produced but does not insert into cell membranes. The effect of Ply within the phagolysosome on *S. pneumoniae* needs exploring, as one hypothesis that may explain the findings in the thesis could be that Ply modifies bacterial components so that they have reduced affinity for phagolysosomal or cytosolic PRR. From the host perspective, a phosphoproteomic approach may establish key cell signalling differences between wild-type and Δ*ply*, to further examine which host cell pathways are differentially activated. If the host

pathways involved were identified, this may allow therapeutic anti-inflammatory manipulation, which could be useful over a spectrum of inflammatory disorders.

In terms of larger scale investigations of *S. pneumoniae*, and the importance of inflammation in disease, I think multiple important gaps bear more detailed investigation:

A fuller understanding of the place of inflammation in disease pathogenesis is required. This should include both bacterial components, but also host elements that were not examined during the course of this thesis. This includes the interplay between innate and adaptive responses, for example how inflammation affects the development of mature T cells and antibodies, the role of innate-like immune cells, as well as *in vivo* examination of soluble components of the host immune response. In terms of more clinically applicable elements, I think more time and money could be spent investigating how inflammation is affected in chronic disease states such as COPD and bronchiectasis, and potentially expanded to the effect of age in general, and how this impacts on morbidity and mortality. This could be extended to further disease categories such as meningitis and septic shock, and also how inflammation impacts on nasopharyngeal colonisation.

8.5 Summary

Streptococcus pneumoniae is an important pathogen, and the host inflammatory response is important in both preventing disease and causing collateral host tissue damage. This thesis presents data that allow further understanding of how specific virulence factors affect the inflammatory response.

The extracellular capsule increases the inflammatory response of human monocyte derived macrophages, as well as in a mouse pneumonia model. While the capsular polysaccharide itself does not induce inflammation, it appears to modify interactions between host cells and other bacterial components. These effects are not dependent on phagocytosis, TLR2, MAPK, NFκB, or recognition by Fc receptors, lectins, and scavenger receptors. More signalling pathways appear to be stimulated by unencapsulated bacteria, possibly including some inhibitory signals.

Cytosolic pneumolysin inhibits inflammatory responses in human monocyte derived macrophages and in the bronchoalveolar compartment of mice. This is dependent on bacterial uptake and partially on pore-forming function. While pneumolysin induces apoptosis, caspase inhibition does not affect the inflammatory response. In mice, early TNF release in particular is inhibited by pneumolysin. Inhibition of TNF release reduces non-cellular host defence factors, allowing more bacterial replication, and so increased virulence.

9 References

Abdullah, Z. and P. A. Knolle (2014). "Scaling of immune responses against intracellular bacterial infection." The EMBO journal **33**(20): 2283-2294.

Akahori, Y, T. Miyasaka, M. Toyama, I. Matsumoto, A. Miyahara, T. Zong, K. Ishii, Y. Kinjo, Y. Miyazaki, S. Saijo, Y. Iwakura and K. Kawakami (2016). "Dectin-2-dependent in host defence in mice infected with serotype 3 *Streptococcus pneumoniae*." BMC Immunology **17:**1.

Albiger, B., S. Dahlberg, A. Sandgren, F. Wartha, K. Beiter, H. Katsuragi, S. Akira, S. Normark and B. Henriques-Normark (2007). "Toll-like receptor 9 acts at an early stage in host defence against pneumococcal infection." Cellular Microbiology **9**(3): 633-644.

Albiger, B., A. Sandgren, H. Katsuragi, U. Meyer-Hoffert, K. Beiter, F. Wartha, M. Hornef, S. Normark and B. H. Normark (2005). "Myeloid differentiation factor 88-dependent signalling controls bacterial growth during colonization and systemic pneumococcal disease in mice." Cellular Microbiology **7**(11): 1603-1615.

Albrich, W., S. Madhi, P. Adrian, N van Niekerk, T Mareletsi, C Cutland, M Wong, M Khoosal, A Karstaedt, P Zhao, A Deatly, M Sidhu, K Jansen, K Klugman (2012). "Use of a rapid test of pneumococcal colonization density to diagnose pneumococcal pneumonia." Clin Infect Dis **54**:601–609.

Alsina, L., E. Israelsson, M. C. Altman, K. K. Dang, P. Ghandil, L. Israel, H. von Bernuth, N. Baldwin, H. Qin, Z. Jin, R. Banchereau, E. Anguiano, A. Ionan, L. Abel, A. Puel, C. Picard, V. Pascual, J. L. Casanova and D. Chaussabel (2014). "A narrow repertoire of transcriptional modules responsive to pyogenic bacteria is impaired in patients carrying loss-of-function mutations in MYD88 or IRAK4." Nat Immunol **15**(12): 1134-1142.

Andre, G. O., W. R. Politano, S. Mirza, T. R. Converso, L. F. Ferraz, L. C. Leite and M. Darrieux (2015). "Combined effects of lactoferrin and lysozyme on *Streptococcus pneumoniae* killing." Microb Pathog **89**: 7-17.

Arango Duque, G. and A. Descoteaux (2014). "Macrophage cytokines: involvement in immunity and infectious diseases." Front Immunol **5**: 491.

Arredouani, M., Z. Yang, Y. Ning, G. Qin, R. Soininen, K. Tryggvason and L. Kobzik (2004). "The scavenger receptor MARCO is required for lung defense against pneumococcal pneumonia and inhaled particles." The Journal of experimental medicine **200**(2): 267-272.

Arredouani, M. S., A. Palecanda, H. Koziel, Y. C. Huang, A. Imrich, T. H. Sulahian, Y. Y. Ning, Z. Yang, T. Pikkarainen, M. Sankala, S. O. Vargas, M. Takeya, K. Tryggvason and L. Kobzik (2005). "MARCO is the major binding receptor for unopsonized particles and bacteria on human alveolar macrophages." Journal of immunology **175**(9): 6058-6064.

Arredouani, M. S., Z. Yang, A. Imrich, Y. Ning, G. Qin and L. Kobzik (2006). "The macrophage scavenger receptor SR-AI/II and lung defense against pneumococci and particles." American journal of respiratory cell and molecular biology **35**(4): 474-478.

Asmat, T. M., V. Agarwal, M. Saleh and S. Hammerschmidt (2014). "Endocytosis of *Streptococcus pneumoniae* via the polymeric immunoglobulin receptor of epithelial cells relies on clathrin and caveolin dependent mechanisms." International journal of medical microbiology : IJMM **304**(8): 1233-1246.

Barocchi, M. A., S. Censini and R. Rappuoli (2007). "Vaccines in the era of genomics: the pneumococcal challenge." Vaccine **25**(16): 2963-2973.

Barocchi, M. A., J. Ries, X. Zogaj, C. Hemsley, B. Albiger, A. Kanth, S. Dahlberg, J. Fernebro, M. Moschioni, V. Masignani, K. Hultenby, A. R. Taddei, K. Beiter, F. Wartha, A. von Euler, A. Covacci, D. W. Holden, S. Normark, R. Rappuoli and B. Henriques-Normark (2006). "A

pneumococcal pilus influences virulence and host inflammatory responses." Proceedings of the National Academy of Sciences of the United States of America **103**(8): 2857-2862.

Basavanna, S., S. Khandavilli, J. Yuste, J. M. Cohen, A. H. Hosie, A. J. Webb, G. H. Thomas and J. S. Brown (2009). "Screening of *Streptococcus pneumoniae* ABC transporter mutants demonstrates that LivJHMGF, a branched-chain amino acid ABC transporter, is necessary for disease pathogenesis." Infection and immunity **77**(8): 3412-3423.

Beisswenger, C., E. S. Lysenko and J. N. Weiser (2009). "Early bacterial colonization induces toll-like receptor-dependent transforming growth factor beta signaling in the epithelium." Infection and immunity **77**(5): 2212-2220.

Beiter, K., F. Wartha, R. Hurwitz, S. Normark, A. Zychlinsky and B. Henriques-Normark (2008). "The capsule sensitizes *Streptococcus pneumoniae* to alpha-defensins human neutrophil proteins 1 to 3." Infect Immun **76**(8): 3710-3716.

Benton, K. A., J. L. VanCott and D. E. Briles (1998). "Role of tumor necrosis factor alpha in the host response of mice to bacteremia caused by pneumolysin- deficient *Streptococcus pneumoniae*." Infection and immunity **66** (2):839 – 842.

Berenson, C. S., R. L. Kruzel, C. T. Wrona, M. J. Mammen and S. Sethi (2015). "Impaired Innate COPD Alveolar Macrophage Responses and Toll-Like Receptor-9 Polymorphisms." PLoS One **10**(9): e0134209.

Berry, A. M., J. Yother, D. E. Briles, D. Hansman and J. C. Paton (1989). "Reduced virulence of a defined pneumolysin-negative mutant of *Streptococcus pneumoniae*." Infection and immunity **57**(7): 2037-2042.

Bewick, T., C. Sheppard, S. Greenwood, M. Slack, C. Trotter, R. George and W. S. Lim (2012). "Serotype prevalence in adults hospitalised with pneumococcal non-invasive community-acquired pneumonia." Thorax **67**(6): 540-545.

Bewley, M. A., M. Naughton, J. Preston, A. Mitchell, A. Holmes, H. M. Marriott, R. C. Read, T. J. Mitchell, M. K. Whyte and D. H. Dockrell (2014). "Pneumolysin activates macrophage lysosomal membrane permeabilization and executes apoptosis by distinct mechanisms without membrane pore formation." mBio **5**(5): e01710-01714.

Bogaert, D., R. De Groot and P. W. Hermans (2004). "*Streptococcus pneumoniae* colonisation: the key to pneumococcal disease." The Lancet Infectious Diseases **4**(3): 144-154.

Bonten, M. J., S. M. Huijts, M. Bolkenbaas, C. Webber, S. Patterson, S. Gault, C. H. van Werkhoven, A. M. van Deursen, E. A. Sanders, T. J. Verheij, M. Patton, A. McDonough, A. Moradoghli-Haftvani, H. Smith, T. Mellelieu, M. W. Pride, G. Crowther, B. Schmoele-Thoma, D. A. Scott, K. U. Jansen, R. Lobatto, B. Oosterman, N. Visser, E. Caspers, A. Smorenburg, E. A. Emini, W. C. Gruber and D. E. Grobbee (2015). "Polysaccharide conjugate vaccine against pneumococcal pneumonia in adults." N Engl J Med **372**(12): 1114-1125.

Bootsma, H. J., M. Egmont-Petersen and P. W. M. Hermans (2007). "Analysis of the *in vitro* transcriptional response of human pharyngeal epithelial cells to adherent *Streptoccocus pneumoniae*: evidence for a distinct response to encapsulated strains." Infect Immun **75**(11):7489-99.

Bowdish, D. M., K. Sakamoto, M. J. Kim, M. Kroos, S. Mukhopadhyay, C. A. Leifer, K. Tryggvason, S. Gordon and D. G. Russell (2009). "MARCO, TLR2, and CD14 are required for macrophage cytokine responses to mycobacterial trehalose dimycolate and Mycobacterium tuberculosis." PLoS pathogens **5**(6): e1000474.

Brady, A. M., J. J. Calix, J. Yu, K. A. Geno, G. R. Cutter and M. H. Nahm (2014). "Low invasiveness of pneumococcal serotype 11A is linked to ficolin-2 recognition of O-acetylated capsule epitopes and lectin complement pathway activation." The Journal of infectious diseases **210**(7): 1155-1165.

Branger, J., S. Knapp, S. Weijer, J. C. Leemans, J. M. Pater, P. Speelman, S. Florquin and T. van der Poll (2004). "Role of Toll-like receptor 4 in gram-positive and gram-negative pneumonia in mice." Infect Immun **72**(2): 788-794.

Braun, J. S., R. Novak, G. Gao, P. J. Murray and J. L. Shenep (1999). "Pneumolysin, a protein toxin of *Streptococcus pneumoniae*, induces nitric oxide production from macrophages." Infection and immunity **67**(8): 3750-3756.

Brealey, D., S. Karyampudy, T. S. Jacques, M. Novelli, R. Stidwill, V. Taylor, R. T. Smolenski and M. Singer (2003). "Mitochondrial dysfunction in a long-term rodent model of sepsis and organ failure." Am J Physiol Integr Comp Physiol **286**: R491-7.

Brouer K., A. Foroushani, M. Laird, C. Chen, A Sribnaia, R. Lo, G. Winsor, R. Hancock, F. Brinkman and D. Lynn (2013). "InnateDB: systems biology of innate immunity and beyond - recent updates and continuing curation." Nuc Acids Res **41**: D1228-D1233.

Brown, J. S., T. Hussell, S. M. Gilliland, D. W. Holden, J. C. Paton, M. R. Ehrenstein, M. J. Walport and M. Botto (2002). "The classical pathway is the dominant complement pathway required for innate immunity to *Streptococcus pneumoniae* infection in mice." Proceedings of the National Academy of Sciences of the United States of America **99**(26): 16969-16974.

Brueggemann, A. B., D. T. Griffiths, E. Meats, T. Peto, D. W. Crook and B. G. Spratt (2003). "Clonal relationships between invasive and carriage *Streptococcus pneumoniae* and serotype- and clone-specific differences in invasive disease potential." J Infect Dis **187**(9): 1424-1432.

Burgos, J., M. Lujan, M. N. Larrosa, D. Fontanals, G. Bermudo, A. M. Planes, M. Puig, J. Rello, V. Falco and A. Pahissa (2014). "Risk factors for respiratory failure in pneumococcal pneumonia: the importance of pneumococcal serotypes." Eur Respir J **43**(2): 545-553.

Burns, T., M. Abadi and L. A. Pirofski (2005). "Modulation of the lung inflammatory response to serotype 8 pneumococcal infection by a human immunoglobulin m monoclonal antibody to serotype 8 capsular polysaccharide." Infection and immunity **73**(8): 4530-4538.

Calbo, E. and J. Garau (2010). "Of mice and men: innate immunity in pneumococcal pneumonia." International Journal of Antimicrobial Agents **35**(2): 107-113.

Camberlein, E., J. M. Cohen, R. Jose, C. J. Hyams, R. Callard, S. Chimalapati, J. Yuste, L. A. Edwards, H. Marshall, N. van Rooijen, M. Noursadeghi and J. S. Brown (2015). "Importance of bacterial replication and alveolar macrophage-independent clearance mechanisms during early lung infection with *Streptococcus pneumoniae*." Infect Immun **83**(3): 1181-1189.

Canton, J., D. Neculai and S. Grinstein (2013). "Scavenger receptors in homeostasis and immunity." Nature reviews. Immunology **13**(9): 621-634.

Cao, J., D. Wang, F. Xu, Y. Gong, H. Wang, Z. Song, D. Li, H. Zhang, L. Zhang, Y. Xia, H. Xu, X. Lai, S. Lin, X. Zhang, G. Ren, Y. Dai and Y. Yin (2014). "Activation of IL-27 signalling promotes development of postinfluenza pneumococcal pneumonia." EMBO Mol Med 6(1): 120-140.

Carratalà, J., A. Marron, A. Fernández-Sevilla J. Liñares and F. Gudiol (1997)**. "**Treatment of Penicillin-Resistant Pneumococcal Bacteremia in Neutropenic Patients with Cancer."Clin Infect Dis **24** (2):148-152.

Cerutti, A., M. Cols and I. Puga (2013). "Marginal zone B cells: virtues of innate-like antibody-producing lymphocytes." Nat Rev Immunol **13**(2): 118-132.

Chain, B., H. Bowen, J. Hammond J, W. Posch, J. Rasaiyaah, J. Tsang J and M. Noursadeghi (2010) "Error, reproducibility and sensitivity: a pipeline for data processing of Agilent oligonucleotide expression arrays." BMC Bioinformatics **11**: 344.

Chapman, S. J., C. C. Khor, F. O. Vannberg, A. Frodsham, A. Walley, N. A. Maskell, C. W. Davies, S. Segal, C. E. Moore, S. H. Gillespie, P. Denny, N. P. Day, D. W. Crook, R. J. Davies and A. V. Hill

(2007). "IkappaB genetic polymorphisms and invasive pneumococcal disease." American journal of respiratory and critical care medicine **176**(2): 181-187.

Chen, L., S. Guo, L. Wu, C. Hao, W. Xu and J. Zhang (2014). "Effects of recombinant IL-17F intranasal inoculation against *Streptococcus pneumoniae* infection in a murine model." Biotechnology and applied biochemistry **62**(3):393-400.

Chimalapati, S., J. M. Cohen, E. Camberlein, N. MacDonald, C. Durmort, H. Baxendale, C. de Vogel, A. van Belkum and J. S. Brown (2011). "Infection with conditionally virulent *Streptococcus pneumoniae* Δ*pab* strains induces antibody to conserved protein antigens but does not protect against systemic infection with heterologous strains." Infect Immun **79**(12): 4965-76.

Chimalapati, S., J. M. Cohen, E. Camberlein, C. Durmort, T. Vernet, P. W. Hermans, T. Mitchell and J. S. Brown (2012). "Effects of deletion of the *Streptococcus pneumoniae* lipoprotein diacylglyceryl transferase gene lgt on ABC transporter function and on growth in vivo." PloS one **7**(7): e41393.

Choi, G., J. J. Hofstra, J. J. Roelofs, A. W. Rijneveld, P. Bresser, J. S. van der Zee, S. Florquin, T. van der Poll, M. Levi and M. J. Schultz (2008). "Antithrombin inhibits bronchoalveolar activation of coagulation and limits lung injury during *Streptococcus pneumoniae* pneumonia in rats." Crit Care Med **36**(1): 204-210.

Clarke, T. B., K. M. Davis, E. S. Lysenko, A. Y. Zhou, Y. Yu and J. N. Weiser (2010). "Recognition of peptidoglycan from the microbiota by Nod1 enhances systemic innate immunity." Nature medicine **16**(2): 228-231.

Clarke, T. B., N. Francella, A. Huegel and J. N. Weiser (2011). "Invasive bacterial pathogens exploit TLR-mediated downregulation of tight junction components to facilitate translocation across the epithelium." Cell host & microbe **9**(5): 404-414.

Clement, C. G., S. E. Evans, C. M. Evans, D. Hawke, R. Kobayashi, P. R. Reynolds, S. J. Moghaddam, B. L. Scott, E. Melicoff, R. Adachi, B. F. Dickey and M. J. Tuvim (2008). "Stimulation of lung innate immunity protects against lethal pneumococcal pneumonia in mice." Am J Respir Crit Care Med **177**(12): 1322-1330.

Coffey, T. J., M. Daniels, M. C. Enright and B. G. Spratt (1999). "Serotype 14 variants of the Spanish penicillin-resistant serotype 9V clone of *Streptococcus pneumoniae* arose by large recombinational replacements of the cpsA-pbp1a region." Microbiology **145 (Pt 8)**: 2023-2031.

Cohen, J. M., S. Khandavilli, E. Camberlein, C. Hyams, H. E. Baxendale and J. S. Brown (2011). "Protective contributions against invasive *Streptococcus pneumoniae* pneumonia of antibody and Th17-cell responses to nasopharyngeal colonisation." PloS one **6**(10): e25558.

Coller, S. P. and D. M. Paulnock (2001). "Signaling pathways initiated in macrophages after engagement of type A scavenger receptors." Journal of leukocyte biology **70**(1): 142-148.

Coutinho, A. and G. Moller (1973). "B cell mitogenic properties of thymus-independent antigens." Nature: New biology **245**(140): 12-14.

Croucher, N. J., S. R. Harris, C. Fraser, M. A. Quail, J. Burton, M. van der Linden, L. McGee, A. von Gottberg, J. H. Song, K. S. Ko, B. Pichon, S. Baker, C. M. Parry, L. M. Lambertsen, D. Shahinas, D. R. Pillai, T. J. Mitchell, G. Dougan, A. Tomasz, K. P. Klugman, J. Parkhill, W. P. Hanage and S. D. Bentley (2011). "Rapid pneumococcal evolution in response to clinical interventions." Science **331**(6016): 430-434.

Cundell, D. R., N. P. Gerard, C. Gerard, I. Idanpaan-Heikkila and E. I. Tuomanen (1995). "*Streptococcus pneumoniae* anchor to activated human cells by the receptor for platelet-activating factor." Nature **377**(6548): 435-438.

Cundell, D. R., J. N. Weiser, J. Shen, A. Young and E. I. Tuomanen (1995). "Relationship between colonial morphology and adherence of *Streptococcus pneumoniae*." Infection and immunity **63**(3): 757-761.

Daniels, C., P. Rogers, C. Shelton (2016). "A review of pneumococcal vaccines: current polysaccharide recommendations and future protein antigens." J Pediatr Pharmacol Ther **21**(1): 27-35.

Das, R., M. I. LaRose, C. B. Hergott, L. Leng, R. Bucala and J. N. Weiser (2014). "Macrophage migration inhibitory factor promotes clearance of pneumococcal colonization." Journal of immunology **193**(2): 764-772.

Dave, S., S. Carmicle, S. Hammerschmidt, M. K. Pangburn and L. S. McDaniel (2004). "Dual roles of PspC, a surface protein of *Streptococcus pneumoniae*, in binding human secretory IgA and factor H." J Immunol **173**(1): 471-477.

Davies, L. C., S. J. Jenkins, J. E. Allen and P. R. Taylor (2013). "Tissue-resident macrophages." Nature Immunol **14**(10): 986-995.

Davis, K. M., H. T. Akinbi, A. J. Standish and J. N. Weiser (2008). "Resistance to mucosal lysozyme compensates for the fitness deficit of peptidoglycan modifications by *Streptococcus pneumoniae*." PLoS pathogens **4**(12): e1000241.

Davis, K. M., S. Nakamura and J. N. Weiser (2011). "Nod2 sensing of lysozyme-digested peptidoglycan promotes macrophage recruitment and clearance of *S. pneumoniae* colonization in mice." The Journal of clinical investigation **121**(9): 3666-3676.

Dempsey, P. W., S. E. Doyle, J. Q. He and G. Cheng (2003). "The signaling adaptors and pathways activated by TNF superfamily." Cytokine Growth Factor Rev **14**(3-4): 193-209.

Dessing, M. C., R. A. Hirst, A. F. de Vos and T. van der Poll (2009). "Role of Toll-like receptors 2 and 4 in pulmonary inflammation and injury induced by pneumolysin in mice." PloS one **4**(11): e7993.

De Vos A. F., M. C. Dessing, A. J. J. Lammers, A. P. N. A. de Porto, S. Florquin, O. J. de Boer, R. de Beer, S. Terpstra, H. J. Bootsma, P. W. Hermans, C. V. Veer and T. van der Poll (2015). The polysaccharide capsule of *Streptococcus pneumoniae* partially impedes MyD88-mediated immunity during pneumonia in mice." PloS one **10**(2): e0118181.

Dixon, B., M. J. Schultz, J. J. Hofstra, D. J. Campbell and J. D. Santamaria (2010). "Nebulized heparin reduces levels of pulmonary coagulation activation in acute lung injury." Crit Care **14**(5): 445.

Dockrell, D. H., H. M. Marriott, L. R. Prince, V. C. Ridger, P. G. Ince, P. G. Hellewell and M. K. Whyte (2003). "Alveolar macrophage apoptosis contributes to pneumococcal clearance in a resolving model of pulmonary infection." Journal of immunology **171**(10): 5380-5388.

Dogan, S., Q. Zhang, A. C. Pridmore, T. J. Mitchell, A. Finn and C. Murdoch (2011). "Pneumolysin-induced CXCL8 production by nasopharyngeal epithelial cells is dependent on calcium flux and MAPK activation via Toll-like receptor 4." Microbes Infect **13**(1): 65-75.

Donkor, E. S., R. A. Stabler, J. Hinds, R. A. Adegbola, M. Antonio and B. W. Wren (2012). "Comparative phylogenomics of *Streptococcus pneumoniae* isolated from invasive disease and nasopharyngeal carriage from West Africans." BMC genomics **13**: 569.

Dopazo, J., A. Mendoza, J. Herrero, F. Caldara, Y. Humbert, L. Friedli, M. Guerrier, E. Grand-Schenk, C. Gandin, M. de Francesco, A. Polissi, G. Buell, G. Feger, E. Garcia, M. Peitsch and J. F. Garcia-Bustos (2001). "Annotated draft genomic sequence from a *Streptococcus pneumoniae* type 19F clinical isolate." Microb Drug Resist **7**(2): 99-125.

Dorrington, M. G., A. M. Roche, S. E. Chauvin, Z. Tu, K. L. Mossman, J. N. Weiser and D. M. Bowdish (2013). "MARCO is required for TLR2- and Nod2-mediated responses to

Streptococcus pneumoniae and clearance of pneumococcal colonization in the murine nasopharynx." Journal of immunology **190**(1): 250-258.

dos Santos, G., M. A. Kutuzov and K. M. Ridge (2012). "The inflammasome in lung diseases." American journal of physiology. Lung cellular and molecular physiology **303**(8): L627-633.

Drummond, R. A. and G. D. Brown (2013). "Signalling C-type lectins in antimicrobial immunity." PLoS pathogens **9**(7): e1003417.

Eberhardt, A., C. N. Hoyland, D. Vollmer, S. Bisle, R. M. Cleverley, O. Johnsborg, L. S. Havarstein, R. J. Lewis and W. Vollmer (2012). "Attachment of capsular polysaccharide to the cell wall in *Streptococcus pneumoniae*." Microbial drug resistance **18**(3): 240-255.

Ely, E. W., P. F. Laterre, D. C. Angus, J. D. Helterbrand, H. Levy, J. F. Dhainaut, J. L. Vincent, W. L. Macias, G. R. Bernard and P. Investigators (2003). "Drotrecogin alfa (activated) administration across clinically important subgroups of patients with severe sepsis." Crit Care Med **31**(1): 12-19.

Engelhard, D., C. Cordonnier, P. J. Shaw, T. Parkalli, C. Guenther, R. Martino, A. W. Dekker, H. Grant Prentice, A. Gustavsson, W. Nurnberger and P. Ljungman (2002). "Early and late invasive pneumococcal infection following stem cell transplantation: a European Bone Marrow Transplantation survey." B J Haem **117** (2): 444–450.

Engelhard, D., S. Pomeranz, R. Gallily, N. Strauss and E. Tuomanen (1997). "Serotype-related differences in inflammatory response to *Streptococcus pneumoniae* in experimental meningitis." The Journal of infectious diseases **175**(4): 979-982.

Fang, R., K. Tsuchiya, I. Kawamura, Y. Shen, H. Hara, S. Sakai, T. Yamamoto, T. Fernandes-Alnemri, R. Yang, E. Hernandez-Cuellar, S. R. Dewamitta, Y. Xu, H. Qu, E. S. Alnemri and M. Mitsuyama (2011). "Critical roles of ASC inflammasomes in caspase-1 activation and host innate resistance to *Streptococcus pneumoniae* infection." Journal of immunology **187**(9): 4890-4899.

Ferrante, A., B. Rowan-Kelly, J. Paton (1984). "Inhibition of in vitro human lymphocyte response by the pneumococcal toxin pneumolysin." Infect Immun **46**(2):585 9.

Ferreira, D. M. and S. B. Gordon (2015). "Mechanisms causing the inflammatory response to *Streptococcus pneumoniae*." Chapter 20, *Streptococcus pneumoniae*: Molecular mechanisms of host pathogen interactions. ed. Brown, J., S. Hammerschmidt, C. Orihuela. Elsevier.

Fillon, S., K. Soulis, S. Rajasekaran, H. Benedict-Hamilton, J. N. Radin, C. J. Orihuela, K. C. El Kasmi, G. Murti, D. Kaushal, M. W. Gaber, J. R. Weber, P. J. Murray and E. I. Tuomanen (2006). "Platelet-activating factor receptor and innate immunity: uptake of gram-positive bacterial cell wall into host cells and cell-specific pathophysiology." Journal of immunology **177**(9): 6182-6191.

Findlay, E. G. and T. Hussell (2012). "Macrophage-mediated inflammation and disease: A focus on the lung." Mediators Inflamm **2012**: 140937.

Fletcher, M. A., H. J. Schmitt, M. Syrochkina and G. Sylvester (2014). "Pneumococcal empyema and complicated pneumonias: global trends in incidence, prevalence, and serotype epidemiology." Eur J Clin Microbiol Infect Dis **33**(6): 879-910.

Foletta, V. C., D. H. Segal and D. R. Cohen (1998). "Transcriptional regulation in the immune system: all roads lead to AP-1." J Leukoc Biol **63**(2): 139-152.

Gabay, C. and I. Kushner (1999). "Acute-phase proteins and other systemic responses to inflammation." The New England journal of medicine **340**(6): 448-454.

Gadola, S. D., H. T. Moins-Teisserenc, J. Trowsdale, W. L. Gross and V. Cerundolo (2000). "TAP deficiency syndrome." Clinical and experimental immunology **121**(2): 173-178.

Gang, T. B., G. A. Hanley and A. Agrawal (2015). "C-reactive protein protects mice against pneumococcal infection via both phosphocholine-dependent and phosphocholine-independent mechanisms." Infect Immun **83**(5): 1845-1852.

Ganz, T. (2004). "Antimicrobial polypeptides." Journal of leukocyte biology **75**(1): 34-38.

Garcia-Suarez Mdel, M., F. Vazquez and F. J. Mendez (2006). "*Streptococcus pneumoniae* virulence factors and their clinical impact: An update." Enferm Infecc Microbiol Clin **24**(8): 512-517.

Garnier, F., R. Janapatla, E. Charpentier, G. Masson, C. Grélaud, J. Stach, F. Denis and M. Ploy (2007). "Insertion Sequence ***1515*** in the ***ply*** Gene of a Type 1 Clinical Isolate of *Streptococcus pneumoniae* Abolishes Pneumolysin Expression." J Clin Micro **45**(7): 2296-7.

Geijtenbeek, T. B. and S. I. Gringhuis (2009). "Signalling through C-type lectin receptors: shaping immune responses." Nature reviews. Immunology **9**(7): 465-479.

Geldhoff, M., B. B. Mook-Kanamori, M. C. Brouwer, D. Troost, J. C. Leemans, R. A. Flavell, A. Van der Ende, T. Van der Poll and D. Van de Beek (2013). "Inflammasome activation mediates inflammation and outcome in humans and mice with pneumococcal meningitis." BMC infectious diseases **13**(1): 358.

Geldhoff, M., B. B. Mook-Kanamori, M. C. Brouwer, M. Valls Seron, F. Baas, A. van der Ende and D. van de Beek (2013). "Genetic variation in inflammasome genes is associated with outcome in bacterial meningitis." Immunogenetics **65**(1): 9-16.

Gerber, J., T. Bottcher, M. Hahn, A. Siemer, S. Bunkowski and R. Nau (2004). "Increased mortality and spatial memory deficits in TNF-alpha-deficient mice in ceftriaxone-treated experimental pneumococcal meningitis." Neurobiol Dis **16**(1): 133-138.

Gibbs, J., L. Ince, L. Matthews, J. Mei, T. Bell, N. Yang, B. Saer, N. Begley, T. Poolman, M. Pariollaud, S. Farrow, F. DeMayo, T. Hussell, G. S. Worthen, D. Ray and A. Loudon (2014). "An epithelial circadian clock controls pulmonary inflammation and glucocorticoid action." Nature medicine **20**(8): 919-926.

Goldblatt, D., M. Hussain, N. Andrews, L. Ashton, C. Virta, A. Melegaro, R. Pebody, R. George, A. Soininen, J. Edmunds, N. Gay, H. Kayhty and E. Miller (2005). "Antibody responses to nasopharyngeal carriage of *Streptococcus pneumoniae* in adults: a longitudinal household study." The Journal of infectious diseases **192**(3): 387-393.

Gomez, J. C., M. Yamada, J. R. Martin, H. Dang, W. J. Brickey, W. Bergmeier, M. C. Dinauer and C. M. Doerschuk (2015). "Mechanisms of interferon-gamma production by neutrophils and its function during *Streptococcus pneumoniae* pneumonia." Am J Respir Cell Mol Biol **52**(3): 349-364.

Grabenstein J. and K Klugman (2012). "A century of pneumococcal vaccination research in humans." Clin Micr & Infect **18**(5): 15-24.

Gray, C., M. S. Ahmed, A. Mubarak, A. V. Kasbekar, S. Derbyshire, M. S. McCormick, M. K. Mughal, P. S. McNamara, T. Mitchell and Q. Zhang (2014). "Activation of memory Th17 cells by domain 4 pneumolysin in human nasopharynx-associated lymphoid tissue and its association with pneumococcal carriage." Mucosal Immunol **7**(3): 705-717.

Greene, N. G., A. R. Narciso, S. R. Filipe and A. Camilli (2015). "Peptidoglycan Branched Stem Peptides Contribute to *Streptococcus pneumoniae* Virulence by Inhibiting Pneumolysin Release." PLoS Pathog **11**(6): e1004996.

Griffin, M. R., Y. Zhu, M. R. Moore, C. G. Whitney and C. G. Grijalva (2013). "U.S. hospitalizations for pneumonia after a decade of pneumococcal vaccination." N Engl J Med **369**(2): 155-163.

Gringhuis, S. I., J. den Dunnen, M. Litjens, B. van Het Hof, Y. van Kooyk and T. B. Geijtenbeek (2007). "C-type lectin DC-SIGN modulates Toll-like receptor signaling via Raf-1 kinase-dependent acetylation of transcription factor NF-kappaB." Immunity **26**(5): 605-616.

Gwyer Findlay, E., L. Danks, J. Madden, M. M. Cavanagh, K. McNamee, F. McCann, R. J. Snelgrove, S. Shaw, M. Feldmann, P. C. Taylor, N. J. Horwood and T. Hussell (2014). "OX40L blockade is therapeutic in arthritis, despite promoting osteoclastogenesis." Proceedings of the National Academy of Sciences of the United States of America **111**(6): 2289-2294.

Haas W., C. J. Hesje, C. M. Sanfilippo and T. W. Morris (2011). "High proportion of non-typeable *Streptococcus pneumoniae* isolates among sporadic , nonoutbreak causes of bacterial conjunctivitis." Curr Eye Res **36**(12):1078-85.

Hahn, I., A. Klaus, A. K. Janze, K. Steinwede, N. Ding, J. Bohling, C. Brumshagen, H. Serrano, F. Gauthier, J. C. Paton, T. Welte and U. A. Maus (2011). "Cathepsin G and neutrophil elastase play critical and nonredundant roles in lung-protective immunity against *Streptococcus pneumoniae* in mice." Infection and immunity **79**(12): 4893-4901.

Hammerschmidt, S., S. Wolff, A. Hocke, S. Rosseau, E. Muller and M. Rohde (2005). "Illustration of pneumococcal polysaccharide capsule during adherence and invasion of epithelial cells." Infection and immunity **73**(8): 4653-4667.

Hanage, W. P., T. Kaijalainen, E. Herva, A. Saukkoriipi, R. Syrjanen and B. G. Spratt (2005). "Using multilocus sequence data to define the pneumococcus." J Bacteriol **187**(17): 6223-6230.

Hanage, W. P., T. H. Kaijalainen, R. K. Syrjanen, K. Auranen, M. Leinonen, P. H. Makela and B. G. Spratt (2005). "Invasiveness of serotypes and clones of *Streptococcus pneumoniae* among children in Finland." Infect Immun **73**(1): 431-435.

Haraguchi, S., N. K. Day, R. P. Nelson, Jr., P. Emmanuel, J. E. Duplantier, C. S. Christodoulou and R. A. Good (1998). "Interleukin 12 deficiency associated with recurrent infections." Proceedings of the National Academy of Sciences of the United States of America **95**(22): 13125-13129.

Harboe, Z. B., R. W. Thomsen, A. Riis, P. Valentiner-Branth, J. J. Christensen, L. Lambertsen, K. A. Krogfelt, H. B. Konradsen and T. L. Benfield (2009). "Pneumococcal serotypes and mortality following invasive pneumococcal disease: a population-based cohort study." PLoS medicine **6**(5): e1000081.

Havarstein, L. S., G. Coomaraswamy, and D. A. Morrison (1995). "An unmodified heptadecapeptide pheromone induces competence for genetic transformation in *Streptococcus pneumoniae*." Proc Natl Acad Sci U. S. A. **92:**11140–11144

Harvey, R. M., C. E. Hughes, A. W. Paton, C. Trappetti, R. K. Tweten and J. C. Paton (2014). "The impact of pneumolysin on the macrophage response to *Streptococcus pneumoniae* is strain-dependent." PloS one **9**(8): e103625.

Harvey, R. M., A. D. Ogunniyi, A. Y. Chen and J. C. Paton (2011). "Pneumolysin with low hemolytic activity confers an early growth advantage to *Streptococcus pneumoniae* in the blood." Infection and immunity **79**(10): 4122-4130.

Haslett, C (1999). "Granulocyte apoptosis and its role in the resolution and control of lung inflammation." American journal of respiratory and critical care medicine **160**(5 Pt 2): S5-11.

Hathaway, L. J., S. D. Brugger, B. Morand, M. Bangert, J. U. Rotzetter, C. Hauser, W. A. Graber, S. Gore, A. Kadioglu and K. Muhlemann (2012). "Capsule type of *Streptococcus pneumoniae* determines growth phenotype." PLoS Pathog **8**(3): e1002574.

Hausdorff, W. P., J. Bryant, C. Kloek, P. R. Paradiso and G. R. Siber (2000). "The contribution of specific pneumococcal serogroups to different disease manifestations: implications for conjugate vaccine formulation and use, part II." Clin Infect Dis **30**(1): 122-140.

Henrichsen, J. (1995). "Six newly recognized types of *Streptococcus pneumoniae*." J Clin Microbiol **33**(10): 2759-2762.

Herbold, W., R. Maus, I. Hahn, N. Ding, M. Srivastava, J. W. Christman, M. Mack, J. Reutershan, D. E. Briles, J. C. Paton, C. Winter, T. Welte and U. A. Maus (2010). "Importance of CXC chemokine receptor 2 in alveolar neutrophil and exudate macrophage recruitment in response to pneumococcal lung infection." Infection and immunity **78**(6): 2620-2630.

Ho, P. L., V. C. Cheng and C. M. Chu (2009). "Antibiotic resistance in community-acquired pneumonia caused by *Streptococcus pneumoniae*, methicillin-resistant Staphylococcus aureus, and Acinetobacter baumannii." Chest **136**(4): 1119-1127.

Hofstra, J. J., A. D. Cornet, B. F. de Rooy, A. P. Vlaar, T. van der Poll, M. Levi, S. A. Zaat and M. J. Schultz (2009). "Nebulized antithrombin limits bacterial outgrowth and lung injury in *Streptococcus pneumoniae* pneumonia in rats." Crit Care **13**(5): R145.

Horiuchi, T., H. Mitoma, S. Harashima, H. Tsukamoto and T. Shimoda (2010). "Transmembrane TNF-alpha: structure, function and interaction with anti-TNF agents." Rheumatology **49**(7): 1215-1228.

Houldsworth, S., P. W. Andrew and T. J. Mitchell (1994). "Pneumolysin stimulates production of tumor necrosis factor alpha and interleukin-1 beta by human mononuclear phagocytes." Infection and immunity **62**(4): 1501-1503.

Hsu, H. E., K. A. Shutt, M. R. Moore, B. W. Beall, N. M. Bennett, A. S. Craig, M. M. Farley, J. H. Jorgensen, C. A. Lexau, S. Petit, A. Reingold, W. Schaffner, A. Thomas, C. G. Whitney and L. H. Harrison (2009). "Effect of pneumococcal conjugate vaccine on pneumococcal meningitis." The New England journal of medicine **360**(3): 244-256.

Hu, D. K., Y. Liu, X. Y. Li and Y. Qu (2015). "In vitro expression of *Streptococcus pneumoniae* ply gene in human monocytes and pneumocytes." Eur J Med Res **20**: 52.

Hughes, C. E., R. M. Harvey, C. D. Plumptre and J. C. Paton (2014). "Development of primary invasive pneumococcal disease caused by serotype 1 pneumococci is driven by early increased type I interferon response in the lung." Infection and immunity **82**(9): 3919-3926.

Huijts, S. M., M. W. Pride, J. M. Vos, K. U. Jansen, C. Webber, W. Gruber, W. G. Boersma, D. Snijders, J. A. Kluytmans, I. van der Lee, B. A. Kuipers, A. van der Ende and M. J. Bonten (2013). "Diagnostic accuracy of a serotype-specific antigen test in community-acquired pneumonia." Eur Respir J **42**(5): 1283-1290.

Hupp, S., C. Fortsch, C. Wippel, J. Ma, T. J. Mitchell and A. I. Iliev (2013). "Direct transmembrane interaction between actin and the pore-competent, cholesterol-dependent cytolysin pneumolysin." Journal of molecular biology **425**(3): 636-646.

Hussain, M., A. Melegaro, R. G. Pebody, R. George, W. J. Edmunds, R. Talukdar, S. A. Martin, A. Efstratiou and E. Miller (2005). "A longitudinal household study of *Streptococcus pneumoniae* nasopharyngeal carriage in a UK setting." Epidemiol Infect **133**(5): 891-898.

Hussell, T. and T. J. Bell (2014). "Alveolar macrophages: plasticity in a tissue-specific context." Nature reviews. Immunology **14**(2): 81-93.

Hyams, C., E. Camberlein, J. M. Cohen, K. Bax and J. S. Brown (2010). "The *Streptococcus pneumoniae* capsule inhibits complement activity and neutrophil phagocytosis by multiple mechanisms." Infection and immunity **78**(2): 704-715.

Hyams, C., S. Opel, W. Hanage, J. Yuste, K. Bax, B. Henriques-Normark, B. G. Spratt and J. S. Brown (2011). "Effects of *Streptococcus pneumoniae* strain background on complement resistance." PloS one **6**(10): e24581.

Hyams, C., K. Trzcinski, E. Camberlein, D. M. Weinberger, S. Chimalapati, M. Noursadeghi, M. Lipsitch and J. S. Brown (2013). "*Streptococcus pneumoniae* capsular serotype invasiveness correlates with the degree of factor H binding and opsonization with C3b/iC3b." Infection and immunity **81**(1): 354-363.

Hyams, C., J. Yuste, K. Bax, E. Camberlein, J. N. Weiser and J. S. Brown (2010). "*Streptococcus pneumoniae* resistance to complement-mediated immunity is dependent on the capsular serotype." Infection and immunity **78**(2): 716-725.

Iliev, A. I., J. R. Djannatian, R. Nau, T. J. Mitchell and F. S. Wouters (2007). "Cholesterol-dependent actin remodeling via RhoA and Rac1 activation by the *Streptococcus pneumoniae* toxin pneumolysin." Proc Natl Acad Sci U S A **104**(8): 2897-2902.

Iovino, F., G. Molema and J. J. Bijlsma (2014). "Platelet endothelial cell adhesion molecule-1, a putative receptor for the adhesion of *Streptococcus pneumoniae* to the vascular endothelium of the blood-brain barrier." Infection and immunity **82**(9): 3555-3566.

Italiani, P. and D. Boraschi (2014). "From Monocytes to M1/M2 Macrophages: Phenotypical vs. Functional Differentiation." Front Immunol **5**: 514.

Ivanov, S., C. Paget and F. Trottein (2014). "Role of non-conventional T lymphocytes in respiratory infections: the case of the pneumococcus." PLoS Pathog **10**(10): e1004300.

Ivanov, S., J. Renneson, J. Fontaine, A. Barthelemy, C. Paget, E. M. Fernandez, F. Blanc, C. De Trez, L. Van Maele, L. Dumoutier, M. R. Huerre, G. Eberl, M. Si-Tahar, P. Gosset, J. C. Renauld, J. C. Sirard, C. Faveeuw and F. Trottein (2013). "Interleukin-22 reduces lung inflammation during influenza A virus infection and protects against secondary bacterial infection." J Virol **87**(12): 6911-6924.

Iwanaszko, M. and M. Kimmel (2015). "NF-kappaB and IRF pathways: cross-regulation on target genes promoter level." BMC Genomics **16**(1): 307.

Jagger, M. P., Z. Huo and P. G. Riches (2002). "Inflammatory cytokine (interleukin 6 and tumour necrosis factor alpha) release in a human whole blood system in response to *Streptococcus pneumoniae* serotype 14 and its capsular polysaccharide." Clinical and experimental immunology **130**(3): 467-474.

Janoff, E. N., C. Fasching, J. M. Orenstein, J. B. Rubins, N. L. Opstad and A. P. Dalmasso (1999). "Killing of *Streptococcus pneumoniae* by capsular polysaccharide-specific polymeric IgA, complement, and phagocytes." J Clin Invest **104**(8): 1139-1147.

M. Jedrzejas (2004). "Extracellular virulence factors of *Streptococcus pneumoniae* (2004). Front Biosci **9**:891-94.

Jefferies, J. M., C. H. Johnston, L. A. Kirkham, G. J. Cowan, K. S. Ross, A. Smith, S. C. Clarke, A. B. Brueggemann, R. C. George, B. Pichon, G. Pluschke, V. Pfluger and T. J. Mitchell (2007). "Presence of nonhemolytic pneumolysin in serotypes of *Streptococcus pneumoniae* associated with disease outbreaks." The Journal of infectious diseases **196**(6): 936-944.

Jensch, I., G. Gamez, M. Rothe, S. Ebert, M. Fulde, D. Somplatzki, S. Bergmann, L. Petruschka, M. Rohde, R. Nau and S. Hammerschmidt (2010). "PavB is a surface-exposed adhesin of *Streptococcus pneumoniae* contributing to nasopharyngeal colonization and airways infections." Molecular microbiology **77**(1): 22-43.

Jeong, D. G., J. H. Seo, S. H. Heo, Y. K. Choi and E. S. Jeong (2015). "Tumor necrosis factor-alpha deficiency impairs host defense against *Streptococcus pneumoniae*." Lab Anim Res **31**(2): 78-85.

Jones, M. R., B. T. Simms, M. M. Lupa, M. S. Kogan and J. P. Mizgerd (2005). "Lung NF-kappaB activation and neutrophil recruitment require IL-1 and TNF receptor signaling during pneumococcal pneumonia." Journal of immunology **175**(11): 7530-7535.

Jonsson, S., D. M. Musher, A. Chapman, A. Goree and E. C. Lawrence (1985). "Phagocytosis and killing of common bacterial pathogens of the lung by human alveolar macrophages." The Journal of infectious diseases **152**(1): 4-13.

Jose, R. J., A. E. Williams, P. F. Mercer, M. G. Sulikowski, J. S. Brown and R. C. Chambers (2015). "Regulation of Neutrophilic Inflammation by Proteinase-Activated Receptor 1 during Bacterial Pulmonary Infection." J Immunol **194**(12): 6024-6034.

Jounblat, R., H. Clark, P. Eggleton, S. Hawgood, P. W. Andrew and A. Kadioglu (2005). "The role of surfactant protein D in the colonisation of the respiratory tract and onset of bacteraemia during pneumococcal pneumonia." Respiratory research **6**: 126.

Jounblat, R., A. Kadioglu, F. Iannelli, G. Pozzi, P. Eggleton and P. W. Andrew (2004). "Binding and agglutination of *Streptococcus pneumoniae* by human surfactant protein D (SP-D) vary between strains, but SP-D fails to enhance killing by neutrophils." Infection and immunity **72**(2): 709-716.

Kadioglu, A., W. Coward, M. J. Colston, C. R. Hewitt and P. W. Andrew (2004). "CD4-T-lymphocyte interactions with pneumolysin and pneumococci suggest a crucial protective role in the host response to pneumococcal infection." Infection and immunity **72**(5): 2689-2697.

Kadioglu, A., K. De Filippo, M. Bangert, V. E. Fernandes, L. Richards, K. Jones, P. W. Andrew and N. Hogg (2011). "The integrins Mac-1 and alpha4beta1 perform crucial roles in neutrophil and T cell recruitment to lungs during *Streptococcus pneumoniae* infection." Journal of immunology **186**(10): 5907-5915.

Kadioglu, A., S. Taylor, F. Iannelli, G. Pozzi, T. J. Mitchell and P. W. Andrew (2002). "Upper and lower respiratory tract infection by *Streptococcus pneumoniae* is affected by pneumolysin deficiency and differences in capsule type." Infection and immunity **70**(6): 2886-2890.

Kadioglu, A., J. N. Weiser, J. C. Paton and P. W. Andrew (2008). "The role of *Streptococcus pneumoniae* virulence factors in host respiratory colonization and disease." Nature Reviews. Microbiology **6**(4): 288-301.

Kafka, D., E. Ling, G. Feldman, D. Benharroch, E. Voronov, N. Givon-Lavi, Y. Iwakura, R. Dagan, R. N. Apte and Y. Mizrachi-Nebenzahl (2008). "Contribution of IL-1 to resistance to *Streptococcus pneumoniae* infection." International immunology **20**(9): 1139-1146.

Kang, Y. S., Y. Do, H. K. Lee, S. H. Park, C. Cheong, R. M. Lynch, J. M. Loeffler, R. M. Steinman and C. G. Park (2006). "A dominant complement fixation pathway for pneumococcal polysaccharides initiated by SIGN-R1 interacting with C1q." Cell **125**(1): 47-58.

Kang, Y. S., J. Y. Kim, S. A. Bruening, M. Pack, A. Charalambous, A. Pritsker, T. M. Moran, J. M. Loeffler, R. M. Steinman and C. G. Park (2004). "The C-type lectin SIGN-R1 mediates uptake of the capsular polysaccharide of *Streptococcus pneumoniae* in the marginal zone of mouse spleen." Proceedings of the National Academy of Sciences of the United States of America **101**(1): 215-220.

Kasanmoentalib, E. S., M. Valls Seron, B. P. Morgan, M. C. Brouwer and D. van de Beek (2015). "Adjuvant treatment with dexamethasone plus anti-C5 antibodies improves outcome of experimental pneumococcal meningitis: a randomized controlled trial." J Neuroinflammation **12**: 149.

Kash, J. C., K. A. Walters, A. S. Davis, A. Sandouk, L. M. Schwartzman, B. W. Jagger, D. S. Chertow, Q. Li, R. E. Kuestner, A. Ozinsky and J. K. Taubenberger (2011). "Lethal synergism of 2009 pandemic H1N1 influenza virus and *Streptococcus pneumoniae* coinfection is associated with loss of murine lung repair responses." mBio **2**(5).

Kawakami, K., N. Yamamoto, Y. Kinjo, K. Miyagi, C. Nakasone, K. Uezu, T. Kinjo, T. Nakayama, M. Taniguchi and A. Saito (2003). "Critical role of Valpha14+ natural killer T cells in the innate phase of host protection against *Streptococcus pneumoniae* infection." European journal of immunology **33**(12): 3322-3330.

Keller, L. E., D. A. Robinson, L. S. McDaniel (2016). "Nonencapsulated *Streptococcus pneumoniae*: Emergence and pathogenesis." mBio **7**(3): e01972-15.

Kerr, A. R., G. K. Paterson, A. Riboldi-Tunnicliffe and T. J. Mitchell (2005). "Innate immune defense against pneumococcal pneumonia requires pulmonary complement component C3." Infect Immun **73**(7): 4245-4252.

Khandavilli, S., K. A. Homer, J. Yuste, S. Basavanna, T. Mitchell and J. S. Brown (2008). "Maturation of *Streptococcus pneumoniae* lipoproteins by a type II signal peptidase is required for ABC transporter function and full virulence." Molecular microbiology **67**(3): 541-557.

Kilian, M., K. Poulsen, T. Blomqvist, L. S. Havarstein, M. Bek-Thomsen, H. Tettelin and U. B. Sorensen (2008). "Evolution of *Streptococcus pneumoniae* and its close commensal relatives." PloS one **3**(7): e2683.

Kilian, M., D. R. Riley, A. Jensen, H. Bruggemann and H. Tettelin (2014). "Parallel evolution of *Streptococcus pneumoniae* and Streptococcus mitis to pathogenic and mutualistic lifestyles." mBio **5**(4): e01490-01414.

Kim, B. J., S. Lee, R. E. Berg, J. W. Simecka and H. P. Jones (2013). "Interleukin-23 (IL-23) deficiency disrupts Th17 and Th1-related defenses against *Streptococcus pneumoniae* infection." Cytokine **64**(1): 375-381.

Kim, J. O. and J. N. Weiser (1998). "Association of intrastrain phase variation in quantity of capsular polysaccharide and teichoic acid with the virulence of *Streptococcus pneumoniae*." The Journal of infectious diseases **177**(2): 368-377.

Kim, Y. J., H. S. Shin, J. H. Lee, Y. W. Jung, H. B. Kim and U. H. Ha (2013). "Pneumolysin-mediated expression of beta-defensin 2 is coordinated by p38 MAP kinase-MKP1 in human airway cells." J Microbiol **51**(2): 194-199.

Kim, Y. S., K. S. Min, S. I. Lee, S. J. Shin, K. S. Shin and E. C. Kim (2010). "Effect of pro-inflammatory cytokines on the expression and regulation of human beta-defensin 2 in human dental pulp cells." J Endod **36**(1): 64-69.

Kinjo, Y., P. Illarionov, J. L. Vela, B. Pei, E. Girardi, X. Li, Y. Li, M. Imamura, Y. Kaneko, A. Okawara, Y. Miyazaki, A. Gomez-Velasco, P. Rogers, S. Dahesh, S. Uchiyama, A. Khurana, K. Kawahara, H. Yesilkaya, P. W. Andrew, C. H. Wong, K. Kawakami, V. Nizet, G. S. Besra, M. Tsuji, D. M. Zajonc and M. Kronenberg (2011). "Invariant natural killer T cells recognize glycolipids from pathogenic Gram-positive bacteria." Nature immunology **12**(10): 966-974.

Kirby, A. C., D. J. Newton, S. R. Carding and P. M. Kaye (2007). "Pulmonary dendritic cells and alveolar macrophages are regulated by gammadelta T cells during the resolution of *S. pneumoniae*-induced inflammation." J Pathol **212**(1): 29-37.

Kirkham, L. A., J. M. Jefferies, A. R. Kerr, Y. Jing, S. C. Clarke, A. Smith and T. J. Mitchell (2006). "Identification of invasive serotype 1 pneumococcal isolates that express nonhemolytic pneumolysin." Journal of clinical microbiology **44**(1): 151-159.

Kirkham, L.S., A.R. Kerr, G.R. Douce, G.K. Paterson, D.A. Dilts, D-F. Liu and T.J. Mitchell (2006). "Construction and immunological characterization of a novel nontoxic protective pneumolysin mutant for use in future pneumococcal vaccines." Infection and Immunity **74**(1): 586–593

Kishore, U., A. L. Bernal, M. F. Kamran, S. Saxena, M. Singh, P. U. Sarma, T. Madan and T. Chakraborty (2005). "Surfactant proteins SP-A and SP-D in human health and disease." Archivum immunologiae et therapiae experimentalis **53**(5): 399-417.

Klein, C., B. Lisowska-Grospierre, F. LeDeist, A. Fischer and C. Griscelli (1993). "Major histocompatibility complex class II deficiency: clinical manifestations, immunologic features, and outcome." The Journal of pediatrics **123**(6): 921-928.

Knapp, S., J. C. Leemans, S. Florquin, J. Branger, N. A. Maris, J. Pater, N. van Rooijen and T. van der Poll (2003). "Alveolar macrophages have a protective antiinflammatory role during murine pneumococcal pneumonia." American journal of respiratory and critical care medicine **167**(2): 171-179.

Knapp, S., C. W. Wieland, C. van 't Veer, O. Takeuchi, S. Akira, S. Florquin and T. van der Poll (2004). "Toll-like receptor 2 plays a role in the early inflammatory response to murine pneumococcal pneumonia but does not contribute to antibacterial defense." Journal of immunology **172**(5): 3132-3138.

Koedel, U., T. Rupprecht, B. Angele, J. Heesemann, H. Wagner, H. W. Pfister and C. J. Kirschning (2004). "MyD88 is required for mounting a robust host immune response to *Streptococcus pneumoniae* in the CNS." Brain : a journal of neurology **127**(Pt 6): 1437-1445.

Koga, T., J. H. Lim, H. Jono, U. H. Ha, H. Xu, H. Ishinaga, S. Morino, X. Xu, C. Yan, H. Kai and J. D. Li (2008). "Tumor suppressor cylindromatosis acts as a negative regulator for *Streptococcus pneumoniae*-induced NFAT signaling." J Biol Chem **283**(18): 12546-12554.

Kopf, M., C. Schneider and S. P. Nobs (2015). "The development and function of lung-resident macrophages and dendritic cells." Nat Immunol **16**(1): 36-44.

Koppe, U., K. Hogner, J. M. Doehn, H. C. Muller, M. Witzenrath, B. Gutbier, S. Bauer, T. Pribyl, S. Hammerschmidt, J. Lohmeyer, N. Suttorp, S. Herold and B. Opitz (2012). "*Streptococcus pneumoniae* stimulates a STING- and IFN regulatory factor 3-dependent type I IFN production in macrophages, which regulates RANTES production in macrophages, cocultured alveolar epithelial cells, and mouse lungs." Journal of immunology **188**(2): 811-817.

Koppe, U., N. Suttorp and B. Opitz (2012). "Recognition of *Streptococcus pneumoniae* by the innate immune system." Cellular Microbiology **14**(4): 460-466.

Koppel, E. A., M. Litjens, V. C. van den Berg, Y. van Kooyk and T. B. Geijtenbeek (2008). "Interaction of SIGNR1 expressed by marginal zone macrophages with marginal zone B cells is essential to early IgM responses against *Streptococcus pneumoniae*." Molecular immunology **45**(10): 2881-2887.

Koppel, E. A., E. Saeland, D. J. de Cooker, Y. van Kooyk and T. B. Geijtenbeek (2005). "DC-SIGN specifically recognizes *Streptococcus pneumoniae* serotypes 3 and 14." Immunobiology **210**(2-4): 203-210.

Koppel, E. A., C. W. Wieland, V. C. van den Berg, M. Litjens, S. Florquin, Y. van Kooyk, T. van der Poll and T. B. Geijtenbeek (2005). "Specific ICAM-3 grabbing nonintegrin-related 1 (SIGNR1) expressed by marginal zone macrophages is essential for defense against pulmonary *Streptococcus pneumoniae* infection." European journal of immunology **35**(10): 2962-2969.

Kota, S., A. Sabbah, T. H. Chang, R. Harnack, Y. Xiang, X. Meng and S. Bose (2008). "Role of human beta-defensin-2 during tumor necrosis factor-alpha/NF-kappaB-mediated innate antiviral response against human respiratory syncytial virus." J Biol Chem **283**(33): 22417-22429.

Kovacs-Simon, A., R. W. Titball and S. L. Michell (2011). "Lipoproteins of bacterial pathogens." Infection and immunity **79**(2): 548-561.

Kragsbjerg, P. and H. Fredlund (2001). "The effects of live *Streptococcus pneumoniae* and tumor necrosis factor-alpha on neutrophil oxidative burst and beta 2-integrin expression." Clin Microbiol Infect **7**(3): 125-129.

Krljanac, B., D. Weih, I. D. Jacobsen, D. Hu, I. Koliesnik, K. Reppe, M. Witzenrath and F. Weih (2014). "NF-kappaB2/p100 deficiency impairs immune responses to T-cell-independent type 2 antigens." European journal of immunology **44**(3): 662-672.

Kruetzmann, S., M. M. Rosado, H. Weber, U. Germing, O. Tournilhac, H. H. Peter, R. Berner, A. Peters, T. Boehm, A. Plebani, I. Quinti and R. Carsetti (2003). "Human immunoglobulin M memory B cells controlling *Streptococcus pneumoniae* infections are generated in the spleen." J Exp Med **197**(7): 939-945.

Kumar, V. and A. Sharma (2010). "Neutrophils: Cinderella of innate immune system." International immunopharmacology **10**(11): 1325-1334.

Kwon, A., D. Arenillas, R. Worsley Hunt and W. Wasserman (2012). "oPOSSUM-3: advanced analysis of regulatory motif over-representation across genes or ChIP-Seq datasets." G3 **2**(9):987-1002.

Lanie, J. A., W. L. Ng, K. M. Kazmierczak, T. M. Andrzejewski, T. M. Davidsen, K. J. Wayne, H. Tettelin, J. I. Glass and M. E. Winkler (2007). "Genome sequence of Avery's virulent serotype 2 strain D39 of *Streptococcus pneumoniae* and comparison with that of unencapsulated laboratory strain R6." J Bacteriol **189**(1): 38-51.

Lanoue, A., M. R. Clatworthy, P. Smith, S. Green, M. J. Townsend, H. E. Jolin, K. G. Smith, P. G. Fallon and A. N. McKenzie (2004). "SIGN-R1 contributes to protection against lethal pneumococcal infection in mice." The Journal of experimental medicine **200**(11): 1383-1393.

Laterre, P. F., G. Garber, H. Levy, R. Wunderink, G. T. Kinasewitz, J. P. Sollet, D. G. Maki, B. Bates, S. C. Yan and J. F. Dhainaut (2005). "Severe community-acquired pneumonia as a cause of severe sepsis: data from the PROWESS study." Critical care medicine **33**(5): 952-961.

Lee, H. Y., A. Andalibi, P. Webster, S. K. Moon, K. Teufert, S. H. Kang, J. D. Li, M. Nagura, T. Ganz and D. J. Lim (2004). "Antimicrobial activity of innate immune molecules against *Streptococcus pneumoniae*, Moraxella catarrhalis and nontypeable Haemophilus influenzae." BMC infectious diseases **4**: 12.

Lee, M. S. and Y. J. Kim (2007). "Signaling pathways downstream of pattern-recognition receptors and their cross talk." Annu Rev Biochem **76**: 447-480.

Lefeber, D. J., B. Benaissa-Trouw, J. F. Vliegenthart, J. P. Kamerling, W. T. Jansen, K. Kraaijeveld and H. Snippe (2003). "Th1-directing adjuvants increase the immunogenicity of oligosaccharide-protein conjugate vaccines related to *Streptococcus pneumoniae* type 3." Infect Immun **71**(12): 6915-6920.

LeMessurier, K., H. Hacker, E. Tuomanen and V. Redecke (2010). "Inhibition of T cells provides protection against early invasive pneumococcal disease." Infect Immun **78**(12): 5287-5294.

LeMessurier, K. S., H. Hacker, L. Chi, E. Tuomanen and V. Redecke (2013). "Type I interferon protects against pneumococcal invasive disease by inhibiting bacterial transmigration across the lung." PLoS pathogens **9**(11): e1003727.

Lemon, J. K., M. R. Miller and J. N. Weiser (2015). "Sensing of interleukin-1 cytokines during *Streptococcus pneumoniae* colonization contributes to macrophage recruitment and bacterial clearance." Infect Immun **83**(8): 3204-3212.

Li, P., J. Shi, Q. He, Q. Hu, Y. Y. Wang, L. J. Zhang, W. T. Chan and W. X. Chen (2015). "*Streptococcus pneumoniae* induces autophagy through the inhibition of the PI3K-I/Akt/mTOR pathway and ROS hypergeneration in A549 cells." PLoS One **10**(3): e0122753.

Li, W., B. Moltedo and T. M. Moran (2012). "Type I interferon induction during influenza virus infection increases susceptibility to secondary *Streptococcus pneumoniae* infection by negative regulation of gammadelta T cells." Journal of virology **86**(22): 12304-12312.

Li, Y., D. M. Weinberger, C. M. Thompson, K. Trzcinski and M. Lipsitch (2013). "Surface charge of *Streptococcus pneumoniae* predicts serotype distribution." Infection and immunity **81**(12): 4519-4524.

Lim, J. H., B. Stirling, J. Derry, T. Koga, H. Jono, C. H. Woo, H. Xu, P. Bourne, U. H. Ha, H. Ishinaga, H. Xu, A. Andalibi, X. H. Feng, H. Zhu, Y. Huang, W. Zhang, X. Weng, C. Yan, Z. Yin, D. E. Briles, R. J. Davis, R. A. Flavell and J. D. Li (2007). "Tumor suppressor CYLD regulates acute lung injury in lethal *Streptococcus pneumoniae* infections." Immunity **27**(2): 349-360.

Littmann, M., B. Albiger, A. Frentzen, S. Normark, B. Henriques-Normark and L. Plant (2009). "*Streptococcus pneumoniae* evades human dendritic cell surveillance by pneumolysin expression." EMBO Mol Med **1**(4): 211-222.

Liu, X., V. S. Chauhan, A. B. Young and I. Marriott (2010). "NOD2 mediates inflammatory responses of primary murine glia to *Streptococcus pneumoniae*." Glia **58**(7): 839-847.

Liu, X., Q. Han and J. Leng (2014). "Analysis of nucleotide-binding oligomerization domain proteins in a murine model of pneumococcal meningitis." BMC infectious diseases **14**(1): 648.

Lock, R, Q. Zhang, A. Berry and J. Paton (1996). "Sequence variation in the *Streptococcus pneumoniae* pneumolysin gene affecting haemolytic activity and electrophoretic mobility of the toxin." Microb Pathog **21**: 71–83.

Lopez, R. and E. Garcia (2004). "Recent trends on the molecular biology of pneumococcal capsules, lytic enzymes, and bacteriophage." FEMS Microbiology Reviews **28**(5): 553-580.

Los, F. C., T. M. Randis, R. V. Aroian and A. J. Ratner (2013). "Role of pore-forming toxins in bacterial infectious diseases." Microbiology and molecular biology reviews : MMBR **77**(2): 173-207.

Lu, J., T. Sun, H. Hou, M. Xu, T. Gu, Y. Dong, D. Wang, P. Chen, C. Wu, C. Liang, S. Sun, C. Jiang, W. Kong and Y. Wu (2014). "Detoxified pneumolysin derivative Plym2 directly protects against pneumococcal infection via induction of inflammatory cytokines." Immunol Invest **43**(7): 717-726.

Lujan, M., M. Gallego and J. Rello (2006). "Optimal therapy for severe pneumococcal community-acquired pneumonia." Intensive Care Medicine **32**(7): 971-980.

Lynch, J. P., 3rd and G. G. Zhanel (2010). "*Streptococcus pneumoniae*: epidemiology and risk factors, evolution of antimicrobial resistance, and impact of vaccines." Current Opinion in Pulmonary Medicine **16**(3): 217-225.

Lysenko, E. S., T. B. Clarke, M. Shchepetov, A. J. Ratner, D. I. Roper, C. G. Dowson and J. N. Weiser (2007). "Nod1 signaling overcomes resistance of *S. pneumoniae* to opsonophagocytic killing." PLoS pathogens **3**(8): e118.

Macedo-Ramos, H., A. F. Batista, A. Carrier-Ruiz, L. Alves, S. Allodi, V. T. Ribeiro-Resende, L. M. Teixeira and W. Baetas-da-Cruz (2014). "Evidence of involvement of the mannose receptor in the internalization of *Streptococcus pneumoniae* by Schwann cells." BMC Microbiol **14**: 211.

Magee, A. D. and J. Yother (2001). "Requirement for capsule in colonization by *Streptococcus pneumoniae*." Infection and immunity **69**(6): 3755-3761.

Malley, R., P. Henneke, S. C. Morse, M. J. Cieslewicz, M. Lipsitch, C. M. Thompson, E. Kurt-Jones, J. C. Paton, M. R. Wessels and D. T. Golenbock (2003). "Recognition of pneumolysin by Toll-like receptor 4 confers resistance to pneumococcal infection." Proceedings of the National Academy of Sciences of the United States of America **100**(4): 1966-1971.

Malley, R., K. Trzcinski, A. Srivastava, C. M. Thompson, P. W. Anderson and M. Lipsitch (2005). "CD4+ T cells mediate antibody-independent acquired immunity to pneumococcal colonization." Proceedings of the National Academy of Sciences of the United States of America **102**(13): 4848-4853.

Marriott, H. M., F. Ali, R. C. Read, T. J. Mitchell, M. K. Whyte and D. H. Dockrell (2004). "Nitric oxide levels regulate macrophage commitment to apoptosis or necrosis during pneumococcal infection." FASEB J **18**(10): 1126-1128.

Marriott, H. M., K. A. Gascoyne, R. Gowda, I. Geary, M. J. Nicklin, F. Iannelli, G. Pozzi, T. J. Mitchell, M. K. Whyte, I. Sabroe and D. H. Dockrell (2012). "Interleukin-1beta regulates CXCL8 release and influences disease outcome in response to *Streptococcus pneumoniae*, defining intercellular cooperation between pulmonary epithelial cells and macrophages." Infection and immunity **80**(3): 1140-1149.

Marriott, H. M., P. G. Hellewell, S. S. Cross, P. G. Ince, M. K. Whyte and D. H. Dockrell (2006). "Decreased alveolar macrophage apoptosis is associated with increased pulmonary inflammation in a murine model of pneumococcal pneumonia." J Immunol **177**(9): 6480-6488.

Martín-Sánchez, F., C. Diamond, M. Zeitler, A. Gomez, A. Baroja-Mazo, J. Bagnall, D. Spiller, M. White, M. Daniels, A. Mortarello, M. Peñalver, P. Paszek, J. Steringer, W. Nickel, D. Brough and P. Pelegrín (2016). "Inflammasome-dependent IL-1β release depends on membrane permabilisation." Cell Death Differ **23**(7):1219-31.

Martin, C. J., K. N. Peters and S. M. Behar (2014). "Macrophages clean up: efferocytosis and microbial control." Curr Opin Micro **17**: 17-23.

Martin, N. G., M. Sadarangani, A. J. Pollard and M. J. Goldacre (2014). "Hospital admission rates for meningitis and septicaemia caused by Haemophilus influenzae, Neisseria meningitidis, and *Streptococcus pneumoniae* in children in England over five decades: a population-based observational study." Lancet Infect Dis **14**(5): 397-405.

Martinon, F., L. Agostini, E. Meylan and J. Tschopp (2004). "Identification of bacterial muramyl dipeptide as activator of the NALP3/cryopyrin inflammasome." Current biology : CB **14**(21): 1929-1934.

Martinot, M., L. Oswald, E. Parisi, E. Etienne, N. Argy, I. Grawey, D. De Briel, M. M. Zadeh, L. Federici, G. Blaison, C. Koebel, B. Jaulhac, Y. Hansmann and D. Christmann (2014). "Immunoglobulin deficiency in patients with *Streptococcus pneumoniae* or Haemophilus influenzae invasive infections." International journal of infectious diseases : IJID : official publication of the International Society for Infectious Diseases **19**: 79-84.

Martner, A., S. Skovbjerg, J. C. Paton and A. E. Wold (2009). "*Streptococcus pneumoniae* autolysis prevents phagocytosis and production of phagocyte-activating cytokines." Infection and immunity **77**(9): 3826-3837.

Marty, V., C. Médina, C. Combe, P Parnet and T Amédée (2005). " ATP binding cassette transporter ABC1 is required for the release of interleukin-1 beta by P2X7 stimulated and lipopolysaccharide-primed mouse Schwann cells." Glia **49**(4):511-9.

Maus, U. A., M. Srivastava, J. C. Paton, M. Mack, M. B. Everhart, T. S. Blackwell, J. W. Christman, D. Schlondorff, W. Seeger and J. Lohmeyer (2004). "Pneumolysin-induced lung injury is independent of leukocyte trafficking into the alveolar space." Journal of immunology **173**(2): 1307-1312.

McIntosh, E. D. and R. R. Reinert (2011). "Global prevailing and emerging pediatric pneumococcal serotypes." Expert Rev Vaccines **10**(1): 109-129.

McKee, A., A. Ives, I. Balfour-Lynn (2011). "Increased incidence of bronchopulmonary fistulas complicating pediatric pneumonia. " Pediat Pulmonol **46**: 70-1

McNeela, E. A., A. Burke, D. R. Neill, C. Baxter, V. E. Fernandes, D. Ferreira, S. Smeaton, R. El-Rachkidy, R. M. McLoughlin, A. Mori, B. Moran, K. A. Fitzgerald, J. Tschopp, V. Petrilli, P. W. Andrew, A. Kadioglu and E. C. Lavelle (2010). "Pneumolysin activates the NLRP3 inflammasome and promotes proinflammatory cytokines independently of TLR4." PLoS pathogens **6**(11): e1001191.

Medeiros, A. I., C. H. Serezani, S. P. Lee and M. Peters-Golden (2009). "Efferocytosis impairs pulmonary macrophage and lung antibacterial function via PGE2/EP2 signaling." J Exp Med **206**(1): 61-68.

Mertens, J., M. Fabri, A. Zingarelli, T. Kubacki, S. Meemboor, L. Groneck, J. Seeger, M. Bessler, H. Hafke, M. Odenthal, J. G. Bieler, C. Kalka, J. P. Schneck, H. Kashkar and W. M. Kalka-Moll (2009). "*Streptococcus pneumoniae* serotype 1 capsular polysaccharide induces CD8CD28 regulatory T lymphocytes by TCR crosslinking." PLoS pathogens **5**(9): e1000596.

Milner, J. D., J. M. Brenchley, A. Laurence, A. F. Freeman, B. J. Hill, K. M. Elias, Y. Kanno, C. Spalding, H. Z. Elloumi, M. L. Paulson, J. Davis, A. Hsu, A. I. Asher, J. O'Shea, S. M. Holland, W. E. Paul and D. C. Douek (2008). "Impaired T(H)17 cell differentiation in subjects with autosomal dominant hyper-IgE syndrome." Nature **452**(7188): 773-776.

Mina, M. J., L. A. Brown and K. P. Klugman (2015). "Dynamics of Increasing IFN-gamma Exposure on Murine MH-S Cell-Line Alveolar Macrophage Phagocytosis of *Streptococcus pneumoniae*." J Interferon Cytokine Res **35**(6): 474-479.

Mitchell, A. J., B. Yau, J. A. McQuillan, H. J. Ball, L. K. Too, A. Abtin, P. Hertzog, S. L. Leib, C. A. Jones, S. K. Gerega, W. Weninger and N. H. Hunt (2012). "Inflammasome-dependent IFN-gamma drives pathogenesis in *Streptococcus pneumoniae* meningitis." J Immunol **189**(10): 4970-4980.

Mitchell, A. M. and T. J. Mitchell (2010). "*Streptococcus pneumoniae*: virulence factors and variation." Clinical microbiology and infection : the official publication of the European Society of Clinical Microbiology and Infectious Diseases **16**(5): 411-418.

Mitzel, D. N., V. Lowry, A. C. Shirali, Y. Liu and H. W. Stout-Delgado (2014). "Age-enhanced endoplasmic reticulum stress contributes to increased Atg9A inhibition of STING-mediated IFN-beta production during *Streptococcus pneumoniae* infection." Journal of immunology **192**(9): 4273-4283.

Moens, U., S. Kostenko and B. Sveinbjornsson (2013). "The Role of Mitogen-Activated Protein Kinase-Activated Protein Kinases (MAPKAPKs) in Inflammation." Genes (Basel) **4**(2): 101-133.

Moffitt, K., M. Skoberne, A. Howard, L. C. Gavrilescu, T. Gierahn, S. Munzer, B. Dixit, P. Giannasca, J. B. Flechtner and R. Malley (2014). "Toll-like receptor 2-dependent protection against pneumococcal carriage by immunization with lipidated pneumococcal proteins." Infection and immunity **82**(5): 2079-2086.

Moffitt, K. L., T. M. Gierahn, Y. J. Lu, P. Gouveia, M. Alderson, J. B. Flechtner, D. E. Higgins and R. Malley (2011). "T(H)17-based vaccine design for prevention of *Streptococcus pneumoniae* colonization." Cell host & microbe **9**(2): 158-165.

Mogensen, T. H. (2009). "Pathogen recognition and inflammatory signaling in innate immune defenses." Clinical Microbiology Reviews **22**(2): 240-273, Table of Contents.

Mogensen, T. H., R. S. Berg, S. R. Paludan and L. Ostergaard (2008). "Mechanisms of dexamethasone-mediated inhibition of Toll-like receptor signaling induced by Neisseria meningitidis and *Streptococcus pneumoniae*." Infection and immunity **76**(1): 189-197.

Mogensen, T. H., S. R. Paludan, M. Kilian and L. Ostergaard (2006). "Live *Streptococcus pneumoniae*, Haemophilus influenzae, and Neisseria meningitidis activate the inflammatory

response through Toll-like receptors 2, 4, and 9 in species-specific patterns." Journal of leukocyte biology **80**(2): 267-277.

Monari, C., F. Bistoni, A. Casadevall, E. Pericolini, D. Pietrella, T. R. Kozel and A. Vecchiarelli (2005). "Glucuronoxylomannan, a microbial compound, regulates expression of co-stimulatory molecules and production of cytokines in macrophages." J Infect Disease **191**(1), 127–137.

Moretti, J. and J. M. Blander (2014). "Insights into phagocytosis-coupled activation of pattern recognition receptors and inflammasomes." Current opinion in immunology **26**: 100-110.

Morona, J. K., R. Morona and J. C. Paton (2006). "Attachment of capsular polysaccharide to the cell wall of *Streptococcus pneumoniae* type 2 is required for invasive disease." Proceedings of the National Academy of Sciences of the United States of America **103**(22): 8505-8510.

Mosser, D. M. and J. P. Edwards (2008). "Exploring the full spectrum of macrophage activation." Nature reviews. Immunology **8**(12): 958-969.

Moynagh, P. N. (2005). "TLR signalling and activation of IRFs: revisiting old friends from the NF-kappaB pathway." Trends Immunol **26**(9): 469-476.

Mukhopadhyay, S., A. Varin, Y. Chen, B. Liu, K. Tryggvason and S. Gordon (2011). "SR-A/MARCO-mediated ligand delivery enhances intracellular TLR and NLR function, but ligand scavenging from cell surface limits TLR4 response to pathogens." Blood **117**(4): 1319-1328.

Mureithi, M. W., A. Finn, M. O. Ota, Q. Zhang, V. Davenport, T. J. Mitchell, N. A. Williams, R. A. Adegbola and R. S. Heyderman (2009). "T cell memory response to pneumococcal protein antigens in an area of high pneumococcal carriage and disease." The Journal of infectious diseases **200**(5): 783-793.

Murphy, J., R. Summer, A. A. Wilson, D. N. Kotton and A. Fine (2008). "The prolonged life-span of alveolar macrophages." American journal of respiratory cell and molecular biology **38**(4): 380-385.

Murray, P. and T. Wynn (2011). "Protective and pathogenic functions of macrophage subsets." Nature Reviews Immunology **11**:723-737.

Musher, D. M. (1992). "Infections caused by *Streptococcus pneumoniae*: clinical spectrum, pathogenesis, immunity, and treatment." Clinical infectious diseases : an official publication of the Infectious Diseases Society of America **14**(4): 801-807.

Musher, D. M., J. E. Groover, M. R. Reichler, F. X. Riedo, B. Schwartz, D. A. Watson, R. E. Baughn and R. F. Breiman (1997). "Emergence of antibody to capsular polysaccharides of *Streptococcus pneumoniae* during outbreaks of pneumonia: association with nasopharyngeal colonization." Clin Infect Dis **24**(3): 441-446.

Musher, D. M., J. E. Groover, J. M. Rowland, D. A. Watson, J. B. Struewing, R. E. Baughn and M. A. Mufson (1993). "Antibody to capsular polysaccharides of *Streptococcus pneumoniae*: prevalence, persistence, and response to revaccination." Clinical infectious diseases : an official publication of the Infectious Diseases Society of America **17**(1): 66-73.

Nakada, T. A., J. A. Russell, J. H. Boyd and K. R. Walley (2011). "IL17A genetic variation is associated with altered susceptibility to Gram-positive infection and mortality of severe sepsis." Crit Care **15**(5): R254.

Nakamatsu, M., N. Yamamoto, M. Hatta, C. Nakasone, T. Kinjo, K. Miyagi, K. Uezu, K. Nakamura, T. Nakayama, M. Taniguchi, Y. Iwakura, M. Kaku, J. Fujita and K. Kawakami (2007). "Role of interferon-gamma in Valpha14+ natural killer T cell-mediated host defense against *Streptococcus pneumoniae* infection in murine lungs." Microbes and infection / Institut Pasteur **9**(3): 364-374.

Naucler, P., J. Darenberg, E. Morfeldt, A. Ortqvist and B. Henriques Normark (2013). "Contribution of host, bacterial factors and antibiotic treatment to mortality in adult patients with bacteraemic pneumococcal pneumonia." Thorax **68**(6): 571-579.

Neill, D. R., W. R. Coward, J. F. Gritzfeld, L. Richards, F. J. Garcia-Garcia, J. Dotor, S. B. Gordon and A. Kadioglu (2014). "Density and duration of pneumococcal carriage is maintained by transforming growth factor beta1 and T regulatory cells." American journal of respiratory and critical care medicine **189**(10): 1250-1259.

Neill, D. R., V. E. Fernandes, L. Wisby, A. R. Haynes, D. M. Ferreira, A. Laher, N. Strickland, S. B. Gordon, P. Denny, A. Kadioglu and P. W. Andrew (2012). "T regulatory cells control susceptibility to invasive pneumococcal pneumonia in mice." PLoS pathogens **8**(4): e1002660.

Nelson, A. L., A. M. Roche, J. M. Gould, K. Chim, A. J. Ratner and J. N. Weiser (2007). "Capsule enhances pneumococcal colonization by limiting mucus-mediated clearance." Infection and immunity **75**(1): 83-90.

Newton, K. and V. M. Dixit (2012). "Signaling in innate immunity and inflammation." Cold Spring Harb Perspect Biol **4**(3).

Nguyen, C. T., E. H. Kim, T. T. Luong, S. Pyo and D. K. Rhee (2014). "ATF3 confers resistance to pneumococcal infection through positive regulation of cytokine production." The Journal of infectious diseases **210**(11): 1745-1754.

Nguyen, C. T., E. H. Kim, T. T. Luong, S. Pyo and D. K. Rhee (2015). "TLR4 mediates pneumolysin-induced ATF3 expression through the JNK/p38 pathway in *Streptococcus pneumoniae*-infected RAW 264.7 cells." Mol Cells **38**(1): 58-64.

Nita-Lazar, M., A. Banerjee, C. Feng, M. N. Amin, M. B. Frieman, W. H. Chen, A. S. Cross, L. X. Wang and G. R. Vasta (2015). "Desialylation of airway epithelial cells during influenza virus infection enhances pneumococcal adhesion via galectin binding." Mol Immunol **65**(1): 1-16.

Noursadeghi, M., J. Tsang, T. Haustein, R. F. Miller, B. M. Chain, D. R. Katz (2008). "Quantitative imaging assay for NFκB translocation in primary human macrophages." J Immunol Methods **329** (1-2):194-200.

Nuorti, J. P., J. C. Butler, M. M. Farley, L. H. Harrison, A. McGeer, M. S. Kolczak and R. F. Breiman (2000). "Cigarette smoking and invasive pneumococcal disease. Active Bacterial Core Surveillance Team." The New England journal of medicine **342**(10): 681-689.

O'Brien, K. L., L. J. Wolfson, J. P. Watt, E. Henkle, M. Deloria-Knoll, N. McCall, E. Lee, K. Mulholland, O. S. Levine and T. Cherian (2009). "Burden of disease caused by *Streptococcus pneumoniae* in children younger than 5 years: global estimates." Lancet **374**(9693): 893-902.

Oeckinghaus, A., M. S. Hayden and S. Ghosh (2011). "Crosstalk in NF-kappaB signaling pathways." Nat Immunol **12**(8): 695-708.

Olliver, M., J. Hiew, P. Mellroth, B. Henriques-Normark and P. Bergman (2011). "Human monocytes promote Th1 and Th17 responses to *Streptococcus pneumoniae*." Infection and immunity **79**(10): 4210-4217.

Olliver, M., L. Spelmink, J. Hiew, U. Meyer-Hoffert, B. Henriques-Normark and P. Bergman (2013). "Immunomodulatory effects of vitamin D on innate and adaptive immune responses to *Streptococcus pneumoniae*." The Journal of infectious diseases **208**(9): 1474-1481.

Opitz, B., A. Puschel, B. Schmeck, A. C. Hocke, S. Rosseau, S. Hammerschmidt, R. R. Schumann, N. Suttorp and S. Hippenstiel (2004). "Nucleotide-binding oligomerization domain proteins are innate immune receptors for internalized *Streptococcus pneumoniae*." The Journal of biological chemistry **279**(35): 36426-36432.

Osler, W (1904). "Medicine in the Nineteenth Century". Aequanimitas with Other Addresses to Medical Students, Nurses and Practitioners of Medicine 260.

Osorio, F. and C. Reis e Sousa (2011). "Myeloid C-type lectin receptors in pathogen recognition and host defense." Immunity **34**(5): 651-664.

Palaniappan, R., S. Singh, U. P. Singh, R. Singh, E. W. Ades, D. E. Briles, S. K. Hollingshead, W. Royal, 3rd, J. S. Sampson, J. K. Stiles, D. D. Taub and J. W. Lillard, Jr. (2006). "CCL5 modulates pneumococcal immunity and carriage." Journal of immunology **176**(4): 2346-2356.

Park, J. Y., H. J. Choi, M. G. Prabagar, W. S. Choi, S. J. Kim, C. Cheong, C. G. Park, C. Y. Chin and Y. S. Kang (2009). "The C-type lectin CD209b is expressed on microglia and it mediates the uptake of capsular polysaccharides of *Streptococcus pneumoniae*." Neurosci Lett **450**(3): 246-251.

Parker, D., F. J. Martin, G. Soong, B. S. Harfenist, J. L. Aguilar, A. J. Ratner, K. A. Fitzgerald, C. Schindler and A. Prince (2011). "*Streptococcus pneumoniae* DNA initiates type I interferon signaling in the respiratory tract." mBio **2**(3): e00016-00011.

Parker, D. and A. Prince (2011). "Innate immunity in the respiratory epithelium." American journal of respiratory cell and molecular biology **45**(2): 189-201.

Parker, D. and A. Prince (2011). "Type I interferon response to extracellular bacteria in the airway epithelium." Trends in immunology **32**(12): 582-588.

Paton, J. C, B. Rowan-Kelly and A. Ferrante (1984). "Activation of human complement by the pneumococcal toxin pneumolysin." Infect Immun **43**(3): 1085-1087.

Penaloza, H. F., P. A. Nieto, N. Munoz-Durango, F. J. Salazar-Echegarai, J. Torres, M. J. Parga, M. Alvarez-Lobos, C. A. Riedel, A. M. Kalergis and S. M. Bueno (2015). "Interleukin-10 plays a key role in the modulation of neutrophils recruitment and lung inflammation during infection by *Streptococcus pneumoniae*." Immunology **146**(1): 100-112.

Pennini, M. E., D. J. Perkins, A. M. Salazar, M. Lipsky and S. N. Vogel (2013). "Complete dependence on IRAK4 kinase activity in TLR2, but not TLR4, signaling pathways underlies decreased cytokine production and increased susceptibility to *Streptococcus pneumoniae* infection in IRAK4 kinase-inactive mice." Journal of immunology **190**(1): 307-316.

Pericone, C. D., K. Overweg, P. W. Hermans and J. N. Weiser (2000). "Inhibitory and bactericidal effects of hydrogen peroxide production by *Streptococcus pneumoniae* on other inhabitants of the upper respiratory tract." Infect Immun **68**(7): 3990-3997.

Picard, C., H. von Bernuth, P. Ghandil, M. Chrabieh, O. Levy, P. D. Arkwright, D. McDonald, R. S. Geha, H. Takada, J. C. Krause, C. B. Creech, C. L. Ku, S. Ehl, L. Marodi, S. Al-Muhsen, S. Al-Hajjar, A. Al-Ghonaium, N. K. Day-Good, S. M. Holland, J. I. Gallin, H. Chapel, D. P. Speert, C. Rodriguez-Gallego, E. Colino, B. Z. Garty, C. Roifman, T. Hara, H. Yoshikawa, S. Nonoyama, J. Domachowske, A. C. Issekutz, M. Tang, J. Smart, S. E. Zitnik, C. Hoarau, D. S. Kumararatne, A. J. Thrasher, E. G. Davies, C. Bethune, N. Sirvent, D. de Ricaud, Y. Camcioglu, J. Vasconcelos, M. Guedes, A. B. Vitor, C. Rodrigo, F. Almazan, M. Mendez, J. I. Arostegui, L. Alsina, C. Fortuny, J. Reichenbach, J. W. Verbsky, X. Bossuyt, R. Doffinger, L. Abel, A. Puel and J. L. Casanova (2010). "Clinical features and outcome of patients with IRAK-4 and MyD88 deficiency." Medicine (Baltimore) **89**(6): 403-425.

Pittet, L. A., L. Hall-Stoodley, M. R. Rutkowski and A. G. Harmsen (2010). "Influenza virus infection decreases tracheal mucociliary velocity and clearance of *Streptococcus pneumoniae*." Am J Respir Cell Mol Biol **42**(4): 450-460.

Pluddemann, A., S. Mukhopadhyay and S. Gordon (2011). "Innate immunity to intracellular pathogens: macrophage receptors and responses to microbial entry." Immunological reviews **240**(1): 11-24.

Price, K. E., N. G. Greene and A. Camilli (2012). "Export requirements of pneumolysin in *Streptococcus pneumoniae*." Journal of bacteriology **194**(14): 3651-3660.

Quinton, L. J., M. R. Jones, B. E. Robson and J. P. Mizgerd (2009). "Mechanisms of the hepatic acute-phase response during bacterial pneumonia." Infection and immunity **77**(6): 2417-2426.

Quinton, L. J., M. R. Jones, B. T. Simms, M. S. Kogan, B. E. Robson, S. J. Skerrett and J. P. Mizgerd (2007). "Functions and regulation of NF-kappaB RelA during pneumococcal pneumonia." Journal of immunology **178**(3): 1896-1903.

Rabes, A., S. Zimmermann, K. Reppe, R. Lang, P. H. Seeberger, N. Suttorp, M. Witzenrath, B. Lepenies and B. Opitz (2015). "The C-type lectin receptor Mincle binds to *Streptococcus pneumoniae* but plays a limited role in the anti-pneumococcal innate immune response." PLoS One **10**(2): e0117022.

Rahman, M. M. and G. McFadden (2006). "Modulation of tumor necrosis factor by microbial pathogens." PLoS pathogens **2**(2): e4.

Ratner, A. J., K. R. Hippe, J. L. Aguilar, M. H. Bender, A. L. Nelson and J. N. Weiser (2006). "Epithelial cells are sensitive detectors of bacterial pore-forming toxins." The Journal of biological chemistry **281**(18): 12994-12998.

Ricci, S., A. Gerlini, A. Pammolli, D. Chiavolini, V. Braione, S. A. Tripodi, B. Colombari, E. Blasi, M. R. Oggioni, S. Peppoloni and G. Pozzi (2013). "Contribution of different pneumococcal virulence factors to experimental meningitis in mice." BMC infectious diseases **13**: 444.

Rijneveld, A. W., G. P. van den Dobbelsteen, S. Florquin, T. J. Standiford, P. Speelman, L. van Alphen and T. van der Poll (2002). "Roles of interleukin-6 and macrophage inflammatory protein-2 in pneumolysin-induced lung inflammation in mice." The Journal of infectious diseases **185**(1): 123-126.

Ring, A., J. N. Weiser and E. I. Tuomanen (1998). "Pneumococcal trafficking across the blood-brain barrier. Molecular analysis of a novel bidirectional pathway." The Journal of clinical investigation **102**(2): 347-360.

Roche, A. M., A. L. Richard, J. T. Rahkola, E. N. Janoff and J. N. Weiser (2015). "Antibody blocks acquisition of bacterial colonization through agglutination." Mucosal Immunol **8**(1): 176-185.

Rodrigo, C., T. Bewick, C. Sheppard, S. Greenwood, T. Mckeever, C. Trotter, M. Slack, R. George, W. Shen Lim (2015). "Impact of infant 13-valent pneumococcal conjugate vaccine on serotypes in adult pneumonia." Eur Resp J **45**:1632-41.

Rogers, P. D., J. Thornton, K. S. Barker, D. O. McDaniel, G. S. Sacks, E. Swiatlo and L. S. McDaniel (2003). "Pneumolysin-dependent and -independent gene expression identified by cDNA microarray analysis of THP-1 human mononuclear cells stimulated by *Streptococcus pneumoniae*." Infection and immunity **71**(4): 2087-2094.

Rosas, M., K. Liddiard, M. Kimberg, I. Faro-Trindade, J. U. McDonald, D. L. Williams, G. D. Brown and P. R. Taylor (2008). "The induction of inflammation by dectin-1 in vivo is dependent on myeloid cell programming and the progression of phagocytosis." J. Immunol. **181(5)**, 3549–3557.

Roy, S., K. Knox, S. Segal, D. Griffiths, C. E. Moore, K. I. Welsh, A. Smarason, N. P. Day, W. L. McPheat, D. W. Crook, A. V. Hill and G. Oxford Pneumoccocal Surveillance (2002). "MBL genotype and risk of invasive pneumococcal disease: a case-control study." Lancet **359**(9317): 1569-1573.

Rubins, J. B., D. Charboneau, J. C. Paton, T. J. Mitchell, P. W. Andrew and E. N. Janoff (1995). "Dual function of pneumolysin in the early pathogenesis of murine pneumococcal pneumonia." The Journal of clinical investigation **95**(1): 142-150.

Rubins, J. B. and C. Pomeroy (1997). "Role of gamma interferon in the pathogenesis of bacteremic pneumococcal pneumonia." Infection and immunity **65**(7): 2975-2977.

Rutherford, T. J., C. Jones, D. B. Davies and A. C. Elliott (1994). "NMR assignment and conformational analysis of the antigenic capsular polysaccharide from *Streptococcus pneumoniae* type 9N in aqueous solution." Carbohydrate research **265**(1): 79-96.

Sandgren, A., K. Sjostrom, B. Olsson-Liljequist, B. Chrsitensson, A. Samuelsson, G. Kronvaal and B. Henriques-Normark (2004). "Effect of clonal and serotype-specific properties on the invasive capacity of *Streptococcus pneumoniae*." J Infect Dis **189**:785–96.

Sandgren, A., B. Albiger, C. J. Orihuela, E. Tuomanen, S. Normark and B. Henriques-Normark (2005). "Virulence in mice of pneumococcal clonal types with known invasive disease potential in humans." The Journal of infectious diseases **192**(5): 791-800.

Sano, H., K. Kuronuma, K. Kudo, H. Mitsuzawa, M. Sato, S. Murakami and Y. Kuroki (2006). "Regulation of inflammation and bacterial clearance by lung collectins." Respirology **11 Suppl**: S46-50.

Sato, S., C. St-Pierre, P. Bhaumik and J. Nieminen (2009). "Galectins in innate immunity: dual functions of host soluble beta-galactoside-binding lectins as damage-associated molecular patterns (DAMPs) and as receptors for pathogen-associated molecular patterns (PAMPs)." Immunological reviews **230**(1): 172-187.

Schaaf, B., J. Rupp, M. Muller-Steinhardt, J. Kruse, F. Boehmke, M. Maass, P. Zabel and K. Dalhoff (2005). "The interleukin-6 -174 promoter polymorphism is associated with extrapulmonary bacterial dissemination in *Streptococcus pneumoniae* infection." Cytokine **31**(4): 324-328.

Scharf, S., J. Zahlten, K. Szymanski, S. Hippenstiel, N. Suttorp and P. D. N'Guessan (2012). "*Streptococcus pneumoniae* induces human beta-defensin-2 and -3 in human lung epithelium." Exp Lung Res **38**(2): 100-110.

Schenk, M., J. T. Belisle and R. L. Modlin (2009). "TLR2 looks at lipoproteins." Immunity **31**(6): 847-849.

Schmeck, B., S. Huber, K. Moog, J. Zahlten, A. C. Hocke, B. Opitz, S. Hammerschmidt, T. J. Mitchell, M. Kracht, S. Rosseau, N. Suttorp and S. Hippenstiel (2006). "Pneumococci induced TLR- and Rac1-dependent NF-kappaB-recruitment to the IL-8 promoter in lung epithelial cells." American journal of physiology. Lung cellular and molecular physiology **290**(4): L730-L737.

Schouten, M., C. van 't Veer, J. J. Roelofs, B. Gerlitz, B. W. Grinnell, M. Levi and T. van der Poll (2011). "Recombinant activated protein C attenuates coagulopathy and inflammation when administered early in murine pneumococcal pneumonia." Thromb Haemost **106**(6): 1189-1196.

Schroder, N. W., S. Morath, C. Alexander, L. Hamann, T. Hartung, U. Zahringer, U. B. Gobel, J. R. Weber and R. R. Schumann (2003). "Lipoteichoic acid (LTA) of *Streptococcus pneumoniae* and Staphylococcus aureus activates immune cells via Toll-like receptor (TLR)-2, lipopolysaccharide-binding protein (LBP), and CD14, whereas TLR-4 and MD-2 are not involved." J Biol Chem **278**(18): 15587-15594.

Scicluna, B. P., M. H. Van Lieshout, D. C. Blok, S. Florquin and T. Van Der Poll (2015). "Modular Transcriptional Networks of the Host Pulmonary Response during Early and Late Pneumococcal Pneumonia." Mol Med **21**(1): 430-441.

Seyoum, B., M. Yano and L. A. Pirofski (2011). "The innate immune response to *Streptococcus pneumoniae* in the lung depends on serotype and host response." Vaccine **29**(45): 8002-8011.

Shainheit, M. G., M. Mule and A. Camilli (2014). "The core promoter of the capsule operon of *Streptococcus pneumoniae* is necessary for colonization and invasive disease." Infection and immunity **82**(2): 694-705.

Shaper, M., S. K. Hollingshead, W. H. Benjamin, Jr. and D. E. Briles (2004). "PspA protects *Streptococcus pneumoniae* from killing by apolactoferrin, and antibody to PspA enhances killing of pneumococci by apolactoferrin [corrected]." Infection and immunity **72**(9): 5031-5040.

Sharif, O., U. Matt, S. Saluzzo, K. Lakovits, I. Haslinger, T. Furtner, B. Doninger and S. Knapp (2013). "The scavenger receptor CD36 downmodulates the early inflammatory response while enhancing bacterial phagocytosis during pneumococcal pneumonia." Journal of immunology **190**(11): 5640-5648.

Sherwin, R. L., S. Gray, R. Alexander, P. C. McGovern, J. Graepel, M. W. Pride, J. Purdy, P. Paradiso and T. M. File, Jr. (2013). "Distribution of 13-valent pneumococcal conjugate vaccine *Streptococcus pneumoniae* serotypes in US adults aged >/=50 years with community-acquired pneumonia." J Infect Dis **208**(11): 1813-1820.

Shin, H. S., I. H. Yoo, Y. J. Kim, H. B. Kim, S. Jin and U. H. Ha (2010). "MKP1 regulates the induction of inflammatory response by pneumococcal pneumolysin in human epithelial cells." FEMS Immunol Med Microbiol **60**(2): 171-178.

Siegel, S. J., E. Tamashiro and J. N. Weiser (2015). "Clearance of Pneumococcal Colonization in Infants Is Delayed through Altered Macrophage Trafficking." PLoS Pathog **11**(6): e1005004.

Simons, J. P., J. M. Loeffler, R. Al-Shawi, S. Ellmerich, W. L. Hutchinson, G. A. Tennent, A. Petrie, J. G. Raynes, J. B. de Souza, R. A. Lawrence, K. D. Read and M. B. Pepys (2014). "C-reactive protein is essential for innate resistance to pneumococcal infection." Immunology **142**(3): 414-420.

Simonsen, L., R. J. Taylor, C. Schuck-Paim, R. Lustig, M. Haber and K. P. Klugman (2014). "Effect of 13-valent pneumococcal conjugate vaccine on admissions to hospital 2 years after its introduction in the USA: a time series analysis." Lancet Respir Med **2**(5): 387-394.

Simpson, S. Q., R. Singh and D. E. Bice (1994). "Heat-killed pneumococci and pneumococcal capsular polysaccharides stimulate tumor necrosis factor-alpha production by murine macrophages." American journal of respiratory cell and molecular biology **10**(3): 284-289.

Sinclair, A., X. Xie, M. Teltscher and N. Dendukuri (2013). "Systematic review and meta-analysis of a urine-based pneumococcal antigen test for diagnosis of community-acquired pneumonia caused by *Streptococcus pneumoniae*." J Clin Microbiol **51**(7): 2303-2310.

Sjostrom, K., C. Spindler, A. Ortqvist, M. Kalin, A. Sandgren, S. Kuhlmann-Berenzon and B. Henriques-Normark (2006). "Clonal and capsular types decide whether pneumococci will act as a primary or opportunistic pathogen." Clinical infectious diseases : an official publication of the Infectious Diseases Society of America **42**(4): 451-459.

Skov Sorensen, U. B., J. Blom, A. Birch-Andersen and J. Henrichsen (1988). "Ultrastructural localization of capsules, cell wall polysaccharide, cell wall proteins, and F antigen in pneumococci." Infection and immunity **56**(8): 1890-1896.

Song, J.-H., R. Dagan, K. P. Klugman and B. Fritzell (2012). "The relationship between pneumococcal serotypes and antibiotic resistance." Vaccine **30**(17): 2728-2737.

Sorrentino, R., P. M. de Souza, S. Sriskandan, C. Duffin, M. J. Paul-Clark and J. A. Mitchell (2008). "Pattern recognition receptors and interleukin-8 mediate effects of Gram-positive and Gram-negative bacteria on lung epithelial cell function." British journal of pharmacology **154**(4): 864-871.

Srivastava, A., H. Casey, N. Johnson, O. Levy and R. Malley (2007). "Recombinant bactericidal/permeability-increasing protein rBPI21 protects against pneumococcal disease." Infection and immunity **75**(1): 342-349.

Srivastava, A., P. Henneke, A. Visintin, S. C. Morse, V. Martin, C. Watkins, J. C. Paton, M. R. Wessels, D. T. Golenbock and R. Malley (2005). "The apoptotic response to pneumolysin is Toll-like receptor 4 dependent and protects against pneumococcal disease." Infection and immunity **73**(10): 6479-6487.

Standish, A. J. and J. N. Weiser (2009). "Human neutrophils kill *Streptococcus pneumoniae* via serine proteases." Journal of immunology **183**(4): 2602-2609.

Statt, S., J. W. Ruan, L. Y. Hung, C. Y. Chang, C. T. Huang, J. H. Lim, J. D. Li, R. Wu and C. Y. Kao (2015). "Statins Enhance Cellular Resistance Against Bacterial Pore-forming Toxins in Airway Epithelial Cells." Am J Respir Cell Mol Biol.

Sun, K. and D. W. Metzger (2008). "Inhibition of pulmonary antibacterial defense by interferon-gamma during recovery from influenza infection." Nature medicine **14**(5): 558-564.

Sun, K., S. L. Salmon, S. A. Lotz and D. W. Metzger (2007). "Interleukin-12 promotes gamma interferon-dependent neutrophil recruitment in the lung and improves protection against respiratory *Streptococcus pneumoniae* infection." Infection and immunity **75**(3): 1196-1202.

Suri, R., J. Periselneris, S. Lanone, P. Zeidler-Erdley, G. Melton, K. Palmer, P. Andujar, J. Antonini, V. Cohignac, A. Erdley, R. Jose, I. Mudway, J. Brown and J. Grigg (2016). Exposure to Welding Fumes and Lower Airway Infection with *Streptococcus pneumoniae*. *J Allergy Clinical Immunol* **137**(2):527-34.

Takashima, K., K. Tateda, T. Matsumoto, Y. Iizawa, M. Nakao and K. Yamaguchi (1997). "Role of tumor necrosis factor alpha in pathogenesis of pneumococcal pneumonia in mice." Infection and immunity **65**(1): 257-260.

Tam, J. C. and D. A. Jacques (2014). "Intracellular immunity: finding the enemy within--how cells recognize and respond to intracellular pathogens." Journal of leukocyte biology **96**(2): 233-244.

Taut, K., C. Winter, D. E. Briles, J. C. Paton, J. W. Christman, R. Maus, R. Baumann, T. Welte and U. A. Maus (2008). "Macrophage Turnover Kinetics in the Lungs of Mice Infected with *Streptococcus pneumoniae*." Am J Respir Cell Mol Biol **38**(1): 105-113.

Tettelin, H., K. E. Nelson, I. T. Paulsen, J. A. Eisen, T. D. Read, S. Peterson, J. Heidelberg, R. T. DeBoy, D. H. Haft, R. J. Dodson, A. S. Durkin, M. Gwinn, J. F. Kolonay, W. C. Nelson, J. D. Peterson, L. A. Umayam, O. White, S. L. Salzberg, M. R. Lewis, D. Radune, E. Holtzapple, H. Khouri, A. M. Wolf, T. R. Utterback, C. L. Hansen, L. A. McDonald, T. V. Feldblyum, S. Angiuoli, T. Dickinson, E. K. Hickey, I. E. Holt, B. J. Loftus, F. Yang, H. O. Smith, J. C. Venter, B. A. Dougherty, D. A. Morrison, S. K. Hollingshead and C. M. Fraser (2001). "Complete genome sequence of a virulent isolate of *Streptococcus pneumoniae*." Science **293**(5529): 498-506.

Thorley, A. J., P. A. Ford, M. A. Giembycz, P. Goldstraw, A. Young and T. D. Tetley (2007). "Differential regulation of cytokine release and leukocyte migration by lipopolysaccharide-stimulated primary human lung alveolar type II epithelial cells and macrophages." Journal of immunology **178**(1): 463-473.

Tomankova, T., E. Kriegova and M. Liu (2015). "Chemokine receptors and their therapeutic opportunities in diseased lung: far beyond leukocyte trafficking." Am J Physiol Lung Cell Mol Physiol **308**(7): L603-618.

Tomlinson, G.S., T. J. Cashmore, P. T. Elkington, J. Yates, R. J. Lehloenya, J. Tsang, M. Brown, R. F. Miller, K. Dheda, D. R. Katz, B. M. Chain and M. Noursadeghi (2011). "Transcriptional

profiling of innate and adaptive human immune responses to mycobacteria in the tuberculin skin test." Eur J Immunol **41**: 3253-3260

Tomlinson, G., S. Chimalapati, T. Pollard, T. Lapp, J. Cohen, E. Camberlein, S. Stafford, J. Periselneris, C. Aldridge, W. Vollmer, C. Picard, J. L. Casanova, M. Noursadeghi and J. Brown (2014). "TLR-Mediated Inflammatory Responses to *Streptococcus pneumoniae* Are Highly Dependent on Surface Expression of Bacterial Lipoproteins." Journal of immunology 193(7): 3736-45.

Travassos, L. H., S. E. Girardin, D. J. Philpott, D. Blanot, M. A. Nahori, C. Werts, and I. G. Boneca (2004). "Toll-like receptor 2-dependent bacterial sensing does not occur via peptidoglycan recognition." EMBO Rep 5: 1000-1006.

Tsang, J., B. M. Chain, R. F. Miller, B. L. Webb, W. Barclay, G. J. Towers, D. R. Katz and M. Noursadeghi (2009). "HIV-1 infection of macrophages is dependent on evasion of innate immune cellular activation." AIDS **23**: 2255-2263.

Tu, A. H., R. L. Fulgham, M. A. McCrory, D. E. Briles and A. J. Szalai (1999). "Pneumococcal surface protein A inhibits complement activation by *Streptococcus pneumoniae*." Infect Immun **67**(9): 4720-4724.

Tuomanen, E., A. Tomasz, B. Hengstler and O. Zak (1985). "The relative role of bacterial cell wall and capsule in the induction of inflammation in pneumococcal meningitis." The Journal of infectious diseases **151**(3): 535-540.

Turner, P., C. Turner, A. Jankhot, N. Helen, S. J. Lee, N. P. Day, N. J. White, F. Nosten and D. Goldblatt (2012). "A longitudinal study of *Streptococcus pneumoniae* carriage in a cohort of infants and their mothers on the Thailand-Myanmar border." PLoS One **7**(5): e38271.

Turvey, S. E. and T. R. Hawn (2006). "Towards subtlety: understanding the role of Toll-like receptor signaling in susceptibility to human infections." Clinical immunology **120**(1): 1-9.

Van Den Boogaard, F. E., X. Brands, M. J. Schultz, M. Levi, J. J. Roelofs, C. Van 't Veer and T. Van Der Poll (2011). "Recombinant human tissue factor pathway inhibitor exerts anticoagulant, anti-inflammatory and antimicrobial effects in murine pneumococcal pneumonia." J Thromb Haemost **9**(1): 122-132.

van den Boogaard, F. E., J. J. Hofstra, C. van 't Veer, M. M. Levi, J. J. Roelofs, T. van der Poll and M. J. Schultz (2015). "Feasibility and Safety of Local Treatment with Recombinant Human Tissue Factor Pathway Inhibitor in a Rat Model of *Streptococcus pneumoniae* Pneumonia." PLoS One **10**(5): e0127261.

van der Poll, T., C. V. Keogh, W. A. Buurman and S. F. Lowry (1997). "Passive immunization against tumor necrosis factor-alpha impairs host defense during pneumococcal pneumonia in mice." American journal of respiratory and critical care medicine **155**(2): 603-608.

van der Poll, T., C. V. Keogh, X. Guirao, W. A. Buurman, M. Kopf and S. F. Lowry (1997). "Interleukin-6 gene-deficient mice show impaired defense against pneumococcal pneumonia." The Journal of infectious diseases **176**(2): 439-444.

van Der Poll, T., A. Marchant and S. J. van Deventer (1997). "The role of interleukin-10 in the pathogenesis of bacterial infection." Clinical microbiology and infection : the official publication of the European Society of Clinical Microbiology and Infectious Diseases **3**(6): 605-607.

van Hoek, A. J., N. Andrews, P. A. Waight, J. Stowe, P. Gates, R. George and E. Miller (2012). "The effect of underlying clinical conditions on the risk of developing invasive pneumococcal disease in England." The Journal of infection **65**(1): 17-24.

van Hoek, A. J., C. L. Sheppard, N. J. Andrews, P. A. Waight, M. P. Slack, T. G. Harrison, S. N. Ladhani and E. Miller (2014). "Pneumococcal carriage in children and adults two years after

introduction of the thirteen valent pneumococcal conjugate vaccine in England." Vaccine **32**(34): 4349-4355.

Van Maele, L., C. Carnoy, D. Cayet, S. Ivanov, R. Porte, E. Deruy, J. A. Chabalgoity, J. C. Renauld, G. Eberl, A. G. Benecke, F. Trottein, C. Faveeuw and J. C. Sirard (2014). "Activation of Type 3 innate lymphoid cells and interleukin 22 secretion in the lungs during *Streptococcus pneumoniae* infection." J Infect Dis **210**(3): 493-503.

Vassal-Stermann, E., M. Lacroix, E. Gout, E. Laffly, C. M. Pedersen, L. Martin, A. Amoroso, R. R. Schmidt, U. Zahringer, C. Gaboriaud, A. M. Di Guilmi and N. M. Thielens (2014). "Human L-ficolin recognizes phosphocholine moieties of pneumococcal teichoic acid." J Immunol **193**(11): 5699-5708.

Verbinnen, B., K. Covens, L. Moens, I. Meyts and X. Bossuyt (2012). "Human CD20+CD43+CD27+CD5- B cells generate antibodies to capsular polysaccharides of *Streptococcus pneumoniae*." The Journal of allergy and clinical immunology **130**(1): 272-275.

Vogel, R. O., R. J. Janssen, M. A. van den Brand, C. E. Dieteren, S. Verkaart, W. J. Koopman, P. H. Willems, W. Pluk, L. P. van den Heuvel, J. A. Smeitink and L. G. Nijtmans (2007). "Cytosolic signaling protein Ecsit also localizes to mitochondria where it interacts with chaperone NDUFAF1 and functions in complex I assembly." Genes Dev **21**(5): 615-624.

von Bernuth, H., C. Picard, Z. Jin, R. Pankla, H. Xiao, C. L. Ku, M. Chrabieh, I. B. Mustapha, P. Ghandil, Y. Camcioglu, J. Vasconcelos, N. Sirvent, M. Guedes, A. B. Vitor, M. J. Herrero-Mata, J. I. Arostegui, C. Rodrigo, L. Alsina, E. Ruiz-Ortiz, M. Juan, C. Fortuny, J. Yague, J. Anton, M. Pascal, H. H. Chang, L. Janniere, Y. Rose, B. Z. Garty, H. Chapel, A. Issekutz, L. Marodi, C. Rodriguez-Gallego, J. Banchereau, L. Abel, X. Li, D. Chaussabel, A. Puel and J. L. Casanova (2008). "Pyogenic bacterial infections in humans with MyD88 deficiency." Science **321**(5889): 691-696.

von Bernuth, H., C. Picard, A. Puel and J. L. Casanova (2012). "Experimental and natural infections in MyD88- and IRAK-4-deficient mice and humans." European journal of immunology **42**(12): 3126-3135.

Vos, Q., A. Lees, Z. Q. Wu, C. M. Snapper and J. J. Mond (2000). "B-cell activation by T-cell-independent type 2 antigens as an integral part of the humoral immune response to pathogenic microorganisms." Immunological reviews **176**: 154-170.

Waight, P. A., N. J. Andrews, N. J. Ladhani, C. L. Sheppard, M. P. Slack and E. Miller (2015). "Effect of the 13-valent pneumococcal conjugate vaccine on invasive pneumococcal disease in England and Wales 4 years after its introduction: an observational cohort study." Lancet Infect Dis **15**(6): 629.

Walker, C. L., I. Rudan, L. Liu, H. Nair, E. Theodoratou, Z. A. Bhutta, K. L. O'Brien, H. Campbell and R. E. Black (2013). "Global burden of childhood pneumonia and diarrhoea." Lancet **381**(9875): 1405-1416.

Wang, I., Y. Bergeron, M. Bergeron (2005). "Ceftriaxone pharmacokinetics in interleukin-10 treated murine pneumococcal pneumonia. J Antimicrob Chem **55**:721-6.

Wang, X. A., R. Zhang, Z. G. She, X. F. Zhang, D. S. Jiang, T. Wang, L. Gao, W. Deng, S. M. Zhang, L. H. Zhu, S. Guo, K. Chen, X. D. Zhang, D. P. Liu and H. Li (2014). "Interferon regulatory factor 3 constrains IKKbeta/NF-kappaB signaling to alleviate hepatic steatosis and insulin resistance." Hepatology **59**(3): 870-885.

Wartha, F., K. Beiter, B. Albiger, J. Fernebro, A. Zychlinsky, S. Normark and B. Henriques-Normark (2007). "Capsule and D-alanylated lipoteichoic acids protect *Streptococcus pneumoniae* against neutrophil extracellular traps." Cellular Microbiology **9**(5): 1162-1171.

Weber, S. E., H. Tian and L. A. Pirofski (2011). "CD8+ cells enhance resistance to pulmonary serotype 3 *Streptococcus pneumoniae* infection in mice." Journal of immunology **186**(1): 432-442.

Weidenmaier, C. and A. Peschel (2008). "Teichoic acids and related cell-wall glycopolymers in Gram-positive physiology and host interactions." Nat Rev Microbiol **6**(4): 276-287.

Weinberger, D. M., Z. B. Harboe, E. A. Sanders, M. Ndiritu, K. P. Klugman, S. Ruckinger, R. Dagan, R. Adegbola, F. Cutts, H. L. Johnson, K. L. O'Brien, J. A. Scott and M. Lipsitch (2010). "Association of serotype with risk of death due to pneumococcal pneumonia: a meta-analysis." Clinical infectious diseases : an official publication of the Infectious Diseases Society of America **51**(6): 692-699.

Weinberger, D. M., R. Malley and M. Lipsitch (2011). "Serotype replacement in disease after pneumococcal vaccination." Lancet **378**(9807): 1962-1973.

Weinberger, D. M., K. Trzcinski, Y. J. Lu, D. Bogaert, A. Brandes, J. Galagan, P. W. Anderson, R. Malley and M. Lipsitch (2009). "Pneumococcal capsular polysaccharide structure predicts serotype prevalence." PLoS pathogens **5**(6): e1000476.

Weiser, J. N., D. Bae, C. Fasching, R. W. Scamurra, A. J. Ratner and E. N. Janoff (2003). "Antibody-enhanced pneumococcal adherence requires IgA1 protease." Proceedings of the National Academy of Sciences of the United States of America **100**(7): 4215-4220.

Welte, T., A. Torres and D. Nathwani (2012). "Clinical and economic burden of community-acquired pneumonia among adults in Europe." Thorax **67**(1): 71-79.

Werner, J. L. and C. Steele (2014). "Innate receptors and cellular defense against pulmonary infections." J Immunol **193**(8): 3842-3850.

Westphalen, K., G. A. Gusarova, M. N. Islam, M. Subramanian, T. S. Cohen, A. S. Prince and J. Bhattacharya (2014). "Sessile alveolar macrophages communicate with alveolar epithelium to modulate immunity." Nature **506**(7489): 503-506.

Whitmarsh, A. J. (2007). "Regulation of gene transcription by mitogen-activated protein kinase signaling pathways." Biochim Biophys Acta **1773**(8): 1285-1298.

Whitsett, J. A. and T. Alenghat (2015). "Respiratory epithelial cells orchestrate pulmonary innate immunity." Nat Immunol **16**(1): 27-35.

Williams, A. E., R. J. Jose, J. S. Brown and R. C. Chambers (2015). "Enhanced inflammation in aged mice following infection with *Streptococcus pneumoniae* is associated with decreased IL-10 and augmented chemokine production." Am J Physiol Lung Cell Mol Physiol **308**(6): L539-549.

Wilson, R., J. M. Cohen, R. J. Jose, C. de Vogel, H. Baxendale and J. S. Brown (2014). "Protection against *Streptococcus pneumoniae* lung infection after nasopharyngeal colonization requires both humoral and cellular immune responses." Mucosal Immunol.

Winter, C., W. Herbold, R. Maus, F. Langer, D. E. Briles, J. C. Paton, T. Welte and U. A. Maus (2009). "Important role for CC chemokine ligand 2-dependent lung mononuclear phagocyte recruitment to inhibit sepsis in mice infected with *Streptococcus pneumoniae*." J Immunol **182**(8): 4931-4937.

Witzenrath, M., F. Pache, D. Lorenz, U. Koppe, B. Gutbier, C. Tabeling, K. Reppe, K. Meixenberger, A. Dorhoi, J. Ma, A. Holmes, G. Trendelenburg, M. M. Heimesaat, S. Bereswill, M. van der Linden, J. Tschopp, T. J. Mitchell, N. Suttorp and B. Opitz (2011). "The NLRP3 inflammasome is differentially activated by pneumolysin variants and contributes to host defense in pneumococcal pneumonia." Journal of immunology **187**(1): 434-440.

Woehrl, B., M. C. Brouwer, C. Murr, S. G. Heckenberg, F. Baas, H. W. Pfister, A. H. Zwinderman, B. P. Morgan, S. R. Barnum, A. van der Ende, U. Koedel and D. van de Beek (2011).

"Complement component 5 contributes to poor disease outcome in humans and mice with pneumococcal meningitis." J Clin Invest **121**(10): 3943-3953.

Wright, A. K., M. Bangert, J. F. Gritzfeld, D. M. Ferreira, K. C. Jambo, A. D. Wright, A. M. Collins and S. B. Gordon (2013). "Experimental human pneumococcal carriage augments IL-17A-dependent T-cell defence of the lung." PLoS pathogens **9**(3): e1003274.

Wunderink, R. G., P. F. Laterre, B. Francois, D. Perrotin, A. Artigas, L. O. Vidal, S. M. Lobo, J. S. Juan, S. C. Hwang, T. Dugernier, S. LaRosa, X. Wittebole, J. F. Dhainaut, C. Doig, M. H. Mendelson, C. Zwingelstein, G. Su, S. Opal and C. T. Group (2011). "Recombinant tissue factor pathway inhibitor in severe community-acquired pneumonia: a randomized trial." Am J Respir Crit Care Med **183**(11): 1561-1568.

Xu, F., D. Droemann, J. Rupp, H. Shen, X. Wu, T. Goldmann, S. Hippenstiel, P. Zabel and K. Dalhoff (2008). "Modulation of the inflammatory response to *Streptococcus pneumoniae* in a model of acute lung tissue infection." American journal of respiratory cell and molecular biology **39**(5): 522-529.

Xu, Q., N. Surendran, D. Verhoeven, J. Klapa, M. Ochs and M. E. Pichichero (2015). "Trivalent pneumococcal protein recombinant vaccine protects against lethal *Streptococcus pneumoniae* pneumonia and correlates with phagocytosis by neutrophils during early pathogenesis." Vaccine **33**(8): 993-1000.

Yamamoto, K., J. D. Ferrari, Y. Cao, M. I. Ramirez, M. R. Jones, L. J. Quinton and J. P. Mizgerd (2012). "Type I alveolar epithelial cells mount innate immune responses during pneumococcal pneumonia." Journal of immunology **189**(5): 2450-2459.

Yamamoto, N., K. Kawakami, Y. Kinjo, K. Miyagi, T. Kinjo, K. Uezu, C. Nakasone, M. Nakamatsu and A. Saito (2004). "Essential role for the p40 subunit of interleukin-12 in neutrophil-mediated early host defense against pulmonary infection with *Streptococcus pneumoniae*: involvement of interferon-gamma." Microbes and infection / Institut Pasteur **6**(14): 1241-1249.

Yang, H., H. J. Ko, J. Y. Yang, J. J. Kim, S. U. Seo, S. G. Park, S. S. Choi, J. K. Seong and M. N. Kweon (2013). "Interleukin-1 promotes coagulation, which is necessary for protective immunity in the lung against *Streptococcus pneumoniae* infection." The Journal of infectious diseases **207**(1): 50-60.

Yoo, I. H., H. S. Shin, Y. J. Kim, H. B. Kim, S. Jin and U. H. Ha (2010). "Role of pneumococcal pneumolysin in the induction of an inflammatory response in human epithelial cells." FEMS Immunol Med Microbiol **60**(1): 28-35.

Yoshimura, A., E. Lien, R. R. Ingalls, E. Tuomanen, R. Dziarski and D. Golenbock (1999). "Cutting edge: recognition of Gram-positive bacterial cell wall components by the innate immune system occurs via Toll-like receptor 2." Journal of immunology **163**(1): 1-5.

Yother, J. (2011). "Capsules of *Streptococcus pneumoniae* and other bacteria: paradigms for polysaccharide biosynthesis and regulation." Annual review of microbiology **65**: 563-581.

Yuste, J., M. Botto, S. E. Bottoms and J. S. Brown (2007). "Serum amyloid P aids complement-mediated immunity to *Streptococcus pneumoniae*." PLoS pathogens **3**(9): 1208-1219.

Yuste, J., M. Botto, J. C. Paton, D. W. Holden and J. S. Brown (2005). "Additive inhibition of complement deposition by pneumolysin and PspA facilitates *Streptococcus pneumoniae* septicemia." Journal of immunology **175**(3): 1813-1819.

Yuste, J., A. Sen, L. Truedsson, G. Jonsson, L. S. Tay, C. Hyams, H. E. Baxendale, F. Goldblatt, M. Botto, and J. S. Brown (2008). "Impaired opsonization with C3b and phagocytosis of *Streptococcus pneumoniae* in serum from subjects with defects in the classical complement pathway." Infect. Immun **76:**3761–3770.

Zamze, S., L. Martinez-Pomares, H. Jones, P. R. Taylor, R. J. Stillion, S. Gordon and S. Y. Wong (2002). "Recognition of bacterial capsular polysaccharides and lipopolysaccharides by the macrophage mannose receptor." The Journal of biological chemistry **277**(44): 41613-41623.

Zhang, J. R., K. E. Mostov, M. E. Lamm, M. Nanno, S. Shimida, M. Ohwaki and E. Tuomanen (2000). "The polymeric immunoglobulin receptor translocates pneumococci across human nasopharyngeal epithelial cells." Cell **102**(6): 827-837.

Zhang, Z., T. B. Clarke and J. N. Weiser (2009). "Cellular effectors mediating Th17-dependent clearance of pneumococcal colonization in mice." The Journal of clinical investigation **119**(7): 1899-1909.

Zwijnenburg, P. J., T. van der Poll, S. Florquin, J. J. Roord and A. M. Van Furth (2003). "IL-1 receptor type 1 gene-deficient mice demonstrate an impaired host defense against pneumococcal meningitis." J Immunol **170**(9): 4724-4730.

10 Appendix: Published Abstracts

Poster presentation ATS 2014

The pro-inflammatory effects of *Streptococcus pneumoniae's* capsule.

J Periselneris, G Tomlinson, T Pollard, S Chimalapati, R José, A Dyson, M Singer, M Noursadeghi, J Brown.

Streptococcus pneumoniae is the second commonest cause of bacterial death world-wide, causing a variety of infections such as community acquired pneumonia, meningitis, and septicaemia. Many of the most serious consequences of infection are due to an over-exuberant inflammatory response. The bacterium is surrounded by a polysaccharide capsule that plays a role in inhibiting opsonophagocytosis. While this is recognised as its most important virulence factor it has not previously been thought to play a role in inducing inflammation.

We have data that shows that the encapsulated wildtype strain, TIGR4, provokes a greater inflammatory response than an unencapsulated mutant of *S. pneumoniae,* P1672. In vitro infection of human monocyte derived macrophages showed increased TNF, IL1β, IL6, and IL8 in response to TIGR4 versus P1672 (see figure). This is despite the unencapsulated mutant activating more NFKB translocation. Microarray analysis of macrophage responses suggest that a wider range of intracellular signalling pathways are stimulated by the unencapsulated mutant. Inhibition of phagocytosis with cytochalasin D did not reduce this difference, suggesting that the inflammatory effects of capsule are not due to reduced phagocytosis. In vivo modelling of mouse pneumonia by intranasal inoculation reproduces the difference between TIGR4 and P1672, in terms of neutrophil infiltrate into the lungs, albumin leak and cytokine levels in bronchoalveolar fluid and lung homogenate. Depleting alveolar macrophages with clodronate diminished some but not all of the differences. Using a rat sepsis model of infection with non-replicating bacteria we have again shown that TIGR4 elicits more pro-inflammatory cytokine release in serum than P1672.

Further work is required to characterise how the unencapsulated mutant causes a more varied transcriptional response. By identifying the mechanisms by which the capsule induces inflammation we may be able to find ways of inhibiting it and thus ameliorating disease.

Oral presentation BTS 2014

The inflammatory response to Streptococcus pneumoniae is exaggerated by the polysaccharide capsule

J N Periselneris, S Chimalapati, G Tomlinson, A Dyson, C Hyams, H Rukke, F Peterson, M Singer, M Noursadeghi, J S Brown

Streptococcus pneumoniae infections characteristically cause a high degree of inflammation. The *S. pneumoniae* polysaccharide capsule prevents opsonophagocytosis and is essential for virulence. The capsule might also be expected to reduce the host's inflammatory response by inhibiting bacterial interactions with pro-inflammatory signalling proteins eg toll-like receptors (TLR), but this has not previously been investigated. Using isogenic unencapsulated strains and *in vitro* and *in vivo* models of infection we have characterised capsule effects on the inflammatory response to *S. pneumoniae.*

Surprisingly, although the unencapsulated (Δ*cps*) *S. pneumoniae* strain was much more sensitive to phagocytosis by macrophages and induced a stronger NFκB response by human monocyte derived macrophages (MDMs) it caused similar levels of stimulation of a TLR2 reporter cell line as the encapsulated strain TIGR4. In addition, microarrays demonstrated increased transcription of pro-inflammatory cytokines by MDMs in response to TIGR4 compared to the Δ*cps* strain, and quantitative PCR and ELISAs confirmed stronger TNF, IL1β, and IL6 responses by MDMs to TIGR4. Furthermore, compared to the Δ*cps* strain the TIGR4 strain caused greater neutrophil recruitment and higher cytokine levels in the lungs in a mouse model of pneumonia, as well as higher serum cytokine levels with worse hypotension in a rat model of sepsis. Additional *in vitro* experiments excluded antibody, complement, pneumolysin, the inflammasome, and lectin-mediated signalling as mechanisms driving differences in inflammatory responses between TIGR4 and Δ*cps*. Expression of the TIGR4 capsule in *Streptococcus mitis* did not increase MDM or murine inflammatory responses. Notably, preventing phagocytosis with cytochalasin D did not alter differences in the inflammatory response between TIGR4 and the Δ*cps* strains, and in silico analysis suggested the Δ*cps* strain activated a wider range of transcription factors.

Overall, the data indicate that unencapsulated *S. pneumoniae* stimulate a wider range of host cell signalling pathways than encapsulated bacteria, some of which are likely to be anti-inflammatory. Hence the capsule, rather than reducing inflammation, causes increased pro-inflammatory responses and subsequent disturbances to host physiology during *S. pneumoniae* infection. Targeting the mechanisms responsible for capsule-dependent inflammation could offer novel treatment options for reducing the morbidity and mortality associated with *S. pneumoniae* infections.

ERS Lung Science & ERS poster abstract 2015

The inflammatory response to *Streptococcus pneumoniae* is exaggerated by the polysaccharide capsule

J N Periselneris, S Chimalapati, G Tomlinson, C Hyams, A Dyson, M Singer, M Noursadeghi, J S Brown

The inflammatory response to bacteria requires the interaction of pattern recognition receptors with bacterial surface constituents. *Streptococcus pneumoniae* has a polysaccharide capsule, an essential virulence factor that would be expected to inhibit these interactions, so reducing inflammatory responses. We tested this hypothesis by characterising the effect of *S. pneumoniae* capsule on the inflammatory response using the TIGR4 strain and its unencapsulated derivative TIGR4cps. Despite being more sensitive to phagocytosis by human macrophages than TIGR4, RNA transcripts and supernatant levels of TNF, IL1β, and IL6 were reduced in response to TIGR4cps. Furthermore, TIGR4 generated greater neutrophilic infiltrate in a mouse pneumonia model than TIGR4cps. Whole genome transcriptome analysis demonstrated a generally reduced pro-inflammatory response to the TIGR4cps strain. Notably, preventing phagocytosis preserved these differences. In vitro experiments excluded differences in TLR2 signalling, antibody recognition, the inflammasome, and lectin signalling as mechanisms driving differences in inflammatory responses between TIGR4 and Δcps. However, a transcription factor array suggested that TIGR4cps activated more transcription factors than TIGR4. These data demonstrate that *S. pneumoniae* capsule causes increased pro-inflammatory responses that are relevant during infection, perhaps by restricting macrophage cell signalling responses. Identifying mechanisms responsible for capsule-dependent inflammation may offer opportunities for adjuvant treatment of *S. pneumoniae* infections.

Oral presentation Europneumo 2015

Inflammation dampening effects of pneumolysin

J Periselneris, T Pollard, T James, M Noursadeghi, J Brown

Streptococcus pneumoniae interactions with alveolar macrophages are important for protective inflammatory responses during early lung infection. Pneumolysin is a well-recognised virulence factor for Streptococcus pneumoniae that has multiple effects on the host immune response that are primarily thought to be pro-inflammatory. We have investigated the effects of pneumolysin on the early macrophage response to *S. pneumoniae* using in vitro culture and an animal model of early pneumonia. Wildtype and non-haemolytic purified pneumolysin induced dose dependent inflammatory cytokine release from human monocyte derived macrophages (MDMs), as expected. However, in contrast, when MDMs were incubated with TIGR4 *S. pneumoniae*, higher levels of TNF and IL6 mRNA and protein were induced in response to pneumolysin deficient bacteria than wildtype. Transcriptome analysis of MDMs after *S. pneumoniae* infection confirmed increased expression of a range of pro-inflammatory genes in response to the pneumolysin mutant. Despite differential cell death in response to wildtype and pneumolysin deficient TIGR4, inhibition of apoptosis or the inflammasome also had no effect on the early MDM cytokine response. Instead, the increase in transcription of pro-inflammatory genes and TNF and IL6 supernatant levels in response to the pneumolysin deficient strain were abrogated by inhibition of S. pneumoniae phagocytosis with cytochalasin D. In a murine model of early pneumonia despite more rapid clearance of the pneumolysin mutant from BALF and lung compared to wildtype TIGR4 at 4 and 24 hours, BALF leukocyte recruitment was increased at 4 hours. These data indicate an unexpected role for pneumolysin as an initial suppressor of macrophage inflammatory responses, which is dependent on phagocytosis. The early inflammation dampening effects of pneumolysin released within the phagolysosome may be an important contribution to *S. pneumoniae* virulence, allowing increased bacterial replication early during the course of infection.

BTS 2015 Oral Presentation

Inflammation dampening effects of pneumolysin

J Periselneris, T James, M Noursadeghi, J Brown.

The inflammatory response to bacteria requires the interaction of pattern recognition receptors with bacterial surface constituents, and humans deficient in components of inflammatory signalling pathways such as IRAK4 are prone to invasive pneumococcal disease. Pneumolysin is a well-recognised virulence factor for *Streptococcus pneumoniae* that has multiple effects on the host immune response that are primarily thought to be pro-inflammatory; including causing IL1β release due to pore formation, and epithelial cell layer breakdown. We hypothesised that pneumolysin deficient TIGR4 (a serotype 4 strain) would induce less inflammatory cytokines than wildtype from human monocyte derived macrophages. While both pore forming and non-cytolytic purified pneumolysin induced dose dependent inflammatory cytokine release, the pneumolysin deficient bacteria induced greater TNF and IL6 than wildtype, by qPCR and ELISA measurement of protein. This was reduced by inhibition of phagocytosis with cytochalasin D. Given the pore forming effects of pneumolysin we assessed whether differential cell death contributed to the differences in inflammatory response. While wildtype bacteria caused more cell death at 24 hours, inhibition of caspases had no effect on the cytokine response suggesting that apoptosis pathways don't directly influence the early inflammatory response. Transcriptome analysis confirmed increased pro-inflammatory and interferon gene signalling with the mutant strain, with reduction of the inflammatory and interferon signature with inhibition of phagocytosis. Wildtype bacteria induced less NFκB translocation, but more IRF3 translocation than Δ*ply*. An in vivo intranasal mouse infection showed wildtype was more virulent, with more bacteria recovered from bronchoalveolar lavage fluid at 4 hours. However, this was associated with reduced TNF compared to Δ*ply*. Neutralising TNF intranasally abrogated the difference in bacteria recovered between wildtype and Δ*ply*. Thus, the early inflammation dampening effects of pneumolysin released within the phagolysosome may be an important contribution to its virulence by allowing bacterial replication at mucosal surfaces. This may be due to IRF3 mediated inhibition of inflammatory cytokine transcription. Better understanding of the biology of pneumolysin may aid in adjuvant treatment of *S. pneumoniae.*

Academy of Medical Sciences 2016, Poster presentation

Anti-inflammatory effects of *Streptococcus pneumoniae* toxin pneumolysin

Jimstan Periselneris, Mahdad Noursadeghi, Jeremy Brown

Background *Streptococcus pneumoniae* is the second commonest cause of bacterial mortality worldwide. Interactions of *S pneumoniae* with alveolar macrophages are important for the protective inflammatory responses during early lung infection. Pneumolysin is a well-recognised virulence factor for *S pneumoniae*; the toxin has multiple effects on the host immune response that are primarily thought to be proinflammatory. Our aim was to characterise the inflammatory effects of pneumolysin on macrophages.

Methods We used in-vitro culture of primary human monocyte-derived macrophages (MDM) with *S pneumoniae* and an isogenic mutant lacking pneumolysin. We measured cytokine production (including tumour necrosis factor [TNF] and interleukin 6) at transcriptional and protein level, as well as transcription factor function, to look at mechanisms of interaction between MDM and bacteria. We extended these data with epithelial cell line work and neutrophil transmigration models. Then we used a murine intranasal infection model to assess functional effects in vivo.

Findings Higher mean concentrations of TNF and interleukin 6 were induced from MDM in response to pneumolysin-deficient bacteria than in response to wild-type bacteria (6014 pg/ml [SD 970] vs 2295 [SD 470] and 821 [SD 374] *vs* 89 [SD 28], respectively). This finding was reflected in TNF mRNA (change in cycle threshold 4·3 *vs* 2·4) and interleukin 6 mRNA (3·5 *vs* 0·4). Transcriptome analysis of MDMs after *S pneumoniae* infection confirmed increased expression of a range of proinflammatory genes, including *IL12*, *IL27*, *CCR7*, *IL5*, and *CCL5*, in response to the pneumolysin mutant. The increase in transcription of proinflammatory genes and concentrations of TNF and interleukin 6 in supernatant in response to the pneumolysin-deficient strain were abrogated by inhibition of phagocytosis. In a murine pneumonia model, despite more rapid clearance of the pneumolysin-deficient mutant (1×10^4 colony-forming units [CFU]/mL) compared with the wild type strain (1×10^5 CFU/ml) from bronchoalveolar lavage fluid (BALF) by 4 h, mean concentrations of TNF were elevated in BALF fluid with the mutant (1336 pg/mL [SD 130] *vs* 6164 [SD 632]). This increase was associated with more rapid neutrophil influx with the pneumolysin-deficient mutant than with the wild-type strain into BALF seen at 2 h (107 neutrophils per mL [SD 39] *vs* 3303 [SD 1624]). Blockade of TNF abrogated the differences in clearance between the pneumolysin mutant and wild-type strain.

Interpretation These data indicate an unexpected role for pneumolysin as an initial suppressor of macrophage inflammatory responses, which is dependent on phagocytosis. The early inflammation dampening effects of pneumolysin released within the phagolysosome might be an important contribution to the virulence of *S pneumoniae*. The inhibition of TNF release allows increased bacterial replication early during the course of infection, and presumably is an evolutionary advantage.